MONASH University

Investigation of Type I Interferon and Immune Signalling in Breast and Ovarian Cancer

By Zoë Rebecca Church Marks
MBBS PhD Candidate

A thesis submitted for the degree of Doctor of Philosophy at
Monash University in 2018
Centre for Innate Immunity & Infectious Diseases
Hudson Institute of Medical Research
Faculty of Medicine, Nursing & Health Sciences

MonashHealth

HUDSON
INSTITUTE OF MEDICAL RESEARCH

Table of Contents

Declaration

This thesis contains no material which has been accepted for the award of any other degree or diploma at any university or equivalent institution and that, to the best of my knowledge and belief, this thesis contains no material previously published or written by another person, except where due reference is made in the text of the thesis. The material in chapter 4 has been submitted for publication and the material in chapter 3 has not yet been submitted.

Signature: 

Print Name: Zoë Rebecca Church Marks

Date: 24/01/2018

List of Abbreviations

ACD	Acid Citrate Destrose
ANOVA	Analysis of Variance
AOCS	Australian Ovarian Cancer Study
AP1	Activating Protein 1
BCS	Body Condition Score
BRCA1	Breast Cancer 1
BRCA2	Breast Cancer 2
C/DTC	Peripherally Disseminated Tumour Cells
CBA	Cytometric Bead Array
CCL2	Chemokine Ligand 2
CCR10	Chemokine Receptor 10
CCL18	Chemokine Ligand 18
CCL22	Chemokine Ligand 22
CCL28	Chemokine Ligand 28
CCR4	Chemokine Receptor 4
CD4	Cluster of Differentiation 4
CD8	Cluster of Differentiation 8
CD11b	Cluster of Differentiation 11b
CD11c	Cluster of Differentiation 11c
CD16	Cluster of Differentiation 16
CD20	Cluster of Differentiation 20
CD25	Cluster of Differentiation 25
CD41	Cluster of Differentiation 41
CD45	Cluster of Differentiation 45

CD45RO	Cluster of Differentiation 45 Varient, Marker of Active T-cells
CD56	Cluster of differentiation 56
CD69	Cluster of Differentiation 69
cDNA	Complementary DNA
cGAS	Cyclic GMP-AMP Synthase
CI	Baseline Cell Index
CK18	Cytokeratin 18
CO_2	Carbon Dioxide
cRNA	Complementary RNA
CSF1	Colony-Stimulating Factor 1
CSIOVDB	Ovarian Cancer Database of the Cancer Science Institute of Singapore
CTC	Circulating Tumour Cell
CXCL8	C-X-C Chemokine 8
CXCL9	C-X-C Chemokine 9
CXCL10	C-X-C Chemokine 10
CXCL14	C-X-C Chemokine 14
CXCR3	Chemokine Receptor 3
DAB	3,3'-Diaminobenzidine
DAPI	4', 6-Diamidino-2-Phenylindole Dihydrochloride
DC	Dendritic Cells
DEPC H_20	Diethyl Pyrocarbonate Water
DMEM	Dulbecco's Modified Eagle's Medium
DMSO	Dimethyl Sulfoxide
DNA	Deoxyribonucleic Acid
DTC	Disseminated tumour cell

EBNA1	Epstein-Barr Virus Nuclear Antigen 1
EBV	Epstein-Barr Virus
EDTA	Ethylenediaminetetraacetic Acid
EGF	Epidermal Growth Factor
ELF3	E74-Like Factor-3
EMT	Epithelial to Mesenchymal Transition
EOC	Epithelial Origin
eQTL	Quantitative Trait Loci
ER	Oestrogen Receptor
ER+/PR-	Oestrogen Receptor Positive/Progesterone Receptor Negative
ETS	E26 Transformation-Specific
FCS	Fetal Calf Serum
FFPE	Formalin Fixed Paraffin Embedded
FoxP3	Forkhead Box P3
FRT	Female Reproductive Tract
FT	Fallopian Tube
GAPDH	Glyceraldehyde 3-Phosphate Dehydrogenase
H_2O_2	Hydrogen Peroxide
HDI	High Dose Interferon
HER2	Human Epidermal Growth Factor Receptor 2
HGSC	High Grade Serous Ovarian Carcinoma
IBC	Invasive Breast Cancer
IFN	Interferon
IFNAR1-/-	Interferon-α/β Recptor 1 Null
IFNAR1/2	Interferon-α/β Recptor 1/2

IFNB1	Interferon Beta 1
IFNGR1/2	Interferon Gamma Receptor 1/2
IFNLR1	Interferon Lambda Receptor 1
IFNα	Interferon Alpha
IFNβ	Interferon Beta
IFNγ	Interferon Gamma
IFNε	Interferon Epsilon
IFNκ	Interferon Kappa
IFNλ	Interferon Lambda
IFNω	Interferon Omega
IgG	Immunoglobulin G
IKKε	Inhibitor of NF-κB Subunit Epsilon
IL-6	Interleukin 6
IL-10	Interleukin 10
IL-10RB	Interleukin 10 Receptor, Beta Subunit
IL-12	Interleukin 12
IL-17	Interleukin 17
IP	Introperitoneal
IRF	Interferon Regulatory Factors
IRF3	Interferon Regulatory Factor 3
IRF7	Interferon Regulatory Factor 7
IRF9	Interferon Regulatory Factor 9
IRG	Interferon Regulated Gene
ISGF3	IFN Stimulated Gene Factor 3
JAK 1	Janus Kinase 1

JAK-STAT	Janus Kinase - Signal Transducers and Activators of Transcription
kCONfab	Kathleen Cunningham Foundation Consortium for Reasearch into Familial Breast Cancer
LPS	Lipopolysaccharides
Ly6C	Lymphocyte Antigen 6 Complex
Ly6G	Lymphocyte Antigen 6 Complex, Locus G6D
M1	M1 Macrophage
M2	M2 Macrophage
MCP-1	Monocyte Chemoattractant Protein-1
MDSC	Myeloid-Derived Suppressor Cells
MEC	Mammary Epithelial Cells
MET	Mesenchymal-Epithelial Transition
MHC	Major Histocompatibility Complex
MHCII	Major Histocompatibility Complex II
MIAME	Minimum Information Essential for Microarray Experiments
M-MLV	Moloney Murine Leukemia Virus
MOSEC	Murine ID8 Ovarian Epithelial Cancer Cells
MRD	Minimal Residual Disease
mRNA	Messenger RNA
MWT	Heated Microwave Treatment
NF-κB	Nuclear Factor Kappa, Enhancer of B Cells
NK	Natural killer Cell
NKG2D	Natural-Killer Group 2, Member D
NKT	Natural killer T Cells
NLR	Nod-Like Receptors

OCP	Oral Contraceptive Pill
OCRF	Ovarian Cancer Research Foundation
PAMP	Pathogen-Associated Molecular Patterns
Pan-CK	Pan Cytokeratin
PBMC	Preipheral Blood Mononuclear Cells
PBS	Phosphate Buffered Saline
PCR	Polymerase Chain Reaction
PD1	Programmed Cell Death Protein 1
pDCs	Plasmacytoid Dendritic Cells
PDGF	Platelet-Derived Growth Factor
PD-L1	Programmed Death Receptor Ligand 1
PDX	Patient Derived Xenograft
PI	Propidium Iodide
PI3K	Phosphatidylinositol 3-Kinase
Poly(A:U)	Polyadenylic-polyuriddylic Acid
Poly(I:C)	Polyinosinic-polycytidylic Acid
PR	Progesterone Receptor
PRR	Pattern Recognition Receptor
PTH-rP	Peptide Parathyroid Hormone-Related Peptide
qRT-PCR	Quantitative Real Time Polymerase Chain Reaction
RAG2-/-	Recombination Activating Gene 2 Null
RAG2-/-X	Recombinant Activating Gene 2 Null Cross with Common Cytokine
Xgammac-/-	Receptor Gamma Null
RANKL	NF-κB Ligand
RB1	Retinoblastoma Protein

RIG-I	Retinoic Acid-Inducible Gene I
RIN	RNA Integrity Number
RLH	RIG-1 Like Helicases
RNA	Ribonucleic Acid
RPMI	Roswell Parks Memorial Institute Media
RT	Reverse Transcriptase
RTCA	Real Time Cell Analysis
SLE	Systemic Lupus Erythematosus
SMa	Smooth Muscle Actin
SPF	Specific Pathogen Free
ssGSEA	Single sample gene set enrichment analysis
STAT1	Signal Transducers and Activators of Transcription 1
STAT2	Signal Transducers and Activators of Transcription 2
STAT3	Signal Transducers and Activators of Transcription 3
STAT4	Signal Transducers and Activators of Transcription 4
STAT5	Signal Transducers and Activators of Transcription 5
TAM	Tumour Associated Macrophage
TAP1	Transporter 1, ATP binding cassette subfamily B
TB	Mycobacterium Tuberculosis
TBK	TANK-Binding Kinase
TBST	Tris Buffered Saline with 0.05% Tween
TGFα	Transforming Growth Factor Alpha
TGFβ	Transforming Growth Factor Beta
TH1	CD4+ Helper Cells
TIL	Tumour Infiltrating Lymphocytes
TLR	Toll-Like Receptor

TLR7	Toll-Like Receptor 7
TLR9	Toll-Like Receptor 9
TMA	Tissue Microarray
TNBC	Triple Negative Breast Cancer
TNFα	Tumour Necrosis Factor Alpha
TNM	Tumour Node Metastasis
TP53	Tumour Protein 53
Treg	Regulatory T cells
TYK2	Tyrosine Kinase 2
VEGF	Vascular Endothelial Growth Factor

Thesis Including Published Works Declaration

I hereby declare that this thesis contains no material which has been accepted for the award of any other degree or diploma at any university or equivalent institution and that, to the best of my knowledge and belief, this thesis contains no material previously published or written by another person, except where due reference is made in the text of the thesis.

This thesis includes 1 original paper submitted and under review at *Cancer Discovery*, a peer-reviewed journal, and 1 publication prepared for submission. The core theme of the thesis is the investigation of Interferon signalling in cancer progression in breast and ovarian cancer. The ideas, development and writing up of all the papers in the thesis were the principal responsibility of myself, the student, working within the Hudson Institute of Medical Research under the supervision of Professor Paul J. Hertzog.

The inclusion of co-authors reflects the fact that the work came from active collaboration between researchers and acknowledges input into team-based research. In the case of Chapters 3 and 4 my contribution to the work involved the following: collecting background information, devising experiments, conducting *in vitro* and *in vivo* experiments, analysis and interpretation of the data, writing and editing of the associated papers and manuscripts. See each Chapter for individual disclosure statements.

Publications submitted to *Cancer Discovery*

Marks Z.C., Mangan N.E., Tate M.D., Matthews A.Y., Rosli S., Bilandzic M., Christie E.L., Stephens A.N., Bowtell D.D.L., de Weerd N.A., Bourke N.M. & Hertzog P.J. "Role of a unique type I interferon, interferon epsilon, in suppressing epithelial ovarian cancer", Submitted Manuscript.

Thesis Chapter	Publication Title	Status *(published, in press, accepted or returned for revision, submitted)*	Nature and % of student contribution	Co-author name(s) Nature and % of Co-author's contribution*	Co-author(s), Monash student Y/N*
4	Role of unique type I interferon, interferon epsilon, in suppressing epithelial ovarian cancer.	Submitted (under review)	70% Conceptualisation, acquisition of data, methodology, data analysis and interpretation and writing, reviewing and editing the manuscript.	Niamh E. Mangan 3% **CMAI* Michelle D. Tate 2% **IA* Anthony Y. Matthews 4% **P* Sarah Rosli 1% **I* Maree Bilandzic 1% **PM* Elizabeth L. Christie 1% **AD* Andrew N. Stephens 1% **PM* David D.L. Bowtell 1% **MDAC* Nicole A. de Weerd 1% **PR* Nollaig M. Bourke 7% **CMAIRE* Paul J. Hertzog 8% ** CMAIRE*	N

**Conceptualisation (C) Methodology (M) Formal Analysis (A) Investigation Aspects (I) Writing (W) Review (R) Editing (E) Provision of Critical resources (P) Data curation (D)*

I have renumbered sections of submitted or published papers in order to generate a consistent presentation within the thesis.

Student signature: [redacted] **Date:** 24/01/2018

The undersigned hereby certify that the above declaration correctly reflects the nature and extent of the student's and co-authors' contributions to this work. In instances where I am not the responsible author I have consulted with the responsible author to agree on the respective contributions of the authors.

Main Supervisor signature:  **Date:** 24/01/18

Acknowledgements

This thesis would not have been possible without the overwhelming support of a great many people. The past four years has taught me a considerable number of lessons, one of which is that the most fulfilling work comes side-by-side with others.

This wisdom can be in large part attributed to my Supervisor, Prof. Paul Hertzog, who champions collaborative work by promoting people as well as science. I'd like to say my warmest thanks for every opportunity I've experienced as a result of his guidance, encouragement & incredible enthusiasm for life. There've been too many occasions to count, even occasionally spanning continents. I am truly grateful for everything, beyond measure.

I must also thank Dr Nollaig Bourke for adopting me as her first PhD student, I could not have been in safer hands. I would love to think I absorbed even a portion of her resilience and drive in the past few years, but I'll settle for all her advice, guidance & care.

I need to extend thanks to everyone at CIIID, present and past. I was incredibly lucky to stumble upon the centre as a BMedSci student, not realising what a unique place it was. But I soon learned. Thank you to all who made it an enjoyable place to work and live. From the Hertzog Lab I must thank Niamh, Michelle, Tony, Jamie & Sarah for helping with the work that has gone into this thesis, but thanks to everyone in the group. Additionally, it's likely that this thesis would not have been quite so enjoyable without drinks on a Friday night so to everyone who made an appearance over the years and raised a bottle, Cheers!

The desire to complete a PhD is undoubtedly a reflection of my admiration for my dad. He is in many ways one of the most curious people I know and continues to research all manner of things. I also look up to my brother Josh, who is effortlessly himself and who inspires me to be the same. To Dean, perhaps my most unexpected discovery, thank you for getting me through, sekoǧas.

Finally,

In loving dedication of Hazel Church.

From her loss, I sought meaning.

Thesis Preface

The work presented in this thesis contains published and submitted manuscripts based on results arising from this study. Chapter 1 contains a review of the literature relevant to the topic of the thesis. Chapter 2 contains a general materials and methods for experiments performed as part of this thesis. Chapter 3 is an experimental chapter in the form of a manuscript that contains a paper prepared for submission. Chapter 4 is an experimental chapter in the form of a manuscript that has been submitted to *Cancer Discovery*. Chapter 5 is a general discussion of all the results presented in this thesis with relevant conclusions.

Abstract

The type I interferons (IFN) are a family of innate immune cytokines known to play vital roles in host defence. The direct & indirect anti-tumour effects of these cytokines have led to considerable investigation into their role in cancer pathogenesis and their use as potential anti-cancer therapeutics. Despite this, the clinical use and benefit of type I IFN therapy has so far been limited to a select number of cancers such as melanoma and haematological malignancies. Notably, the success of IFN treatment has varied widely among patients and cancer types including many solid tumours where IFN therapy has exhibited poor efficacy and is largely restricted by dose-limited toxicity. The greater potential of these cytokines as anti-cancer agents has yet to be realised and to this end, there is a clear need to further understand the complexities of type I IFN signalling in cancer development and progression.

New insights into the molecular pathways underlying cancer progression reveal further evidence of dysregulated type I IFN signalling. Specifically, the presence of constitutive IFN signalling in mammary epithelium as well as primary breast tumours has been shown to be suppressed in bone metastases. Here, suppression of constitutive IFN was characterised as a critical mechanism of immune evasion facilitating successful breast cancer metastasis, although the processes underlying this metastatic pathway remained unclear. Meanwhile, a distinct type I IFN, IFNε, has been characterised as constitutively expressed in epithelial cells of the female reproductive tract (FRT), with previously unexplored anti-tumour properties, potentially critical in restricting FRT malignancies such as ovarian cancer. The significance of continuous IFN activity in the pathogenesis and additionally, the metastasis of these tumours remains to be characterised. The central aims of this thesis were to use these two models of cancer, breast and ovarian, to firstly: determine whether characterising IFN

signatures in peripheral blood could provide further insight into cancer metastasis or derive novel biomarkers for patient stratification; and secondly: to investigate the previously unknown anti-tumour potential of a distinctly constitutive type I IFN, IFNε.

In breast cancer, this work investigated local, systemic and distant signatures to characterise the processes underlying metastasis and map a continuum of disease progression from normal tissue to metastases. Blood transcriptomics revealed a strong enrichment of platelet activity, T cell suppression and broad IFN involvement, which were further investigated by multiplexed staining of tumour tissue to correlate key immune-tumour cell interactions with metastatic potential. In ovarian cancer, this work demonstrated patterns of constitutive IFNε expression never before characterized – in the tissue of origin of high grade serous ovarian carcinomas (HGSC). In addition, this study demonstrated the first evidence of the loss of constitutive IFNε in human HGSC development and has also revealed IFNε to be an effective anti-metastatic therapy in mouse models of orthotopic and disseminated ovarian cancer, through both intrinsic and extrinsic pathways of tumour suppression providing the basis for the use of IFNε as an anti-cancer therapy.

Thus, this thesis contributes to the knowledge of constitutive type I IFN in tumorigenesis and tumour progression and demonstrates the potential use of endogenous IFN signalling and immune signatures for patient stratification in cancer progression as well as targeted anti-metastatic exogenous IFN therapy.

CHAPTER 1: LITERATURE REVIEW

'I have so much I want to tell you, and nowhere to begin.'[*]

~

1.1 Introduction

Cancer occurs when a cell loses the regulatory mechanisms that govern basic survival resulting in uninhibited growth, loss of biological function & the ability to evade cell death. There are currently over 4 million cancer-related publications worldwide (Pubmed 2017) and 2,957 clinical cancer trials ongoing in Australia (1), making it one of the most widely researched areas of drug discovery & development. The magnitude of investigation into this disease process is driven by the inescapable fact that when a rogue cell is able to grow unchallenged, multiply *in situ* & spread to distant organs, it is likely to overwhelm the body & kill its host.

The processes involved in carcinogenesis, initially described as intrinsic properties acquired by or common to almost all cancers (2), include the ability to sustain growth via autocrine feedforward loops through secreting growth factors such as platelet-derived growth factor (PDGF) & transforming growth factor alpha (TGFα) (3). Additionally, intrinsic properties common to cancers include sustained angiogenesis, limitless proliferative potential, the ability to evade cell death & anti-growth signals, and the potential to invade surrounding tissue & metastasise to secondary sites (2). Recently, two additional hallmarks have been identified (Figure 1.1): the ability to reprogram cellular metabolism & the evasion of immune detection & destruction (2, 4). By acquiring these properties, tumour cells are able to bypass the regulatory signals that govern homeostasis. Considering that the progression of cancer cells in the body is dependent on avoiding the immune system to propagate and survive, the cancer cells mirror the spread of a pathogen, as it masks itself from host defences & accordingly, these two diseases share a vital enemy – the host immune system.

[*] J. D. Salanger

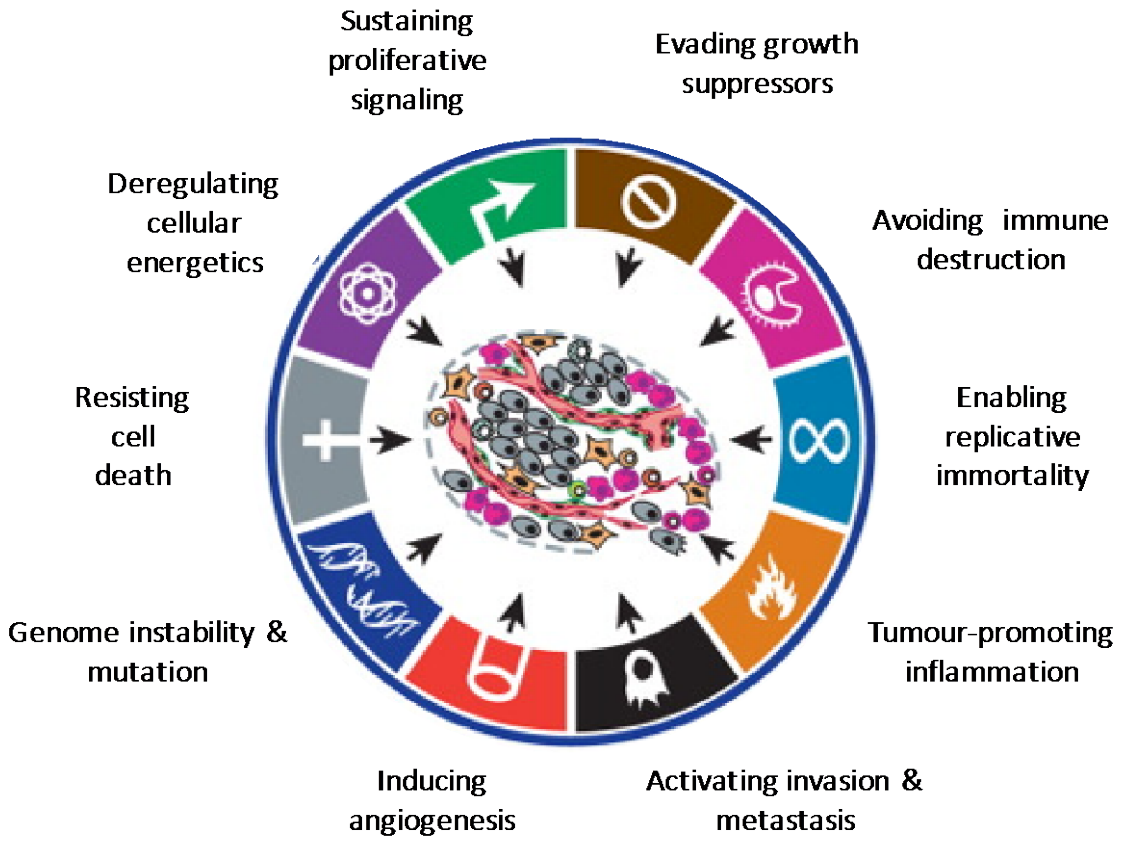

Figure 1.1: The Hallmarks of Cancer.

These hallmarks describe the key properties common to all cancer cells and required for tumour cell survival and progression in the body (image adapted from (4))

The immune system, and the vast array of cell types, signals and secreted factors that it comprises, is capable of a complex repertoire of responses to different pathogens and pathogenic stimuli. Both innate immunity, which until recently was regarded as a broad, first-line response including dendritic cells (DC), natural killer cells (NK) and natural killer T cells (NKT), and adaptive immunity, traditionally viewed as a more sophisticated and finely-tuned response involving T & B lymphocytes, are vital components of host defence. It has long been established that both innate & adaptive cells are present in the tumour microenvironment, are able to interact with tumour cells and influence disease outcome (5).

Our understanding of the role of the immune system in cancer is rapidly expanding and with it, an appreciation of its duality – on the one hand tumour-supressing, and on the other tumour promoting. In some instances, specific immune cells such as regulatory T cells (Treg) and myeloid derived suppressor cells (MDSC) have demonstrated to have regulatory functions that are vital in establishing an immunosuppressive microenvironment in solid tumours including ovarian cancer (6). This immunosuppressive microenvironment diminishes the anti-tumour activity of other immune cells, & instead either directly or indirectly facilitates effector T cell exhaustion (7). In these cases, the presence of tumour infiltrating lymphocytes (TIL) does not necessarily correlate with a positive prognosis for the patient, rather the specific ratios of subsets of TILs may better predict outcome (8-10). In addition to regulatory immune cells, the immune system appears to shape a heterogeneous tumour into a more resistant phenotype. Through eliminating tumour cells that are easily detected by immune cells the immune system protects against early-stage, immune-naïve malignancy, however in doing so it facilitates the survival of less immunogenic cells, which are more likely to evade immune control & metastasise (11). This process constitutes the basic principles of cancer immune-editing (12-16).

Born out of the observation that tumours grow more readily in immunodeficient mice & demonstrate higher immunogenicity (17) the theory of immune-editing is described in terms of three distinctly chronological stages shown in Figure 1.2. The first stage is elimination where innate & adaptive immune cells detect and destroy microscopic tumour formation, followed by the second stage termed equilibrium, a subclinical period where tumour cells of low immunogenicity that have survived elimination remain dormant and are subject to constant immune-driven selective pressure (18). The final stage is escape, where less immunogenic tumour sub-clones or tumour cells that have evolved strategies for immunosuppression are able to metastasise (11). Despite their primary anti-tumour functions, cells of both innate & adaptive immunity are able to play a vital role in shaping tumour progression. Methods for harnessing the immune system's primary ability to suppress tumour cells while more effectively targeting tumour-acquired immunosuppression constitute the principle aims of successful immunotherapy. These strategies involve boosting anti-tumour immunity by activating endogenous T cells, depleting immunosuppressive cells, targeting tumour antigens, modulating cytokines to boost anti-tumour response including type I interferon therapies and inducers, or inhibiting immune checkpoints (19).

This thesis explores the role of endogenous, constitutive host defence proteins, the type I interferons, in cancer progression and aims to further characterise the anti-tumour, immunotherapeutic potential of these cytokines.

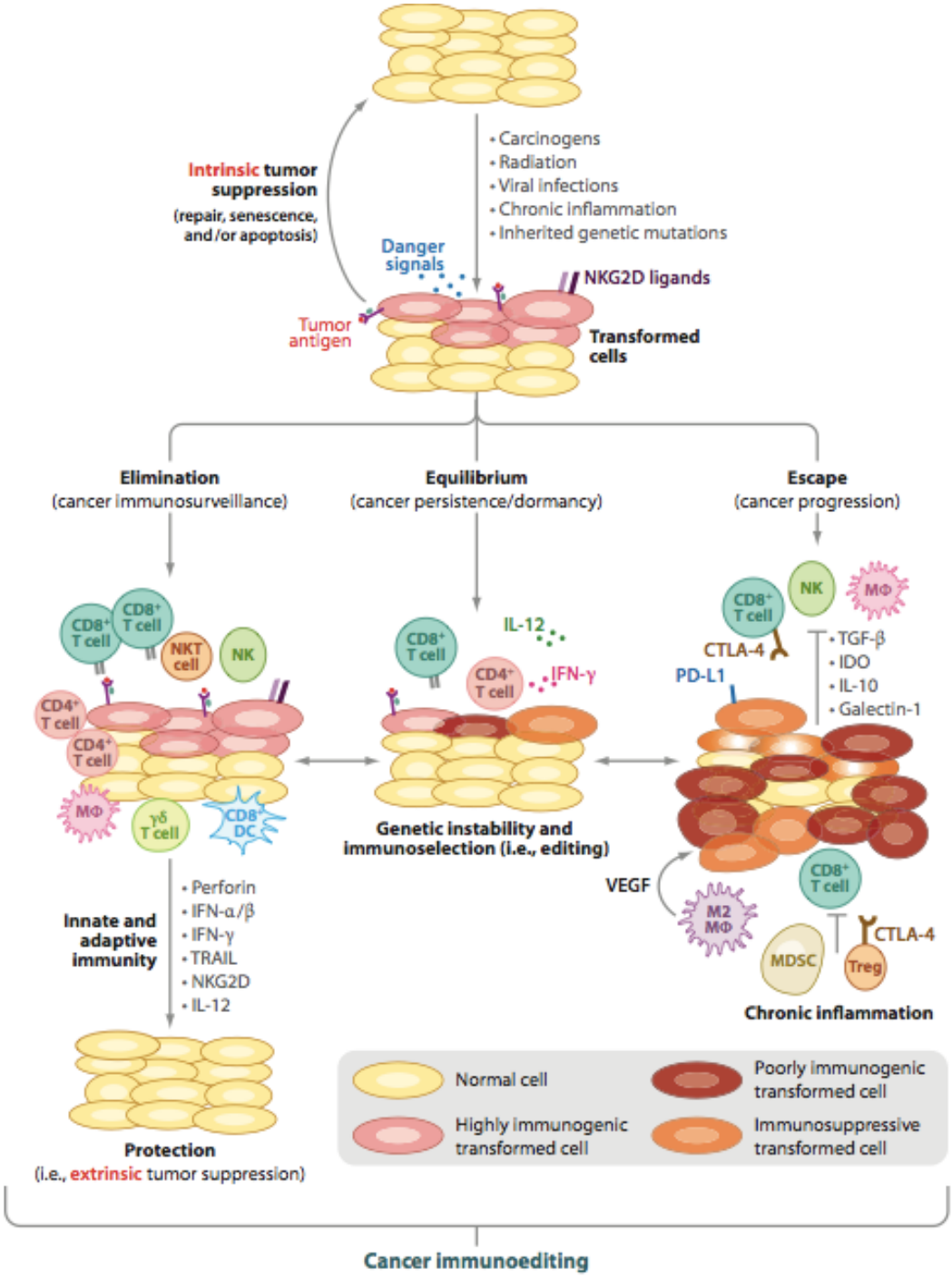

Figure 1.2: The three stages of immunoediting and the various immune cells and cytokines that contribute.

The interaction between tumour cells and host immune cells designated into three distinct stages, elimination, in which immune cells detect and destroy some tumour cells; equilibrium, in which the surviving tumour cells remain dormant; and escape, in which tumour cells of low immunogenicity evade immune detection and invade secondary tissue. A number of host immune cells and cytokines are active in each stage (image adapted from (5)).

1.2 Metastasis, Tumour Dissemination & Immunity

Successful cancer therapies, such as surgical resection or chemotherapies, have shown improvements in patient outcomes. Interestingly, these therapeutic strategies have seen the greatest clinical benefit in patients that have their cancer subtype localised in the primary organ. Indeed, such diseases as breast cancer and melanoma have survival outcomes of over 90% if localised in the primary site. Significantly, these prognoses drop drastically if there is presence of metastasis with survival rates plummeting to under 20% for these same cancer subtypes (20-22). This has led to the overwhelming cause of death in these patients to be mass organ failure that has occurred due to the metastatic burden. The impact of metastasis on survival necessitates a shift to focus on prevention of the spread from primary sites to distal organs. One such approach is indirect suppression of the primary tumour cell spread through therapeutically inducing immune activation to counter the immunosuppressive microenvironment created by the cancer cells limiting its potential to metastasise.

The onset of metastasis is quite complex, firstly cells from the primary tumour must undergo a series of migratory steps that involve cell autonomous processes. This often reflects an altered gene expression and distinct mutational burden of metastatic tumour cells compared to matched primary populations, as well as recruitment of both local and systemic host immune cell populations. This enables safe voyage of migrating tumour cells and prepares a supportive environment for distant metastases. The cell intrinsic processes required for tumour cells to migrate and disseminate involve phenotypic changes described as epithelial to mesenchymal transition (EMT) (23), whereby tumour cells undergo de-differentiation associated with a stem cell phenotype (24, 25), as well as a re-differentiation process termed mesenchymal-epithelial transition (MET) (26-28). These processes allow a very select proportion of tumour cells to leave the primary site, survive transit through blood, lymphatics or other compartments to

colonise distant sites and ultimately, lead to death. Understanding these processes and targeting this very small proportion of cancer cells remains one of the biggest challenges facing therapeutic innovation in cancer.

1.2.1 Routes of Metastasis

Cancer cells do not always spread via the same physiological processes. In fact, the Greek term 'metastasis' translates as 'rapid transition from one point to another' (Oxford University Press 2017), hints at the 'what', 'where' and 'when' of tumour spread, but omits 'how' cells are able to do this, and thus it is used to describe a number of distinct pathways by which migrating tumour cells travel from the primary site. A well-established characterisation of these pathways are hematogenous and/or lymphatic metastasis, where tumour cells migrate from the primary tumour via the blood stream or lymphatic drainage. This process requires a number of migratory steps shown in Figure 1.3 (29).

In short, a select population of tumour cells located at the leading edge of the tumour invade the lymphatic or vascular systems, evade immunosurveillance* (30), survive transit to the site of metastasis, then adhere to endothelial cells of the vascular wall and undergo extravasation before colonising secondary tissue (31, 32). Hematogenous metastasis is a frequent and fatal pathway of spread for many malignancies including breast cancer where metastases often occur in bone and lung (33).

* The concept of 'immunosurveillance', introduced by Burnet in the 1960s, suggests that circulating lymphocytes patrol tissues & play a key role in eliminating neoplastic or transforming cells, likely through recognition of tumour-associated antigens (Burnet FM. Lancet 1967).

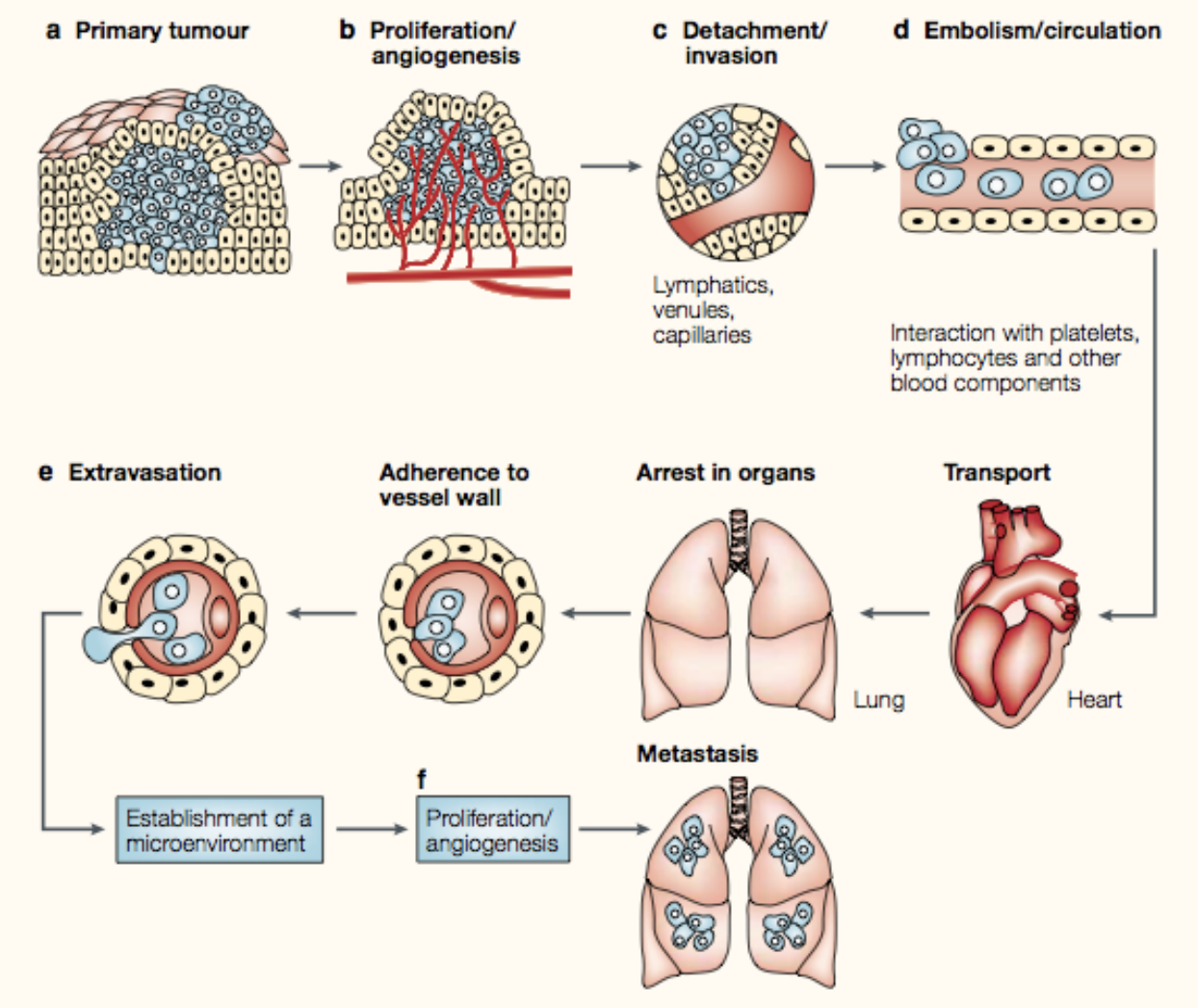

Figure 1.3: Multistep process of metastasis from primary tumour to secondary organs.

A) First primary tumour cells undergo proliferation. B) The primary tumour is highly vascular and develops a network of blood vessels through angiogenesis. C) Primary tumour cells may then detach from the tumour mass and invade into either the lymphatic or vascular systems depending on the primary tumour type. D) This enables transport to distant sites. E) Tumour cells adhere to the luminal surface of vessels then invade into secondary organs where they undergo proliferation and establish macrometastases (image adapted from (34)).

In malignancies that arise in tissues within the peritoneal cavity such as ovarian cancer, rather than travel via the blood or lymphatics, ovarian cancer cells more frequently undergo transcoelomic spread. Here, various processes including blockage of the lymphatic drainage & increased vascular leakage leads to the accumulation of ascites fluid in the peritoneal cavity into which cancer cells on the growing edge of the primary tumour simply shed and are able to disseminate freely throughout the peritoneum. The peritoneal cavity provides an environment rich in immune cells, cytokines and secreted factors (35) and therefore, a unique microenvironment for tumour cells (36).

Importantly, circulating tumour cells remain vulnerable to host defence, indeed each migratory step undertaken by a cancer cell may be rate limiting if the host environment including local & systemic immunity is able to inhibit further progression (34). This illustrates that the immune system and the factors that regulate it, are collectively one of the most critical defence systems against the fundamental cause of cancer fatality.

1.3 Overview of the Key Immune Cell Populations in Metastasis

Many immune cell types have been implicated in various stages of metastasis & tumour dissemination. While it is well established that the adaptive immune system, specifically T cells, actively contribute to the process of immune-editing, more recent studies have investigated the role of the innate immunity in regulating tumour cell immunogenicity and metastasis (37). Using RAG2-/- x γc-/- mice deficient in cells of both adaptive and innate immune systems compared to RAG2-/- mice lacking only adaptive immune cells (17, 38), it was demonstrated that tumour incidence was highest when both immune systems were absent and that tumours derived from these mice had the highest rate of rejection when transplanted into an immunocompetent host (37). This suggests that the degree of tumour cell susceptibility

to immune suppression is affected by the immune status of the environment from which the tumour cells are derived.

Both immune systems must be present for successful tumour suppression (37). However, the mechanisms utilised by tumour cells to successfully evade or suppress different immune cells vary widely. This is largely a reflection of a complex and dynamic relationship involving an array of immune cell types, which directly or indirectly interact with tumour cells and may, depending on finely-tuned signalling and the surrounding environmental factors, suppress or promote tumour progression. Additionally, some tumours demonstrate immune naïve or 'cold' phenotypes while others have extensive immune infiltrate or 'hot' phenotypes, which demonstrates an immune privileged environment (shown in Figure 1.4). These data emphasise the importance of tailoring therapy to the individual tumour and its specific immune environment.

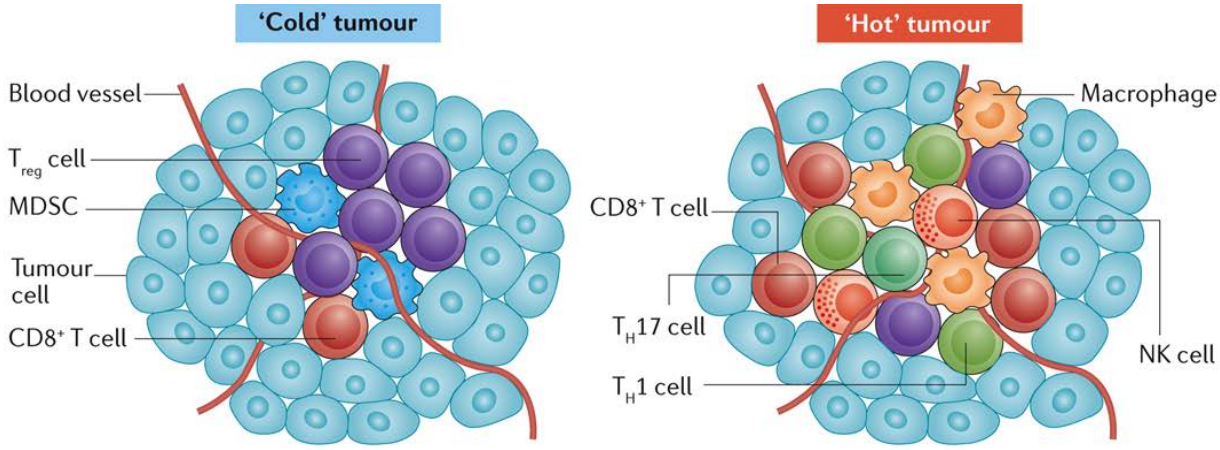

Figure 1.4: Distinct immune phenotypes of tumour microenvironment.

In an effort to develop and target effective immunotherapies as well as satisfy a growing need for precision medicine, extensive molecular characterisations of individual tumours have been performed. These reveal complex heterogeneity of immune phenotypes of tumours and their microenvironments, reflected by both detection of infiltrating immune populations as well as transcriptional signatures of tumour cells. This image shows the distinction between immunologically sparse or 'cold' tumours compared to tumours with a high proportion of infiltrating immune cells or 'hot' tumours. These phenotypes may be used to stratify treatment for patients. (Image adapted from (39)).

Below is a brief overview of some of the key immune cell populations involved in regulating tumour progression, however, knowledge of the full repertoire of immune responses to cancer continues to expand. For the purposes of this thesis, a select proportion of these cells are outlined:

1.3.1 T Lymphocytes

Several cancers have demonstrated susceptibility to the anti-tumour effects of the adaptive immune system where the presence of TILs in the primary tumour correlates with improved survival. Whether the same effector cells are able to successfully inhibit primary tumour cells, circulating cells, or peripherally disseminated tumour cells (C/DTCs) and if so how some CTCs are able to escape this, is less clear. Anti-tumour T cells include CD8+ cytotoxic and CD4+ helper (T_H1) cells that are well established components of the anti-tumour immune response, however immune-driven tumour suppression cannot be solely attributed to either cell type. CD4+ lymphocytes are often involved in priming responses either as a result of interaction with major histocompatibility complex II (MHC-II) expressed on tumour cells themselves or MHC-II on antigen presenting cells such as dendritic cells whereas Tregs have been found to play a key role in suppressing effector cells to contribute to an immune suppressive tumour microenvironment.

CD8+ lymphocytes demonstrate well-established anti-tumour effects including host rejection of transplantable tumours (40), suppression of highly antigenic tumour cells (17) and suppression of tumour growth during the equilibrium stage of immunoediting (18). They also have a vital impact on the efficacy of some anti-cancer therapeutics including radiotherapy (41) and cytokine therapy such as recombinant IFN (42, 43). The presence of CD8+ T cell infiltrate in metastases has been found to indicate patient prognosis in some cancers (44, 45). However, the survival benefit or disadvantage differs between cancer types and may be a reflection of

the specific tumour-associated phenotypes of CD8+ T cells in found in different tumour microenvironments including dysfunctional and senescent CD8+ T cells (46).

1.3.2 B Lymphocytes

Primary tumour B cell infiltrate has correlated with improved patient outcomes in a number of human cancers including melanoma, pharyngeal carcinoma and ovarian cancer (47-49). In metastases from human high grade serous ovarian carcinoma (HGSC), B cell infiltrate in metastatic stroma was associated with a strong memory phenotype and correlated with increased T cell-dependent anti-tumour responses (50). The anti-tumour effects of lymphocytes have generally been linked to their ability to prime DCs with immunoglobulin G (IgG) bound tumour antigen and in turn, promote DC-activation of cytotoxic cells (51). A subset of B cells has also been found to have regulatory or immunosuppressive effects on anti-tumour immunity and aid in tumour progression (52). Tumour cells themselves are able to promote switching of B cell phenotypes through production of transforming growth factor β (TGF-β) and drive B cell secretion of immunosuppressive factors such as interleukin 10 (IL-10) as well as promote B cell expression of immune checkpoints, cell surface proteins which inhibit immune activation and suppress anti-tumour immunity such as programmed death receptor ligand 1 (PD-L1) (53, 54).

1.3.3 Natural Killer Cells

Natural killer (NK) cells are part of the innate immune system and are known for their ability to protect against pathogens either by targeted cell lysis or cytokine production (55). These lymphocytes are classified according to their expression of cell surface markers such as cluster of differentiation 56 (CD56) and CD16 in humans, which correspond to its phenotype. In cancer, NK cells act as sensors and suppressors of tumour spread. NK cells detect tumour cells in a number of ways including deficiency in MHC I expression on the surface of tumour cells,

detection of stress ligands which activate NK cells via their naturally killer group 2D (NKG2D) receptor or detection of tumour antigens (56). Once activated, NKs are able to release cytolytic granules containing granzyme B and perforin, and initiate tumour apoptosis (57). Tumour cells must therefore maintain expression of MHC-I to evade NK-mediated lysis, however, they must also simultaneously avoid presentation of tumour-associated antigens in the context of MHC-I, which would in turn drive the anti-tumour functions in effector T cells.

1.3.4 Monocytes/Macrophages

Macrophages are phagocytes that are part of the innate, nonspecific response to pathogens, however, they have the capacity to help activate adaptive immune cells. In cancer, macrophages have been broadly studied, which has led to the classification by anti-tumour or tumour-associated phenotypes. They are often simply characterised as type 1 (M1) or type 2 (M2) phenotypes, describing polar ends of a spectrum of functional phenotypes adopted by macrophages as a result of environmental factors including tumour-derived cytokines (58). M1 cells suppress tumours and pathogens, produce large amounts of pro-inflammatory cytokines such as IFNγ, interleukin 12 (IL-12) and tumour necrosis factor alpha (TNF-α), and highly express MHC molecules. M2 phenotypes secrete TGF-β and IL-10 to suppress immune responses, and promote angiogenesis through secretion of growth factors including vascular endothelial growth factor (VEGF) as well as interleukins such as IL-17. In other instances, M2 macrophages or pro-tumorigenic macrophages are indicated by the term tumour-associated macrophages (TAMs). Additionally, immature myeloid cells are often associated with pro-tumorigenic/M2 properties. The term 'myeloid-derived suppressor cell' (MDSC) is used to describe these cells in terms of origin but also their immune-suppressive phenotype (59, 60). MDSCs are able to promote tumour growth and suppress anti-tumour immunity through several processes including expression of PD-L1 and recruiting of Tregs (61). The

classification and effect of these cells are at times overlapping and depend on tissue localisation as well as molecular & functional phenotype.

1.3.5 Platelets

Platelets are small, non-nuclear blood cells that are predominantly involved in blood clotting in response to injury. However, these cells have been shown to secrete a vast range of factors that can promote tumour survival including pro-angiogenic growth factors such as VEGFs and platelet derived growth factor (PDGF) (reviewed in (62)). Increasing evidence demonstrates a key role played by platelets during tumour metastasis. In peripheral blood, platelets are able to interact directly with circulating tumour cells and protect them from immune suppression including elimination by NK cells, a phenomenon that has been identified in a number of cancers as well as a general increase in platelet activity in the blood of cancer patients (62-65). These activated platelets form cross-links that allow them to aggregate with tumour cells and thus, effectively shield tumour cells from immune suppression in circulation. In addition, platelets promote tumour intrinsic pro-metastatic processes such as EMT (66).

1.4 The Role of the Tumour Microenvironment in Regulating Tumour & Immune Compartments

1.4.1 Chemokines

Chemokines are a large subfamily of cytokines known for their vital role in lymphoid development and immune trafficking. However, in the context of cancer, chemokines are able to recruit immune cells into & function within the tumour microenvironment (reviewed in (39, 67)). In this environment, these small proteins may be secreted by tumour cells as well as immune and stromal cells. They in turn, regulate migration of immune cells including anti-tumour effector populations such as CD8+ T cells, T_H 1 cells & NK cells which all express the

C-X-C motif chemokine receptor 3 (CXCR3) receptor and migrate in response to chemokine (C-X-C motif) ligand 9 (CXCL9) & CXCL10. Additionally, chemokines have been shown to recruit regulatory immune cells such as Tregs which express CC chemokine receptor 4 (CCR4) & CCR10 and migrate in response to chemokine (CC motif) ligand 22 (CCL22) produced by macrophages & tumour cells (6), and CCL28 in hypoxic conditions (68), respectively. Chemokines directly regulate tumour cell intrinsic function such as pro-proliferative (CCL2) and pro-invasiveness (CCL18), while others suppress tumours by inhibiting proliferation (CXCL14) and promoting immunogenicity (CXCL8). Thus, chemokines contribute to the complex signalling occurring in the tumour microenvironment and have the capacity to regulate tumour progression both directly, by targeting tumour cell intrinsic function, but also indirectly, by recruiting immune cells.

1.4.2 Glucose & Metabolic Factors

The metabolic niche of the tumour microenvironment can have a considerable effect on the function of infiltrating immune cells. CD8+ T cells have been shown to require aerobic glycolysis, the process of converting glucose into lactate in the presence of oxygen, for optimal effector function including production of IFNγ and granzyme B (69). These cells must compete with the tumour for glucose, which is rapidly metabolised by tumour cells themselves undergoing aerobic glycolysis (70). The demand for glucose can therefore limit T cell function in the tumour microenvironment as tumour cells glucose-restrict surrounding immune cells leading to hypo-responsive T cells which fail to suppress even highly antigenic tumours (71). Further, tumour cell-derived lactate can impair effector T cell metabolism & function by blocking their lactic acid export leading to a significant decrease in proliferation & cytokine production as well as cytotoxic function (72).

1.4.3 Growth Factors

Soluble growth factors such as epidermal growth factor (EGF), VEGF and transforming growth factors (TGFα & β) are proteins, which under normal physiological conditions, such as embryogenesis & wound repair, can be secreted by immune cells, the epithelium, the endothelium and/or stroma to signal via transmembrane receptors on neighbouring cells in a paracrine manner (3). In tumour cells however, normal paracrine growth factor signalling is often replaced by an intrinsic ability to both secrete and respond to self-produced growth factor – an autocrine mechanism of sustained growth or clonal expansion (73). Additionally, tumour cells may overexpress growth factor receptors to maintain a hyper-responsive phenotype, for example, in breast cancer cells overexpressing human epidermal growth factor receptor 2 (HER2) (74), has been associated with more aggressive, highly metastatic tumours (75).

1.4.4 Interferons (IFN)

Another family of secreted proteins capable of regulating both tumour cell intrinsic and immune cell function, are the IFNs. These cytokines were first characterised by their anti-viral properties and are named for their ability to suppress viral replication via what is known as an 'interference' reaction (76). To date, three major types of IFNs have been identified, each of which signal via specific cognate cell surface receptors: type I (including 13 distinct IFNα's, IFNβ, IFNε, IFNκ & IFNω), which signal via IFNAR1/2 and are the most widely active type of IFNs, capable of being produced by & signal to most cells of the body. Type II (IFNγ), which signals via IFNGR1/2 and whose expression is somewhat more restricted to T cells and NK cell predominantly; & type III (three subtypes of IFNλ), which, while expressed by a broad range of cell types, has limited effects due to sparse expression of their cognate receptors IFNLR1 & IL-10Rβ (77).

All IFNs have the capacity to elicit an anti-tumour response either directly, by regulating tumour intrinsic function or indirectly, by regulating an anti-tumour immune response. In fact, the long-established anti-tumour properties of IFNs have led to their use in clinical trials of melanoma (78-87), renal cell carcinoma (88, 89), colorectal cancer (90, 91) , pancreatic cancer (92), prostate cancer (93), breast cancer (94-96) (extensively reviewed in (97)) & ovarian cancer (98-104). A selection of trials using type I IFNs are listed in Table 1.1. However, the success and routine administration of IFN therapy in cancer has been limited due to the cytotoxic side effects associated with high dose IFN (HDI) therapy which include flu-like symptoms, nausea, anorexia and depression.

In an effort to maximise the efficacy of IFN therapy while avoiding toxicity, agonists of the IFN pathway have been trialled as a way of inducing an IFN response *in vivo* without administering exogenous protein. Trails using pattern recognition receptor (PRR) agonists polyadenylic-polyuridylic acid (poly(A:U)) and polyinosinic-polycytidylic acid (poly(I:C)) in solid tumours (105, 106) demonstrated efficacy against non-metastatic, operable tumours with only mild toxicity. The use of IFN pathway agonists may prove to be an improved form of IFN therapy, however further trials are needed to understand the full mechanism of action and characterise their potential benefits over recombinant IFN.

Table 1.1 An overview of clinical trials of type I IFNs in cancer

Recombinant IFN			
Cancer	Agent	Response	Ref
Melanoma	IFNα-2b	Prolonged relapse-free survival (p=0.0023) and OS (0.0237) Dose modification due to toxicity in majority of patients	Kirkwood et al. 1996 (78)
	High dose IFNα-2b	RFS & OS benefit (p =0.0015 & p = 0.009)	Kirkwood et al. 2001 (79)
	High dose IFNα-2b	11/20 patients had objective clinical response, 3/20 had complete pathological response Responders had increased endotumoural CD11c+ & CD3+ cells and fewer CD83+ cells	Moschos et al. 2006 (80)
	IFNβ ($6x10^5$ IU continuous IV daily)	No significant effect on overall patient outcome and no side effects	Voelter-Mahlknecht et al. 2006 (81)
	PEGylated IFNα-2b (induction 6ug/kg per week for 8 weeks, then maintenance 3ug/kg)	RFS benefit with IFN (HR=0.82, p=0.01) Treatment discontinued due to toxicity in 31% of patients	Eggermont et al. 2008 (82)
	IFN-β1a ($12\text{-}18x10^6$ IU s.c. daily)	No overall clinical benefit Severe adverse effects in 13/21 patients	Borden et al. 2011 (83)
	Low dose IFNβ ($3x10^6$ IU/day s.c. for 10 days)	RFS & OS benefit in IFN compared to observation groups (p=0.024 & p=0.029)	Aoyagi et al. 2012 (84)
	Intermittent high dose IFNα-2b compared to standard HDI ($20x10^6$IU 5xweekly IV)	No survival benefit for iHDI compared to standard HDI Safety & quality of life improved in iHDI	Mohr et al. 2015 (85)
	High dose IFNα-2b compared to complete lymph node dissection	No DFS or OS benefit in patients with or without tumour-positive sentinel lymph nodes at start of trial	McMasters et al. 2016 (86)
	IFNα-2b ($10x10^6$IU initial 4-week regime with $5\text{-}10x10^6$IU 12 -24 month follow up treatment)	RFS (p=0.0008), DMFS (p=0.0003) & OS (p=0.0007) for 25 month regime in patients with ulcerated primary tumours	Eggermont et al. 2016 (87)
Renal cell carcinoma	Naptumomab estafenatox (Nap) + IFNα (9 million units s. c. three times weekly compared to IFN monotherapy	Median overall survival of 17 months and no difference between treatment groups No severe toxicities. Stratifying patients showed survival benefit in a select subgroup	Hawkins et al. 2016 (88)
Colorectal cancer	PEGylated IFN-α-2b (Pegintron, 1 μg/kg body weight) in combination with synthetic peptide vaccine	Combination induced significantly more IFNγ-producing T cells (patients previously successfully treated for metastatic disease)	Zeestraten et al. 2013 (90)

	IFNα ($3x10^6$ IU) in combination with 21urviving-2B80-88 plus IFA	4/8 patients had two-fold increase in CTL	Kameshima et al. 2011 (91)
Pancreatic cancer	IFNα ($3x10^6$ IU) in combination with 21urviving-2B80-88 plus IFA	50% of patients had positive clinical responses and positive immunological effects seen in CD8+ T lymphocytes	Kameshima et al. 2013 (92)
Prostate cancer	IFNα-2b/13-cis retinoic acid with paclitaxel or mitoxantrone, estramustine or vinorelbine (MEV)	IFN therapy had lower response rates and overall survival than MEV-treated patients IFN significantly decreased quality of life compared to MEV (p=0.01)	DiPaola et al. 2010 (93)
Breast cancer	Partially purified HuIFNβ 3-6 $x10^6$ U i.m. daily	Moderate toxicity reported and 16% pathological response	Borden et al. 1982 (94)
	Fibroblast IFNβ 6 – 60 $x10^6$ U for at least 6 weeks	No responses were seen and moderate to severe toxicity was frequent	Bruntsch et al. 1984 (95)
	IFNα-2a in combination with IL2 $7.5x10^6$ U 3xweekly s.c.	Moderate toxicity and low pathological response rates	Kimmick et al. 2004 (96)
Ovarian Cancer	IP IFN-2α alternated with cisplatin to treat minimal residual disease	7/14 patients demonstrated complete remission via laparotomy median follow up 22 months with minimal toxicity	Nardi et al. 1990 (98)
	Stage III minimal disease patients treated with weekly i.p. carboplatin and IFNα-2b (30 million units) for 12 weeks	Mild toxicity commonly reported and 5 patients had severe dose-limiting reactions. 91% of patients with tumours <5mm had complete responses.	Frasci et al. 1994 (99)
	Determine the maximum tolerated dose of i.p. IFNα-2b in combination with i.v. cisplatin plus cyclophosphamide	No patients completed the planned schedule. Toxicity was reported in all patients and dose-limiting myelosuppression disrupted treatment cycles. The maximum tolerated dose was 20 million units a week apart	Moore et al. 1995 (100)
	IFN-2α ($25x10^6$ U) in combination with carboplatin i.p. for 3x 28 day courses	Toxicity was more frequent and severe in IFN treated patients with no significant survival or progression-free benefit	Bruzzone et al. 1997 (101)
	IFNα in combination with continuous cyclosporine infucion and carboplatin	In recurrent ovarian cancer 3/84 patients showed a partial response. 9 patients stable for >4 months. Toxicity reported as nausea, headache, myelosuppression. Combination not recommended further.	Morgan et al. 2007 (102)
	Pegintron (IFNα) in combination with gemcitabine and p53 synthetic long peptide vaccine	No patients experienced dose-limiting toxicity, though reports of nauseas, mild-moderate fatigue and flu-like symptoms. Combination therapy increased circulating CD4+ & CD8+ T cells but not Tregs	Dijkgraaf et al. 2015 (103)

Abbreviations: RFS = relapse-free survival, OS = overall survival, DMFS = distant metastasis free survival, IU = international units, IV = intravenous, IP = intra-peritoneal, s.c. = subcutaneous, HDI = high dose IFN, iHDI = intermittent HDI

The type I IFNs are known to be critical in immunosurveilance and specifically, immune elimination (reviewed in (107)). Evidence suggests that the potent anti-tumour effects of type I IFNs reflect their action on host immune cells predominantly, rather than tumour cells. Specifically, experiments performed by Dunn et al. using highly immunogenic sarcomas demonstrated that mice treated with specific antibodies against the type I IFN receptor developed progressive tumour growth while mice with intact receptor signalling were able to reject tumours (108). Additionally, tumours deficient in the type I IFN receptor were predominantly rejected when transplanted into naïve mice. In tumours that progressed, restoring type I IFN receptor signalling did not achieve tumour rejection.

Fine-tuning the clinical efficacy of exogenous IFN therapy lies in an improved understanding of their endogenous role and mechanisms of action. These include their tumour cell intrinsic and extrinsic effects. The central thesis & experimental data contained within this body of work explores these unanswered questions, and will hereafter focus on the anti-tumour properties, endogenous protection and pre-clinical efficacy of members of the type I IFN family.

1.5 Type I IFNs

1.5.1 Type I IFN Signalling & Regulation

All type I IFNs signal via the Janus kinase – signal transducers and activators of transcription (JAK-STAT) pathway (99), shown in Figure 1.5. Type I IFNs bind to interferon alpha receptor (IFNAR) chains, IFNAR1 and IFNAR2, which are pre-associated with the kinases tyrosine kinase 2 (TYK2) and JAK1, respectively (109). Once these two JAKs are activated, they phosphorylate residues on the receptors; allowing STAT2 to bind to the intracellular portion of the IFNAR2 chain and subsequently recruit STAT1 (110).

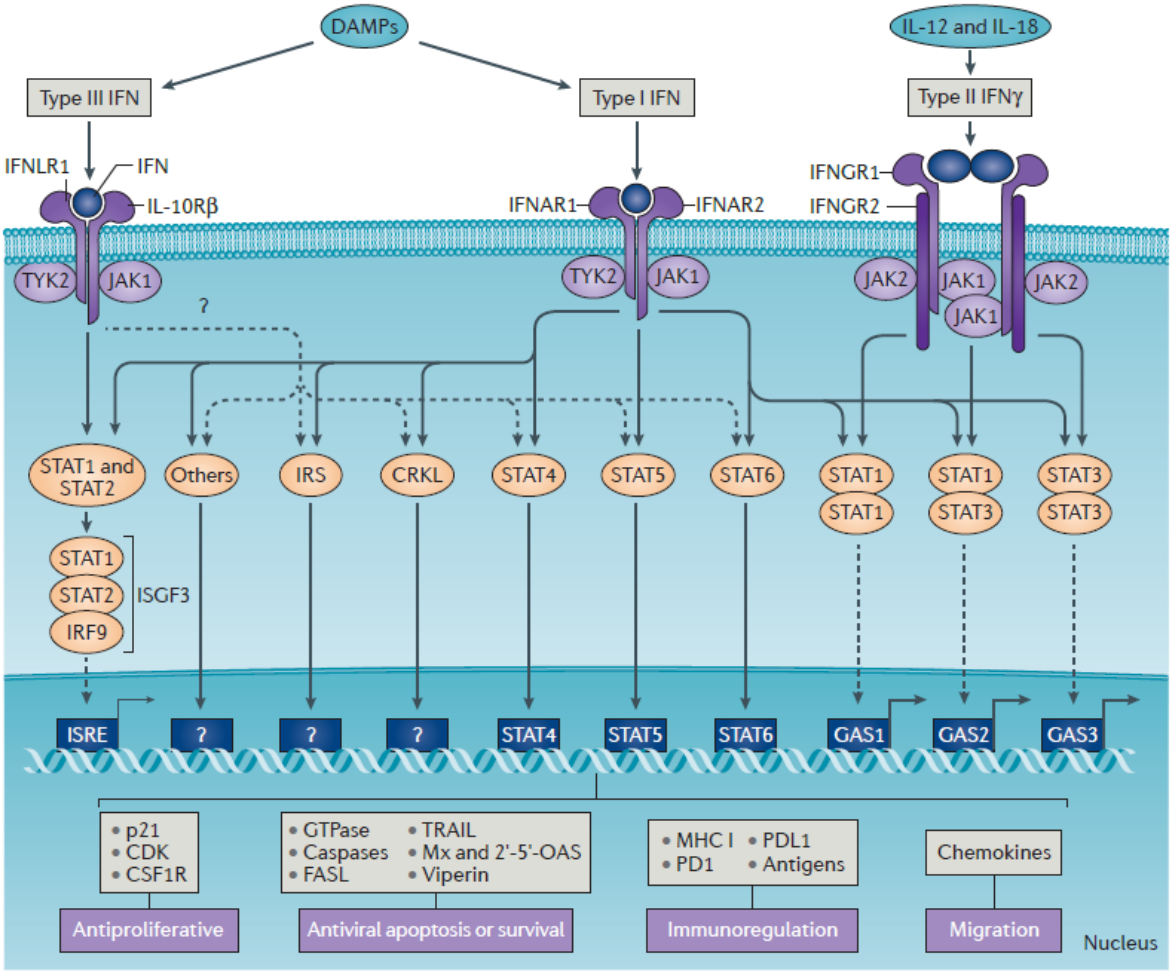

Figure 1.5: Type I IFN signalling via the JAK-STAT pathway

Type I IFNs bind to IFNAR receptor chains on the cell surface and activate the JAK-STAT signalling cascade. Once the receptor chains are phosphorylated by TYK2 and JAK1, STAT2 binds to the intracellular portions of IFNAR receptor chains and recruits STAT1 to form a heterodimer, which dissociates from the receptor chains. STAT1/STAT2 then bind IRF9 to form ISGF3, which translocates to the nucleus, binds to promoter sequences and induces IFN regulated gene expression (image adapted from (97)).

Both STATs bind together and undergo phosphorylation to become a heterodimer, which dissociates from IFNAR receptor chains and together with interferon regulatory factor 9 (IRF9), form the transcription factor known as IFN stimulated gene factor 3 (ISGF3) (111). Once ISGF3 has translocated to the nucleus, it induces gene expression (112). Importantly, type I IFNs do not exclusively signal via the STAT1/STAT2 pathway; indeed, many other IFN signalling pathways exist. These vary depending on tissue and pathophysiological state and may contribute to anti-tumour activity (77, 113, 114) with pathways shown to involve STAT4 (115), STAT3 and STAT5 (116) as well as non-STAT molecules such as mitogen-activated protein kinase p38 and phosphatidylinositol 3-kinase (PI3K) (117), others remain to be characterised. Type I IFN signalling results in the regulation (induction and suppression) of expression of thousands of IFN regulated genes (IRGs), which encode the effector proteins of the IFN response mediating antiviral, cell growth regulation, survival and immune activation activities (118).

Microarrays and more recently RNA-Seq are powerful technologies that enables simultaneous genome-wide expression analysis on a single sample. Such analysis has enabled the extensive study of IFN-driven pathways and subsequently, resulted in the characterisation of IRGs. The INTERFEROME database is a compilation of microarray datasets performed on cells or organisms following stimulation with type I, II & III IFNs and provides a complete list of IRGs with accompanying tools/features to characterise IRG regulation pathways (119). This computational tool has the capacity to reveal IFN signatures across different diseases including chronic viral infection, autoimmune disorders, bacterial infection and various types of cancer (113, 114). These analyses have shaped an understanding of the myriad of biological pathways regulated by type I IFNs leading to identification of IFN mechanism and may constitute effective biomarkers of disease states.

1.5.2 Type I IFN Functions

Since their discovery in 1957, IFNs have been shown to exhibit pleiotropic activity within cells (120). Of the many functions of type I IFNs it is their anti-tumour capabilities that have the potential to combat cancer. Type I IFNs are known to act in an anti-tumour capacity both directly, by acting upon tumour cells (121, 122); and indirectly, through immune cell activation (123) as well as affecting cells in the tumour microenvironment (115) (summarised in Figure 1.6).

Recently, many studies have investigated the indirect anti-malignant capacity of type I IFNs, indeed large emphasis now revolves around the immunomodulatory actions of type I IFNs and how they contribute to cancer immunosurveillance (124) (summarised in Table 1.2). As touched on earlier, of the immune response. Specifically, tumour cells from mice deficient in both IFNAR1 and IFNGR1 were not rejected when type I IFN sensitivity was restored, however restored sensitivity to type II IFN facilitated tumour rejection (108). Additionally, type I IFNs were shown to target host hematopoietic cells to enhance anti-tumour responses, emphasising the indirect action of type I IFNs in cancer suppression, as distinct from IFNγ, which directly targets both tumour and host cells (108, 125, 126). A selection of these anti-tumour immunoregulatory effects are summarized in Table 1.2.

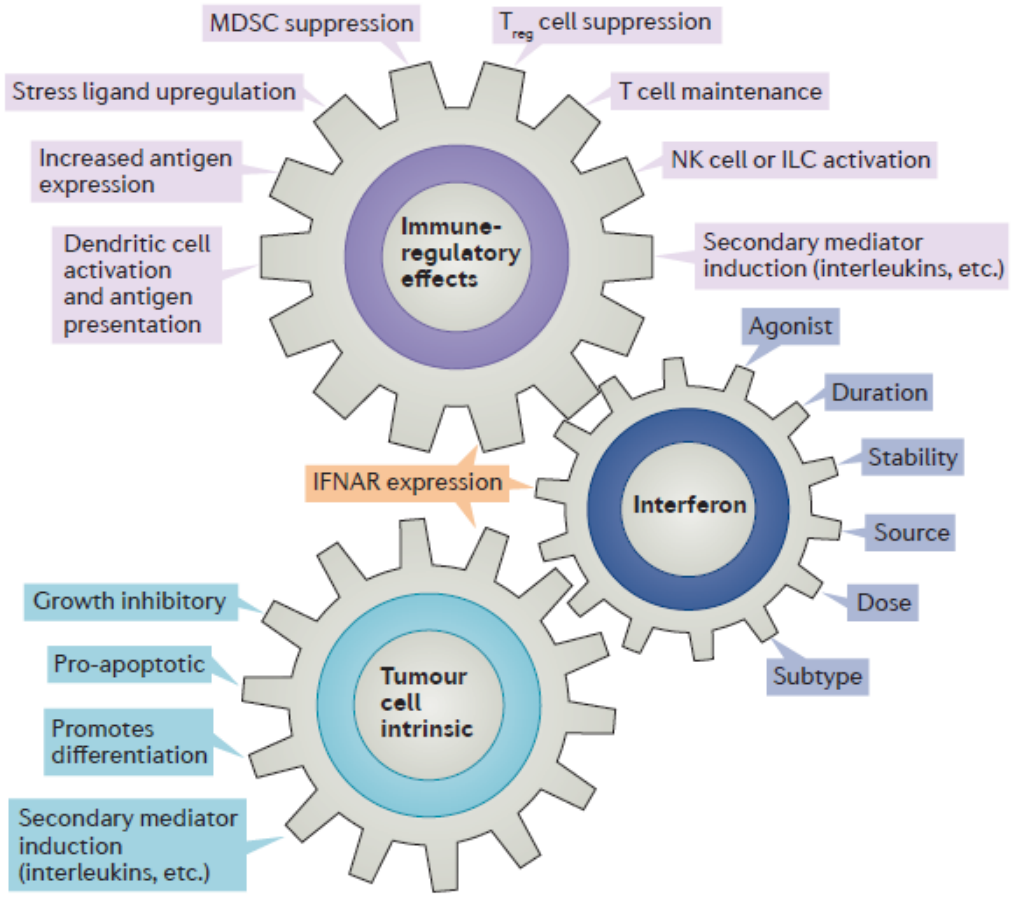

Figure 1.6: Intrinsic & Extrinsic anti-tumour actions of type I IFN.

Type I IFN anti-tumour activities are facilitated through expression of IRGs, many of which encode specific effector proteins with anti-malignant function. For instance, IRGs such as p15 and Cyclin D have been shown to exhibit anti-proliferative activity through their regulation of cell cycle (108), while pro-apoptotic function include the IRGs Bak and Bax (127) and protein kinase R (PKR) (128) (image adapted from (97)).

Table 1.2 The anti-tumour immunoregulatory effects of the type I IFNs.

Immune cell type	IFN action on cell	Reference
NK cells	Increase cytotoxicity & effector function	Biron et al Annu. Rev Immunol 1999 (129)
	Promote proliferation	Biron et al. J Leukoc Biol 1984 (130)
Dendritic cells	Increase activation & cross presentation	Schiavoni et al. Front Immunol 2013 (131)
Effector T lymphocytes	Increase activation	Marrack et al. J Exp Med 1999 (132)
	Promote effector function	Curtsinger & Mescher Curr Opin Immunol 2010 (133), Fuertes et al. J Exp Med 2011 (134)
	Increase proliferation	Zhang et al. Immunity 1998 (135)
B lymphocyte	Increase activation and lower threshold for induction	Braun et al. Int Immunol 2002 (136)
	Increase antibody response	Le Bon et al. J Immunol 2006 (137)
	Promote antibody class switching	Swanson J Exp Med 2010 (138)
T regulatory cells	Decrease immunosuppressive activity	Pace et al. J Immunol 2010 (139)

1.5.3 Cell Intrinsic Anti-Tumour Effects of the Type I IFNs

The type I IFNs are also capable of regulating several cell intrinsic processes that are vital for tumour survival and progression including proliferation, apoptosis, expression of tumour antigens, migration and invasion (reviewed in (97)). Early *in vitro* studies demonstrated that the direct anti-proliferative effects of type I IFNs on tumour cell lines, specifically breast cancer cell lines treated with lymphoblastoid IFN, prolonged all cell cycle phases (140). IFNα has been shown to upregulate p21, an inhibitor of cyclin dependent kinases, on prostate cancer cell lines and inhibit cell cycle (141).

The type I IFNs are also able to regulate both pathways of apoptotic cell death including the death receptor mediated pathway involving caspase 8 activation and the mitochondrial pathway involving the release of cytochrome c which activates cytoplasmic caspases (142-144). Additionally, type I IFNs are able to promote tumour antigen presentation on the surface of tumour cells (145) and upregulate proteins associated with antigen presentation such as transporter 1, ATP binding cassette subfamily B member (TAP1) (146). Finally, type I IFNs have been shown to modulate the expression of immune checkpoints on tumour cells including PD-L1 (147). Thus, type I IFNs directly regulate tumour cell function and immunogenicity

1.5.4 Type I IFNs as Anti-Cancer Therapy

One of the earliest human trials of recombinant IFNα in cancer was against Kaposi's sarcoma (123). Additional trials have since used IFNα alone and as adjuvant therapy against malignancies such as chronic myeloid leukaemia (148), renal cell carcinoma (149, 150) and melanoma (151-155), among others (156, 157). Treatment with IFNα alone demonstrated some anti-tumour capacity when treating a portion of these malignancies, however its efficacy varies between cancer types and is limited by the significant adverse effects that accompany

long-term IFN therapy such as fever, headache, myalgia, nausea and fatigue and signs of autoimmunity (158, 159).

Early trials of type I IFNs in breast cancer used treatment with IFNα as adjuvant therapy in human patients (160, 161). These trials demonstrated some positive results, Gutterman *et al*.'s study resulted in 6 of 17 breast cancer patients exhibiting partial remission (>50% tumour size reduction) when treated with intramuscular IFNα (94, 162) and Borden *et al*. had similar results with 5 of 23 patients demonstrating partial responses to intra muscular IFNα (162). Despite these initial results, however subsequent *in vivo* studies trialling type I IFNs alone or as adjuvant therapy have been largely unsuccessful (94).

Crucially it must be acknowledged that in many studies there was a limited capacity for therapeutic response as only primary tumour response was examined and patients were treated at an advanced stage disease. For example, Kimmick *et al*.'s study used adjuvant subcutaneous IFNα treatment against 40 human metastatic breast tumours *in vivo* (96, 163, 164). No complete responses were observed and only one patient exhibited a partial response (3%, C. I. 0-16) (96). However, given that this patient cohort comprised women post-chemotherapy for inoperable metastatic breast cancer, it was unlikely that any clinical benefit would be observed. As previously mentioned, another obstacle to measuring IFN efficacy is their severe dose-limiting cytotoxic effects.

1.5.5 Type I IFN Production

Type I IFNs production can occur in most cell types of the body under the control of a diverse range of stimuli. The cells and localisation of type I IFN production are important determinants of the physiological role of IFN and in the context of cancer, the ability of type I IFNs to regulate intrinsic or extrinsic tumour suppression.

1.5.5.1 Type I IFN Production: Lymphoid

Plasmacytoid dendritic cells (pDCs) are major producers of type I IFNs, in particular in response to viral RNA & DNA that stimulate toll-like receptor 7 (TLR7) and TLR9, respectively (165-167). However, pDCs may also produce type I IFNs in response to host-derived signals, for instance, during wound healing and in response to injury (168). Indeed, almost all cell types can produce type I IFNs in response to pattern recognition receptor (PRR) activation, these include TLRs, which detect bacterial lipopolysaccharides (TLR1, 2, 4, 5, 6) or nucleic acids (TLR3, 7, 8, 9); RIG-I like helicases (RLHs) in response to viral nucleic acids; cyclic GMP-AMP synthase (cGAS); Nod-like receptors (NLRs); and C-type lectins. Regarding pathogen-driven type I IFN production, macrophages, NK cells, DCs, lymphocytes and fibroblasts are capable of producing type I IFNs, predominantly an acute phase response.

1.5.5.2 Type I IFN Production: Epithelial

Epithelial cells provide a physical barrier against pathogenic entry and colonisation of the host. Mucosal epithelial cells including those that line the luminal surfaces of the respiratory, gastrointestinal and female reproductive tracts have been shown to produce type I IFNs as part of the local first line of defence against invading pathogens. Epithelial type IFN production is likely regulated by ETS factor binding sites in the IFNε promoter such as ELF3 (E74-like factor-3) important for terminal differentiation of intestinal epithelium (169). These transcriptional regulators may account for unconventional cell type specific patterns of expression, for instance, constitutive expression of IFNβ in bronchial epithelial cells has been reported as critical for late anti-viral responses and viral clearance (170). Moreover, IFNβ may be produced by the gastrointestinal epithelium to protect against bacterial infection and the more recently characterised type I IFN, IFNε, is produced by the epithelial lining of the female

reproductive tract and has been shown to protect against viral and bacterial sexually transmitted infections (171).

1.5.5.3 Type I IFN Production: Acute Phase

Type I IFN production can be triggered by a variety of 'danger' signals. The best characterised inducers of IFN are conserved components of pathogens referred to as pathogen-associated molecular patterns (PAMPs), particularly PAMPs of viral or bacterial origin (96). These stimuli are detected by PRRs and activate signal transduction pathways leading to activation of transcription factors, such as nuclear factor kappa, enhancer of B cells (NFκB) and interferon regulatory factors (IRFs), which induce pro-inflammatory cytokines and IFNs, respectively (122). The stimuli for IFN production during tumourigenesis remains unknown, but could involve a number of pathways. Other 'danger' signals that induce IFN include DNA from dying cells and immune complexes in autoimmune diseases (122).

Acute phase IFN production in response to pathogen involves a rapid, usually transient, expression of IFN genes (122). These genes are regulated transcriptionally upon activation by signalling molecules such as IRFs & NF-kB that bind to specific IFN gene promoter sequences (172). To date, nine interferon regulatory factors (IRFs) have been recognised: IRF1, IRF2, IRF3, IRF4, IRF5, IRF6, IRF7, IRF8 and IRF9 (173). IRFs were originally characterised in IFN induction, however, it is now known that IRFs are critical within host immunity with IRF5 and IRF9 shown to facilitate T helper 1 development (174) and STAT signalling, respectively (175). IRFs & NF-kB are considered major transcriptional regulators of type I IFN expression in response to pathogens, however it is important to consider that not all type I IFN promoters comprise different binding sites that potentially provide further insight into alternate patterns of expression of these IFNs.

1.6 Constitutive Type I IFN Signalling & Host Defence

Type I IFN signalling is rarely detected at high constitutive levels in human tissues in the absence of a pathogenic stimulus. However, constitutive type I IFN signalling and activity has been found to be critical in the body where it has been implicated as a vital tissue resident component preventing pathogenic invasion via priming immune responses or suppressing metastatic spread of cancer cells. In 1981, Bocci described an 'acute' and 'physiological' IFN response (176) and suggested not only that locally, physiologically produced IFN may be critical for homeostasis, but that the age-associated progressive decline of constitutive IFN may favour the development of diseases such as cancer. At the time, the hypothesis of constitutive IFN production was difficult to prove due to an inability to detect evidence of peripheral IFN activity and a lack of understanding of what constituted a non-pathogenic inducer of IFN.

1.6.1 Constitutive or Physiological Type I IFN

In fact, while type I IFN productions is often classified as a transient process in response to pathogenic or cell death signalling, type I IFN signalling has been described as a physiological process that involves constitutive cytokine production which aids in maintaining homeostasis. In addition to typical IRF binding sites, the *IFNB1* gene promoter contains NF-kB & activating protein 1 (AP1) binding sites (97). Physiological expression of IFNβ can be found in myeloid cells upon stimulation with colony-stimulating factor 1 (CSF1) (177) and in osteoclasts in response to receptor activator of NF-kB ligand (RANKL) via the AP1 pathway (178).

Constitutive IFNβ has also been detected in mononuclear phagocytes in the colon, where it has been shown to be important for producing anti-inflammatory signals, promoting Treg function and maintaining gut homeostasis (179). Additionally, high constitutive IFNβ has been detected in murine thymus and been implicated to regulate T cell development (180).

Furthermore, in the female reproductive tract, constitutive IFNε (whose promoter contains ELF3 and hormone receptor binding sites) is under hormonal regulation and expression of IFNε in the epithelial tissue, which fluctuates across the menstrual cycle positively correlating with peaks in oestrogen and negatively correlating with progesterone (171). This initial evidence provides insight into the role of constitutive IFN in maintaining homeostasis and protecting against infections, however, the physiological role of IFN production in preventing tumourigenesis remains poorly understood and is a considerable focus of investigation for this thesis.

To study the role of constitutive IFN in host defence particularly tumour suppression, it is critical to consider discrete components of the IFN production & signalling cascade (Figure 1.7). Firstly, understanding how IFN production is induced in the absence of pathogenic stimuli and whether this involves classical PRR signalling or alternative pathways (such as CSF1 and RANKL Figure 1.7, Box 1). Secondly, it is unknown how physiological or constitutive IFN production is regulated transcriptionally (Figure 1.7, Box 2) or when constitutive IFN production is detectable and in which cells. Furthermore, the mechanism of action on these cells or peripheral cell populations remains poorly understood (Figure 1.7, Box 3). Finally, there is scope to investigate a constitutive IFN signature and identify IRGs regulated by physiological IFN signalling and the differences compared to the acute phase response genes (Figure 1.7, Box 4).

'It is suggested that the physiological interferon response, although previously overlooked, has great biological importance because production of interferon at strategic sites can maintain active defence systems essential for survival.'

– Bocci V. Biol Rev 1981

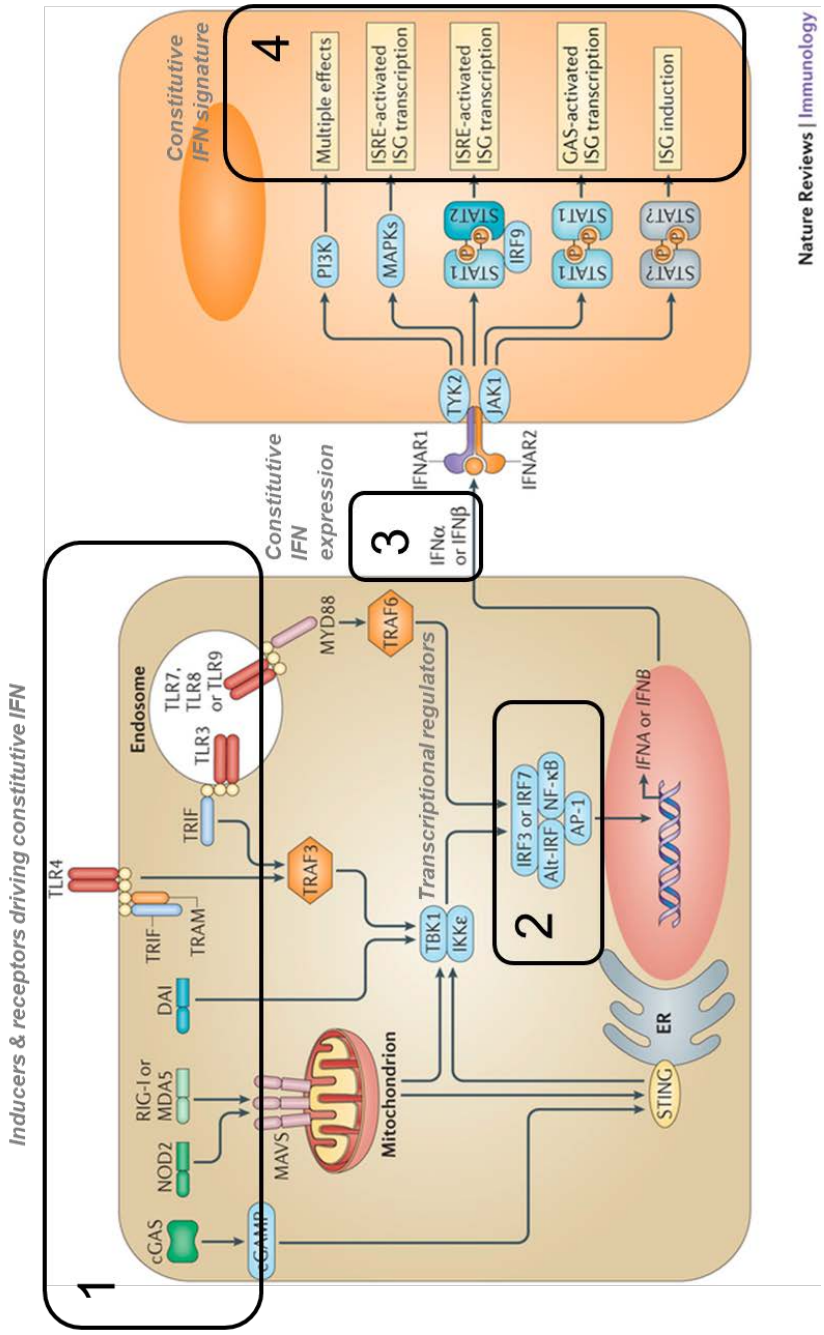

Figure 1.7: The discrete components of constitutive IFN signalling.

1) Inducers and their receptors which are involved in detecting signals which drive constitutive IFN signalling are likely to be cell type specific and remain poorly defined. 2) The transcriptional signals driving constant IFN expression such as IRF7 which in turn is an IRG and is involved in a positive feedforward loop with type I IFNs. 3) Detection of constitutive type I IFN, specific subtypes and their distinct expression and modes of action have yet to be fully characterised across tissues of the body. 4) Downstream products of constitutive IFN signalling, for example, expression of specific IRGs constituting a constitutive IFN signature. Image adapted from (181).

1.7 Type I IFN Signatures in PBMC & Epithelial Tissue

Human peripheral blood comprises a mixed population of cells. Peripheral blood mononuclear cells (PBMCs) include monocytes/macrophages, B & T lymphocytes and NK cells. Gene expression in peripheral blood has been shown to indicate disease progression in a number of infections (174), autoimmune diseases (182) and cancers (183). Primary tumour IFN signatures have been investigated in a number of cancer types including renal cell carcinoma, melanoma and hepatocellular carcinoma as well as haematological malignancies, however there is a distinct lack of literature on IFN signatures in peripheral blood cells for solid tumours. One study investigated IFN-regulated gene expression in PBMCs of melanoma patients (184) and some of the IRGs found to be expressed in PBMCs of melanoma patients included STAT1, STAT2, IFIT1, IFIT2 and OAS3. However, this study focused on dose response and used these genes merely as an indication of IFN response rather than characterising an IFN signature in human PBMCs. In the absence of appropriate cancer studies, IFN signatures in peripheral blood cells of non-cancer disease states, including autoimmunity and infection, provide an insight into the genes controlled by IFN in circulating blood cells, disease progression and can be studied with respect to their possible importance in cancer.

1.7.1 IFN Blood Signatures in Disease

1.7.1.1 Systemic Lupus Erythematous

Variations in IFN signatures that occur from patients with the same disease state have been correlated to disease severity. Baechler *et al*. performed gene expression analysis on the PBMCs of 48 patients diagnosed with systemic lupus erythematosus (SLE) compared to non-disease control samples. Of the 161 genes up regulated in SLE, 23 genes associated with

IFN were overexpressed and were subsequently used as an IFN gene expression 'signature' (184). Interestingly, expression intensity of this signature seemed to correlate with the severity of disease, patients demonstrating higher levels of IFN stimulated gene expression were more likely to have more clinical disease manifestations or multiple organ involvement ($p<0.0002$) (183). Bennett *et al*. also identified an IFN signature in PBMCs taken from paediatric patients with SLE (183). These SLE studies demonstrate that in a disease where production of IFN is considered to contribute to the pathological process, a resulting IRG signature is detectable in PBMCs. Critically, this work has led to a clinical program of blocking type I IFN signalling in patients who are stratified by signature.

1.7.1.2 Mycobacterium Tuberculosis

Berry *et al*. demonstrated a similar application of systemic IFN signatures in Mycobacterium tuberculosis (TB), though rather than simply comparing diseased blood signatures to healthy samples they used two disease states; active and latent TB, as well as healthy controls (185). Of the 393 genes they identified as up regulated in active TB, a third were shown to be IRGs in the INTERFEROME database (182), suggesting the importance of IFN in this disease process and further, identifying variations in IFN signatures as an indication of severity of disease.

These examples demonstrate the successful use of IFN signatures in peripheral blood of diseased patients to indicate disease progression and severity. This boosts the feasibility of finding a signature of constitutive IFN signalling in cancer metastasis, which may guide precision therapy to suppress tumour progression.

1.7.2 A Constitutive IFN Signature in Mammary Epithelium

1.7.2.1 Constitutive Interferon Regulatory Factor 7 (IRF7) Expression

A major advancement in the understanding of breast cancer metastasis was a study by our lab in collaboration with the Parker lab at Peter MacCallum Institute in 2012 by demonstrating the importance of the IRF7 pathway in suppressing breast cancer metastasis to bone through a combination of gene expression and ontological analysis (42, 120). Using mice that develop primary breast tumours and distant metastases when inoculated orthotopically (into the mammary tissue from which the tumour originated) with the breast cancer cell-line 4T1.2, Bidwell *et al*. analysed gene expression in tumour cells purified from bone metastases compared to primary breast tumour cells. A list of genes down regulated in bone metastases were analysed using the INTERFEROME database, an online database pooling IRGs from publically available microarray datasets (42).

Of the 2,500 genes down regulated in bone metastases, 540 were identified as IRGs and a further 208 had predicted IRF7-binding sites in their proximal promoter sequences (113, 114). Additionally, Bidwell *et al*. analysed human datasets of primary breast tumours and known first sites of distant metastases, and found a linear correlation between expression of the 208 putative IRF7 target genes and bone metastasis-free survival, demonstrating a preliminary translation of the findings into human data. Bidwell *et al*. then went on to perform immunohistochemical staining using IRF7 antibodies on sections from both primary breast tumours and matched bone metastases.

Expression of IRF7 was found to be present in primary breast tumour cells but absent in bone metastases (42). IRF7 is a transcription factor known to be a major regulator of IFN production in both systemic innate and local adaptive immune responses (42). The *IRF7* gene was first investigated in the context of Epstein-Barr virus latency, due to the role played by IRF7 protein in transcriptionally regulating EBV nuclear antigen 1 (*EBNA1)* expression (186, 187). *IRF7* shares the highest sequence homology with *IRF3* and as such their pathways

and effector protein functions overlap to an extent (188). IRF7 is induced when exposed to a number of stimuli including viral infection, IFNs and lipopolysaccharides (LPS) (189). As an inducible factor IRF7 is rarely constitutively expressed in most cells, the exception being pDCs (190) that express high levels of IFNs very rapidly (191), and mammary epithelium, which Bidwell et al. demonstrated in human tissue through immunohistochemical staining, however, the mechanism of constitutive expression in this tissue remains unknown (42).

IRF7 can be regulated in two ways; either induced by type I IFN or activated via phosphorylation in response to viral and bacterial infection (165). It is important to acknowledge that IRF7 and type I IFN contribute to a positive feedback loop (shown in Figure 1.8) and as such these two pathways for IRF7 regulation are not mutually exclusive. When exposed to a virus, various transcription factors, including IRF7, are activated via PRR activated cascades (192). These cascades involve activation of the kinases IKKξ and TBK, which phosphorylate IRF7 (192). Activated IRF7 then dimerises, translocates to the nucleus and binds to various promoters to induce the expression of type I IFNs (193). Production of IRF7 is subsequently induced via IFNAR receptor binding and activation of the STAT signalling pathway. This loop will remain active until the stimulus is cleared from the cell (192).

IRF7 emerged as a key regulator of type I IFN production in both the innate and adaptive immune systems largely through *IRF7* knockout mice (*IRF7*$^{-/-}$) experiments (194). When examining both cytosolic viral detection and TLR pathways, *IRF7*$^{-/-}$ mice have been shown to be consistently more susceptible to viral infection correlating with a decrease in IFNα/β production (187). Sato *et al.* demonstrated that IFN expression in response to viral stimulus was completely absent in mice lacking both IRF7 and IRF3 (187). Restoration of normal IFN responsiveness was only observed when both factors were reintroduced, reflecting the critical role both IRF7 and IRF3 play in regulating type I IFN (186).

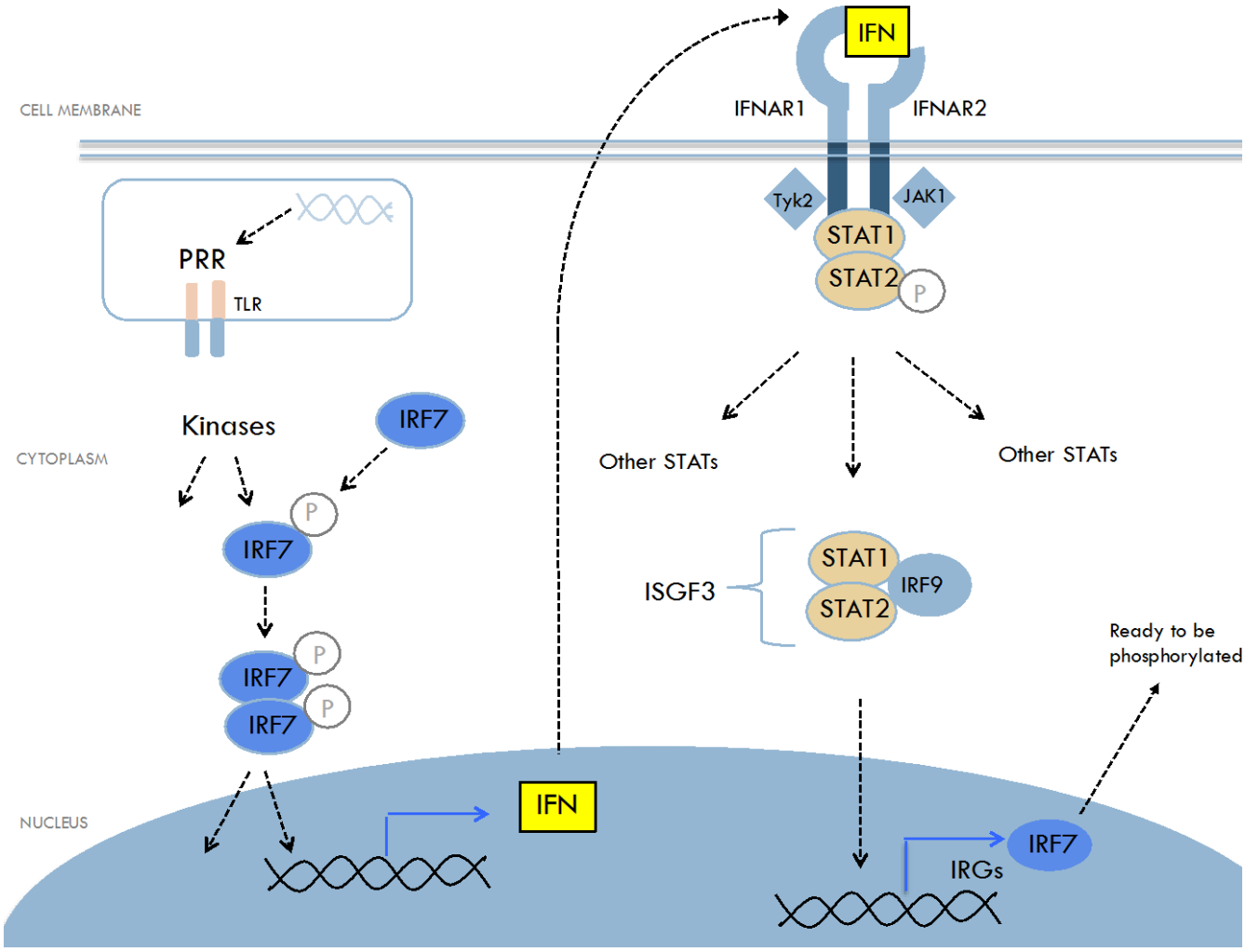

Figure 1.8: Positive Regulatory loop involving IRF7 & type I IFN.

Type I IFN and IRF7 are engaged in a positive regulatory loop, which is initiated when a PRR detects pathogenic stimuli and subsequently stimulates a signalling pathway. Intracellular kinases are activated and in turn phosphorylate IRF7, which then dimerises and translocates to the nucleus to bind to various promoter sequences and induce type I IFN expression. Type I IFN is then secreted out of the cell and binds to cell surface receptors IFNAR1/IFNAR2, which initiate the JAK-STAT pathway. Activation of the JAK-STAT pathway results in induction of IRF7 expression. If IRF7 is phosphorylated it will lead to further IFN production. This regulatory loop will continue until the pathogen stimuli is removed (image adapted from (192)).

Other studies using *IRF7*$^{-/-}$ mice have further investigated IRF7 signalling *in vivo*, for instance, Honda *et al.* showed that without IRF7, induction of IFNβ was diminished compared to wild type, and IFNα was completely inhibited (186). Subsequently, IRF7 was shown to play a significant role in type I IFN induction in a number of cells via different mechanisms (187, 189). Induction of IFNα via cytosolic PRRs has been shown to rely on both IRF7 and IRF3 while type I IFN induction in pDCs utilises toll-like receptors (TLR7 and TLR9) that rely exclusively on IRF7 (189, 195). In comparison to other types of dendritic cells, pDCs constitutively expresses large amounts of IRF7 (187), which likely accounts for the distinctly large amounts of type I IFNs produced by these cells (191). IRF7 has been shown to induce a broader range of type I IFNs than IRF3. One study demonstrated that IFNβ and two IFNα subtypes (IFNα1 and IFNα2) were inducible through either IRF7 or IRF3 expression, while a further three IFNα subtypes (IFNα4/7/14) were exclusively induced by IRF7 (196).

Given the known indirect anti-tumour function of type I IFNs through immune cell stimulation (190), it was hypothesized that the absence of IRF7 in bone metastases may correspond with decreased type I IFN activation of host immune cells. Restoring IRF7 should therefore increase type I IFN levels and subsequent immune cell mediated suppression of bone metastasis. Bidwell *et al*. demonstrated that restoring IRF7 either through overexpression of IRF7, or treating with recombinant type I IFN did not have any effect on primary tumour growth, however, it did result in reduced spinal metastases. Indeed 60% of non-IRF7 overexpressing mice had spinal metastases while no spinal metastases were detected in IRF7-overexpressing mice. Restoring IRF7 by treating mice with IFNα for 5 weeks prolonged survival compared to those treated with saline (42). Importantly, restoring IRF7 was only able to suppress bone metastases in mice with an intact IFN signalling pathway, Bidwell *et al*. showed that Irf7over-expression in *Ifnar1-/-* mice did not suppress bone metastasis (115). This highlights that type I IFN-induced signalling in 'host' cells is essential for suppressing bone

metastasis and agrees with evidence that type I IFN anti-tumour effects are predominantly enacted via effects on host cells rather than tumour (108).

Bidwell *et al*. examined the relationship between type I IFNs and immune cells in eliciting this anti-tumour response by showing that mice treated with IFNα for 6 weeks had much lower levels of immune-suppressing cells (myeloid-derived suppressor cells) in their bone marrow and peripheral blood compared to mice treated with saline. Additionally, mice over-expressing Irf7 had increased populations of CD4+ and CD8+ T lymphocytes and NK cells in their peripheral blood compared to non-overexpressing mice, suggesting that Irf7-driven IFN stimulates immune cell proliferation in the blood stream. Additionally, they showed that mice over-expressing Irf7 yet deplete of immune cells (CD8+ T and NK cells) did not have significantly reduced metastasis-free survival compared to non-immunocompromised mice.

Together these findings support the hypothesis that IRF7 inducing type I IFNs in primary breast tumour cells leads to the secretion of IFN into the blood, resulting in activation of host immune cells, which then suppress metastatic cells, though much remains unclear about this pathway. For example, at what point in the metastatic pathway to bone is IRF7 lost. Despite these unknowns, Bidwell *et al*. have demonstrated the importance of constitutive Irf7 in facilitating immune-driven suppression of bone metastases.

1.7.2.2 Constitutive IFNε Signalling in the Female Reproductive Tract Epithelium

A recent study by our lab provided the latest characterisation of a novel member of the type I IFNs, IFNε (9). Previously, the IFNε gene had been located on chromosome 9p in the type I IFN locus (12). It shares roughly 30% sequence homology with IFNα and IFNβ, and *in vitro* studies demonstrated IFNε signals through the characteristic type I IFN receptors IFNAR1 and IFNAR2 (68), however its potential anti-tumour properties have not been addressed.

Interestingly, unlike other type I IFNs, which remain at undetectable levels or lowly constitutively expressed in cells until pathogen-induced, IFNε has been found to be highly constitutively expressed primarily in organs of the female reproductive tract (FRT) such as uterus, cervix vagina and ovary (9, 12). IFNε expression is localised to luminal and glandular epithelial cells of the FRT and is unaltered in the absence of haemopoietic cells, which traditionally express other type I IFNs.

Regulation of IFNε is distinct from other type I IFNs. Unlike Ifnα and Ifnβ, Ifnε expression is largely unaltered in response to pathogenic stimuli (9, 12, 69, 70)Instead, Ifnε expression significantly varies across stages of the murine estrous cycle, with expression levels 3-fold higher during estrus than diestrus, an expression pattern that is reflected in human tissue during the menstrual cycle (9). This indicates that unlike other type I IFNs, Ifnε is hormonally regulated, which provides novel insight in respect to ovarian cancer, a disease where for previously unknown reasons hormonal based contraception was shown to decrease the lifetime risk of developing disease (71). Furthermore, post-menopausal women are the highest at-risk group for developing ovarian cancer, correlating with almost undetectable expression of the potentially anti-tumour IFNε (9).

The generation of Ifnε-/- mice allowed for investigation into the role of Ifnε in the physiology and pathology of the FRT. Primary uterine epithelial cells from knockout mice proliferate *in vitro* at significantly higher levels compared to WT (Hertzog lab, unpublished), consistent with the intrinsic, anti-proliferative functions of this new type I IFN. These data, in conjunction with the unique expression profile of Ifnε in the FRT and its ability to signal via IFNARs to elicit typical type I IFN functions, suggest that Ifnε may play a key role in both intrinsic and extrinsic suppression of FRT malignancies such as ovarian cancer.

The suppression of constitutive IFN signalling has recently been shown to be important in breast tumour progression in the mammary gland, yet the role of IFNε in breast homeostasis

and cancer development remains poorly understood. Nevertheless, it is a compelling argument that constitutive IFNε in the FRT may guard against FRT tumour development and hence suppression of its constitutive signalling may be important for tumour progression in both FRT-specific malignancies, the most fatal of which is epithelial ovarian cancer. Therefore, these two cancers constitute common models for investigation of two critical examples of the importance of constitutive type I IFN in tissue homeostasis and its loss in tumourigenesis.

1.8 Type I IFNs & Cancer- Perspective on Breast Cancer

Breast cancer is currently the number one cancer affecting Australian women and second most commonly diagnosed cancer worldwide (42). In 2012, 1.67 million cases were diagnosed and 522,000 breast cancer fatalities were reported achieving the fifth highest overall cancer mortality rate (197). Primary breast tumours have shown to be treatable however, there are few therapeutic options that are effective on distant metastases, the formation of which are a hallmark of end stage cancer and ultimately, are the cause of breast cancer fatality (197).

1.8.1 Metastasis from Breast Cancer

Two common sites of metastasis from breast cancer are lung and bone (198) and both are associated with severely reduced survival, mainly due to their difficulty to treat. Of these two, bone metastasis is linked to the worst overall patient survival (198). Bone metastasis occurs as a result of the general metastatic pathway previously discussed, and is a process by which circulating tumour cells invade the bone marrow cavity and ultimately destroy the normal bone architecture (199). The majority of breast cancer bone metastases are osteolytic, which involves stimulation of osteoclasts that destroy normal bone tissue (200). Many factors influence this specific metastatic pathway including the stimulation of osteoclasts by

production of tumour peptide parathyroid hormone-related peptide (PTH-rP), resulting in bone destruction (200). This site of metastasis of breast cancer is a clear example of the devastation of metastatic spread in cancer. It is largely incurable, but it is also associated with severe bone pain, increased risk of pathological fractures and can significantly decrease quality of life for the patient (201).

1.8.2 Breast Cancer Development & Classification

Normal mammary gland tissue contains a network of ductal branches spreading outwards from the nipple, which are comprised of mammary epithelial cells (MECs) (201). During pregnancy and lactation, these cells undergo ordered proliferation, which is reversible during involution, when widespread-programmed cell death restores breast tissue to pre-pregnancy morphology (202). This contrasts to the unrestrained epithelial cell division that occurs during breast tumour oncogenesis (203, 204). This pathological process is thought to result from a combination of genetic abnormalities and epigenetic factors (5).

Generally, breast cancer can be classified as invasive or non-invasive (205). Ductal carcinoma *in situ* is a non-invasive breast tumour, which arises in and is confined to mammary ducts (198). Among invasive breast cancers (IBCs), those expressing features of both ductal and lobular disease are known as invasive mammary carcinomas, which expand beyond the ductal system and invade the healthy surrounding tissue (198). These tumours are more likely to metastasise to distant organs and thus are associated with poorer prognosis (206).

Despite the use of clinical and histological classifications of breast cancer, which include the Tumour Node Metastasis (TNM) staging system (198) and histological Grades I, II and III to indicate spread and degree of differentiation, respectively (207), it remains difficult to accurately predict the behaviour & likely progression of each tumour and thus, survival for each patient. As with all solid malignancies, breast cancer is a heterogeneous disease (208) and

despite a range of therapeutic options such as surgery, chemotherapy and radiation, not all tumours will respond to standard treatments calling for further molecular classification of each individual tumour (209).

One class of the molecular features that allows for personalised treatment of breast cancer is hormone receptor status. The vast majority of breast cancers are luminal characterised by expression of oestrogen (ER) and progesterone receptors (PR). For this reason, luminal cancers are associated with better prognosis (209) as they are responsive to receptor-targeted therapies. Inversely, non-luminal cancers are ER and PR negative. These subsets of breast cancer can further be divided based on expression of human epidermal growth factor receptor type 2 (HER2). HER2 negative cancers often have a worse clinical outcome due to poorer levels of tumour cell differentiation (210). Breast tumours that lack all three of these receptors are termed 'triple negative'. This subset accounts for 10-20% of breast cancers and is generally associated with the worst patient prognosis. These tumours exhibit rapid aggressive growth and are associated with an increased metastatic risk. The molecular features of triple negative cancers are poorly understood and targeted therapies have yet to be developed. Currently, chemotherapy is the only systemic therapeutic option for triple negative breast cancers and it is often difficult to predict whether these tumours will be responsive.

1.8.3 Gene Signatures in Breast Cancer

In the past two decades, many gene expression studies have performed genome-wide analysis of thousands of women with breast cancer (211) shown in Table 1.3. Of these studies, most have investigated gene expression in primary tumours, rather than peripheral blood signatures, and none have specifically focused on IFN signatures. However, collectively they provide a valuable resource for future data mining.

1.8.4 Primary Breast Tumour Cells

It is important to note that breast cancers of the same stage, histological grade and hormone receptor status often produce different clinical outcomes and for this reason, a number of studies have used gene signatures in primary breast tumour cells to investigate prognosis. Ascierto *et al*. performed transcriptional analysis of primary human breast tumour cells from 17 patients grouped according to number of years of relapse-free survival (1-5 years and >7 years) (212-217). Of the genes expressed in these tumour cells, *STAT1* was among a number of genes found to be the best predictors of relapse-free survival ($p<0.001$), which, as STAT1 is a known IRG and a driver of IRGs (218), indirectly implicates an IFN pathway involvement in breast cancer outcomes.

Another study analysed gene expression in 98 primary breast tumours in an attempt to classify tumours according to their likelihood of metastasising (218). They were able to cluster these primary tumours into two discrete groups according to the similarities in gene expression and correlate gene expression to follow-up data on clinical outcome (219). Importantly, 70% of the primary tumours in the first group came from patients who were diagnosed with metastatic breast cancer within 5 years while only 34% of patients in the second group had metastatic disease in the same time period (219), shaping the basis of a 'poor-prognosis' gene expression group compared to a 'good-prognosis' equivalent. Functional annotation of the genes upregulated in the poor prognosis signature identified enrichment of genes involved in invasion and metastasis, however they did not report on genes downregulated in poor prognosis that may have exhibited immune function. Collectively, these studies demonstrate the importance of gene signatures to predict prognosis in primary breast tumours and metastatic potential, some of which implicate the role of IFN in tumour suppression.. However, few studies have investigated gene signatures in peripheral blood of breast cancer patients as an indication of prognosis (Table 1.3).

Table 1.3: Breast cancer signature studies; investigating gene expression in breast cancer primary tumours or peripheral blood cells of breast cancer patients

Study First Author (ref)	Tissue type	Signature Type or Definition
Sharma et al. (219)	PBMCs	Early detection of BC
Aaroe et al. (220)	PBMCs	Early detection of BC
Tudoranet al. (221)	PBMCs	Identify differential signature in TNBC
Ascierto et al. (209)	Primary tumour	Identify relapse-free survival signature
Van t'Veer et al. (218)	Primary tumour	Identify poor-prognosis signature
Minn et al. (219)	Primary tumour	Predict metastasis to lung
Kang et al. (222)	Primary tumour	Predict metastasis to bone
Perou et al. (223)	Primary tumour	Classification of tumours based on molecular phenotype
Gruvberger et al. (212)	Primary tumour	Classification of ER positive tumours
Martin et al. (214)	Primary tumour	Classification of tumours
Gatza et al. (215)	Primary tumour	Classification of tumours
Wang et al. (224)	Primary tumour	ClinicoMolecular Triad Classification
Curtis et al. (225)	Primary tumour	METABRIC – clustering 2,000 primary tumours

The prognosis of breast cancer patients is only partially informed on by the primary tumour. Tumour cells are known to interact with surrounding tissue and circulating blood cells to elicit responses that may either promote or suppress tumour growth. The immune system has a large part to play in tumour regulation, suppression and even promotion. The direct and indirect interaction between primary breast tumour cells and the immune system may therefore be crucial in determining prognosis. Additionally, even when successful suppression of primary tumour is achieved, few therapeutic options are effective on distant breast metastases (20).

Two common sites of metastasis from breast cancer are lung and bone (226). Bone metastasis is a process by which circulating tumour cells invade the bone marrow cavity and ultimately destroy the normal bone architecture (198). Bone metastases are osteolytic or oestoblastic in nature, however the majority of breast cancer bone metastases are osteolytic, which involves stimulation of osteoclasts that destroy normal bone tissue (200). Many factors influence this specific metastatic pathway including the stimulation of osteoclasts by production of tumour peptide PTH-rP, resulting in bone destruction. This process is a hallmark of advanced breast cancer with devastating consequences for the patient (201), including severe bone pain, increased risk of pathological fractures and can significantly decrease quality of life for the patient (227).

Currently, there is a distinct lack of studies investigating stratification of breast cancer patients based on their peripheral blood status. Furthermore, no studies have yet focused on IFN regulated gene signatures in breast cancer, despite the clear hormonal regulation of IFNε, which may serve as a regulator of immune responses and a possible pathway for tumour suppression.

1.9 Type I IFNs & Cancer- Perspective on Ovarian Cancer

Ovarian cancer is a complex, heterogeneous disease comprising a number of molecularly distinct tumours that arise not only from ovarian cells but from cells of the fallopian tubes or surrounding tissue as well (228). Projections of tumour incidence from 1982-2006 estimated that 1,434 new cases of ovarian cancer would be diagnosed in Australia in 2015 (229). Many of these women will already have advanced stage disease at first presentation and of those who respond to treatment, more than half will relapse and die within 5 years (229).

The vast majority of ovarian cancers are of epithelial origin (EOC), together having the fourth highest female cancer fatality rate (228). EOC is classified based on histological subtype including mucinous, clear cell, endometrioid and serous carcinomas, each of which are associated with a distinct morphology, mutational profile, cell of origin & prognosis. Serous carcinomas are the most commonly diagnosed EOC and there is increasing evidence to suggest this EOC is derived from the secretory epithelial lining of the distal fallopian tube (230-233). The standard therapeutic options, surgical resection and platinum-based chemotherapy, are often ineffective as many women with advanced disease are not surgical candidates and chemoresistence leads to increasing rates of recurrence (228).

1.9.1 Mouse Models of Ovarian Cancer

To date, a number of mouse models have been used to study epithelial ovarian cancer (234-238). Patient-derived xenograft (PDX) models, that use single-cell suspensions injected subcutaneously or IP, have demonstrated successful EOC formation, ascites and metastasis (239), however this model is dependent on an immunocompromised host and thus, is inappropriate for investigation into the role of IFN signaling in immuno-regulation of EOC. Connolly et al. developed a transgenic model of EOC, however tumour

formation was only seen in half of the mice and may not accurately model human disease (237). A syngeneic, orthotopic mouse model of EOC has been successfully used to establish EOC formation as well as metastatic IP lesions and extensive ascites (236, 238). This model not only allows for the study of tumour formation in an immunocompetent host environment, but also utilizes intrabursal injections of murine ID8 ovarian epithelial cancer cells (MOSEC) that directly interact with ovarian stroma during tumourigenesis, therefore more closely mimicking human disease than previously used intraperitoneal injections.

1.9.2 Molecular Profiling

Extensive molecular profiling of ovarian cancers has shown that mutations in BRCA1/2 genes confer significantly increased risk of high-grade serous carcinoma (HGSC), the most common and lethal EOC (240). BRCA1 & BRCA2 are both documented IFN regulated genes (25) and play important roles in the homologous recombination repair pathway of DNA (241), somatic and germline mutations of which contribute to overall chromosomal instability. Molecular profiling has also identified that HGSC with higher expression of immune-associated genes such as CD8A, Granzyme B and CXCL9, designated the immunologic subtype, demonstrate the best overall survival (242), highlighting the potential benefit of immune-driven suppression in this cancer, evident at a transcriptional level.

Further molecular based analysis has revealed similarities in the mutational profile of basal-like breast cancers and serous ovarian cancers with high frequency of TP53, BRCA1 & BRCA2 mutations, down-regulation of RB1 and the amplification of cyclin E1 is common to both (243). Additionally, while the role of hormones in ovarian cancer tumourigenesis remains unclear, there is evidence of poor prognosis in PR negative patients irrespective of ER expression (244), which bears similarities to reports of poor prognosis in breast cancer patients with either triple negative breast cancer (TNBC) or oestrogen receptor positive/progesterone

receptor negative (ER+/PR-) cancers (245).

1.9.3 Type I IFNs & Ovarian Cancer

Clinical trials using type I IFNs, specifically IFNα and IFNβ, in ovarian cancer have been underwhelming, largely due to the dose-limiting toxicity preventing high-dose therapy in late stage disease (246-254). Some success has been reported using intraperitoneal IFNα in the treatment of malignancy ascites from ovarian cancer (255, 256) (listed in Table 1.2) and while the mechanisms underlying IFN's efficacy against ascites remain unclear, they likely involve both intrinsic (acting directly on tumour cells) and extrinsic (acting indirectly via activation of anti-tumour immune cells) IFN pathways of tumour suppression. What we learned from our breast cancer work (published by Bidwell et al.,) was that in general terms it is important to understand the role of IFNs in disease pathogenesis in order to best direct therapy (i.e. in that case metastases therapy administered in an adjuvant setting is efficacious). Furthermore, examining immunomodulation at different stages of therapy in addition to direct effects on tumour cells may hold the key to IFN efficacy.

1.10 Loss of Constitutive Type I IFN Signalling

There is evidence that components of constitutive type I IFN signaling are detectable in the local tissue of origin of both breast and ovarian cancers, however the significance of continuous IFN activity in the pathogenesis of these diseases and additionally, the metastasis of these tumours, remains to be characterized. Therefore, we have an opportunity to study firstly the *consequences* of the loss of constitutive type I IFN in these tissues, develop a method of *measurement* of constitutive IFN activity, and implement a course *action* for cancer patients in an effort to suppress fatal metastasis.

1.11 Rationale for the Research

The direct & indirect anti-tumour effects of type I interferons (IFN), along with convincing evidence of dysregulated IFN signalling in cancer - for instance, the presence of constitutive IFN signalling in tumourigenesis & its loss in metastases, make these cytokines attractive candidates for a role in suppressing tumourigenesis and agents for cancer therapy. Limited only by our understanding of the role of finely-tuned IFN signalling & function in cancer, further investigation into these processes may hold the key to developing better therapeutics for these devastating diseases.

The IFNs are a family of innate immune cytokines so named for their ability to 'interfere' with viral replication (257). It is now known that type I IFNs induce pleiotropic activities within cells, in fact, they are potent regulators of many distinct biological processes not limited to anti-viral immunity. Importantly, endogenous IFNs exhibit anti-tumour functions both intrinsically, through regulation of anti-proliferative (258, 259), pro-apoptotic (260, 261) pathways and potentially modifying the immunogenicity of tumour cells, and extrinsically, by activating anti-tumour immune cells (167), mechanisms which many tumours evolve strategies to evade. Exogenous IFNs have been trialled in the treatment of a number of different malignancies, however the success of IFN treatment has varied widely and in particular, IFNs have exhibited poor efficacy against some solid tumours such as breast cancer and ovarian cancer. Additionally, HDI is limited by severe systemic side effects (125).

New insights into IFN signalling provide a case for a role in development and potential therapy of breast and other malignancies such as ovarian cancers that are highly prevalent among women worldwide and both associated with high fatality rates, thus representing unmet medical needs. Furthermore, it is likely that within these patient populations, at least a proportion could benefit from IFN immunotherapy, however, it is difficult to predict and

monitor this particular subset of patients. To solve this problem, there is a need to better understand the role of IFNs in the development of these tumours. Recent work has identified that an unexpected, critical defect in IFN signalling, specifically the loss of a constitutive IFN signature, promotes breast cancer metastasis to bone (7), a lethal end-stage of disease progression.

Meanwhile, the discovery and characterisation of a novel type I IFN, IFNε, whose constitutive expression in the FRT (171), unusual regulation and likely classical type I IFN anti-tumour properties led to the hypothesis that this novel type I IFN may play a critical role in the pathogenesis of cancer originating in the FRT organ system. Moreover, the potential benefit of IFN immunotherapy in breast and ovarian cancers warrants further investigation, particularly with a targeted focus on treating or suppressing metastases. Constitutive expression of this IFN in the FRT implies a tissue-specific tolerance that may potentially bypass the main obstacle to IFN therapy in cancer, the severe dose-limiting side effects. The ability to devise IFN signatures, based on new understanding of the pathophysiological role of type I IFNs and its mechanism of signalling and gene regulation, may enable the identification of patients who would benefit from IFN based immunotherapy.

1.12 Research Aims

1. In breast cancer - a model where constitutive IFN signaling activates anti-tumour immunity - determine whether type I IFN blood signatures provide further insight into the metastatic processes and/or represent a biomarker for stratifying patients.

2. In ovarian cancer – a model where constitutive IFN regulation of anti-tumour immunity has not yet been established - investigate whether this is the case and specifically, if constitutively expressed IFNε, has a role in the development and/or treatment of epithelial ovarian cancer.

CHAPTER 2:
MATERIALS & METHODS

2.1 Ethics Statements

2.1.1 Human Ethics

The study was approved by the Human Research Ethics Panel at Monash Health in accordance with the ethical guidelines of the 1975 Declaration of Helsinki. Approval provided access to utilise patient samples & data previously collected and stored by the Kathleen Cunningham Foundation Consortium for Research into Familial Breast Cancer (kConFab) tissue bank (262) (NMA Reference No. LNR/16/MonH/194) and the use of patient samples collected and stored by the Ritchie Centre Human Tissue Bank (HREC 01067B/14227L) for this study. Additionally, the Department of Defence Human Ethics Committee (No.15246A) approved the use of patient samples in this study collected and stored by both the Ovarian Cancer Research Foundation (OCRF) and the Australian Ovarian Cancer Study (AOCS). Written informed consent had previously been obtained from all participants to utilise these samples for research purposes in accordance with the ethical and scientific principles set out by the National Health and Research Council of Australia.

2.1.2 Animal Ethics

All animal experimentation presented in this thesis, was approved by the Monash Animal Ethics Committee (Project No. MMCA/2015/61). Subsequently, two minor amendments to these ethics were sought and granted (June 2016 and July 2016). Any data obtained from animals described herein compile with these approvals.

2.2 Human Cohorts & Sample Processing

2.2.1 Kathleen Cunningham Foundation Consortium of Research into Familial Breast Cancer (kConFab)

Human samples collected and stored by kConFab (262) (Project No. 157) including preserved PBMCs and tissue microarray (TMA) samples were obtained for analysis. For breast cancer patient PBMC processing, the chief selection criteria applied was the diagnosis of at least one additional metastatic site prior to blood collection, whilst exclusion criteria included other types of primary cancer present in patients other than breast cancer. Furthermore, family pedigree data from kConFab was used to select at least one of two controls from within the same family which were: i) breast cancer patients who had not been diagnosed with metastasis and/or ii) donors who had not been diagnosed with cancer. From this, a total of 231 PBMC samples were selected, these consisted of samples from patients with metastatic breast cancer (n = 28), patients with non-metastatic breast cancer (n = 36) and unaffected donors (n = 29), collectively representing 35 families. All participants had been previously recruited and consented by trained kConFab research nurses to give 9 - 10mls peripheral blood collected in acid citrate destrose (ACD) tubes. All blood was kept at room temperature until processed and processed within 24 - 48 hours of collection. The kConFab bio-specimen protocol for processing for PBMC isolation and storage is described in Section 2.3.1.

For breast cancer tissue staining and analysis, TMA slides cut from formalin fixed paraffin embedded (FFPE) blocks containing primary tumour biopsies from 231 breast cancer patients were obtained from kConFab. Of these, 20 patients had been diagnosed with metastatic tumours and 211 patients had been diagnosed with primary breast cancer only.

Tissue cores from patients were arranged on TMAs in grids containing 60 – 120 cores each, a single tissue core per patient.

2.2.2 Control Human Fallopian Tube Samples

Human fallopian tube specimens were obtained with approval from the Institutional Human Research Committee to access samples from the Ritchie Centre Human Tissue Bank collected from women undergoing hysterectomy. Samples were collected by a trained research nurse and stored in phosphate-buffered saline (PBS) at 4°C and processed within 24 hrs. To process for histology, excess surrounding tissue was cut away from the fallopian tubes and discarded. Fallopian tube tissue was then fixed for 24 hours in 10% neutral buffered formalin (Orion Laboratories, Australia), then washed in 70% ethanol, and taken to the Monash Histology Facility for processing (paraffin-embedding) and sectioning.

2.2.3 Ovarian Cancer TMAs

TMA slides containing sectioned biopsies from low grade and high grade serious carcinomas were obtained from the Ovarian Cancer Research Foundation (OCRF) in collaboration with the Ovarian Cancer Biomarkers Lab at the Hudson Institute of Medical Research.

2.2.4 In silico Analysis of Datasets Obtained from Australian Ovarian Cancer Study (AOCS) & the Ovarian Cancer Database of the Cancer Science Institute of Singapore (CSIOVDB)

RNAseq data containing 93 human high grade serous carcinoma (HGSC) samples and 7 human fallopian tube epithelium collected and processed by the Australian Ovarian Cancer Study (263) was analysed in collaboration with the Cancer Genomics and Genetics Program, Peter MacCallum Cancer Centre. Additional analysis was then performed on microarray data

consisting of 707 ovarian cancer samples made publically available online by the Ovarian Cancer Database of the Cancer Science Institute of Singapore (CSIOVDB) (264).

2.3 Tissue Culture

2.3.1 PBMC Isolation & Storage

As per the kConFab bio-specimen collection protocol for PBMC isolation and storage, blood was centrifuged 1300-1500 rpm for 10-15 minutes to separate plasma, then transferred into a 50ml falcon tube containing 10mls Roswell Parks Memorial Institute (RPMI) media (Life Technologies, USA) before being layered onto 3mls Ficoll-Paque^{TM} PLUS (GE Healthcare Bio-sciences, USA) and immediately centrifuged at 1600 rpm for 30 minutes without a brake. Separated PBMCs were then collected using a sterile pipette and mixed with 10mls RPMI media and centrifuged at 1600 rpm for 10 minutes. Supernatant was then discarded and PBMCs frozen in sterile solution containing 70% RPMI, 20% (v/v) fetal calf serum (FCS, Life Technologies, USA) and 10% DMSO. PBMCs were frozen and stored at -70°C.

2.3.2 Cell lines & Cell Culture

Ovarian cancer lines ID8 (murine; Roby KF, et al., Carcinogenesis 2000), CAOV3 (human; ATCC, Virginia), and OVCAR4 (human; National Cancer Institute) were used for *in vitro* assays. ID8 & OVCAR4 cell lines were cultured in RPMI 1640 (GibcoBRL, Ontario, Canada) while the CAOV3 were cultured in DMEM (GibcoBRL) supplemented with 4% (ID8) or 10% (CaOV3, OVCAR4) heat-activated fetal calf serum (FCS; GibcoBRL). All cells were incubated at 37°C in an atmosphere of 5% (v/v) carbon dioxide (CO_2). Cells were confirmed Mycoplasma negative according to MycoAlert™ PLUS Mycoplasma Detection Kit (ratio <1; Lonza, Basel).

2.3.3 Cellular Stimulations

Viable cells were counted using trypan blue on a haemacytometer under a bright field microscope (Nikon, Japan). Cell lines were plated ($1.5x10^5$ cells/well) in 12 well plates, 24 hours prior to stimulation with recombinant IFNε or IFNβ (see appendix I for recombinant protein production) at 0 – 1000IU/ml with resuspension buffer (see Appendix I) or vehicle control (PBS). Cells were then incubated at 37°C for 3 hrs prior to harvesting.

2.3.4 Cellular Growth Assays

Cellular proliferation was performed on the xCELLigence platform (ACEA Biosciences, Inc., San Diego, CA, USA) for real-time cell analysis (RTCA). 50 µl of cell culture medium was initially added to each well in a 96 well E- plate (ACEA Biosciences, Inc.) for the impedance background measurement. Cells were then added (ID8 – $6x10^3$ cells/well, CAOV3 & OVCAR4 – $1x10^5$ cells/well) to a volume of 100 µl in serum-free culture media and allowed to adhere overnight. Recombinant IFN or vehicle control was diluted in culture media supplemented with serum and added to the cells up to a final volume of 200µL. The E-Plates were incubated at 37°C with 5% CO_2 and impedance measured on the RTCA system at 15-minute time intervals for up to 72 hours with or without treatment. For data analysis, the baseline cell index (CI) was determined by subtracting the CI for a cell-containing well from the CI of a well with only culture media. To facilitate the statistical evaluation of the results, impedance measurements from each well were normalised to the time of stimulation with IFN, termed 'normalised cell index'. Three independent experiments were performed in technical quadruplicate and analysed for doubling-time & slope (1/hr) of growth curves, indicative of rate of proliferation, using RCTA software (265).

2.3.5 Migration Assays

Migration assays were performed and analysed for a provisional patent on IFNε as an anti-cancer therapeutic. The results are presented in the patent specification (in Thesis Appendices). To perform single cell tracking assays, ID8 cells were plated in serum free media at $2.5x10^4$ cells/well in a 48 well plate and allowed to adhere overnight. Individual cells were then tracked via fluorescence to measure the overall distance travelled by each cell (track length) and direct displacement length from the initial to final position of each cell (track displacement) over 12 hours. The mean distance travelled was then compared in technical triplicate.

To further assess cellular migration, scratch assays were utilized to measure the percentage surface area closure of a scratch (empty space) over 12 hours. ID8 cells were plated in a 48 well plate and allowed to reach confluence and the coated wells were scratched using a P10 filter tip (Axygen Scientific, California). Cells were stained using CellTrace™ CFSE Cell Proliferation Kit (ThermoFischer Scientific, Massachusetts) as per the manufacturer's instructions, then washed in PBS and treated with recombinant IFN. Fluorescent images were captured every 30 minutes for 12 hours using a confocal microscope and analysed using Imaris software.

2.3.6 Apoptosis Assays

ID8 cells were plated in a 12 well plate ($3.5x10^4$ cells/well) in 2mls of media and left to adhere overnight. Cells were stimulated with recombinant murine Ifnε or vehicle control for 48 hours. Hydrogen peroxide (H_2O_2) was used a positive control for induction of apoptosis at a concentration of 1 – 5 mM. Following stimulation, cells were trypsinised and washed in PBS and analysed for the proportions of live cells and apoptotic cells using flow cytometry (see Section 2.7.3).

2.3.7 mRNA Extraction & Purification

Frozen PBMCs were thawed briefly prior to RNA extraction. Total cellular RNA was extracted using Trizol (GIBCO/BRL, Invitrogen) and further purified over Qiagen miRNeasy Mini columns as per manufacturer's instructions (Qiagen Inc, Germany), including an on-column DNase digestion using the QIAGEN RNase-free DNase Set (Qiagen Inc, Germany) according to manufacturer's instructions. RNA samples with an RNA integrity number (RIN) ≥ 7.0 by Bioanalyzer assessment were of an acceptable quality for microarray analysis.

For cell lines, RNA was extracted using a QIAGEN RNeasy mini-kit (Invitrogen, USA) as per the manufacturer's protocol. Cells were harvested in 1% betamercaptoethanol in RLT buffer and homogenized using a 1 mL syringe and a 23-gauge needle. RNA was on-column DNase treated using the QIAGEN RNase-free DNase Set (Qiagen Inc, Germany) according to manufacturer's instructions. RNA yield and quality was then assessed using a NanoDrop® ND-1000 spectrophotometer and stored at -80°C.

2.3.8 cDNA Synthesis

A total of 500 ng of RNA was made up to 7µl with diethylpyrocarbonate (DEPC) treated Milli-Q H_2O. For low yield RNA samples, 500ng of RNA was concentrated to a volume >7µl using a rotational-vacuum-concentrator (Christ, Germany). RNA was then reverse-transcribed into cDNA using M-MLV reverse transcriptase (Promega, USA), according to manufacturer's instructions. cDNA samples were stored at -20°C. A negative reverse transcriptase control was included for each sample.

2.3.9 GAPDH Polymerase Chain Reaction

A GAPDH PCR was performed on cDNA samples and reverse transcriptase negative controls were included to ensure there was no genomic DNA contamination of samples.

1µl of cDNA was added to 5X GoTaq Green buffer,magnesium chloride, forward and reverse GAPDH primers, 10mM dNTPs, GoTaq enzyme (Promega, USA) and a total volume of 25µl was made up with DEPC treated H_2O. All PCR reactions were carried out in a MyCycler™ Thermal Cycler (BIO-RAD) using the following cycle reaction conditions:

- Denaturation: 94°C, 2 minutes — 1 cycle
- Denaturation: 94°C, 30 secs
- Annealing: 55°C, 30 secs — 35 cycles
- Extension: 72°C, 30 secs
- Extension: 72°C, 7 minutes — 1 cycle

Each PCR product was then loaded onto a 1.5% agarose gel and run at 100V for 30 minutes.

2.3.10 Quantitative Real Time PCR (qRT-PCR)

Primers were designed to be intron-spanning where possible. Primers were designed using Primer Express® v3.0 software (Applied Biosystems, USA). Each reaction was performed in a total of 10µl comprising 2µl of cDNA, 5µl Sybr Green PCR Master Mix (Applied Biosystems, USA), 0.2µl of each 10mM stocks of relevant forward and reverse primers and DEPC H_2O. Samples were loaded in triplicate onto a MicroAmp™ Optical 384-well reaction plate and sealed with MicroAmp™ Optical adhesive film. Additionally, two RT negative reactions and a no transcript control were included on each plate. Amplification of a single PCR product was confirmed by analysing dissociations curves and visualisation on agarose gels. For a list of primers sequences see appendix II.

All reactions were processed using a 7900HT Fast Real Time PCR machine (Applied Biosystems, USA) using the following thermal cycling protocol: 50°C for 2 minutes, 95°C for

10 minutes followed by 40 cycles of 95°C for 15 seconds and 60°C for 1 minute. Cycle threshold (Ct) values for all probes were exported and data analysis was carried out using the 2−ΔΔCT method (266). For figures, gene amplifications were normalized to the expression of 18S, an internal control gene stably expressed in cells. Then values of fold-change were expressed relative to value for untreated samples (which was 1).

2.4 Microarray Procedure

The processing of samples, RNA extraction and performance of microarray analysis were performed according to MIAME**-compliant protocols as described in M&M section and in the attached report (in Thesis Appendices). These data are routinely formatted ready for uploading into 'Array Express' at the time of publication.

** MIAME = Minimum Information Essential for Microarray Experiments

2.4.1 Agilent One-Colour Spike

Microarray was performed at the Monash Health Translational Precinct, Medical Genomics Facility. Agilent One-Colour Spike-In kit was used to provide positive controls for monitoring microarray processing. Briefly, 100 ng of mRNA was diluted in a total volume of 1.5µl with RNase-free H_2O. The Agilent One-Colour Spike mix was prepared by heating to 37°C for 5 minutes. Three-fold serial dilutions of the Spike mix (Agilent Technologies, USA) were prepared and 2µl was added to each 1.5µl mRNA sample along with 1.8µl T7 promoter primer to a final volume of 5.3µl. The samples were denatured by incubating at 65°C for 10 minutes followed by ice for 5 minutes and a pulse/spin.

2.4.2 cDNA synthesis

cDNA master mix was made up with 2µl 5X first strand buffer, 1µl 0.1M DTT, 0.5µl 10mM dNTP mix and 1.2µl AffinityScript RNase Block Mix (Agilent Technologies, USA). 4.7µl cDNA mix was added to each RNA sample making a total volume of 10µl. Each sample was mixed by pipetting and incubated in a 40°C water bath for 2 hours. To heat inactivate, each sample was heated at 70°C for 15 minutes followed by ice for 5 minutes and a pulse/spin. Samples were stored at -20°C until the next step.

2.4.3 Labeling & Transcription

Transcription mix was made up with 0.75 µl nuclease free water, 3.2 µl 5X Transcription buffer, 0.6 µl 0.1M DTT, 1 µl NTP mix, 0.21 µl T7 RNA polymerase blend and 0.24 µl Cy3-CTP. A total of 6 µl of transcription mix was then added to each RNA sample making a total of 16µl. Each sample was mixed by pipetting and incubated in a 40°C water bath for 2 hours.

2.4.4 cRNA Purification & Quantification

A QIAGEN RNeasy mini kit (QIAGEN, USA) was used to purify Cy3 labelled cRNA as per the manufacturer's instructions. 1 µl of cRNA was read by Nanodrop using the RNA-40.Cy3 microarray measurement. Requirements were yield >0.825 µg and specific activity >6.0 pmol/µg.

Yield (µg cRNA) = ng/µl cRNA x 30µl (elution volume) /1000

Specific activity = [(pmol/ng Cy3) / (ng/µl cRNA)] x 1000

2.4.5 Chip Hybridisation

8 x 60K microarrays were performed through hybridizing via the Agilent Gene Expression Hybridization Kit (Agilent Technologies, USA). Fragmentation mix made up with 600 ng of

Cy3 labelled cRNA was added to 5 µl 10X Blocking agent and 1 µl 25X Fragmentation buffer. Fragmentation mix was then made up to a total volume of 25µl with water. The samples were incubated at 60°C for 30 minutes and then immediately iced for 1 min. Each reaction was stopped by adding 25µl 2X GE Hybridisation buffer. The samples were then centrifuged at 13,000rpm for 1 minute. 40µl of sample was placed on ice and then used immediately for hybridisation onto the microarray slide. Samples were hybridized at 67°C for 17 hours at 20 rpm.

2.4.6 Microarray Slide Wash & Scan

Disassembly of the slides and an initial wash was performed at room temperature in GE wash buffer 1 (GE Healthcare, USA) with washes performed for 1 minute. A second wash was performed in pre-warmed GE wash buffer 2 (GE Healthcare, USA) for 1 minute. The microarray slide was removed slowly from the second wash and scanned immediately. The slide was loaded into a Version B slide holder (Agilent Technologies, USA) and scanned in a G2505B Series Microarray scanner (Agilent Technologies, USA) using the one-colour scan setting for 8x60K microarray slides (61x21.6 scan region, 3µm scan resolution, 20 bit Tiff, dye channel was set to green and green PMT selected at 100%). The scanned microarray slides were analysed by the Feature Extraction Software 9.5.3.1 (Agilent Technologies, USA) and log intensity values for each spot were calculated.

2.5 Microarray Analysis

Microarray analysis was performed by Dr Linden J Gearing (CIIID Bioinformatics group) using R (v3.4.3). The data and accompanying sample annotation was imported and processed using the limma package (v3.32.10) (267). Probe annotation was obtained from GEO using the GEOquery package (v2.42.0), with the GEO

platform identifier GPL21185. For data normalisation, 'normexp' background correction and quantile normalisation were performed. Probes were filtered out using the microarray negative control probes. For each sample, the 95% percentile of expression for the negative controls was calculated. Any probes with expression values at least 10% greater than this were taken as expressed in that sample. Probes were kept only if they were expressed in greater than or equal to 28 samples (the number of samples in the smallest group). Finally, any remaining duplicate probes (with the same ID and therefore the same sequence) were then averaged using 'avereps'. These steps reduced the number of probes from 62,976 to 32,801.

Array weights were calculated using an intercept design matrix (268) and were incorporated into the linear model. Samples were grouped according to tumour type, Unaffected, Primary (non-metastatic breast cancer) or Metastasis (metastatic breast cancer), using family as a blocking factor. This was to adjust tumour type for differences between families. Moderated *t*-statistics were calculated using the 'eBayes' method (269). The Benjamini-Hochberg adjustment method and 'global' multiple-testing method were used to adjust *P*-values for probes and across contrasts between the different tumour types. Differentially expressed probes were selected with an adjusted *P*-value < 0.05.

For gene set enrichment, Entrez gene IDs were used as identifiers and competitive gene set testing was performed using 'camera' (270) from the limma package using a set of transcriptional modules (271, 272). The ssGSEA method was used to assign a score to each sample (273), based on its expression of the module gene sets, using the GSVA package (274). For analysis of IRG expression, the INTERFEROME database (114) was searched for genes up-regulated in human blood cells more than twofold. The resulting genes were matched with microarray probes by Entrez gene ID.

2.6 Tissue Staining

2.6.1 Immunohistochemistry

Human fallopian tubes, mouse organs and tumour samples were fixed for 24 hours in 10% neutral buffered formalin (Orion Laboratories, Australia), then washed in 70% ethanol, and taken to the Monash Histology Facility for processing and sectioning. Samples were embedded in paraffin and sectioned at 4-μm thickness using a microtome. Sections were stained for Haematoxylin and Eosin by the Monash Histology Facility with subsequent sequential sectioning. To investigate tissue expression of proteins of interest histological sections were deparaffinised and rehydrated. Antigen retrieval was performed by heat in 10 mM Tris/1 mM EDTA (pH 9.0) for 6 minutes. After inhibition of endogenous peroxidase activity with 3% (vol/vol) hydrogen peroxide, tissues were blocked in CAS-Block™ (ThermoFisher Scientific) for 1 hour. Tissues were then incubated overnight at 4°C with relevant antibodies: anti-IFNε (1:210; Novus Biologicals, Colorado), anti-SMa (1:100; Dako Omnis, Santa Clara), anti-Ck18 (1:50; Dako Omnis) and rabbit IgG (1:200; Vector Laboratories, California) or mouse IgG1 (1:37; Vector Laboratories) as isotype controls. Biotinylated anti-rabbit or anti-mouse IgGs (both 1:250 dilution; Vector Laboratories) were diluted in the same buffer and incubated for 1 hour. Slides were then washed in 0.05% Tween/PBS and incubated with avidin and biotinylated horseradish peroxidase (VECTASTAIN® Elite® ABC Kit, Vector Laboratories) as per the manufacturer's instructions. Slides were washed with 0.05% Tween/PBS then incubated with diaminobenzidine tetrahydrochloride (DAB; DAB+ Substrate Chromogen System, Dako Omnis) as per the manufacturer's instructions. Sections were counterstained with Haematoxylin for 45 seconds then dehydrated and placed under coverslip with dibutylphthalate dolystyrene xylene (DPX; Merck, Germany). Staining intensity was

calculated using the positive pixel analysis tool in Imagescope software or the Aperio Cell Imaging Software.

2.6.2 Multiplexed Immunohistochemistry

Multiplexed staining using the Opal protocol was performed by Natasha K. Brockwell at the Cancer Microenvironment and Immunology Lab, La Trobe University. Firstly, tissue microarrays (TMAs) generated by kConFab were de-paraffinized in histolene and rehydrated in ethanol. Antigen retrieval was performed as per antibody specifications in either pH 6.0 or pH 9.0 (Perkin Elmer) using heated microwave treatment (MWT). Antibodies, blocking buffers, secondary antibodies, opal fluorophores and diluents used were from the Opal 7 Tumor Infiltrating Lymphocyte (TIL) kits (Perkin Elmer) except CD20 was swapped for CD41 and staining was performed as per manufacturers protocol. Following pH 9.0 heated MWT, slides were blocked for 10 minutes and then incubated with anti-CD8 (1:200) for 1hr in a humidified chamber at room temperature (RT). Slides were washed with TBST (tris buffered saline + 0.05% tween (v/v)) before addition of secondary antibody for 10 minutes followed by further washing and incubation with Opal-570 TSA (1:50) diluted in amplification diluent for 10 minutes. Slides were then subjected to heated MWT with pH 6.0 buffer and staining was performed as per above with anti-FoxP3 (1:100) and Opal-620. Slides were subjected to heated MWT (15 minutes at 20% power) with pH 6.0 buffers and staining performed as above except primary antibody, anti-CD41(1:250) was left on overnight at 4 degrees in a humidified chamber, staining resumed as per normal the following day with Opal-540 being used. Slides were subjected to heated MWT pH 6.0 and staining was performed as above with anti-CD45RO (1:150) and Opal 650. Slides were subjected to heated MWT with pH 6.0 and staining performed as per above except primary antibody, anti-pan-CK (1:500) was left on overnight at 4 degrees in a humidified chamber, staining resumed as per normal the following day with Opal-690. Slides were subjected to

heated MWT pH 9.0 and staining was performed as per above with anti-CD4 (1:150) and Opal 520. Slides were then subjected to heated MWT pH 6.0 and stained with DAPI solution for 3 minutes. Slides were then ounted using VECTASHIELD HardSet Antifade mounting medium (Vectorlabs). Slides were then imaged using the VECTRA microscope (PerkinElmer) where whole slide scans were performed and regions of interest captured at 200x magnification.

2.6.3 Multispectral Analysis

InForm image analysis software (Perkin Elmer) was used to spectrally unmix and analyse images. Briefly, InForm was trained to segment tissue regions within each individual TMA core between tumor epithelium and surrounding stroma compartments, using DAPI and nuclei size (275). The core was further segmented into individual cells using DAPI staining. Cell scoring was based on expression of said marker and scoring was given as percentage positivity per tissue section, with cells being classed as either single or double positive. H scores were also generated for cytokeratin and CD41 positive tumour cells.

2.7 Flow Cytometry

2.7.1 Immunophenotyping

Peritoneal exudate cells were isolated from C57BL6/J mice by flushing the peritoneal cavity with 5 ml ice cold PBS. Cell pellets were obtained by centrifugation at 1,000 rpm for 5 mins and stained for surface antigen expression using a panel of monoclonal antibodies directly conjugated with fluorochromes. In order to prevent non-specific binding, cell surface receptors were blocked with Anti-mouse CD16/CD32 Fcγ III/II Receptor blocking antibody (BD PharMingen, California). Surface cell staining was performed with the various combinations of fluorochrome-labelled antibodies: panel 1 – APC conjugated CD45, APC-Cy7 conjugated

CD8, FITC conjugated NK-1.1, PE conjugated CD69, Pacific Blue conjugated CD4; panel 2 – APC conjugated CD25, APC-Cy7 conjugated CD8, FITC conjugated CD45, PE conjugated Pan CK, PE-Cy7 conjugated CD4 and Pacific Blue conjugated FoxP3; panel 3 – APC conjugated CD45, APC-Cy7 conjugated CD11b, FITC conjugated Ly6C, PE conjugated I-Ab, PE-Cy7 conjugated CD11c and Pacific Blue Ly6G. Cells were analysed using a FACSCanto™ II flow cytometer (BD Biosciences) and Flo-Jo software.

2.7.2 Cytometric bead array (CBA)

Cytometric bead array (BD CBA Mouse Inflammation Kit; BD Pharmingen) was used to determine cytokine levels in the supernatant of peritoneal exudate cells from mice injected with ID8 cells as per the manufacturer's instructions. FACSCanto™ II flow cytometer (BD Biosciences) and Flo-Jo software were used to examine levels of MCP-1, IFNγ, IL-6, IL-10, IL-12p70, or TNF-α.

2.7.3 Annexin V/PI

Following cell stimulation and trypsinisation, single cell suspensions were stained with FITC conjugated Annexin V and propidium iodide (PI). Cells were stained using the FITC Annexin V Apoptosis Detection kit II (BD Biosciences, New Jersey), as per the manufacturer's instructions and analysed by flow cytometry using a FACSCanto™ II flow cytometer (BD Biosciences) and Flo-Jo software. The different phases of apoptosis were defined as i) live cells (Annexin V-/PI-), ii) early apoptotic (Annexin V+/PI-), iii) late apoptotic (AnnexinV+/PI+), and iv) necrotic cells (Annexin V-/PI+) (Andree HA, et al., J Biol Chem 1990).

2.8 In Vivo Models

2.8.1 Mice

IFNε$^{-/-}$ (171) and Ifnar1$^{-/-}$ (276) on a C57BL6/J background and wild-type mice (Monash Animal Research Facility) were housed in standard specific pathogen free (SPF) conditions.

2.8.2 Intrabursal (orthotopic) Ovarian Cancer Model

Female (10 weeks of age) C57BL6/J wild-type (Ifnε +/+) and Ifnε deficient mice (Ifnε $^{-/-}$) were anaesthetized by inhalation of isoflurane (5% in oxygen) in an induction chamber, and anesthesia maintained at 2.5-3.0% isoflurane delivered via nosecone during all procedures. Mice were subcutaneously injected with the analgesic Carprofen (5mg/kg) prior to surgery. A small incision was made at the dorso-medial position directly above the ovarian fat pad, with a secondary small incision through the peritoneal wall. The ovarian fat pad was externalised and stabilized with a bull clip, and a dissecting microscope was used to locate the oviduct in the exposed ovary. ID8 cells ($1x10^6$) were injected underneath the left ovarian bursa. The peritoneal wall was sutured closed using 6/0 suture prior to topical Bupivacaine administration and closure of the incision closed with surgical staples. Analgesia (Carprofen 5mg/kg body weight) was provided in drinking water for 3 days thereafter. Mice were monitored for body weight, Body Condition Score (BCS) and culled within 13 weeks post-ID8 injection.

2.8.3 Intraperitoneal (disseminated) Ovarian Cancer Model

Female (6 to 8 weeks of age) C57BL6/J wild-type (Ifnε +/+) mice were injected intraperitoneal with $5x10^6$ ID8 cells. Mice were monitored for body weight, body condition score (BCS) and clinical signs and culled 8 weeks post-ID8 injection. At autopsy, the overall spread and tumour burden of each mouse was documented (number of tumour nodules, sites of nodule deposits

recorded and photographed), ascites fluid was drained from the peritoneum for volume measurement and cell counts and tissue harvested (spleen, diaphragm, peritoneal wall, mesenteric fat, female reproductive tract) for weight measurements and immunohistochemical analysis.

2.8.4 Intraperitoneal Recombinant IFN Administration

IFN treatments were commenced 3 days post-intraperitoneal ID8 cell injections. Mice either received recombinant murine Ifnε injected intraperitoneally 3 times a week at a dose of 500IU/injection or Ifnβ at 500IU/injection or vehicle for 8 weeks. At autopsy, the orthotopic 'primary" tumour was collected along with metastases (diaphragmatic & peritoneal), spleen, ascites fluid (volume and cell counts) and peritoneal lavage and samples weighed, photographed and processed for immunohistochemical analysis.

2.9 Statistical Analysis

Data were graphed in GraphPad Prism 7. Significance for parametric data were determined using Student's Unpaired T Test or one-way ANOVA and non-paramteric data were determined using Mann-Whitney *t* test. Differences were considered significant if the P value was < 0.05 and significance is indicated as *$p<0.05$, **$p<0.01$, ***$p<0.001$, ****$p<0.0001$. Specific details of statistical data are indicated for each figure.

CHAPTER 3:

Analysis of Systemic and Local Responses Reveals Novel IFN and Immune Signatures in Breast Cancer

3.1 Declaration

Monash University

Declaration for Thesis Chapter 3

Declaration by candidate

In the case of Chapter 3, the nature and extent of my contribution to the work was the following:

Nature of contribution	**Extent of contribution (%)**
Acquisition of data, analysis and interpretation and writing, reviewing and editing the manuscript	70 %

The following co-authors contributed to the work. If co-authors are students at Monash University, the extent of their contribution in percentage terms must be stated:

Name	**Nature of Contribution**	Extent of contribution (%) Authors Only
Linden J. Gearing	See statement below	
Natasha K. Brockwell		
Jodee A. Gould		
kConFab		
Nollaig M. Bourke		
Belinda S. Parker		
Paul J. Hertzog		

AUTHOR CONTRIBUTIONS

Conception and Design: Z.C.M, L.J.G, N.M.B., B.S.P and P.J.H

Development of Methodology: Z.C.M, L.J.G., N.K.B., B.S.P and P.J.H.

Acquisition of Data: Z.C.M, L.J.G., N.K.B., J.A.G., kCONfab and P.J.H.

Analysis and Interpretation of Data: Z.C.M, L.J.G. and P.J.H.

Writing, Review and/or Editing of the Manuscript: Z.C.M, L.J.G, N.K.B., N.M.B and P.J.H.

Study Supervision: N.M.B, B.S.P and P.J.H.

The undersigned hereby certify that the above declaration correctly reflects the nature and extent of the candidate's and co-authors' contributions to this work.

Candidate's Signature	[redacted]	**Date 24/01/2018**
Main Supervisor's Signature	[redacted]	**Date 24/01/2018**

3.2 Analysis of Systemic and Local Responses Reveal Novel IFN and Immune Signatures in Breast Cancer Metastasis

Zoë C. Marks, Linden J. Gearing, Natasha K. Brockwell, Jodee A. Gould, The Kathleen Cunningham Foundation Consortium for research into Familial Breast Cancer, Nollaig M. Bourke, Belinda S. Parker and Paul J. Hertzog, *Prepared Manuscript*

Analysis of systemic and local responses reveals novel IFN and immune signatures in breast cancer metastasis

Zoe C. Marks[1,2], Linden J. Gearing[1], Natasha K. Brockwell[3], Jodee A. Gould[1], The Kathleen Cunningham Foundation Consortium for research into Familial Breast Cancer[4], Nollaig M. Bourke[5], Belinda S. Parker[3], Paul J. Hertzog[1]

[1] Centre for Innate Immunity and Infectious Diseases; Hudson Institute of Medical Research; Clayton, Victoria, 3168; Australia.

[2] Department of Molecular and Translational Science; Monash University; Clayton, Victoria, 3168; Australia.

[3] Department of Biochemistry and Genetics, La Trobe Institute for Molecular Science, La Trobe University; Bundoora, Victoria, 3083; Australia.

[4]Peter MacCallum Cancer Centre; Melbourne, Victoria, 3000; Australia.

[5] Department of Medical Gerontology, School of Medicine, Trinity Translational Medicine Institute; Trinity College Dublin; The University of Dublin, College Green, Dublin 2; Ireland

* Correspondence: [redacted]

Acknowledgements:

We wish to thank Heather Thorne, Eveline Niedermayr, all the kConFab research nurses and staff, the heads and staff of the Family Cancer Clinics, and the Clinical Follow Up Study (which has received funding from the NHMRC, the National Breast Cancer Foundation, Cancer Australia, and the National Institute of Health (USA)) for their contributions to this resource, and the many families who contribute to kConFab. kConFab is supported by a grant from the National Breast Cancer Foundation, and previously by the National Health and Medical Research Council (NHMRC), the Queensland Cancer Fund, the Cancer Councils of New South Wales, Victoria, Tasmania and South Australia, and the Cancer Foundation of Western Australia

ACKNOWLEDGEMENTS

This work was supported by project grants from the National Health and Medical research Council of Australia (NHMRC) to PJH,. ZCM is supported by an Australian Postgraduate Award; PJH is supported by NHMRC Senior Principal Research fellowship.

In conducting research using animals, the investigators adhered to the laws of Australia and received ethical approval for this research from the Monash University Animal Ethics Committee A.

In conducting research using human tissues, the investigators adhered to the laws of Australia and receive ethical approval for this research from the Monash Health Human Research Ethics Committee (ratified by the Monash University Human Research Ethics Committee).

The authors would like to acknowledge Rebecca Smith for assistance with preparation of the manuscript.

This work is supported from the Operational Infrastructure Fund of the State Government of Victoria.

AUTHOR CONTRIBUTIONS

ZRM was involved in conceptualisation, methodology, formal analysis, investigation aspects of the project and in writing the original draft, review and editing the manuscript

LJG - formal analysis, data synthesis, graphic design, contribution to original manuscript, review

NKB - investigation, formal analysis, contribtuion to original manuscript

JAG - investigation, formal analysis, contribtuion to original manuscript, review

kConFab - conceptualisation, sample and data provision

NMB – conceptualisation, methodology, formal analysis, investigation, contribution to original draft, review and editing manuscript, supervision and acquisition of funding

BSP - conceptualisation, methodology, formal analysis, resources, contribution to original draft, review and editing manuscript, supervision and acquisition of funding

PJH– conceptualisation, methodology, formal analysis, resources, contribution to original draft, review and editing manuscript, supervision and acquisition of funding

*All authors had input into review or editing the manuscript.

DECLARATION OF INTERESTS

The authors declare no competing interests.

ABSTRACT

The processes that govern breast cancer metastasis remain poorly understood and is the overwhelming cause of death in breast cancer patients. Previous evidence published by our lab revealed a constitutive type I IFN signature, driven by IRF7, which was present in mammary epithelium and primary breast tumours, but lost in bone metastases. Restoring this IFN pathway regulated peripheral anti-tumour immunity and suppressed metastases, however it remained unclear at what point on the metastatic pathway this signalling could be detected and whether this signature may indicate metastatic potential or immune processes occurring in the primary or metastatic sites. In this study, we investigated local, systemic and distant signatures during breast cancer metastasis by analysing blood transcriptomics from matched familial breast cancer patients and multiplex staining of primary and secondary tumour microarrays. We demonstrate the benefit of using familial controls for transcriptomic analysis and identify distinct 'metastasis-associated' blood signatures enriched in platelet activity, T cell suppression and a broad contribution of IFN signalling. We also demonstrate distinct cell signatures in primary and secondary breast tumour tissue, which reflect transcriptional changes seen in the blood. These findings contribute to a greater insight into the processes underlying breast cancer metastasis from local through to distant sites, and support future development of the use of blood transcriptomics to classify breast cancer patient prognosis.

INTRODUCTION

Considerable advances in screening, diagnosis, classification and treatment of primary breast cancers have improved patient outcomes, however breast cancer metastases remain both difficult to predict and treat, and therefore constitute the overwhelming cause of death for patients (1). Thus, there is an urgent need to better understand the processes underlying breast cancer metastasis down to the molecular events occurring not only at the primary tumour site, but also in the systemic vasculature and secondary organs.

Genomic analyses including transcriptomics continue to reveal key pathways in breast cancer pathogenesis and progression (2-6). In fact, we previously showed that in comparison to primary breast tumours, bone metastases express a distinct transcriptome. Further characterisation of this bone metastasis signature revealed a key regulatory pathway involved in breast cancer pathogenesis, specifically metastases, an improved understanding of which may provide insight into potential biomarkers and novel therapy (7). Our experiments revealed interferon regulatory factor 7 (IRF7), a transcription factor known to be a major regulator of type I IFN signalling (8, 9), was unexpectedly highly expressed in primary breast tumours, where it regulated the expression of numerous immunoregulatory genes including the type I IFNs. Moreover, IRF7 expression and a cluster of genes predicted to be regulated by IRF7 were substantially decreased in bone metastases. Through a series of investigations, it was shown that primary tumour cells produced IRF7-driven type I IFNs, which acted on immune cells to prevent metastasis, most specifically to bone. Conversely, loss of this pathway was essential for metastases. Furthermore, expression of the IRF7/IFN pathway in primary tumour samples was found to correlate with patient prognosis, demonstrating that while it showed no impact on the primary breast tumour, the anti-metastatic effects of this pathway have a significant clinical benefit (7).

In order to better understand the mechanisms underlying this pathway and identify potential clinical biomarkers, it is important to establish whether this IFN production detectable locally in primary tumours, is reflected systemically. How the IFN pathway impacts the cells in peripheral blood, the cells known to be key in regulating metastasis (10), is unknown. These findings prompted the following questions: i) does IFN produced by primary tumour cells induce an 'IFN signature' in peripheral blood cells, and ii) could other signatures be identified in peripheral blood, which may or may not be related to IRF7 or IFN, that would modify or reflect the metastatic potential of primary tumour cells and thus, patient prognosis?

Blood transcriptomic analysis has proved a useful tool in characterising disease severity and prognosis in a range of diseases including breast cancer (11-14), however to date, there has been no targeted investigation of the role of this IFN pathway in metastatic blood signatures. We herein aim to further our understanding of these processes by characterising peripheral blood transcriptomes in breast cancer patients with or without metastases, and correlate with immune and cellular infiltrate in primary and metastatic breast tumours to examine each stage and location during the process of metastasis.

METHODS

Patient Cohort- The study was approved by the Human Research Ethics Panel at Monash Health in accordance with the ethical guidelines of the 1975 Declaration of Helsinki. This authorised the use of patient samples & data previously collected and stored by the Kathleen Cunningham Foundation Consortium for research into Familial Breast Cancer (kConFab) tissue bank (15) (NMA Reference No. LNR/16/MonH/194, kConFab Project No. 157) including preserved peripheral blood mononuclear cells (PBMCs) and tissue microarray (TMA) samples. Written informed consent had previously been obtained from each participant

for research purposes in accordance with the ethical and scientific principles set out by the National Health and Research Council of Australia.

From the available kConFab patient cohort (15), a subset of cases was selected for this study. The chief selection criteria were breast cancer patients who had a known diagnosis of at least one site of metastasis prior to blood collection. Exclusion criteria included other types of primary cancer other than breast cancer. Additionally, family pedigree data from kConFab was used to select at least one of two controls from within the same family, i) breast cancer patients who had not been diagnosed with metastasis and/or ii) donors who had not been diagnosed with cancer. From this, a total of 231 PBMC samples were selected, these consisted of samples from patients with metastatic breast cancer (n = 28), patients with non-metastatic breast cancer (n = 36) and unaffected donors (n = 29), collectively representing 35 families. All participants had been previously recruited and consented by trained kConFab research nurses to give 9 - 10 ml peripheral blood collected in Acid Citrate Dextrose (ACD) tubes. All blood was kept at room temperature until processed within 24-48 hours of collection. As per the kConFab bio-specimen collection protocol for PBMC isolation and storage, blood was centrifuged 1300-1500 rpm for 10-15 mins to separate plasma, then transferred into a 50ml falcon tube containing 10 ml Roswell Parks Memorial Institute (RPMI) media (Life Technologies, USA) before being layered onto 3 ml Ficoll-Paque^{TM} PLUS (GE Healthcare Bio-sciences, USA) and immediately centrifuged at 1600 rpm for 30 mins without a brake. Separated PBMCs were then collected using a sterile pipette and mixed with 10 ml RPMI media and centrifuged at 1600 rpm for 10 mins. Supernatant was then discarded and PBMCs frozen in sterile solution containing 70% RPMI, 20% (v/v) fetal calf serum (FCS, Life Technologies, USA) and 10% DMSO. PBMCs were frozen and stored at -70°C.

For breast cancer tissue staining and analysis, TMA slides constructed from formalin fixed paraffin embedded (FFPE) blocks containing primary tumour biopsies from 231 breast

cancer patients were obtained from kConFab. Of these, 20 patients had been diagnosed with metastatic tumours and 211 patients had been diagnosed with primary breast cancer only. Tissue cores from patients were arranged on TMAs in grids containing 60 – 120 cores each, a single tissue core per patient.

RNA Extraction & Chip Hybridisation- The processing of samples, RNA extraction and performance of microarray analysis were performed according to MIAME**-compliant protocols as described in M&M section and in the attached report (in thesis Appendices). These data are routinely formatted ready for uploading into 'Array Express' at the time of publication.

** MIAME = Minimum Information Essential for Microarray Experiments

Frozen PBMCs were thawed briefly prior to RNA extraction. Total cellular RNA was extracted using Trizol (GIBCO/BRL, Invitrogen) and further purified over Qiagen miRNeasy Mini columns (Qiagen Inc.). Bioanalyzer assessment (Agilent Technologies) was used to measure RNA quality and samples with an RNA integrity number (RIN) $\geq$ 6.0 were of an acceptable quality for microarray (Schroeder et al. 2006). Purified Cy3-labelled cRNA was generated and hybridized onto Agilent arrays, Agilent-072363 SurePrint G3 Human GE v3 8x60K microarrays (Agilent Technologies) at 67°C for 17 hours at 20 rpm.

Microarray slide wash & scan- Disassembly of the slides was performed at room temperature in GE wash buffer 1. The microarray slide was then washed at room temperature in GE wash buffer 1 for 1 minute. The second wash was performed in pre-warmed GE wash buffer 2 for 1 minute. The microarray slide was removed slowly from the second wash and scanned immediately. The slide was loaded into a Version B slide holder (Agilent Technologies, USA) and scanned in a G2505B Series Microarray scanner (Agilent Technologies, USA) using the one-colour scan setting for 8x60K microarray slides (61x21.6 scan region, 3µm scan resolution,

20-bit Tiff, dye channel was set to green and green PMT selected at 100%). Feature Extraction Software 9.5.3.1 (Agilent Technologies, USA) was used to analyse the scanned images and log intensity values for each spot were calculated.

Microarray and Statistical Analysis- Microarray analysis was performed using R (v3.4.3). The data and accompanying sample annotation was imported and processed using the limma package (v3.32.10) (16). Probe annotation was obtained from GEO using the GEOquery package (v2.42.0), with the GEO platform identifier GPL21185. For data normalisation, 'normexp' background correction and quantile normalisation were performed. Probes were filtered out using the microarray negative control probes. For each sample, the 95% percentile of expression for the negative controls was calculated. Any probes with expression values at least 10% greater than this were taken as expressed in that sample. Probes were kept only if they were expressed in greater than or equal to 28 samples (the number of samples in the smallest group). Finally, data from any remaining duplicate probes (with the same ID and therefore the same sequence) were then averaged using 'avereps'. These steps reduced the number of probes from 62,976 to 32,801. Array quality weights were calculated using an intercept design matrix (17) and were incorporated into the linear model. Samples were grouped according to tumour type, 'Unaffected', 'Primary' (non-metastatic breast cancer) or 'Metastasis' (metastatic breast cancer), using family as a blocking factor. This was to adjust tumour type for differences between families. Alternatively, potential confounding clinical variables were tested in the linear model instead of family. Moderated *t*-statistics were calculated using the 'eBayes' method (18). The Benjamini-Hochberg adjustment (BH-adjusted) method and 'global' multiple-testing method were used to adjust *P*-values for probes and across contrasts between the different tumour types. Differentially expressed probes with an adjusted *P*-value < 0.05 were selected for further analysis.

For gene set enrichment, Entrez gene IDs were used as identifiers and competitive gene set testing was performed using 'camera' (19) from the limma package using a collection of transcriptional modules (20, 21). The ssGSEA method was used to assign a score to each sample (22), based on its expression of the module gene sets, using the GSVA package (23). Gene ontology (GO) analyses were performed using the PANTHER Classification System (24). For analysis of IRG expression, the INTERFEROME database V 2.0 (25) was searched for genes up- or down-regulated more than twofold in human cells in response to recombinant IFN stimulation. The resulting genes were matched with microarray probes by Entrez gene ID.

Multiplex immunohistochemistry- Multiplexed staining using the Opal protocol was performed at the Cancer Microenvironment and Immunology Lab, La Trobe University. Firstly, tissue microarrays (TMAs) generated by kConFab were de-paraffinized in histolene and rehydrated in ethanol. Antigen retrieval was performed as per antibody specifications in either pH 6.0 or pH 9.0 (Perkin Elmer) using heated microwave treatment (MWT). Antibodies, blocking buffers, secondary antibodies, opal fluorophores and diluents used were from the Opal 7 Tumor Infiltrating Lymphocyte (TIL) kits (Perkin Elmer) except CD20 was swapped for CD41 and staining was performed as per manufacturers protocol. Following pH 9.0 heated MWT, slides were blocked for 10 minutes and then incubated with anti-CD8 (1:200) for 1hr in a humidified chamber at room temperature (RT). Slides were washed with TBST (tris buffered saline + 0.05% tween (v/v)) before addition of secondary antibody for 10 minutes followed by further washing and incubation with Opal-570 TSA (1:50) diluted in amplification diluent for 10 minutes. Slides were then subjected to heated MWT with pH 6.0 buffer and staining was performed as per above with anti-FoxP3 (1:100) and Opal-620. Slides were subjected to heated MWT (15 minutes at 20% power) with pH 6.0 buffers and staining performed as above except primary antibody, anti-CD41(1:250) was left on overnight at 4 degrees in a humidified

chamber, staining resumed as per normal the following day with Opal-540 being used. Slides were subjected to heated MWT pH 6.0 and staining was performed as above with anti-CD45RO (1:150) and Opal 650. Slides were subjected to heated MWT with pH 6.0 and staining performed as per above except primary antibody, anti-pan-CK (1:500) was left on overnight at 4 degrees in a humidified chamber, staining resumed as per normal the following day with Opal-690. Slides were subjected to heated MWT pH 9.0 and staining was performed as per above with anti-CD4 (1:150) and Opal 520. Slides were then subjected to heated MWT pH 6.0 and stained with DAPI solution for 3 minutes. Slides were then counted using VECTASHIELD HardSet Antifade mounting medium (Vectorlabs). Slides were then imaged using the VECTRA microscope (PerkinElmer) where whole slide scans were performed and regions of interest captured at 200x magnification.

Multispectral analysis- InForm image analysis software (Perkin Elmer) was used to spectrally unmix and analyse images. Briefly, InForm was trained to segment tissue regions within each individual TMA core between tumor epithelium and surrounding stroma compartments, using DAPI and nuclei size (26). The core was further segmented into individual cells using DAPI staining. Cell scoring was based on expression of said marker and scoring was given as percentage positivity per tissue section, with cells being classed as either single or double positive. H scores were also generated for cytokeratin and CD41 positive tumour cells.

RESULTS

Patient clinical information- A total of 64 breast cancer patients and 29 unaffected donors were included in this study (Table 1). Of the breast cancer patients, 28 patients had been diagnosed with metastatic breast cancer (for the purposes of this study these patients will be referred to as the 'metastasis' group) and 36 patients had been diagnosed with only primary breast cancer (and as such will be referred to as the 'primary' group). Patient information and clinical data was used to inform experimental design and transcriptome analysis (Table 1 and Table 2). Additionally, samples were selected using kConFab family pedigree records so that sets of patients from within the same family could be used as familial controls. In total, 23 complete family sets were selected, each included one breast cancer patient with metastases ('metastasis' group), one female relative with primary breast cancer ('primary group) and one female relative without cancer ('unaffected' group) (Table 3). The remaining 24 patients used in the study come from 12 incomplete family sets from which at least one patient ('metastasis', 'primary' or 'unaffected') was selected. By using familial controls, we were able adjust patient groups for differences between families before applying statistics.

As shown in Table 1 and Table 2, of the 13 clinical parameters studied, only 4 were significantly different across patient groups. These included the number of patient deaths, age at blood sampling, menopausal status and oral contraceptive (OCP) use (Table 1.) Three of these parameters including age, menopause and OCP, were only significantly different in unaffected donors compared to breast cancer patients and showed no difference between breast cancer groups with or without metastases. In comparison to unaffected donors, 70.3% of breast cancer patients were over 50 years old and only 5.6% were younger than 40 years, compared to 34.5% and 48.3% of unaffected donors, respectively (Fisher's Exact test $p=0.0015$) (Table 1). Additionally, 62.5% of breast cancer patients compared to 24.1% of unaffected donors were post-menopausal at the time of blood sampling (Fisher's Exact test $p=0.0008$) and none

of the breast cancer patients used the OCP compared to 17.2% of unaffected donors (Fisher's Exact Test p=0.0023). These variables were subject to analysis as potential confounding factors and will be discussed below.

With the exception of one patient in the 'metastasis' group, all patient samples came from females, none of whom were pregnant or taking the oral contraceptive pill at the time of blood collection (Table 1). As expected, a significantly higher proportion of breast cancer patients were deceased (42%) compared to unaffected donors (all of whom were alive at the time of analyses). Of the deceased breast cancer patients, 81.5% patients were from the 'metastasis' group compared to 18.5% 'primary' patients. Cancer was determined the cause of death (COD) for 17 patients from the 'metastasis' group compared to 2 of the 'primary' patients, thus patients with unknown COD were removed from survival analyses (n=1 'metastasis' patient and n =2 'primary' patient). Unsurprisingly, breast cancer patients with metastasis had poorer survival (63%) compared to patients without metastases (6%) (Fisher's Exact test $p<0.00001$), highlighting the lethality of metastatic spread of breast cancer. Importantly, within the breast cancer patient groups, no significant difference was seen in any clinical information including primary histological type, treatment received or interval between last treatment and blood collection (Table 2) and therefore, these parameters were not considered confounding variables in the comparison of blood transcriptomic evidence of the metastatic potential of primary tumours.

Potential confounding variables in transcriptome analyses- Peripheral blood mononuclear cells (PBMCs) from each patient were assessed for gene expression using microarrays. Multidimensional scaling (MDS) analyses were used to examine the distribution of samples (Fig. 1A), which demonstrated that the majority of samples plotted in close proximity with no clear separation between sample groups.

We also interrogated the data by adjusting for potential confounding variables to see what impact this had on the number of significantly differentially expressed probes. These variables included patient age at time of blood collection ('age'), which we knew to be significantly lower in unaffected donors compared to both cancer groups (Fig. 1B), as well as the gender of the patients ('gender'), the matched family set they belonged to ('family'), the array chip the sample was run on ('chip'), the patients' OCP use ('OCP') and menopausal status at the time of blood collection ('menopause') and the length of time PBMCs were kept frozen prior to this study ('storage time') (Fig. 1C). A total of 648 probes (219 up-regulated probes and 429 downregulated probes) were significantly differentially expressed between 'metastasis' samples and 'unaffected' samples when patient group was the sole variable considered in the model (Fig. 1C, right-hand column). This was the largest set of differentially expressed probes between any of the patient groups and thus, encompasses the largest variance in the experiment. Adjusting for other variables such as storage time, gender and chip had little impact on differential probe expression and were not considered confounding variables. In contrast, age, menopause and OCP each had a noticeable impact on differential probe expression and combining a third variable into the analysis ('group' + 'age' + 'chip') negated all differentially expressed probes indicating that the model needed more sample power to incorporate this many variables. The effect of age (which also correlates with menopausal status and OCP use) could not be delineated from the presence of cancer. However, there was no significant difference in ages of patients in either breast cancer group, thus any potential effect of age did not impact the key analysis of differences between 'metastasis' and 'primary'.

Additionally, analysis of variables demonstrated that adjusting for family set data yielded the highest number of differentially expressed probes between 'metastasis' and 'unaffected' patient groups: a total of 1,397 probes (524 upregulated probes and 823 downregulated probes) (Fig. 1C). A comparison of paired and unpaired analysis results is

shown in Supplementary Fig. 1, demonstrating an increase in differentially expressed probes for all group comparisons when the samples are matched by familial controls. Family sets therefore provided a method of controlling for population variance and was adopted for all subsequent analyses, a distinct strength of this study.

Peripheral blood signatures in metastatic breast cancer- The expression of a total of 32,801 probes were compared across each of our patient groups using moderated *t*-statistics and adjusted *P* values (BH-adjusted with 'global' multiple-testing adjustment). Differentially expressed probes were determined by an adjusted *P* value <0.05. A comprehensive list of differentially expressed probes, corresponding transcript names, fold changes and *P* values are listed in Supplementary Table S1-S6*. Overall, our analysis identified 171 probes with differential expression in PBMCs from 'primary' compared to 'unaffected' donors (29 upregulated and 142 downregulated probes) (Fig. 2Ai) while 1,397 probes were differentially expressed in PBMCs from 'metastasis' patients compared to 'unaffected' donors (524 upregulated and 823 downregulated probes) (Fig. 2Aii) and 146 probes differentially expressed between 'metastasis' and 'primary' breast cancer patients (123 upregulated and 23 downregulated probes) (Fig. 2Aiii). These differentially expressed probes were plotted in Venn diagrams to identify those that were expressed significantly higher (Fig. 2Bi) or lower across one or more groups (Fig. 2Bii). The genes in each comparison are listed in Supplementary Table S7-S16. Collectively, Supplementary Tables 1-16 contain lists of probes and gene IDs in the respective categories from which individual examples can be identified as having associations to cancer. For the purposes of this study we have directed our focus to the overall processes reflected by these gene sets.

*For the purposes of this thesis the supplementary tables S1-S28 are located in the Appendices.

Gene ontology enrichment analyses were performed on each gene set using PANTHER overrepresentation tests. Biological processes were considered significantly enriched by Fisher's exact test with FDR correction $p < 0.05$. This analysis revealed that among the 73 genes expressed higher in PBMCs from 'metastasis' patients compared to 'primary' and 'unaffected' patients (including *PDGFA*, *TSPAN33* and *XK* (Table S10)), the most significantly enriched biological terms included 'platelet degranulation', 'blood coagulation', 'coagulation' and 'hemostasis' (Fig. 2Ci, Supplementary Table 17). Similar processes were enriched in the 350 genes expressed significantly higher in blood from 'metastasis' patients compared to 'unaffected' donors (Supplementary Table 18), suggesting that blood from patients with metastatic breast cancer shows more platelet activation, aggregation, degranulation, endothelial cell proliferation, blood coagulation and hemostasis compared to blood from women without cancer and blood from breast cancer patients whose tumour is not yet circulating or forming macro-metastases. In contrast, the only set of genes expressed at lower levels in group comparisons large enough to return a significant ontology enrichment was the set of 594 genes expressed lower in PBMCs from 'metastasis' patients compared to 'unaffected' donors (Fig, 2Bii). Gene ontology analyses found the biological processes overrepresented in this gene set were predominantly molecular processes vital for cell function including 'gene expression', 'RNA metabolic process' and 'transcription' (Fig. 1Cii) as well as many processes involved in biosynthesis and cellular metabolic pathways (Supplementary Table 19). As expected, similar cellular and metabolic processes were the predominant ontologies significantly underrepresented (fold enrichment <1, FDR <0.05) in genes expressed higher in PBMCs from 'metastasis' patients compared to 'unaffected' donors (Supplementary Table 18). While the only underrepresented ontology in genes expressed lower in PBMCs from 'metastasis' patients compared to 'unaffected' donors was 'response to stimulus' (Fig. 2Cii).

Collectively, these ontologies depict a biological snapshot of the processes occurring in the blood during breast cancer metastasis including an increase in platelet activity, blood coagulation and growth of vasculature, and a decrease in cell transcription and metabolic processes.

Platelets and T cell enriched blood signatures in breast cancer metastasis- To better understand the biological processes underlying the distinct blood signatures during breast cancer metastasis, competitive gene set testing was performed using a set of co-dependent immune-focused transcriptional modules (20, 21), to identify those modules that were significantly enriched in the comparisons between the three groups. Probes were annotated by their corresponding set of co-dependent genes or module (listed in Supplementary Table 1 – 6). Similar to the results of PANTHER gene ontology analyses (which identified platelet activity & blood coagulation as the most enriched biological processes during breast cancer metastases), the most prevalent cellular immune modules identified were attributed to platelets. 'M1.1_Platelets' were the most significantly positively enriched module found in PBMCs from patients with metastatic breast cancer compared to both unaffected donors (Fig. 3Ai,) and non-metastatic breast cancer (Fig. 3Aii,), which further validated the findings of PANTHER enrichment. 'Inflammation' was also significantly positively enriched in metastatic breast cancer compared to both other patient groups (Fig. 3Ai, ii) and other modules including 'cell cycle' and 'mitochondrial stress response' were significantly enriched in PBMCs from 'metastasis' patients compared to 'primary' patients (Fig. 3Aii). In contrast, T cell modules were significantly negatively enriched in PBMCs from 'metastasis' patients compared to both 'unaffected' donors (Fig. 3Ai) and 'primary' patients (Fig. 3Aii). Additionally, 'interferon' modules were significantly negatively enriched gene sets in metastatic breast cancer compared to non-metastatic (Fig. 3Aii), however no individual probes from the 'M1.2_Interferon' or

'M3.4_Interferon' modules were significantly differentially expressed. Analyses revealed that this enrichment reflected a global decrease in IFN signalling in PBMCs from patients with metastases, likely due to a collection of IFN-related transcripts showing similar trends in lower expression.

To complement this analysis, gene sets were compared by single sample gene set enrichment analysis (ssGSEA) assigning an enrichment score to each patient across all three groups and thus demonstrate a continuum of disease progression from unaffected to primary cancer to metastases (Fig. 3Bi,ii). This demonstrates the progressive increase in platelet signatures and decrease in T cell signatures throughout disease progression. Similarly, an analysis of individual genes is exemplified by including transcripts such as *TSPAN33,* a member of the tetraspanin family identified in platelet membrane proteomics (27) (Fig. 3Ci), and *EDAR,* ectodysplasin-A receptor for T cell signatures (Fig. 3Cii).

Together, these enrichment analyses contribute further to our appreciation of the molecular events occurring in peripheral blood cells which reflect the metastatic process of breast cancer. Specifically, these data suggest an environment whereby platelet activity is increased, T cells and potentially other known anti-tumour cell populations are suppressed along with a broad suppression of IFN signalling, which may reflect a continuing process of disease progression.

Interferon signalling in blood during breast cancer metastasis- We used a series of analyses to further investigate interferon-related differences in blood signatures from metastatic and non-metastatic breast cancer. Probes differentially expressed in PBMCs from 'metastasis' patients compared to 'primary' patients were plotted on a heat map showing the relative expression compared to the average expression across all samples in each patient group (Fig. 4). Hierarchical clustering was used to separate these 146 probes into 5 clusters (C1 – C5),

each of which contained probes with similar expression patterns across the experiment (Fig. 4, right y axis). Aligned with these clusters are the immune-focused modules to which each transcript was assigned (Fig 4. left y axis). We also used the INTERFEROME, an online tool developed by the Hertzog Lab comprising an extensive catalogue of published IFN experiments and characterising an exhaustive list of genes which constitute a transcriptional IFN response across a range of conditions, *in vitro* and *in vivo*, as well as different species and different subtypes of IFN (25, 28). This database contains over 4,000 genes that are potentially IFN regulated. As such it represents a broader definition of IFN responsive genes and thus, a more in-depth interrogation of IRG enrichment than the transcriptional modules defined above. We used this tool to search our differentially expressed probe lists for IFN responsive genes and thus, broadly characterise peripheral IFN signalling during breast cancer metastasis. The total 131 genes differentially expressed in metastatic compared to non-metastatic breast cancer were searched against the INTERFEROME database to determine which were IFN-regulated genes (IRGs). Genes were considered IRGs if they existed in the INTERFEROME database with a 2-fold increase or decrease in response to IFN treatment. Table 4 provides an abbreviated list of each cluster, the total number of probes in each, examples of genes within each cluster and whether these genes were determined IRGs by the INTERFEROME (the full set of clusters are listed in Supplementary Table 20). In total, 50 out of 131 (38.2%) differentially expressed genes in PBMCs from 'metastasis' patients compared to 'primary' patients were identified as IRGs (45 expressed higher and 5 expressed lower in 'metastasis' patients) (Supplementary Table 25 & 26).

Further INTERFEROME analyses revealed that a total of 412 out of 1,210 (34.0%) genes differentially expressed in PBMCs across any of our patient groups were identified as IRGs (Fig. 5A, Supplementary Table 21 - 26). The total 412 differentially expressed genes in our study identified using the INTERFEROME as IRGs were plotted in a Venn diagram for

comparison (Fig. 5Bi). This revealed that distinct subsets of IRGs were expressed in PBMCs according to patient pathology (a full list of these subgroups is available in Supplementary Table 27). A subset of 28 IRGs were significantly differentially expressed in PBMCs from breast cancer patients regardless of metastases and thus constitute a 'cancer-associated' signature including *ATM*, a known breast cancer susceptibility gene (29). A subset of 15 IRGs were differentially expressed solely in 'primary' patients compared to 'unaffected' donors and thus were considered as a chronic disease IRG subset, including genes such as *GBP1* & *GBP1L1* which have been associated with vascular dysfunction in chronic inflammatory diseases (30). Additionally, three distinct subsets of 'metastasis'-associated IRGs were identified: 319 that were solely differentially expressed in 'metastasis' patients compared to 'unaffected' donors (an acute cancer/disease-associated subset); 37 that were differentially expressed in 'metastasis' patients compared to both other groups (a 'metastasis-specific' subset); and 12 that were expressed differentially between 'metastasis' and 'primary' patients but that did not differ to 'unaffected'. All metastasis-associated subsets of IRGs were combined (312 'cancer-associated' IRGs, 36 'metastasis-specific' IRGs and 12 'non-primary cancer-associated' IRGs) and analysed using PANTHER for gene ontology enrichment. Interestingly, the most significantly enriched ontologies amongst IRG expression in the blood during metastasis remained platelet activation, degranulation and hemopoiesis pathways (Fig. 4Bii, Supplementary Table 28), demonstrating that IFN signalling may play a role in the systemic processes vital to metastasis in less well-characterised IFN functions.

Collectively these data demonstrate that transcriptional signatures indicate the vast molecular processes occurring in peripheral blood of patients with metastatic breast cancer. Specifically, these signatures demonstrate differences in systemic IFN signalling with a global decline in well-characterised IFN module expression during breast cancer metastasis, while in contrast, revealing an enrichment of IRGs contributing to metastasis-associated pathways such

as platelet activity. This highlights the vital role IFN signalling may play during disease progression and the importance of characterising broad-spectrum IFN responses as a means to better understand the complex processes underlying metastasis and potentially develop novel biomarkers.

Distinct cell signatures reflect the metastatic potential of primary breast tumours- To understand the local molecular processes underlying breast cancer metastasis from the primary tumour and to contextualise our findings in peripheral blood, we stained tissue microarrays (TMAs) using multiplex immunohistochemistry to visualise different cell populations in primary tumour samples from 231 breast cancer patients (TMAs accessed via kConFab (15)). Of these, 211 breast cancer patients had not been diagnosed with metastases and 20 patients either had already been diagnosed with metastases at the time of tissue collection or went on to develop metastatic cancer. This was an opportunity to examine cell differences in primary breast tumours that may drive metastasis or indicate metastatic potential, and be reflected systemically by our metastasis-associated signatures. Within the limitations of this study, priority was given to the analysis of established cell markers including pan-cytokeratin (pan-CK) for tumour cells (31), CD8 for CD8+ T cells (32), CD45RO for activation of effector cells or memory phenotype (33), CD41 for platelets (34), CD4 for CD4+ T cells and FoxP3 (35). Direct markers of IFN response for multiplex analysis require further development at the time of preparation of this thesis. The combination of these allowed us to translate our findings in peripheral blood signatures by investigating the most significantly positively and negatively enriched blood cell pathways in primary tissue.

Here we show, composite (multispectral stain overlaying all markers) and "pathology" (deconvoluted single CD45RO+ stain) images of multiplex staining from three representative TMA cores taken from patients with non-metastatic breast cancer (i – iii) or patients with

metastatic breast cancer (iv – vi). The composite images show the overall tissue architecture of each core including the spatial relationship between tumour cells (CK+) and stromal tissue as well as the concentration of immune cells in the stroma and density of cellular content. By comparing the composite morphology of non-metastatic primary tumours (Fig. 6Ai-iii) and primary tumour with metastatic potential (Fig. 6Aiv-vi) there was a trend towards non-metastatic tumours forming large, clustered tumour nodules some of which were double positive for epithelial and platelet markers (CK+CD41+), suggesting that in some cases platelets may aggregate around or coat primary tumour cells. Overall, the structure of non-metastatic primary tumours was well-organised with frequent evidence of immune infiltrate in the stroma surrounding tumour nodules. The stroma often stained positive for CD8 T cells (CD8+), which displayed a high frequency of activation (CD8+CD45RO+) (Fig. 6Ai-iii). By deconvoluting CD45RO+ cells into a single stain, we found that immune activation was present within the stroma of non-metastatic primary tumours, often occurring in concentrated areas of immune infiltrate. In contrast, primary tumours with metastatic potential, showed distinct tissue morphology (Fig. 6Aiv-vi). These tumours (CK+) were more diffusely distributed across the tissue core, with scattered tumour clusters, usually containing fewer tumour cells per cluster, yet overall demonstrating more CK+ cells per tissue core than non-metastatic primary tumours. The structure of the tumour microenvironments was disorganised in primary tumours with metastatic potential and showed some CD8+ stroma, however there were significantly fewer total CD8 T cells per stromal region compared to non-metastatic tumours as well as fewer activated CD8 T cells and no clear arrangement or distinction between tumour clusters and stroma.

As expected, the patient tissue cores varied in an extent in tumour content and structure difficult to quantify by visual observation alone. We therefore used multispectral analyses to systematically quantify staining positivity for each marker across all patient samples. For

tumour and platelet markers, the percentage of positive cells per total cells in each tissue core was calculated and for immune markers, the percentage of positive cells per cells in the stromal region was calculated. Overall, primary breast tumours with metastatic potential (MP) had significantly higher proportions of tumour cells per core (Fig. 6Bi), which corresponded with a trend towards an increase in tumour-associated platelets (Fig. 6Bii) compared to non-metastatic (Non-M) primary breast tumours. In contrast, MP primary tumours had a significantly lower proportion of stromal CD8+ T cells (Fig. 6Biii), which were also less activated demonstrating a lower proportion of CD8+CD45RO+ cells compared to Non-M primary tumours (Fig. 6Biv). Further classification of the six representative patient cores (i – vi) showed a trend towards Non-M primary tumour samples having a higher stromal content per tissue core (average 77.44% per core), longer metastasis-free survival (average 7,550 days) and overall prognosis (average 33% of patients deceased) compared to 56.8% stroma per core, 4,106 days MFS and 66% mortality for patients with MP primary tumours, respectively (Fig. 6C). This integration of clinical and cell signature data, while needing further expansion beyond this study, demonstrates the potential benefit and application of these signatures in understanding the nature of each tumour and stratifying patients based on metastatic potential.

Taken together, these data show distinct differences in the tissue architecture, proportion of cell types and spatial relationship between cells in primary breast tumours as an indication of metastatic potential. Primary breast tumours which have already or are certain to metastasise and thus have high metastatic potential, have disorganised tumour clusters throughout the tissue, which also stain positive for platelets, sparse stromal regions containing few total effector T cells as well as poor activation in contrast to primary non-metastatic tumours. Overall, these local cell signatures reflect our systemic transcriptome data which demonstrated that in PBMCs from patients with metastatic breast cancer there was a strong enrichment of platelet activity partially regulated by our broadly classified IFN responsive genes, a

suppression of T cell signalling as well as a suppression of a subset of well-characterised IFN signalling and cellular functions such as transcription and metabolism, which may prevent processes such as immune activation. Here, we demonstrate that systemic transcriptome data may indeed reflect processes occurring at the primary tumour site and indicate metastatic potential.

Distant metastases maintain an immunocompromised status and lose platelet signature- To correlate our data on local cell signatures in the primary tumour and systemic transcriptomic data with the processes occurring at the site of distant metastases, we investigated the same panel of cell marker staining in TMAs containing secondary/metastatic tumour samples alongside our primary tumour cohort. Given the difficulty of accessing metastases from terminally ill patients the study was limited at this stage to staining secondary tumours from 7 breast cancer patients (in technical replicates n = 1-3, each averaged). Figure 7 shows composite images, score maps (a comparison of CK+CD41+ overlap) and deconvoluted pathology images for CK+ and CD41+ cells of multispectral stains in secondary tumour and primary tumour samples divided into metastatic potential (MP) tumours and non-metastatic (Non-M) tumours. The example secondary tumour shown shows a well-established tumour mass with densely populated tumour cells growing in close proximity and a distinct lack of extracellular space or stromal tissue and immune infiltrate in contrast to primary tumour samples (Fig. 7A). The overlapped score map shows the breakdown of CK+CD41- cells (shown in red), CD41+CK- cells (green), double positive cells (yellow) and double negative cells (blue), combined with individual pathology stains demonstrates that secondary tumour samples generally showed a higher proportion of tumour cells (CK+) that were negative for the platelet marker (CD41-), which corresponded with an overall decrease in the proportion of CD41 + cells in comparison to primary breast tumours. As expected, individual patient samples

varied to an extent and thus we did not rely solely on visual observation. These observations were combined with multispectral analyses which revealed that, in contrast to primary breast tumours, secondary breast tumours showed a significant reduction in total platelets (CD41+) (Fig. 7Bi) and more specifically, a decrease in tumour cells positive for platelet marker staining (CK+CD41+) (Fig. 7Bii), and inversely, an increase in tumours cells negative for platelet marker staining (CK+CD41-) (Fig. 7Biii). Additionally, we found that secondary tumour samples demonstrated a similar immune infiltrate pattern to primary tumours with metastatic potential with a trend towards a decrease in total CD4+ T cells (Fig. 7iv) as well as trend towards a decrease in total CD8+ T cells (Fig. 7Bv) and activated CD8+ T cells (CD8 +CD45RO+) (Fig. 7Bvi).

Interestingly, these data on cell signatures in distant secondary tumours partly align with our findings in local and systemic metastatic signatures, which reveal a decrease in infiltrating T cells in primary breast tumours that metastasise and loss of T cell signatures in peripheral blood cells from breast cancer patients with metastasis compared to patients with non-metastatic breast cancer. Here, we see a similar trend in few infiltrating immune cells, potentially reflective of an established immunosuppressive microenvironment. In contrast, secondary tumours show a decrease in the overall platelet signature that was enriched in both primary tumour tissue staining and peripheral signatures from patients with metastatic breast cancer. This may suggest that the role of platelets in promoting metastasis and the close physical association between tumour cells and platelets throughout the initiation and systemic circulation of breast cancer metastasis is no longer required once tumour cells seed secondary sites, supported by an immunosuppressed microenvironment. These data further contribute to our knowledge of the distinctions between local, systemic and secondary signatures during metastasis.

DISCUSSION

The processes involved in breast cancer metastasis occur as co-ordinated molecular events located not only at the primary tumour site, but also throughout the metastatic pathway including in the peripheral vasculature and secondary organs. These processes, driven by cells at the primary tumour site, in circulation and at the site of micro-metastases, may already be at work long before medical detection or intervention (36-39), and overwhelmingly contribute to patient mortality. Gene expression profiling studies have provided insight into the severity and prognosis of several cancers including breast cancer (2-4, 6, 11, 12, 40, 41), however most of these have focused on characterising the primary tumour transcriptome and thus, omitted the corresponding events occurring systemically as well as at secondary sites. Our lab and collaborators previously characterised a specific IFN signature present in primary tumour cells, the loss of which was critical in suppressing systemic anti-tumour immune responses and facilitating breast cancer metastasis to bone (7). Our aim here was to further characterise this pathway, specifically investigate whether the presence of this signature in primary tumour cells would influence the systemic transcriptome or metastatic tumour signatures, and thus provide a mapped pathway analysis of breast cancer metastasis that would both inform our understanding of processes occurring in the circulation and generate a systemic signature that could serve as a disease biomarker.

One of the strengths of the analyses of blood transcriptomics in this study was the use of matched familial samples, which allowed for paired analyses across patient groups. As we showed, the use of paired familial samples enabled an increased analytical power of transcriptomic differences across groups of human samples in part, because a proportion of the human transcriptome is highly heritable (42, 43). By incorporating paired familial controls into our analyses, we found more than a 2-fold increase in the number of differentially expressed probes detected in PBMCs from patients with metastatic breast cancer compared to

unaffected donors, and most importantly, almost an 8-fold increase in detection of differentially expressed probes between breast cancer patients with or without metastases. This suggests that studies investigating blood transcriptomics in breast cancer may benefit from familial controls, which have not previously been adopted.

Overall, we identified gene expression signatures in peripheral blood immune cells (PBMCs) associated with breast cancer metastasis. Among genes significantly up-regulated in blood from metastatic compared to non-metastatic breast cancer patients and unaffected donors, several biological processes were enriched (FDR <0.05) including platelet degranulation (GO:0002576), blood coagulation (GO:0007596, GO:0050817) and hemostasis (GO:0007599). Too few genes were down-regulated in blood from metastatic patients compared to non-metastatic patients for gene enrichment analyses to be performed. However, in comparison to unaffected donors, genes down-regulated in blood from metastatic patients were significantly enriched in gene expression/transcription (GO:0010467, GO:0006351, GO:0097659) and RNA metabolic process (GO:0016070), while the only significantly negatively enriched process among down-regulated genes was response to stimulus (GO:0050896).

Platelet degranulation leads to the secretion of growth factors and lipids into the blood. This in turn recruits more platelets which form aggregates as well as promote blood coagulation, two of the key processes required to shield circulating tumour cells from immune detection and aid adherence to endothelial surfaces at secondary site for metastasis (44, 45). Increased platelet activity has been identified in a number of cancers including breast cancer (46) and associated with poor prognosis (47). Our findings align with previous evidence to suggest this pathway is active and enriched in blood during breast cancer metastasis. Additionally, our data agree with previous reports that cell processes such as metabolism are

suppressed in peripheral blood signatures in breast cancer (11) and may reflect the broad metabolic changes observed during cancer (48).

Immune cells effect tumour spread at each stage of the metastatic pathway: i) during primary tumour development and growth *in situ*; ii) during migration and circulation of tumour cells in systemic vasculature; and iii) in successful colonisation of secondary tissue. The significant contribution of the cells of immune system to this process has both the potential to suppress, but also aid tumour metastasis. Characterisation of the properties of both paradoxical roles of the immune system are the subject of much investigation. We investigated the contribution of the immune system to our metastatic blood signature through gene module enrichment (20, 21). This analysis firstly, validated a significant enrichment of platelet signatures in the blood of metastatic breast cancer patients in comparison to both non-metastatic patients and unaffected donors, which corresponded with a mild increase in inflammation. It also validated the suppression of cell processes such as cell cycle (M3.5, M4.7) and protein synthesis (M4.3), however in addition it identified a significant suppression in several T cell modules (M4.1, M4.15) as well as multiple well-characterised interferon (IFN) modules (M3.4, M1.2). IFNs are known to have potent anti-tumour effects, in part through activation of anti-tumour immune responses including T cells (49), which we previously demonstrated in preventing breast cancer bone metastasis (7). In our previous study, expression of IFN in primary breast tissue had no impact on primary growth, instead having a purely anti-metastatic effect via peripheral immune activation. Our present data on suppression of systemic IFN/immune signatures in patients with metastatic compared to non-metastatic breast cancer further corroborate the processes occurring systemically during metastasis.

Further investigation of IFN signalling via the INTERFEROME tool for expansive identification of IFN response genes demonstrated that while well-defined IFN modules were systemically suppressed during metastasis, IFN signalling was a considerable component of

the metastasis-associated blood signature found in breast cancer patients. Furthermore, the most significantly enriched biological processes represented by the GO's of these less-characterised IRGs associated with metastasis- were platelet degranulation, activation (GO:0030168) and blood coagulation as well as cell-cell adhesion (GO:0034109) and cell junction assembly and organisation (GO:0034329, GO:0034330). The higher number of genes identified by the INTERFEROME analysis suggests that not only is classical IFN signalling suppressed systemically during metastasis, in support of our previous findings, but that broader, less characterised IFN signalling contributes to the processes critical for successful tumour cell circulation such as key platelet-related pathways: activation and the promotion of epithelial-mesenchymal-like transition (EMT) and adhesion to endothelial surfaces for extravasation (50).

Finally, we combined our blood transcriptomics data with multiplex immune staining in primary breast tumours divided by metastatic potential and secondary tumour samples. Interestingly, the vast majority of primary breast tumour nodules stained positive for a platelet marker, CD41, suggesting that platelets were in fact present in most primary breast tumours prior to or regardless of metastatic burden. Primary breast tumours with metastatic potential demonstrated a significantly higher proportion of tumour cells with a trend towards a higher proportion of double positive CK+CD41+ tumours. These findings correspond with previous detection of platelets surround primary tumour samples in pancreatic cancer (51). Additionally, in breast cancer, platelet staining in primary tumours correlated with response to chemotherapy (52), suggesting that the local presence of platelets coating tumour cells may occur much earlier than detection of macro-metastases and aid in survival and progression of the primary tumour. In contrast, this platelet cell signature was significantly reduced in secondary tumour samples, demonstrated by reduced numbers of both individual total platelet and tumour-associated platelet staining in metastases samples as well as an increase in non-

coated tumour cells. This may reflect the fact that once seeded in secondary sites, which may even have been platelet-primed for colonisation (53, 54), tumour cells no longer rely as heavily on platelet aggregation and signalling to survive. We also found decreases in total CD4+ and CD8+ T cells as well as activated CD8+ T cells in both primary breast tumours with metastatic potential as well as secondary tumours, supporting our hypothesis that immune activity (potentially IFN-driven) is suppressed during successful metastatic pathways.

CONCLUSION

This study investigates local, systemic and distant signatures during breast cancer metastasis and reveals significant differences in metastasis-associated peripheral blood transcriptomic signatures in breast cancer patients matched to familial controls including an enrichment of platelet activity, T cell suppression and a broad contribution of IFN signalling. We show a distinct cell signatures in primary and secondary breast tumour tissue, which reflect changes seen in the blood and provide a map of metastasis from local through to distant sites. Further interrogation of signatures in breast cancer will likely provide greater insight into the mechanisms including cell subsets, signals and secreted factors underlying these changes and potentially support the development of "liquid biopsy" for classifying metastatic potential.

REFERENCES

1. Downs-Holmes C, Silverman P. Breast Cancer: overview & updates. Nurse Pract. 2011;36(12):20-6.

2. Ascierto ML, Kmieciak M, Idowu MO, Manjili R, Zhao Y, Grimes M, et al. A signature of immune function genes associated with recurrence-free survival in breast cancer patients. Breast Cancer Res Treat. 2012;131(3):871-80.

3. Minn AJ, Gupta GP, Siegel PM, Bos PD, Shu W, Giri DD, et al. Genes that mediate breast cancer metastasis to lung. Nature. 2005;436(7050):518-24.

4. van t'Veer LJ, Dai H, van de Vijver MJ, He YD, Hart AA, Mao M, et al. Gene expression profiling predicts clinical outcome of breast cancer. Nature. 2002;415(6871):530-6.

5. Curtis C, Shah SP, Chin SF, Turashvili G, Rueda OM, Dunning MJ, et al. The genomic and transcriptomic architecture of 2,000 breast tumours reveals novel subgroups. Nature. 2012;486(7403):346-52.

6. Kang Y, Siegel PM, Shu W, Drobnjak M, Kakonen SM, Cordón-Cardo C, et al. A multigenic program mediating breast cancer metastasis to bone. Cancer Cell. 2003;3(6):537-49.

7. Bidwell BN, Slaney CY, Withana NP, Forster S, Cao Y, Loi S, et al. Silencing of Irf7 pathways in breast cancer cells promotes bone metastasis through immune escape. Nat Med. 2012;18(8):1224-31.

8. Honda K, Yanai H, Negishi H, Asagiri M, Sato M, Mizutani T, et al. IRF-7 is the master regulator of type-I interferon-dependent immune responses. Nature. 2005;434(7034):772-7.

9. Sato M, Suemori H, Hata N, Asagiri M, Ogasawara K, Nakao K, et al. Distinct and essential roles of transcriptions factors IRF-3 and IRF-7 in response to viruses for IFN-α/β gene induction. Immunity. 2000;13(4):539-48.

10. Mohme M, Riethdorf S, Pantel K. Circulating and disseminated tumour cells - mechanisms of immune surveillance and escape. Nat Rev Clin Oncol. 2017;14(3):155-67.

11. Aaroe J, Lindahl T, Dumeaux V, Saebo S, Tobin D, Hagen N, et al. Gene expression profiling of peripheral blood cells for early detection of breast cancer. Breast Cancer Res. 2010;12(1):R7.

12. Sharma P, Sahni NS, Tibshirani R, Skaane P, Urdal P, Berghagen H, et al. Early detection of breast cancer based on gene-expression patterns in peripheral blood cells. Breast Cancer Res. 2005;7(5):R634-44.

13. Tudoran O, Virtic O, Balacescu L, Pop L, Dragla F, Eniu A, et al. Differential peripheral blood gene expression profile based on Her2 expression on primary tumors of breast cancer patients. PLoS One. 2014;9(7):e102764.

14. Mohr S, Liew CC. The peripheral-blood transcriptome: new insights into disease and risk assessment. Trends Mol Med. 2007;13(10):422-32.

15. Mann GJ, Thorne H, Balleine RL, Butow PN, Clarke CL, Edkins E, et al. Analysis of cancer risk and BRCA1 and BRCA2 mutation prevalence in the kConFab familial breast cancer resource. Breast Cancer Res. 2006;8(1).

16. Ritchie ME, Phipson B, Wu D, Hu Y, Law CW, Shi W, et al. Limma powers differential expression analyses for RNA-sequencing and microarray studies. Nucleic Acids Res. 2015;43(7):e47.

17. Ritchie ME, Diyagama D, Neilson J, van Laar R, Dobrovic A, Holloway A, et al. Empirical array quality weights in the analysis of microarray data. BMC Bioinformatics. 2006;7.

18. Phipson B, Lee S, Majewski IJ, Alexander WS, Smyth GK. Robust hyperparameter estimation protects against hypervariable genes and improves power to detect differential expression. Annals of Applied Statistics. 2016;10(2):946-63.

19. Wu D, Smyth GK. Camera: A competitive gene set test accounting for inter-gene correlation. Nucleic Acids Res. 2012;40(17).

20. Chaussabel D, Quinn C, Shen J, Patel P, Glaser C, Baldwin N, et al. A Modular Analysis Framework for Blood Genomics Studies: Application to Systemic Lupus Erythematosus. Immunity. 2008;29(1):150-64.

21. Chaussabel D, Baldwin N. Democratizing systems immunology with modular transcriptional repertoire analyses. Nature Reviews Immunology. 2014;14(4):271-80.

22. Barbie DA, Tamayo P, Boehm JS, Kim SY, Moody SE, Dunn IF, et al. Systematic RNA interference reveals that oncogenic KRAS-driven cancers require TBK1. Nature. 2009;462(7269):108-12.

23. Hänzelmann S, Castelo R, Guinney J. GSVA: Gene set variation analysis for microarray and RNA-Seq data. BMC Bioinformatics. 2013;14.

24. Mi H, Muruganujan A, Casagrande JT, Thomas PD. Large-scale gene function analysis with the panther classification system. Nat Protoc. 2013;8(8):1551-66.

25. Rusinova I, Forster S, Yu S, Kannan A, Masse M, Cumming H, et al. Interferome v2.0: an updated database of annotated interferon-regulated genes. Nucleic Acids Res. 2013;41(Database issue):D1040-6.

26. Hendry S, Salgado R, Gevaert T, Russell PA, John T, Thapa B, et al. Assessing Tumor-infiltrating Lymphocytes in Solid Tumors: A Practical Review for Pathologists and Proposal for a Standardized Method from the International Immunooncology Biomarkers Working Group: Part 1: Assessing the Host Immune Response, TILs in Invasive Breast Carcinoma and Ductal Carcinoma in Situ, Metastatic Tumor Deposits and Areas for Further Research. Adv Anat Pathol. 2017;24(5):235-51.

27. Lewandrowski U, Wortelkamp S, Lohrig K, Zahedi RP, Wolters DA, Walter U, et al. Platelet membrane proteomics: a novel repository for functional research. Blood. 2009;114(1):e10-9.

28. Samarajiwa SA, Forster S, Auchettl K, Hertzog PJ. INTERFEROME: the database of interferon regulated genes. Nucleic Acids Res. 2009;37(Database issue):D852-7.

29. Ahmed M, Rahman N. ATM and breast cancer susceptibility. Oncogene. 2006;25(43):5906-11.

30. Hammon M, Herrmann M, Bleiziffer O, Pryymachuk G, Andreoli L, Munoz LE, et al. Role of guanylate binding protein-1 in vascular defects associated with chronic inflammatory diseases. J Cell Mol Med. 2011;15(7):1582-92.

31. Lu S-H, Tsai W-S, Chang Y-H, Chou T-Y, Pang S-T, Lin P-H, et al. Identifying cancer origin using circulating tumor cells. Cancer Biol Ther. 2016;17(4):430-8.

32. Appay V, van Lier RAW, Sallusto F, Roederer M. Phenotype and function of human T lymphocyte subsets: Consensus and issues. 2008;73A(11):975-83.

33. Hu G, Wang S. Tumor-infiltrating CD45RO(+) Memory T Lymphocytes Predict Favorable Clinical Outcome in Solid Tumors. Sci Rep. 2017;7(1):10376.

34. Galindo M, Gonzalo E, Martinez-Vidal MP, Montes S, Redondo N, Santiago B, et al. Immunohistochemical detection of intravascular platelet microthrombi in patients with lupus nephritis and anti-phospholipid antibodies. Rheumatology (Oxford). 2009;48(8):1003-7.

35. deLeeuw RJ, Kost SE, Kakal JA, Nelson BH. The prognostic value of FoxP3+ tumor-infiltrating lymphocytes in cancer: a critical review of the literature. Clin Cancer Res. 2012;18(11):3022-9.

36. Pantel K, Alix-Panabieres C. Bone marrow as a reservoir for disseminated tumor cells: a special source for liquid biopsy in cancer patients. BoneKEy reports. 2014;3:584.

37. Pantel K, Brakenhoff RH, Brandt B. Detection, clinical relevance and specific biological properties of disseminating tumour cells. Nat Rev Cancer. 2008;8(5):329-40.

38. Braun S, Naume B. Circulating and disseminated tumor cells. J Clin Oncol. 2005;23(8):1623-6.

39. Bidard FC, Kirova YM, Vincent-Salomon A, Alran S, de Rycke Y, Sigal-Zafrani B, et al. Disseminated tumor cells and the risk of locoregional recurrence in nonmetastatic breast cancer. Ann Oncol. 2009;20(11):1836-41.

40. Perou CM, Jeffrey SS, van de Rijn M, Rees CA, Eisen MB, Ross DT, et al. Distinctive gene expression patterns in human mammary epithelial cells and breast cancers. Proc Natl Acad Sci U S A. 1999;96(16):9212-17.

41. Dumeaux V, Ursini-Siegel J, Flatberg A, Fjosne HE, Frantzen JO, Holmen MM, et al. Peripheral blood cells inform on the presence of breast cancer: a population-based case-control study. Int J Cancer. 2015;136(3):656-67.

42. Wright FA, Sullivan PF, Brooks AI, Zou F, Sun W, Xia K, et al. Heritability and genomics of gene expression in peripheral blood. Nat Genet. 2014;46(5):430-7.

43. Huan T, Liu C, Joehanes R, Zhang X, Chen BH, Johnson AD, et al. A systematic heritability analysis of the human whole blood transcriptome. Hum Genet. 2015;134(3):343-58.

44. Gay LJ, Felding-Habermann B. Contribution of platelets to tumour metastasis. Nat Rev Cancer. 2011;11(2):123-34.

45. Menter DG, Tucker SC, Kopetz S, Sood AK, Crissman JD, Honn KV. Platelets and cancer: a casual or causal relationship: revisited. Cancer Metastasis Rev. 2014;33(1):231-69.

46. Blann AD, Gurney D, Wadley M, Bareford D, Stonelake P, Lip GY. Increased soluble P-selectin in patients with haematological and breast cancer: a comparison with fibrinogen, plasminogen activator inhibitor and von Willebrand factor. Blood Coagul Fibrinolysis. 2001;12(1):43-50.

47. Taucher S, Salat A, Gnant M, Kwasny W, Mlineritsch B, Menzel R-C, et al. Impact of pretreatment thrombocytosis on survival in primary breast cancer. Thromb Haemost. 2003;89(6):1098-106.

48. Tisdale MJ. Cachexia in cancer patients. Nat Rev Cancer. 2002;2(11):862-71.

49. Parker BS, Rautela J, Hertzog PJ. Antitumour actions of interferons: Implications for cancer therapy. Nature Reviews Cancer. 2016;16(3):131-44.

50. Gay LJ, Felding-Habermann B. Platelets alter tumor cell attributes to propel metastasis: programming in transit. Cancer Cell. 2011;20(5):553-4.

51. Miyashita T, Tajima H, Makino I, Nakagawara H, Kitagawa H, Fushida S, et al. Metastasis-promoting role of extravasated platelet activation in tumor. J Surg Res. 2015;193(1):289-94.

52. Ishikawa S, Miyashita T, Inokuchi M, Hayashi H, Oyama K, Tajima H, et al. Platelets surrounding primary tumor cells are related to chemoresistance. Oncol Rep. 2016;36(2):787-94.

53. Boucharaba A, Serre CM, Gres S, Saulnier-Blache JS, Bordet JC, Guglielmi J, et al. Platelet-derived lysophosphatidic acid supports the progression of osteolytic bone metastases in breast cancer. J Clin Invest. 2004;114(12):1714-25.

54. Leblanc R, Lee SC, David M, Bordet JC, Norman DD, Patil R, et al. Interaction of platelet-derived autotaxin with tumor integrin alphaVbeta3 controls metastasis of breast cancer cells to bone. Blood. 2014;124(20):3141-50.

Table 1. Characteristics of the human cohort used for PBMC transcriptome analyses including breast cancer patients and unaffected donors.

	Breast Cancer N(%)			Unaffected N(%)	Fisher Exact test	
	Metastases		Total		Metastasis V Primary	Cancer V Unaffected
	Yes 'Metastasis'	No 'Primary'				
	28 (43.7)	36 (56.3)	64 (100.0)	29 (100.0)		
Gender						
F	27 (96.4)	36 (100.0)	63 (98.4)	29 (100.0)	0.4375	>0.9999
M	1 (3.6)	0 (0.0)	1 (1.6)	0 (0.0)		
Deceased						
Y	22 (78.6)	5 (13.9)	27 (42.2)	0 (0.0)	<0.00001	<0.00001
N	6 (21.4)	31 (81.1)	37 (57.8)	29 (100.0)		
Cancer COD	N (% of deceased)					
Y	17 (77.3)	2 (40.0)	19 (70.4)	NA	0.5212	NA
N	4 (18.2)	1 (20.0)	5 (18.5)	NA		
Unknown	1 (4.5)	2 (40.0)	3 (11.1)	NA		
At time of sampling						
Age (years)						
0 - 50	9 (32.2)	10 (27.8)	19 (39.7)	19 (48.3)	0.7858	0.0015
51 - 90	19 (67.8)	26 (72.2)	45 (70.3)	10 (34.5)		
Pregnant						
Y	0 (0.0)	0 (0.0)	0 (0.0)	0 (0.0)	>0.9999	>0.9999
N	28 (100.0)	36 (100.0)	64 (100.0)	29 (100.0)		
Menopause						
Y	20 (71.8)	20 (55.6)	40 (62.5)	7 (24.1)	0.2979	0.0008
N	8 (28.2)	16 (44.4)	24 (37.5)	22 (75.9)		
OCP						
Y	0 (0.0)	0 (0.0)	0 (0.0)	5 (17.2)	>0.9999	0.0023
N	28 (100.0)	36 (100.0)	64 (100.0)	24 (82.8)		

**Data are expressed as number of participants and percentage of the total cohort for each column (unless otherwise specified). F – female, M – male, COD – cause of death, Y – yes, N– no, OCP – oral contraceptive pill. Significance was determined by Fisher's Exact Test and P values are indicated.*

Table 2. Clinical information of breast cancer patients used for PBMC transcriptional analyses.

	Breast Cancer N(%)			Fisher Exact Test
	Metastases		Total	
	Yes	No		
	28 (43.7)	36 (56.3)	64 (100.0)	0.2158
Clinical nodal status				
N0	12 (42.9)	13 (36.1)	25 (39.1)	0.6145
N1	5 (17.9)	5 (13.9)	10 (15.6)	0.7367
N2-3	2 (7.1)	2 (5.6)	4 (6.2)	>0.9999
Unknown	9 (32.1)	16 (44.4)	25 (39.1)	0.4392
Primary clinical tumour grade				
I	2 (7.1)	7 (19.4)	9 (14.1)	0.2778
II	6 (21.4)	13 (36.1)	19 (29.7)	0.2729
III	9 (32.1)	6 (16.7)	15 (23.4)	0.2338
Unknown	11 (39.3)	10 (27.8)	21 (32.8)	0.4232
Primary histological type				
Ductal	22 (78.6)	26 (72.2)	48 (75.0)	0.7718
Lobular	3 (10.7)	3 (8.3)	6 (9.4)	>0.9999
Other	2 (7.1)	3 (8.3)	5 (7.8)	>0.9999
Unknown	1 (3.6)	4 (11.1)	5 (7.8)	0.3753
Primary breast cancer subtype				
Luminal A	3 (10.7)	4 (11.1)	7 (10.9)	>0.9999
Luminal B	1 (3.6)	1 (2.8)	2 (3.1)	>0.9999
HER2+	1 (3.6)	1 (2.8)	2 (3.1)	>0.9999
Basal-like	2 (7.1)	0 (0.0)	2 (3.1)	0.1875
Unknown	21 (75.0)	30 (83.3)	51 (79.7)	0.5342
Treatment received				
Chemotherapy	10 (35.7)	10 (27.8)	20 (31.2)	0.4310
Radiation	12 (42.9)	13 (36.1)	25 (39.1)	0.6145
Anti-hormone	14 (50.0)	13 (26.1)	27 (42.2)	0.3134
Other	2 (7.1)	2 (5.6)	4 (6.2)	>0.9999
None	6 (21.4)	10 (27.8)	16 (25.0)	0.7718
Time between treatment & sampling				
0 - 1 years	6 (21.4)	5 (13.9)	11 (17.2)	0.5127
1 - 5 years	10 (35.7)	8 (22.2)	18 (28.1)	0.2717
>5 years	5 (17.9)	10 (27.8)	15 (23.4)	0.3904

**Data are expressed as number of participants and percentage of the total cohort for each column. Significance is determined by Fisher's Exact Test and P values are indicated.*

Figure 1.

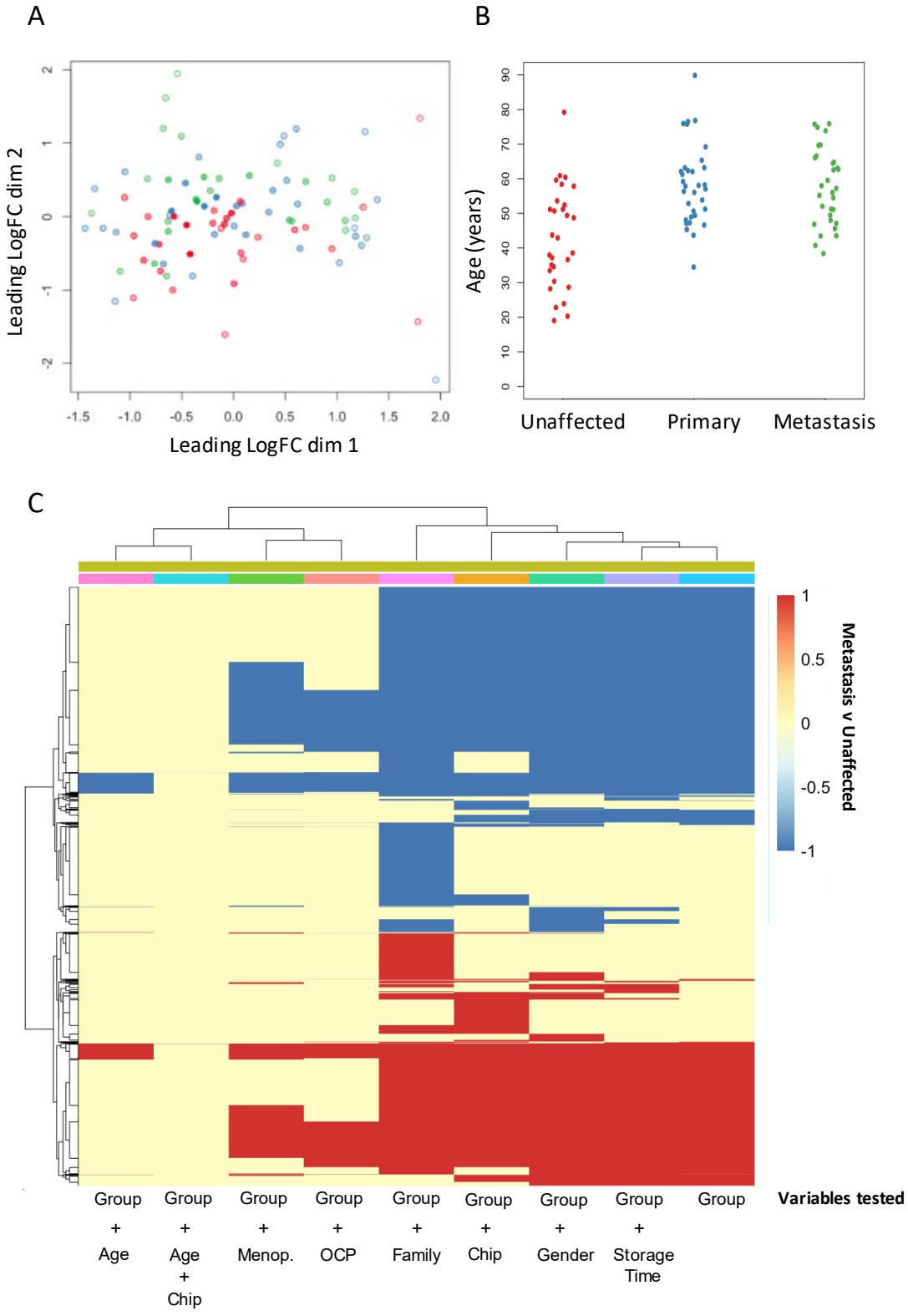
A
B
Leading LogFC dim 2
Leading LogFC dim 1
Age (years)
Unaffected
Primary
Metastasis
C
Metastasis v Unaffected
Variables tested
Group + Age
Group + Age + Chip
Group + Menop.
Group + OCP
Group + Family
Group + Chip
Group + Gender
Group + Storage Time
Group

Figure 1. Analysis of transcriptional variance and confounding variables in PBMC microarray. *Microarray analysis was performed using PBMCs from breast cancer patients with metastases ('metastasis'), breast cancer patients with no metastases ('primary') and unaffected donors. (A) Multidimensional scaling (MDS) plot shows the relationship between individual samples based on transcriptional similarity, coloured by patient group and shaded by array quality weighting. (B) Plot shows ages of individual patients in each group at time of blood collection. (C) Heat map shows significantly differentially expressed probes in PBMCs from 'metastasis' patients compared to unaffected donors ('group' analysis, right hand column) along with adjustment for potential confounding variables (shown on the x axis). Each column shows the probes that were significantly differentially expressed incorporating the indicated variables into the linear model. Probes are coloured by whether they significantly regulated (+1) or downregulated (-1). Significance was determined using BH-adjusted P value < 0.05.*

Table 3. Distribution of human samples across patient pathology and matched family groups.

Patient Pathology			No. of families	No. of samples
Metastases	Primary	Unaffected		
0	1	0	1	1
1	1	0	3	6
0	2	0	2	4
1	0	1	2	4
0	1	1	3	6
1	1	1	23	69
0	2	1	1	3
Total			35	93

**A total of 93 PBMC samples were used for transcriptome analyses. These samples came from breast cancer patients with and without metastatases ('metastases' and 'primary' groups, respectively) and unaffected donors. Overall, the samples used in the study came from 35 matched family groups, the majority of which were represented by one sample per pathology group.*

Figure 2.

A

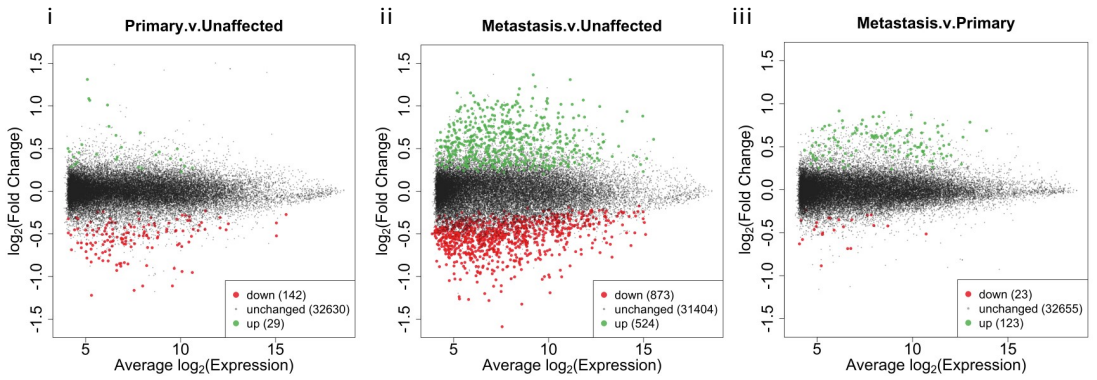

B

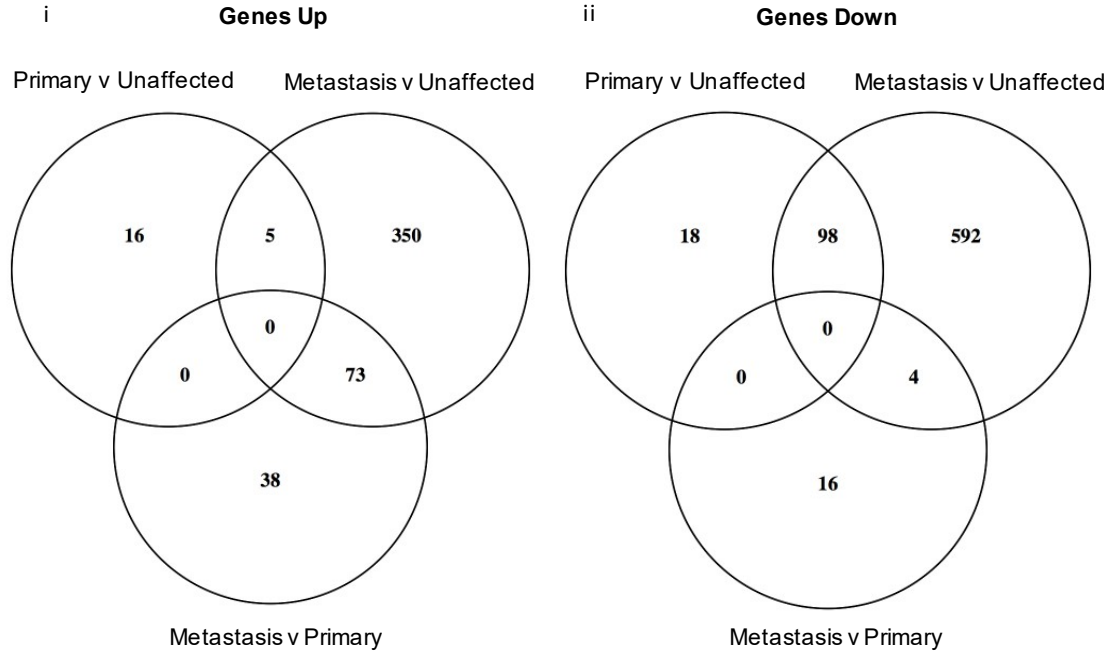

C

i 73 genes 'up' in Metastasis v Primary/Unaffected

GO biological process	Fold Enrichment	FDR
learning (GO:0007612)	13.76	1.90E-02
platelet degranulation (GO:0002576)	12.45	4.70E-02
blood coagulation (GO:0007596)	8.65	3.56E-02
coagulation (GO:0050817)	8.59	2.49E-02
hemostasis (GO:0007599)	8.5	2.01E-02

ii 592 genes 'down' in Metastasis v Unaffected

GO biological process	Fold Enrichment	FDR
gene expression (GO:0010467)	1.64	6.52E-05
RNA metabolic process (GO:0016070)	1.64	2.20E-04
transcription, DNA-templated (GO:0006351)	1.62	7.46E-03
nucleic acid-templated transcription (GO:0097659)	1.62	6.83E-03
response to stimulus (GO:0050896)	0.72	4.89E-03

Figure 2. Changes in PBMC transcriptomes during breast cancer metastasis. (*A) i-iii) Plots show differentially expressed probes in PBMCs from i) breast cancer patients with no metastases ('primary') compared to unaffected donors; ii) breast cancer patients with metastases ('metastasis') compared to unaffected donors; and iii) 'metastasis' compared to 'primary' breast cancer patients. Probes are plotted on a log_2 scale for fold change and expression. Probes significantly higher are coloured in green ('up') and probes expressed significantly lower are coloured red ('down') for each comparison. The number and direction of differentially expressed probes are indicated for each comparison. Significance was determined using a BH-adjusted P-value < 0.05. (B) Venn diagrams show the overlap between i) genes expressed significantly higher 'genes up' in any comparison and ii) genes expressed significantly lower in any comparison. (C) i) The top 5 most enriched gene ontologies in 73 gene 'up' in 'metastasis' compared to 'primary' and 'unaffected'. GO terms are ranked by fold enrichment. Significance determined by Fisher Exact with FDR <0.05.*

Figure 3.

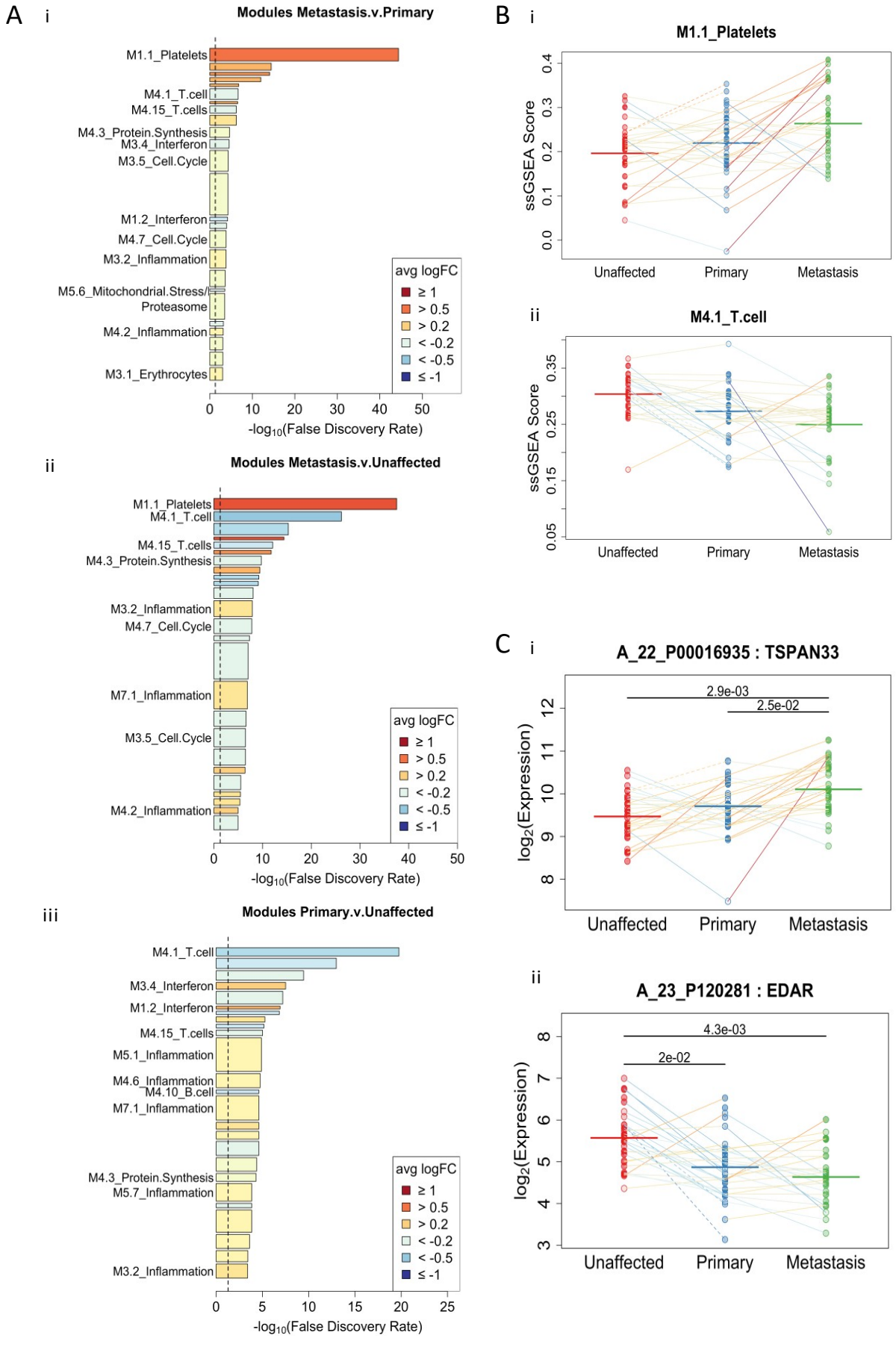
A
i
Modules Metastasis.v.Primary
M1.1_Platelets
M4.1_T.cell
M4.15_T.cells
M4.3_Protein.Synthesis
M3.4_Interferon
M3.5_Cell.Cycle
M1.2_Interferon
M4.7_Cell.Cycle
M3.2_Inflammation
M5.6_Mitochondrial.Stress/ Proteasome
M4.2_Inflammation
M3.1_Erythrocytes
avg logFC
≥ 1
> 0.5
> 0.2
< -0.2
< -0.5
≤ -1
0 10 20 30 40 50
-log10(False Discovery Rate)
ii
Modules Metastasis.v.Unaffected
M1.1_Platelets
M4.1_T.cell
M4.15_T.cells
M4.3_Protein.Synthesis
M3.2_Inflammation
M4.7_Cell.Cycle
M7.1_Inflammation
M3.5_Cell.Cycle
M4.2_Inflammation
avg logFC
≥ 1
> 0.5
> 0.2
< -0.2
< -0.5
≤ -1
0 10 20 30 40 50
-log10(False Discovery Rate)
iii
Modules Primary.v.Unaffected
M4.1_T.cell
M3.4_Interferon
M1.2_Interferon
M4.15_T.cells
M5.1_Inflammation
M4.6_Inflammation
M4.10_B.cell
M7.1_Inflammation
M4.3_Protein.Synthesis
M5.7_Inflammation
M3.2_Inflammation
avg logFC
≥ 1
> 0.5
> 0.2
< -0.2
< -0.5
≤ -1
0 5 10 15 20 25
-log10(False Discovery Rate)
B
i
M1.1_Platelets
ssGSEA Score
0.0 0.1 0.2 0.3 0.4
Unaffected Primary Metastasis
ii
M4.1_T.cell
ssGSEA Score
0.05 0.15 0.25 0.35
Unaffected Primary Metastasis
C
i
A_22_P00016935 : TSPAN33
2.9e-03
2.5e-02
log2(Expression)
8 9 10 11 12
Unaffected Primary Metastasis
ii
A_23_P120281 : EDAR
4.3e-03
2e-02
log2(Expression)
3 4 5 6 7 8
Unaffected Primary Metastasis

Figure 3. Immune module enrichment in blood during breast cancer metastasis. *Analysis of module gene set expression using competitive gene set testing. (A) i-iii) Graphs show gene modules enriched in PBMCs from i) 'metastasis' breast cancer patients compared to 'primary' patients; ii) 'metastasis' compared to 'unaffected' donors; and iii) 'primary' breast cancer patients compared to 'unaffected' donors. Enriched modules are listed on the y axis and ranked by false discovery rate. The length of each bar shows the* $-\log_{10}$*(FDR) for the gene set. The width of each bar shows the relative gene set size and the colour shows the average log fold change of the probes in gene set (red indicates that the gene set is positively enriched; blue that the gene set is negatively enriched; yellow indicates that the average log fold change is zero). (B) i-ii) Plots show ssGSEA-assigned gene set scores for each sample based on the expression of genes within a set of interest. Plots shows individual samples within each patient group linked to other members of the same family (lines are coloured by* $\log_2$ *fold change, dotted lines indicate samples with only two family members). Samples are shaded by array weighting. Mean scores per group are indicated. (C) i-ii) Plots show transcript expression for TSPAN33 & EDAR across groups. Significance was determined using a BH-adjusted P-value < 0.05 and indicated on each plot.*

Figure 4.

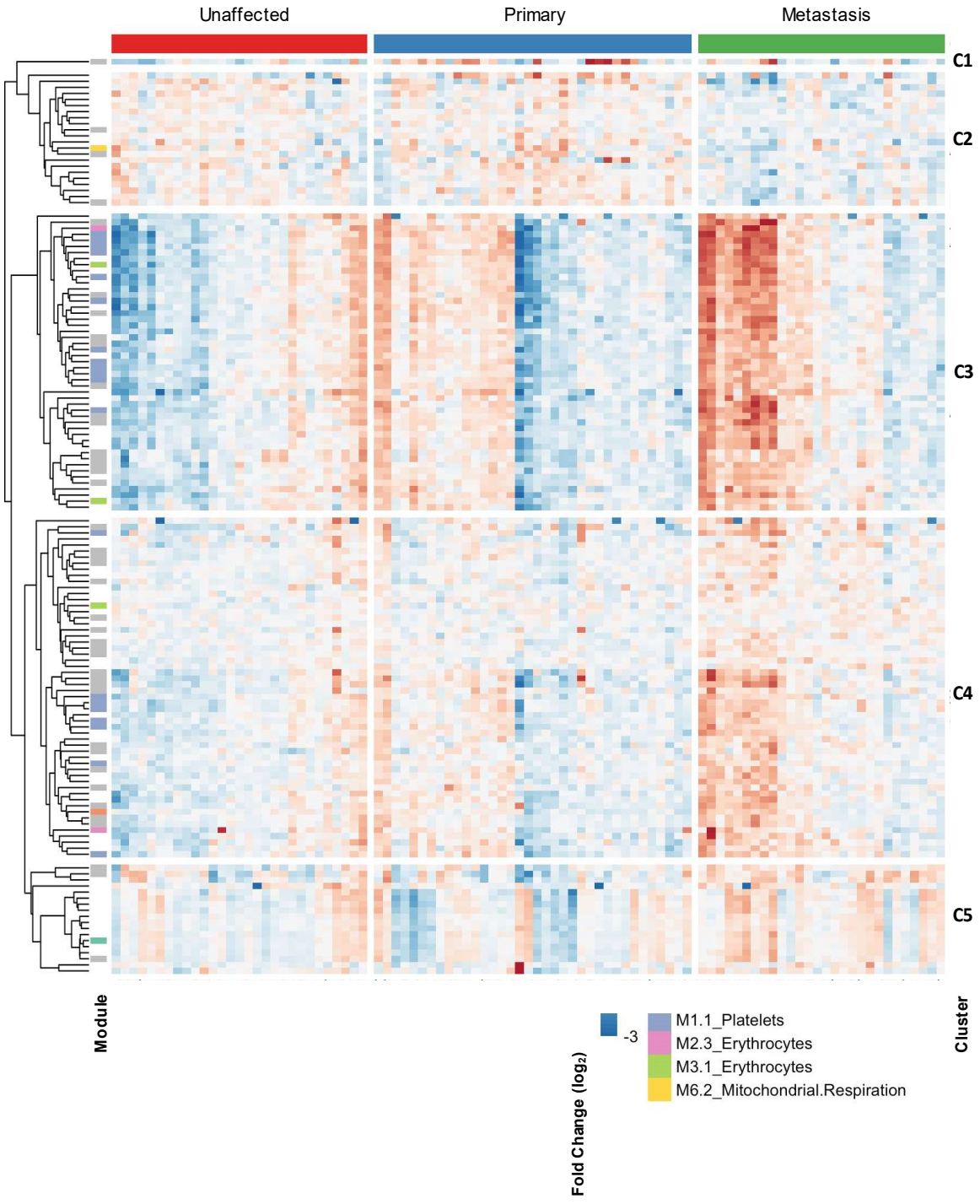
Unaffected
Primary
Metastasis
C1
C2
C3
C4
C5
Module
Cluster
Fold Change (log2)
-3
M1.1_Platelets
M2.3_Erythrocytes
M3.1_Erythrocytes
M6.2_Mitochondrial.Respiration

Figure 4. Clustered blood signatures in breast cancer metastasis. *Heat map shows hierarchical clustering (C1 – C5) and the expression of 146 probes significantly differentially expressed in 'metastasis' patients compared to 'primary' patients. Samples are arranged by group indicated on the x axis and corresponding gene set modules for each probe are displayed on the left y axis. the significance and direction of probe expression for each comparison is indicated in the y axis. Probes show expression level relative to the average of each probe across all the samples. Significance was determined using a BH-adjusted P-value < 0.05.*

Table 4. Clustered probes differentially expressed in blood during breast cancer metastasis.

Cluster	No. of probes	Genes of interest	Module	IFN regulated gene in Interferome database
C1	1	*KCNJ2*	Other	Yes
C2	22	*GXYLT1* *AQR* *MRPS18C* *BCDIN3D*	Other Mitochondrial Resp. Other Other	Yes
C3	49	*XK* *TREML1* *ALOX12* *F13A1* *EGF* *FAXDC2* *NRGN* *ASAP2* *ACRBP* *TMEM40* *ABLIM3* *TGFB1I1* *PBX1*	Erythrocytes Platelets Platelets Platelets Platelets Erythrocytes Platelets Platelets Platelets Platelets Platelets Other Erythrocytes	 Yes Yes Yes Yes Yes Yes Yes Yes
C4	56	*ATP2C1* *TFPI* *MAX* *R3HDM4* *TNNC2* *TSAN33* *GRAP2* *MMD* *HDGF* *ACTN1* *TRIM10* *HIST1H2AG*	Other Platelets Other Erythrocytes Platelets Platelets Platelets Platelets Other Inflammation Erythrocytes Platelets	Yes Yes Yes Yes Yes Yes Yes Yes Yes
C5	18	*KLF6* *FOSB* *ADRA1A* *CBX7*	Other Other Cell Cycle Other	Yes Yes Yes Yes

Figure 5.

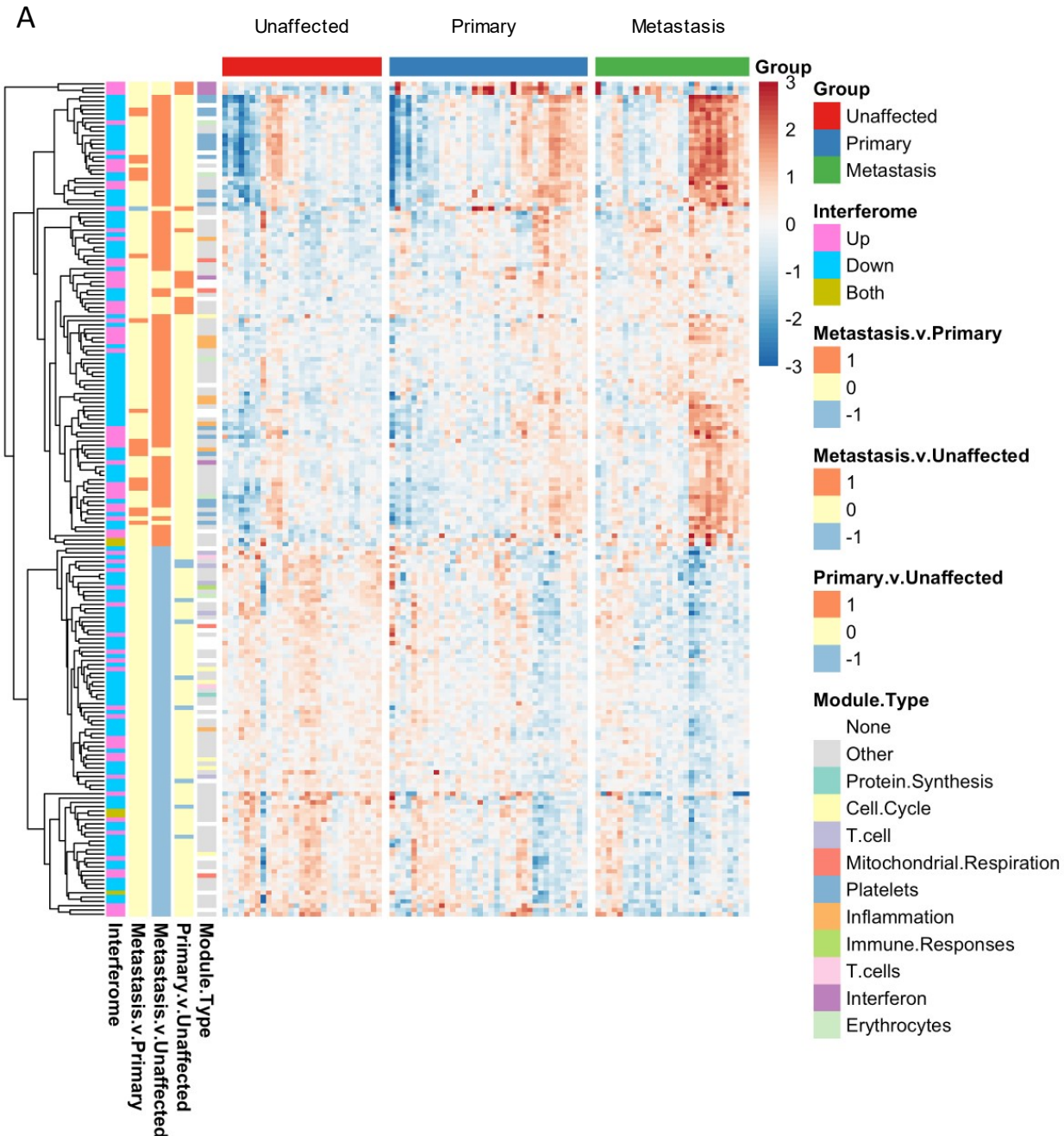
A
Unaffected
Primary
Metastasis
Group
3
2
1
0
-1
-2
-3
Group
Unaffected
Primary
Metastasis
Interferome
Up
Down
Both
Metastasis.v.Primary
1
0
-1
Metastasis.v.Unaffected
1
0
-1
Primary.v.Unaffected
1
0
-1
Module.Type
None
Other
Protein.Synthesis
Cell.Cycle
T.cell
Mitochondrial.Respiration
Platelets
Inflammation
Immune.Responses
T.cells
Interferon
Erythrocytes
Interferome
Metastasis.v.Primary
Metastasis.v.Unaffected
Primary.v.Unaffected
Module.Type

B i

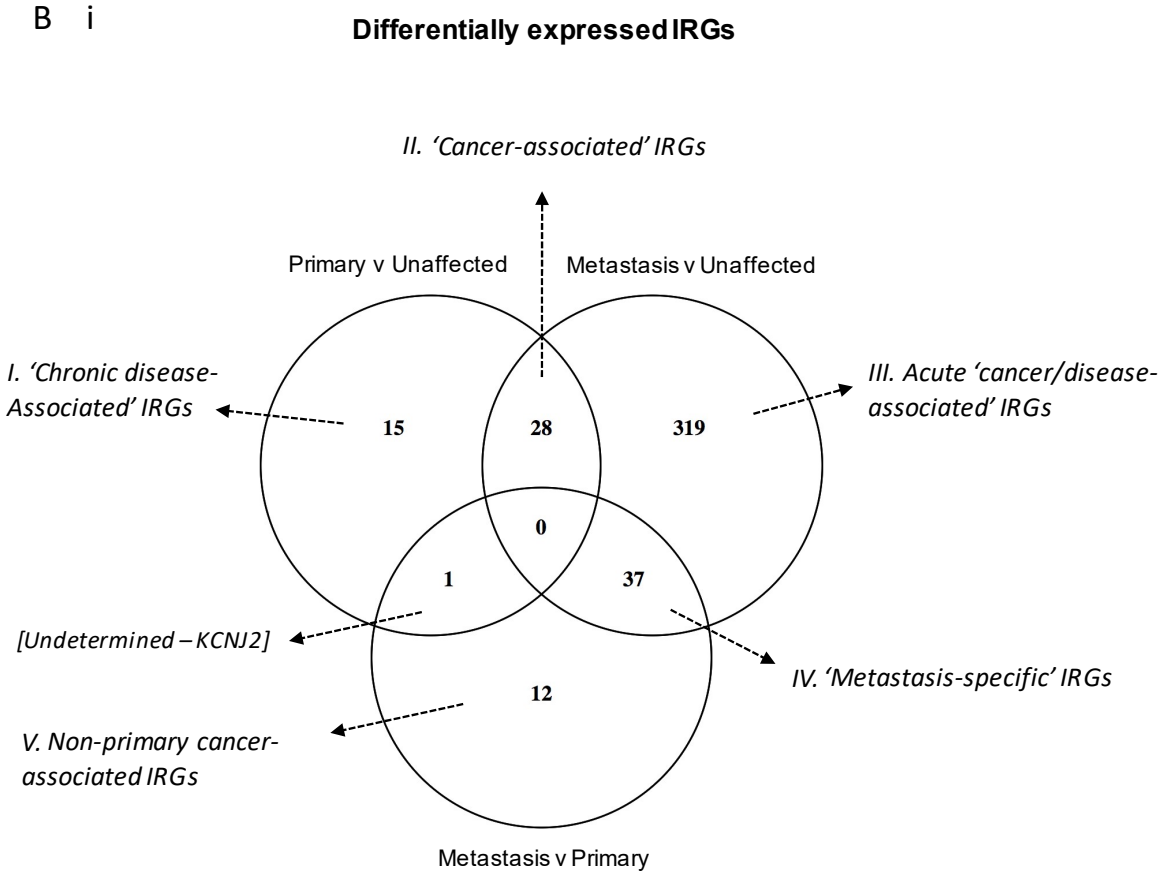

ii Combined 368 metastasis-associated IRGs

GO biological process	Fold Enrichment	FDR
platelet degranulation (GO:0002576)	9.13	1.16E-08
homotypic cell-cell adhesion (GO:0034109)	7.87	3.74E-02
platelet activation (GO:0030168)	5.76	1.29E-03
cell junction assembly (GO:0034329)	5.05	1.39E-02
regulation of muscle contraction (GO:0006937)	4.5	2.48E-02
cell junction organization (GO:0034330)	4.38	6.10E-03
blood coagulation (GO:0007596)	3.96	1.14E-03
coagulation (GO:0050817)	3.94	1.08E-03

Figure 5. Distinct peripheral interferon signatures in breast cancer metastasis. *A) Heat map shows IRGs that were significantly differentially expressed across any patient group comparison and were present in the INTERFEROME database query (human blood cell genes up- or down- regulated ≥ 2 fold in response to IFN treatment). The direction of regulation of the gene within the INTERFEROME is shown on the left y axis as well as whether the probe was significantly up or down in the three comparisons between the groups and the corresponding gene set modules for each gene. Probes are expressed as fold change (log_2). Significance was determined using a BH-adjusted P-value < 0.05. (B) i) Venn diagram shows the overlap between IRGs that were significantly differentially expressed across each group comparison and arrows point to descriptive term for each set. ii) Table shows the top 8 most enriched gene ontologies in combined 368 'metastasis-associated' IRGs. GO terms are ranked by fold enrichment. Significance determined by Fisher Exact with FDR <0.05.*

Figure 6.

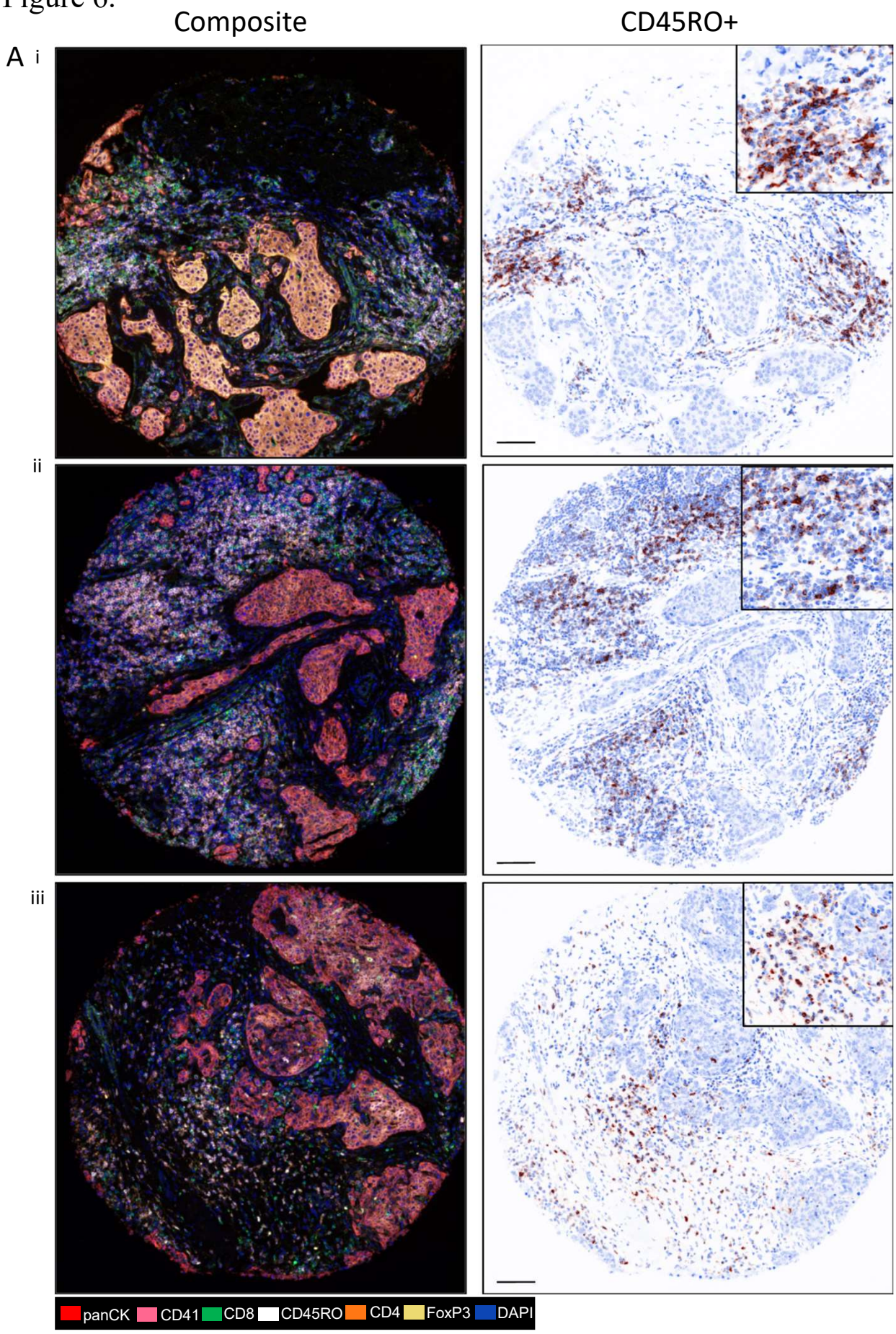
Composite
CD45RO+
A i
ii
iii
panCK
CD41
CD8
CD45RO
CD4
FoxP3
DAPI

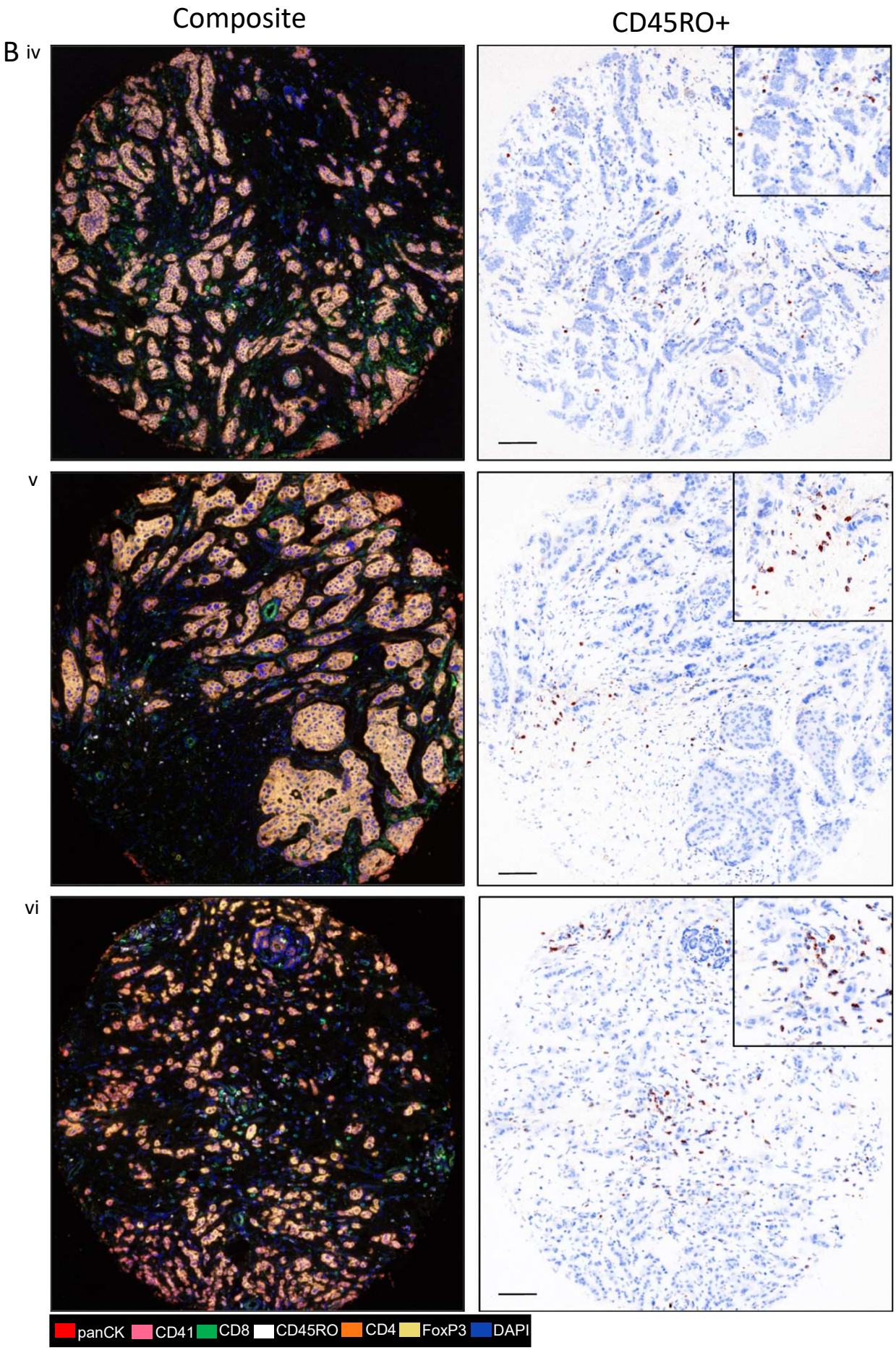
Composite
CD45RO+
B iv
v
vi
panCK
CD41
CD8
CD45RO
CD4
FoxP3
DAPI

B

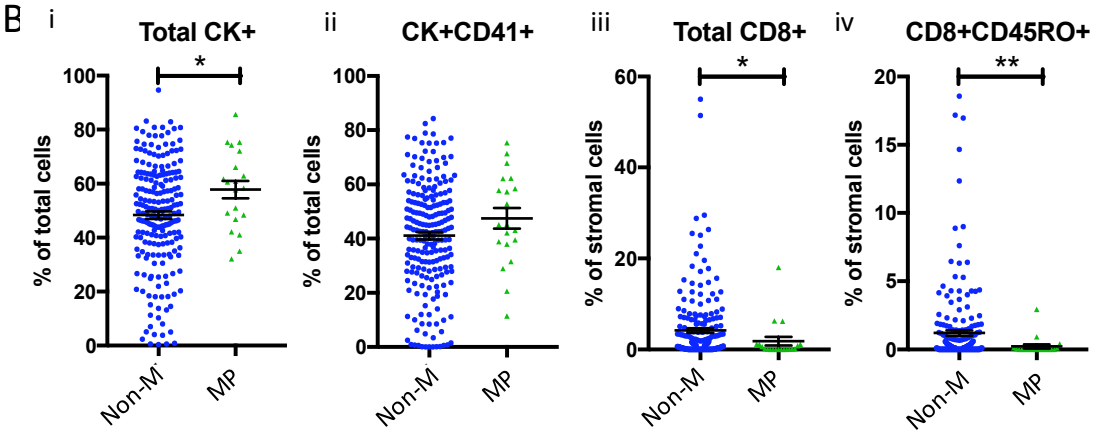

C

Patient	Primary Tumour Group	Stromal region	Metastasis-free survival (days)	Mortality
i	Non-M	73.03%	9885	Deceased
ii	Non-M	82.78%	5131	Alive
iii	Non-M	76.51%	7633	Alive
iv	MP	58.69%	4397	Deceased
v	MP	48.43%	7434	Alive
vi	MP	63.39%	488	Deceased

Figure 6. Local cell signatures in primary breast tumours reflect metastatic potential. *Tissue microarrays from primary breast tumours were multiplex stained for a panel of markers: panCK, CD41, CD4, FoxP3, CD8, CD45RO and DAPI. (A) Images show composite (all markers) and pathology (deconvoluted CD45RO+) stains from i – iii) three non-metastatic breast cancer patients and iv-vi) three breast cancer patients with metastatic potential. (B) i – ii) Graphs show quantification of mutlispectral analysis using InForm software for percentage positive cells per total cells in the core for panCK+ and CD41+, or per stromal content for CD8+ and CD8+CD45RO+. (C) Table shows patient number, tumour group, percentage of stromal cells per tissue core, number of days until diagnosis with metastasis (MFS) or time of tissue biopsy (for non-metastatic patients) and recorded patient mortality at time of study. Scale bars for IHC images black=100um. Significance was determined by Mann-Whitney t tests **p<0.01, *p<0.05.*

Figure 7.

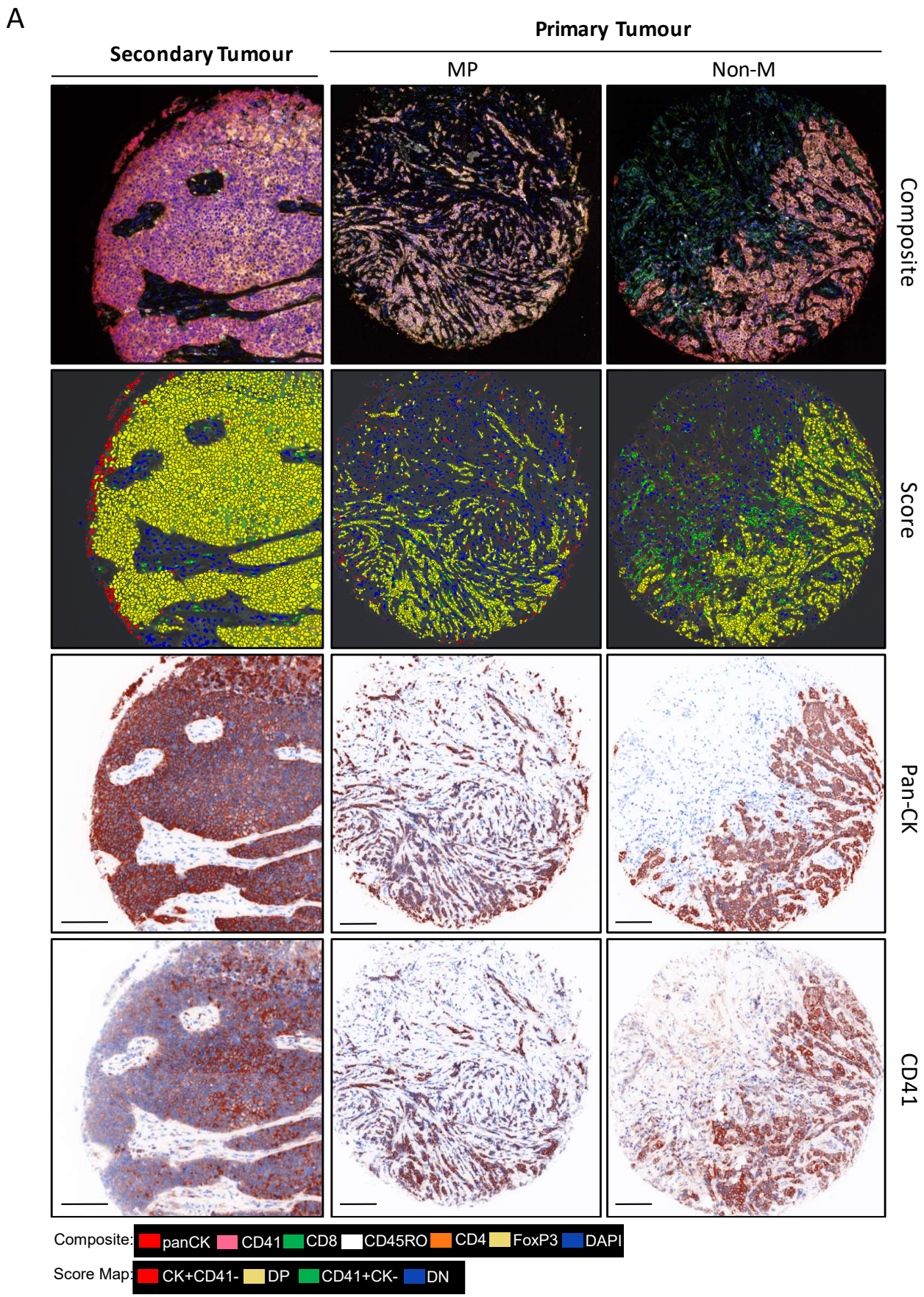
A
Secondary Tumour
Primary Tumour
MP
Non-M
Composite
Score
Pan-CK
CD41
Composite: panCK CD41 CD8 CD45RO CD4 FoxP3 DAPI
Score Map: CK+CD41- DP CD41+CK- DN

B

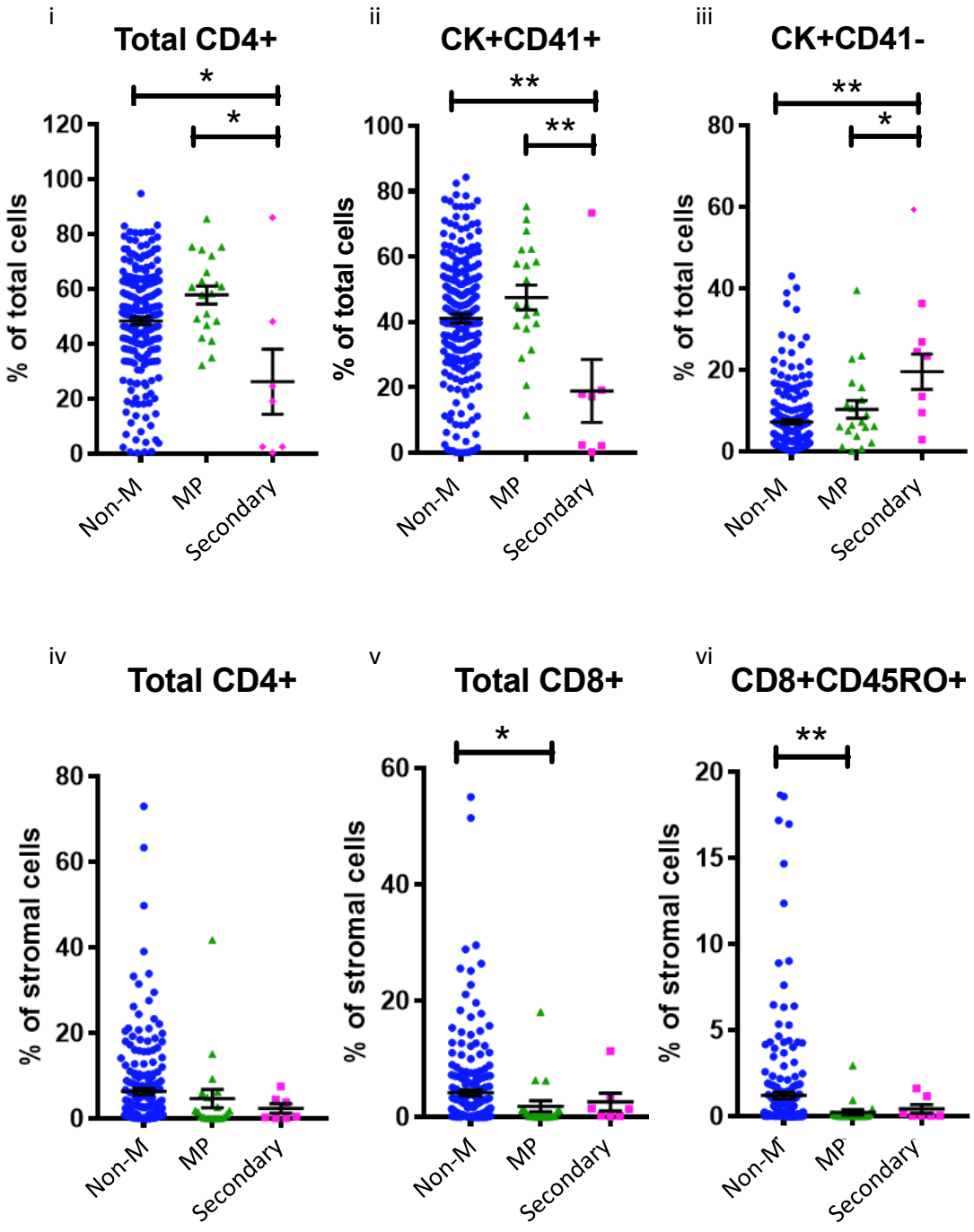
i
Total CD4+
% of total cells
Non-M
MP
Secondary
ii
CK+CD41+
% of total cells
Non-M
MP
Secondary
iii
CK+CD41-
% of total cells
Non-M
MP
Secondary
iv
Total CD4+
% of stromal cells
Non-M
MP
Secondary
v
Total CD8+
% of stromal cells
Non-M
MP
Secondary
vi
CD8+CD45RO+
% of stromal cells
Non-M
MP
Secondary

Figure 7. Distant signatures in breast cancer metastases. *Tissue microarrays from secondary and primary breast tumours multiplex stained for a panel of markers: panCK, CD41, CD4, FoxP3, CD8, CD45RO and DAPI. (A) Images show composite (all markers) and pathology (deconvoluted CD45RO+) stains from i – iii) three non-metastatic breast cancer patients and iv-vi) three breast cancer patients with metastatic potential. (B) i – ii) Graphs show quantification of mutlispectral analysis using InForm software for percentage positive cells per total cells in the core for panCK+ and CD41+, or per stromal content for CD8+ and CD8+CD45RO+. (C) Table shows patient number, tumour group, percentage of stromal cells per tissue core, number of days until diagnosis with metastasis (MFS) or time of tissue biopsy (for non-metastatic patients) and recorded patient mortality at time of study. Scale bars for IHC images black=100um. Significance was determined by Mann-Whitney t tests ****p<0.0001, **p<0.01, *p<0.05.*

Supplementary Figure 1.

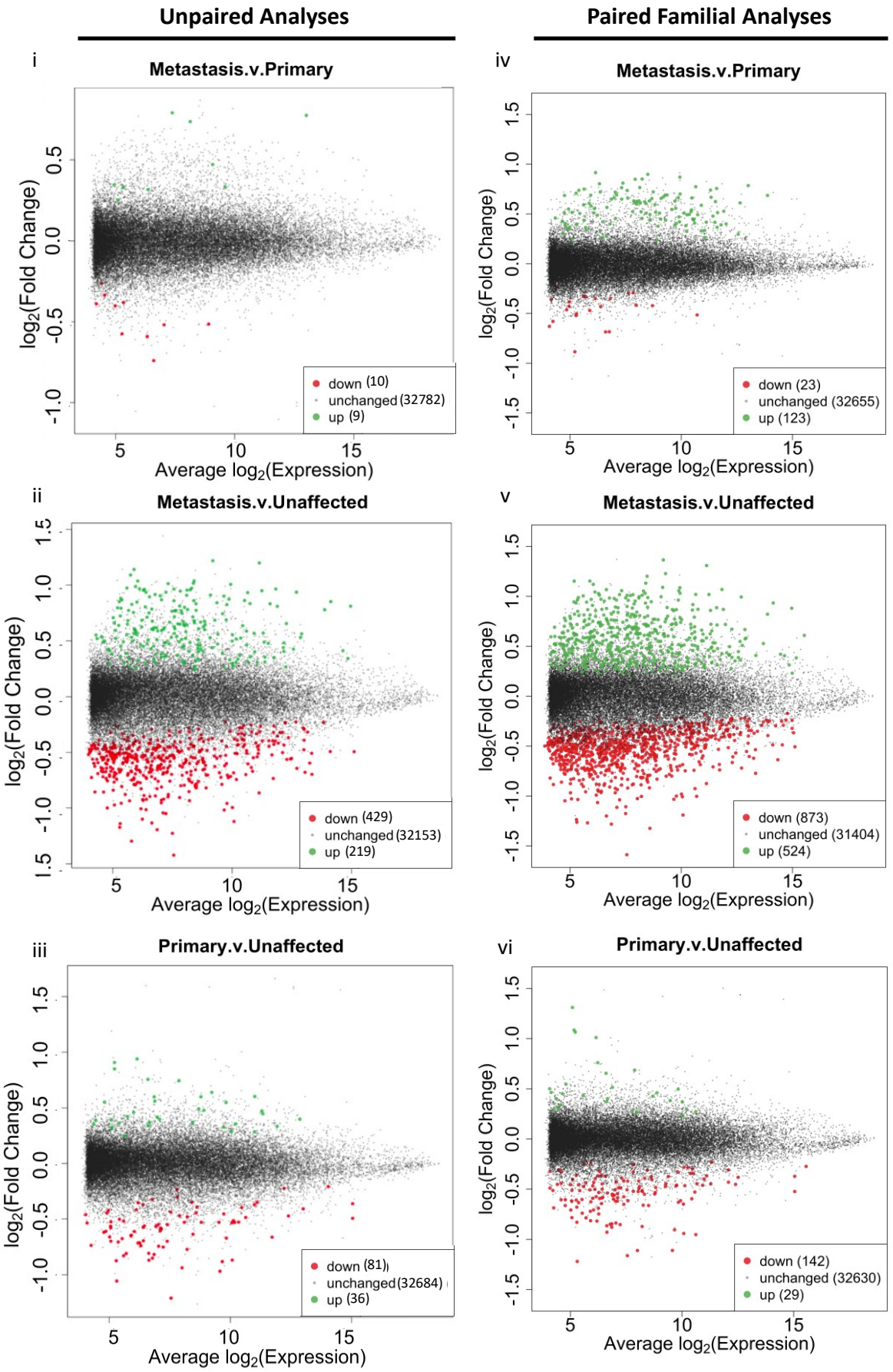

Supplementary Figure 1. Increased analytical power of analyses of blood transcriptomics using matched familial controls. *i-iii) Plots show differentially expressed probes analysed using unpaired analyses of PBMCs from i) breast cancer patients with no metastases ('primary') compared to unaffected donors; ii) breast cancer patients with metastases ('metastasis') compared to unaffected donors; and iii) 'metastasis' compared to 'primary' breast cancer patients.*
iv–vi) Plots show differentially expressed probes analysed using familial paired analyses of PBMCs from from the same patient comparison as (i-iii). Probes are plotted on a log_2 *scale for fold change and expression. Probes significantly higher are coloured in green ('up') and probes expressed significantly lower are coloured red ('down') for each comparison. The number and direction of differentially expressed probes are indicated for each comparison.*

CHAPTER 4:

Role of a Unique Type I Interferon, Interferon Epsilon, in Suppressing Epithelial Ovarian Cancer

4.1 Declaration

Monash University

Declaration for Thesis Chapter 4

Declaration by candidate

In the case of Chapter 4, the nature and extent of my contribution to the work was the following:

Nature of contribution	**Extent of contribution (%)**
Acquisition of data, analysis and interpretation and writing, reviewing and editing the manuscript	70 %

The following co-authors contributed to the work. If co-authors are students at Monash University, the extent of their contribution in percentage terms must be stated:

Name	**Nature of Contribution**	Extent of contribution (%) Authors Only
Niamh E. Mangan	See statement below	
Michelle D. Tate		
Anthony Y. Matthews		
Sarah Rosli		
Maree Bilandzic		
Elizabeth L. Christie		
Andrew N. Stephens		
David. D.L. Bowtell		
Nicole A. de Weerd		
Nollaig M. Bourke		
Paul J. Hertzog		

AUTHOR CONTRIBUTIONS

Conception and Design: Z.C.M, N.E.M, D.D.L.B, N.M.B and P.J.H

Development of Methodology: Z.C.M, N.E.M, M.D.T, A.Y.M, M.B, A.N.S, N.A.dW, N.M.B and P.J.H.

Acquisition of Data: Z.C.M, N.E.M, M.D.T, S.R, N.M.B and P.J.H.

Analysis and Interpretation of Data: Z.C.M, N.E.M, M.D.T, E.L.C, D.D.L.B, N.M.B and P.J.H.

Writing, Review and/or Editing of the Manuscript: Z.C.M, N.M.B and P.J.H.

Study Supervision: N.M.B and P.J.H.

The undersigned hereby certify that the above declaration correctly reflects the nature and extent of the candidate's and co-authors' contributions to this work.

Candidate's Signature	[redacted]	**Date 24/01/2018**

Main Supervisor's Signature	[redacted]	**Date 24/01/2018**

4.2 Role of a Unique Type I Interferon, Interferon Epsilon, in Suppressing Epithelial Ovarian Cancer

Zoë C. Marks, Niamh E. Mangan, Michelle D. Tate, Anthony Y. Matthews, Sarah Rosli, Maree Bilandzic, Elizabeth L. Christie, Andrew N. Stephens, David D.L. Bowtell, Nicole A. de Weerd, Nollaig M. Bourke and Paul J. Hertzog. Submitted Manuscript.

Role of a unique type I interferon, interferon epsilon, in suppressing epithelial ovarian cancer

Zoe C. Marks[1,2], Niamh E. Mangan[1], Michelle D. Tate[1], Antony Y. Matthews[1], Sarah Rosli[1] Maree Bilandzic[2,3], Elizabeth L. Christie[4], Andrew N. Stephens[2,3], David D.L. Bowtell[4], Nicole A. de Weerd[1], Nollaig M. Bourke[1,5,6,] & Paul J. Hertzog[1,2,6,*]

[1] Centre for Innate Immunity and Infectious Diseases; Hudson Institute of Medical Research; Clayton, Victoria, 3168; Australia.

[2] Department of Molecular and Translational Science; Monash University; Clayton, Victoria, 3168; Australia.

[3] Centre for Cancer Research; Hudson Institute of Medical Research; Clayton, Victoria, 3168; Australia.

[4] Cancer Genomics and Genetics Program; Peter McCallum Cancer Centre; Melbourne, Victoria, 3000; Australia.

[5] Department of Medical Gerontology, School of Medicine, Trinity Translational Medicine Institute; Trinity College Dublin; The University of Dublin, College Green, Dublin 2; Ireland

[6] These authors contributed equally to this work.

* Correspondence: [redacted]

ACKNOWLEDGEMENTS

This work was supported by project grants from the National Health and Medical research Council of Australia (NHMRC) to PJH, MDT, DDLB. ZCM is supported by an Australian Postgraduate Award; MB and ANS are supported by the Ovarian Cancer Foundation of Australia; NEM is supported by a Fielding Foundation Fellowship; PJH is supported by NHMRC Senior Principal Research fellowship.

This work was also supported by the United States of America's Office of the Assistant Secretary of Defense for Health Affairs through the Ovarian Cancer Research Program under Award No. W81XWH-15-1-0106. Opinions, interpretations, conclusions and recommendations are those of the author and are not necessarily endorsed by the United States of America's Department of Defense.

In conducting research using animals, the investigators adhered to the laws of Australia and received ethical approval for this research from the Monash University Animal Ethics Committee A and the United States of America's Department of Defense.

In conducting research using human tissues, the investigators adhered to the laws of Australia and receive ethical approval for this research from the Monash Health Human Research Ethics Committee (ratified by the Monash University Human Research Ethics Committee).

The authors would like to acknowledge Rebecca Smith for assistance with preparation of the manuscript.

This work is supported from the Operational Infrastructure Fund of the State Government of Victoria.

AUTHOR CONTRIBUTIONS

ZRM was involved in conceptualisation, methodology, formal analysis, investigation aspects of the project and in writing the original draft, review and editing the manuscript

NEM – conceptualisation, methodology, formal analysis and investigation of experiments

MDT – investigation, formal analysis

AYM – provisional of critical resources

SR - investigation

MB - resources and methodology

ELC – Formal analysis and data curation

ANS - resources and methodology

DDLB – methodology, data curation and analysis, and conceptualisation

NAdW –provision of resources and review of manuscript

NMB – conceptualisation, methodology, formal analysis, investigation, contribution to original draft, review and editing manuscript, supervision and acquisition of funding

PJH– conceptualisation, methodology, formal analysis, resources, contribution to original draft, review and editing manuscript, supervision and acquisition of funding

*All authors had input into review or editing the manuscript.

DECLARATION OF INTERESTS

The authors declare no competing interests.

Summary:

IFNε is a distinct type I interferon (IFN), uniquely regulated and constitutively expressed in female reproductive tract epithelium, where it protected from infection. We present the first evidence of anti-tumour functions of IFNε. Epithelial IFNε was reduced in high grade serous carcinoma (HGSC); residual expression correlated with survival. In orthotopic ovarian cancer models, mice lacking endogenous IFNε had increased peritoneal metastases and exogenous IFNε suppressed metastases in models of developing, established and advanced cancer. The mechanism of action of IFNε was in part, via direct tumour cell growth suppression, shown *in vitro* and in IFNAR$^{-/-}$ mice. Furthermore, both endogenous and exogenous IFNε regulated immune response inducing activation and expression of PD1/PDL1. Collectively our data demonstrates a critical role for IFNε in the development and potential treatment of HGSC.

Significance:

HGSC is the most lethal reproductive tract cancer with late stage peritoneal metastases and poor treatment options resulting in a poor survival. We demonstrate a new cytokine involved in tumour development and potential treatment. IFNε, is unique type I IFN constitutively expressed in the FRT epithelium from which HGSC arise, had intrinsic and extrinsic anti-tumour activities. We showed the first evidence for the suppressive role of endogenous IFNε in models of tumourigenesis and progression. In preclinical, orthotopic models our recombinant IFNε□inhibited□via mechanisms including direct effects on tumour cells. The distinct characteristics of IFNε especially its tolerated, continuous expression in the FRT, and correlation of endogenous levels with improved survival, make it an attractive therapeutic option, fit for purpose in that location. Additionally, IFNε activates immune effector cells and

stimulates PD1 and PDL1 expression, making it also, an attractive candidate for combination therapy.

INTRODUCTION

Understanding the inventory and mechanism of action of factors that modulate the development and pathogenesis of tumours is key to devising new treatments in particular for intractable cancers. Ovarian cancer is the most lethal female reproductive cancer (U.S. Cancer Statistics Working Group, 2017). Epithelial ovarian cancer is a complex, heterogeneous disease comprising a number of molecularly distinct tumour types arising in the peritoneal cavity (Jayson et al., 2014; Tothill et al., 2008; Vaughan et al., 2011), the most common of which are high grade serous carcinomas (HGSC). Currently, standard therapy includes debulking surgery and platinum-based chemotherapy, however ovarian tumours often develop platinum resistance (Patch et al., 2015). Furthermore, due to the lack of effective screening for this disease and a predominance of vague, abdominal symptoms, many women first present with late-stage, metastatic disease associated with malignant ascites. These factors contribute to an estimated 5-year survival rate which is usually below $50^{\%}$. Consequently, a greater understanding of the pathogenesis of this disease to facilitate novel targeted therapies is urgently needed to improve outcomes for HGSC.

The type I interferons (IFNs) are a family of cytokines known to have pleiotropic functions including the ability to exhibit anti-cancer effects via tumour cell intrinsic and extrinsic immunomodulatory signalling (Parker et al., 2016). While these anti-cancer properties have held promise in the clinical treatment of cancer, the successes have been limited to haematological malignancies such as leukaemia (Anguille et al., 2011) and solid tumours such as melanoma (Akman et al., 2014; Ascierto et al., 2014; Kirkwood et al., 2001; Mocellin et al., 2010; Pasquali and Mocellin, 2010). Indeed, to date, type I IFN therapy has yielded little clinical benefit against ovarian cancer (Alberts et al., 2006; Berek et al., 1985; Berek et al., 1999; Bruzzone et al., 1997; Frasci et al., 1994; Hall et al., 2004; Markman et al., 2004;

Markman et al., 1992; Moore et al., 1995; Willemse et al., 1990), restricted by the same issues that limit high dose IFN use in other solid malignancies. These reflect the biological function of type I IFNs – evolved as potent, rapidly-responding, acute acting, innate immune cytokines that protect the host from invading pathogens but whose sustained presence or excessive amounts are toxic. It is likely that the conventional members of this family are therefore limited in their use as high-dose, long-term therapies required to eradicate diffuse, metastatic tumours.

IFNε is a distinct type I IFN that appears to have evolved to protect mucosa, particularly in the female reproductive tract (FRT), by novel mechanisms (Fung et al., 2013; Hardy et al., 2004). We have demonstrated it to be a type I IFN that signals through Ifnar1 and Ifnar2 activating the JAK-STAT pathway to induce conventional IFN regulated genes (IRGs) and associated anti-viral, anti-bacterial and immunoregulatory activities using in vitro assays (Stifter et al., 2017). Unlike conventional IFNs, our studies have shown it constitutively expressed in endometrial epithelium and regulated by hormones (Fung et al., 2013). We characterised its role in protecting the FRT from infection by mechanisms including regulation of immune effector cells (Fung et al., 2013) that are also important in anti-tumour immunity. However, the anti-tumour properties of IFNε have not been previously addressed, so we herein examined the role of this well tolerated IFNε in the development of ovarian cancer. We demonstrate for the first time that IFNε has anti-tumour intrinsic and extrinsic actions. Specifically, we demonstrate that IFNε is constitutively and strongly expressed within the epithelium of the fallopian tube which contains the putative cell of origin of HGSC, the secretory epithelial cells (Perets et al., 2013), that this expression is lost in HGSC and this suppression correlates with poor survival. We show that IFNε has anti-proliferative, pro-apoptotic effects on ovarian cancer cells *in vitro* and have generated compelling data using *in vivo* mouse models of ovarian cancer, that endogenous and exogenous IFNε strongly inhibit

the growth of metastatic ovarian cancer through cell intrinsic as well as extrinsic anti-tumour effects by modulating immune responses.

RESULTS

Reduced expression of Fallopian tube epithelial IFNε in High Grade Serous Ovarian cancer correlates with poor prognosis

To identify the potential role of IFNε in ovarian cancer, it was important to first characterise its endogenous expression in human fallopian tube (FT) epithelium which contains secretory epithelial cells (SEC), which are the putative cells of origin of many HGSCs (Kurman and Shih Ie, 2011). Using immunohistochemistry, we showed IFNε expression in apparently all epithelia including the SEC (Fig. 1A, panels i-ii). This expression pattern was similar to that of an epithelial marker, cytokeratin 18 and contrasted with smooth muscle actin (SMa), which stained predominately non-epithelial tissue (Sup. Fig1). We next confirmed this expression by analyzing a transcriptome dataset of human FT secretory cells and primary FT epithelium for expression of IFNs (Fig. 1A iii), demonstrating that IFNε was the only IFN highly and constitutively expressed in these cells (Fig 1A iii) (Fung et al., 2013; Bourke et al, unpublished).

This constitutive expression of IFNε was significantly suppressed in human HGSCs compared to normal FT epithelium. This was first demonstrated by staining of tissue microarrays for IFNε which showed suppressed expression in low grade serous carcinoma (LGSC) & HGSC both qualitatively (Fig. 1B i,ii) and quantitatively (Fig 1Biii). Secondly, we found significantly lower IFNε transcript levels in the Australian Ovarian Cancer Study cohort (Patch et al., 2015) of HGSC samples from 93 patients (Fig. 1C i, ii). Other type I IFNs such as IFNβ were essentially undetectable in normal and tumour epithelium (Figure 1Ci). Thirdly, we validated these findings by analyzing microarray data from an external cohort of a publically available, Cancer Science Institute of Singapore Ovarian Cancer Database (Tan et

al., 2015) of 707 samples of ovarian cancer and non-tumour tissues (Fig. 1Di). These analyses confirm the expression of IFNε in FT epithelium and its loss in HGSC.

To determine whether IFNε expression has an impact on clinical outcome, we interrogated clinical survival data on both the HGSC AOCS cohort of 93 cases and the CSIOVDB cohort of 707 cases. We identified that high IFNε expression HGSC correlates with increased progression-free and overall survival in both cohorts (Fig. 1Ciii and 1Dii, iii). Taken together these data demonstrate that IFNε a unique type I IFN constitutively expressed in normal epithelium, supressed in ovarian cancer where the lower levels correlate with poor prognosis.

IFNε has potent anti-tumour effects in a syngeneic, orthotopic model of ovarian cancer

Since the above data implies IFNε has anti-tumour properties and in the absence of any prior studies to demonstrate this, we first investigated IFNε activity in an *in vivo,* syngeneic, orthotopic model of ovarian cancer. The murine ovarian cancer cells, ID8 are injected, into the intrabursal space in the ovaries of immunocompetent mice (Greenaway et al., 2008;). This model enables the assessment of the direct and indirect anti-tumour effects of IFNε via tumour cell intrinsic and extrinsic (immunoregulatory) mechanisms on the 'primary' orthotopic tumour growth in the bursa and the different stages and locations of metastatic spread and growth in the peritoneal cavity.

Treatment with intraperitoneal injections of recombinant murine (rmu) IFNε significantly suppressed, in a dose-dependent manner, the growth of peritoneal metastases. This was evident firstly in the development of malignant, haemorrhagic ascites (Fig. 2A,) - a key characteristic of end-stage disease in the model that closely mimics the progression of human disease. Secondly, IFNε significantly reduced metastatic tumour deposits throughout

the peritoneal cavity quantified as tumour burden score in the mesentery and total number of metastases throughout the peritoneum (Fig. 2B, Ci, iii). Thirdly, IFNε also reduced haemorrhaging in the peritoneal cavity (Fig. 2A, Cii), another indication of advanced stage disease. Interestingly, despite marked reduction of tumour spread, IFNε had little effect on orthotopic, primary tumour growth with only a slight reduction in primary tumour size or weight (Fig. 2Di, ii), which did not reach significance (Fig 2 Dii). These results constitute the first demonstration that IFNε clearly has anti-tumour actions and that these are against ovarian cancer metastases.

Since conventional type I IFNs can exert their anti-tumour actions via immune cell recruitment and activation, we investigated IFNε induction of these parameters in this model. Tumour bearing mice had increased numbers and proportions of total leukocytes, $CD4^+$, $CD8^+$ and B lymphocytes as well as NK cells compared to non-tumour bearing mice (NT) (Supplementary Fig. 2A, B). A manual correlation of all parameters of 'primary' and metastatic tumour burden and responses of immune cells highlighted that this immunogenic tumour model triggered host defences, marked by elevated levels of immune cells that strongly correlated with disease progression in our model (Sup. Fig. 2B, 3- correlations with disease scoring). Crucially, while total immune cell numbers reflected more the presence of disease rather than differences between treatment groups, mice treated with IFNε had significantly higher proportions of activated immune cells and expression of checkpoint molecules, demonstrated by induction of CD69 and PD-1 on $CD4^+$ T cells, $CD8^+$ T cells, NK cells and B cells (Fig. 2Ei-iv). Indeed, disease suppression by IFNε correlated with activation of certain cell types, including $CD4^+CD69^+PD1^+$ T cells and $B220^+CD69^+$ B cells (Sup. Fig. 3A and B). These results show that tumour elicits a significant immune cell recruitment, but these immune cells appear not to be effective at clearing tumour burden unless activated by IFNε treatment. Thus,

we demonstrate for the first time, that the novel type I IFNε has potent anti-tumour and immune activation activity *in vivo*.

In order to demonstrate the anti-tumour actions of IFNε in a more clinically relevant setting, we examined its activity on an established tumour and compared activity to a conventional type I IFN, IFNβ. Remarkably, delaying onset of IFN treatment by 4 weeks (to allow more established orthotopic tumours to form) did not diminish overall IFNε efficacy. Delayed-onset IFNε therapy suppressed peritoneal spread of ovarian cancer as evident from mesenteric tumour burden, peritoneal haemorrhaging and overall metastatic score (Fig 3B); but was ineffective at suppressing orthotopic 'primary' tumour development (Fig. 3A). In contrast, mice receiving delayed-onset IFNβ therapy did not exhibit reduced primary or peritoneal tumour burden (Fig. 3A). Strikingly, IFNε treatment was also significantly more effective than IFNβ at activating the majority of peritoneal immune populations, inducing CD69 and or the checkpoint molecule, PD1 on $CD4^+$ and $CD8^+$ T cells and B cells, whereas both IFNs significantly activated NK cells (Fig. 3Ci - iv).

Thus IFNε demonstrates anti-tumour activity on the peritoneal spread of both developing and established ovarian cancer, more so than equivalent units of IFNβ; and furthermore, IFNε activates immune cells including CD4 and CD8 T cells and NK cells and expression of checkpoint markers.

IFNε suppresses ascites and metastasis in a model of advanced ovarian cancer

Since the vast majority of HGSCs present as late-stage metastatic disease, we assessed the efficacy of exogenous IFNε treatment in a model recapitulating this advanced disease by injecting ID8 cells directly into the peritoneum. Mice displayed extensive disseminated tumour growth throughout the peritoneum, with adhesions & growth of tumour nodules on multiple

organs mimicking the characteristic spread of ovarian cancer in humans such as to the peritoneal wall, throughout the mesentery and on the diaphragm (Fig. 4A) as well as hemorrhagic malignant ascites. Treatment with IFNε significantly suppressed peritoneal tumour dissemination in this model with reduced tumour growth in the mesentery (Fig. 4A, B & Sup. Fig 4) and fewer tumour nodules adhered to diaphragm and peritoneal wall (Fig. 4A & 4Bi). Additionally, IFNε treated mice showed reduced malignant ascites development whereby peritoneal fluid was reduced in volume (Fig. 4Bii), markedly less hemorrhagic (Fig. 4Biii), and contained fewer circulating epithelial tumour cells (Fig. 4Biv). IFNε treatment resulted in lower levels of inflammatory cytokine levels, such as the chemokine MCP1 (CCL2) (Supplementary Fig. 4). Strikingly, administration of IFNβ had no effect on ascites tumour growth by any measure (Fig. 4).

Similar to our results in our orthotopic ovarian cancer model, we found that in this advanced tumour model, total immune cells such as leukocytes, $CD4^+$ and $CD8^+$ T cells correlated with the presence of advanced disease in mice injected i/p. with ovarian tumour cells, but that these populations did not differ between treatment groups (Sup. Fig. 5C). However, IFNε treatment significantly increased the proportion of activated $CD4^+$ and $CD8^+$ T cells in the peritoneum of these mice (Fig. 4Ci-iv), typified by CD25 or CD69 and PD1 induction on CD4 T cells (Fig 4Ci-iii) and CD8 T cells (Fig 4Civ), which correlated with decreases in overall tumour burden and ascites development.

Endogenous and exogenous IFNε regulate immune cells in vivo

Together the above results demonstrate that IFNε maintains efficacy against peritoneal spread of developing, established and advanced models of ovarian cancer, however the mechanism of action, specific to IFNε not shared with IFNβ, was unknown. Since conventional type I IFNs

can exert anti-tumour actions either directly on tumour cells or indirectly via immune cells, we first sought to define the hitherto unknown, intrinsic, *in vivo* immunomodulatory effects of IFNε, independently of the presence of a tumour, but in the peritoneal cavity, the site of ovarian cancer metastasis. IFNε treatment did not regulate $CD4^+$ T cell numbers and showed only a small but significant increase in $CD8^+CD4^-$ cells (Sup Fig 6) but did activate CD4 cell expression of PD1, CD69 and CD25 (Fig 5A). IFNε treatment also increased total peritoneal leukocytes, inflammatory macrophages and dendritic cells (Sup. Fig. 6B).

We next determined whether endogenous IFNε regulated immune cells in the peritoneum which could impact on tumour development at this site, by comparing WT and IFNε-/- mice. While there was no significant difference in the number of peritoneal leukocytes or total T cells, in $IFN\varepsilon^{-/-}$ compared to WT mice, consistent with data above, there were fewer NK cells (Fig. 5B, Sup. Fig. 6). Furthermore, there were increased levels of activated cells including NK, and CD4T cells expressing CD69 and or PD1(Fig 5B), which were lower in the IFNε null mice. These results show that endogenous IFNε maintains the levels and activation status of certain peritoneal immune cells, suitable for immune surveillance.

Endogenous IFNε suppresses ovarian cancer metastases

We next investigated whether endogenous IFNε played a role in tumourigenesis by comparing orthotopic tumour development & dissemination in WT and $IFN\varepsilon^{-/-}$ mice. By 13 weeks post-ID8 implantation, $IFN\varepsilon^{-/-}$ mice developed peritoneal haemorrhaging & ascites accumulation, large nodular orthotopic tumours and multiple metastatic tumour deposits throughout the peritoneal cavity (Fig. 6A-C). Strikingly, tumour cells disseminated throughout the peritoneum more readily in the absence of endogenous IFNε as shown by increased peritoneal metastases by all three measures (Fig. 6B and Cii-iv), whereas the 'primary' orthotopic tumour growth (fig 6B) was similar in WT and $IFN\varepsilon^{-/-}$ mice as demonstrated by similar ovarian weight

(Fig 6Ci). To gain insight into the effect of this endogenous IFNε in early tumour development, we compared tumour burden in mice 6 weeks post-ID8 implantation at which time, IFNε$^{-/-}$ mice developed relatively small, less nodular orthotopic tumours (Fig. 6D). However, although we showed there was no significant difference in primary tumour weight between WT and IFNε$^{-/-}$ mice at this early stage (Fig. 6Ei), we demonstrated an increase in tumour dissemination and metastatic growth in IFNε$^{-/-}$ mice, as measured by increased tumour metastases on the peritoneal wall & total metastases found in the peritoneal cavity (Fig. 6Eii, iii).

At 6 weeks post-tumour implantation, IFNε$^{-/-}$ mice had increased numbers of total leukocytes, CD4 and CD8 lymphocytes compared to their non-tumour bearing (NT) genotype controls (Sup. Fig. 7), an increase which was not seen in WT mice. Our data suggest that a combination of the presence of a tumour plus the absence of suppressive signals from endogenous IFNε, resulted in increased tumour growth. Importantly, IFNε$^{-/-}$ mice had significantly lower proportions of activated immune cells than WT mice demonstrated by markers expressed on CD4 and CD8 T cells including CD69 as well as PD1 (Fig. 6F). These data demonstrate that although there is no significant effect of the absence of endogenous IFNε at the site of tumour cell implantation, endogenous IFNε signaling does influence the activation state of immune cells and suppresses the tumour-elicited influx of immune cells. These differences conferred by endogenous IFNε signaling have a significant impact on the ability of tumour cells to disseminate throughout the peritoneum and establish macro-metastases on peritoneal tissues.

Differentiating direct and indirect anti-tumour effects of IFNε on peritoneal metastases

In order to further dissect the mechanism of action of exogenous and endogenous IFNε in the ovarian cancer models, we characterised tumour development in mice lacking IFNAR1 ($Ifnar1^{-/-}$ mice), where the immune cells cannot respond to type I IFN. At 8 weeks post-ID8 injection, $Ifnar1^{-/-}$ mice demonstrated characteristic peritoneal haemorrhaging, ascites accumulation and nodular tumour deposits throughout the mesentery and adhered to the peritoneal wall (Fig. 7A & B). There were several indications of more advanced disease in tumour-bearing $Ifnar1^{-/-}$ mice relative to WT mice, in particular, a larger number of epithelial peritoneal tumour cells (Fig 7Bii), total peritoneal leukocytes (Fig 7Ci)), CD4 and CD8 cells (Fig. 7Cii and iii). In addition, there were trends towards increases in ascites volume (Fig 7Biii) and peritoneal haemorrhage (Fig 7Biv).

Crucially, exogenous IFNε significantly suppressed overall tumour metastatic burden (Fig. 7A & Bi) in $Ifnar1^{-/-}$ mice. Consistent with previous data, the proportion of activated cells such as CD69 positive CD4 cells and B220 positive cells was not affected (Sup. Fig 8A, B) indicating that this is a direct effect of IFNε. By contrast, the numbers of CD4, CD8 cells were still reduced by exogenous IFNε in the $Ifnar1^{-/-}$ mice, indicating that this effect occurs via the tumour cells (the only IFN responsive cells present) (Fig 7Cii, iii) - consistent with data generated above showing indirect immunoregulatory role of exogenous IFNε on the levels of anti-tumour immune cells.

Overall these results indicate that firstly, that endogenous IFN signalling via IFNAR1, likely by IFNε, suppresses tumour development, consistent with data in the section above. Secondly, the anti-tumour efficacy of exogenous IFNε treatment is still evident in Ifnar1 null mice indicating a direct action by this IFN on tumour cells.

IFNε regulates intrinsic anti-tumour activities on ovarian cancer cells

While the mechanism of IFNε-driven tumour suppression in this model is suggested to be via direct, tumour intrinsic mechanisms, these had not been demonstrated for this IFN. Therefore, we sought to define the repertoire of direct anti-tumour effects of IFNε *in vitro* in the mouse ovarian cancer cell line ID8. Treatment of ID8 cells with rmuIFNε significantly regulated expression of genes involved in cancer-related biological pathways including immune response, *PDL1, Tap1*; cell death, *Casp1* & *Bcl-2*; cell cycle, *Ccne1* & *Cdc20* (Fig. 8A) and chemotaxis, *Cxcl10 (*Sup. Fig. 9*)*. Recombinant muIFNε exhibited a dose-dependent anti-proliferative effect as shown by diminished growth rate & prolonged doubling time measured using xCELLigence (Fig. 8B), which was further confirmed using MTT assay (Fig. 8C). Additionally, rmuIFNε induced of increased apoptosis in these cells as demonstrated by increased Annexin V/PI staining (Fig. 8D, E). Collectively, these results demonstrate that murine ovarian cancer cells respond to direct stimulation with recombinant IFNε through classical IFN signaling pathways including induction of IRGs involved in cancer-related pathways. Regulation of such pathways also correlates with functional assays demonstrating that *in vitro*, IFNε has intrinsic anti-cancer properties including anti-proliferative and pro-apoptotic effects, which may therefore, be one of its mechanisms of action *in vivo*, consistent with the results from Ifnar null mice presented above.

In order to consolidate that these indications from our mouse model were relevant to human ovarian cancers, and given the strong clinical indications for a tumour suppressive role for IFNε in women with ovarian cancer (Fig 1), and in the absence of published data on the anti-tumour properties of this relatively new cytokine, we tested its direct anti-tumour effects on human ovarian cancer cell lines. We used our recombinant human IFNε (rhIFNε) on two

human ovarian cancer cell lines, CaOV3 & OVCAR4, shown previously to be representative of human HGSC (Domcke et al., 2013). Firstly, we showed that these cells were directly responsive to rhIFNε stimulation, which elicited a dose-dependent induction of classical IRGs such as *ISG15* and *IFIT1,* as did IFNβ (Sup. Fig 9), Accordingly, since these data showed that rhIFNε exerted classical type I IFN signaling, we determined the anti-tumour effects using functional assays; the results showed that rhIFNε regulated cellular proliferation and directly suppress human ovarian cancer cell growth. IFNε had significant dose-dependent anti-proliferative effects on both cell lines over 48 & 72 hours as measured by doubling times (Sup. Fig 10). These results suggest that novel IFNε may prolong survival in HGSC by regulating tumour cell intrinsic pathways as indicated in our preclinical animal models.

DISCUSSION

IFNε is the most recently discovered type I IFN (Fung et al., 2013; Hardy et al., 2004), whose constitutive expression in FRT epithelium was known to play a critical role in the regulation of local immune responses that protect against FRT infections (Fung et al., 2013). This IFN is a member of the type I IFN family of cytokines whose other 'classical' members (IFNα,β, etc.) exert anti-tumour responses by direct action on tumour cells or indirect activation of immune responses. However, despite its distinct biological expression and activity, there have been no previous investigations into the role of IFNε during tumourigenesis or as a cancer therapy. Aiming to address this, we here demonstrate the first evidence for IFNε as an endogenous tumour suppressor and effective anti-tumour therapeutic in an aggressive FRT tumour - epithelial ovarian cancer, and we elucidate aspects of its mechanism of action.

In the ID8 orthotopic model, exogenous IFNε treatment caused a marked reduction in overall disease progression & metastatic tumour burden, despite little effect on 'primary' orthotopic ovarian tumour growth. This effect on metastasis not primary tumour, is consistent with evidence in other cancer models such as breast cancer, where IFNα treatment bears no effect on orthotopic, primary tumour development but was critical in suppressing specific pathways of metastatic spread (Bidwell et al., 2012). These data might be explained on a pharmacokinetic basis whereby this cytokine has better access to cells undergoing metastatic spread relative to restricted access to target cells in the primary solid tumour, or differences in the nature of tumour cells growing in a solid mass and the immune cell infiltrate (Parker et al., 2016). It is well-established that the peritoneal cavity provides a self-contained compartment rich in immune cells, cytokines and secreted factors (Capobianco et al., 2017) and thus, peritoneal tumours are therefore afforded a unique microenvironment whereby metastatic trajectory can be determined by a number of mechanisms (Mitra, 2016; Worzfeld et al., 2017); and collectively, depict an

environment of balanced immune suppression and activation (Charbonneau et al., 2013) – all of which suggest that the peritoneum may be a particularly suitable place for IFNε action.

While we demonstrate that IFNε has the capacity to directly modulate tumour cell proliferation and survival *in vivo* and *in vitro*, as well as to modulate the immune response, one of the key findings from this study is the ability of IFNε to directly exert anti-tumour effects by regulating tumour cell intrinsic functions. This was demonstrated *in vivo* using Ifnar1$^{-/-}$ mice (where the immune cells cannot respond to the IFN), yet IFNε was still effective, at least in part. This was supported by gene induction and antiproliferative effects of IFN□ε*in vitro* using representative human cell lines. Furthermore, IFNε stimulation of cultured ID8 cells regulated the expression of critical genes involved in cancer-related biological pathways including immune regulation (PD-L1), cell cycle & cell death genes and chemotaxis (e.g. *CXCL10).* IFNε also regulated the corresponding biological effects such as inhibition of proliferation and activation of apoptosis in those cell lines as well as tumour-derived immunoregulatory factors such as CXCL10. CXCL10 expression correlates with decreased tumour burden in mice (K Au et al., 2017), improved survival in human HGSC (Bronger et al., 2016), and is usually responsible for recruitment of activated T cells and NK cells into sites of inflammation (Lande et al 2003) and thus may contribute to the tumour cell extrinsic actions of IFNε defined herein, that complement its intrinsic actions.

While the ID8 orthotopic model elicits an influx of immune cells into the peritoneum these immune cells appear not effective at clearing tumour burden. Importantly, if activated, as shown here with IFNε treatment (but interestingly not IFNβ), these cells can mount effective anti-tumour responses capable of suppressing metastatic peritoneal tumour spread from the

orthotopic 'primary' tumour. Indeed, we demonstrate that IFNε has potent immunoregulatory effects *in vivo* whereby it activates effector cells including CD4, CD8, NK and B cells, as evidenced by the markers CD69 and CD25. Total tumour-infiltrating lymphocytes have been shown to correlate with improved survival in human disease (Zhang et al., 2003), however subsequent investigations have highlighted the prognostic importance of distinguishing the proportions of suppressive cells such as regulatory T cells from effector immune responses (Curiel et al., 2004). Others have used the ID8 syngeneic mouse model of ovarian cancer to study tumour infiltrating leucocytes (TIL) exhaustion and combined blockade of check point inhibitors, PD1 or PD-L1, with myeloid- targeted vaccinations and found that upregulated effector T cell signaling cleared the majority of tumour (Duraiswamy et al., 2013a). PD-L1 expression on tumour cells and macrophages, positively correlated with TILs and improved outcome in HGSC (Webb et al., 2016). Most recently, epigenetic therapy using the ID8 mouse model demonstrated tumour suppression and increased immune activation in a type I IFN-dependent manner (Stone et al., 2017) and suggest this may be a key method to sensitise suppressed microenvironment to checkpoint blockade therapy. Here using the same model, we show that IFNε not only effectively cleared tumour burden, but also directly regulated expression of PD-L1 on tumour cells and PD1 on immune cell populations. Therefore, IFNε may constitute an effective immunotherapy with a potential additive efficacy in combination with therapies that simultaneously target the PD-L1/PD1 axis checkpoint inhibitors.

The data herein constitute compelling evidence not only that **exogenous IFNε** inhibits tumour growth in the peritoneum, but also that **endogenous IFNε** suppresses tumourigenesis. 1) IFNε is constitutively expressed in the putative cell of origin of HGSC, human fallopian tube epithelium (Ducie et al., 2017; Perets and Drapkin, 2016); 2) this expression is decreased in a significant proportion of HGSCs; 3) in preclinical mouse models, loss of IFNε (IFNε$^{-/-}$ mice)

or the ability to respond to IFNε (IFNAR1-/- mice) results in increased tumours in the peritoneum and reduced levels of activated immune cells (Fig 6). There are several possible mechanisms underlying loss of IFNε expression in ovarian tumours. Interestingly, IFNε loss has also been characterized in the FRT of post-menopausal women who lack the reproductive hormones which normally regulate IFNε expression (Fung et al., 2013). Postmenopausal women are in fact the highest at-risk group for ovarian cancer development (Howlander et al 2017). Conversely, use of the combined oral contraceptive pill significantly reduces the risk of serous carcinoma (Webb et al., 2017; Webb and Jordan, 2017; Wentzensen et al., 2016), suggesting that enhanced regulation of IFNε may prevent tumourigenesis. Since this is not consistent with the rest of our data, this observation may reflect an IFNε - independent effect of hormones. Importantly, we have recently characterized the regulation of constitutive IFNε to be mediated by the transcription factor E74-like factor 3 (*ELF3*), an epithelial-specific Ets factor (Fung et al. unpublished). In support of this, ELF3 was recently identified as a positive prognostic marker in transcriptome analysis of epithelial components of human ovarian tumours (Yeung et al., 2017), which corresponds with our *in silico* analysis indicating that expression of *IFNε* transcript is a predictor of disease-free survival in two independent human ovarian cancer cohorts (AOCS & CSIOVDB) and may suggest a key upstream signal in IFNε regulation worthy of further investigation in ovarian cancer. Loss of endogenous IFNε in a (high) proportion of HGSCs may in fact demonstrate a key driving factor in the development and progression of these tumours and critically, may also identify patients who may most benefit from recombinant IFNε therapy in a disease where prolonged disease-free survival following surgery has a significant cumulative effect (Kurta et al., 2014).

Strikingly, IFNε showed a marked difference from IFNβ in many aspects of this study, namely loss in human tumours and its correlation with improved survival; inhibition of tumour and

activation of immune response after delayed IFNε treatment, inhibition of tumour growth and activation of immune response in an advanced ovarian cancer metastasis model, *in vitro* inhibition of proliferation and regulation of apoptosis, and *in vivo* immune cell activation (e.g. CD25 and PD1 surface expression). This reflects critical differences in their respective receptor interactions and binding affinities (Stifter et al., 2017). This vital difference in efficacy may also reflect the distinct biological roles of these two type I IFNs. Conventional type I IFNs (α's and β) have evolved to act as acute phase cytokines produced mostly by inflammatory cells in a transient manner to avoid toxicity. By contrast, IFNε has evolved as a constitutive, protective cytokine expressed by normal epithelia where continuous action is tolerated, perhaps even preferred. These properties make IFNε a unique type I IFN cytokine, fit for purpose to protect the reproductive tract from tumourigenesis and our data also support it as a potential therapeutic alone or in combination, for HGSC.

METHODS

Cell lines & cell culture- Ovarian cancer lines ID8 (murine; Roby KF, et al., Carcinogenesis 2000), CAOV3 (human; ATCC, Virginia), and OVCAR4 (human; National Cancer Institute) were used for in vitro assays. ID8 & OVCAR4 cell lines were cultured in RPMI 1640 (GibcoBRL, Ontario, Canada) and CAOV3 in DMEM (GibcoBRL) supplemented with 4% (ID8) or 10% (CaOV3, OVCAR4) heat-activated fetal calf serum (FCS; GibcoBRL). All cells were cultured at 37°C in an atmosphere of 5% (v/v) carbon dioxide (CO_2). Cells were confirmed Mycoplasma negative according to MycoAlert™ PLUS Mycoplasma Detection Kit (ratio <1; Lonza, Basel).

Interferons- Recombinant murine IFNε and IFNβ were expressed in-house in insect cells, affinity purified and quality controlled by physicochemical procedures and bioactivity was determined by a reporter assay calibrated against an international IFNα/β reference standard in a cytopathic effect-reduction bioassay as described elsewhere (Stifter et al., 2017). Recombinant human IFNα was expressed in E.Coli, purified by affinity and gel filtration chromatography, and refolded and tested to have endotoxin levels < 0.01 units per my using the limulus assay (S. Lim, de Weerd and Hertzog et al., unpublished).

Cell stimulations- Cell lines were plated ($1.5x10^5$ cells/well) in a 12 well plate in normal media 24 hour prior to stimulation with recombinant IFNε or IFNβ at 0 – 1000IU/ml or PBS as vehicle controls. Cells were then incubated at 37°C for 3 hrs prior to mRNA extraction.

Cell growth assays- Cellular proliferation was measured using the xCELLigence system (ACEA Biosciences, Inc., San Diego, CA, USA) for real-time cell analysis (RTCA). Fifty microliters of cell culture medium was added to each well in a 96 well E- plate (ACEA

Biosciences, Inc.) for the impedance background measurement. Cells were then added (ID8 – $6x10^3$ cells/well, CAOV3 & OVCAR4 – $1x10^5$ cells/well) to a volume of 100µL in serum-free culture media and allowed to adhere overnight. Recombinant IFN or vehicle was added to the cells up to a final volume of 200µL of normal culture media. The E-Plates were incubated at 37°C with 5% CO_2 and impedance measured on the RTCA system at 15-minute time intervals for up to 72 hours with or without treatment. For data analysis, the baseline cell index (CI) is determined by subtracting the CI for a cell-containing well from the CI of a well with only culture media. To facilitate the statistical evaluation of the results, impedance measurements from each well were normalised to the time of stimulation with IFN, termed 'normalised cell index'. We performed three independent experiments in technical quadruplicate and analysed for doubling-time & slope (1/hr) of growth curves, indicative of rate of proliferation, using RCTA software.

Apoptosis assays- ID8 cells were plated in a 12 well plate ($3.5x10^4$ cells/well) in 2ml and left to adhere overnight. Cells were stimulated with recombinant murine Ifnε or vehicle control for 48 hours. Hydrogen peroxide (H_2O_2) was used a positive control for induction of apoptosis at 1 – 5mM. Following stimulation, cells were trypsinised and washed in PBS. Single cell suspensions were stained with FITC conjugated Annexin V and propidium iodide (PI) using the FITC Annexin V Apoptosis Detection kit II (BD Biosciences, New Jersey), as per the manufacturer's instructions and analysed by flow cytometry using a FACSCanto™ II flow cytometer (BD Biosciences) and Flo-Jo software. The different phases of apoptosis were defined as i) live cells (FITC-labelled Annexin V-/PI-), ii) early apoptotic (FITC-labelled Annexin V+/PI-), iii) late apoptotic (FITC AnnexinV+/PI+), and iv) necrotic cells (FITC Annexin V-/PI+) (Andree HA, et al., J Biol Chem 1990).

Immunohistochemistry- Human fallopian tubes, mouse organs and tumour samples were fixed for 24 hours in 10% neutral buffered formalin, then washed in 70% ethanol, and embedded in

paraffin. Tissue was sectioned at 4-μm thickness and stained for H&E, smooth muscle actin (SMa), cytokeratin 18(Ck18) & IFNε. Briefly, histological tissue sections were deparaffinised and rehydrated. Antigen retrieval was performed by heat in 10 mM Tris/1 mM EDTA (pH 9.0) for 6 mins. After inhibition of endogenous peroxidase activity with 3% (vol/vol) hydrogen peroxide, tissues were blocked in CAS-Block™ (ThermoFisher Scientific) for 1 hour. Tissues were then incubated overnight at 4°C with anti-IFNε (1:210; Novus Biologicals, Colorado), anti-SMa (1:100; Dako Omnis, Santa Clara), anti-Ck18 (1:50; Dako Omnis) and rabbit IgG (1:200; Vector Laboratories, California) or mouse IgG1 (1:37; Vector Laboratories) as isotype controls. Biotinylated anti-rabbit or anti-mouse IgGs (both 1:250 dilution; Vector Laboratories) were diluted in the same buffer and incubated for 1 hour. Slides were then washed in 0.05% Tween/PBS and incubated with avidin and biotinylated horseradish peroxidase (VECTASTAIN® Elite® ABC Kit, Vector Laboratories) as per the manufacturer's instructions and washed again. Slides were then incubated with diaminobenzidine tetrahydrochloride (DAB; DAB+ Substrate Chromogen System, Dako Omnis) as per the manufacturer's instructions. Sections were counterstained with Haematoxylin for 45 seconds then dehydrated and placed under coverslip with dibutylphthalate dolystyrene xylene (DPX; Merck, Germany). Staining intensity was calculated using the positive pixel analysis tool in Imagescope software.

Immunophenotyping- Single cell suspensions were obtained from peritoneal lavage cells of C57BL/J mice studied for surface antigen expression using a panel of monoclonal antibodies directly conjugated with fluorochromes. In order to prevent non-specific binding, cell surface receptors were blocked with Anti-mouse CD16/CD32 Fcγ III/II Receptor blocking antibody (BD PharMingen, California). For surface staining, cells were stained with the various combinations of fluorochrome-labelled antibodies: panel 1 – APC conjugated CD45, APC-Cy7 conjugated CD8, FITC conjugated NK-1.1, PE conjugated CD69, Pacific Blue conjugated

CD4; panel 2 – APC conjugated CD25, APC-Cy7 conjugated CD8, FITC conjugated CD45, PE conjugated Pan CK, PE-Cy7 conjugated CD4 and Pacific Blue conjugated FoxP3; panel 3 – APC conjugated CD45, APC-Cy7 conjugated CD11b, FITC conjugated Ly6C, PE conjugated I-Ab, PE-Cy7 conjugated CD11c and Pacific Blue Ly6G. Cells were analysed using a FACSCanto™ II flow cytometer (BD Biosciences) and Flo-Jo software.

Cytometric bead array (CBA)- Cytometric bead array (BD CBA Mouse Inflammation Kit; BD Pharmingen) was used to determine levels of MCP-1, IFNγ, IL-6, IL-10, IL-12p70, and TNF-α. in the supernatant of peritoneal exudate cells from mice injected with ID8 cells (see intraperitoneal model of ovarian cancer below) as per the manufacturer's instructions. A FACSCanto™ II flow cytometer (BD Biosciences) and Flo-Jo software was used to examine levels of MCP-1, IFNγ, IL-6, IL-10, IL-12p70, or TNF-α.

Mice- IFNε$^{-/-}$ (Fung K, Mangan N, et al., Science 2013) and Ifnar1$^{-/-}$ (Hwang, Hertzog et al., PNAS 1995) on a C57bl6 background and wild-type mice (Monash Animal Research Facility) were housed in standard specific pathogen free (SPF) conditions.

Intrabursal (orthotopic) ovarian cancer model- Female mice (10 weeks of age) were anaesthetized by inhalation of isoflurane (5% in oxygen) in an induction chamber, and anesthesia maintained at 2.5-3.0% isoflurane delivered *via* nosecone during all procedures. Mice were subcutaneously injected with Carprofen (5mg/kg) prior to surgery. A small incision was made at the dorso-medial position directly above the ovarian fat pad, with a secondary small incision through the peritoneal wall. The ovarian fat pad was externalised and stabilized with a bull clip, and a dissecting microscope used to locate the oviduct in the exposed ovary. ID8 cells ($1x10^6$) were injected underneath the left ovarian bursa. The peritoneal wall was sutured closed using 6/0 suture prior to topical Bupivacaine administration and closure of the incision closed with surgical staples. Analgesia (Carprofen 5mg/kg body weight) was provided

in drinking water for 3 days thereafter. Mice were monitored for body weight, Body Condition Score (BCS) defined as: BCS 1 Thin – Skeletal structure prominent and vertebral bodies protruding, BCS 2 Under-conditioned – segmentation of vertebral column evident but not protruding, and BCS3 Well-conditioned – vertebrae not evident without palpation, as well as clinical signs (see Appendix C) and culled 13 weeks post-ID8 injection.

Intraperitoneal (disseminated) ovarian cancer model- Female (6 to 8 weeks of age) mice were injected intraperitoneally with $5x10^6$ ID8 cells. Mice were monitored for body weight, BCS and clinical signs and culled 8 weeks post-ID8 injection. At autopsy, the overall spread and tumour burden of each mouse was documented (number of tumour nodules, sites of nodule deposits recorded and photographed), ascites fluid was drained from the peritoneum for volume measurement and cell counts and tissue harvested (spleen, diaphragm, peritoneal wall, mesenteric fat, female reproductive tract) for weight measurements and immunohistochemical analysis. All analysis of mice phenotypes was performed blinded.

Intraperitoneal recombinant IFN therapy- IFN treatments were commenced 3 days post-intraperitoneal ID8 cell injections. Mice either received recombinant murine Ifnε injected intraperitoneally 3 times a week at a dose of 500IU/injection or Ifnβ at 500IU/injection or vehicle for 8 weeks. At autopsy, the orthotopic 'primary" tumour was collected along with metastases (diaphragmatic & peritoneal), spleen, ascites fluid (volume and cell counts) and peritoneal lavage and samples weighed, photographed and processed for immunohistochemical analysis.

Statistical analysis- Data were graphed in GraphPad Prism 7. Significance for parametric data were determined using Student's Unpaired T Test and non-paramteric data were determined using Mann-Whitney *t* test. Differences were considered significant if the P value was < 0.05

and significance is indicated as *p<0.05, **p<0.01, ***p<0.001, ****p<0.0001. Details of statistical data are indicated for each figure.

References.

Akman, T., Oztop, I., Unek, I. T., Koca, D., Unal, O. U., Salman, T., Yavuzsen, T., Yilmaz, A. U., Somali, I., Demir, N., and Ellidokuz, H. (2014). Long-term outcomes and prognostic factors of high-risk malignant melanoma patients after surgery and adjuvant high-dose interferon treatment: a single-center experience. Chemotherapy *60*, 228-238.

Alberts, D. S., Markman, M., Muggia, F., Ozols, R. F., Eldermire, E., Bookman, M. A., Chen, T., Curtin, J., Hess, L. M., Liebes, L.*, et al.* (2006). Proceedings of a GOG workshop on intraperitoneal therapy for ovarian cancer. Gynecologic oncology *103*, 783-792.

Anguille, S., Lion, E., Willemen, Y., Van Tendeloo, V. F., Berneman, Z. N., and Smits, E. L. (2011). Interferon-alpha in acute myeloid leukemia: an old drug revisited. Leukemia *25*, 739-748.

U.S. Cancer Statistics Working Group. (2017). United States Cancer Statistics: 1999-2014 Incidence and Mortality Web-based Report. In, (Atlanta (GA): Department of Health and Human Services, Centers for Disease Control and Prevention, and National Cancer Institute).

Ascierto, P. A., Chiarion-Sileni, V., Muggiano, A., Mandala, M., Pimpinelli, N., Del Vecchio, M., Rinaldi, G., Simeone, E., and Queirolo, P. (2014). Interferon alpha for the adjuvant treatment of melanoma: review of international literature and practical recommendations from an expert panel on the use of interferon. Journal of chemotherapy *26*, 193-201.

Berek, J. S., Hacker, N. F., Lichtenstein, A., Jung, T., Spina, C., Knox, R. M., Brady, J., Greene, T., Ettinger, L. M., Lagasse, L. D., and et al. (1985). Intraperitoneal recombinant alpha-interferon for "salvage" immunotherapy in stage III epithelial ovarian cancer: a Gynecologic Oncology Group Study. Cancer research *45*, 4447-4453.

Berek, J. S., Markman, M., Stonebraker, B., Lentz, S. S., Adelson, M. D., DeGeest, K., and Moore, D. (1999). Intraperitoneal interferon-alpha in residual ovarian carcinoma: a phase II gynecologic oncology group study. Gynecologic oncology *75*, 10-14.

Bidwell, B. N., Slaney, C. Y., Withana, N. P., Forster, S., Cao, Y., Loi, S., Andrews, D., Mikeska, T., Mangan, N. E., Samarajiwa, S. A.*, et al.* (2012). Silencing of Irf7 pathways in breast cancer cells promotes bone metastasis through immune escape. Nature Medicine *18*, 1224-1231.

Bronger, H., Singer, J., Windmuller, C., Reuning, U., Zech, D., Delbridge, C., Dorn, J., Kiechle, M., Schmalfeldt, B., Schmitt, M., and Avril, S. (2016). CXCL9 and CXCL10 predict survival and are regulated by cyclooxygenase inhibition in advanced serous ovarian cancer. British journal of cancer *115*, 553-563.

Bruzzone, M., Rubagotti, A., Gadducci, A., Catsafados, E., Foglia, G., Brunetti, I., Giannessi, P. G., Carnino, F., Iskra, L., Rosso, R.*, et al.* (1997). Intraperitoneal carboplatin with or without interferon-alpha in advanced ovarian cancer patients with minimal residual disease at second look: a prospective randomized trial of 111 patients. G.O.N.O. Gruppo Oncologic Nord Ovest. Gynecologic oncology *65*, 499-505.

Capobianco, A., Cottone, L., Monno, A., Manfredi, A. A., and Rovere-Querini, P. (2017). The peritoneum: healing, immunity, and diseases. The Journal of pathology *243*, 137-147.

Charbonneau, B., Goode, E. L., Kalli, K. R., Knutson, K. L., and Derycke, M. S. (2013). The immune system in the pathogenesis of ovarian cancer. Critical reviews in immunology *33*, 137-164.

Curiel, T. J., Coukos, G., Zou, L., Alvarez, X., Cheng, P., Mottram, P., Evdemon-Hogan, M., Conejo-Garcia, J. R., Zhang, L., Burow, M*., et al.* (2004). Specific recruitment of regulatory T cells in ovarian carcinoma fosters immune privilege and predicts reduced survival. Nature medicine *10*, 942-949.

Domcke, S., Sinha, R., Levine, D. A., Sander, C., and Schultz, N. (2013). Evaluating cell lines as tumour models by comparison of genomic profiles. Nature communications *4*, 2126.

Ducie, J., Dao, F., Considine, M., Olvera, N., Shaw, P. A., Kurman, R. J., Shih, I. M., Soslow, R. A., Cope, L., and Levine, D. A. (2017). Molecular analysis of high-grade serous ovarian carcinoma with and without associated serous tubal intra-epithelial carcinoma. Nature communications *8*, 990.

Duraiswamy, J., Freeman, G. J., and Coukos, G. (2013a). Therapeutic PD-1 pathway blockade augments with other modalities of immunotherapy T-cell function to prevent immune decline in ovarian cancer. Cancer research *73*, 6900-6912.

Duraiswamy, J., Kaluza, K. M., Freeman, G. J., and Coukos, G. (2013b). Dual blockade of PD-1 and CTLA-4 combined with tumor vaccine effectively restores T-cell rejection function in tumors. Cancer research *73*, 3591-3603.

Frasci, G., Tortoriello, A., Facchini, G., Conforti, S., Persico, G., Mastrantonio, P., Cardone, A., and Iaffaioli, R. V. (1994). Carboplatin and alpha-2b interferon intraperitoneal combination as first-line treatment of minimal residual ovarian cancer. A pilot study. European journal of cancer *30A*, 946-950.

Fung, K. Y., Mangan, N. E., Cumming, H., Horvat, J. C., Mayall, J. R., Stifter, S. A., De Weerd, N., Roisman, L. C., Rossjohn, J., Robertson, S. A.*, et al.* (2013). Interferon-epsilon protects the female reproductive tract from viral and bacterial infection. Science *339*, 1088-1092.

Greenaway, J., Moorehead, R., Shaw, P., and Petrik, J. (2008). Epithelial-stromal interaction increases cell proliferation, survival and tumorigenicity in a mouse model of human epithelial ovarian cancer. Gynecologic oncology *108*, 385-394.

Hall, G. D., Brown, J. M., Coleman, R. E., Stead, M., Metcalf, K. S., Peel, K. R., Poole, C., Crawford, M., Hancock, B., Selby, P. J., and Perren, T. J. (2004). Maintenance treatment with interferon for advanced ovarian cancer: results of the Northern and Yorkshire gynaecology group randomised phase III study. British journal of cancer *91*, 621-626.

Hardy, M. P., Owczarek, C. M., Jermiin, L. S., Ejdeback, M., and Hertzog, P. J. (2004). Characterization of the type I interferon locus and identification of novel genes. Genomics *84*, 331-345.

Howlader N, Noone AM, Krapcho M, Miller D, Bishop K, Kosary CL, Yu M, Ruhl J, Tatalovich Z, Mariotto A, Lewis DR, Chen HS, Feuer EJ, Cronin KA (eds). (2016) SEER Cancer Statistics Review, 1975-2014, National Cancer Institute. Bethesda MD, https://seer.cancer.gov/csr/1975_2014/, based on November 2016 SEER data submission, posted to the SEER web site, April 2017.

Hwang* SY, Hertzog* PJ, Holland KA, Sumarsono SH, Tymms MJ, Hamilton JA, Whitty G, Bertoncello I, Kola I. (1995). A null mutation in the gene encoding a type I interferon receptor component eliminates antiproliferative and antiviral responses to interferons alpha and beta and alters macrophage responses. Proc Natl Acad Sci U S A. 92(24):11284-8

Jayson, G. C., Kohn, E. C., Kitchener, H. C., and Ledermann, J. A. (2014). Ovarian cancer. Lancet *384*, 1376-1388.

K Au, K., Peterson, N., Truesdell, P., Reid-Schachter, G., Khalaj, K., Ren, R., Francis, J. A., Graham, C. H., Craig, A. W., and Koti, M. (2017). CXCL10 alters the tumour immune microenvironment and disease progression in a syngeneic murine model of high-grade serous ovarian cancer. Gynecologic oncology *145*, 436-445.

Kirkwood, J. M., Ibrahim, J. G., Sosman, J. A., Sondak, V. K., Agarwala, S. S., Ernstoff, M. S., and Rao, U. (2001). High-dose interferon alfa-2b significantly prolongs relapse-free and overall survival compared with the GM2-KLH/QS-21 vaccine in patients with resected stage

IIB-III melanoma: results of intergroup trial E1694/S9512/C509801. Journal of clinical oncology : official journal of the American Society of Clinical Oncology *19*, 2370-2380.

Kurman, R. J., and Shih Ie, M. (2011). Molecular pathogenesis and extraovarian origin of epithelial ovarian cancer--shifting the paradigm. Human pathology *42*, 918-931.

Kurta, M. L., Edwards, R. P., Moysich, K. B., McDonough, K., Bertolet, M., Weissfeld, J. L., Catov, J. M., Modugno, F., Bunker, C. H., Ness, R. B., and Diergaarde, B. (2014). Prognosis and conditional disease-free survival among patients with ovarian cancer. Journal of clinical oncology : official journal of the American Society of Clinical Oncology *32*, 4102-4112.

Lande R., Giacomini E., Grassi T., Remoli M. E., Iona E., Miettinen E., Julkunen I and Coccia E.M. (2003). IFN-αβ Released by *Mycobacterium tuberculosis*-Infected Human Dendritic Cells Induces the Expression of CXCL10: Selective Recruitment of NK and Activated T Cells. J. Immunol 170 (3) 1174-1182.

Markman, M., Belinson, J., Webster, K., Zanotti, K., Morrison, B., Jacobs, B., Borden, E., and Lindner, D. (2004). Phase 2 trial of interferon-beta as second-line treatment of ovarian cancer, fallopian tube cancer, or primary carcinoma of the peritoneum. Oncology *66*, 343-346.

Markman, M., Berek, J. S., Blessing, J. A., McGuire, W. P., Bell, J., and Homesley, H. D. (1992). Characteristics of patients with small-volume residual ovarian cancer unresponsive to cisplatin-based ip chemotherapy: lessons learned from a Gynecologic Oncology Group phase II trial of ip cisplatin and recombinant alpha-interferon. Gynecologic oncology *45*, 3-8.

Mitra, A. K. (2016). Ovarian Cancer Metastasis: A Unique Mechanism of Dissemination. In Tumor Metastasis, K. Xu, ed. (DOI: 10.5772/64700: InTech).

Mocellin, S., Pasquali, S., Rossi, C. R., and Nitti, D. (2010). Interferon alpha adjuvant therapy in patients with high-risk melanoma: a systematic review and meta-analysis. Journal of the National Cancer Institute *102*, 493-501.

Moore, D. H., Valea, F., Walton, L. A., Soper, J., Clarke-Pearson, D., and Fowler, W. C., Jr. (1995). A phase I study of intraperitoneal interferon-alpha 2b and intravenous cis-platinum plus cyclophosphamide chemotherapy in patients with untreated stage III epithelial ovarian cancer: a Gynecologic Oncology Group pilot study. Gynecologic oncology *59*, 267-272.

Parker, B. S., Rautela, J., and Hertzog, P. J. (2016). Antitumour actions of interferons: implications for cancer therapy. Nature reviews Cancer *16*, 131-144.

Pasquali, S., and Mocellin, S. (2010). The anticancer face of interferon alpha (IFN-alpha): from biology to clinical results, with a focus on melanoma. Current medicinal chemistry *17*, 3327-3336.

Patch, A. M., Christie, E. L., Etemadmoghadam, D., Garsed, D. W., George, J., Fereday, S., Nones, K., Cowin, P., Alsop, K., Bailey, P. J.*, et al.* (2015). Whole-genome characterization of chemoresistant ovarian cancer. Nature *521*, 489-494.

Perets, R., and Drapkin, R. (2016). It's Totally Tubular....Riding The New Wave of Ovarian Cancer Research. Cancer research *76*, 10-17.

Perets, R., Wyant, G. A., Muto, K. W., Bijron, J. G., Poole, B. B., Chin, K. T., Chen, J. Y., Ohman, A. W., Stepule, C. D., Kwak, S.*, et al.* (2013). Transformation of the fallopian tube secretory epithelium leads to high-grade serous ovarian cancer in Brca;Tp53;Pten models. Cancer cell *24*, 751-765.

Stifter, S. A., Matthews, A. Y., Mangan, N. E., Fung, K. Y., Drew, A., Tate, M. D., Soares da Costa, T. P., Hampsey, D., Mayall, J., Hansbro, P. M.*, et al.* (2017). Defining the distinct, intrinsic properties of the novel type I interferon, epsilon. J Biol Chem. Nov 29. [Epub ahead of print]

Stone, M. L., Chiappinelli, K. B., Li, H., Murphy, L. M., Travers, M. E., Topper, M. J., Mathios, D., Lim, M., Shih, I. M., Wang, T. L.*, et al.* (2017). Epigenetic therapy activates type I interferon signaling in murine ovarian cancer to reduce immunosuppression and tumor burden. Proceedings of the National Academy of Sciences of the United States of America.

Tan, T. Z., Yang, H., Ye, J., Low, J., Choolani, M., Tan, D. S., Thiery, J. P., and Huang, R. Y. (2015). CSIOVDB: a microarray gene expression database of epithelial ovarian cancer subtype. Oncotarget *6*, 43843-43852.

Tothill, R. W., Tinker, A. V., George, J., Brown, R., Fox, S. B., Lade, S., Johnson, D. S., Trivett, M. K., Etemadmoghadam, D., Locandro, B.*, et al.* (2008). Novel molecular subtypes of serous and endometrioid ovarian cancer linked to clinical outcome. Clinical cancer research : an official journal of the American Association for Cancer Research *14*, 5198-5208.

Vaughan, S., Coward, J. I., Bast, R. C., Jr., Berchuck, A., Berek, J. S., Brenton, J. D., Coukos, G., Crum, C. C., Drapkin, R., Etemadmoghadam, D.*, et al.* (2011). Rethinking ovarian cancer: recommendations for improving outcomes. Nature reviews Cancer *11*, 719-725.

Webb, J. R., Milne, K., Kroeger, D. R., and Nelson, B. H. (2016). PD-L1 expression is associated with tumor-infiltrating T cells and favorable prognosis in high-grade serous ovarian cancer. Gynecologic oncology *141*, 293-302.

Webb, P. M., Green, A. C., and Jordan, S. J. (2017). Trends in hormone use and ovarian cancer incidence in US white and Australian women: implications for the future. Cancer causes & control : CCC *28*, 365-370.

Webb, P. M., and Jordan, S. J. (2017). Epidemiology of epithelial ovarian cancer. Best practice & research Clinical obstetrics & gynaecology *41*, 3-14.

Wentzensen, N., Poole, E. M., Trabert, B., White, E., Arslan, A. A., Patel, A. V., Setiawan, V. W., Visvanathan, K., Weiderpass, E., Adami, H. O.*, et al.* (2016). Ovarian Cancer Risk Factors by Histologic Subtype: An Analysis From the Ovarian Cancer Cohort Consortium. Journal of clinical oncology : official journal of the American Society of Clinical Oncology *34*, 2888-2898.

Willemse, P. H., de Vries, E. G., Mulder, N. H., Aalders, J. G., Bouma, J., and Sleijfer, D. T. (1990). Intraperitoneal human recombinant interferon alpha-2b in minimal residual ovarian cancer. European journal of cancer *26*, 353-358.

Worzfeld, T., Pogge von Strandmann, E., Huber, M., Adhikary, T., Wagner, U., Reinartz, S., and Muller, R. (2017). The Unique Molecular and Cellular Microenvironment of Ovarian Cancer. Frontiers in oncology *7*, 24.

Yeung, T. L., Leung, C. S., Wong, K. K., Gutierrez-Hartmann, A., Kwong, J., Gershenson, D. M., and Mok, S. C. (2017). ELF3 is a negative regulator of epithelial-mesenchymal transition in ovarian cancer cells. Oncotarget *8*, 16951-16963.

Zhang, L., Conejo-Garcia, J. R., Katsaros, D., Gimotty, P. A., Massobrio, M., Regnani, G., Makrigiannakis, A., Gray, H., Schlienger, K., Liebman, M. N.*, et al.* (2003). Intratumoral T cells, recurrence, and survival in epithelial ovarian cancer. The New England journal of medicine *348*, 203-213.

Figure 1.

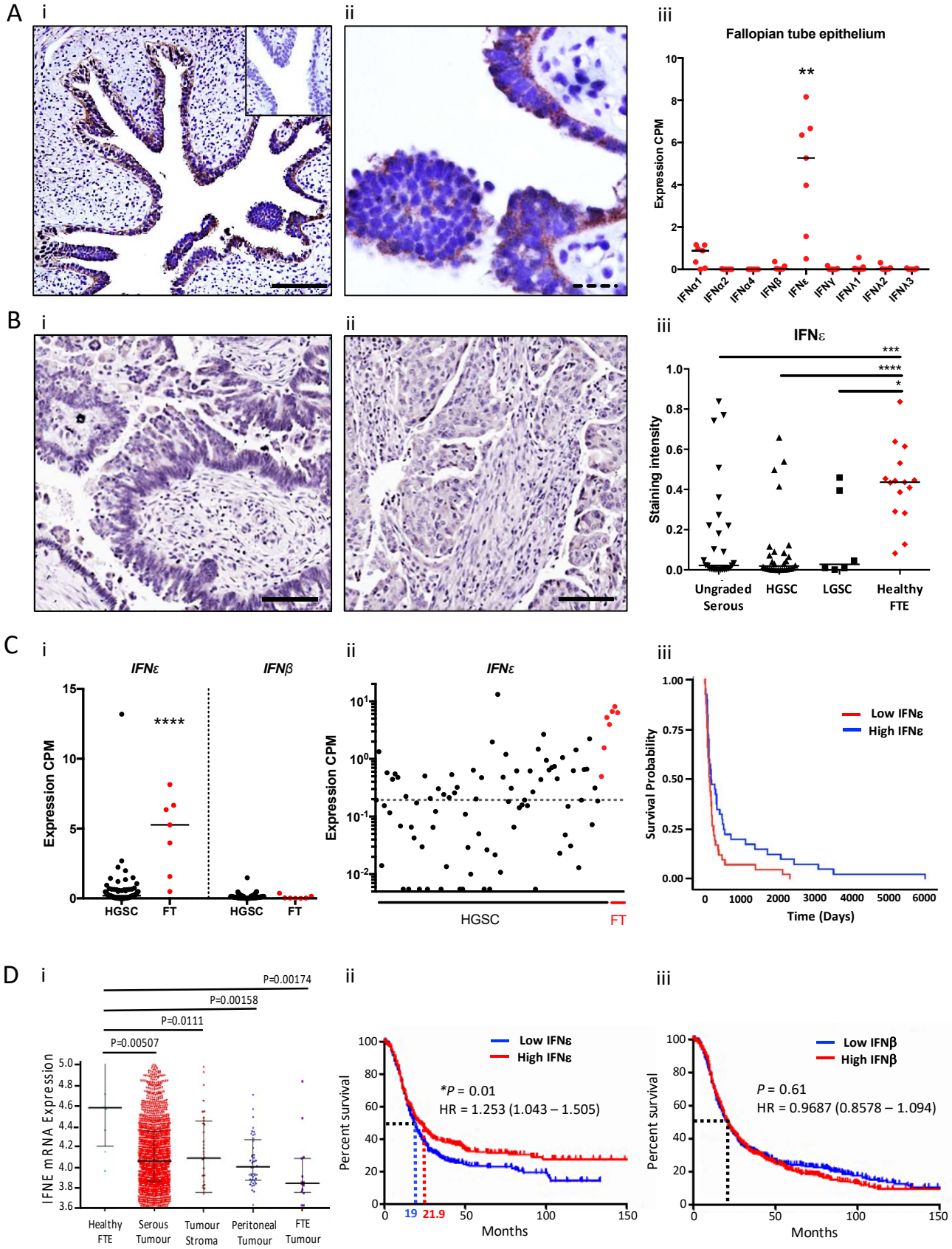
A
i
ii
iii
Fallopian tube epithelium
Expression CPM
**
IFNα1
IFNα2
IFNα4
IFNβ
IFNε
IFNγ
IFNλ1
IFNλ2
IFNλ3
B
i
ii
iii
IFNε
Staining intensity
***
****
*
Ungraded Serous
HGSC
LGSC
Healthy FTE
C
i
IFNε
IFNβ
Expression CPM
****
HGSC
FT
HGSC
FT
ii
IFNε
Expression CPM
HGSC
FT
iii
Survival Probability
Low IFNε
High IFNε
Time (Days)
D
i
P=0.00174
P=0.00158
P=0.0111
P=0.00507
IFNE mRNA Expression
Healthy FTE
Serous Tumour
Tumour Stroma
Peritoneal Tumour
FTE Tumour
ii
Low IFNε
High IFNε
Percent survival
*P = 0.01
HR = 1.253 (1.043 – 1.505)
19
21.9
Months
iii
Low IFNβ
High IFNβ
Percent survival
P = 0.61
HR = 0.9687 (0.8578 – 1.094)
Months

Figure 1. Suppressed expression of Fallopian tube epithelial IFNε in High Grade Serous Ovarian cancer correlates with poor prognosis. *(A) i-ii) Immunohistochemical (IHC) staining of human fallopian tube cross sections for IFNε, using rabbit anti-hu IFNε, or (image insert) rabbit IgG control. iii) mRNA expression of IFNs in human fallopian tube epithelium (RNAseq data derived from AOCS control samples, Cancer Genomics and Genetics Program at Peter MacCallum Cancer Centre[23]). (B) IHC staining for IFNε in i) low grade serous carcinoma, ii) high grade serous carcinoma representative of participants plotted in iiii) staining intensity of IFNε detection in n=20 human FT control epithelium, n=6 low grade, n=30 high grade serous carcinoma & n=28 ungraded serous samples analysed using positive pixel analysis in Imagescope software to quantify staining intensity in epithelial derived tissue components. Data are expressed as mean intensity scores for each sample stained in technical duplicates on tissue microarrays, analysed using individual Mann-Whitney tests, **p<0.01, ****p<0.0001. (C) i-ii) Plot showing normalised expression (by RNAseq analysis) of IFNε & IFNβ in AOCS samples (n=93 HGSC samples and n=7 FT epithelium). ii) Individual expression for IFNε, median expression in tumour samples indicated by dotted line. iii) Disease-free survival for AOCS cohort determined by expression of IFNε above or below the median. D) i) mRNA expression of IFNε in CSIOVDB cohort[24]. ii) Disease-free survival for CSIOVDB cohort determined by expression of IFNε and IFNβ (iii) above or below the median. Scale bars for IHC images black=100um, dashed=20um.*

Figure 2.

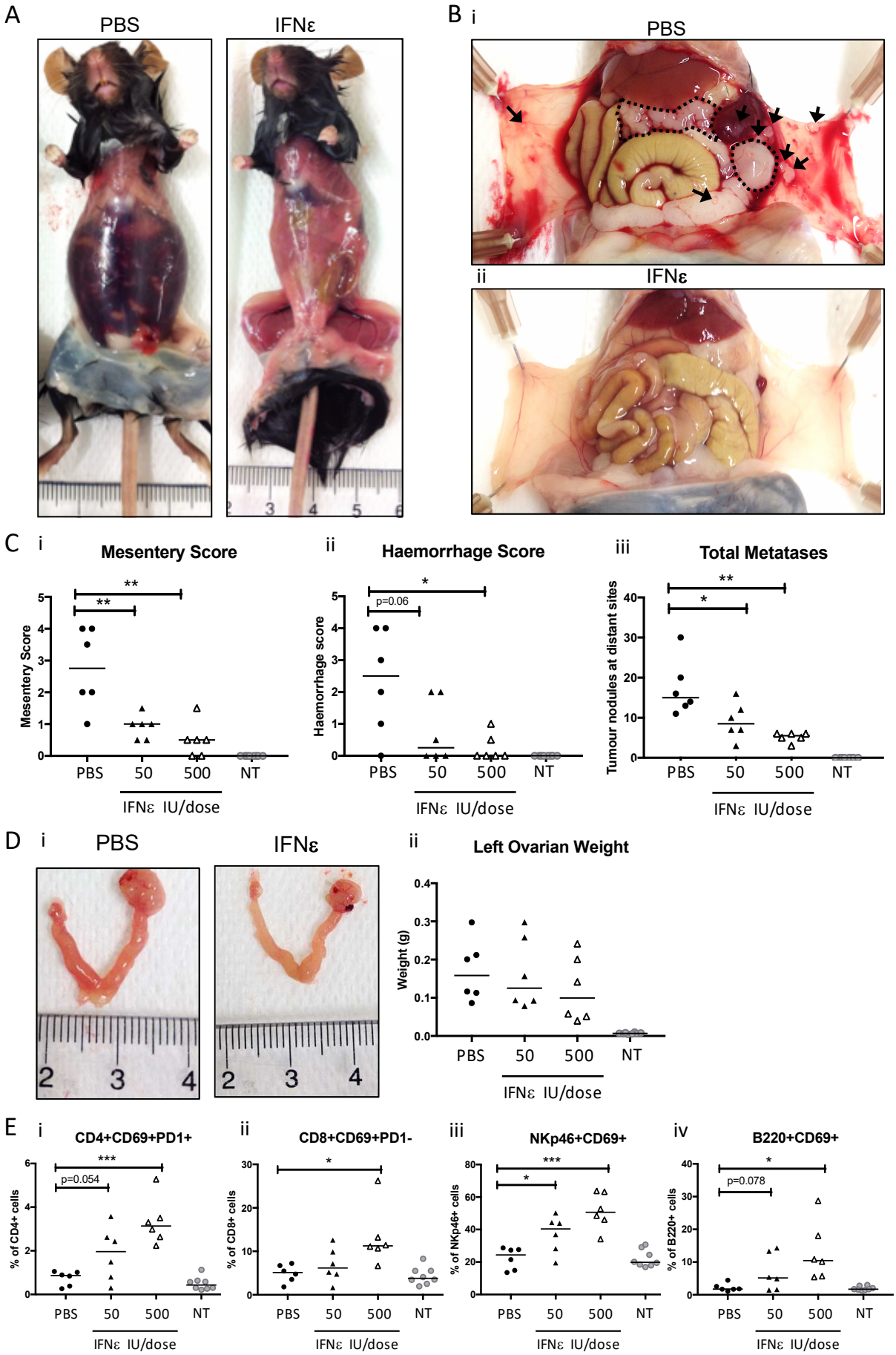
A
PBS
IFNε
B i
PBS
ii
IFNε
C i
Mesentery Score
Mesentery Score
PBS
50
500
NT
IFNε IU/dose
ii
Haemorrhage Score
Haemorrhage score
p=0.06
iii
Total Metatases
Tumour nodules at distant sites
D i
PBS
IFNε
ii
Left Ovarian Weight
Weight (g)
E i
CD4+CD69+PD1+
% of CD4+ cells
p=0.054
ii
CD8+CD69+PD1-
% of CD8+ cells
iii
NKp46+CD69+
% of NKp46+ cells
iv
B220+CD69+
% of B220+ cells
p=0.078

Figure 2. Anti-tumour activity of IFNε in a preclinical orthotopic model of ovarian cancer. *ID8 cells were implanted into C57BL6J mice via intrabursal injection (1x10^6 cells/mouse) to form orthotopic ovarian tumours & peritoneal metastases. (A) Images show peritoneal haemorrhagic ascites development in mice treated with PBS (left) compared to 500IU recombinant murine IFNε (right) 3x weekly via i.p. injections. NT is non tumour bearing mice. (B) Characteristic haemorrhaging & metastatic tumour deposits throughout the peritoneal cavity (black arrows & dotted outlines) of i) PBS- compared to ii) IFNε-treated mice. (C) i) Scoring of mesenteric tumour burden, ii) scoring of red blood cell content of lavage samples, iii) quantification of total number of metastatic deposits found in the peritoneal cavity of mice treated with PBS, 50 or 500 iu/ml IFNε. (D) i) Images show excised ovaries and uterine horn of PBS- and IFNε- treated mice, (ii) weights of orthotpic tumour-bearing ovaries are graphed. (E) Peritoneal lavage samples stained for immune markers and measured by multi-coloured flow cytometry - proportion of activated leukocytes including i) activated CD4 T cells (CD69+PD1+), ii – iv) CD8 T cells, NK cells & B cells (all CD69+). Data are presented as individual data points with median, n=6 mice per treatment. Significance was determined by Student's T test ****p<0.0001, ***p<0.001, **p<0.01, *p<0.05.*

Figure 2.

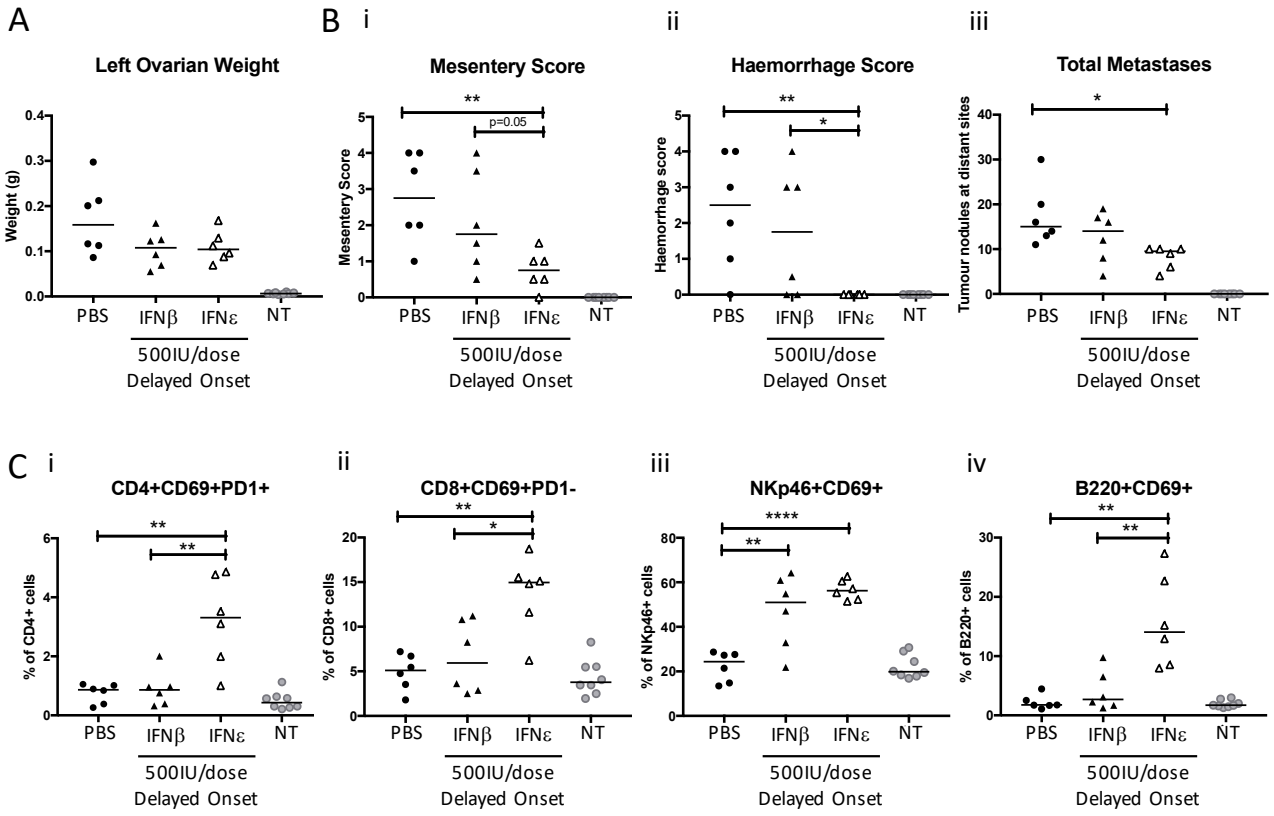
A
Left Ovarian Weight
Weight (g)
0.4
0.3
0.2
0.1
0.0
PBS
IFNβ
IFNε
NT
500IU/dose
Delayed Onset
B i
Mesentery Score
Mesentery Score
**
p=0.05
5
4
3
2
1
0
PBS
IFNβ
IFNε
NT
500IU/dose
Delayed Onset
ii
Haemorrhage Score
Haemorrhage score
**
*
5
4
3
2
1
0
PBS
IFNβ
IFNε
NT
500IU/dose
Delayed Onset
iii
Total Metastases
Tumour nodules at distant sites
*
40
30
20
10
0
PBS
IFNβ
IFNε
NT
500IU/dose
Delayed Onset
C i
CD4+CD69+PD1+
% of CD4+ cells
**
**
6
4
2
0
PBS
IFNβ
IFNε
NT
500IU/dose
Delayed Onset
ii
CD8+CD69+PD1-
% of CD8+ cells
**
*
20
15
10
5
0
PBS
IFNβ
IFNε
NT
500IU/dose
Delayed Onset
iii
NKp46+CD69+
% of NKp46+ cells
****
**
80
60
40
20
0
PBS
IFNβ
IFNε
NT
500IU/dose
Delayed Onset
iv
B220+CD69+
% of B220+ cells
**
**
30
20
10
0
PBS
IFNβ
IFNε
NT
500IU/dose
Delayed Onset

Figure 3. Delayed onset IFNε effectively suppresses pre-established orthotopic ovarian tumours. *ID8 cells were implanted into C57BL6J mice via intrabursal injection (1x10^6 cells/mouse) to form orthotopic 'primary' ovarian tumours & peritoneal metastases for 4 weeks prior to commencing recombinant IFNε or IFNβ therapy (500IU/dose i.p. injected 3x weekly for an additional 4 weeks). (A) Weights of excised left ID8-implanted ovaries compared to right PBS-implanted non-tumour controls. (B) i) Scoring of mesenteric tumour burden, ii) scoring of red blood cell content of peritoneal lavage samples, iii) quantification of total number of metastatic deposits found in the peritoneal cavity. (C) Peritoneal lavage samples stained for immune markers and measured by multi-coloured flow cytometry - proportion of activated leukocytes including i) activated CD4 T cells (CD69+PD1+), ii-iv) CD8 T cells, NK cells & B cells (all CD69+). Data are presented as median of individual data points, n=6 mice per treatment. Significance was determined by Student's T test ****p<0.0001, ***p<0.001, **p<0.01, *p<0.05.*

Figure 4.

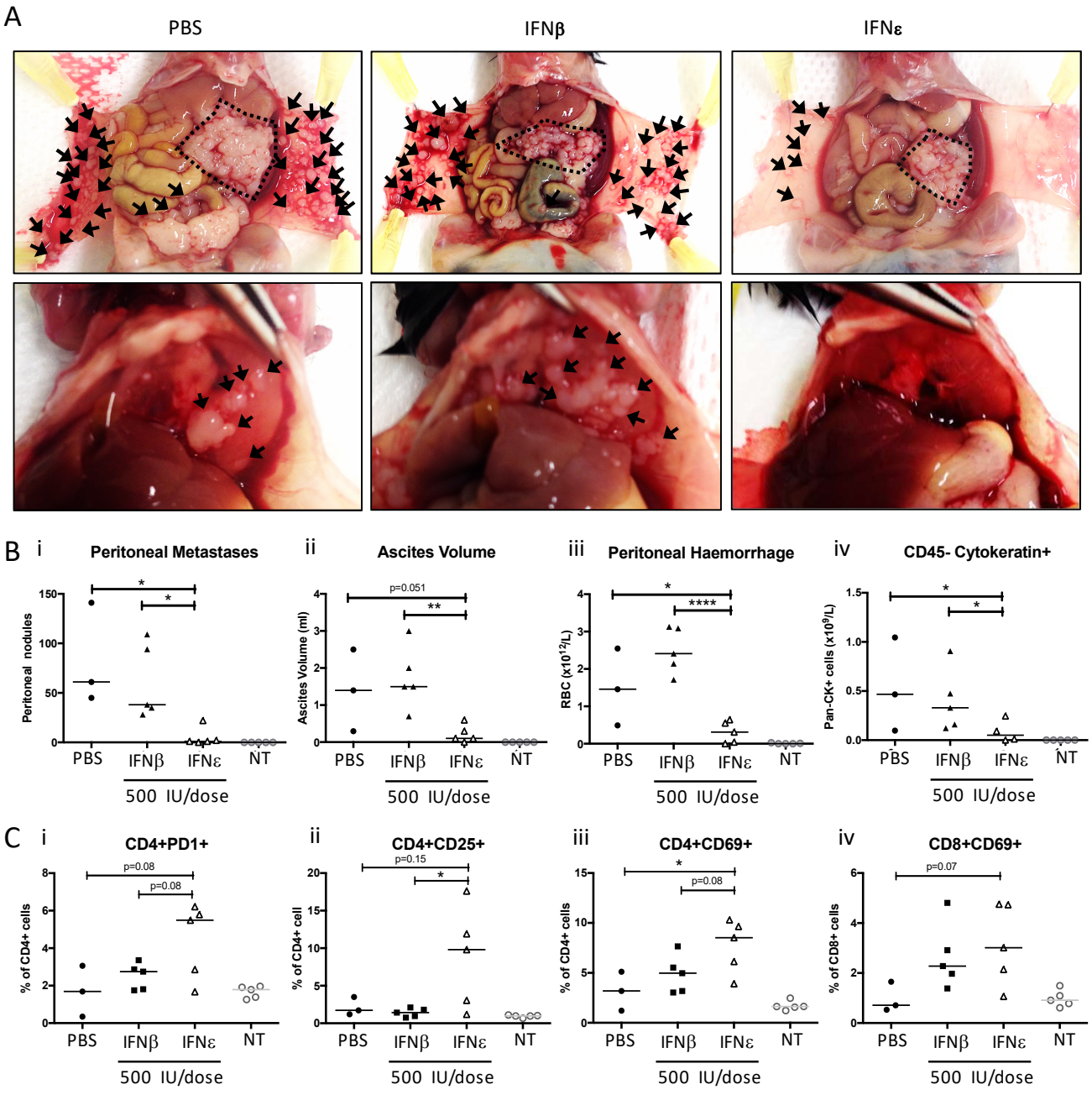
A
PBS
IFNβ
IFNε
B
i
Peritoneal Metastases
Peritoneal nodules
ii
Ascites Volume
Ascites Volume (ml)
p=0.051
iii
Peritoneal Haemorrhage
RBC (x10^12/L)
iv
CD45- Cytokeratin+
Pan-CK+ cells (x10^9/L)
PBS
IFNβ
IFNε
NT
500 IU/dose
C
i
CD4+PD1+
% of CD4+ cells
p=0.08
ii
CD4+CD25+
p=0.15
% of CD4+ cell
iii
CD4+CD69+
iv
CD8+CD69+
% of CD8+ cells
p=0.07

Figure 4. IFNε suppresses ascites & metastasis in a model of advanced ovarian cancer. *Dissemination & tumour growth of ID8 cells 8-weeks post-intraperitoneal injection of IFNε or IFNβ into C57BL6J mice. (A) Characteristic nodule formation throughout the mesentery (black dotted outlines; top row) and adhered to the peritoneal wall (black arrows; top row) and diaphragm (black arrows; bottom row) of mice injected with ID8 cells then treated with i.p. i) PBS, ii) IFNβ or iii) IFNε at 500IU/dose 3 times weekly for 8 weeks. (B) i) Quantified metastatic nodules on the peritoneal wall, ii) volume of ascites drained from the peritoneum, iii) number of red blood cells in ascites fluid measured by Sysmex Cell Counter, and iv) number of epithelial (pan-CK+) tumour cells in peritoneal lavage fluid measured by flow cytometry. (C) Peritoneal lavage samples from C57BL/6J mice 8 weeks post-intraperitoneal injection with ID8 cells stained for immune markers and measured by multi-coloured flow cytometry. Proportion of activated leukocytes in these mice including i-iii) activated CD4 T cells (CD25+, CD69+ or PD1+), and iv) CD8 T cells (CD69+). Data are presented as median of individual data points, n=5 mice per IFN treatment group, n=5 non-tumour bearing mice, and n=3 tumour-bearing mice treated with PBS. Significance was determined by Student's T test ****p<0.0001, ***p<0.001, **p<0.01, *p<0.05.*

Figure 5.

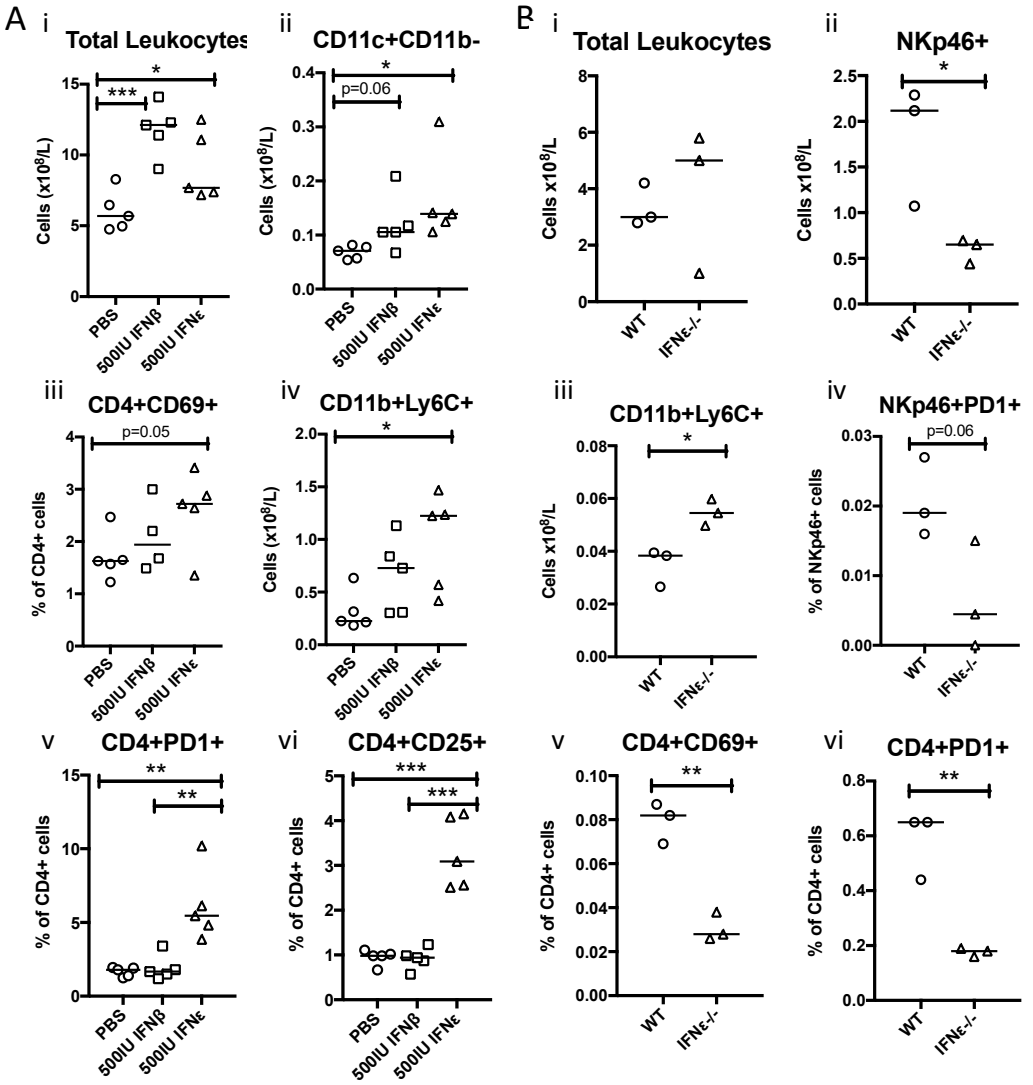
A
i
Total Leukocytes
Cells (x10⁸/L)
PBS
500IU IFNβ
500IU IFNε
ii
CD11c+CD11b-
p=0.06
iii
CD4+CD69+
p=0.05
% of CD4+ cells
iv
CD11b+Ly6C+
v
CD4+PD1+
vi
CD4+CD25+
B
i
Total Leukocytes
Cells x10⁸/L
WT
IFNε-/-
ii
NKp46+
iii
CD11b+Ly6C+
iv
NKp46+PD1+
% of NKp46+ cells
v
CD4+CD69+
vi
CD4+PD1+

Figure 5. Endogenous and exogenous IFNε regulate immune cells in vivo. *Peritoneal lavage samples from non-tumour bearing C57BL6J mice stained for immune cell identification and activation markers and measured by multi-coloured flow cytometry. (A) i - vi) WT mice treated with PBS, IFNβ or IFNε (500IU/dose i.p. injected 3 times weekly for 8 weeks). (B) i - vi) WT compared to IFNε$^{-/-}$ mice. Leukocyte populations include total leukocytes (CD45+), NK cells (CD45+NKp46+), dendritic cells (CD45+CD11c+CD11b-) and inflammatory monocytes (CD45+CD11b+Ly6C+) and proportions of activated CD4 T cells (CD25+, CD69+ or PD1+) in these mice. Data are presented as median of individual data points, n=3 mice per genotype comparison group (endogenous IFNε) and n=5 mice per i.p. treatment group (exogenous IFNε). Significance was determined by Student's T test ***p<0.001, **p<0.01, *p<0.05.*

Figure 6.

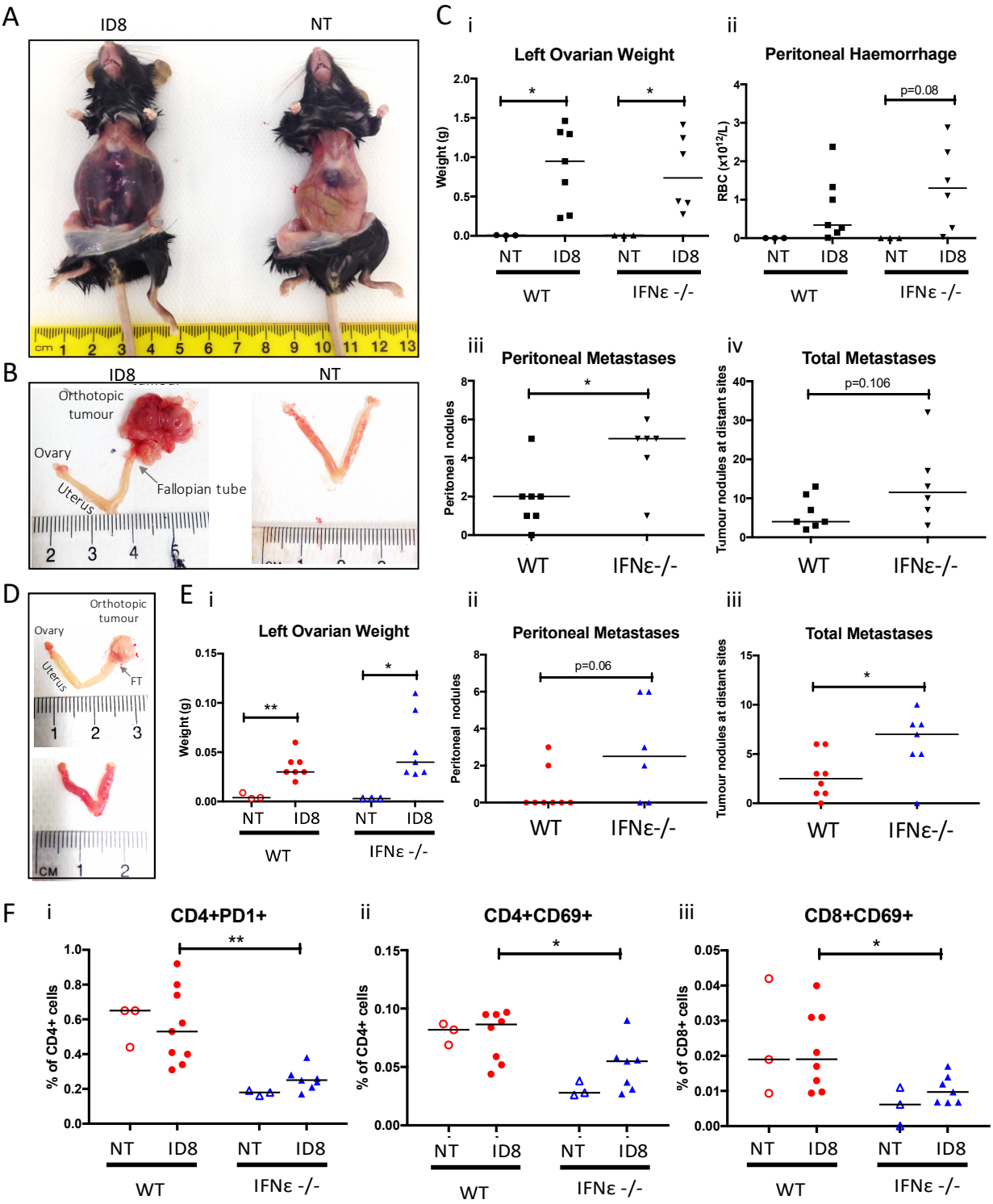
A
ID8
NT
B
ID8
NT
Orthotopic tumour
Ovary
Uterus
Fallopian tube
C i
Left Ovarian Weight
Weight (g)
NT
ID8
WT
IFNε -/-
C ii
Peritoneal Haemorrhage
RBC (x10^12/L)
p=0.08
C iii
Peritoneal Metastases
Peritoneal nodules
WT
IFNε-/-
C iv
Total Metastases
Tumour nodules at distant sites
p=0.106
D
Orthotopic tumour
Ovary
Uterus
FT
E i
Left Ovarian Weight
E ii
Peritoneal Metastases
p=0.06
E iii
Total Metastases
F i
CD4+PD1+
% of CD4+ cells
F ii
CD4+CD69+
F iii
CD8+CD69+
% of CD8+ cells

Figure 6. Endogenous IFNε suppresses ovarian cancer metastases. *Mouse ovarian cancer cells (ID8) were injected into the left ovarian bursa of female C57BL/6 wild-type (IFNε$^{+/+}$) and IFNε deficient mice (IFNε$^{-/-}$). A –B) At 13 weeks post-intrabursal ID8 injection WT & IFNε$^{-/-}$ mice demonstrate advanced haemorrhagic ascites & primary tumours. (C) i) Weights of excised left ID8-implanted ovaries compared to right PBS-implanted non-tumour controls, ii) number of red blood cells in peritoneal lavage samples, iii) number of metastatic nodules adhered to the peritoneal wall, iv) quantification of total number of metastatic deposits found in the peritoneal cavity. (D) Orthotopic tumour growth at 6 weeks post-intrabursal ID8 injection WT & IFNε$^{-/-}$ mice. (E) i) Weights of excised left ID8-implanted ovaries compared to PBS-implanted non-tumour controls, ii) number of metastatic nodules adhered to the peritoneal wall, iii) quantification of total number of metastatic deposits found in the peritoneal cavity. (F) Immunophenotyping flow cytometry was performed on peritoneal cells from WT & IFNε$^{-/-}$ mice 6 weeks post-intrabursal ID8 injection. Proportion of activated leukocytes in these mice including i-ii) activated CD4 T cells (PD1^{+}CD69^{+}) & iii) CD8 T cells (CD69^{+}). Data are presented as median of individual data points, n=3 non-tumour bearing mice per genotype, 13-week model: n=6 ID8-injected mice per genotype, 6-week model: n=8 WT ID8-injected mice and n=7 IFNε$^{-/-}$ ID8-injected mice. Significance was determined by Student's T test ***p<0.001, **p<0.01, *p<0.05.*

Figure 7.

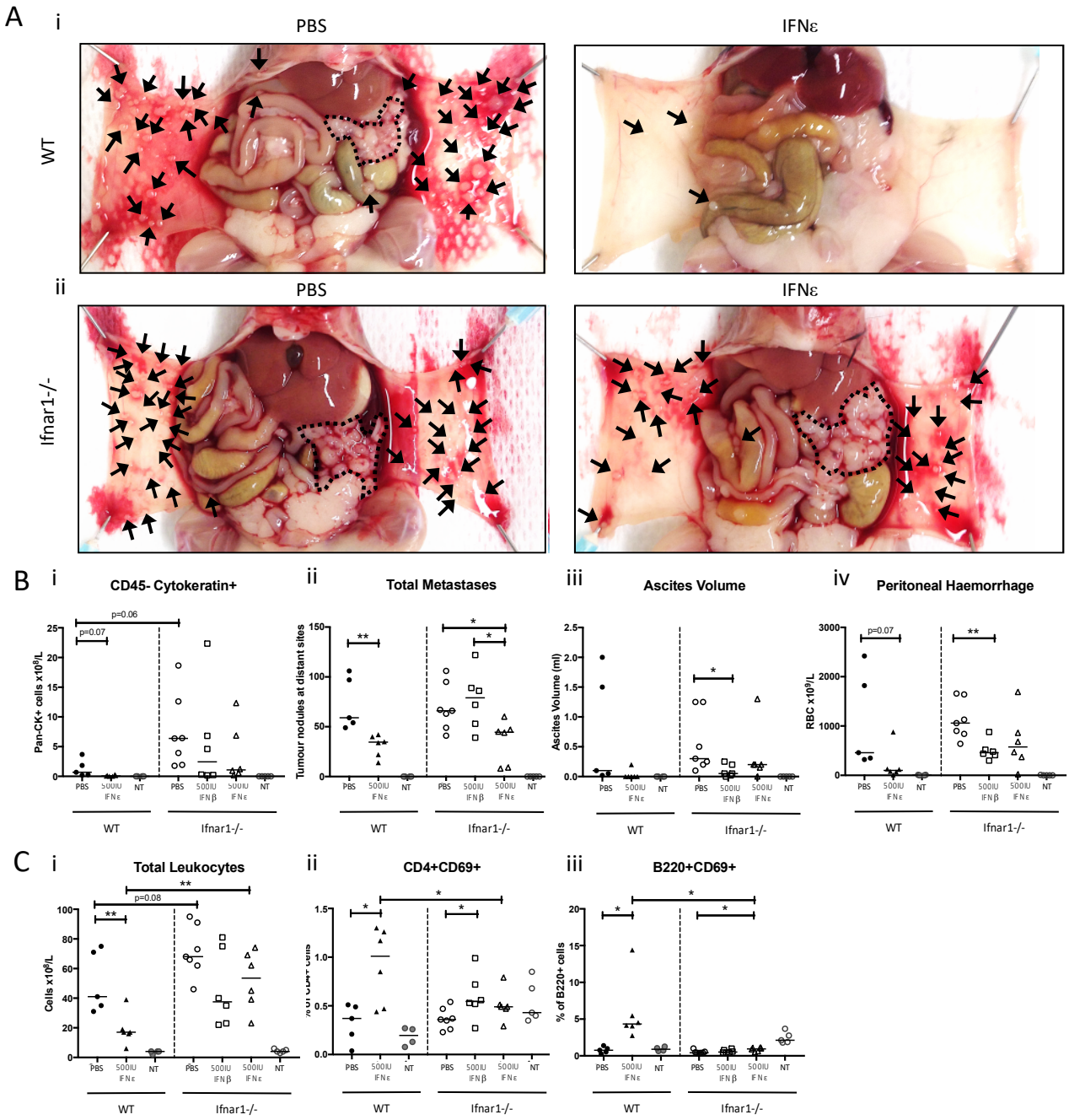
A
i
PBS
IFNε
WT
ii
PBS
IFNε
Ifnar1-/-
B
i
CD45- Cytokeratin+
Pan-CK+ cells x10⁶/L
ii
Total Metastases
Tumour nodules at distant sites
iii
Ascites Volume
Ascites Volume (ml)
iv
Peritoneal Haemorrhage
RBC x10⁹/L
PBS
500IU IFNε
500IU IFNβ
NT
WT
Ifnar1-/-
C
i
Total Leukocytes
Cells x10⁶/L
ii
CD4+CD69+
iii
B220+CD69+
% of B220+ cells

Figure 7. The mechanism of IFN suppression of peritoneal anti-tumour immunity. . *Dissemination & tumour growth of ID8 cells 8-weeks post-intraperitoneal injection into WT or Ifnar1-/- C57BL6J mice. (A) Characteristic nodule formation throughout the mesentery (black dotted outlines) and adhered to the peritoneal wall (black arrows) and diaphragm (black arrows) of i) WT mice or ii) Ifnar1-/- mice injected with ID8 cells then treated with i.p. PBS or IFNε at 500IU/dose 3 times weekly for 8 weeks. (B) i) quantified total metastatic nodules ii) number of epithelial (pan-CK+) tumour cells in peritoneal lavage fluid measured by flow cytometry, iii) volume of ascites drained from the peritoneum, iv) number of red blood cells in ascites fluid measured by Sysmex Cell Counter. (C) Peritoneal lavage samples from C57BL6J mice 8 weeks post- intraperitoneal injection with ID8 cells stained for immune markers and measured by multi-coloured flow cytometry. i) Total live leukocytes (CD45+), ii) CD4 T cells & iii) CD8 T cells (CD69+). Data are presented as median of individual data points, n=5 mice per IFN treatment group, n=5 non-tumour bearing mice, and n=3 tumour-bearing mice treated with PBS. Significance was determined by Student's T test ****p<0.0001, ***p<0.001, **p<0.01, *p<0.05.*

Figure 8.

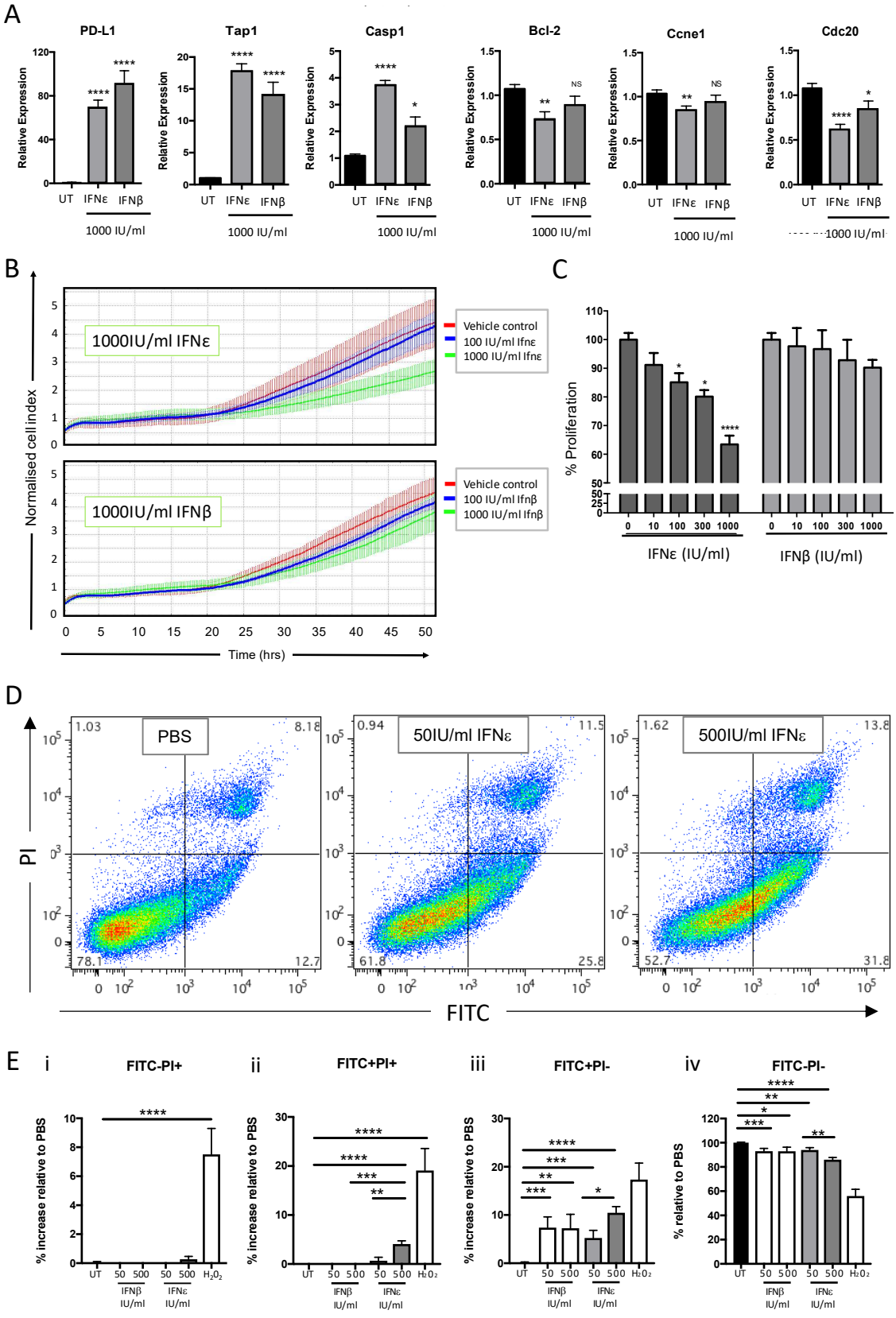
A
PD-L1
Tap1
Casp1
Bcl-2
Ccne1
Cdc20
Relative Expression
UT
IFNε
IFNβ
1000 IU/ml
B
1000IU/ml IFNε
1000IU/ml IFNβ
Vehicle control
100 IU/ml Ifnε
1000 IU/ml Ifnε
100 IU/ml Ifnβ
1000 IU/ml Ifnβ
Normalised cell index
Time (hrs)
C
% Proliferation
IFNε (IU/ml)
IFNβ (IU/ml)
D
PBS
50IU/ml IFNε
500IU/ml IFNε
PI
FITC
E
i FITC-PI+
ii FITC+PI+
iii FITC+PI-
iv FITC-PI-
% increase relative to PBS
% relative to PBS
IFNβ IU/ml
IFNε IU/ml
H2O2

Figure 8. Direct anti-tumour effects of IFNε on murine ovarian cancer cells in vitro. *(A) Graphs show expression of PD-L1, Tap1, Casp1, Bcl-2, Ccne1 and Cdc20 in response to stimulation of ID8 cells with 1000 IU/ml IFNε (light grey bar) or IFNβ (dark grey bar) for 3 hours. Gene expression was measured by qRT-PCR, expression calculated by dCT standardised to 18s and relative expression show here determined in relation to expression at t0. Data are presented as mean +/- SEM of n=3 independent experiments, each done in technical triplicates. (B) Plots show inhibition of proliferation of ID8 cells treated with 100–1000 IU/ml of IFNε (top panel) or IFNβ (bottom panel) for 48 hours. Cell proliferation was measured by xCELLigence. Graphs show the mean cell index across each well +/- SD. (C) Plot shows inhibition of proliferation of ID8 cells treated with 0-1000 IU/ml of IFNε (dark grey bars) or IFNβ (light grey bars) for 48 hours. Cell proliferation was measured by MTT assay. Plot shows the proliferation measured as end point absorbance and calculated as percentage of untreated cells +/- SEM.(D) Scatter plots show induction of apoptosis (Annexin V-FITC/PI staining) in ID8 cells treated with 50-500 IU/ml of IFNε or PBS for 48 hours measured by flow cytometry. (E) Graphs show Annexin V-FITC/PI staining for i) necrotic cells (FITC-PI+), ii) late apoptotic/dead cells (FITC+PI+), iii) early apoptotic cells (FITC+PI-) and iv) live cells (FITC-PI-). Data shown as percentage positive cells after treatment with IFNε or IFNβ relative to PBS-treated. Data are presented as mean +/- SEM. All experiments done using ID8 cells, n=3 independent experiments done in technical triplicates (RT-PCR, xCELLigence, MTT) or duplicates (Annexin V/PI). Significance was determined by Student's T test ****p<0.0001, ***p<0.001, **p<0.01, *p<0.05.*

Supplementary Figure 1.

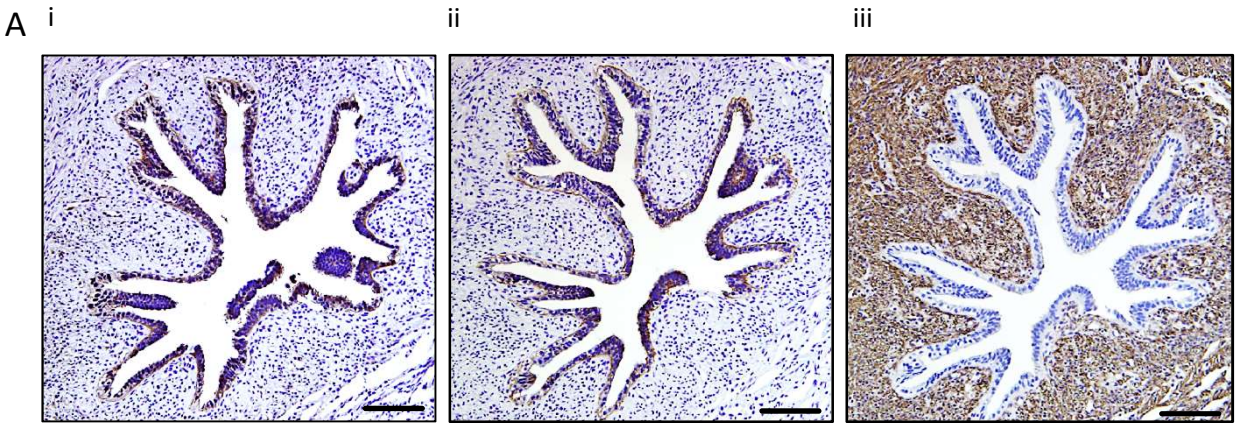

Supplementary Figure 1. IFN expression co-localises with cytokeratin-18 in the human fallopian tube epithelium. *(A) Images show immunohistochemical staining of human fallopian tube cross sections for i) IFNε, using rabbit anti-hu IFNε, ii) cytokeratin-18, iii) smooth muscle actin. Representative of n=10 fallopian tube samples. Scale bars 100um.*

Supplementary Figure 2.

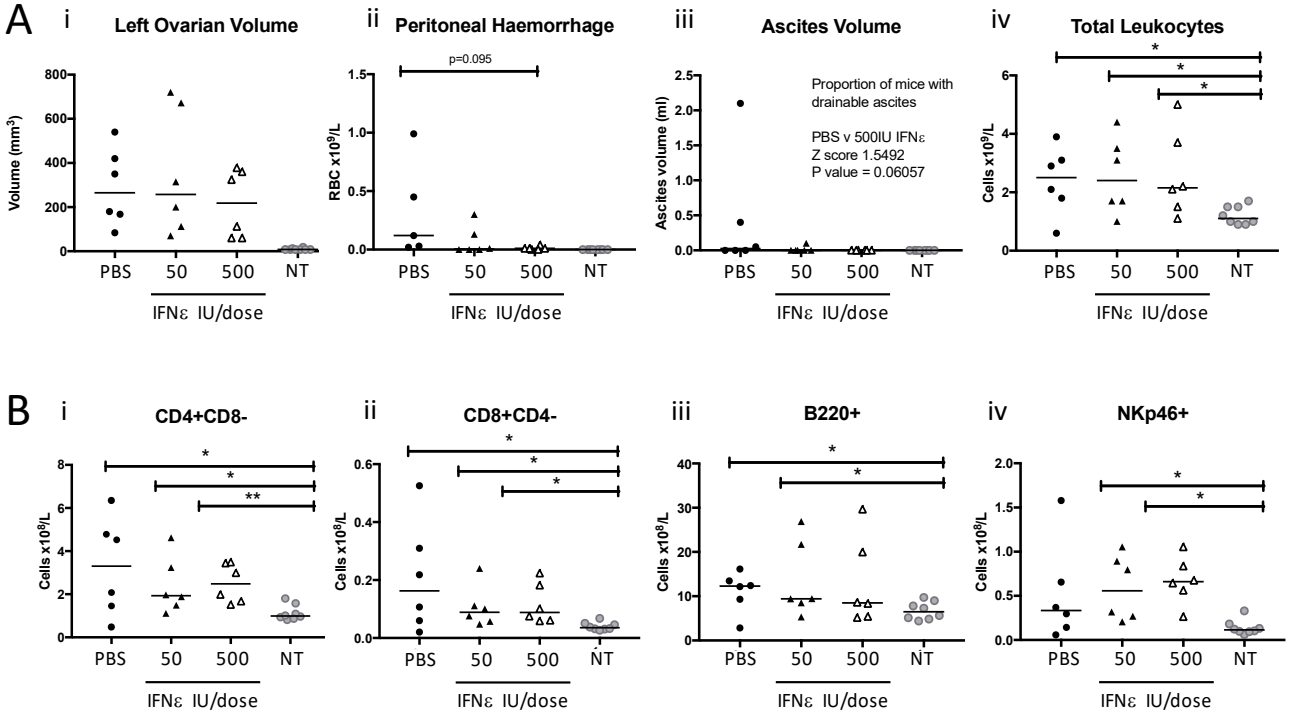

Supplementary Figure 2. Dose response of anti-tumour activity of IFNε in an orthotopic model of ovarian cancer. *ID8 cells were implanted into C57BL6J mice via intrabursal injection (1x10^6 cells/mouse) to form orthotopic 'primary' ovarian tumours and peritoneal metastases. (A) Additional disease quantification including volumes of excised left ID8-implanted ovaries compared to PBS-implanted non-tumour controls, red blood cell content of peritoneal ascites & lavage fluid, volume of peritoneal ascites and total number of leukocytes in peritoneal fluid of tumour-bearing mice treated with a dose-range of IFNε compared to PBS and non-tumour controls. (B) Peritoneal lavage samples stained for immune markers and measured by multi-coloured flow cytometry – total number of leukocytes populations including CD4 T cells (CD45+CD4+CD8-), CD8 T cells (CD45+CD8+CD4-), B cells (CD45+B220+) & NK cells (CD45+NKp46+). Data are shown as median of individual data points, n=6 mice per treatment. Significance was determined by Student's T test ****p<0.0001, ***p<0.001, **p<0.01, *p<0.05.*

Supplementary Figure 3.

		Haemorrhage Score	Mesentery Score	CD8	MCP1	Total Mets	CD4	CD11cMHCII	IL6	CD11bLy6G	NK Cells	CD11bLy6C	TNF
Tumour burden	Mesentery Score	0.91		0.78	0.79	0.74	0.70	0.55	0.51	0.42	0.30	0.24	0.47
	Haemorrhage Score		0.91	0.84	0.84	0.70	0.78	0.60	0.51	0.54	0.42	0.39	0.34
	Total Mets	0.70	0.74	0.47	0.57		0.43	0.40	0.37	0.40	0.08	0.24	0.23
Total Immune Cells	CD4	0.78	0.70	0.91	0.70	0.43		0.71	0.55	0.47	0.74	0.39	0.40
	CD8	0.84	0.78		0.82	0.47	0.91	0.63	0.74	0.64	0.70	0.50	0.47
	B Cells	0.21	0.17	0.46	0.10	-0.08	0.57	0.51	0.01	0.02	0.50	0.10	0.06
	NK Cells	0.42	0.30	0.70	0.50	0.08	0.74	0.67	0.57	0.64		0.64	0.26
	CD11bLy6C	0.39	0.24	0.50	0.56	0.24	0.39	0.55	0.60	0.90	0.64		0.14
	CD11bLy6G	0.54	0.42	0.64	0.67	0.40	0.47	0.42	0.81		0.64	0.90	0.26
	CD11cMHCII	0.60	0.55	0.63	0.52	0.40	0.71		0.24	0.42	0.67	0.55	0.07
Immune Activation	CD4 PD1	-0.02	-0.06	0.16	0.01	-0.15	0.41	0.66	-0.20	-0.09	0.49	0.21	-0.10
	CD4 CD69	0.25	0.13	0.30	0.01	-0.02	0.52	0.45	-0.02	0.05	0.45	0.06	0.05
	CD4 CD25	-0.04	0.03	0.11	-0.08	-0.08	0.38	0.55	-0.22	-0.19	0.43	0.01	-0.01
	CD4 Foxp3	0.03	0.06	0.19	0.01	-0.08	0.47	0.44	-0.12	-0.13	0.52	-0.02	0.15
	CD4 CD25+ Foxp3+	0.02	0.11	0.15	-0.06	-0.01	0.42	0.51	-0.19	-0.20	0.44	-0.08	0.02
	CD4 CD25- Foxp3+	0.03	0.02	0.19	0.04	-0.10	0.44	0.36	-0.07	-0.08	0.52	0.01	0.21
	CD4 CD25+ Foxp3-	-0.23	-0.23	-0.07	-0.13	-0.25	0.08	0.42	-0.22	-0.06	0.21	0.33	-0.11
	CD4 CD69+ PD1+	-0.52	-0.45	-0.39	-0.31	-0.36	-0.30	-0.05	-0.25	-0.26	-0.18	0.01	-0.05
	CD4 PD1+ Foxp3-	-0.40	-0.36	-0.30	-0.24	-0.26	-0.07	0.20	-0.33	-0.32	0.05	-0.05	-0.18
	CD4 PD1+ Foxp3+	-0.24	-0.21	-0.24	-0.15	-0.13	-0.04	0.19	-0.28	-0.21	0.16	-0.07	-0.05
	CD4 PD1- Foxp3+	-0.28	-0.11	-0.25	-0.26	-0.14	-0.03	-0.06	-0.27	-0.39	0.05	-0.40	0.09
	B220+ CD69+	-0.53	-0.49	-0.23	-0.34	-0.39	-0.30	-0.11	-0.21	-0.12	0.02	0.03	-0.10
	NK CD69+	-0.21	-0.25	0.02	-0.06	-0.22	0.13	0.41	-0.04	0.15	0.63	0.32	0.00
	CD11bintMHCIIint	0.21	0.26	0.03	0.05	0.43	0.20	0.41	-0.18	-0.10	0.01	-0.06	-0.19
Cytokines	IFNgamma	-0.12	-0.07	-0.11	-0.01	0.01	-0.11	-0.19	0.03	-0.03	-0.16	-0.07	0.32
	IL6	0.51	0.51	0.74	0.68	0.37	0.55	0.24		0.81	0.57	0.60	0.46
	IL10	0.12	0.12	0.18	0.25	-0.11	0.14	0.00	0.14	0.12	0.18	0.11	0.28
	IL12	-0.40	-0.24	-0.22	-0.34	-0.21	-0.15	-0.38	-0.17	-0.33	-0.17	-0.35	0.23
	MCP1	0.84	0.79	0.82		0.57	0.70	0.52	0.68	0.67	0.50	0.56	0.50
	TNF	0.34	0.47	0.47	0.50	0.23	0.40	0.07	0.46	0.26	0.26	0.14	
		1/A						1/B			2		
		High tumour correlation **AND** MCP1/IL6 **AND** total immune counts - **Negative** immune activation						**Moderate** tumour correlation **AND** total immune			**Weak** tumour correlation - **high** total immune		

		CD11bintMHCIIint	CD4 CD69	B Cells	CD4 Foxp3	CD4 CD25- Foxp3+	CD4 CD25+ Foxp3+	CD4 PD1	CD4 CD25	CD4 PD1- Foxp3+	CD4 PD1+ Foxp3+	CD4 CD25+ Foxp3-	NK CD69+	CD4 PD1+ Foxp3-	CD4 CD69+ PD1+	IL12	B220+ CD69+
Tumour burden	Mesentery Score	0.26	0.13	0.17	0.06	0.02	0.11	-0.06	0.03	-0.11	-0.21	-0.23	-0.25	-0.36	-0.45	-0.24	-0.49
	Haemorrhage Score	0.21	0.25	0.21	0.03	0.03	0.02	-0.02	-0.04	-0.28	-0.24	-0.23	-0.21	-0.40	-0.52	-0.40	-0.53
	Total Mets	0.43	-0.02	-0.08	-0.08	-0.10	-0.01	-0.15	-0.08	-0.14	-0.13	-0.25	-0.22	-0.26	-0.36	-0.21	-0.39
Total Immune Cells	CD4	0.20	0.52	0.57	0.47	0.44	0.42	0.41	0.38	-0.03	-0.04	0.08	0.13	-0.07	-0.30	-0.15	-0.30
	CD8	0.03	0.30	0.46	0.19	0.19	0.15	0.16	0.11	-0.25	-0.24	-0.07	0.02	-0.30	-0.39	-0.22	-0.23
	B Cells	0.17	0.42		0.59	0.56	0.54	0.57	0.53	-0.04	-0.13	0.26	0.19	-0.14	-0.27	-0.03	0.19
	NK Cells	0.01	0.45	0.50	0.52	0.52	0.44	0.49	0.43	0.05	0.16	0.21	0.63	0.05	-0.18	-0.17	0.02
	CD11bLy6C	-0.06	0.06	0.10	-0.02	0.01	-0.08	0.21	0.01	-0.40	-0.07	0.33	0.32	-0.05	0.01	-0.35	0.03
	CD11bLy6G	-0.10	0.05	0.02	-0.13	-0.08	-0.20	-0.09	-0.19	-0.39	-0.21	-0.06	0.15	-0.32	-0.26	-0.33	-0.12
	CD11cMHCII	0.41	0.45	0.51	0.44	0.36	0.51	0.66	0.55	-0.06	0.19	0.42	0.41	0.20	-0.05	-0.38	-0.11
Immune Activation	CD4 PD1	0.30	0.37	0.57	0.77	0.71	0.75		0.83	0.34	0.44	0.72	0.57	0.68	0.31	0.09	0.11
	CD4 CD69	0.30		0.42	0.47	0.36	0.57	0.37	0.54	0.20	0.12	0.21	0.25	0.08	-0.10	-0.17	-0.13
	CD4 CD25	0.51	0.54	0.53	0.84	0.69	0.97	0.83		0.61	0.47	0.65	0.54	0.52	0.23	0.18	0.02
	CD4 Foxp3	0.29	0.47	0.59		0.97	0.88	0.77	0.84	0.68	0.44	0.33	0.52	0.38	-0.04	0.23	-0.08
	CD4 CD25+ Foxp3+	0.52	0.57	0.54	0.88	0.73		0.75	0.97	0.70	0.47	0.46	0.51	0.42	0.09	0.19	-0.05
	CD4 CD25- Foxp3+	0.13	0.36	0.56	0.97		0.73	0.71	0.69	0.61	0.38	0.24	0.48	0.32	-0.11	0.23	-0.08
	CD4 CD25+ Foxp3-	0.24	0.21	0.26	0.33	0.24	0.46	0.72	0.65	0.06	0.27		0.40	0.61	0.62	0.04	0.25
	CD4 CD69+ PD1+	-0.09	-0.10	-0.27	-0.04	-0.11	0.09	0.31	0.23	0.17	0.41	0.62	0.23	0.74		0.33	0.31
	CD4 PD1+ Foxp3-	0.11	0.08	-0.14	0.38	0.32	0.42	0.68	0.52	0.46	0.62	0.61	0.47		0.74	0.25	0.13
	CD4 PD1+ Foxp3+	0.10	0.12	-0.13	0.44	0.38	0.47	0.44	0.47	0.61		0.27	0.58	0.62	0.41	0.11	-0.02
	CD4 PD1- Foxp3+	0.20	0.20	-0.04	0.68	0.61	0.70	0.34	0.61		0.61	0.06	0.37	0.46	0.17	0.46	-0.13
	B220+ CD69+	-0.38	-0.13	0.19	-0.08	-0.08	-0.05	0.11	0.02	-0.13	-0.02	0.25	0.40	0.13	0.31	0.10	
	NK CD69+	-0.01	0.25	0.19	0.52	0.48	0.51	0.57	0.54	0.37	0.58	0.40		0.47	0.23	0.07	0.40
	CD11bintMHCIIint		0.30	0.17	0.29	0.13	0.52	0.30	0.51	0.20	0.10	0.24	-0.01	0.11	-0.09	-0.11	-0.38
Cytokines	IFNgamma	-0.14	0.05	-0.02	-0.04	0.06	-0.24	-0.22	-0.26	-0.11	-0.26	-0.21	-0.19	-0.21	-0.16	-0.17	0.10
	IL6	-0.18	-0.02	0.01	-0.12	-0.07	-0.19	-0.20	-0.22	-0.27	-0.28	-0.22	-0.04	-0.33	-0.25	-0.17	-0.21
	IL10	-0.29	0.04	-0.01	-0.01	-0.01	-0.01	-0.06	0.00	-0.06	-0.07	0.01	0.13	-0.08	0.00	0.12	0.09
	IL12	-0.11	-0.17	-0.03	0.23	0.23	0.19	0.09	0.18	0.46	0.11	0.04	0.07	0.25	0.33		0.10
	MCP1	0.05	0.01	0.10	0.01	0.04	-0.06	0.01	-0.08	-0.26	-0.15	-0.13	-0.06	-0.24	-0.31	-0.34	-0.34
	TNF	-0.19	0.05	0.06	0.15	0.21	0.02	-0.10	-0.01	0.09	-0.05	-0.11	0.00	-0.18	-0.05	0.23	-0.10
		3/A			3/B					3/C				4			
		No tumour correlation - some total immune AND CD4 activation			**No** tumour correlation - shift to total B cells **AND** CD4 activation					**No** tumour correlation - shift away from total cells, some immune activation				**Negative** tumour correlation **AND** MCP1			

Supplementary Figure 3. Correlations between immune cell populations, inflammatory cytokines and tumour burden in a model of ovarian cancer. *ID8 cells implanted into C57BL6J mice via intrabursal injection ($1x10^6$ cells/mouse), forming orthotopic ovarian tumours & peritoneal metastases over 8 weeks. A – B) Tables show Pearson r correlations between various parameters determining tumour burden (mesentery & haemorrhage score, total metastatic nodules), total immune cell populations (CD4+ & CD8+ T cells, B cells, NK cells, monocytes, neutrophils, dendritic cells), markers of immune activation (PD1, CD69, CD25, MHCII) and inflammatory cytokines IFNγ, IL6, IL10, IL12, MCP1, TNF) as measured at endpoint. Correlations are coloured if $p<0.05$, blue $r<0$, yellow $r<0.5$, orange $0.5>r<0.7$, red $r>0.8$. Correlations were calculated on results from n=6 PBS-treated, IFNε-treated & IFNβ-treated mice. Non-tumour bearing mice were excluded from analysis.*

Supplementary Figure 4.

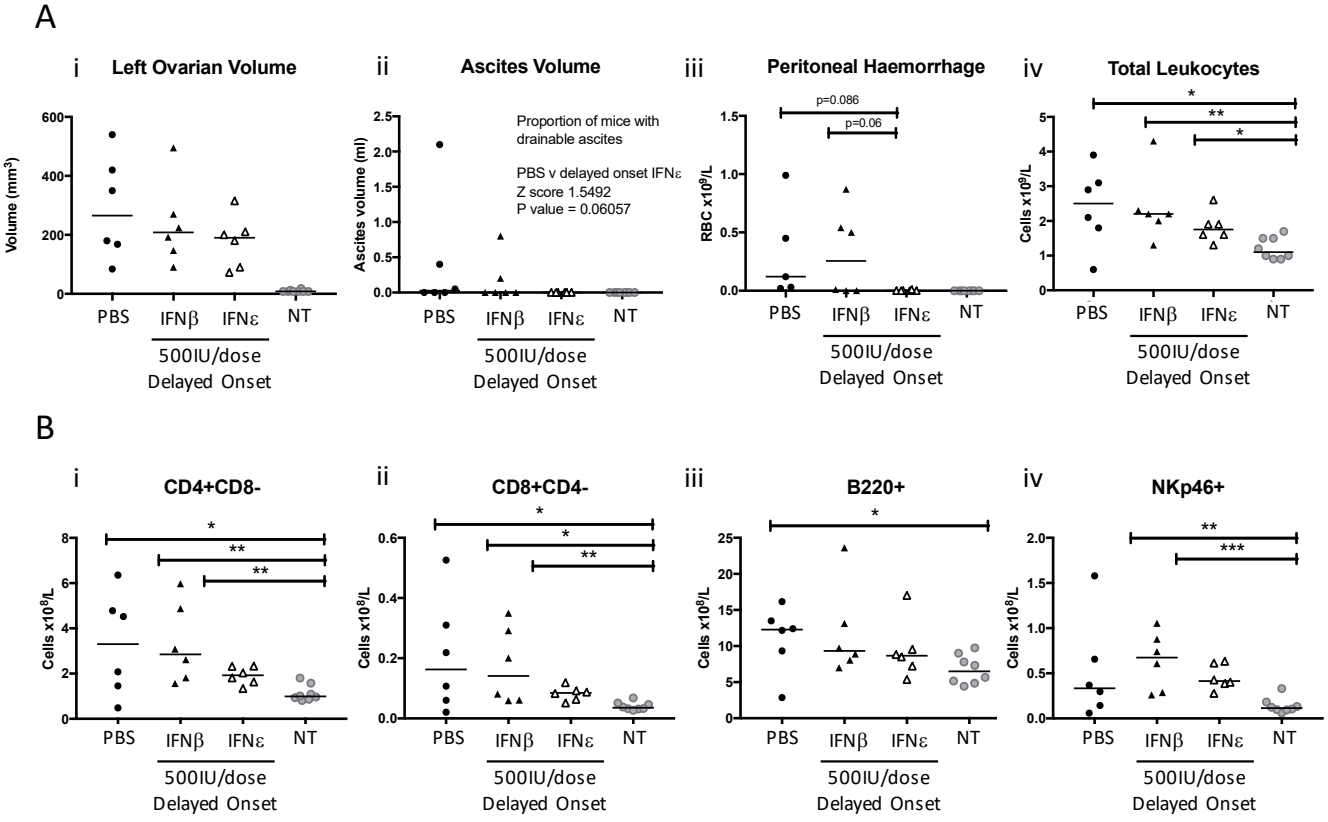

Supplementary Figure 4. Anti-tumour activity of IFNε compared to IFNβ in a model of ovarian cancer. *Dissemination & tumour growth of ID8 cells 8-weeks post-intraperitoneal injection into C57BL6J mice. (A) Scoring of mesenteric tumour burden mice injected with ID8 cells then treated with IP PBS, IFNβ or IFNε at 500IU/dose 3 times weekly for 8 weeks. (B) The concentration of cytokines MCP-1, IL-6 & IL-10 detected in peritoneal fluid by cytometric bead array. (C) Peritoneal lavage samples from C57BL6J mice 8 weeks post-intraperitoneal injection with ID8 cells stained for immune markers and measured by multi-coloured flow cytometry. Total leukocyte populations in these mice including total leukocytes (CD45+), CD4 T cells (CD45+ CD4+CD8-), CD8 T cells (CD45+CD8+CD4-). Cytokine bead array data are shown as mean +/- SEM, otherwise shown as median of individual data points, n=5 mice per IFN treatment group, n=5 non-tumour bearing mice, and n=3 tumour-bearing mice treated with PBS. Significance was determined by Student's T test ****p<0.0001, ***p<0.001, **p<0.01, *p<0.05*

Supplementary Figure 5.

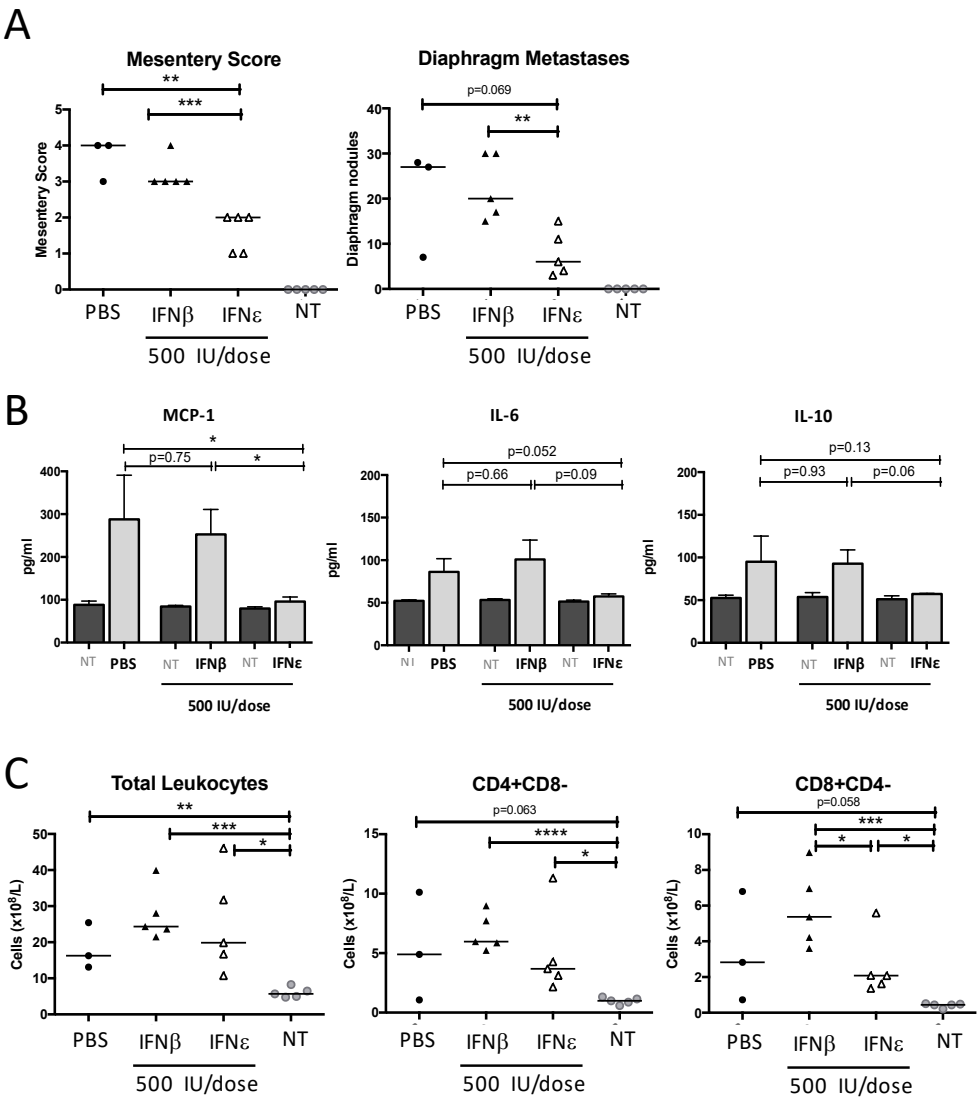

Supplementary Figure 5. IFNε effectively suppresses tumour progression in mice with pre-existing 4 week-old orthotopic ovarian cancer. *ID8 cells were implanted into C57BL6J mice via intrabursal injection (1x10^6 cells/mouse) to form orthotopic ovarian tumours & peritoneal metastases over 4 weeks prior to commencing recombinant IFNε or IFNβ therapy (500IU/dose i.p. injected 3x weekly for additionally 4 weeks). (A) Additional disease quantification including volumes of excised left ID8-implanted ovaries compared to PBS-implanted non-tumour controls, red blood cell content of peritoneal ascites & lavage fluid, volume of peritoneal ascites and total number of leukocytes in peritoneal fluid of tumour-bearing mice treated with 500IU/ml of IFNε or IFNβ compared to PBS and non-tumour controls. (B) Peritoneal lavage samples stained for immune markers and measured by multi-coloured flow cytometry – total number of leukocytes populations including CD4 T cells (CD45+CD4+CD8-), CD8 T cells (CD45+CD8+CD4-), B cells (CD45+B220+) & NK cells (CD45+NKp46+). Data are shown as median of individual data points, n=6 mice per treatment. Significance was determined by Student's T test ****p<0.0001, ***p<0.001, **p<0.01, *p<0.05.*

Supplementary Figure 6.

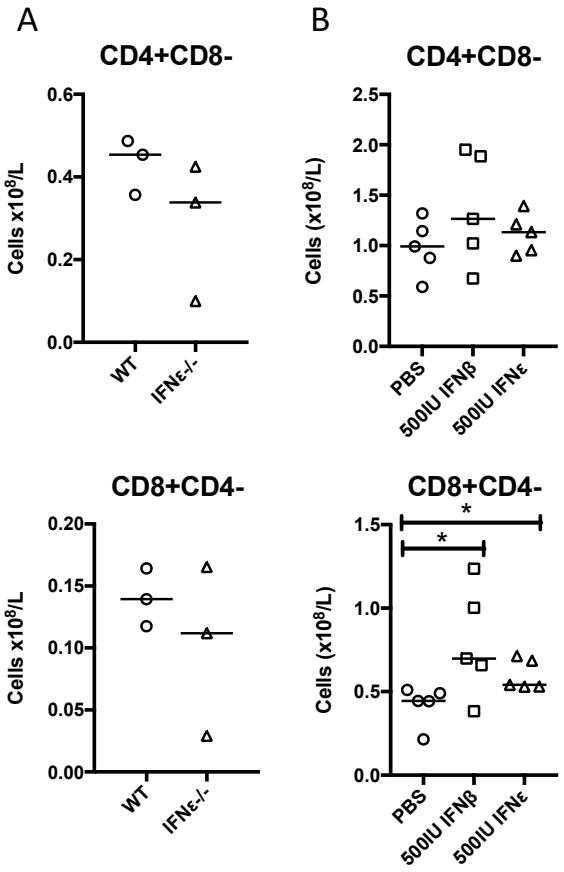

Supplementary Figure 6. Endogenous and exogenous IFNε regulates immune cells in mice. *Peritoneal lavage samples from non-tumour bearing C57BL6J mice stained for immune markers and measured by multi-coloured flow cytometry. (A) Wild-type compared to IFNε knock out mice. (B) Wild-type mice treated with PBS, IFNβ or IFNε (500IU/dose i.p. injected 3 times weekly for 8 weeks). Leukocyte populations include CD4+ and CD8+ T lymphocytes. Data are shown as median of individual data points, n=3 mice per genotype comparison group (endogenous IFNε) and n=5 mice per i.p. treatment group (exogenous IFNε). Significance was determined by Student's T test ***p<0.001, **p<0.01, *p<0.05.*

Supplementary Figure 7.

A

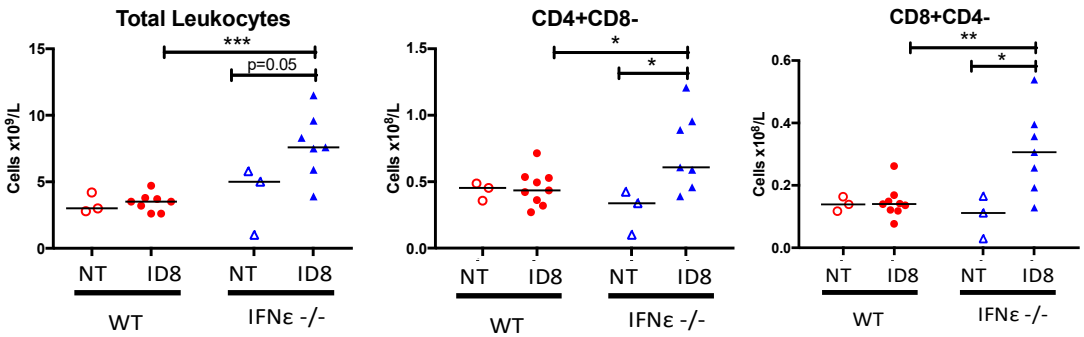

Supplementary Figure 7. Early-stage orthotopic models of murine ovarian cancer in mice lacking endogenous IFN. *Female C57BL/6 wild-type (Ifnε +/+) and Ifnε deficient mice (Ifnε -/-) were intrabursally injected with 1x10⁶ mouse ovarian cancer cells (ID8) into the left ovarian bursa. Immunophenotyping flow cytometry was performed on peritoneal cells from WT & Ifnε deficient mice 6 weeks post-intrabursal ID8 injection. Total number of peritoneal lavage leukocytes, C4 T cells (CD45+CD4+CD8-) and CD8 T cells (CD45+CD8+CD4-) were detected by immunostaining and flow cytometry. Data are shown as median of individual data points, n=3 non-tumour bearing mice per genotype, n=8 WT ID8-injected mice and n=7 Ifnε-/- ID8-injected mice. Significance was determined by Student's T test ***p<0.001, **p<0.01, *p<0.05.*

Supplementary Figure 8.

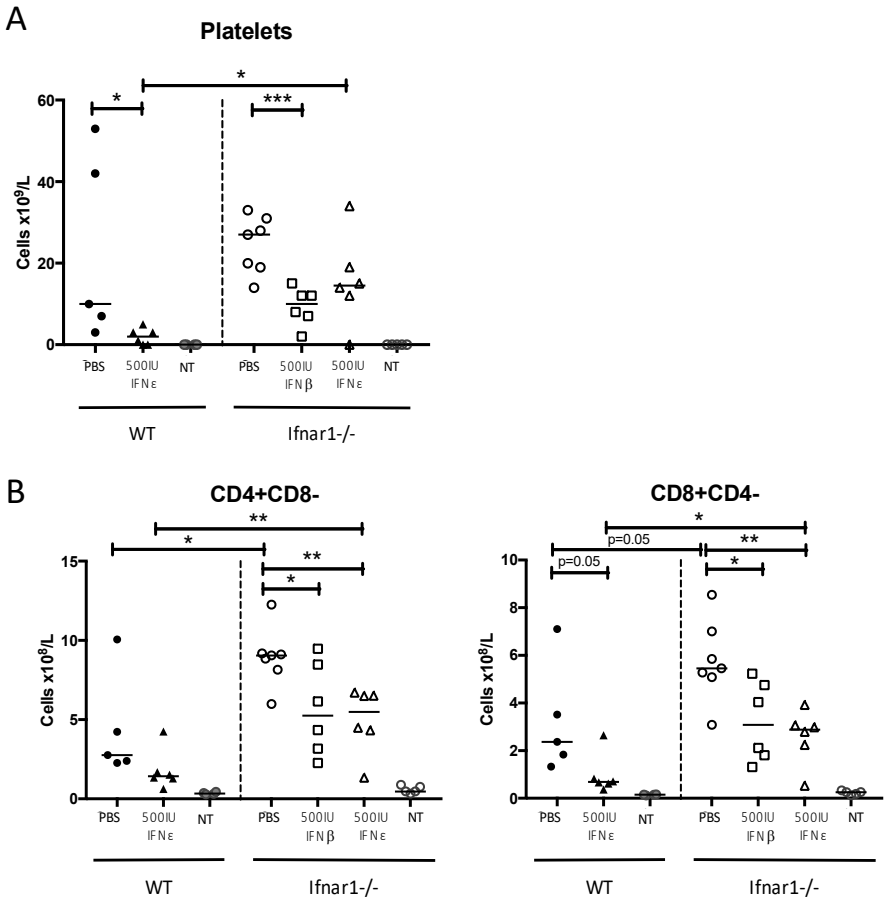

Supplementary Figure 8. The mechanism of IFN modulation in peritoneal anti-tumour immunity. *Quantified total volume of ascites and red blood cells in peritoneal fluid of WT mice or Ifnar1-/- mice injected intrabursally with ID8 cells then treated with i.p. PBS, IFNβ or IFNε at 500IU/dose 3 times weekly for 8 weeks. (A) CD4 T cells and (B) Number of platelets in peritoneal fluid quantified by immunostaining flow cytometry and Sysmex Cell Counter, respectively. Data are shown as median of individual data points, n=5 mice per IFN treatment group, n=5 non-tumour bearing mice, and n=3 tumour-bearing mice treated with PBS. Significance was determined by Student's T test ****p<0.0001, ***p<0.001, **p<0.01, *p<0.05.*

Supplementary Figure 9.

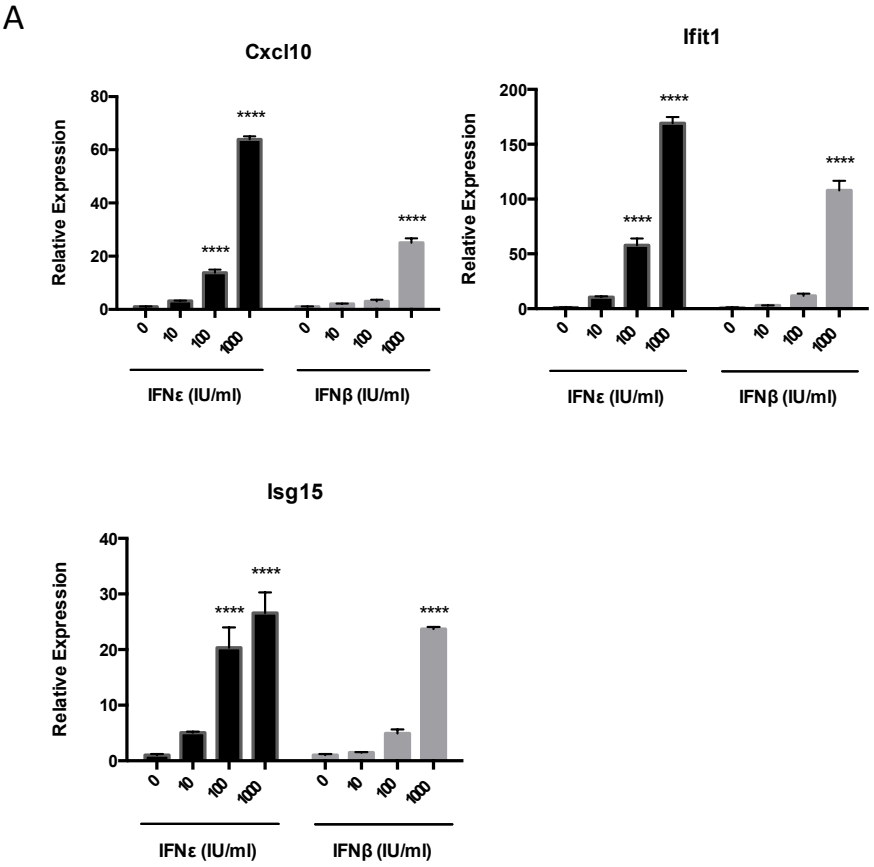

Supplementary Figure 9. Induction of IRGs in ID8 cells by IFNε & IFNβ. *Graph shows a 3 hour dose response of 10-1000 IU/ml IFNε (left panels shown in black) and IFN β(right panels in grey) induction of Cxcl10, Ifit1 and Isg15. Gene expression was measured by qRT-PCR, expression calculated by dCT standardised to 18s and relative expression shown here determined in relation to expression at t0. Data are shown as mean +/- SEM of n=3 independent experiments, each done in technical triplicates. Significance was determined by Student's T test ****p<0.0001.*

Supplementary Figure 10.

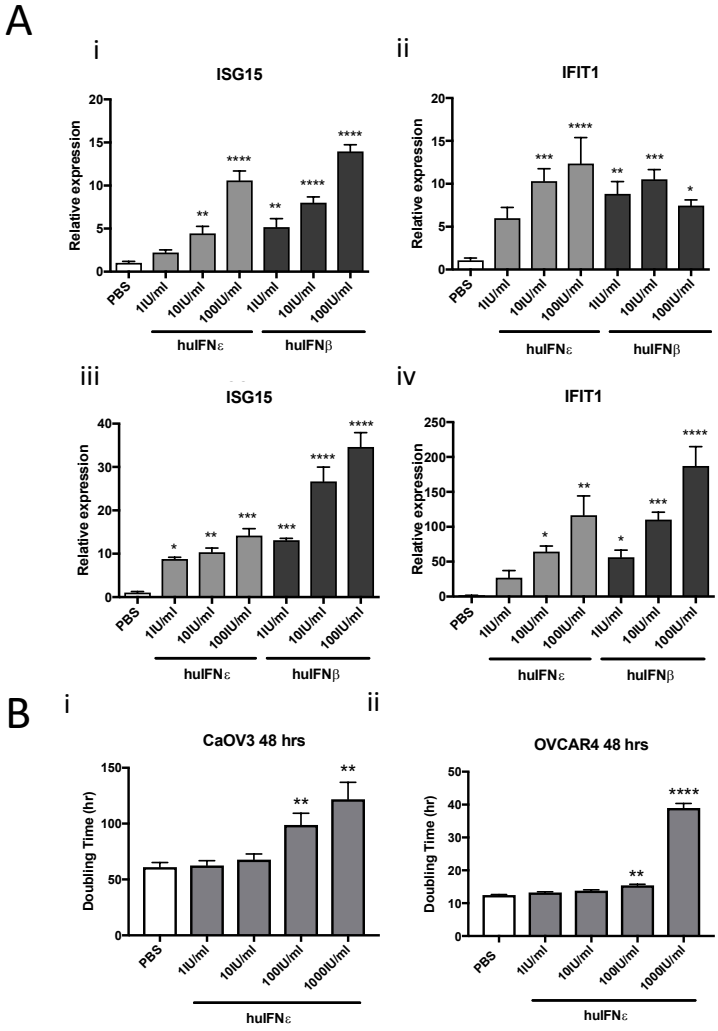

Supplementary Figure 10. Direct anti-tumour activity of IFNε in vitro on human ovarian cancer cell lines. *(A) Graphs show doubling times of CaOV3 & OVCAR4 cells treated with 1-1000 IU/ml of IFNε for 48 hours. Cell proliferation was measured using xCELLigence and displayed as doubling time. Data are representative of n=3 independent experiments, shown as mean +/- SEM. Significance was determined by Student's T test ****p<0.0001, ***p<0.001, **p<0.01, *p<0.05.*

CHAPTER 5: DISCUSSION

'Little by little, one travels far.'[†]

~

5.1 Overview

Metastases are the most difficult to treat and subsequently, most lethal consequence of cancer growth, whereby a select population of discrete tumour cells are able to steal into the human body and colonise distant sites. The collection of processes facilitating the survival and spread of these tumour cells may in fact stem from intrinsic properties common to all cancers including the ability to regulate cell proliferation, cell death, vascular growth, reprogramming cell metabolism, invading surrounding tissue and evading immune elimination (2, 4). Type I IFN signalling has been linked to each of these cellular processes as a key family of regulatory cytokines in caner with the ability to regulate both tumour cell intrinsic functions and also tumour extrinsic immune responses (97).

The promise of these anti-tumour properties has led to use of exogenous IFNα and IFNβ to be utilised in clinical trials against cancer. As a result, type I IFN therapy has proved clinically beneficial in haematological malignancies (277) these benefits were partly attributed to direct effects on circulating tumour cells (278, 279). IFN therapy has shown some promise in solid tumours as well, such as melanoma, where adjuvant treatment of late-stage disease improved relapse-free and overall survival (79, 280-283). However, despite its promise, broad therapeutic application of type I IFN has largely been limited by adverse clinical effects including HDI-associated cytotoxicity that include flu-like symptoms, anorexia and even depression. Evidence of a selective benefit in treating with type I IFN in an adjuvant setting compared to advanced metastatic disease (281) has been interpreted as a demonstration of the immunoregulatory anti-tumour effects on disseminated tumour cells or minimal residual

[a] From the Spanish 'poco a poco, se va lejos'. Popularly attributed to J.R.R. Tolkien

disease (MRD) (97), however this remains to be established. Further characterisation of type I IFN signalling is needed to understand its role in cancer and effectively harness its anti-tumour effects.

Endogenous IFN plays a vital role in regulating the tumour microenvironment and can be produced either by tumour cells themselves, stromal cells or immune cells (42, 284). In breast cancer, dysregulation in endogenous type I IFN signalling has been detected in immune cells (285) and identified as a vital mechanism by which tumour cells suppress anti-tumour immune responses and thus, are able to spread (42). This study also highlights the successful use of exogenous IFN as a substitute for deficient or compromised IFN signalling. This suggests the potential benefit of developing IFN–associated biomarkers to identify patients that may respond to anti-metastatic IFN replacement therapy. Constitutive IFN signalling has been detected in epithelial cells of the female reproductive tract (FRT), where a distinct member of the type I IFN family, IFNε, is constitutively expressed (171). This constitutive IFNε signalling has been shown to regulate epithelial function and protect against pathogens via immune regulation (171), however prior to this study its role in FRT malignancies remained unknown.

Using breast and ovarian cancer as models, the aims of this thesis were to study the loss of constitutive type I IFN in these tissues, investigate detection of constitutive type I IFN activity and investigate the anti-metastatic effects of type I IFN. Subsequently, the work presented in this thesis contributes some of the first evidence of the importance of constitutive type I IFN signalling during specific pathways of cancer development and metastatic dissemination, detection of broad, systemic IFN activity during metastasis and effective anti-metastatic therapy.

5.2 Constitutive Type I IFN Signalling in Cancer Development & Progression

One of the key findings of this thesis was the detection of constitutive IFNε expression in human fallopian tube (FT) epithelium, presented in Chapter 4. Prior to this, our Lab had reported *IFNε* mRNA was constitutively expressed in both murine and human lower FRT and IFNε protein expression was detected specifically in murine uterine epithelial cells (171). However, the expression of IFNε in FT epithelium remained unknown. The immunohistochemistry data presented in this thesis, together with *in silico* analyses of human transcriptomic data, clearly show IFNε is expressed in human FT epithelium. This finding constitutes the first evidence that type I IFN signalling is constitutively active among cells including the putative cell of origin of human HGSC (230-233). This finding complements evidence that type I IFN is constitutively expressed in normal mammary tissue from which breast tumours arise (42), highlighting that constitutive type I IFN signalling in the epithelium, may play an important role in restricting development of both cancers. Interestingly, the upstream regulation of constitutive IFN differs between these two sites: IRF7 drives expression of IFN in mammary epithelium, but is not responsible for constitutive IFNε expression in FRT epithelium as the IFNε promote lacks IRF binding sites and thus, is not regulated by PRR signalling (171).

Further analyses revealed that IFNε mRNA and protein expression was significantly suppressed in human HGSC samples compared to normal FT epithelium and critically, stratifying HGSC patients based on IFNε mRNA expression significantly correlated with patient disease-free survival. While further work will be required to explore the mechanisms underlying IFNε suppression in ovarian cancer development and progression these data suggest that loss of endogenous constitutive IFNε may be a key mechanism of tumour progression.

Given that IFNε is regulated by hormones within the FRT (171), IFNε loss may be a consequence of menopause. Incidence of ovarian cancer increases with age with median age at diagnosis of 63 years (286), the majority of new cases occur in postmenopausal women, in whom IFNε expression is lost (171). Additionally, among premenopausal women there is evidence that oral contraceptive pill (OCP) use reduces the risk of ovarian cancer with a 20-30% reduction per 5 years of use (287), which may reflect an oestrogen-driven upregulation of IFNε which is yet to be investigated.

5.3 Detection of Local, Systemic & Secondary IFN/Immune Signatures during Metastasis

The finding that constitutive IFN signalling may be a key component in restricting development and progression of cancer highlights the need for methods of detecting and measuring IFN activity as a means of stratifying patients for personalised IFN therapy. To address this, we have performed transcriptomic analyses on peripheral blood cells from a cohort of familial breast cancer patients with or without metastases and unaffected donors each selected from matched family groups. The use of familial controls allowed for paired analyses of human samples, in lieu of obtaining multiple samples taken from the same patient across the course of metastasis, an invasive procedure for individuals with a life-threatening illness. In fact, the results of these analyses presented in Chapter 3, demonstrate that the use of familial paired analysis significantly increased analytical power of differential transcriptomic analyses. It is likely that this experimental design controls for reported population variance in the blood transcriptome (288, 289). There is evidence to suggest that a proportion of the human transcriptome is highly heritable (290), which can attributed to expression Quantitative Trait Loci (eQTL) and genetic polymorphisms that regulate gene expression (291-295).

The results in Chapter 3 demonstrate some of the key pathways active in local, systemic and distant tissue during breast cancer metastasis as detected by peripheral blood transcriptome analyses and multiplex tissue staining. Our aim was to detect and characterise an expression signature in blood as an indication of a loss of constitutive IFN activity and thus, metastatic potential. The results demonstrate that well-characterised interferon-related signatures were significantly negatively enriched in blood from patients with metastases compared to those without. This supports the hypothesis that the constitutive IFN signalling detectable in primary tumour cells is suppressed during tumour metastasis (42), though previously it was unknown whether this occurred prior to tumour intravasation, in circulation or post-extravasation.

Suppression of IFN signalling was accompanied by a significant systemic suppression in T cell gene enrichment during breast cancer metastasis. T cells have been shown to be critical in effecting IFN-driven anti-metastatic effects in breast cancer (42). Additionally, impairment of T cell function has been identified in peripheral blood lymphocytes from breast cancer patients (285) the mechanism of which has been suggested a loss of CD4+ Helper cells which in turn leads to less effector cell priming (296). In a murine ovarian cancer cell model, suppression of tumour dissemination was associated with increased CD8+ T cell activation (297). Therefore, the fact that IFN associated T cell activation is associated with metastases suppression across both our models suggests that immune regulation is indeed a critical anti-tumour mechanism in type I IFN suppression of tumour progression.

The findings of this thesis consistently suggest that anti-tumour immunoregulation driven by type I IFN signalling, both endogenous and exogenous, is critical in metastatic spread of both breast and ovarian cancer. Firstly, in breast cancer our blood transcriptome analyses and multiplex immune staining demonstrates that during metastasis or in tumours with assured metastatic potential, primary breast tumour cells are closely, physically associated with platelets. The role of platelets in chaperoning tumour cells throughout metastasis has been

shown in a number of cancers including breast cancer (62-65), where platelets have been detected trafficking tumour cells in the blood stream. Additionally, platelets in close proximity to cells within the primary tumour have been shown to promote chemoresistance (298) that our data corroborated as we observed the presence and close association between primary tumour cells and platelets. This association was present in primary tumours regardless of metastatic potential, though exclusively positively enriched in blood from breast cancer patients with metastases. This potentially indicates that platelets are recruited to the site of primary tumour long before the establishment and diagnosis of macro-metastases. This significance of this observation in terms of pathogenesis or diagnosis of metastases requires further investigation.

Platelets have been identified as key cells involved in priming pre-metastatic niches in secondary organs (299). In this study, platelet-tumour cell association was markedly reduced in a proportion of secondary breast tumours. This interaction potentially decreases as tumour cells establish macro-metastases in secondary organs and no longer require platelet aid, however further work is needed to explore this relationship further. Interestingly, we also found a platelet-associated phenotype in ovarian cancer dissemination. Haemorrhagic malignant ascites development in the peritoneal cavity is the end-stage of human ovarian cancer progression, in fact thrombocytosis, or high platelet counts & activity, has been reported in roughly 30% of newly diagnosed women (300). Evidence *in vitro* demonstrates that co-culture with platelets acts as a chemoattractant and promotes migration in human ovarian cancer cells (301). In our mouse model of ovarian cancer dissemination, we found recombinant IFNε treatment significantly reduced peritoneal haemorrhaging (an indirect association with platelet burden) which correlated with suppressed tumour dissemination.

Using the INTERFEROME tool, we were able to demonstrate that while modules of select numbers of well-characterised interferon genes were significantly negatively enriched among our metastatic and non-metastatic blood signatures, many broadly classified IFN

responsive genes were in fact contributing to the key biological enrichments demonstrated in blood during breast cancer metastasis. We were able to classify a subset of 'metastasis-associated' IRGs, which when divided into up or down regulation during metastasis, were in fact significantly positively enriched for platelet activity and negatively enriched for cell processes including metabolism and transcription.

Metabolic processes such as hypoxia are known to impact immune function in the tumour microenvironment, a growing field of research (302, 303). Recent work has shown that type I IFNs can activate immune cells via metabolic processes including fatty acid oxidation and oxidative phosphorylation (304). While further work is needed to explore potential IFN-driven pathways revealed in metastasis, the findings of this thesis highlights the complexity of IFN signalling and the array of biological functions effected by IRG expression. In future, combining these data with further gene set characterisation such as transcription factor binding site prediction (305) might reveal the specific IFN-associated pathways mediating these distinct effects and contribute to the growing body of knowledge on IFNs in cancer.

5.4 Anti-Metastatic Effects of Type I IFNs

5.4.1 Endogenous Type I IFN

As was demonstrated by Bidwell et al., constitutive IFN signalling present in primary breast tumour samples had no effect on the growth of the primary tumour itself, but rather the anti-tumour effects of type I IFN signalling suppressed bone metastasis (42). This is consistent with findings that IFNα therapy is more effective as an adjuvant therapy to surgery rather than a treatment for advanced metastatic disease (281). This potentially reflects that type I IFN therapy is most effective when able to exert immunoregulatory effects on target tumour cells (97, 306), rather than solely elicit a direct anti-proliferative or pro-apoptotic effect on tumour cells within established metastatic masses likely in the context of an immunosuppressive

microenvironment. Our data in IFNε-/- mice using an orthotopic ID8 model of murine ovarian cancer, demonstrates that endogenous IFNε has little overt effect on primary 'orthotopic' tumour growth, but instead reduces peritoneal tumour dissemination. However, the tumour cells used in this study were not deficient in IFNε and demonstrated low expression *in vitro*. Therefore, in future work it will be important to study tumour development in the absolute absence of IFNε (by generating IFNε$^{-/-}$ tumour cells using CRISPr/Cas9) and thus, delineate the role endogenous IFNε expression in tumour cells and host cells.

Additionally, further characterisation of the effects of endogenous IFNε could be discerned from genetically modifying tumour cells to overexpress IFNε in this model or alternatively, using an IFNε inducer to upregulate endogenous protein expression. Similar approaches have been trailed clinically using PRR agonists to induce type I IFN in several cancers with promising effects (105, 106, 307), however further work is needed to identify potential therapeutic inducers of endogenous IFNε, a potential area for drug development.

An important outcome from this work combined with further characterisation of anti-metastatic effects of endogenous type I IFN, could be the identification of novel IFN biomarkers for cancer development and progression. Methods of patient stratification and targeted/precision therapy approaches in cancer are currently the subject of much investigation and development (308, 309). While many studies have utilised mutational profiles of tumours for patient stratification and outcome prediction, transcriptome data-mining and tumour phenotyping also demonstrate growing promise (310). Work presented in this thesis demonstrates the potential use of 'metastasis-associated' transcriptional blood signatures in breast cancer, which consist of IRGs and reflect cell profiles of primary and secondary tumours. Meanwhile, the loss of endogenous IFNε in fallopian tube epithelial cells may prove to be a key method of stratifying women more likely to develop ovarian cancer. Combined with principles developed from previous mouse modelling of breast cancer metastasis, where

restoring the loss of endogenous IFN suppressed bone metastases (42), work from this thesis suggest a way of identifying patients who may benefit from replacement IFN therapy.

5.4.2 Exogenous Type I IFN

Improved knowledge of the endogenous anti-tumour properties of type I IFN helps guide more effective, targeted exogenous IFN-based therapy. This thesis applied knowledge of the endogenous functions of IFNε, previously demonstrated during FRT infections (171) and tissue-specific expression of IFNε, to investigate its role in FRT cancer and test its therapeutic potential. Here, recombinant IFNε therapy showed that exogenous IFNε had little effect on primary growth but marked reduction in peritoneal total metastases. This correlated with an increased in the activation status of a number of peritoneal immune populations such as CD4+ T cells, CD8+ T cells and NKs and thus, supports the proposal and observation that type I IFN efficacy against solid tumours lies in its anti-metastatic effects, at least in part due to extrinsic immunoregulatory effects. An interesting point of distinction in our findings came from the use of IFNAR1-/- mice, which maintained some ability to clear ovarian cancer metastases when treated with exogenous IFNε and thus, demonstrate that the direct or cell intrinsic anti-tumour effects of the type I IFNs remain important in the anti-metastatic pathway of early ovarian cancer dissemination. Critically, these findings constitute the first evidence of IFNε as an anti-cancer therapeutic and have subsequently formed the basis of a provisional patent on IFNε as a means of treating cancer (refer to Thesis Appendices).

The clear potential for IFNε as a therapy poses several key considerations for future drug development. The findings presented in this thesis demonstrate IFNε as a potential single agent therapy for suppressing tumour dissemination in both orthotropic and advanced metastatic ID8 models of ovarian cancer. However, future work will need to expand on these findings using other ovarian cancer models. Importantly, the use of CRISPR/Cas9

gene editing has enabled the recent generation of ID8 sublines which bear a mutational profile similar to human ovarian cancer (both Tp53-/- and Brca2-/- lines) and result in more aggressive disease progression and exhibit distinct tumour microenvironments (238). These new models would provide critical tools for studying the effects of IFNε in human disease. Additionally, future work should employ patient-derived xenografts (PDXs) and spontaneous murine tumour models arising from induced oncogenic mutations to provide more insight into the direct effects of recombinant human IFNε on tumour cells (259).

To date type I IFNs have shown little benefit as single agent therapies in solid tumours, largely due to their severe dose-limiting side effects. The findings presented here, suggest that IFNε is in fact well tolerated and can be used at effective doses in mice for at least two months. While further characterisation IFNε tolerance is needed, its potential advantage in efficacy over toxicity may be a reflection of the key properties of IFNε that make it a unique type I IFN. Recently, IFNε has been shown to have a low affinity interaction with the type I IFN receptor (311), which may contribute to lower toxicity but also enable constitutive IFN activity while maintaining receptor expression on the target cell surface.

Finally, these findings highlight the potential for IFNε as an adjunct therapy in cancer. Adjuvant type I IFN therapy has already demonstrated promise in combination with other standard cancer therapies including radiation, hormones and chemotherapy. Interestingly, response to chemotherapy appears to be dependent on successful induction of type I IFN production in malignant cells to activate anti-tumour immunity (312).

The findings reported here, demonstrate consistent IFNε-driven immune activation in mouse models of early and late stage ovarian cancer progression and suggest that adjuvant IFNε may further provide clinical benefit in combination with therapies that elicit anti-tumour immune responses as an additive activating signal. Alternatively, adjunct IFNε

therapy could potentially be used to overcome immunosuppression when administered in combination with immune checkpoint inhibitors as demonstrated by IFNε-regulated PD1 and PD-L1 expression on tumour and immune cells, respectively. These applications require further investigation but critically, the efficacy and tolerance of IFNε cancer therapy, demonstrated for the first time in this thesis, constitute an exciting area for novel IFN therapy in cancer, which has the potential to supress disseminated peritoneal disease and thus significantly improve patient outcome.

5.5 Concluding Remarks

The central aim of this thesis was to explore the role of constitutive type I IFN in tumour development and progression. In breast cancer, a model where constitutive type I IFN is critical for suppression of metastasis, this work investigated local, systemic and distant signatures that revealed key processes occurring in breast cancer metastasis and mapped these as a continuum of disease progression from normal tissue to primary tumour to metastases.

In ovarian cancer, a tumour model where constitutive type I IFN had not previously been investigated, the work presented here demonstrated patterns of constitutive IFNε expressed never before characterized – in the tissue of origin of HGSC. In addition to the first evidence of the loss of constitutive IFNε in human HGSC development, this work has for the first time revealed IFNε to be an effect anti-metastatic therapy in mouse models of orthotopic and disseminated ovarian cancer. The results of which are now the basis for the use of IFNε as an anti-cancer therapy, not only in ovarian cancer, but with the potential to be used as a distinct, novel type I IFN therapy in any malignancy. This work contributes to the fundamental knowledge of the role of type I IFN in tumorigenesis and tumour progression, the implications of which provide means for patient stratification and could reimagine type I IFN therapy at the forefront of cancer immunotherapy.

REFERENCES

1. Cancer Australia. Australian Cancer Trials [Internet]. Surry Hills NSW: Cancer Australia; 2018 [updated 2018 Jan 22; cited 2018 Jan 23]. Available from: http://www.australiancancertrials.gov.au/search-clinical-trials/.

2. Hanahan D, Weinberg RA. The Hallmarks of Cancer. Cell. 2000;100:57-70.

3. Witsch E, Sela M, Yarden Y. Roles for growth factors in cancer progression. Physiology (Bethesda). 2010;25(2):85-101.

4. Hanahan D, Weinberg RA. Hallmarks of cancer: the next generation. Cell. 2011;144(5):646-74.

5. Vesely MD, Kershaw MH, Schreiber RD, Smyth MJ. Natural innate and adaptive immunity to cancer. Annu Rev Immunol. 2011;29:235-71.

6. Curiel TJ, Coukos G, Zou L, Alvarez X, Cheng P, Mottram P, et al. Specific recruitment of regulatory T cells in ovarian carcinoma fosters immune privilege and predicts reduced survival. Nat Med. 2004;10(9):942-9.

7. Wherry EJ. T cell exhaustion. Nat Immunol. 2011;131(6):492-9.

8. Sato E, Olson SH, Ahn J, Bundy B, Nishikaway H, Qian F, et al. Intraepithelial CD8+ tumor-infiltrating lymphocytes and a high CD8+/regulatory T cell ratio are associated with favorable prognosis in ovarian cancer. Proc Natl Acad Sci U S A. 2005;102(51):18538-43.

9. Gooden MJ, de Bock GH, Leffers N, Daemen T, Nijman HW. The prognostic influence of tumour-infiltrating lymphocytes in cancer: a systematic review with meta-analysis. Br J Cancer. 2011;105(1):93-103.

10. Li J, Wang J, Chen R, Bai Y, Lu X. The prognostic value of tumor-infiltrating T lymphocytes in ovarian cancer. Oncotarget 2017;8(9):15621-31.

11. Dunn GP, Bruce AT, Ikeda H, Old LJ, Schreiber RD. Cancer immunoediting: from immunosurveillance to tumor escape. Nat Immunol. 2002;3(11):991-8.

12. Marcus A, Gowen BG, Thompson TW, Iannello A, Ardolino M, Deng W, et al. Recognition of tumors by the innate immune system and natural killer cells. Adv Immunol. 2014;122:91-128.

13. Dunn GP, Old LJ, Schreiber RD. The three Es of cancer immunoediting. Annu Rev Immunol. 2004;22:329-60.

14. Dunn GP, Old LJ, Schreiber RD. The immunobiology of cancer immunosurveillance and immunoediting. Immunity. 2004;21(2):137-48.

15. Schreiber RD, Old LJ, Smyth MJ. Cancer immunoediting: integrating immunity's roles in cancer suppression and promotion. Science. 2011;331(6024):1565-70.

16. Mittal D, Gubin MM, Schreiber RD, Smyth MJ. New insights into cancer immunoediting and its three component phases-elimination, equilibrium and escape. Curr Opin Immunol. 2014;27C:16-25.

17. Shankaran V, Ikeda H, Bruce AT, White JM, Swanson PE, Old LJ, et al. IFN gamma and lymphocytes prevent primary tumour development and shape tumour immunogenecity. Nature. 2001;410(6832):1107-11.

18. Koebel CM, Vermi W, Swann JB, Zerafa N, Rodig SJ, Old LJ, et al. Adaptive immunity maintains occult cancer in an equilibrium state. Nature. 2007;450(7171):903-7.

19. Pardoll DM. The blockade of immune checkpoints in cancer immunotherapy. Nat Rev Cancer. 2012;12(4):252-64.

20. Cianfrocca M, Goldstein LJ. Prognostic and predictive factors in early-stage breast cancer. The Oncologist. 2004;9:606-16.

21. Parise CA, Caggiano V. Breast Cancer Survival Defined by the ER/PR/HER2 Subtypes and a Surrogate Classification according to Tumor Grade and Immunohistochemical Biomarkers. J Cancer Epidemiol. 2014;2014:469251.

22. Shaikh WR, Dusza SW, Weinstock MA, Oliveria SA, Geller AC, Halpern AC. Melanoma Thickness and Survival Trends in the United States, 1989 to 2009. J Natl Cancer Inst. 2016;108(1).

23. Brabletz T. EMT and MET in metastasis: where are the cancer stem cells? Cancer Cell. 2012;22(6):699-701.

24. Mani SA, Guo W, Liao MJ, Eaton EN, Ayyanan A, Zhou AY, et al. The epithelial-mesenchymal transition generates cells with properties of stem cells. Cell. 2008;133(4):704-15.

25. Morel AP, Lievre M, Thomas C, Hinkal G, Ansieau S, Puisieux A. Generation of breast cancer stem cells through epithelial-mesenchymal transition. PLoS One. 2008;3(8):e2888.

26. Tsai JH, Donaher JL, Murphy DA, Chau S, Yang J. Spatiotemporal regulation of epithelial-mesenchymal transition is essential for squamous cell carcinoma metastasis. Cancer Cell. 2012;22(6):725-36.

27. Tsai JH, Yang J. Epithelial-mesenchymal plasticity in carcinoma metastasis. Genes Dev. 2013;27(20):2192-206.

28. Ocana OH, Corcoles R, Fabra A, Moreno-Bueno G, Acloque H, Vega S, et al. Metastatic colonization requires the repression of the epithelial-mesenchymal transition inducer Prrx1. Cancer Cell. 2012;22(6):709-24.

29. Fidler IJ. The pathogenesis of cancer metastasis: the 'seed and soil' hypothesis revisited. Nat Rev Cancer. 2003;3(6):453-8.

30. Burnet FM. Immunological aspects of malignant disease. Lancet. 1967;1(7501):1171-4.

31. Makrilia N, Kollias A, Manolopoulos L, Syrigos K. Cell adhesion molecules: role and clinical significance in cancer. Cancer Invest. 2009;26(10):1023-37.

32. Li D-M, Feng Y-M. Signaling mechanism of cell adhesion molecules in breast cancer metastasis: Potential therapeutic targets. Breast Cancer Res Treat. 2011;128(1):7-21.

33. Weigelt B, Hu Z, He X, Livasy C, Carey LA, Ewend MG, et al. Molecular portraits and 70-gene prognosis signature are preserved throughout the metastatic process of breast cancer. Cancer Res. 2005;65(20):9155-8.

34. Fidler IJ. The organ microenvironment and cancer metastasis. Differentiation. 2002;70(9-10):498-505.

35. Capobianco A, Cottone L, Monno A, Manfredi AA, Rovere-Querini P. The peritoneum: healing, immunity, and diseases. J Pathol. 2017;243(2):137-47.

36. Charbonneau B, Goode EL, Kalli KR, Knutson KL, Derycke MS. The immune system in the pathogenesis of ovarian cancer. Crit Rev Immunol. 2013;33(2):137-64.

37. O'Sullivan T, Saddawi-Konefka R, Vermi W, Koebel CM, Arthur C, White JM, et al. Cancer immunoediting by the innate immune system in the absence of adaptive immunity. J Exp Med. 2012;209(10):1869-82.

38. Mazurier F, Fontanellas A, Salesse S, Taine L, Landriau S, Moreau-Gaudry F, et al. A Novel Immunodeficient Mouse Model-RAG2 gamma Cytokine Receptor Chain Double Mutants-Requiring Exogenous Cytokine Administration for Human Hematopoietic Stem Cell Engraftment Common. J Interferon Cytokine Res. 1999;19(5):533-41.

39. Nagarsheth N, Wicha MS, Zou W. Chemokines in the cancer microenvironment and their relevance in cancer immunotherapy. Nat Rev Immunol. 2017;17(9):559-72.

40. Udono H, Mieno M, Shiku H, Nakayama E. The roles of CD8+ and CD4+ cells in tumour rejection. Jpn J Cancer Res. 1989;80(7):649-54.

41. Burnette BC, Liang H, Lee Y, Chlewicki L, Khodarev NN, Weichselbaum RR, et al. The efficacy of radiotherapy relies upon induction of type i interferon-dependent innate and adaptive immunity. Cancer Res. 2011;71(7):2488-96.

42. Bidwell BN, Slaney CY, Withana NP, Forster S, Cao Y, Loi S, et al. Silencing of Irf7 pathways in breast cancer cells promotes bone metastasis through immune escape. Nat Med. 2012;18(8):1224-31.

43. Gresser I, Maury C, Carnaud C, De Maever E, Maunoury M-T, Belardelli F. Anti-tumor effects of interferon in mice injected with interferon-sensitive and interferon-resistant friend erythroleukemia cells. VIII. Role of the immune system in the inhibition of visceral metastases. Int J Cancer. 1990;46(3):468-74.

44. Remark R, Alifano M, Cremer I, Lupo A, Dieu-Nosjean MC, Riquet M, et al. Characteristics and clinical impacts of the immune environments in colorectal and renal cell carcinoma lung metastases: influence of tumor origin. Clin Cancer Res. 2013;19(15):4079-91.

45. Erdag G, Schaefer JT, Smolkin ME, Deacon DH, Shea SM, Dengel LT, et al. Immunotype and immunohistologic characteristics of tumor-infiltrating immune cells are associated with clinical outcome in metastatic melanoma. Cancer Res. 2012;72(5):1070-80.

46. Apetoh L, Smyth MJ, Drake CG, Abastado JP, Apte RN, Ayyoub M, et al. Consensus nomenclature for CD8(+) T cell phenotypes in cancer. Oncoimmunology. 2015;4(4):e998538.

47. Ladanyi A, Kiss J, Mohos A, Somlai B, Liszkay G, Gilde K, et al. Prognostic impact of B-cell density in cutaneous melanoma. Cancer Immunol Immunother. 2011;60(12):1729-38.

48. Pretscher D, Distel LV, Grabenbauer GG, Wittlinger M, Buettner M, Niedobitek G. Distribution of immune cells in head and neck cancer: CD8+ T-cells and CD20+ B-cells in metastatic lymph nodes are associated with favourable outcome in patients with oro- and hypopharyngeal carcinoma. BMC Cancer. 2009;9:292.

49. Nielsen JS, Sahota RA, Milne K, Kost SE, Nesslinger NJ, Watson PH, et al. CD20+ tumor-infiltrating lymphocytes have an atypical CD27- memory phenotype and together with CD8+ T cells promote favorable prognosis in ovarian cancer. Clin Cancer Res. 2012;18(12):3281-92.

50. Montfort A, Pearce O, Maniati E, Vincent BG, Bixby L, Bohm S, et al. A Strong B-cell Response Is Part of the Immune Landscape in Human High-Grade Serous Ovarian Metastases. Clin Cancer Res. 2017;23(1):250-62.

51. Carmi Y, Spitzer MH, Linde IL, Burt BM, Prestwood TR, Perlman N, et al. Allogeneic IgG combined with dendritic cell stimuli induce antitumour T-cell immunity. Nature. 2015;521(7550):99-104.

52. Sarvaria A, Madrigal JA, Saudemont A. B cell regulation in cancer and anti-tumor immunity. Cell Mol Immunol. 2017;14(8):662-74.

53. Shalapour S, Font-Burgada J, Di Caro G, Zhong Z, Sanchez-Lopez E, Dhar D, et al. Immunosuppressive plasma cells impede T-cell-dependent immunogenic chemotherapy. Nature. 2015;521(7550):94-8.

54. Khan AR, Hams E, Floudas A, Sparwasser T, Weaver CT, Fallon PG. PD-L1hi B cells are critical regulators of humoral immunity. Nature communications. 2015;6:5997.

55. Cooper MA, Fehniger TA, Caligiuri MA. The biology of human natural killer-cell subsets. Trends Immunol. 2001;22(11):633-40.

56. Morvan MG, Lanier LL. NK cells and cancer: you can teach innate cells new tricks. Nat Rev Cancer. 2016;16(1):7-19.

57. Voskoboinik I, Whisstock JC, Trapani JA. Perforin and granzymes: function, dysfunction and human pathology. Nat Rev Immunol. 2015;15(6):388-400.

58. Mantovani A, Sozzani S, Locati M, Allavena P, Sica A. Macrophage polarization: tumor-associated macrophages as a paradigm for polarized M2 mononuclear phagocytes. Trends Immunol. 2002;23(11):549-55.

59. Gabrilovich DI, Bronte V, Chen SH, Colombo MP, Ochoa A, Ostrand-Rosenberg S, et al. The terminology issue for myeloid-derived suppressor cells. Cancer Res. 2007;67(1):425; author reply 6.

60. Gabrilovich DI. Myeloid-Derived Suppressor Cells. Cancer Immunol Res. 2017;5(1):3-8.

61. Kumar V, Patel S, Tcyganov E, Gabrilovich DI. The Nature of Myeloid-Derived Suppressor Cells in the Tumor Microenvironment. Trends Immunol. 2016;37(3):208-20.

62. Menter DG, Tucker SC, Kopetz S, Sood AK, Crissman JD, Honn KV. Platelets and cancer: a casual or causal relationship: revisited. Cancer Metastasis Rev. 2014;33(1):231-69.

63. Gay LJ, Felding-Habermann B. Contribution of platelets to tumour metastasis. Nat Rev Cancer. 2011;11(2):123-34.

64. Blann AD, Gurney D, Wadley M, Bareford D, Stonelake P, Lip GY. Increased soluble P-selectin in patients with haematological and breast cancer: a comparison with fibrinogen, plasminogen activator inhibitor and von Willebrand factor. Blood Coagul Fibrinolysis. 2001;12(1):43-50.

65. Taucher S, Salat A, Gnant M, Kwasny W, Mlineritsch B, Menzel R-C, et al. Impact of pretreatment thrombocytosis on survival in primary breast cancer. Thromb Haemost. 2003;89(6):1098-106.

66. Labelle M, Begum S, Hynes RO. Direct signaling between platelets and cancer cells induces an epithelial-mesenchymal-like transition and promotes metastasis. Cancer Cell. 2011;20(5):576-90.

67. Balkwill F. Cancer and the chemokine network. Nat Rev Cancer. 2004;4(7):540-50.

68. Facciabene A, Peng X, Hagemann IS, Balint K, Barchetti A, Wang LP, et al. Tumour hypoxia promotes tolerance and angiogenesis via CCL28 and T(reg) cells. Nature. 2011;475(7355):226-30.

69. Cham CM, Driessens G, O'Keefe JP, Gajewski TF. Glucose deprivation inhibits multiple key gene expression events and effector functions in CD8+ T cells. Eur J Immunol. 2008;38(9):2438-50.

70. Warburg O. On the origin of cancer cells. Science. 1956;123(3191):309-14.

71. Chang CH, Qiu J, O'Sullivan D, Buck MD, Noguchi T, Curtis JD, et al. Metabolic Competition in the Tumor Microenvironment Is a Driver of Cancer Progression. Cell. 2015;162(6):1229-41.

72. Fischer K, Hoffman P, Voelkl S, Meivenbauer N, Ammer J, Edinger M, et al. Inhibitory effect of tumor cell-derived lactic acid on human T cells. Blood. 2007;109(9):3812-9.

73. Sporn MB, Todaro GJ. Autocrine Secretion and Malignant Transformation of Cells. N Engl J Med. 1980;303(15):878-80.

74. Burstein HJ. The Distinctive Nature of HER2-Positive Breast Cancers. N Engl J Med. 2005;353(16):1652-4.

75. Tan M, Yao J, Yu D. Overexpression of the c-erbB-2 gene enhanced intrinsic metastasis potential in human breast cancer cells without increasing their transformation abilities. Cancer Res. 1997;57(6):1199-205.

76. Isaacs A, Lindenmann J. Virus Interfernce. I. The Interferon. Proc R Soc Lond B Biol Sci. 1957;147(927):258-67.

77. Pestka S, Krause CD, Walter MR. Interferons, interferon-like cytokines, and their receptors. Immunol Rev. 2004;202:8-32.

78. Kirkwood J, Strawderman M, Ernstoff MS, Smith T, Borden EC, Blum RH. Interferon alfa-2b adjuvant therapy of high-risk resected cutaneous melanoma: the Eastern Cooperative Oncology Group Trial EST 1684. J Clin Oncol. 1996;14(1):7-17.

79. Kirkwood J, Ibrahim J, Sosman JA, Sondak VK, Agarwala S, Ernstoff MS, et al. High-Dose Interferon Alfa-2b Significantly Prolongs Relapse-Free and Overall Survival Compared With the GM2-KLH/QS-21 Vaccine in Patients With Resected Stage IIB-III Melanoma: Results of Intergroup Trial E1694/S9512/C509801. J Clin Oncol. 2001;19(9):2370-80.

80. Moschos SJ, Edington HD, Land SR, Rao UN, Jukic D, Shipe-Spotloe J, et al. Neoadjuvant Treatment of Regional Stage IIIB Melanoma With High-Dose Interferon Alfa-2b Induces Objective Tumor Regression in Association With Modulation of Tumor Infiltrating Host Cellular Immune Responses. J Clin Oncol. 2006;24(19):3164-71.

81. Voelter-Mahlknecht S, Mahlknecht U, Letzel S, Fierlbeck G. Phase 2 trial of the continuous IV administration of interferon-beta in patients with disseminated malignant melanoma. Skinmed. 2006;5(6):271-6.

82. Eggermont AM, Suciu S, Santinami M, Testori A, Kruit WH, Marsden J, et al. Adjuvant therapy with pegylated interferon alfa-2b versus observation alone in resected stage III melanoma: final results of EORTC 18991, a randomised phase III trial. The Lancet. 2008;372(9633):117-26.

83. Borden EC, Jacobs B, Hollovary E, Rybicki L, Elson P, Olencki T, et al. Gene regulatory and clinical effects of interferon β in patients with metastatic melanoma: A phase II trial. J Interferon Cytokine Res. 2011;31(5):433-40.

84. Aoyagi S, Hata H, Homma E, Shimizu H. Sequential local injection of low-dose interferon-beta for maintenance therapy in stage II and III melanoma: A single-institution matched case-control study. Oncology. 2012;82(3):139-46.

85. Mohr P, Hauschild A, Trefzer U, Enk A, Tilgen W, Loquai C, et al. Intermittent high-dose intravenous interferon alfa-2b for adjuvant treatment of stage III melanoma: Final analysis of a randomized phase III dermatologic cooperative oncology group trial. J Clin Oncol. 2015;33(34):4077-84.

86. McMasters KM, Jr., Egger ME, Edwards MJ, Ross MI, Reintgen DS, Noyes RD, et al. Final Results of the Sunbelt Melanoma trial: A multi-institutional prospective randomized phase III study evaluating the role of adjuvant high-dose interferon alfa-2b and completion lymph node dissection for patients staged by sentinel lymph node biopsy. J Clin Oncol. 2016;34(10):1079-86.

87. Eggermont AMM. Adjuvant ipilimumab in stage III melanoma: New landscape, new questions. Eur J Cancer. 2016;69:39-42.

88. Hawkins RE, Gore M, Shparyk Y, Bondar V, Gladkov O, Ganev T, et al. A randomized phase II/III study of naptumomab estafenatox + IFNα versus IFNα in renal cell carcinoma: Final analysis with baseline biomarker subgroup and trend analysis. Clin Cancer Res. 2016;22(13):3172-81.

89. Artaç M, Çoşkun HŞ, Korkmaz L, Koçer M, Turhal NS, Engin H, et al. Using Interferon Alfa Before Tyrosine Kinase Inhibitors May Increase Survival in Patients With Metastatic Renal Cell Carcinoma: A Turkish Oncology Group (TOG) Study. Clin Genitourin Cancer. 2016;14(4):e347-e53.

90. Zeestraten ECM, Speetjens FM, Welters MJP, Saadatmand S, Stynenbosch LFM, Jongen R, et al. Addition of interferon-α to the p53-SLP® vaccine results in increased production of interferon-γ in vaccinated colorectal cancer patients: A phase I/II clinical trial. Int J Cancer. 2013;132(7):1581-91.

91. Kameshima H, Tsuruma T, Torigoe T, Takahashi A, Hirohashi Y, Tamura Y, et al. Immunogenic enhancement and clinical effect by type-I interferon of anti-apoptotic protein, survivin-derived peptide vaccine, in advanced colorectal cancer patients. Cancer Sci. 2011;102(6):1181-7.

92. Kameshima H, Tsuruma T, Kutomi G, Shima H, Iwayama Y, Kimura Y, et al. Immunotherapeutic benefit of α-interferon (IFNα) in survivin2B-derived peptide vaccination for advanced pancreatic cancer patients. Cancer Sci. 2013;104(1):124-9.

93. DiPaola RS, Chen YH, Stein M, Vaughn D, Patrick-Miller L, Carducci M, et al. A randomized phase II trial of mitoxantrone, estramustine and vinorelbine or bcl-2 modulation with 13-cis retinoic acid, interferon and paclitaxel in patients with metastatic castrate-resistant prostate cancer: ECOG 3899. J Transl Med. 2010;8.

94. Borden EC, Holland JF, Dao TL, Gutterman JU, Wiener L, Chang YC, et al. Leukocyte-derived interferon (alpha) in human breast carcinoma. The American Cancer Society phase II trial. Annuls of Internal Medicine. 1982;97(1):1-6.

95. Bruntsch U, Groos G, Tigges FJ, Hofschneider PH, Gallmeier WM. Lack of response in nine patients with breast cancer treated with fibroblast interferon. Cancer Chemother Pharmacol. 1984;13(1):39-42.

96. Kimmick G, Ratain MJ, Berry D, Woolf S, Norton L, Muss HB, et al. Subcutaneously administered recombinant human interleukin-2 and interferon alfa-2a for advanced breast cancer: a phase II study of the Cancer and Leukemia Group B (CALGB 9041). Invest New Drugs. 2004;22(1):83-9.

97. Parker BS, Rautela J, Hertzog PJ. Antitumour actions of interferons: Implications for cancer therapy. Nature Reviews Cancer. 2016;16(3):131-44.

98. Nardi M, Cognetti F, Pollera CF, Della Giulia M, Lombardi A, Atlante G, et al. Intraperitoneal recombinant alpha-2-interferon alternating with cisplatin as salvage therapy for minimal residual-disease ovarian cancer: A phase II study. J Clin Oncol. 1990;8(6):1036-41.

99. Frasci G, Tortoriello A, Facchini G, Conforti S, Persico G, Mastrantonio P, et al. Carboplatin and a-2b Interferon Intraperitoneal Combination as First-line Treatment of Minimal Residual Ovarian Cancer. A Pilot Study. Eur J Cancer. 1994;30A(7):946-50.

100. Moore DH, Valea F, Walton LA, Soper J, Clarke-Pearson D, Fowler WCJ. A Phase I Study of Intraperitoneal Interferon-a2b and Intravenous cis-Platinum plus Cyclophosphamide Chemotherapy in Patients with Untreated Stage III Epithelial Ovarian Cancer: A Gynecologic Oncology Group Pilot Study. Gynecol Oncol. 1995;59(2):267-72.

101. Bruzzone M, Rubagotti A, Gadducci A, Catsafados E, Foglia G, Brunetti I, et al. Intraperitoneal Carboplatin with or without Interferon-a in Advanced Ovarian Cancer Patients with Minimal Residual Disease at Second Look: A Prospective Randomized Trial of 111 Patients. Gynecol Oncol. 1997;65(3):499-505.

102. Morgan Jr RJ, Synold TW, Gandara D, Muggia F, Scudder S, Reed E, et al. Phase II trial of carboplatin and infusional cyclosporine with alpha-interferon in recurrent ovarian cancer: A California Cancer Consortium Trial. Int J Gynecol Cancer. 2007;17(2):373-8.

103. Dijkgraaf EM, Santegoets SJAM, Reyners AKL, Goedemans R, Wouters MCA, Kenter GG, et al. A phase I trial combining carboplatin/doxorubicin with tocilizumab, an anti-IL-6R monoclonal antibody, and interferon-α2b in patients with recurrent epithelial ovarian cancer. Ann Oncol. 2015;26(10):2141-9.

104. Lawal AO, Musekiwa A, Grobler L. Interferon after surgery for women with advanced (Stage II-IV) epithelial ovarian cancer. The Cochrane database of systematic reviews. 2013;6.

105. Jeung HC, Moon YW, Rha SY, Yoo NC, Roh JK, Noh SH, et al. Phase III trial of adjuvant 5-fluorouracil and adriamycin versus 5-fluorouracil, adriamycin, and polyadenylic-polyuridylic acid (poly A:U) for locally advanced gastric cancer after curative surgery: Final results of 15-year follow-up. Ann Oncol. 2008;19(3):520-6.

106. Kemeny N, Yagoda A, Wang Y, Field K, Wrobleski H, Whitmore W. Randomized trial of standard therapy with or without poly I:C in patients with superficial bladder cancer. Cancer. 1981;48(10):2154-7.

107. Dunn GP, Koebel CM, Schreiber RD. Interferons, immunity and cancer immunoediting. Nat Rev Immunol. 2006;6(11):836-48.

108. Dunn GP, Bruce AT, Sheehan KC, Shankaran V, Uppaluri R, Bui JD, et al. A critical function for type I interferons in cancer immunoediting. Nat Immunol. 2005;6(7):722-9.

109. Stark GR, Kerr IM, Williams BR, Silverman RH, Schreiber RD. How cells respond to interferons. Annu Rev Biochem. 1998;67:227-64.

110. de Weerd NA, Samarajiwa SA, Hertzog PJ. Type I interferon receptors: biochemistry and biological functions. J Biol Chem. 2007;282(28):20053-7.

111. Li X, Leung S, Kerr IM, Stark GR. Functional subdomains of STAT2 required for preassociation with the alpha interferon receptor and for signaling. Mol Cell Biol. 1997;17(4):2048-56.

112. Fu X-Y, Kessler DS, Veals SA, Levy DE, Darnell Jr. JE. ISGF3, the transcriptional activator induced by interferon a, consists of multiple interacting polypeptide chains. Proc Natl Acad Sci U S A. 1990;87(21):8555-9.

113. Samarajiwa SA, Forster S, Auchettl K, Hertzog PJ. INTERFEROME: the database of interferon regulated genes. Nucleic Acids Res. 2009;37(Database issue):D852-7.

114. Rusinova I, Forster S, Yu S, Kannan A, Masse M, Cumming H, et al. Interferome v2.0: an updated database of annotated interferon-regulated genes. Nucleic Acids Res. 2013;41(Database issue):D1040-6.

115. Grumbach IM, Mayer IA, Uddin S, Lekmine F, Majchrzak B, Yamauchi H, et al. Engagement of the CrkL adaptor in interferon alpha signalling in BCR-ABL-expressing cells. Br J Haematol. 2001;112(2):327-36.

116. Nguyen KB, Watford WT, Salomon R, Hofmann SR, Pien GC, Morinobu A, et al. Critical role for STAT4 activation by type 1 interferons in the interferon-gamma response to viral infection. Science. 2002;297(5589):2063.

117. Su L, David M. Distinct mechanisms of STAT phosphorylation via the interferon-alpha/beta receptor. Selective inhibition of STAT3 and STAT5 by piceatannol. J Biol Chem. 2000;275(17):12661-6.

118. Platanias LC. Mechanisms of type-I- and type-II-interferon-mediated signalling. Nat Rev Immunol. 2005;5(5):375-86.

119. Hertzog P, Forster S, Samarajiwa S. Systems biology of interferon responses. J Interferon Cytokine Res. 2011;31(1):5-11.

120. Forster S. Interferon signatures in immune disorders and disease. Immunol Cell Biol. 2012;90(5):520-7.

121. Swann JB, Smyth MJ. Immune surveillanc of tumours. J Clin Invest. 2007;117(5):1137-46.

122. Hertzog PJ, Williams BR. Fine tuning type I interferon responses. Cytokine Growth Factor Rev. 2013;24(3):217-25.

123. Clemens MJ. Interferons and apoptosis. J Interferon Cytokine Res. 2003;23(6):277-92.

124. Zhang T, Sun HC, Zhou HY, Luo JT, Zhang BL, Wang P, et al. Interferon alpha inhibits hepatocellular carcinoma growth through inducing apoptosis and interfering with adhesion of tumor endothelial cells. Cancer Lett. 2010;290(2):204-10.

125. Bracarda S, Eggermont AM, Samuelsson J. Redefining the role of interferon in the treatment of malignant diseases. Eur J Cancer. 2010;46(2):284-97.

126. Swann JB, Hayakawa Y, Zerafa N, Sheehan KC, Scott B, Schreiber RD, et al. Type I IFN contributes to NK cell homeostasis, activation, and antitumor function. J Immunol. 2007;178(12):7540-9.

127. Sangfelt O, Erickson S, Castro J, Heiden T, Gustafsson A, Einhorn S, et al. Molecular mechanisms underlying interferon-alpha-induced G0/G1 arrest: CKI-mediated regulation of G1 Cdk-complexes and activation of pocket proteins. Oncogene. 1999;18(18):2798-810.

128. Panaretakis T, Pokrovskaja K, Shoshan MC, Grander D. Interferon-alpha-induced apoptosis in U266 cells is associated with activation of the proapoptotic Bcl-2 family members Bak and Bax. Oncogene. 2003;22(29):4543-56.

129. Biron CA, Nguyen KB, Pien GC, Cousens LP, Salazar-Mather TP. Natural killer cells in antiviral defense: Function and regulation by innate cytokines. Annu Rev Immunol1999. p. 189-220.

130. Biron CA, Sonnenfeld G, Welsh RM. Interferon induces natural killer cell blastogenesis in vivo. J Leukoc Biol. 1984;35(1):31-7.

131. Schiavoni G, Mattei F, Gabriele L. Type I interferons as stimulators of DC-mediated cross-priming: Impact on anti-tumor response. Front Immunol. 2013;4(DEC).

132. Marrack P, Kappler J, Mitchell T. Type I interferons keep activated T cells alive. J Exp Med. 1999;189(3):521-9.

133. Curtsinger JM, Mescher MF. Inflammatory cytokines as a third signal for T cell activation. Curr Opin Immunol. 2010;22(3):333-40.

134. Fuertes MB, Kacha AK, Kline J, Woo SR, Kranz DM, Murphy KM, et al. Host type I IFN signals are required for antitumor CD8+ T cell responses through CD8{alpha}+ dendritic cells. J Exp Med. 2011;208(10):2005-16.

135. Zhang X, Sun S, Hwang I, Tough DF, Sprent J. Potent and selective stimulation of memory-phenotype CD8+ T cells in vivo by IL-15. Immunity. 1998;8(5):591-9.

136. Braun D, Caramalho I, Demengeot J. IFn-α/β enhances BCR-dependent B cell responses. Int Immunol. 2002;14(4):411-9.

137. Le Bon A, Thompson C, Kamphuis E, Durand V, Rossmann C, Kalinke U, et al. Cutting edge: Enhancement of antibody responses through direct stimulation of B and T cells by type I IFN. J Immunol. 2006;176(4):2074-8.

138. Swanson CL, Wilson TJ, Strauch P, Colonna M, Pelanda R, Torres RM. Type I IFN enhances follicular B cell contribution to the T cell-independent antibody response. J Exp Med. 2010;207(7):1485-500.

139. Pace L, Vitale S, Dettori B, Palombi C, La Sorsa V, Belardelli F, et al. APC activation by IFN-α decreases regulatory T cell and enhances Th cell functions. J Immunol. 2010;184(11):5969-79.

140. Balkwill F, Watling D, Taylor‐Papadimitriou J. Inhibition by lymphoblastoid interferon of growth of cells derived from the human breast. Int J Cancer. 1978;22(3):258-65.

141. Hobeika AC, Subramaniam PS, Johnson HM. IFNα induces the expression of the cyclin-dependent kinase inhibitor p21 in human prostate cancer cells. Oncogene. 1997;14(10):1165-70.

142. Choi EA, Lei H, Maron DJ, Wilson JM, Barsoum J, Fraker DL, et al. Stat1-dependent induction of tumor necrosis factor-related apoptosis-inducing ligand and the cell-surface death signaling pathway by interferon β in human cancer cells. Cancer Res. 2003;63(17):5299-307.

143. Thyrell L, Erickson S, Zhivotovsky B, Pokrovskaja K, Sangfelt O, Castro J, et al. Mechanisms of interferon-alpha induced apoptosis in malignant cells. Oncogene. 2002;21(8):1251-62.

144. Fulda S, Debatin KM. 5-Aza-2′-deoxycytidine and IFN-γ cooperate to sensitize for TRAIL-induced apoptosis by upregulating caspase-8. Oncogene. 2006;25(37):5125-33.

145. Greiner JW, Hand PH, Schlom J, Noguchi P, Fisher PB, Pestka S. Enhanced Expression of Surface Tumor-associated Antigens on Human Breast and Colon Tumor Cells after Recombinant Human Leukocyte α-Interferon Treatment. Cancer Res. 1984;44(8):3208-14.

146. Heise R, Amann PM, Ensslen S, Marquardt Y, Czaja K, Joussen S, et al. Interferon alpha signalling and its relevance for the upregulatory effect of transporter proteins associated with antigen processing (TAP) in patients with malignant melanoma. PLoS One. 2016;11(1).

147. Schreiner B, Mitsdoerffer M, Kieseier BC, Chen L, Hartung HP, Weller M, et al. Interferon-β enhances monocyte and dendritic cell expression of B7-H1 (PD-L1), a strong inhibitor of autologous T-cell activation: Relevance for the immune modulatory effect in multiple sclerosis. J Neuroimmunol. 2004;155(1-2):172-82.

148. Paredes J, Krown SE. Interferon-α therapy in patients with Kaposi's sarcoma and the acquired immunodeficienct syndrome. Int J Immunopharmacol. 1991;13(SUPPL. I):77-81.

149. Radin AI, Kim HT, Grant BW, Bennett JM, Kirkwood JM, Stewart JA, et al. Phase II study of alpha2 interferon in the treatment of the chronic myeloproliferative disorders (E5487): a trial of the Eastern Cooperative Oncology Group. Cancer. 2003;98(1):100-9.

150. Kiladjian JJ, Chomienne C, Fenaux P. Interferon-alpha therapy in bcr-abl-negative myeloproliferative neoplasms. Leukemia. 2008;22(11):1990-8.

151. Quesada JR, Rios A, Swanson D, Trown P, Gutterman JU. Antitumour activity of recombinant-derived interferon alpha in metastatic renal cell carcinoma. J Clin Oncol. 1985;3(11):1522-8.

152. Kirkwood JM, Harris JE, Vera R, Sandler S, Fischer DS, Khandekar J, et al. A randomized study of low and high doses of leukocyte α-interferon in matastatic renal cell

carcinoma: The American Cancer Society Collaborative Trial. Cancer Res. 1985;45(2):863-71.

153. Muss HB, Costanzi JJ, Leavitt R, Williams RD, Kempf RA, Pollard R, et al. Recombinant alfa interferon in renal cell carcinoma: A randomized trial of two routes of administration. J Clin Oncol. 1987;5(2):286-91.

154. Kriegmair M, Oberneder R, Hostetter A. Interferon alfa and vinblastine versus medroxyprogesterone acetate in the treatment of metastatic renal cell carcinoma. Urology. 1995;45(5):758-62.

155. Mendiratta SK, Quezada A, Matar M, Thull NM, Bishop JS, Nordstrom JL, et al. Combination of interleukin 12 and interferon α gene therapy induces a synergistic antitumor response against colon and renal cell carcinoma. Hum Gene Ther. 2000;11(13):1851-62.

156. Kirkwood JM, Tarhini AA, Panelli MC, Moschos SJ, Zarour HM, Butterfield LH, et al. Next generation of immunotherapy for melanoma. J Clin Oncol. 2008;26(20):3445-55.

157. Atkins MB, Hsu J, Lee S, Cohen GI, Flaherty LE, Sosman JA, et al. Phase III trial comparing concurrent biochemotherapy with cisplatin, vinblastine, dacarbazine, interleukin-2, and interferon alfa-2b with cisplatin, vinblastine, and dacarbazine alone in patients with metastatic malignant melanoma (E3695): a trial coordinated by the Eastern Cooperative Oncology Group. J Clin Oncol. 2008;26(35):5748-54.

158. Agarwal C, Hembree JR, Rorke EA, Eckert RL. Interferon and retinoic acid suppress the growth of human papillomarvirus type 16 immortalized cervical eptihelial cells, but only

interferon suppresses the level of the human papillomavirus transforming oncogenes. Cancer Res. 1994;54:2108-12.

159. Kotredes KP, Gamero AM. Interferons as inducers of apoptosis in malignant cells. J Interferon Cytokine Res. 2013;33(4):162-70.

160. Young HA, Bream JH. IFN-gamma: recent advances in understanding regulation of expression, biological functions, and clinical applications. Curr Top Microbiol Immunol. 2007;316:97-117.

161. Ascierto PA, Gogas HJ, Algarra SM, Mohr P, Hansson J, Hauschild A. Adjuvant interferon alfa in malignant melanoma: an interdisciplinary and multinational expert review. Crit Rev Oncol Hematol. 2013;85(2):149-61.

162. Gutterman JU, Blumenschein GR, Alexanian R, Yap HY, Buzdar AU, Cabanillas F, et al. Leukocyte interferon-induced tumor regression in human metastatic breast cancer, multiple myeloma, and malignant lymphoma. Annuls of Internal Medicine. 1980;93(3):399-406.

163. Macheledt JE, Buzdar AU, Hortobagyi GN, Frye DK, Gutterman JU, Holmes FA. Phase II evaluation of interferon added to tamoxifen in the treatment of metastatic breast cancer. Breast Cancer Res Treat. 1991;18(3):165-70.

164. Repetto L, Giannessi PG, Campora E, Pronzato P, Vigani A, Naso C, et al. Tamoxifen and interferon-beta for the treatment of metastatic breast cancer. Breast Cancer Res Treat. 1996;39(2):235-8.

165. Siegal FP, Kadowaki N, Shodell M, Fitzgerald-Bocarsly P, Shah K, Ho S, et al. The nature of the prinicipal type 1 interferon-producing cells in human blood. Science. 1999;284(5421):1835-7.

166. Asselin-Paturel C, Boonstra A, Dalod M, Durand I, Yessaad N, Dezutter-Dambuyant C, et al. Mouse type I IFN-producing cells are immature APCs with plasmacytoid morphology. Nat Immunol. 2001;2(12):1144-50.

167. Zitvogel L, Galluzzi L, Kepp O, Smyth MJ, Kroemer G. Type I interferons in anticancer immunity. Nature Reviews Immunology. 2015;15(7):405-14.

168. Gregorio J, Meller S, Conrad C, Di Nardo A, Homey B, Lauerma A, et al. Plasmacytoid dendritic cells sense skin injury and promote wound healing through type i interferons. J Exp Med. 2010;207(13):2921-30.

169. Ng AYN, Waring P, Ristevski S, Wang C, Wilson T, Pritchard M, et al. Inactivation of the transcription factor Elf3 in mice results in dysmorphogenesis and altered differentiation of intestinal epithelium. Gastroenterology. 2002;122(5):1455-66.

170. Hsu ACY, Parsons K, Barr I, Lowther S, Middleton D, Hansbro PM, et al. Critical role of constitutive type i interferon response in bronchial epithelial cell to influenza infection. PLoS One. 2012;7(3).

171. Fung KY, Mangan NE, Cumming H, Horvat JC, Mayall JR, Stifter SA, et al. Interferon-epsilon protects the female reproductive tract from viral and bacterial infection. Science. 2013;339(6123):1088-92.

172. Levy DE, Marie I, Prakash A. Enhancement and diversification of IFN induction by IRF-7-mediated positive feedback. Journal of Interferon and Cytokine Research : the official journal of the International Society for Interferon and Cytokine Research. 2002;22(1):87-93.

173. Lu R, Au W-C, Yeow W-S, Hageman N, Pitha P-M. Regulation of the promoter activity of interferon regulatory factor-7 gene. Activation by interferon and silencing by hypermethylation. J Biol Chem. 2000;275(41):31805-12.

174. Savitsky D, Tamura T, Yanai H, Taniguchi T. Regulation of immunity and oncogenesis by the IRF transcription factor family. Cancer Immunol Immunother. 2010;59(4):489-510.

175. Paun A, Bankoti R, Joshi T, Pitha PM, Stager S. Critical role of IRF-5 in the development of T helper 1 responses to Leishmania donovani infection. PLoS Pathog. 2011;7(1):e1001246.

176. Bocci V. Production and role of interferon in physiological conditions. Biol Rev Camb Philos Soc. 1981;56(1):49-85.

177. Hamilton JA, Whitty GA, Kola I, Hertzog PJ. Endogenous IFN-αβ suppresses colony-stimulating factor (CSF)-1-stimulated macrophage DNA synthesis and mediates inhibitory effects of lipopolysaccharide and TNF-α. J Immunol. 1996;156(7):2553-7.

178. Takayanagi H, Kim S, Matsuo K, Suzuki H, Suzuki T, Sato K, et al. RANKL maintains bone homeostasis through c-fos-dependent induction of interferon-β. Nature. 2002;416(6882):744-9.

179. Kole A, He J, Rivollier A, Silveira DD, Kitamura K, Maloy KJ, et al. Type I IFNs regulate effector and regulatory T cell accumulation and anti-inflammatory cytokine production during T cell-mediated colitis. J Immunol. 2013;191(5):2771-9.

180. Lienenklaus S, Cornitescu M, Ziętara N, Łyszkiewicz M, Gekara N, Jabłońska J, et al. Novel reporter mouse reveals constitutive and inflammatory expression of IFN-β in vivo. J Immunol. 2009;183(5):3229-36.

181. McNab F, Mayer-Barber K, Sher A, Wack A, O'Garra A. Type I interferons in infectious disease. Nature Reviews Immunology. 2015;15(2):87-103.

182. Berry MP, Graham CM, McNab FW, Xu Z, Bloch SA, Oni T, et al. An interferon-inducible neutrophil-driven blood transcriptional signature in human tuberculosis. Nature. 2010;466(7309):973-7.

183. Baechler EC, Batliwalla FM, Karypis G, Gaffney PM, Ortmann WA, Espe KJ, et al. Interferon-inducible gene expression signature in peripheral blood cells of patients with severe lupus. Proc Natl Acad Sci U S A. 2003;100(5):2610-5.

184. Zimmerer JM, Lehman AM, Ruppert AS, Noble CW, Olencki T, Walker MJ, et al. IFN-alpha-2b-induced signal transduction and gene regulation in patient peripheral blood mononuclear cells is not enhanced by a dose increase from 5 to 10 megaunits/m2. Clin Cancer Res. 2008;14(5):1438-45.

185. Bennett L, Palucka AK, Arce E, Cantrell V, Borvak J, Banchereau J, et al. Interferon and granulopoiesis signatures in systemic lupus erythematosus blood. J Exp Med. 2003;197(6):711-23.

186. Sato M, Suemori H, Hata N, Asagiri M, Ogasawara K, Nakao K, et al. Distinct and essential roles of transcriptions factors IRF-3 and IRF-7 in response to viruses for IFN-α/β gene induction. Immunity. 2000;13(4):539-48.

187. Honda K, Yanai H, Negishi H, Asagiri M, Sato M, Mizutani T, et al. IRF-7 is the master regulator of type-I interferon-dependent immune responses. Nature. 2005;434(7034):772-7.

188. Zhang L, Pagano JS. IRF-7, a new interferon regulatory factor associated with Epstein-Barr virus latency. Mol Cell Biol. 1997;17(10):5748-57.

189. Honda K, Taniguchi T. IRFs: master regulators of signalling by Toll-like receptors and cytosolic pattern-recognition receptors. Nat Rev Immunol. 2006;6(9):644-58.

190. Lin R, Genin P, Mamane Y, Hiscott J. Selective DNA Binding and Association with the CREB Binding Protein Coactivator Contribute to Differential Activation of Alpha/Beta Interferon Genes by Interferon Regulatory Factors 3 and 7. Mol Cell Biol. 2000;20(17):6342-53.

191. Izaguirre A, Barnes BJ, Amrute S, Yeow WS, Megjugorac N, Dai J, et al. Comparative analysis of IRF and IFN-alpha expression in human plasmacytoid and monocyte-derived dendritic cells. J Leukoc Biol. 2003;74(6):1125-38.

192. Marie I, Durbin JE, Levy DE. Differential viral induction of distinct interferon-alpha genes by positive feedback through interferon regulatory factor-7. EMBO J. 1998;17(22):6660-9.

193. Yang H, Lin CH, Ma G, Baffi MO, Wathelet MG. Interferon regulatory factor-7 synergizes with other transcription factors through multiple interactions with p300/CBP coactivators. J Biol Chem. 2003;278(18):15495-504.

194. Erickson AK, Gale M, Jr. Regulation of interferon production and innate antiviral immunity through translational control of IRF-7. Cell Res. 2008;18(4):433-5.

195. Hiscott J. Triggering the innate antiviral response through IRF-3 activation. J Biol Chem. 2007;282(21):15325-9.

196. Kawai T, Akira S. Innate immune recognition of viral infection. Nat Immunol. 2006;7(2):131-7.

197. Ferlay J, Soerjomataram I, Ervik M, Dikshit R, Eser S, Mathers C, et al. Cancer Incidence and Mortality Worldewide Lyon, France: International Agency for Research on Cancer; 2013 [cited 2014 15/04/2014]. Available from: http://globocan.iarc.fr/.

198. Downs-Holmes C, Silverman P. Breast Cancer: overview & updates. Nurse Pract. 2011;36(12):20-6.

199. Howlader N, Noone AM, Krapcho M, Garshell J, Miller D, Altekruse SF, et al. SEER Cancer Statisitcs Review, 1975-2011. 2013 April 2014.

200. Mundy GR. Metastasis to bone: causes, consequences and therapeutic opportunities. Nat Rev Cancer. 2002;2(8):584-93.

201. Mundy GR. Mechanisms of bone metastasis. Cancer. 1997;80(8):1546-56.

202. Coussens LM, Pollard JW. Leukocytes in mammary development and cancer. Cold Spring Harb Perspect Biol. 2011;3(3).

203. Clarkson RW, Wayland MT, Lee J, Freeman T, Watson CJ. Gene expression profiling of mammary gland development reveals putative roles for death receptors and immune mediators in post-lactational regression. Breast Cancer Res. 2004;6(2):R92-109.

204. Watson CJ, Oliver CH, Khaled WT. Cytokine signalling in mammary gland development. J Reprod Immunol. 2011;88(2):124-9.

205. Robert J. Comparative study of tumourigenesis and tumour immunity in invertebrates and nonmammalian vertebrates. Dev Comp Immunol. 2010;34:915-25.

206. Australian Institute of Health and Welfare, Australian Association of Cancer Registeries, National Breast and Ovarian Cancer Centre. Breast cancer survival by size and nodal stutus in Australia. Canberra: AIHW; 2007. Contract No.: CAN 34.

207. Singletary SE. Revision of the American Joint Committee on Cancer Staging System for Breast Cancer. J Clin Oncol. 2002;20(17):3628-36.

208. Bloom HJ, Richardson WW. Histological grading and prognosis in breast cancer; a study of 1409 cases of which 359 have been followed for 15 years. Br J Cancer. 1957;11(3):359-77.

209. Tudoran O, Virtic O, Balacescu L, Pop L, Dragla F, Eniu A, et al. Differential peripheral blood gene expression profile based on Her2 expression on primary tumors of breast cancer patients. PLoS One. 2014;9(7):e102764.

210. Friedenreich CM, Woolcott CG, McTiernan A, Ballard-Barbash R, Brant RF, Stanczyk FZ, et al. Alberta physical activity and breast cancer prevention trial: sex hormone changes in a year-long exercise intervention among postmenopausal women. J Clin Oncol. 2010;28(9):1457-66.

211. Cooke T, Reeves J, Lanigan A, Stanton P. HER2 as a prognotic and predictive marker for breast cancer. Ann Oncol. 2001;12(SUPPL. 1):S23-S8.

212. Perou CM, Jeffrey SS, van de Rijn M, Rees CA, Eisen MB, Ross DT, et al. Distinctive gene expression patterns in human mammary epithelial cells and breast cancers. Proc Natl Acad Sci U S A. 1999;96(16):9212-17.

213. Perou CM, Sorlie T, Eisen MB, van de Rijn M, Jeffrey SS, Rees CA, et al. Molecular portraits of human breast tumours. Nature. 2000;406(6797):747-52.

214. Gruvberger S, Ringner M, Chen Y, Panavally S, Saal LH, Borg A, et al. Estrogen receptor status in breast cancer is associated with remarkably distinct gene expression patterns. Cancer Res. 2001;61(16):5979-84.

215. Martin KL, Kritzman BM, Price LM, Koh B, Kwan CP, Zhang X, et al. Linking gene expression patterns to therapeutic groups in breast cancer. Cancer Res. 2000;60(8):2232-8.

216. Zajchowski DA, Bartholdi MF, Gong Y, Webster L, Liu HL, Munishkin A, et al. Identification of gene expression profiles that predict aggressive behaviour of breast cancer cells. Cancer Res. 2001;61(13):5168-78.

217. Sorlie T, Perou CM, Tibishirani R, Aas T, Geisler S, Johnsen H, et al. Gene expression patterns of breast carcinomas distinguish tumor subclasses with clinical implications. Proc Natl Acad Sci U S A. 2001;98(19):10869-74.

218. Ascierto ML, Kmieciak M, Idowu MO, Manjili R, Zhao Y, Grimes M, et al. A signature of immune function genes associated with recurrence-free survival in breast cancer patients. Breast Cancer Res Treat. 2012;131(3):871-80.

219. van t'Veer LJ, Dai H, van de Vijver MJ, He YD, Hart AA, Mao M, et al. Gene expression profiling predicts clinical outcome of breast cancer. Nature. 2002;415(6871):530-6.

220. Sharma P, Sahni NS, Tibshirani R, Skaane P, Urdal P, Berghagen H, et al. Early detection of breast cancer based on gene-expression patterns in peripheral blood cells. Breast Cancer Res. 2005;7(5):R634-44.

221. Aaroe J, Lindahl T, Dumeaux V, Saebo S, Tobin D, Hagen N, et al. Gene expression profiling of peripheral blood cells for early detection of breast cancer. Breast Cancer Res. 2010;12(1):R7.

222. Minn AJ, Gupta GP, Siegel PM, Bos PD, Shu W, Giri DD, et al. Genes that mediate breast cancer metastasis to lung. Nature. 2005;436(7050):518-24.

223. Kang Y, Siegel PM, Shu W, Drobnjak M, Kakonen SM, Cordón-Cardo C, et al. A multigenic program mediating breast cancer metastasis to bone. Cancer Cell. 2003;3(6):537-49.

224. Gatza ML, Lucas JE, Barry WT, Kim JW, Wang Q, Crawford MD, et al. A pathway-based classification of human breast cancer. Proc Natl Acad Sci U S A. 2010;107(15):6994-9.

225. Wang DY, Done SJ, McCready DR, Boerner S, Kulkarni S, Leong WL. A new gene expression signature, the ClinicoMolecular Triad Classification, may improve prediction and prognostication of breast cancer at the time of diagnosis. Breast Cancer Res. 2011;13(5):R92.

226. Curtis C, Shah SP, Chin SF, Turashvili G, Rueda OM, Dunning MJ, et al. The genomic and transcriptomic architecture of 2,000 breast tumours reveals novel subgroups. Nature. 2012;486(7403):346-52.

227. Solomayer EF, Diel IJ, Meyberg GC, Gollan C, Bastert G. Metastatic breast cancer: clinical course, prognosis and therapy related to the first site of metastasis. Breast Cancer Res Treat. 2000;59(3):271-8.

228. Jayson GC, Kohn EC, Kitchener HC, Ledermann JA. Ovarian cancer. The Lancet. 2014;384(9951):1376-88.

229. AIHW. Ovarian cancer in Australia: an overview, 2010. Cancer series 52 Cat no CAN 48 2010.

230. Kurman RJ, Shih IM. Molecular pathogenesis and extraovarian origin of epithelial ovarian cancer- Shifting the paradigm. Hum Pathol. 2011;42(7):918-31.

231. Perets R, Wyant G, Muto K, Bijron J, Poole B, Chin K, et al. Transformation of the

Fallopian Tube Secretory Epithelium Leads to High-Grade Serous Ovarian Cancer in Brca;Tp53;Pten Models. Cancer Cell. 2013;24(6):751-65.

232. Perets R, Drapkin R. It's totally tubular…. Riding the new wave of ovarian cancer research. Cancer Res. 2016;76(1):10-7.

233. Ducie J, Dao F, Considine M, Olvera N, Shaw PA, Kurman RJ, et al. Molecular analysis of high-grade serous ovarian carcinoma with and without associated serous tubal intra-epithelial carcinoma. Nature communications. 2017;8(1).

234. Greenaway J, Moorehead R, Shaw P, Petrik J. Epithelial-stromal interaction increases cell proliferation, survival and tumorigenicity in a mouse model of human epithelial ovarian cancer. Gynecol Oncol. 2008;108(2):385-94.

235. Connolly DC, Hensley HH. Xenograft and transgenic mouse models of epithelial ovarian cancer and non-invasive imaging modalities to monitor ovarian tumor growth in situ: applications in evaluating novel therapeutic agents. Curr Protoc Pharmacol. 2009;Chapter 14:Unit14 2.

236. Cho S, Sun Y, Soisson AP, Dodson MK, Peterson CM, Jarboe EA, et al. Characterization and evaluation of pre-clinical suitability of a syngeneic orthotopic mouse ovarian cancer model. Anticancer Res. 2013;33(4):1317-24.

237. Szabova L, Bupp S, Kamal M, Householder DB, Hernandez L, Schlomer JJ, et al.

Pathway-Specific Engineered Mouse Allograft Models Functionally Recapitulate Human Serous Epithelial Ovarian Cancer. Katoh M, ed. PLoS ONE. 2014;9(4):e95649. doi:10.1371/journal.pone.0095649.

238. Walton J, Blagih J, Ennis D, Leung E, Dowson S, Farquharson M, et al. CRISPR/ Cas9-mediated Trp53 and Brca2 knockout to generate improved murine models of ovarian high grade serous carcinoma. Cancer research. 2016;76(20):6118-6129.

239. Shaw TJ, Senterman MK, Dawson K, Crane CA, Vanderhyden BC. Characterization of intraperitoneal, orthotopic, and metastatic xenograft models of human ovarian cancer. Mol Ther. 2004;10(6):1032-42.

240. Gilbert L, Basso O, Sampalis J, Karp I, Martins C, Feng J, et al. Assessment of symptomatic women for early diagnosis of ovarian cancer: results from the prospective DOvE pilot project. Lancet Oncol2012;13:285-91.

241. Venkitaraman AR. Cancer Suppression by the Chromosome Custodians, BRCA1 and BRCA2. Science. 2014;343(6178):1470-5.

242. Tothill RW, Tinker AV, George J, Brown R, Fox SB, Lade S, et al. Novel molecular subtypes of serous and endometrioid ovarian cancer linked to clinical outcome. Clin Cancer Res. 2008;14(16):5198-208.

243. Cancer Genome Atlas Network. Comprehensive molecular portraits of human breast tumours. Nature. 2012;490(7418):61-70.

244. Sieh W, Kobel M, Longacre TA, Bowtell DD, deFazio A, Goodman MT, et al.

Hormonereceptor expression and ovarian cancer survival: an Ovarian Tumor Tissue Analysis consortium study. The Lancet Oncology. 2013;14(9):853-62.

245. Thakkar JP, Mehta DG. A review of an unfavorable subset of breast cancer: estrogen receptor positive progesterone receptor negative. Oncologist. 2011;16(3):276-85.

246. Berek JS, Hacker NF, Lichtenstein A, Jung T, Spina C, Knox RM, et al. Intraperitoneal Recombinant A-Interferon for "Salvage" Immunotherapy in Stage III Epithelial Ovarian Cancer: A Gynecologic Oncology Group Study. Cancer Res. 1985;45:4447-53.

247. Willemse PHB, De Vries EGE, Mulder NH, Aalders JG, Bouma J, Sleijfer DTH. Intraperitoneal human recombinant interferon alpha-2b in minimal residual ovarian cancer. Eur J Cancer Clin Oncol. 1990;26(3):353-8.

248. Marman M, Berek JS, Blessing JA, McGuire WP, Bell J, Homesley HD. Characteristics of Patients with Small-Volume Residual Ovarian Cancer Unresponsive to Cisplatin-Based ip Chemotherapy: Lessons Learned from a Gynecologic Oncology Group Phase II Trial of ip Cisplatin and Recombinant a-lnterferon. Gynecol Oncol. 1992;45(1):3-8.

249. Frasci G, Tortoriello A, Facchini G, Conforti S, Persico G, Mastrantonio P, et al. Carboplatin and a-2b Interferon Intraperitoneal Combination as First-line Treatment of Minimal Residual Ovarian Cancer. A Pilot Study. Eur J Cancer. 1994;30A(7):946-50.

250. Bruzzone M, Rubagotti A, Gadducci A, Catsafados E, Foglia G, Brunetti I, et al. Intraperitoneal Carboplatin with or without Interferon-a in Advanced Ovarian Cancer

Patients with Minimal Residual Disease at Second Look: A Prospective Randomized Trial of 111 Patients. Gynecol Oncol. 1997;65(3):499-505.

251. Moore DH, Valea F, Walton LA, Soper J, Clarke-Pearson D, Fowler WCJ. A Phase I Study of Intraperitoneal Interferon-a2b and Intravenous cis-Platinum plus Cyclophosphamide Chemotherapy in Patients with Untreated Stage III Epithelial Ovarian Cancer: A Gynecologic Oncology Group Pilot Study. Gynecol Oncol. 1995;59(2):267-72.

252. Berek JS, Markman M, Stonebraker B, Lentz SS, Adelson MD, DeGeest K, et al. Intraperitoneal interferon-α in residual ovarian carcinoma: A phase II gynecologic oncology group study. Gynecol Oncol. 1999;75(1):10-4.

253. Markman M, Belinson J, Webster K, Zanotti K, Morrison B, Jacobs B, et al. Phase 2 trial of interferon-beta as second-line treatment of ovarian cancer, fallopian tube cancer, or primary carcinoma of the peritoneum. Oncology. 2004;66(5):343-6.

254. Hall GD, Brown JM, Coleman RE, Stead M, Metcalf KS, Peel KR, et al. Maintenance treatment with interferon for advanced ovarian cancer: results of the Northern and Yorkshire gynaecology group randomised phase III study. Br J Cancer. 2004;91(4):621-6.

255. Bezwoda WR, Golombick T, Dansey R, Keeping J. Treatment of Malignant Ascites due to Recurrent/Refractory Ovarian Cancer: the Use of Interferon-a or Interferon-a Plus Chemotherapy in vivo and in vitro. Eur J Cancer. 1991;27(11):1423-9.

256. Sartori S, Nielsen I, Tassinari L, Abbasciano V, Malacarne P. Evaluation of a standardized protocol of intracavitary recombinant interferon alpha-2b in the palliative

treatment of malignant peritoneal effusions. A prospective pilot study. Oncology. 2001;61(3):192-6.

257. Isaacs A, Lindenmann J. Virus Interfernce. I. The Interferon. Proc R Soc Lond B Biol Sci. 1957;147(927):258-67.

258. Gresser I, Bourali C, Levy JP, Fontaine-Brouty-Boye D, Thomas MT. Increased survival in mice inoculated with tumour cells and treated with interferon preparations. Proc Natl Acad Sci U S A. 1969;63(1):51-7.

259. Rehberg E, Kelder B, Hoal EG, Pestka S. Specific molecular activities of recombinant and hybrid leukocyte interferons. J Biol Chem. 1982;257(19):11497-502.

260. Thyrell L, Hjortsberg L, Arulampalam V, Panaretakis T, Uhles S, Dagnell M, et al. Interferon alpha-induced apoptosis in tumor cells is mediated through the phosphoinositide 3-kinase/mammalian target of rapamycin signaling pathway. J Biol Chem. 2004;279(23):24152-62.

261. Porta C, Hadj-Slimane R, Nejmeddine M, Pampin M, Tovey MG, Espert L, et al. Interferons alpha and gamma induce p53-dependent and p53-independent apoptosis, respectively. Oncogene. 2005;24(4):605-15.

262. Mann GJ, Thorne H, Balleine RL, Butow PN, Clarke CL, Edkins E, et al. Analysis of cancer risk and BRCA1 and BRCA2 mutation prevalence in the kConFab familial breast cancer resource. Breast Cancer Res. 2006;8(1).

263. Patch AM, Christie EL, Etemadmoghadam D, Garsed DW, George J, Fereday S, et al. Whole-genome characterization of chemoresistant ovarian cancer. Nature.

2015;521(7553):489-94.

264. Tan TZ, Yang H, Ye J, Low J, Choolani M, Tan DS, et al. CSIOVDB: a microarray gene expression database of epithelial ovarian cancer subtype. Oncotarget. 2015;6(41):43843-52.

265. Ke N, Wang X, Xu X, Abassi YA. The xCELLigence system for real-time and label-free monitoring of cell viability. Methods Mol Biol. 2011;740:33-43.

266. Schmittgen TD, Livak KJ. Analyzing real-time PCR data by the comparative C(T) method. Nat Protoc. 2008;3(6):1101-8.

267. Ritchie ME, Phipson B, Wu D, Hu Y, Law CW, Shi W, et al. Limma powers differential expression analyses for RNA-sequencing and microarray studies. Nucleic Acids Res. 2015;43(7):e47.

268. Ritchie ME, Diyagama D, Neilson J, van Laar R, Dobrovic A, Holloway A, et al. Empirical array quality weights in the analysis of microarray data. BMC Bioinformatics. 2006;7.

269. Phipson B, Lee S, Majewski IJ, Alexander WS, Smyth GK. Robust hyperparameter estimation protects against hypervariable genes and improves power to detect differential expression. Annals of Applied Statistics. 2016;10(2):946-63.

270. Wu D, Smyth GK. Camera: A competitive gene set test accounting for inter-gene correlation. Nucleic Acids Res. 2012;40(17).

271. Chaussabel D, Quinn C, Shen J, Patel P, Glaser C, Baldwin N, et al. A Modular

Analysis Framework for Blood Genomics Studies: Application to Systemic Lupus Erythematosus. Immunity. 2008;29(1):150-64.

272. Chaussabel D, Baldwin N. Democratizing systems immunology with modular transcriptional repertoire analyses. Nature Reviews Immunology. 2014;14(4):271-80.

273. Barbie DA, Tamayo P, Boehm JS, Kim SY, Moody SE, Dunn IF, et al. Systematic RNA interference reveals that oncogenic KRAS-driven cancers require TBK1. Nature. 2009;462(7269):108-12.

274. Hänzelmann S, Castelo R, Guinney J. GSVA: Gene set variation analysis for microarray and RNA-Seq data. BMC Bioinformatics. 2013;14.

275. Hendry S, Salgado R, Gevaert T, Russell PA, John T, Thapa B, et al. Assessing Tumor-infiltrating Lymphocytes in Solid Tumors: A Practical Review for Pathologists and Proposal for a Standardized Method from the International Immunooncology Biomarkers Working Group: Part 1: Assessing the Host Immune Response, TILs in Invasive Breast Carcinoma and Ductal Carcinoma in Situ, Metastatic Tumor Deposits and Areas for Further Research. Adv Anat Pathol. 2017;24(5):235-51.

276. Hwang SY, Hertzog PJ, Holland KA, Sumarsono SH, Tymms MJ, Hamilton JA, et al. A null mutation in the gene encoding a type I interferon receptor component eliminates antiproliferative and antiviral responses to interferons alpha and beta and alters macrophage responses. Proc Natl Acad Sci U S A. 1995;92(24):11284-8.

277. Anguille S, Lion E, Willemen Y, Van Tendeloo VF, Berneman ZN, Smits EL. Interferon-alpha in acute myeloid leukemia: an old drug revisited. Leukemia. 2011;25(5):739-48.

278. Platanias LC. Interferons and their antitumor properties. J Interferon Cytokine Res. 2013;33(4):143-4.

279. Stein BL, Tiu RV. Biological rationale and clinical use of interferon in the classical BCR-ABL-negative myeloproliferative neoplasms. J Interferon Cytokine Res. 2013;33(4):145-53.

280. Akman T, Oztop I, Unek IT, Koca D, Unal OU, Salman T, et al. Long-term outcomes and prognostic factors of high-risk malignant melanoma patients after surgery and adjuvant high-dose interferon treatment: a single-center experience. Chemotherapy. 2014;60(4):228-38.

281. Ascierto PA, Chiarion-Sileni V, Muggiano A, Mandala M, Pimpinelli N, Del Vecchio M, et al. Interferon alpha for the adjuvant treatment of melanoma: review of international literature and practical recommendations from an expert panel on the use of interferon. J Chemother. 2014;26(4):193-201.

282. Mocellin S, Pasquali S, Rossi CR, Nitti D. Interferon alpha adjuvant therapy in patients with high-risk melanoma: a systematic review and meta-analysis. J Natl Cancer Inst. 2010;102(7):493-501.

283. Pasquali S, Mocellin S. The anticancer face of interferon alpha (IFN-alpha): from biology to clinical results, with a focus on melanoma. Curr Med Chem. 2010;17(29):3327-36.

284. De Lustig ES, Cortade de De La Pena N, Canonico A. Interferon in breast cancer. Tumori. 1977;63(2):155-62.

285. Critchley-Thorne RJ, Simons DL, Yan N, Miyahira AK, Dirbas FM, Johnson DL, et al. Impaired interferon signaling is a common immune defect in human cancer. Proc Natl Acad Sci U S A. 2009;106(22):9010-5.

286. Howlander N, Noone AM, Krapcho M, Miller D, Bishop JS, Kosary CL, et al. SEER Cancer Statistics Review, 1975-2014. Bethesda, MD: National Cancer Institute; 2017 April 2017.

287. Moorman PG, Calingaert B, Palmieri RT, Iversen ES, Bentley RC, Halabi S, et al. Hormonal risk factors for ovarian cancer in premenopausal and postmenopausal women. Am J Epidemiol. 2008;167(9):1059-69.

288. Tabassum R, Nath A, Preininger M, Gibson G. Geographical, environmental and pathophysiological influences on the human blood transcriptome. Current genetic medicine reports. 2013;1(4):203-11.

289. Whitney AR, Diehn M, Popper SJ, Alizadeh AA, Boldrick JC, Relman DA, et al. Individuality and variation in gene expression patterns in human blood. Proc Natl Acad Sci U S A. 2003;100(4):1896-901.

290. Cheung VG, Conlin LK, Weber TM, Arcaro M, Jen KY, Morley M, et al. Natural variation in human gene expression assessed in lymphoblastoid cells. Nat Genet. 2003;33(3):422-5.

291. Lloyd-Jones LR, Holloway A, McRae A, Yang J, Small K, Zhao J, et al. The Genetic Architecture of Gene Expression in Peripheral Blood. Am J Hum Genet. 2017;100(2):371.

292. Zhang W, Duan S, Kistner EO, Bleibel WK, Huang RS, Clark TA, et al. Evaluation of genetic variation contributing to differences in gene expression between populations. Am J Hum Genet. 2008;82(3):631-40.

293. Dimas AS, Deutsch S, Stranger BE, Montgomery SB, Borel C, Attar-Cohen H, et al. Common regulatory variation impacts gene expression in a cell type-dependent manner. Science. 2009;325(5945):1246-50.

294. Nica AC, Parts L, Glass D, Nisbet J, Barrett A, Sekowska M, et al. The architecture of gene regulatory variation across multiple human tissues: the MuTHER study. PLoS genetics. 2011;7(2):e1002003.

295. Price AL, Helgason A, Thorleifsson G, McCarroll SA, Kong A, Stefansson K. Single-tissue and cross-tissue heritability of gene expression via identity-by-descent in related or unrelated individuals. PLoS genetics. 2011;7(2):e1001317.

296. Gruber I, Landenberger N, Staebler A, Hahn M, Wallwiener D, Fehm T. Relationship between circulating tumor cells and peripheral T-cells in patients with primary breast cancer. Anticancer Res. 2013;33(5):2233-8.

297. Stone ML, Chiappinelli KB, Li H, Murphy LM, Travers ME, Topper MJ, et al. Epigenetic therapy activates type I interferon signaling in murine ovarian cancer to reduce immunosuppression and tumor burden. Proc Natl Acad Sci U S A. 2017;114(51):E10981-e90.

298. Ishikawa S, Miyashita T, Inokuchi M, Hayashi H, Oyama K, Tajima H, et al. Platelets surrounding primary tumor cells are related to chemoresistance. Oncol Rep. 2016;36(2):787-94.

299. Peinado H, Zhang H, Matei IR, Costa-Silva B, Hoshino A, Rodrigues G, et al. Pre-metastatic niches: organ-specific homes for metastases. Nat Rev Cancer. 2017;17(5):302-17.

300. Stone RL, Nick AM, McNeish IA, Balkwill F, Han HD, Bottsford-Miller J, et al. Paraneoplastic thrombocytosis in ovarian cancer. N Engl J Med. 2012;366(7):610-8.

301. Orellana R, Kato S, Erices R, Bravo ML, Gonzalez P, Oliva B, et al. Platelets enhance tissue factor protein and metastasis initiating cell markers, and act as chemoattractants increasing the migration of ovarian cancer cells. BMC Cancer. 2015;15:290.

302. Buck MD, Sowell RT, Kaech SM, Pearce EL. Metabolic Instruction of Immunity. Cell. 2017;169(4):570-86.

303. Taylor CT, Colgan SP. Regulation of immunity and inflammation by hypoxia in immunological niches. Nat Rev Immunol. 2017;17(12):774-85.

304. Wu D, Sanin DE, Everts B, Chen Q, Qiu J, Buck MD, et al. Type 1 Interferons Induce Changes in Core Metabolism that Are Critical for Immune Function. Immunity. 2016;44(6):1325-36.

305. Matys V, Kel-Margoulis OV, Fricke E, Liebich I, Land S, Barre-Dirrie A, et al. TRANSFAC and its module TRANSCompel: transcriptional gene regulation in eukaryotes. Nucleic Acids Res. 2006;34(Database issue):D108-10.

306. Slaney CY, Rautela J, Parker BS. The emerging role of immunosurveillance in dictating metastatic spread in breast cancer. Cancer Res. 2013;73(19):5852-7.

307. Hartman LL, Crawford JR, Makale MT, Milburn M, Joshi S, Salazar AM, et al.

Pediatric phase II trials of poly-ICLC in the management of newly diagnosed and recurrent brain tumors. J Pediatr Hematol Oncol. 2014;36(6):451-7.

308. Reuben A, Spencer CN, Prieto PA, Gopalakrishnan V, Reddy SM, Miller JP, et al. Genomic and immune heterogeneity are associated with differential responses to therapy in melanoma. NPJ genomic medicine. 2017;2.

309. Salgado R, Moore H, Martens JWM, Lively T, Malik S, McDermott U, et al. Steps forward for cancer precision medicine. Nature reviews Drug discovery. 2018;17(1):1-2.

310. Jeong E, Moon SU, Song M, Yoon S. Transcriptome modeling and phenotypic assays for cancer precision medicine. Arch Pharm Res. 2017;40(8):906-14.

311. Stifter SA, Matthews AY, Mangan NE, Fung KY, Drew A, Tate MD, et al. Defining the distinct, intrinsic properties of the novel type I interferon, epsilon. J Biol Chem. 2017.

312. Sistigu A, Yamazaki T, Vacchelli E, Chaba K, Enot DP, Adam J, et al. Cancer cell-autonomous contribution of type I interferon signaling to the efficacy of chemotherapy. Nat Med. 2014;20(11):1301-9.

Appendix I - PRIMER SEQUENCES

Mouse

Isg15	F	TGAGAGCAAGCAGCCAGAAG
Isg15	R	ACGGACACCAGGAAATCGTT
Cxcl10	F	CTGAATCCGGAATCTAAGACCA
Cxcl10	R	GAGGCTCTCTGCTGTCCATC
Ifit1	F	TCAAGGCAGGTTTCTGAGGA
Ifit1	R	ACCTGGTCACCATCAGCATT
Cdc20	F	GTCACTCCGCTCGAGTAAGC
Cdc20	R	GCCCACATACTTCCTGGCTA
Tap1	F	CGCAACATATGGCTCATGTC
Tap1	R	GCCCGAAACACCTCTCTGT
Ccne1	F	CCTCCAAAGTTGCACCAGTT
Ccne1	R	AGAGGGCTTAGACGCCACTT
Bcl2	F	CCGGGAGAACAGGGTATGATAA
Bcl2	R	CCCACTCGTAGCCCCTCTG
Caspase1	F	ACGCCATGGCTGACAAGATCCTG
Caspase1	R	GGTCCCGTGCCTTGTCCATAGC
Gapdh	F	CATGGCCTTCCGTGTTCCTA
Gapdh	R	GCGGCACGTCAGATCCA
Cd274	F	CTGCAACACATCCTCCACAG
Cd274	R	AACGCCACATTTCTCCACAT

Human

I8S	F	GTAACCCGTTGAACCCCATT
I8S	R	CCATCCAATCGGTAGTAGCG

CXCL10	F	TTCCTGCAAGCCATTTTGT
CXCL10	R	TTCTTGATGGCCTTCGATTC
ISG15	F	GCGAACTCATCTTTGCCAGT
ISG15	R	AGCATCTTCACCGTCAGGTC
IFIT1	F	AGCTTACACCATTGGCTGCT
IFIT1	R	CCATTTGTACTCATGGTTGCTGT

18 May 2017

Quality Report – Reference Quotation – Breast Cancer

Dear Zoe Marks

The following quality report details methodologies used for your project.

Samples received from client: March 2017

Number of samples received: 95 total RNA samples

Microarray requested: Human Gene Expression v3 – 8 x 60K: 072363

Label Protocol:

- Cyanine-3 (Cy3) labelled cRNA was prepared from 0.1ug total RNA using the One-Color Low input Quick Amp labelling Kit (Agilent) according to the manufacturer's instructions, followed by RNeasy column purification (Qiagen). Dye incorporation and cRNA yield were checked with the NanoDrop ND-1000 Spectrophotometer.

Hybridisation Protocol:

- 600ng of Cy3 labeled cRNA (specific activity > 6 pmol Cy3/ug cRNA) was fragmented at 60ºC for 30 minutes in a reaction volume of 25ul containing 1x Agilent fragmentation buffer and 2x Agilent blocking agent following the manufacturer's instructions. On completion 25ul of 2x Agilent gene expression hybridisation buffer was added and 42ul of sample hybridised for 17 hours at 65oC in a rotating Agilent hybridisation oven. After hybridisation, microarrays were washed 1 minute at room temperature with GE wash buffer 1(Agilent) and 1 minute with 37oC GE wash buffer 2(Agilent).

Scan Protocol:

- Slides were scanned immediately after washing on the Agilent C, DNA microarray scanner using one color scan settings for 8x60k array slides; scan area 61x21.6mm, scan resolution 3um, dye channel is set to Green and 20 bit Tiff.

Data Processing:

- The scanned images were analysed with Feature Extraction Software 11.0.1.1 (Agilent) using default parameters (protocol GE1-1100_Jul11 and Grid: (072363_D_F_20150612) to obtain background subtracted and spatially detrended Processed Signal intensities.

	Sample Name	Group	Feature Extracted files
1	04.002.0006 04/7673MH	1	257236314222_201703240945_SO1_GE1_1100_Jul11_1_1.txt
2	04.002.0007 04/7438JK	1	257236314212_201703240957_SO1_GE1_1100_Jul11_1_2.txt
3	04.002.0008 04/7496DE	1	257236314213_201703241009_SO1_GE1_1100_Jul11_1_3.txt
4	06.007.0495 06/8835JO	2	257236314212_201703240957_SO1_GE1_1100_Jul11_1_3.txt
5	06.007.0499 06/8882JM	2	257236314213_201703241009_SO1_GE1_1100_Jul11_1_4.txt
6	06.007.0503 06/8886KL	2	257236314222_201703240945_SO1_GE1_1100_Jul11_2_1.txt
8	06.004.0304 06/9829SW	4	257236314213_201703241009_SO1_GE1_1100_Jul11_1_2.txt
9	06.004.0305 07/10732JM	4	257236314222_201703240945_SO1_GE1_1100_Jul11_1_3.txt
10	06.004.0256 06/9751LF	4	257236314212_201703240957_SO1_GE1_1100_Jul11_2_1.txt
11	06.002.0246 06/9388ES	5	257236314222_201703240945_SO1_GE1_1100_Jul11_2_3.txt
12	06.002.0250 06/9437WR	5	257236314212_201703240957_SO1_GE1_1100_Jul11_2_4.txt
13	06.002.0146 06/9099ST	5	257236314213_201703241009_SO1_GE1_1100_Jul11_2_1.txt
14	99.005.0159 14/13837RW	6	257236314212_201703240957_SO1_GE1_1100_Jul11_2_2.txt
15	99.005.1222 09/11951AG	6	257236314222_201703240945_SO1_GE1_1100_Jul11_1_4.txt
16	99.0060258 98/1056KM	7	257236314213_201703241009_SO1_GE1_1100_Jul11_2_2.txt
17	99.006.0269 04/7007TW	7	257236314222_201703240945_SO1_GE1_1100_Jul11_2_2.txt
18	99.006.0263 98/770MM	7	257236314212_201703240957_SO1_GE1_1100_Jul11_1_4.txt
19	01.008.0343 01/3781JC	8	257236314222_201703240945_SO1_GE1_1100_Jul11_2_4.txt
20	07.0080002 07/10362EM	8	257236314213_201703241009_SO1_GE1_1100_Jul11_1_1.txt
21	01.008.0344 01/3868HB	8	257236314212_201703240957_SO1_GE1_1100_Jul11_2_3.txt
23	03.010.0437 03/6762BM	9	257236314213_201703241009_SO1_GE1_1100_Jul11_2_3.txt
24	04.010.0289 04/7405AM	9	257236314222_201703240945_SO1_GE1_1100_Jul11_1_2.txt
7	99.002.0594 98/668PF	18	257236314212_201703240957_SO1_GE1_1100_Jul11_1_1.txt
22	99.002.0586 98/602AF	18	257236314213_201703241009_SO1_GE1_1100_Jul11_2_4.txt
25	06.006.0910 07/10062LR	10	257236314223_201704060841_SO1_GE1_1100_Jul11_1_1.txt
26	00.006.0968 07/10125DR	10	257236314217_201704060854_SO1_GE1_1100_Jul11_1_2.txt
27	06.006.0788 06/9916JL	10	257236314218_201704060906_SO1_GE1_1100_Jul11_1_3.txt
28	01.007.0501 01/4467JM	11	257236314223_201704060841_SO1_GE1_1100_Jul11_2_2.txt
30	01.007.0480 02/4628AM	11	257236314217_201704060854_SO1_GE1_1100_Jul11_2_3.txt
29	01.007.0475 01/4359DB	11	257236314218_201704060906_SO1_GE1_1100_Jul11_2_4.txt
32	00.003.1364 00/2584DM	13	257236314217_201704060854_SO1_GE1_1100_Jul11_1_3.txt
33	00.003.1353 00/2787FM	13	257236314218_201704060906_SO1_GE1_1100_Jul11_1_4.txt
34	00.003.1365 00/2616JH	13	257236314223_201704060841_SO1_GE1_1100_Jul11_2_1.txt
35	08.007.0168 14/13744HC	14	257236314217_201704060854_SO1_GE1_1100_Jul11_2_4.txt
36	09.007.0181 10/12174WC	14	257236314218_201704060906_SO1_GE1_1100_Jul11_2_2.txt
37	09.007.0179 10/12082AC	14	257236314223_201704060841_SO1_GE1_1100_Jul11_1_3.txt
38	01.009.0443 01/4337SC	15	257236314218_201704060906_SO1_GE1_1100_Jul11_1_2.txt
39	01.009.0457 02/4850KF	15	257236314223_201704060841_SO1_GE1_1100_Jul11_2_4.txt
40	01.009.0442 01/4229CK	15	257236314217_201704060854_SO1_GE1_1100_Jul11_1_1.txt
41	03.007.0429 03/6065MS	16	257236314218_201704060906_SO1_GE1_1100_Jul11_2_1.txt
42	03.007.0436 03/6189BG	16	257236314223_201704060841_SO1_GE1_1100_Jul11_1_2.txt
43	03.007.0435 03/6213JN	16	257236314217_201704060854_SO1_GE1_1100_Jul11_2_2.txt
31	04.004.0534 05/8019VK	17	257236314223_201704060841_SO1_GE1_1100_Jul11_1_4.txt
44	04.004.0533 05/7995JB	17	257236314217_201704060854_SO1_GE1_1100_Jul11_2_1.txt
45	04.004.0532 05/7957SJ	17	257236314218_201704060906_SO1_GE1_1100_Jul11_2_3.txt
46	00.005.0458 00/2687SS	19	257236314217_201704060854_SO1_GE1_1100_Jul11_1_4.txt
47	00.005.0464 00/2688CW	19	257236314218_201704060906_SO1_GE1_1100_Jul11_1_1.txt
48	00.005.0463 00/2646MP	19	257236314223_201704060841_SO1_GE1_1100_Jul11_2_3.txt

	Sample Name	Group	Feature Extracted files
49	06.003.02248 06/9131BR	12	257236314182_201704211102_SO1_GE1_1100_Jul11_1_2.txt
50	06.003.0237 06/9005LN	12	257236314192_201704211038_SO1_GE1_1100_Jul11_2_1.txt
51	02.006.0675 02/5115JE	20	257236314182_201704211102_SO1_GE1_1100_Jul11_1_3.txt
52	02.006.0643 02/5116JL	20	257236314192_201704211038_SO1_GE1_1100_Jul11_1_1.txt
53	02.006.0639 02/5114KA	20	257236314183_201704211050_SO1_GE1_1100_Jul11_2_3.txt
54	03.006.0785 03/6564JF	21	257236314192_201704211038_SO1_GE1_1100_Jul11_1_2.txt
55	03.006.0758 03/6711WG	21	257236314183_201704211050_SO1_GE1_1100_Jul11_2_1.txt
56	03.006.0750 03/6253HC	21	257236314182_201704211102_SO1_GE1_1100_Jul11_2_2.txt
57	01.006.0977 01/4426IW	22	257236314183_201704211050_SO1_GE1_1100_Jul11_1_3.txt
58	01.006.1012 01/4396AL	22	257236314182_201704211102_SO1_GE1_1100_Jul11_1_1.txt
59	01.006.0985 02/4641SD	22	257236314192_201704211038_SO1_GE1_1100_Jul11_1_3.txt
60	10.007.0342 10/12357IM	23	257236314183_201704211050_SO1_GE1_1100_Jul11_2_2.txt
61	10.007.0345 10/12439HU	23	257236314192_201704211038_SO1_GE1_1100_Jul11_2_4.txt
62	00.002.0703 00/3402AU	24	257236314182_201704211102_SO1_GE1_1100_Jul11_2_1.txt *
63	01.002.0184 06/9322AI	24	257236314183_201704211050_SO1_GE1_1100_Jul11_1_4.txt
64	00.002.0723 01/3497MI	24	257236314192_201704211038_SO1_GE1_1100_Jul11_2_2.txt
65	02.009.0691 02/5606JW	25	257236314192_201704211038_SO1_GE1_1100_Jul11_2_3.txt
66	02.009.0692 02/5639MA	25	257236314183_201704211050_SO1_GE1_1100_Jul11_1_1.txt
67	02.009.0685 02/5707GP	25	257236314182_201704211102_SO1_GE1_1100_Jul11_1_4.txt
68	03.005.1077 04/7679PH	26	257236314183_201704211050_SO1_GE1_1100_Jul11_2_4.txt
69	03.005.1094 047735DC	26	257236314182_201704211102_SO1_GE1_1100_Jul11_2_3.txt
70	99.004.1017 05/7993CK	27	257236314192_201704211038_SO1_GE1_1100_Jul11_1_4.txt
71	99.004.1015 06/9410LM	27	257236314182_201704211102_SO1_GE1_1100_Jul11_2_4.txt
72	99.004.0976 98/104IA	27	257236314183_201704211050_SO1_GE1_1100_Jul11_1_2.txt *
73	01.888.1253 07/10706EA	28	257236316809_201705180952_SO1_GE1_1100_Jul11_1_1.txt
74	01.888.1250 07/10678 BO	28	257236316808_201705181005_SO1_GE1_1100_Jul11_2_2.txt *
75	04.006.1087 04/7797LM	29	257236316807_201705181017_SO1_GE1_1100_Jul11_1_2.txt
76	04.006.1098 10/12233KW	29	257236316809_201705180952_SO1_GE1_1100_Jul11_2_1.txt
77	04.006.1094 04/7732CW	29	257236316808_201705181005_SO1_GE1_1100_Jul11_1_4.txt
78	10.007.0149 10/12435SM	30	257236316809_201705180952_SO1_GE1_1100_Jul11_1_3.txt
79	05.007.0443 06/8870AS	30	257236316808_201705181005_SO1_GE1_1100_Jul11_1_1.txt
80	05.007.0434 06/8806NM	30	257236316807_201705181017_SO1_GE1_1100_Jul11_1_3.txt
81	99.008.0968 99/1671RP	31	257236316808_201705181005_SO1_GE1_1100_Jul11_1_2.txt
82	99.008.0976 08/11516LP	31	257236316807_201705181017_SO1_GE1_1100_Jul11_1_4.txt
83	02.005.1303 04/7490DP	32	257236316808_201705181005_SO1_GE1_1100_Jul11_2_1.txt
84	04.005.0421 04/7510FP	32	257236316807_201705181017_SO1_GE1_1100_Jul11_2_2.txt
85	02.005.1301 04/7368DO	32	257236316809_201705180952_SO1_GE1_1100_Jul11_1_2.txt
86	99.005.2064 99/1980LA	33	257236316807_201705181017_SO1_GE1_1100_Jul11_2_3.txt
87	99.005.2069 99/1976VA	33	257236316808_201705181005_SO1_GE1_1100_Jul11_1_3.txt
88	99.005.2099 99/2019LV	33	257236316809_201705180952_SO1_GE1_1100_Jul11_1_4.txt
89	15.007.129 15/14048VP	34	257236316809_201705180952_SO1_GE1_1100_Jul11_2_2.txt
90	15.007.115 15/14024AS	34	257236316807_201705181017_SO1_GE1_1100_Jul11_1_1.txt
91	00.008.0068 00/2822DR	35	257236316808_201705181005_SO1_GE1_1100_Jul11_2_3.txt
92	00.008.0067 00/3010JL	35	257236316809_201705180952_SO1_GE1_1100_Jul11_2_4.txt
93	00.008.0071 00/2448FL	35	257236316807_201705181017_SO1_GE1_1100_Jul11_2_1.txt
94	99.005.0290 04/14126MA	36	257236316807_201705181017_SO1_GE1_1100_Jul11_2_4.txt
95	99.005.0243 04/7212HH	36	257236316808_201705181005_SO1_GE1_1100_Jul11_2_4.txt
96	99.004.0976 98/104IA	27repeat	257236316809_201705180952_SO1_GE1_1100_Jul11_2_3.txt

***** QC metrics detected issues with these 3 samples.

Yours Sincerely

Ms Jodee Gould
Microarray Manager
Next Generation Sequencing Specialist
MHTP Medical Genomics Facility

Appendix III – Differentially Probe/Gene List From Chapter 3

Supplementary Table 1. Probes up in 'Primary' v 'Unaffected'

ProbeName	GENE_SYMBOL	Avg. log2 exp.	log2 FC	p.value	adjusted.p.value	GeneSets.Modules
A_23_P329261	KCNJ2	5.22	1.07	1.37E-05	0.006703865	M7.16_Not.Determined
A_22_P00024322	lnc-GBP6-1	6.60	0.65	4.71E-04	0.037246084	NA
A_23_P62890	GBP1	7.88	0.69	6.15E-04	0.042276045	M3.4_Interferon
A_24_P303091	CXCL10	5.09	1.31	3.37E-04	0.031967627	M1.2_Interferon
A_23_P105144	SCUBE2	4.14	0.46	1.34E-04	0.021010396	NA
A_33_P3343175	CXCL10	5.17	1.09	4.81E-04	0.037639737	M1.2_Interferon
A_33_P3310864		4.43	0.32	2.97E-04	0.030214105	NA
A_23_P374322	LACC1	4.64	0.45	3.88E-04	0.034025543	NA
A_19_P00320729	CDYL2	9.47	0.38	3.55E-04	0.03265178	NA
A_23_P74928	MR1	7.78	0.28	4.66E-04	0.037232052	M8.2_Not.Determined
A_33_P3286789		4.36	0.40	7.74E-06	0.005374337	NA
A_32_P44453	INPP1	6.61	0.37	4.14E-04	0.035419346	M8.45_Undetermined
A_32_P138004	FAM45A	10.62	0.27	2.42E-04	0.027608238	M7.1_Inflammation
A_23_P97795	ACBD5	10.21	0.29	7.67E-04	0.046792473	M8.37_Undetermined
A_21_P0000015	PARP9	9.83	0.50	7.44E-04	0.046141468	M3.4_Interferon
A_22_P00020739		4.56	0.34	2.49E-04	0.02784477	NA
A_24_P98555	FAM45A	7.97	0.27	6.71E-04	0.043937034	M7.1_Inflammation
A_23_P138680	IL15RA	8.88	0.46	6.66E-04	0.04390981	M9.23_Undetermined
A_21_P0008516	lnc-SIPA1L1-1	4.07	0.50	6.06E-04	0.04196584	NA
A_33_P3338071		4.80	0.55	4.46E-05	0.011787934	NA
A_23_P371865	CDYL2	6.66	0.40	4.86E-05	0.012138801	NA
A_33_P3332215	MUC1	4.26	0.28	2.92E-04	0.030056343	M7.29_Not.Determined
A_24_P287691	AP3S2	10.02	0.37	4.59E-04	0.037001062	NA

A_33_P3411628	CDKN2A	5.57	0.43	4.18E-04	0.035509032	NA
A_21_P0011804	LOC100507006	6.23	0.76	5.02E-04	0.03855304	NA
A_24_P40626	GREM2	6.15	1.01	1.92E-05	0.007842799	NA
A_23_P137856	MUC1	6.88	0.51	7.96E-04	0.04755026	M7.29_Not.Determined
A_24_P42681	PSMD2	10.04	0.23	4.32E-04	0.035909384	M6.17_Not.Determined
A_33_P3734384	lnc-MYO1G-1	8.69	0.43	5.91E-04	0.041641944	NA

Supplementary Table 2. Probes down in 'Primary' v 'Unaffected'

ProbeName	GENE_SYMBOL	Avg. log2 exp.	log2 FC	p.value	adjusted.p.value	GeneSets.Modules
A_23_P392470	NR3C2	7.11	-0.62	7.84E-04	0.047129627	M7.12_Undetermined
A_21_P0003889	FLJ36777	5.92	-0.24	5.38E-04	0.039927058	NA
A_33_P3262376	OTUD7A	6.96	-0.56	5.75E-04	0.04133617	NA
A_23_P170679	COL4A3	4.77	-0.66	1.54E-04	0.022495222	M9.6_Undetermined
A_23_P24922	LIPT2	8.21	-0.52	5.92E-04	0.041641944	M9.9_Undetermined
A_22_P00005659	LOC101060038	8.00	-1.11	3.67E-07	0.002123715	NA
A_33_P3227400	COL4A4	6.86	-0.85	1.55E-04	0.022509114	M9.32_Undetermined
A_21_P0007822	lnc-EIF2S3L.1-2	6.63	-0.86	2.52E-04	0.027889246	NA
A_33_P3294583	LOC256880	5.00	-0.46	1.12E-04	0.019191864	NA
A_23_P30163	KLF3-AS1	6.31	-0.59	4.40E-04	0.036162723	NA
A_33_P3715843	MGC40069	5.52	-0.60	3.42E-04	0.032169999	NA
A_33_P3272563	NMT2	8.10	-0.47	4.12E-04	0.035419346	M4.15_T.cells
A_33_P3311971		7.25	-0.49	5.63E-04	0.041061307	NA
A_32_P324933	LINC00282	5.29	-0.83	7.97E-04	0.04755026	NA
A_23_P204751	ASIC1	5.91	-0.81	2.07E-04	0.025822209	M9.11_Undetermined
A_33_P3391796	NOG	7.55	-1.16	3.09E-05	0.00994877	M8.25_Undetermined
A_33_P3387106		4.09	-0.32	4.20E-04	0.03557475	NA
A_21_P0006502	lnc-ZC3H12B-2	10.57	-0.53	2.03E-04	0.025604539	NA
A_33_P3423721	JPH3	15.05	-0.52	5.39E-04	0.039978773	NA
A_23_P21495	FCGBP	9.57	-1.11	7.85E-07	0.002428258	M7.12_Undetermined
A_33_P3377239	LOC100270804	8.06	-0.42	4.56E-04	0.036809485	NA
A_33_P3329737		8.32	-0.55	5.02E-04	0.03855304	NA
A_21_P0006057		5.07	-0.78	2.03E-05	0.007912019	NA
A_22_P00013078	LINC01089	8.65	-0.40	7.09E-04	0.045198427	M5.11_Not.Determined|M9.19_Undetermined
A_21_P0000208	SNORD22	10.37	-0.34	5.13E-04	0.038911264	NA
A_33_P3329356	lnc-HADH-1	6.64	-0.93	9.89E-06	0.006042892	NA
A_33_P3346972		7.00	-0.51	8.74E-05	0.016935314	NA
A_24_P9090	HNRNPDL	11.11	-0.37	7.65E-05	0.015714455	M5.8_Not.Determined|M6.9_Not.Determined
A_33_P3306948	LRP6	6.25	-0.69	4.97E-04	0.038361321	NA
A_22_P00014395	LOC102723346	5.07	-0.51	3.49E-04	0.032411077	NA
A_23_P151059	FAM90A1	5.92	-0.63	2.52E-06	0.003939264	NA
A_23_P212511	TTC14	10.09	-0.28	7.23E-04	0.045598798	M9.7_Undetermined
A_21_P0010094	lnc-ARFGEF2-2	5.62	-0.24	7.11E-04	0.045198427	NA
A_22_P00022504	KRT73-AS1	4.25	-0.69	3.67E-05	0.010858652	NA
A_23_P211244	PRMT2	9.28	-0.44	5.85E-04	0.041641944	M7.18_Undetermined|M9.17_Undetermined
A_23_P153676	TLE2	8.78	-0.55	4.70E-04	0.037246084	NA
A_21_P0002980	LOC100506990	7.30	-0.39	8.14E-04	0.048163559	NA
A_21_P0005923	LOC100506990	7.06	-0.43	2.40E-04	0.027601504	NA
A_33_P3253792	CXorf67	5.87	-0.51	7.81E-04	0.04707844	NA
A_33_P3883985	LMF1	10.08	-0.94	4.50E-05	0.011787967	NA
A_22_P00000215	PIK3IP1-AS1	10.44	-0.60	7.38E-05	0.015368244	NA
A_23_P133543	KLHL3	8.82	-0.48	5.43E-04	0.040136182	M4.1_T.cell
A_23_P209360	KLHL29	7.23	-0.85	3.13E-06	0.004301154	NA
A_33_P3316313	MTERF4	9.82	-0.33	6.89E-04	0.0445019	NA

A_22_P00006901	SCARNA10	10.66	-0.45	2.44E-04	0.027719634	NA
A_22_P00025447	PIK3IP1-AS1	6.65	-0.54	3.59E-05	0.010796968	NA
A_23_P254978	TATDN1	7.80	-0.26	4.02E-04	0.03491255	M5.5_Not.Determined
A_33_P3273490		6.42	-0.45	5.81E-04	0.041395106	NA
A_23_P163161	SDR39U1	11.31	-0.23	5.41E-04	0.040040156	M9.11_Undetermined
A_33_P3319987	SCML4	7.11	-0.54	5.12E-04	0.038911264	M9.25_Undetermined
A_21_P0000451	SNORD116-27	6.01	-0.47	2.68E-04	0.028461171	NA
A_21_P0006503	ZC3H12B	5.69	-0.44	5.65E-04	0.041087337	M9.11_Undetermined
A_33_P3307253	AK5	6.27	-0.75	6.04E-04	0.041964446	M9.11_Undetermined
A_23_P120281	EDAR	5.02	-0.71	1.25E-04	0.020137974	M4.1_T.cell
A_21_P0012654	LOC101928803	9.76	-0.46	4.53E-04	0.036666132	NA
A_33_P3422289	lnc-TMED5-1	11.29	-0.45	4.29E-04	0.035872788	NA
A_32_P208823	PLXDC1	6.88	-0.55	2.50E-04	0.02784477	M9.5_Undetermined
A_22_P00000386	KLF3-AS1	5.59	-0.47	7.37E-04	0.045981674	NA
A_23_P34546	SDCCAG8	7.82	-0.33	2.59E-04	0.028169994	M9.17_Undetermined
A_33_P3261408	TMIE	5.37	-0.63	1.56E-04	0.022642288	NA
A_33_P3385842	CCDC7	9.38	-0.37	5.05E-04	0.038669168	NA
A_21_P0000882	RNF157-AS1	5.70	-0.79	1.08E-04	0.018740165	NA
A_33_P3388618	TNK1	7.82	-0.52	6.01E-04	0.041787724	NA
A_21_P0005656	LOC100506990	7.57	-0.42	7.27E-04	0.045694403	NA
A_22_P00001320	ANTXRL	15.56	-0.27	5.11E-04	0.038911264	NA
A_21_P0005794	lnc-PRAGMIN.1-3	7.39	-0.42	6.52E-04	0.043474196	NA
A_21_P0013168	XLOC_l2_013267	6.15	-0.57	3.15E-04	0.030888204	NA
A_21_P0000454	SNORD116-29	5.10	-0.40	3.75E-04	0.033412059	NA
A_22_P00007532	lnc-HADH-1	6.04	-0.71	1.35E-05	0.006663874	NA
A_33_P3415888	TEPP	5.06	-0.62	3.27E-05	0.010368477	NA
A_21_P0012368	XLOC_l2_009639	7.12	-0.58	4.40E-04	0.036162723	NA
A_22_P00005927	ACTN1-AS1	5.42	-0.51	1.73E-04	0.023561031	NA
A_33_P3308512	SLC16A10	6.00	-0.59	3.62E-04	0.032924428	M4.1_T.cell
A_33_P3589722	ATM	10.49	-0.34	2.50E-04	0.02784477	NA
A_23_P34375	TCEA3	8.50	-0.66	5.15E-04	0.038912744	M4.1_T.cell
A_22_P00008745	TRAF3IP2-AS1	7.39	-0.65	2.00E-04	0.025393065	NA
A_21_P0010595	FBXO25	10.26	-0.28	5.77E-04	0.04133617	NA
A_21_P0000893	IQCH-AS1	6.41	-0.59	7.99E-04	0.047607064	NA
A_32_P170925	TXNRD3	4.58	-0.44	8.17E-04	0.048243011	NA
A_33_P3312466	BTNL9	4.77	-0.60	2.10E-04	0.025894909	NA
A_22_P00024240	lnc-FPGS-1	8.22	-0.52	1.21E-04	0.019955581	NA
A_33_P3324814	SATB1-AS1	9.84	-0.63	2.69E-04	0.028461171	NA
A_22_P00007531	LEF1-AS1	8.21	-0.87	3.76E-05	0.010880565	M9.5_Undetermined
A_33_P3212630	FAM90A1	4.50	-0.31	3.47E-04	0.032376572	NA
A_23_P259741	SATB1	12.51	-0.38	5.22E-04	0.039113257	M9.6_Undetermined
A_22_P00016257	lnc-TMED5-1	12.08	-0.43	6.87E-04	0.044477347	NA
A_33_P3424636		6.90	-0.56	1.17E-04	0.019505265	NA
A_21_P0014428	LOC101927372	9.73	-0.47	2.11E-04	0.025894909	NA
A_21_P0000450	SNORD116-26	6.05	-0.43	6.17E-05	0.0139321	NA
A_24_P211565	C1QTNF6	8.33	-0.39	6.31E-04	0.042885639	M9.1_Undetermined|M9.5_Undetermined
A_21_P0014024	SATB1-AS1	8.80	-0.53	4.00E-04	0.034793686	NA
A_21_P0009485	lnc-WDR7-2	4.59	-0.61	7.56E-04	0.0465739	NA
A_23_P8834	EPHX2	9.67	-0.90	1.62E-04	0.022922284	M4.1_T.cell
A_22_P00002610	LMF1	5.89	-0.72	3.43E-05	0.010556801	NA
A_21_P0001480	lnc-C1orf201-2	9.93	-0.61	3.62E-04	0.032924428	NA
A_23_P428640	PPP1R3E	8.03	-0.52	4.07E-04	0.035159279	M7.13_Not.Determined
A_23_P306890	POLI	8.44	-0.31	6.81E-04	0.044200216	NA
A_24_P119685	OBSCN	8.26	-0.66	7.57E-04	0.0465739	M9.5_Undetermined
A_23_P91001	ASNSD1	12.08	-0.31	4.69E-04	0.037232052	M6.5_Not.Determined
A_23_P13364	NUCB2	10.99	-0.40	4.55E-05	0.011814108	M5.6_Mitochondrial.Stress/Proteasome
A_21_P0012456	LOC101927056	5.26	-0.36	2.61E-04	0.028222508	NA
A_23_P342709	FBXO15	6.45	-0.58	1.59E-05	0.007282873	NA
A_21_P0003911	lnc-DCTD-1	7.39	-0.58	6.80E-05	0.014815771	NA
A_33_P3321657	HSPG2	7.58	-0.62	2.17E-04	0.026381819	NA
A_33_P3331314		5.37	-0.46	2.74E-04	0.028849847	NA
A_33_P3402646		6.11	-0.39	4.68E-04	0.037232052	NA
A_24_P196592	MMP28	6.93	-0.60	9.91E-07	0.002787148	NA
A_21_P0014339	lnc-AC009113.1-1	6.19	-0.82	5.73E-06	0.004619028	NA
A_24_P169092	MAML2	7.54	-0.51	4.56E-05	0.011814108	NA

A_33_P3313810	CELA1	6.78	-0.85	3.66E-06	0.004304929	M9.9_Undetermined
A_33_P3357591	ATHL1	8.07	-0.49	2.26E-04	0.026848316	M8.44_Undetermined
A_21_P0000891	SDCBP2-AS1	6.40	-0.36	5.68E-05	0.013338946	NA
A_33_P3294459	COPG2IT1	5.29	-0.68	6.51E-04	0.043474196	NA
A_33_P3280801	LMO7	6.57	-0.37	8.42E-04	0.049166483	NA
A_23_P143981	FBLN2	6.10	-0.50	6.86E-04	0.044441637	M9.30_Undetermined
A_33_P3228807	SPEG	5.26	-0.61	1.97E-04	0.025247134	M9.5_Undetermined
A_23_P417282	IGF1R	10.06	-0.65	9.51E-05	0.017548582	M5.14_Not.Determined|M9.34_Undetermined
A_33_P3217495	SLC5A2	6.24	-0.37	6.66E-04	0.04390981	NA
A_33_P3404546	OBSCN	7.15	-0.49	2.00E-04	0.025393065	M9.5_Undetermined
A_24_P273157	OBSCN	7.02	-0.62	1.23E-04	0.020080023	M9.5_Undetermined
A_23_P423457	SERINC5	8.61	-0.38	3.31E-04	0.03181727	NA
A_23_P24433	CTSF	10.92	-0.46	5.78E-04	0.04133617	M9.11_Undetermined
A_24_P678104	STMN3	9.26	-0.47	2.13E-04	0.026137352	M4.1_T.cell|M9.12_Undetermined
A_33_P3299329		6.42	-0.50	6.81E-04	0.044200216	NA
A_22_P00000635	LINC00304	6.27	-0.53	5.98E-04	0.041714788	NA
A_24_P252364	NRCAM	5.31	-1.22	6.41E-06	0.004889364	M9.11_Undetermined
A_21_P0008352	lnc-EXD2-1	6.85	-0.88	4.93E-06	0.00441379	NA
A_32_P183904	SHF	4.42	-0.45	1.95E-04	0.024996864	NA
A_33_P3301514	NRCAM	5.06	-0.62	4.67E-05	0.011942253	M9.11_Undetermined
A_22_P00000382	KRT73-AS1	7.04	-0.84	6.59E-06	0.004986098	NA
A_21_P0013532	XLOC_l2_014098	6.30	-0.32	7.19E-04	0.045416944	NA
A_23_P33984	TMEM27	4.60	-0.33	6.75E-04	0.044072389	NA
A_23_P211212	COL18A1	10.62	-0.95	1.85E-04	0.02446447	M5.14_Not.Determined
A_22_P00000284	lnc-AC009113.1-1	6.40	-0.64	5.93E-06	0.004744485	NA
A_33_P3337485	CD248	5.53	-0.74	1.10E-04	0.018965996	M4.1_T.cell
A_23_P116743	LINC01089	12.40	-0.45	2.08E-04	0.025822209	M5.11_Not.Determined|M9.19_Undetermined
A_33_P3272330	DNMT3A	10.13	-0.46	5.63E-04	0.041061307	M9.3_Undetermined|M9.7_Undetermined
A_23_P64058	RASGRP2	15.05	-0.37	2.78E-04	0.029184293	M6.10_Not.Determined
A_22_P00002090	HULC	4.22	-0.51	1.50E-04	0.022135108	NA
A_33_P3256031		6.89	-0.56	4.46E-04	0.036436529	NA
A_24_P943922	CACHD1	4.09	-0.49	4.05E-04	0.035049568	M9.11_Undetermined
A_21_P0000020	RBM19	10.47	-0.30	7.52E-04	0.046439041	NA

Supplementary Table 3. Probes up in 'Metastasis' v 'Unaffected'

ProbeName	GENE_SYMBOL	Avg. log2 exp.	log2 FC	p.value	adjusted.p.value	GeneSets.Modules
A_23_P47410	ESAM	7.80	0.88	1.27E-06	2.97E-03	M8.39_Undetermined
A_23_P216023	ANGPT1	5.89	0.49	3.73E-04	3.34E-02	M9.31_Undetermined
A_23_P215479	CLIP2	8.66	0.50	1.96E-05	7.84E-03	M6.14_Not.Determined
A_22_P00012038	MTURN	9.66	0.60	2.04E-04	2.57E-02	M1.1_Platelets
A_22_P00025822	LOC100130264	5.96	0.46	2.96E-04	3.02E-02	NA
A_24_P16913	ABCC4	5.87	0.78	1.67E-06	3.35E-03	M8.18_Undetermined
A_23_P43810	LTBP1	6.28	1.03	1.03E-05	6.09E-03	M8.1_Not.Determined
A_24_P82880	TPM4	10.92	0.66	1.61E-05	7.28E-03	NA
A_23_P132285	MPST	11.03	0.39	8.10E-05	1.62E-02	M9.4_Undetermined
A_23_P19624	BMP6	8.49	0.80	1.81E-04	2.42E-02	M1.1_Platelets
A_22_P00014471	lnc-SHANK2-1	5.98	0.60	1.26E-04	2.01E-02	NA
A_33_P3229918	PTCRA	11.89	0.87	1.24E-05	6.52E-03	M8.18_Undetermined
A_22_P00002171	LINC00958	4.79	0.44	1.27E-04	2.03E-02	NA
A_23_P143817	MYLK	9.70	0.77	2.62E-04	2.82E-02	M1.1_Platelets
A_23_P81934	C6orf25	6.99	0.98	1.14E-05	6.24E-03	M8.52_Undetermined
A_23_P137697	SELP	8.09	0.98	6.29E-06	4.84E-03	M1.1_Platelets
A_22_P00003469	lnc-CCDC68-1	7.72	0.64	1.95E-05	7.84E-03	NA
A_23_P29124	GP1BB	14.13	0.93	2.03E-05	7.91E-03	M1.1_Platelets
A_33_P3321025	PLXNA4	4.71	0.52	5.49E-05	1.31E-02	NA
A_22_P00017811		5.34	0.48	5.84E-05	1.35E-02	NA
A_21_P0014150	LOC101928489	4.14	0.59	1.37E-05	6.70E-03	NA
A_24_P160104	TUBA8	11.61	0.71	4.60E-05	1.19E-02	NA
A_24_P277657	GMPR	8.39	0.93	4.41E-06	4.41E-03	M2.3_Erythrocytes
A_19_P00315452	LOC100130938	9.87	0.96	1.29E-06	2.97E-03	NA
A_22_P00011004		5.89	1.15	8.99E-08	8.81E-04	NA
A_24_P151	KCNAB2	9.59	0.40	3.34E-05	1.05E-02	M9.3_Undetermined
A_22_P00017386	lnc-VAMP1-1	6.85	0.43	5.96E-04	4.17E-02	NA
A_21_P0001291	lnc-CYP4A22-2	6.34	0.35	4.03E-04	3.50E-02	NA
A_33_P3417150	P2RY1	5.06	0.71	7.59E-06	5.37E-03	M9.21_Undetermined
A_21_P0009255	lnc-LUC7L3-1	6.86	0.64	3.30E-04	3.18E-02	NA
A_23_P99906	HOMER2	6.52	0.81	2.17E-05	8.10E-03	M1.1_Platelets
A_32_P168349	C6orf25	11.83	1.07	1.87E-05	7.78E-03	M8.52_Undetermined
A_23_P121564	GUCY1B3	6.43	0.87	1.14E-04	1.93E-02	M8.39_Undetermined
A_23_P106042	CMTM5	9.94	1.03	6.09E-05	1.38E-02	M1.1_Platelets
A_21_P0000865	LINC01016	7.02	0.28	2.89E-04	2.99E-02	NA
A_21_P0008340	lnc-C14orf101-1	4.19	0.44	2.93E-04	3.01E-02	NA
A_23_P200001	NEXN	8.97	0.55	2.19E-04	2.65E-02	M8.18_Undetermined
A_23_P17130	C2orf88	8.87	0.65	8.65E-05	1.69E-02	M5.3_Not.Determined
A_33_P3317073	MOB1B	6.89	0.41	1.07E-04	1.87E-02	M5.2_Not.Determined
A_22_P00008020	LOC101929089	8.55	0.48	3.28E-05	1.04E-02	NA
A_23_P151907	PCSK6	6.12	1.04	4.92E-06	4.41E-03	M8.39_Undetermined
A_23_P11025	ZNF185	8.94	0.63	5.74E-04	4.13E-02	M6.14_Not.Determined
A_23_P102109	TUBA4A	13.35	0.41	5.79E-04	4.13E-02	M8.2_Not.Determined
A_33_P3361398	C19orf26	5.63	0.31	2.00E-04	2.54E-02	NA
A_22_P00010174	FGD5-AS1	6.03	0.52	9.17E-05	1.72E-02	NA
A_33_P3391418	TMEM40	8.00	0.84	1.86E-05	7.77E-03	M1.1_Platelets
A_23_P45496	GDI1	12.25	0.28	1.18E-05	6.37E-03	M9.15_Undetermined
A_33_P3363420	FRMD3	9.06	0.70	3.35E-04	3.19E-02	M8.39_Undetermined
A_33_P3384562	PDLIM7	10.98	0.62	6.41E-05	1.43E-02	M3.2_Inflammation|M4.13_Inflammation
A_23_P152995	SLC6A4	7.23	1.02	6.90E-07	2.34E-03	M8.18_Undetermined
A_33_P3304655	LTBP1	5.80	0.87	4.11E-05	1.13E-02	M8.1_Not.Determined
A_33_P3383226	GP9	12.69	0.99	1.03E-05	6.09E-03	M1.1_Platelets
A_23_P217428	ARHGAP6	6.31	0.74	1.05E-04	1.86E-02	M9.22_Undetermined
A_23_P216966	PTGS1	9.55	0.72	2.40E-04	2.76E-02	M8.18_Undetermined
A_24_P277367	CXCL5	9.66	0.86	1.48E-04	2.19E-02	M1.1_Platelets
A_23_P359277	ELOVL7	7.71	0.80	1.60E-04	2.28E-02	M8.18_Undetermined
A_22_P00014053	DGKD	9.90	0.36	2.45E-04	2.78E-02	M6.10_Not.Determined
A_33_P3332955	CLEC1B	9.97	0.74	1.81E-04	2.42E-02	M1.1_Platelets
A_24_P319736	MEIS1	7.91	0.70	1.07E-04	1.87E-02	M1.1_Platelets
A_33_P3242863	NT5M	11.37	0.65	3.50E-04	3.24E-02	M1.1_Platelets
A_33_P3351836	C2orf73	6.14	0.39	6.04E-04	4.20E-02	NA

A_22_P00023250	lnc-NBPF3-4	6.48	0.61	6.85E-05	1.48E-02	NA
A_33_P3413558	CD226	7.47	0.57	1.84E-04	2.44E-02	NA
A_24_P64167	PTGS1	10.01	0.77	8.03E-05	1.62E-02	M8.18_Undetermined
A_24_P921366	CALD1	7.16	0.89	1.18E-04	1.96E-02	M1.1_Platelets
A_33_P3372666	PDGFA	5.90	0.63	4.37E-05	1.17E-02	NA
A_33_P3292896	SFXN5	7.14	0.29	7.72E-04	4.69E-02	M9.15_Undetermined
A_23_P8906	LRP12	6.43	0.71	7.90E-07	2.43E-03	NA
A_23_P25246	AVPR1A	5.10	0.58	1.36E-04	2.12E-02	NA
A_33_P7477724	lnc-VAMP1-1	6.23	0.37	3.40E-04	3.20E-02	NA
A_24_P943301	PEAR1	5.90	0.81	9.24E-05	1.73E-02	NA
A_32_P210642	EGFL7	6.73	0.72	1.52E-05	7.17E-03	NA
A_22_P00024586		6.14	0.26	2.19E-04	2.65E-02	NA
A_22_P00014623	lnc-SLC16A3-1	6.86	0.82	6.45E-04	4.34E-02	NA
A_24_P156113	EHD2	5.25	0.52	3.34E-04	3.19E-02	NA
A_23_P148422	PCYT1B	4.98	0.57	7.11E-04	4.52E-02	NA
A_23_P29939	SNCA	9.76	0.72	7.15E-04	4.53E-02	M2.3_Erythrocytes
A_33_P3236071	CLEC1B	9.32	0.77	1.51E-04	2.22E-02	M1.1_Platelets
A_33_P3265030	GP1BB	14.96	0.88	3.70E-05	1.09E-02	M1.1_Platelets
A_33_P3232552	GUCY1B3	5.19	0.61	2.97E-04	3.02E-02	M8.39_Undetermined
A_33_P3329686		6.54	0.95	5.52E-05	1.31E-02	NA
A_21_P0001290	LINC00853	7.99	0.69	1.39E-04	2.14E-02	NA
A_33_P3303372	PARD3	7.55	0.76	9.42E-05	1.74E-02	NA
A_24_P76675	MFAP3L	6.63	0.78	1.68E-06	3.35E-03	M8.18_Undetermined
A_23_P256205	ABLIM3	8.52	0.71	5.67E-04	4.12E-02	M1.1_Platelets
A_33_P3461416	GP6	7.83	1.02	9.49E-06	5.84E-03	M1.1_Platelets
A_23_P105562	VWF	8.40	1.13	2.17E-05	8.10E-03	M1.1_Platelets
A_23_P215913	CLU	11.24	1.02	2.00E-05	7.90E-03	NA
A_21_P0010978		10.60	0.64	1.95E-05	7.84E-03	NA
A_33_P3401647	PPP1R14A	6.70	0.49	4.29E-04	3.59E-02	M7.26_Undetermined
A_33_P3404779	TCTEX1D4	5.95	0.41	3.95E-04	3.45E-02	NA
A_24_P41864	ARHGAP6	4.87	0.51	3.04E-04	3.04E-02	M9.22_Undetermined
A_33_P3382924	SPARC	8.96	0.77	7.30E-04	4.57E-02	NA
A_24_P251534	CTDSPL	7.62	0.96	6.85E-05	1.48E-02	M1.1_Platelets
A_23_P154065	TUBA4A	14.46	0.42	3.58E-04	3.28E-02	M8.2_Not.Determined
A_23_P89902	RTN2	6.83	0.69	4.91E-06	4.41E-03	M7.1_Inflammation
A_23_P166633	ITGB5	8.65	0.95	4.85E-05	1.21E-02	M1.1_Platelets
A_23_P151133	TSPAN9	5.63	0.81	1.42E-04	2.17E-02	M1.1_Platelets
A_23_P30020	PLA2G12A	9.08	0.45	5.30E-04	3.95E-02	M6.14_Not.Determined
A_32_P122754	MSANTD3	7.99	0.34	2.46E-04	2.78E-02	M8.51_Undetermined
A_33_P3231557	CDC14B	6.88	0.53	7.33E-04	4.58E-02	M8.51_Undetermined
A_23_P382835	P2RY1	6.77	0.98	4.68E-06	4.41E-03	M9.21_Undetermined
A_33_P3339100	SELP	7.56	1.01	1.12E-05	6.24E-03	M1.1_Platelets
A_33_P3214334	LY6G6F	8.30	1.05	2.10E-05	8.09E-03	M1.1_Platelets
A_33_P3236065	CLEC1B	10.42	0.72	3.08E-04	3.06E-02	M1.1_Platelets
A_23_P104804	ZBTB16	9.60	0.72	3.13E-04	3.08E-02	M8.31_Undetermined|M9.15_Undetermined
A_23_P350591	BEND2	4.74	0.59	7.64E-04	4.67E-02	NA
A_22_P00004088		6.18	0.55	3.75E-04	3.34E-02	NA
A_24_P93633	DENND4C	6.59	0.37	7.96E-04	4.76E-02	NA
A_23_P377214	HEXIM2	10.99	0.56	3.55E-04	3.27E-02	M9.13_Undetermined
A_22_P00001342	NEAT1	10.74	0.47	3.74E-04	3.34E-02	M9.4_Undetermined
A_24_P209171	SH3BGRL2	7.77	0.82	3.34E-04	3.19E-02	NA
A_19_P00318761		4.12	0.36	1.87E-04	2.46E-02	NA
A_24_P372134	TMEM140	8.44	0.48	3.96E-04	3.45E-02	M5.12_Interferon
A_24_P318656	ITGB3	11.14	1.31	5.71E-06	4.62E-03	M6.1_Not.Determined
A_23_P42975	PRKAR2B	10.58	0.79	4.39E-04	3.62E-02	NA
A_21_P0010882	lnc-MBL2-3	6.10	0.66	3.65E-04	3.30E-02	NA
A_33_P3242973	IGF2BP2	4.97	0.44	6.34E-04	4.30E-02	M2.3_Erythrocytes
A_21_P0000833	SENCR	7.60	0.62	2.54E-04	2.80E-02	NA
A_24_P945059	MYCT1	5.66	0.76	3.81E-06	4.35E-03	M9.14_Undetermined
A_23_P206960	SEC14L1	12.57	0.45	5.68E-05	1.33E-02	M7.31_Undetermined
A_22_P00005046	XKR5	4.87	0.42	2.76E-04	2.90E-02	NA
A_24_P219785	CALM3	11.44	0.45	2.27E-04	2.69E-02	M7.8_Undetermined
A_33_P3392921	CTTN	4.71	0.63	2.54E-04	2.80E-02	M1.1_Platelets
A_23_P360240	MYEOV	5.83	0.54	3.16E-06	4.30E-03	NA
A_24_P176079	WASF3	5.20	0.82	1.83E-05	7.72E-03	M8.18_Undetermined

A_23_P160546	FAM63A	10.60	0.70	3.27E-04	3.17E-02	NA
A_23_P84448	TUBA4A	12.04	0.44	6.96E-04	4.48E-02	M8.2_Not.Determined
A_32_P58407	KCND3	7.35	0.35	1.83E-04	2.43E-02	NA
A_23_P54488	ACSBG1	7.12	0.59	8.04E-05	1.62E-02	M1.1_Platelets
A_19_P00318418	TBXAS1	5.90	0.59	1.24E-04	2.01E-02	M5.1_Inflammation
A_33_P3223958	NAT8B	8.11	1.00	2.10E-06	3.62E-03	NA
A_23_P43412	HEMGN	7.24	0.67	2.33E-05	8.48E-03	M6.18_Erythrocytes
A_23_P16944	SDC1	7.07	0.47	5.26E-04	3.93E-02	M6.1_Not.Determined
A_21_P0003640	lnc-UGT8-4	6.64	0.88	7.40E-05	1.54E-02	NA
A_23_P344451	HDGFRP3	7.48	0.67	8.44E-06	5.57E-03	M9.17_Undetermined
A_23_P417942	FNBP1L	5.91	0.58	1.02E-04	1.84E-02	M6.14_Not.Determined
A_24_P369232	CCDC3	5.75	0.94	3.12E-04	3.08E-02	NA
A_23_P57658	HRASLS	7.50	0.99	6.64E-05	1.47E-02	M6.14_Not.Determined
A_33_P3310780	CTTN	10.50	0.86	1.94E-04	2.50E-02	M1.1_Platelets
A_23_P126613	AQP10	9.19	1.36	5.11E-07	2.34E-03	NA
A_23_P393080	CALML3	8.58	0.53	3.21E-05	1.02E-02	NA
A_23_P111701	GNG11	12.86	0.67	7.84E-04	4.71E-02	M1.1_Platelets
A_23_P336612	C15orf26	6.39	0.97	1.19E-05	6.42E-03	M9.41_Undetermined
A_22_P00018077		6.01	0.91	1.14E-05	6.24E-03	NA
A_22_P00005043	LINC00534	5.85	0.72	2.87E-04	2.98E-02	NA
A_23_P40718	PARVB	8.81	0.67	4.47E-06	4.41E-03	M1.1_Platelets
A_23_P210425	MYL9	9.16	1.09	3.26E-04	3.17E-02	M1.1_Platelets|M8.51_Undetermined
A_24_P100277	CYB5R3	7.15	0.49	1.32E-05	6.60E-03	M7.1_Inflammation
A_33_P3238290	FAM65C	5.68	0.58	5.91E-04	4.16E-02	M4.4_Not.Determined
A_24_P385313	PTPRF	5.59	1.00	5.73E-06	4.62E-03	NA
A_23_P73114	PROS1	6.63	1.07	4.83E-05	1.21E-02	M1.1_Platelets
A_24_P308506	NAT8B	7.56	0.90	3.35E-06	4.30E-03	NA
A_23_P143173	SLA2	9.25	0.60	2.46E-04	2.78E-02	M7.18_Undetermined
A_24_P79403	PF4	15.53	0.61	5.95E-04	4.17E-02	NA
A_23_P435833	FUBP3	5.61	0.30	5.71E-04	4.13E-02	M5.4_Not.Determined
A_24_P167654	SLC8A3	5.44	0.55	6.99E-04	4.50E-02	M1.1_Platelets
A_24_P376707	HDGF	11.37	0.34	1.69E-05	7.50E-03	M4.4_Not.Determined
A_33_P3421515		12.17	0.50	4.09E-05	1.13E-02	NA
A_33_P3226755	FLNA	5.12	0.49	9.72E-05	1.78E-02	M4.16_Not.Determined
A_33_P3248765	ADIPOR1	8.72	0.34	3.74E-04	3.34E-02	M3.1_Erythrocytes
A_24_P65373	ITGA2B	9.30	1.23	3.11E-05	9.96E-03	M1.1_Platelets
A_33_P3348288	RHOBTB1	8.49	0.89	4.19E-06	4.38E-03	NA
A_22_P00000203		5.33	0.37	2.32E-04	2.70E-02	NA
A_33_P3223121	HIPK2	8.84	0.66	1.02E-04	1.84E-02	M7.26_Undetermined
A_23_P129221	FAH	8.58	0.49	7.15E-04	4.53E-02	M7.33_Undetermined
A_21_P0011314	INAFM2	11.21	0.46	4.18E-04	3.55E-02	NA
A_24_P475349	RAB6B	5.02	0.78	4.12E-06	4.38E-03	NA
A_19_P00318409	NEAT1	10.52	0.46	3.11E-04	3.07E-02	M9.4_Undetermined
A_22_P00013249	lnc-ROM1-3	4.13	0.42	6.22E-04	4.26E-02	NA
A_24_P79054	TGFB1	12.41	0.35	1.93E-04	2.50E-02	NA
A_22_P00013776		7.58	0.69	6.66E-04	4.39E-02	NA
A_19_P00317612	LINC00211	5.30	0.62	4.01E-05	1.13E-02	NA
A_23_P210330	LGALSL	10.52	0.92	4.28E-05	1.15E-02	M1.1_Platelets
A_23_P502224	CYB5R3	14.64	0.41	8.29E-06	5.57E-03	M7.1_Inflammation
A_23_P139198	LGALS12	8.72	0.64	1.79E-04	2.42E-02	M9.12_Undetermined
A_23_P250156	IGF2BP2	7.69	0.57	7.52E-05	1.56E-02	M2.3_Erythrocytes
A_22_P00023924	lnc-OBFC2A-5	4.15	0.31	7.60E-04	4.67E-02	NA
A_33_P3238997	AGFG1	10.00	0.51	4.22E-04	3.56E-02	M7.23_Undetermined
A_33_P3395219	NEXN-AS1	4.83	0.40	4.30E-04	3.59E-02	NA
A_33_P3418597	GAS2L1	8.81	0.77	8.07E-05	1.62E-02	M8.18_Undetermined
A_24_P47182	VCL	11.33	0.72	2.65E-04	2.84E-02	M8.39_Undetermined
A_23_P84219	LIPH	5.23	0.62	5.96E-04	4.17E-02	NA
A_33_P3381870	DMTN	11.98	0.72	6.13E-04	4.22E-02	M3.1_Erythrocytes
A_23_P46627	ADIPOR1	11.37	0.34	2.18E-04	2.64E-02	M3.1_Erythrocytes
A_24_P753476	GAS2L1P2	8.33	0.72	4.41E-04	3.62E-02	NA
A_24_P414999	LAPTM4B	5.78	0.59	9.28E-05	1.73E-02	M9.4_Undetermined
A_22_P00023374	INAFM2	11.82	0.43	3.48E-04	3.24E-02	NA
A_33_P3285809	SSX2IP	7.36	0.47	4.75E-05	1.20E-02	NA
A_22_P00004848	LOC100133669	4.41	0.32	7.26E-04	4.57E-02	NA
A_21_P0004992	lnc-C6orf146-2	9.33	0.25	2.87E-04	2.98E-02	NA

A_33_P3350828	EPS15L1	9.13	0.29	3.46E-04	3.24E-02	M8.60_Undetermined
A_32_P134968	SPTB	7.09	0.96	1.21E-04	2.00E-02	M6.18_Erythrocytes
A_33_P3396159	CCDC6	9.43	0.44	3.56E-04	3.27E-02	M5.5_Not.Determined
A_33_P3375451	NYNRIN	8.56	0.43	7.30E-05	1.53E-02	NA
A_23_P31532	ZC3HAV1L	6.29	0.23	6.68E-04	4.39E-02	NA
A_33_P3223631		6.42	0.29	1.78E-04	2.40E-02	NA
A_33_P3368159	SLA2	7.77	0.69	2.50E-04	2.78E-02	M7.18_Undetermined
A_21_P0014624	LOC102725057	6.37	0.70	6.11E-06	4.81E-03	NA
A_23_P167096	VEGFC	5.35	0.85	4.10E-05	1.13E-02	NA
A_23_P102950	RSPH1	6.32	0.53	5.75E-04	4.13E-02	NA
A_23_P79978	SLC24A3	8.46	1.20	3.90E-05	1.11E-02	M1.1_Platelets
A_33_P3298024	ABCC3	8.08	0.68	1.65E-04	2.30E-02	NA
A_24_P140204	PXK	10.30	0.30	2.88E-04	2.98E-02	M8.37_Undetermined
A_23_P16866	VIL1	6.69	0.75	5.71E-04	4.13E-02	M9.41_Undetermined
A_23_P167856	TMEM63B	7.68	0.35	7.47E-04	4.62E-02	M3.1_Erythrocytes
A_23_P65506	SPTB	4.36	0.51	7.39E-04	4.60E-02	M6.18_Erythrocytes
A_24_P333993	OR2W3	4.65	0.64	1.86E-04	2.45E-02	M2.3_Erythrocytes
A_23_P330070	TFPI	5.18	0.94	4.02E-04	3.49E-02	M1.1_Platelets|M8.39_Undetermined
A_23_P423864	PHC2	12.91	0.58	1.26E-04	2.01E-02	M3.2_Inflammation
A_24_P189997	PCSK6	5.33	0.96	6.66E-06	5.00E-03	M8.39_Undetermined
A_33_P3239736	WDR44	8.00	0.32	1.14E-05	6.24E-03	M8.43_Undetermined
A_23_P80122	WRB	7.78	0.49	4.86E-04	3.79E-02	M8.36_Undetermined
A_22_P00011730		4.60	0.58	1.06E-04	1.86E-02	NA
A_24_P358305		6.96	0.61	2.49E-04	2.78E-02	NA
A_24_P74371	CTSA	13.69	0.53	2.57E-04	2.82E-02	M7.1_Inflammation
A_22_P00014572	lnc-SLA2-2	5.22	0.54	4.81E-04	3.76E-02	NA
A_23_P149992	PDLIM1	8.48	0.57	4.52E-04	3.66E-02	M1.1_Platelets
A_33_P3238250	F11R	8.59	0.43	2.54E-05	8.90E-03	M8.10_Undetermined
A_23_P414273	SMIM3	12.27	0.67	4.48E-04	3.64E-02	M8.39_Undetermined
A_24_P415624	MLXIP	8.18	0.53	6.81E-04	4.42E-02	NA
A_23_P210886	BCL2L1	7.58	0.59	8.55E-06	5.57E-03	M2.3_Erythrocytes|M3.1_Erythrocytes
A_22_P00019419		5.80	0.35	5.73E-04	4.13E-02	NA
A_23_P158053	C9orf16	9.83	0.27	7.32E-04	4.58E-02	M9.16_Undetermined
A_21_P0003155	LINC00635	5.47	0.31	6.35E-04	4.30E-02	NA
A_23_P58396	PDGFC	7.97	0.63	1.10E-04	1.90E-02	M7.10_Undetermined
A_22_P00021288		6.79	0.69	1.18E-04	1.96E-02	NA
A_33_P3413038	PLXNB3	4.80	0.76	2.40E-04	2.76E-02	NA
A_33_P3343972	RSPH1	5.54	0.54	2.10E-04	2.59E-02	NA
A_33_P3225313	FAM91A1	7.36	0.38	2.37E-04	2.75E-02	M4.9_Not.Determined
A_24_P189533	ENDOD1	9.57	0.67	1.63E-04	2.30E-02	M1.1_Platelets
A_24_P295245	ASPH	9.60	0.87	3.54E-04	3.27E-02	M7.10_Undetermined
A_22_P00024273		7.65	0.22	5.14E-04	3.89E-02	NA
A_23_P348911	LINC01126	6.86	0.34	4.11E-04	3.54E-02	NA
A_23_P212696	FSTL1	7.88	0.92	3.37E-04	3.20E-02	M1.1_Platelets
A_23_P371239	CMIP	9.83	0.43	2.86E-04	2.98E-02	M9.15_Undetermined
A_24_P226008	MGLL	10.75	0.87	5.69E-05	1.33E-02	M1.1_Platelets|M6.14_Not.Determined
A_23_P255444	DAPP1	10.32	0.34	3.35E-04	3.19E-02	M5.2_Not.Determined
A_33_P3292829	SCYL2	8.28	0.32	3.63E-04	3.29E-02	M5.1_Inflammation
A_22_P00013508	LOC102725057	6.21	0.54	6.62E-05	1.46E-02	NA
A_23_P49376	CETP	5.74	0.71	7.01E-04	4.51E-02	M9.24_Undetermined
A_33_P3319760	TAGLN2	12.66	0.36	6.78E-04	4.41E-02	M8.44_Undetermined|M8.52_Undetermined
A_24_P55225	RSPH9	5.34	0.56	5.09E-04	3.88E-02	M9.4_Undetermined
A_23_P418373	BCL2L2	9.60	0.43	1.38E-04	2.14E-02	M7.22_Undetermined
A_21_P0013885		9.20	0.32	6.16E-04	4.23E-02	NA
A_23_P33683		9.23	0.62	3.81E-04	3.37E-02	M4.4_Not.Determined
A_23_P208788	C19orf33	9.89	1.06	1.17E-04	1.95E-02	M6.14_Not.Determined
A_33_P3232006	UBL4A	9.26	0.37	7.04E-04	4.52E-02	M8.80_Undetermined
A_24_P391260	PTTG1IP	9.48	0.49	6.87E-05	1.48E-02	M5.1_Inflammation
A_33_P3212959	SPANXN4	4.88	0.56	3.71E-04	3.33E-02	NA
A_33_P3783812	C8orf60	11.13	0.58	3.38E-04	3.20E-02	NA
A_24_P185186	SAMD14	6.05	1.12	2.08E-05	8.07E-03	M1.1_Platelets
A_24_P816384	UBE2Q2P1	9.40	0.30	7.61E-04	4.67E-02	M7.2_Not.Determined
A_33_P3399443	SH3TC1	5.90	0.46	5.13E-04	3.89E-02	M8.62_Undetermined
A_33_P3354564	GPD2	7.55	0.31	5.12E-04	3.89E-02	M7.30_Undetermined
A_22_P00020277	lnc-GCNT3-1	5.24	0.28	8.17E-04	4.82E-02	NA

A_33_P3358037		9.86	0.30	2.41E-04	2.76E-02	NA
A_21_P0006297	CDC14B	4.24	0.45	4.93E-04	3.84E-02	M8.51_Undetermined
A_23_P105066	ILK	10.61	0.51	4.25E-05	1.15E-02	M5.1_Inflammation
A_23_P76364	CD9	8.38	1.03	4.89E-06	4.41E-03	M6.14_Not.Determined
A_23_P77145	RAB11A	8.46	0.31	6.50E-04	4.35E-02	M7.9_Undetermined
A_23_P25684	RDH11	11.01	0.30	5.77E-04	4.13E-02	M6.2_Mitochondrial.Respiration
A_23_P77630	MAP1LC3B	10.27	0.34	8.48E-04	4.93E-02	M5.1_Inflammation
A_21_P0012079	MIR4435-1HG	12.87	0.57	6.36E-07	2.34E-03	NA
A_23_P163087	NID2	5.11	0.43	1.77E-04	2.39E-02	NA
A_23_P346006	CCPG1	6.57	0.33	4.82E-04	3.77E-02	M3.2_Inflammation
A_24_P270829	GP1BA	4.59	0.52	2.56E-05	8.94E-03	M8.39_Undetermined
A_24_P273143	LINC00152	11.30	0.62	1.22E-06	2.97E-03	NA
A_23_P434518	LFNG	7.74	0.33	3.64E-04	3.30E-02	M7.18_Undetermined
A_23_P3592	HSF4	6.04	0.37	1.22E-05	6.47E-03	NA
A_33_P3307068	GOLGA2	6.72	0.46	4.31E-04	3.59E-02	M7.26_Undetermined
A_33_P3335966	TPM1	7.98	0.73	3.50E-04	3.24E-02	M7.33_Undetermined
A_33_P3281795	MGLL	9.78	0.87	4.38E-05	1.17E-02	M1.1_Platelets|M6.14_Not.Determined
A_33_P3299982	USF2	14.98	0.23	1.62E-04	2.30E-02	M6.10_Not.Determined|M9.50_Undetermined
A_24_P374244	GATA1	6.27	0.74	1.14E-04	1.93E-02	M3.1_Erythrocytes
A_33_P3275070		6.03	0.75	1.88E-04	2.46E-02	NA
A_33_P3279353	AZU1	6.84	0.54	1.90E-04	2.48E-02	M5.15_Neutrophils
A_33_P3212555	PROS1	4.53	0.59	5.97E-04	4.17E-02	M1.1_Platelets
A_32_P206899	DNAH2	5.25	0.62	5.64E-04	4.11E-02	NA
A_23_P8763	PTPN12	12.14	0.41	1.46E-04	2.18E-02	M8.60_Undetermined
A_32_P231086	GOLGA6L9	9.74	0.20	6.56E-04	4.36E-02	NA
A_21_P0001196	lnc-SERPINC1-3	7.40	0.35	8.68E-04	4.99E-02	NA
A_32_P141238	ANO2	5.10	0.68	1.46E-04	2.18E-02	NA
A_24_P44462	TPM1	7.96	0.80	3.89E-04	3.41E-02	M7.33_Undetermined
A_33_P3316026	USF2	9.68	0.29	1.40E-04	2.15E-02	M6.10_Not.Determined|M9.50_Undetermined
A_24_P246173	MYO9B	12.28	0.39	5.03E-04	3.86E-02	M7.3_Not.Determined
A_22_P00000933		7.06	0.36	2.51E-04	2.78E-02	NA
A_33_P3366161	ABAT	4.67	0.34	4.14E-04	3.54E-02	M8.44_Undetermined
A_23_P1691	MMP1	5.19	1.15	6.82E-05	1.48E-02	NA
A_23_P137173	TMSB15A	5.29	0.57	7.45E-04	4.61E-02	M9.21_Undetermined
A_33_P3339531	CHADL	7.58	0.62	3.47E-04	3.24E-02	NA
A_23_P31686	CCAR2	8.77	0.32	7.56E-04	4.66E-02	M5.5_Not.Determined|M7.10_Undetermined
A_24_P180680	LAPTM4B	8.49	0.61	2.63E-04	2.82E-02	M9.4_Undetermined
A_33_P3212022	RGS6	4.41	0.38	5.90E-04	4.16E-02	NA
A_21_P0014785	VIM-AS1	7.24	0.41	3.09E-05	9.95E-03	NA
A_33_P3235335	MTMR3	8.20	0.43	1.35E-04	2.10E-02	M4.13_Inflammation|M7.27_Undetermined
A_23_P359636	BROX	8.30	0.31	2.66E-04	2.84E-02	M4.9_Not.Determined
A_23_P146572	NPDC1	10.62	0.59	5.93E-04	4.16E-02	M7.4_Not.Determined
A_33_P3297244	GAS2L2	5.11	0.43	4.64E-04	3.72E-02	NA
A_22_P00001341	MIR612	8.33	0.61	4.97E-04	3.84E-02	NA
A_22_P00007974	lnc-IDH3G-1	5.52	0.24	8.16E-04	4.82E-02	NA
A_23_P216448	NFIB	4.91	0.65	3.65E-04	3.30E-02	M6.14_Not.Determined
A_33_P3258777		4.30	0.52	2.23E-06	3.66E-03	NA
A_33_P3404126	PCGF3	9.90	0.42	4.51E-04	3.66E-02	NA
A_23_P118427	MAP2K3	10.71	0.41	2.48E-04	2.78E-02	M3.1_Erythrocytes|M9.8_Undetermined
A_21_P0001959		6.92	0.69	6.05E-05	1.38E-02	NA
A_33_P3243683	DIAPH1	8.00	0.30	1.02E-05	6.09E-03	NA
A_33_P3212257	MMRN1	6.15	0.80	4.48E-04	3.64E-02	NA
A_33_P3369262	FGFR1OP2	7.18	0.34	4.05E-04	3.50E-02	M5.2_Not.Determined
A_33_P3367970		7.68	0.45	2.05E-04	2.57E-02	NA
A_23_P104509	FAM53B	6.84	0.50	9.73E-05	1.78E-02	M8.102_Undetermined
A_21_P0006672	lnc-ZNF37A-3	7.92	0.33	3.30E-04	3.18E-02	NA
A_23_P204375	LPAR5	6.16	0.44	5.49E-04	4.04E-02	M9.9_Undetermined
A_33_P3285540	CLDN5	9.39	0.80	4.52E-04	3.66E-02	M1.1_Platelets
A_21_P0014427	lnc-CHADL-1	6.22	0.64	2.53E-04	2.79E-02	NA
A_23_P897	C1orf116	5.59	0.59	6.15E-05	1.39E-02	M8.77_Undetermined
A_21_P0005609	KMT2E-AS1	9.41	0.60	3.39E-05	1.05E-02	NA
A_33_P3406413		6.10	0.42	5.85E-04	4.16E-02	NA
A_33_P3316293	CAB39	8.43	0.25	2.31E-04	2.70E-02	M5.1_Inflammation
A_33_P3280213	CTSA	11.42	0.53	7.98E-04	4.76E-02	M7.1_Inflammation
A_23_P126388	SH3BGRL3	15.17	0.38	6.46E-04	4.34E-02	M7.31_Undetermined

A_33_P3382919	LOC100130587	5.70	0.39	5.71E-04	4.13E-02	NA
A_33_P3238993	AGFG1	8.84	0.57	2.51E-04	2.78E-02	M7.23_Undetermined
A_23_P45475	GLA	11.75	0.37	1.46E-04	2.18E-02	M4.6_Inflammation
A_23_P202905	TIRAP	5.82	0.40	6.06E-04	4.20E-02	NA
A_23_P154874	DSCR3	7.19	0.27	8.25E-04	4.85E-02	M7.21_Undetermined
A_23_P159920	IKBKG	10.01	0.29	2.51E-04	2.78E-02	NA
A_33_P3386099	ELK1	5.65	0.41	5.07E-04	3.88E-02	M6.17_Not.Determined
A_23_P37598	NPTN	8.78	0.39	1.04E-04	1.85E-02	M8.2_Not.Determined
A_23_P361820	ATG2A	10.49	0.51	8.52E-04	4.94E-02	M7.15_Undetermined
A_33_P3275751	SEC14L1	12.17	0.41	2.49E-04	2.78E-02	M7.31_Undetermined
A_23_P73239	NCKAP1	6.63	0.56	6.24E-05	1.40E-02	M6.14_Not.Determined
A_23_P129367	DRC7	4.75	0.50	2.51E-04	2.78E-02	M6.1_Not.Determined
A_24_P944964	GP5	4.96	0.47	8.39E-04	4.91E-02	NA
A_22_P00011372		6.96	0.84	5.62E-04	4.10E-02	NA
A_33_P3318581	PLOD2	5.38	0.99	3.50E-05	1.07E-02	M8.51_Undetermined
A_23_P64044	FERMT3	11.28	0.40	7.63E-04	4.67E-02	M5.1_Inflammation
A_22_P00022843	ST3GAL6-AS1	4.69	0.48	9.77E-05	1.78E-02	NA
A_24_P73370	ULK1	11.37	0.49	9.98E-05	1.81E-02	M7.1_Inflammation
A_33_P3286349	DNAAF3	4.32	0.60	7.38E-04	4.60E-02	M9.8_Undetermined
A_22_P00001057		7.06	0.30	3.61E-04	3.29E-02	NA
A_24_P297539	UBE2C	6.74	0.52	7.02E-04	4.51E-02	M3.3_Cell.Cycle
A_24_P383850	EIF4G3	9.39	0.45	3.58E-04	3.28E-02	M7.21_Undetermined
A_23_P67399	STRN4	10.78	0.36	5.18E-04	3.90E-02	M6.10_Not.Determined
A_33_P3565133	LINC00642	6.34	0.73	3.15E-04	3.09E-02	NA
A_22_P00010555	lnc-NCOA5-1	4.66	0.29	3.70E-04	3.33E-02	NA
A_23_P141394	WIPI1	10.92	0.56	3.78E-04	3.35E-02	M7.10_Undetermined
A_33_P3382267	SEC16A	6.90	0.41	3.76E-04	3.35E-02	NA
A_23_P43490	CDKN2A	8.35	0.38	1.26E-05	6.53E-03	NA
A_23_P140614	GOLGA8O	7.51	0.43	3.79E-04	3.35E-02	M9.52_Undetermined
A_23_P103070	YWHAH	9.89	0.52	1.69E-04	2.32E-02	M8.106_Undetermined
A_33_P3404651	TTC7A	9.72	0.34	2.86E-04	2.98E-02	NA
A_22_P00025652	LOC100288846	5.82	0.41	4.54E-04	3.67E-02	NA
A_33_P3360392	LINC00092	6.38	0.30	1.64E-04	2.30E-02	NA
A_21_P0010793	LOC100132287	6.48	0.33	3.61E-04	3.29E-02	NA
A_21_P0008062	lnc-LRCH1-1	4.86	0.31	1.29E-04	2.05E-02	NA
A_23_P372834	AQP1	6.00	0.65	5.93E-04	4.16E-02	M9.33_Undetermined
A_23_P331253	XPNPEP1	9.16	0.42	7.08E-05	1.50E-02	M6.2_Mitochondrial.Respiration
A_23_P122375	ZFAND3	8.30	0.35	4.68E-04	3.72E-02	M7.31_Undetermined
A_33_P3226492	RAB7A	5.69	0.36	6.24E-05	1.40E-02	M5.1_Inflammation
A_23_P48596	RNASE1	7.16	0.84	3.69E-04	3.32E-02	M9.1_Undetermined
A_23_P338325	ELK3	7.23	0.45	3.39E-04	3.20E-02	NA
A_23_P218646	TNFRSF6B	7.04	0.32	6.60E-04	4.37E-02	NA
A_22_P00014902	lnc-SLC9A4-1	7.65	0.70	2.57E-04	2.82E-02	NA
A_32_P129288	RAB1B	10.65	0.33	6.84E-05	1.48E-02	M7.1_Inflammation
A_33_P3380236		6.93	0.37	2.54E-04	2.80E-02	NA
A_33_P3349883	LGALS8	5.64	0.34	6.47E-04	4.34E-02	M9.21_Undetermined
A_24_P271363	CDS2	9.03	0.26	5.13E-04	3.89E-02	M7.21_Undetermined
A_23_P99397	ZDHHC20	10.16	0.30	5.05E-04	3.87E-02	M7.10_Undetermined
A_33_P3301010	SPIRE1	5.31	0.72	1.86E-04	2.45E-02	M7.17_Undetermined
A_23_P367899	EPOR	7.70	0.32	8.02E-04	4.78E-02	M7.33_Undetermined
A_32_P35969	CHRNA7	7.72	1.01	1.63E-04	2.30E-02	NA
A_33_P3353360	BRK1	4.96	0.36	1.49E-04	2.21E-02	M7.11_Undetermined
A_21_P0008109	lnc-FARP1-1	5.99	0.51	5.76E-05	1.34E-02	NA
A_22_P00007936		5.70	0.28	3.60E-04	3.29E-02	NA
A_23_P345118	PIM1	12.74	0.51	2.35E-04	2.73E-02	M4.4_Not.Determined
A_33_P3418000	RELL1	7.83	0.53	7.07E-04	4.52E-02	NA
A_23_P4494	DSC2	5.95	0.97	6.49E-05	1.44E-02	M9.15_Undetermined
A_24_P914495	MARK2	7.91	0.34	1.35E-04	2.11E-02	M9.22_Undetermined|M9.40_Undetermined
A_22_P00018323	SSPO	7.34	0.23	5.58E-04	4.08E-02	NA
A_33_P3228190	KCNAB2	8.58	0.35	3.45E-04	3.23E-02	M9.3_Undetermined
A_23_P96976	ZCCHC17	10.31	0.37	1.67E-04	2.32E-02	M6.4_Not.Determined
A_33_P7278111	LAPTM4B	6.46	0.61	2.13E-04	2.61E-02	M9.4_Undetermined
A_23_P213562	F2R	8.06	0.58	2.30E-04	2.70E-02	NA
A_23_P42931	CLEC2L	5.02	0.73	5.70E-04	4.13E-02	M9.41_Undetermined
A_33_P3376454	LOC100133299	7.16	0.63	2.96E-04	3.02E-02	NA

A_23_P101707	PLIN3	9.06	0.50	2.40E-04	2.76E-02	M6.13_Cell.Death
A_23_P144465	PAPSS1	7.84	0.38	3.52E-04	3.25E-02	M7.23_Undetermined
A_24_P391568	ARNT	7.44	0.26	6.41E-04	4.32E-02	M8.97_Undetermined
A_24_P316019	GOLGA8R	7.13	0.36	3.54E-04	3.26E-02	NA
A_22_P00009864		6.70	0.64	5.73E-05	1.34E-02	NA
A_23_P108082	CREB3L3	4.53	0.52	4.97E-04	3.84E-02	NA
A_21_P0010823	XLOC_l2_001569	5.16	0.63	7.30E-04	4.57E-02	NA
A_24_P80204	MALL	4.74	0.70	2.77E-05	9.44E-03	NA
A_33_P3284939	TMEM189	10.63	0.31	8.36E-04	4.89E-02	NA
A_23_P201295	CASZ1	6.13	0.39	7.88E-04	4.73E-02	M7.26_Undetermined
A_33_P3406449	SLC15A4	10.01	0.50	4.29E-04	3.59E-02	M5.7_Inflammation
A_33_P3407657	MGRN1	5.55	0.38	2.92E-04	3.01E-02	NA
A_24_P163920	FAR1	7.92	0.42	3.34E-04	3.19E-02	M8.7_Undetermined
A_23_P215735	ST7	6.62	0.38	8.58E-04	4.96E-02	M5.3_Not.Determined|M9.4_Undetermined
A_33_P3313519	CHRFAM7A	5.10	0.48	5.35E-04	3.98E-02	NA
A_23_P54576	KIFC3	6.44	0.52	8.55E-05	1.68E-02	M9.19_Undetermined
A_24_P393864	PHTF1	7.88	0.51	1.29E-05	6.57E-03	M3.2_Inflammation
A_33_P3231065		5.75	0.30	4.13E-04	3.54E-02	NA
A_33_P3320888	CREB3L2	7.70	0.37	4.19E-04	3.55E-02	M7.19_Undetermined
A_33_P3220570	UBTD1	9.57	0.47	8.19E-04	4.83E-02	M4.13_Inflammation
A_21_P0003908	lnc-SCRG1-1	4.31	0.44	3.01E-04	3.04E-02	NA
A_33_P3239860	ANKDD1A	7.13	0.69	7.37E-04	4.60E-02	NA
A_24_P244944	MCTP2	8.05	0.51	6.45E-04	4.34E-02	M4.2_Inflammation
A_23_P80032	E2F1	6.79	0.47	7.71E-04	4.69E-02	M8.39_Undetermined
A_23_P65789	MCTP2	7.45	0.48	1.29E-04	2.05E-02	M4.2_Inflammation
A_19_P00321461		5.73	0.28	5.54E-04	4.06E-02	NA
A_24_P873414	PLEKHB2	12.56	0.39	6.38E-04	4.31E-02	M4.9_Not.Determined|M7.9_Undetermined
A_23_P416686	GPR137	7.65	0.29	7.42E-04	4.61E-02	M2.2_Cell.Cycle
A_33_P3329607	RAB1B	8.34	0.40	1.81E-04	2.42E-02	M7.1_Inflammation
A_33_P3240348	NF1	5.80	0.46	4.49E-04	3.65E-02	M9.14_Undetermined
A_22_P00012110	lnc-POFUT2-3	4.53	0.27	7.67E-04	4.68E-02	NA
A_24_P254850	SEC14L5	4.99	0.80	1.20E-04	1.98E-02	NA
A_23_P372848	P2RX1	9.59	0.52	7.44E-04	4.61E-02	M7.10_Undetermined
A_33_P3377130	MAP3K5	8.71	0.25	5.13E-04	3.89E-02	M7.1_Inflammation
A_23_P317184	LRRFIP2	9.21	0.35	3.05E-04	3.05E-02	M5.1_Inflammation
A_21_P0012236	NF1	7.19	0.46	5.13E-04	3.89E-02	M9.14_Undetermined
A_23_P41365	SMR3A	5.20	0.28	2.17E-04	2.64E-02	NA
A_22_P00010840	LOC101927272	4.73	0.47	6.05E-04	4.20E-02	NA
A_24_P336276	SLCO3A1	8.82	0.36	7.60E-05	1.57E-02	M4.6_Inflammation|M7.27_Undetermined|
A_22_P00021963	lnc-NLRP12-2	7.60	0.50	3.35E-04	3.19E-02	NA
A_22_P00015402	KMT2E-AS1	8.23	0.49	2.31E-04	2.70E-02	NA
A_23_P16214	FBXW9	6.71	0.32	3.88E-05	1.11E-02	M9.13_Undetermined
A_23_P60227	CCIN	7.98	0.44	3.94E-04	3.45E-02	NA
A_23_P351757	PLCD3	4.31	0.69	2.06E-04	2.58E-02	NA
A_24_P184555	PXN	14.85	0.31	3.62E-04	3.29E-02	NA
A_33_P3390357	SPIRE1	7.95	0.68	2.32E-04	2.70E-02	M7.17_Undetermined
A_24_P141214	STOM	11.34	0.48	1.00E-04	1.82E-02	M7.10_Undetermined|M7.29_Not.Determined
A_32_P525524	ITPRIPL1	7.57	0.45	7.12E-04	4.52E-02	M9.12_Undetermined
A_23_P350451	PRDM1	10.60	0.58	2.00E-04	2.54E-02	M7.19_Undetermined|M9.14_Undetermined
A_33_P3333146	RAP1GAP2	6.01	0.52	1.64E-04	2.30E-02	M9.1_Undetermined
A_24_P129417	BMP1	4.82	0.42	5.60E-04	4.10E-02	M9.1_Undetermined
A_21_P0001902	LOC101928173	8.44	0.70	5.93E-04	4.16E-02	NA
A_33_P3417810	NOL10	10.06	0.27	3.09E-04	3.06E-02	NA
A_33_P3250278	AGXT	4.35	0.30	6.23E-04	4.26E-02	NA
A_21_P0014465	LOC101928173	7.83	0.68	7.24E-04	4.56E-02	NA
A_23_P252681	PCYT1A	9.71	0.33	3.94E-04	3.45E-02	NA
A_33_P3370600	SMIM6	4.74	0.41	1.27E-04	2.03E-02	NA
A_22_P00013971	lnc-RTN2-1	7.38	0.74	4.14E-05	1.14E-02	NA
A_23_P309837	STON2	5.63	0.75	1.34E-05	6.64E-03	NA
A_22_P00002271	lnc-C10orf31-2	4.78	0.37	1.11E-04	1.91E-02	NA
A_24_P128308	KLF6	8.00	0.62	2.37E-05	8.50E-03	M7.2_Not.Determined|M7.15_Undetermined|
A_32_P198923	YWHAZ	11.61	0.31	4.67E-04	3.72E-02	M4.9_Not.Determined|M9.44_Undetermined
A_33_P3258274	TFPI	5.93	0.65	1.64E-04	2.30E-02	M1.1_Platelets|M8.39_Undetermined
A_23_P151662	MAX	11.05	0.28	6.35E-04	4.30E-02	M6.14_Not.Determined|M7.30_
A_33_P3322539	BEND2	8.01	0.65	4.17E-05	1.14E-02	NA

A_23_P2414	SPX	7.04	0.89	2.07E-06	3.62E-03	NA
A_24_P414658	HIST1H2AG	5.86	0.57	2.40E-04	2.76E-02	M1.1_Platelets
A_23_P90357	TBXA2R	9.28	0.75	2.90E-05	9.58E-03	M9.41_Undetermined
A_23_P169437	LCN2	8.13	0.81	4.63E-05	1.19E-02	NA
A_21_P0009522		5.10	0.46	4.38E-04	3.62E-02	NA
A_33_P3341429	NEXN	8.10	0.63	1.23E-04	2.01E-02	M8.18_Undetermined
A_22_P00016935	TSPAN33	9.75	0.73	1.05E-06	2.88E-03	M1.1_Platelets
A_23_P141974	TPM4	11.51	0.53	2.08E-06	3.62E-03	NA
A_22_P00005011	FAM212B-AS1	5.61	0.69	1.27E-05	6.54E-03	NA
A_23_P62953	PBX1	4.93	0.57	8.83E-05	1.70E-02	M3.1_Erythrocytes
A_23_P143902	P2RY12	7.60	0.83	3.72E-06	4.31E-03	M9.21_Undetermined
A_23_P405295	LCE3C	4.66	0.52	8.42E-06	5.57E-03	NA
A_21_P0000061	CGREF1	6.80	0.43	5.12E-05	1.26E-02	NA
A_23_P67864	ADCY3	10.91	0.34	1.14E-04	1.93E-02	M7.29_Not.Determined
A_24_P95822	NPTN	9.07	0.55	7.13E-06	5.20E-03	M8.2_Not.Determined
A_33_P3273136	MCUR1	9.92	0.44	1.16E-04	1.94E-02	M8.51_Undetermined
A_23_P380208	VEPH1	6.36	0.74	1.33E-04	2.09E-02	M9.21_Undetermined
A_33_P3231670	RNF208	7.87	0.82	3.11E-06	4.30E-03	NA
A_33_P3396370	ACRBP	12.64	0.55	7.54E-04	4.65E-02	M1.1_Platelets
A_23_P216845	GFI1B	8.74	0.77	8.33E-05	1.65E-02	M6.14_Not.Determined
A_33_P3304983	PRKAR2B	11.59	0.89	1.97E-05	7.86E-03	NA
A_23_P501831	FAXDC2	10.65	1.02	2.44E-06	3.94E-03	M3.1_Erythrocytes|M4.4_Not.Determined
A_19_P00317360	ATP2C1	6.66	0.76	1.91E-06	3.62E-03	M7.17_Undetermined|M8.36_Undetermined
A_22_P00002303	lnc-C11orf30-1	8.49	0.99	6.55E-05	1.45E-02	NA
A_33_P3275722	LY6G6D	6.48	0.55	3.62E-06	4.30E-03	M9.21_Undetermined
A_21_P0012452		5.27	0.93	3.34E-06	4.30E-03	NA
A_33_P3236858	TGFB1I1	8.35	0.79	7.04E-06	5.17E-03	M9.19_Undetermined
A_33_P3363620	TMEM91	10.26	0.56	4.08E-05	1.13E-02	NA
A_33_P3379669	RNF208	6.06	0.59	3.35E-05	1.05E-02	NA
A_33_P3244274	RNF208	7.89	0.80	4.69E-06	4.41E-03	NA
A_23_P251173	EIF2AK1	11.05	0.32	1.84E-05	7.72E-03	M4.4_Not.Determined
A_33_P3223116	HIPK2	7.04	0.61	3.18E-06	4.30E-03	M7.26_Undetermined
A_33_P3247858	MPP1	8.68	0.74	6.06E-05	1.38E-02	M7.33_Undetermined
A_24_P365901	TSPAN33	10.44	0.68	4.89E-06	4.41E-03	M1.1_Platelets
A_24_P123408	ABLIM3	5.40	0.81	9.04E-05	1.72E-02	M1.1_Platelets
A_22_P00005519	lnc-EBF3-6	8.58	0.61	5.14E-04	3.89E-02	NA
A_23_P145238	HIST1H2BK	11.63	0.48	7.45E-04	4.62E-02	M7.16_Not.Determined
A_23_P420831	TRIM10	6.23	0.47	4.97E-04	3.84E-02	M2.3_Erythrocytes|M4.4_Not.Determined
A_33_P3398526	BCL2L11	10.36	0.58	3.37E-05	1.05E-02	NA
A_23_P142631	FKBP1B	8.41	0.71	1.41E-06	3.08E-03	NA
A_23_P210358	LIMS1	10.74	0.50	2.92E-04	3.01E-02	M6.14_Not.Determined|M8.39_Undetermined
A_33_P3337019	LOC728975	9.20	0.62	8.19E-04	4.83E-02	NA
A_23_P104199	ITGB1	10.24	0.39	3.00E-05	9.80E-03	M5.4_Not.Determined|M7.3_Not.Determined
A_23_P202004	PRTFDC1	5.94	0.64	9.21E-05	1.73E-02	M8.18_Undetermined
A_33_P3235400	HDGF	8.96	0.36	5.88E-04	4.16E-02	M4.4_Not.Determined
A_33_P3263666	ANKRD9	10.48	0.63	7.09E-04	4.52E-02	M9.26_Undetermined
A_23_P155979	EGF	6.32	1.01	1.29E-05	6.57E-03	M1.1_Platelets
A_33_P3249414	TRIM58	11.31	0.86	5.00E-05	1.24E-02	NA
A_23_P107612	RAB27B	7.81	0.67	1.04E-05	6.09E-03	M1.1_Platelets|M6.14_Not.Determined
A_23_P152906	ALOX12	8.24	1.01	3.61E-05	1.08E-02	M1.1_Platelets
A_23_P128598	TUBA3C	8.59	0.63	1.15E-05	6.27E-03	NA
A_33_P3232955	F2RL3	8.42	0.72	3.71E-05	1.09E-02	NA
A_33_P3381777	TREML1	9.94	1.09	1.79E-05	7.72E-03	M1.1_Platelets
A_22_P00019581		6.09	0.60	1.67E-04	2.32E-02	NA
A_23_P116264	NRGN	13.88	0.82	3.63E-05	1.08E-02	M1.1_Platelets
A_23_P102731	SMOX	9.95	0.79	9.85E-05	1.79E-02	M7.33_Undetermined
A_33_P3423270	TMEM40	8.15	0.63	3.12E-04	3.08E-02	M1.1_Platelets
A_23_P120435	WFDC3	6.63	0.27	7.73E-04	4.69E-02	NA
A_33_P3342528	P2RY1	7.32	1.06	3.50E-06	4.30E-03	M9.21_Undetermined
A_23_P45304	XK	7.93	0.95	1.08E-04	1.87E-02	M2.3_Erythrocytes
A_23_P25974	TTC7B	9.36	0.89	1.40E-05	6.77E-03	NA
A_23_P217319	FGF13	4.34	0.53	8.40E-05	1.66E-02	M7.29_Not.Determined|M9.15_Undetermined
A_24_P941353	PCYT1B	4.75	0.78	9.40E-05	1.74E-02	NA
A_24_P362540	ASAP2	6.85	0.76	5.74E-05	1.34E-02	M1.1_Platelets
A_19_P00321743	LOC100130938	9.09	1.00	6.41E-07	2.34E-03	NA

A_23_P19987	IGF2BP3	10.13	0.51	5.00E-04	3.85E-02	M7.16_Not.Determined
A_23_P113701	PDGFA	6.98	0.76	8.80E-05	1.70E-02	NA
A_33_P3416097	F13A1	7.57	0.81	1.56E-04	2.26E-02	M1.1_Platelets
A_33_P3343316	SH3BGRL2	7.09	0.76	1.77E-04	2.39E-02	NA
A_24_P40626	GREM2	6.15	0.86	2.15E-04	2.62E-02	NA
A_23_P137856	MUC1	6.88	0.60	1.25E-04	2.01E-02	M7.29_Not.Determined
A_24_P42681	PSMD2	10.04	0.26	9.10E-05	1.72E-02	M6.17_Not.Determined
A_33_P3734384	lnc-MYO1G-1	8.69	0.42	7.04E-04	4.51E-02	NA

Supplementary Table 4. Probes down in 'Metastasis' v 'Unaffected'

ProbeName	GENE_SYMBOL	Avg. log2 exp.	log2 FC	p.value	adjusted. p.value	GeneSets.Modules
A_23_P392470	NR3C2	7.11	-1.11	2.85E-08	8.81E-04	M7.12_Undetermined
A_23_P170679	COL4A3	4.77	-1.05	2.64E-08	8.81E-04	M9.6_Undetermined
A_23_P24922	LIPT2	8.21	-0.82	2.90E-07	1.91E-03	M9.9_Undetermined
A_22_P00005659	LOC101060038	8.00	-0.70	6.70E-04	4.39E-02	NA
A_33_P3227400	COL4A4	6.86	-1.28	7.40E-08	8.81E-04	M9.32_Undetermined
A_33_P3294583	LOC256880	5.00	-0.66	1.32E-07	1.09E-03	NA
A_23_P30163	KLF3-AS1	6.31	-0.88	6.52E-07	2.34E-03	NA
A_33_P3715843	MGC40069	5.52	-0.88	6.67E-07	2.34E-03	NA
A_33_P3272563	NMT2	8.10	-0.69	8.43E-07	2.51E-03	M4.15_T.cells
A_33_P3311971		7.25	-0.72	1.26E-06	2.97E-03	NA
A_32_P324933	LINC00282	5.29	-1.24	1.94E-06	3.62E-03	NA
A_33_P3391796	NOG	7.55	-1.59	6.36E-08	8.81E-04	M8.25_Undetermined
A_21_P0006502	lnc-ZC3H12B-2	10.57	-0.74	6.35E-07	2.34E-03	NA
A_23_P21495	FCGBP	9.57	-0.80	1.91E-04	2.48E-02	M7.12_Undetermined
A_33_P3377239	LOC100270804	8.06	-0.59	2.18E-06	3.63E-03	NA
A_33_P3329737		8.32	-0.78	2.52E-06	3.94E-03	NA
A_21_P0006057		5.07	-1.03	8.92E-08	8.81E-04	NA
A_33_P3329356	lnc-HADH-1	6.64	-1.20	4.71E-08	8.81E-04	NA
A_33_P3346972		7.00	-0.67	5.71E-07	2.34E-03	NA
A_24_P9090	HNRNPDL	11.11	-0.49	5.00E-07	2.34E-03	M5.8_Not.Determined|M6.9_Not.Determined
A_33_P3306948	LRP6	6.25	-0.94	4.65E-06	4.41E-03	NA
A_22_P00014395	LOC102723346	5.07	-0.69	3.24E-06	4.30E-03	NA
A_23_P151059	FAM90A1	5.92	-0.79	1.49E-08	8.81E-04	NA
A_23_P212511	TTC14	10.09	-0.38	8.47E-06	5.57E-03	M9.7_Undetermined
A_22_P00022504	KRT73-AS1	4.25	-0.88	3.10E-07	1.91E-03	NA
A_23_P211244	PRMT2	9.28	-0.60	7.65E-06	5.37E-03	M7.18_Undetermined|M9.17_Undetermined
A_23_P153676	TLE2	8.78	-0.73	6.86E-06	5.08E-03	NA
A_21_P0002980	LOC100506990	7.30	-0.52	1.40E-05	6.77E-03	NA
A_21_P0005923	LOC100506990	7.06	-0.56	3.61E-06	4.30E-03	NA
A_33_P3253792	CXorf67	5.87	-0.68	1.40E-05	6.77E-03	NA
A_33_P3883985	LMF1	10.08	-1.19	6.26E-07	2.34E-03	NA
A_23_P133543	KLHL3	8.82	-0.63	1.14E-05	6.24E-03	M4.1_T.cell
A_23_P209360	KLHL29	7.23	-1.04	4.29E-08	8.81E-04	NA
A_33_P3316313	MTERF4	9.82	-0.43	1.60E-05	7.28E-03	NA
A_22_P00006901	SCARNA10	10.66	-0.57	5.05E-06	4.47E-03	NA
A_23_P254978	TATDN1	7.80	-0.33	1.06E-05	6.09E-03	M5.5_Not.Determined
A_33_P3273490		6.42	-0.57	1.81E-05	7.72E-03	NA
A_33_P3319987	SCML4	7.11	-0.69	1.66E-05	7.41E-03	M9.25_Undetermined
A_21_P0000451	SNORD116-27	6.01	-0.59	8.48E-06	5.57E-03	NA
A_21_P0006503	ZC3H12B	5.69	-0.56	1.96E-05	7.84E-03	M9.11_Undetermined
A_33_P3307253	AK5	6.27	-0.95	2.11E-05	8.10E-03	M9.11_Undetermined
A_23_P120281	EDAR	5.02	-0.88	3.85E-06	4.35E-03	M4.1_T.cell
A_21_P0012654	LOC101928803	9.76	-0.58	1.62E-05	7.30E-03	NA
A_32_P208823	PLXDC1	6.88	-0.69	8.74E-06	5.61E-03	M9.5_Undetermined
A_22_P00000386	KLF3-AS1	5.59	-0.60	3.29E-05	1.04E-02	NA
A_33_P3261408	TMIE	5.37	-0.78	6.26E-06	4.84E-03	NA
A_21_P0000882	RNF157-AS1	5.70	-0.96	4.23E-06	4.38E-03	NA
A_33_P3388618	TNK1	7.82	-0.65	2.84E-05	9.48E-03	NA
A_21_P0005656	LOC100506990	7.57	-0.52	3.72E-05	1.09E-02	NA
A_21_P0005794	lnc-PRAGMIN.1-3	7.39	-0.52	3.53E-05	1.07E-02	NA
A_21_P0013168	XLOC_l2_013267	6.15	-0.70	1.60E-05	7.28E-03	NA

A_21_P0000454	SNORD116-29	5.10	-0.49	2.19E-05	8.13E-03	NA
A_22_P00007532	lnc-HADH-1	6.04	-0.83	6.21E-07	2.34E-03	NA
A_33_P3415888	TEPP	5.06	-0.73	1.67E-06	3.35E-03	NA
A_21_P0012368	XLOC_l2_009639	7.12	-0.71	2.87E-05	9.52E-03	NA
A_22_P00005927	ACTN1-AS1	5.42	-0.62	1.06E-05	6.09E-03	NA
A_33_P3308512	SLC16A10	6.00	-0.71	2.45E-05	8.68E-03	M4.1_T.cell
A_33_P3589722	ATM	10.49	-0.41	1.81E-05	7.72E-03	NA
A_23_P34375	TCEA3	8.50	-0.80	4.19E-05	1.14E-02	M4.1_T.cell
A_22_P00008745	TRAF3IP2-AS1	7.39	-0.77	1.57E-05	7.28E-03	NA
A_21_P0010595	FBXO25	10.26	-0.34	5.16E-05	1.26E-02	NA
A_21_P0000893	IQCH-AS1	6.41	-0.70	7.78E-05	1.58E-02	NA
A_32_P170925	TXNRD3	4.58	-0.53	8.24E-05	1.64E-02	NA
A_33_P3312466	BTNL9	4.77	-0.71	1.95E-05	7.84E-03	NA
A_22_P00024240	lnc-FPGS-1	8.22	-0.61	1.10E-05	6.23E-03	NA
A_33_P3324814	SATB1-AS1	9.84	-0.74	2.60E-05	9.01E-03	NA
A_22_P00007531	LEF1-AS1	8.21	-1.00	3.22E-06	4.30E-03	M9.5_Undetermined
A_21_P0014428	LOC101927372	9.73	-0.54	2.34E-05	8.48E-03	NA
A_21_P0000450	SNORD116-26	6.05	-0.49	6.76E-06	5.04E-03	NA
A_21_P0014024	SATB1-AS1	8.80	-0.62	5.45E-05	1.31E-02	NA
A_21_P0009485	lnc-WDR7-2	4.59	-0.70	1.15E-04	1.93E-02	NA
A_23_P8834	EPHX2	9.67	-1.03	2.23E-05	8.21E-03	M4.1_T.cell
A_22_P00002610	LMF1	5.89	-0.81	4.84E-06	4.41E-03	NA
A_21_P0001480	lnc-C1orf201-2	9.93	-0.70	6.38E-05	1.43E-02	NA
A_23_P428640	PPP1R3E	8.03	-0.59	7.74E-05	1.58E-02	M7.13_Not.Determined
A_23_P306890	POLI	8.44	-0.35	1.44E-04	2.17E-02	NA
A_24_P119685	OBSCN	8.26	-0.74	1.69E-04	2.32E-02	M9.5_Undetermined
A_23_P91001	ASNSD1	12.08	-0.34	1.02E-04	1.84E-02	M6.5_Not.Determined
A_23_P13364	NUCB2	10.99	-0.44	8.82E-06	5.61E-03	M5.6_Mitochondrial.Stress/Proteasome
A_21_P0012456	LOC101927056	5.26	-0.40	5.78E-05	1.34E-02	NA
A_23_P342709	FBXO15	6.45	-0.63	3.41E-06	4.30E-03	NA
A_21_P0003911	lnc-DCTD-1	7.39	-0.52	2.59E-04	2.82E-02	NA
A_33_P3321657	HSPG2	7.58	-0.55	7.80E-04	4.71E-02	NA
A_24_P196592	MMP28	6.93	-0.56	4.16E-06	4.38E-03	NA
A_21_P0014339	lnc-AC009113.1-1	6.19	-0.88	1.33E-06	2.97E-03	NA
A_24_P169092	MAML2	7.54	-0.55	1.14E-05	6.24E-03	NA
A_33_P3313810	CELA1	6.78	-0.91	9.23E-07	2.67E-03	M9.9_Undetermined
A_33_P3357591	ATHL1	8.07	-0.45	6.50E-04	4.35E-02	M8.44_Undetermined
A_21_P0000891	SDCBP2-AS1	6.40	-0.33	1.71E-04	2.34E-02	NA
A_33_P3294459	COPG2IT1	5.29	-0.74	2.42E-04	2.76E-02	NA
A_33_P3280801	LMO7	6.57	-0.40	3.52E-04	3.25E-02	NA
A_33_P3228807	SPEG	5.26	-0.57	4.33E-04	3.59E-02	M9.5_Undetermined
A_23_P417282	IGF1R	10.06	-0.69	4.04E-05	1.13E-02	M5.14_Not.Determined|M9.34_Undetermined
A_33_P3217495	SLC5A2	6.24	-0.39	3.06E-04	3.06E-02	NA
A_33_P3404546	OBSCN	7.15	-0.52	8.89E-05	1.71E-02	M9.5_Undetermined
A_24_P273157	OBSCN	7.02	-0.58	2.59E-04	2.82E-02	M9.5_Undetermined
A_23_P423457	SERINC5	8.61	-0.40	1.57E-04	2.27E-02	NA
A_24_P678104	STMN3	9.26	-0.50	1.02E-04	1.84E-02	M4.1_T.cell|M9.12_Undetermined
A_33_P3299329		6.42	-0.52	3.80E-04	3.36E-02	NA
A_24_P252364	NRCAM	5.31	-1.26	3.35E-06	4.30E-03	M9.11_Undetermined
A_21_P0008352	lnc-EXD2-1	6.85	-0.85	8.83E-06	5.61E-03	NA
A_32_P183904	SHF	4.42	-0.44	3.07E-04	3.06E-02	NA
A_33_P3301514	NRCAM	5.06	-0.64	2.83E-05	9.48E-03	M9.11_Undetermined
A_22_P00000382	KRT73-AS1	7.04	-0.81	1.04E-05	6.09E-03	NA
A_21_P0013532	XLOC_l2_014098	6.30	-0.34	4.71E-04	3.72E-02	NA
A_23_P33984	TMEM27	4.60	-0.34	4.65E-04	3.72E-02	NA
A_23_P211212	COL18A1	10.62	-0.93	2.63E-04	2.83E-02	M5.14_Not.Determined
A_22_P00000284	lnc-AC009113.1-1	6.40	-0.66	3.93E-06	4.36E-03	NA
A_33_P3337485	CD248	5.53	-0.72	1.50E-04	2.21E-02	M4.1_T.cell
A_23_P116743	LINC01089	12.40	-0.44	2.61E-04	2.82E-02	M5.11_Not.Determined|M9.19_Undetermined
A_33_P3272330	DNMT3A	10.13	-0.47	4.61E-04	3.71E-02	M9.3_Undetermined|M9.7_Undetermined
A_23_P64058	RASGRP2	15.05	-0.37	3.26E-04	3.17E-02	M6.10_Not.Determined
A_22_P00002090	HULC	4.22	-0.51	1.73E-04	2.36E-02	NA
A_33_P3256031		6.89	-0.56	5.02E-04	3.86E-02	NA
A_24_P943922	CACHD1	4.09	-0.49	3.87E-04	3.40E-02	M9.11_Undetermined
A_21_P0000020	RBM19	10.47	-0.30	7.61E-04	4.67E-02	NA

A_21_P0014136		5.27	-0.49	8.05E-05	1.62E-02	NA
A_23_P338233	BCDIN3D	7.97	-0.45	6.76E-05	1.48E-02	M7.24_Undetermined
A_23_P33607	TEFM	7.62	-0.32	1.46E-04	2.18E-02	NA
A_23_P501372	MIEF2	7.84	-0.41	2.08E-06	3.62E-03	NA
A_24_P548060		6.77	-0.75	1.39E-04	2.14E-02	NA
A_33_P3235731	LOC101930072	4.95	-0.43	4.22E-04	3.56E-02	NA
A_23_P403335	EXPH5	6.81	-0.58	4.50E-05	1.18E-02	NA
A_21_P0008620	SRP14-AS1	5.85	-0.33	2.74E-05	9.37E-03	NA
A_23_P252700	UNC50	9.74	-0.24	6.60E-04	4.37E-02	M7.8_Undetermined
A_22_P00008837		7.32	-0.72	2.95E-04	3.02E-02	NA
A_33_P3423425	ZNF770	9.69	-0.36	3.74E-05	1.09E-02	NA
A_33_P3439765	ZC3H14	10.41	-0.32	1.11E-05	6.24E-03	M5.5_Not.Determined
A_22_P00022427	NUPR1L	4.71	-0.69	3.50E-05	1.07E-02	NA
A_33_P3299872	HINT3	10.41	-0.45	2.02E-05	7.91E-03	M7.16_Not.Determined
A_33_P3418417	SLC3A1	4.09	-0.55	1.34E-04	2.10E-02	NA
A_33_P3366850		6.33	-0.61	2.57E-04	2.82E-02	NA
A_22_P00013300		4.19	-0.48	4.96E-05	1.23E-02	NA
A_33_P3387365	PXMP4	6.66	-0.63	2.95E-05	9.69E-03	NA
A_23_P72770	USP44	4.62	-0.60	1.64E-05	7.38E-03	NA
A_33_P3387771	USP9X	7.65	-0.36	5.14E-04	3.89E-02	M5.1_Inflammation
A_32_P231493	DOCK9-AS2	7.42	-0.59	1.41E-04	2.16E-02	NA
A_23_P383118	ZSWIM5	5.12	-0.61	2.44E-04	2.78E-02	NA
A_33_P3359543	ZNF561	8.86	-0.34	9.75E-05	1.78E-02	NA
A_33_P3289422	ZNF765	8.82	-0.43	2.79E-04	2.93E-02	NA
A_23_P134814	THAP1	8.71	-0.44	4.79E-06	4.41E-03	M5.4_Not.Determined|M7.3_Not.Determined
A_23_P252100	TAS2R5	4.23	-0.47	4.36E-05	1.16E-02	NA
A_21_P0001023	SDHC	4.87	-0.75	2.67E-06	4.10E-03	M5.13_Not.Determined|M7.11_Undetermined|
A_33_P3229161	UTP14C	7.20	-0.32	7.33E-04	4.58E-02	NA
A_21_P0014623	SNHG21	9.18	-0.40	6.21E-06	4.84E-03	NA
A_24_P82957	RNF114	9.52	-0.30	1.94E-04	2.50E-02	M7.3_Not.Determined
A_33_P3258191	C16orf91	10.49	-0.36	1.40E-04	2.15E-02	M5.10_Mitochondrial.Respiration
A_33_P3263170	SNRPG	13.90	-0.26	2.36E-04	2.75E-02	M6.2_Mitochondrial.Respiration
A_24_P274831	GIMAP7	12.32	-0.61	2.16E-05	8.10E-03	M5.5_Not.Determined
A_22_P00017623	SNHG21	8.19	-0.29	1.13E-04	1.92E-02	NA
A_23_P31135	ACAT2	10.49	-0.27	7.85E-05	1.59E-02	M3.5_Cell.Cycle
A_32_P46765	C12orf29	7.60	-0.47	3.38E-06	4.30E-03	M4.7_Cell.Cycle
A_23_P356554	BAG2	7.96	-0.68	9.85E-08	8.81E-04	NA
A_22_P00016432	lnc-TMEM35-1	4.26	-0.32	1.58E-04	2.27E-02	NA
A_33_P3412055	ZNF582	4.40	-0.47	4.88E-05	1.21E-02	NA
A_22_P00014909	TPBGL	5.94	-0.73	6.13E-05	1.39E-02	NA
A_33_P3344816	ZNF813	6.21	-0.35	7.08E-04	4.52E-02	NA
A_23_P94095	ANKRD46	6.36	-0.52	2.69E-04	2.85E-02	M4.7_Cell.Cycle
A_23_P380815	KIAA1279	7.35	-0.38	7.76E-04	4.69E-02	M5.6_Mitochondrial.Stress/Proteasome
A_23_P58877	GOPC	8.85	-0.44	7.39E-05	1.54E-02	M6.7_Not.Determined
A_32_P104432	LINC00087	7.04	-0.92	5.77E-08	8.81E-04	NA
A_23_P128663	SACS	8.72	-0.43	2.62E-04	2.82E-02	M9.28_Undetermined
A_23_P417383	ASPRV1	8.39	-0.48	1.44E-05	6.89E-03	M5.12_Interferon
A_21_P0008949		4.72	-0.74	2.99E-05	9.80E-03	NA
A_33_P3369939	DNAJC21	7.68	-0.24	2.00E-04	2.54E-02	NA
A_23_P501080	ZNF92	9.97	-0.32	2.70E-04	2.85E-02	NA
A_23_P19322	SAYSD1	8.14	-0.35	2.48E-04	2.78E-02	M7.24_Undetermined
A_23_P65068	EID3	9.01	-0.36	1.74E-04	2.36E-02	M7.25_Undetermined
A_22_P00015597	STXBP5	7.91	-0.73	2.33E-07	1.77E-03	M5.7_Inflammation
A_24_P372217	ERLIN2	7.05	-0.26	6.46E-04	4.34E-02	M6.17_Not.Determined|M9.14_Undetermined
A_24_P791669	ZNF879	5.17	-0.49	3.97E-05	1.12E-02	NA
A_22_P00018831	lnc-PPM1D-1	4.65	-0.45	1.37E-04	2.13E-02	NA
A_23_P115824	HNRNPH3	11.19	-0.28	3.69E-05	1.09E-02	M7.3_Not.Determined
A_24_P51061	DCBLD2	4.59	-0.73	2.97E-07	1.91E-03	NA
A_24_P379693	DNPEP	7.37	-0.36	1.74E-05	7.64E-03	M5.10_Mitochondrial.Respiration
A_23_P29575	MRPS36	12.22	-0.24	1.11E-04	1.91E-02	M9.46_Undetermined
A_33_P3301940	PDE7B	4.21	-0.63	5.46E-05	1.31E-02	M9.12_Undetermined
A_24_P89911	NAIF1	9.49	-0.35	8.47E-05	1.67E-02	M9.18_Undetermined
A_33_P3261818	MDH1	11.82	-0.24	7.38E-04	4.60E-02	M5.10_Mitochondrial.Respiration
A_24_P59607	C17orf51	7.29	-0.73	3.67E-06	4.30E-03	NA
A_32_P219116	CENPJ	8.00	-0.37	7.98E-04	4.76E-02	M7.7_Undetermined

A_22_P00002833	lnc-C2orf78-1	4.79	-0.51	8.51E-04	4.94E-02	NA
A_23_P435697	EDRF1	7.89	-0.50	1.70E-06	3.35E-03	M6.5_Not.Determined
A_23_P309850	RPUSD2	11.05	-0.50	3.20E-06	4.30E-03	M4.12_Not.Determined
A_33_P3257187	PRKAA1	6.92	-0.35	1.63E-04	2.30E-02	M5.1_Inflammation
A_24_P406245		7.14	-0.33	8.33E-04	4.88E-02	NA
A_32_P150876	LINC00667	7.68	-0.40	2.08E-04	2.58E-02	NA
A_32_P145010	LOC729683	9.36	-0.55	7.75E-07	2.43E-03	NA
A_24_P326739	GLS2	5.05	-0.73	3.35E-05	1.05E-02	NA
A_33_P3379492	LOC100131581	4.90	-0.45	4.69E-05	1.19E-02	NA
A_22_P00012831	lnc-RASA1-3	7.14	-0.32	2.10E-04	2.59E-02	NA
A_23_P320159	TCEANC	8.62	-0.41	1.84E-05	7.72E-03	NA
A_24_P268893	THAP6	7.13	-0.32	2.87E-04	2.98E-02	M6.3_Not.Determined
A_21_P0005447	PAXIP1-AS1	7.12	-0.38	3.74E-05	1.09E-02	NA
A_33_P3407638	ARL14EP	9.99	-0.38	2.08E-04	2.58E-02	NA
A_33_P3369079	CHKB-AS1	5.69	-0.52	2.04E-04	2.56E-02	NA
A_33_P3256902		12.02	-0.29	4.42E-04	3.62E-02	NA
A_23_P501435	CSRP2BP	9.68	-0.57	2.26E-04	2.68E-02	M7.11_Undetermined|M9.6_Undetermined
A_33_P3221234	IPP	5.15	-0.37	5.93E-04	4.16E-02	NA
A_21_P0001781	LOC101927156	5.03	-0.54	9.41E-05	1.74E-02	NA
A_24_P40907	PPAPDC2	6.35	-0.60	3.09E-05	9.95E-03	M8.74_Undetermined
A_24_P15898	C1orf145	4.38	-0.62	1.20E-06	2.97E-03	NA
A_33_P3369461	AMIGO1	8.18	-0.81	3.95E-06	4.36E-03	NA
A_23_P69877	ZFP62	10.60	-0.52	3.61E-05	1.08E-02	NA
A_23_P46819	BTRC	6.74	-0.37	1.55E-04	2.26E-02	M9.2_Undetermined
A_32_P326819	KRR1	6.32	-0.24	6.74E-04	4.41E-02	M7.28_Undetermined
A_23_P9662	IPP	7.07	-0.43	1.81E-04	2.42E-02	NA
A_23_P162127	CCDC90B	10.40	-0.32	4.76E-04	3.74E-02	M5.2_Not.Determined
A_24_P759674	OBFC1	6.80	-0.48	3.40E-04	3.21E-02	M7.11_Undetermined|M9.6_Undetermined
A_22_P00025612	LINC01395	4.75	-0.64	5.28E-05	1.29E-02	NA
A_24_P98161	KRIT1	4.51	-0.28	8.40E-04	4.91E-02	NA
A_23_P403521	YAE1D1	6.63	-0.50	7.48E-04	4.62E-02	M5.6_Mitochondrial.Stress/Proteasome
A_22_P00012945		5.97	-0.65	7.24E-06	5.24E-03	NA
A_22_P00003080	lnc-C8orf56-1	4.28	-0.49	8.88E-05	1.71E-02	NA
A_22_P00013894	HCG25	6.37	-0.26	7.77E-04	4.70E-02	NA
A_23_P200216	MAGOH	11.05	-0.19	5.23E-04	3.91E-02	M5.13_Not.Determined
A_23_P328766	ZNF519	6.43	-0.39	1.69E-04	2.32E-02	M9.46_Undetermined
A_24_P137434	DCBLD2	4.62	-0.86	5.71E-07	2.34E-03	NA
A_33_P3285639	TSGA10	4.70	-0.49	7.36E-05	1.54E-02	M8.8_Undetermined
A_23_P17103	TSGA10	5.02	-0.54	2.92E-04	3.01E-02	M8.8_Undetermined
A_24_P372553	EDRF1	6.90	-0.45	1.49E-05	7.06E-03	M6.5_Not.Determined
A_21_P0014057	lnc-RGS5-1	5.76	-0.67	1.07E-04	1.87E-02	NA
A_32_P109604	ANKRD20A12P	4.14	-0.62	3.01E-04	3.04E-02	NA
A_23_P10870	DOLK	7.24	-0.44	1.66E-05	7.41E-03	M6.12_Mitochondrial.Stress
A_23_P85188	ARMCX5	9.26	-0.30	2.41E-04	2.76E-02	M7.12_Undetermined|M9.2_Undetermined
A_22_P00009553	lnc-MAP3K3-1	5.56	-0.60	3.60E-06	4.30E-03	NA
A_33_P3419460	VAPA	5.65	-0.33	2.01E-04	2.54E-02	M7.2_Not.Determined|M8.52_Undetermined
A_23_P62840	YRDC	11.75	-0.26	1.22E-04	2.00E-02	NA
A_33_P3351101	TYSND1	6.39	-0.77	1.67E-06	3.35E-03	M7.24_Undetermined
A_33_P3413335		7.67	-0.50	8.90E-05	1.71E-02	NA
A_23_P42738	FAM220A	8.35	-0.43	2.67E-04	2.85E-02	M6.7_Not.Determined
A_33_P3264416		7.11	-0.55	3.60E-05	1.08E-02	NA
A_23_P356139	FAM178A	5.25	-0.41	7.94E-04	4.75E-02	M6.4_Not.Determined
A_33_P3306679	PLEKHG7	4.90	-0.64	1.23E-05	6.52E-03	NA
A_22_P00024074	LOC101927531	3.87	-0.50	1.90E-04	2.48E-02	NA
A_23_P50217	ZNF671	9.92	-0.36	2.89E-04	2.99E-02	M4.12_Not.Determined
A_22_P00023027	lnc-UTS2D-1	4.66	-0.64	7.01E-05	1.49E-02	NA
A_22_P00015387	lnc-SREK1-2	4.11	-0.82	1.20E-06	2.97E-03	NA
A_33_P3369520	MAGI3	5.39	-0.58	4.28E-04	3.59E-02	NA
A_33_P3285235	ZNF507	5.84	-0.37	6.01E-04	4.18E-02	NA
A_23_P163117	C14orf169	10.23	-0.48	2.13E-06	3.62E-03	M7.5_Undetermined
A_33_P3250953	SLC35B4	7.07	-0.46	2.00E-04	2.54E-02	NA
A_22_P00025125	lnc-FAM98A-1	4.99	-0.53	5.90E-04	4.16E-02	NA
A_23_P80643	SETMAR	8.37	-0.48	1.31E-04	2.07E-02	NA
A_24_P419300	PP7080	8.65	-0.54	7.99E-06	5.50E-03	M8.40_Undetermined
A_24_P652502		5.61	-0.57	2.00E-05	7.90E-03	NA

A_19_P00319698		6.09	-0.49	5.98E-04	4.17E-02	NA
A_21_P0014652	lnc-STX3-2	6.07	-0.28	6.53E-04	4.35E-02	NA
A_23_P133359	ZFP2	5.04	-0.60	2.17E-04	2.64E-02	NA
A_23_P77714	CLUAP1	7.84	-0.44	7.44E-04	4.61E-02	M6.19_Not.Determined|M7.25_Undetermined|
A_23_P411612	SPRYD4	8.54	-0.43	6.91E-05	1.48E-02	M9.9_Undetermined
A_23_P123905	EXOSC3	7.91	-0.27	1.59E-04	2.27E-02	M7.8_Undetermined
A_22_P00020742	LOC101928101	4.98	-0.56	8.32E-05	1.65E-02	NA
A_24_P193295	RAB15	8.91	-0.83	1.04E-05	6.09E-03	M9.11_Undetermined
A_22_P00006058	LINC00087	5.89	-0.74	2.09E-06	3.62E-03	NA
A_33_P3368555	AHSA2	6.95	-0.29	1.64E-04	2.30E-02	M7.2_Not.Determined
A_23_P135465	HARBI1	7.91	-0.51	6.68E-04	4.39E-02	NA
A_23_P379034	BAIAP2L2	8.27	-0.42	3.30E-04	3.18E-02	M9.5_Undetermined
A_21_P0012500		4.00	-0.50	9.16E-05	1.72E-02	NA
A_22_P00005575		11.54	-0.39	1.30E-05	6.57E-03	NA
A_22_P00001976	LOC101928714	4.92	-0.74	6.06E-06	4.81E-03	NA
A_33_P3402763	NIFK	9.56	-0.30	8.09E-05	1.62E-02	M4.7_Cell.Cycle
A_33_P3321993		4.63	-0.45	3.88E-04	3.40E-02	NA
A_23_P348146	SLAIN1	7.84	-0.39	4.39E-04	3.62E-02	M4.7_Cell.Cycle
A_24_P252078	BTN3A2	10.69	-1.00	3.63E-04	3.29E-02	M5.4_Not.Determined|M6.10_Not.Determined
A_21_P0008284	LINC01550	4.84	-0.47	1.82E-04	2.42E-02	NA
A_23_P40989	USP13	6.54	-0.47	1.18E-04	1.96E-02	M9.27_Undetermined
A_21_P0006615		4.74	-0.77	1.03E-04	1.85E-02	NA
A_33_P3311668		4.58	-0.45	3.68E-04	3.31E-02	NA
A_23_P210829	PCMTD2	8.30	-0.44	1.09E-04	1.88E-02	M7.17_Undetermined
A_21_P0004295	CDC42SE2	5.48	-0.52	2.16E-05	8.10E-03	M5.4_Not.Determined
A_23_P342000	RBM11	5.35	-0.70	2.40E-05	8.58E-03	M9.19_Undetermined
A_22_P00003766		8.27	-0.55	3.40E-05	1.05E-02	NA
A_24_P316430	NT5E	4.45	-0.50	3.60E-04	3.29E-02	M9.11_Undetermined
A_21_P0001771	LINC00954	6.68	-0.49	8.99E-05	1.71E-02	M7.13_Not.Determined
A_32_P226858		12.64	-0.38	2.71E-04	2.86E-02	NA
A_22_P00015933	LOC101929132	4.77	-0.51	2.82E-05	9.48E-03	NA
A_33_P3235611	SLC46A1	5.68	-0.74	1.16E-04	1.94E-02	NA
A_24_P349616	UBTF	8.21	-0.37	5.84E-05	1.35E-02	M9.3_Undetermined
A_24_P254084	ZNF69	4.81	-0.32	8.44E-04	4.92E-02	NA
A_23_P37391	CCDC85C	6.74	-0.43	5.68E-04	4.12E-02	M8.40_Undetermined
A_23_P133386	RASGRF2	5.94	-0.69	1.55E-05	7.25E-03	NA
A_33_P3228868		5.45	-0.48	3.07E-04	3.06E-02	NA
A_24_P93754	KDM4C	5.94	-0.43	2.31E-04	2.70E-02	M8.8_Undetermined
A_21_P0010939	SLC9B1	4.79	-0.68	1.26E-05	6.53E-03	NA
A_33_P3312807	IPW	5.96	-0.56	3.93E-05	1.11E-02	NA
A_33_P3807593	LOC286437	10.51	-0.37	2.85E-05	9.48E-03	NA
A_32_P204239	CDHR3	4.74	-0.53	3.68E-04	3.31E-02	NA
A_21_P0013652	XLOC_l2_015213	5.21	-0.40	5.24E-04	3.92E-02	NA
A_33_P3447441	lnc-WDR1-1	10.58	-0.36	6.88E-04	4.45E-02	NA
A_21_P0004274	lnc-RASA1-3	7.46	-0.72	4.50E-05	1.18E-02	NA
A_24_P283324	ALDH8A1	5.65	-0.49	7.90E-04	4.74E-02	NA
A_23_P144999	RAPGEF6	8.69	-0.43	5.68E-04	4.12E-02	M5.5_Not.Determined
A_23_P394166	CNOT7	10.04	-0.22	8.69E-04	4.99E-02	M6.7_Not.Determined|M7.5_Undetermined
A_23_P143474	ATP5O	14.76	-0.17	5.49E-04	4.04E-02	M6.2_Mitochondrial.Respiration
A_33_P3399363	GPR155	8.78	-0.48	6.15E-04	4.23E-02	M7.14_Undetermined
A_33_P3339336	FAM86FP	5.36	-0.39	5.70E-04	4.13E-02	NA
A_33_P3305780	CCNI2	5.00	-0.40	4.71E-04	3.73E-02	NA
A_22_P00017466	lnc-VSIG2-1	4.92	-0.45	1.46E-04	2.18E-02	NA
A_33_P3323842	BDNF-AS	5.01	-0.54	4.33E-04	3.59E-02	NA
A_33_P3403773	ZNF569	8.32	-0.47	7.65E-04	4.67E-02	NA
A_33_P3324786	TCFL5	6.62	-0.32	1.55E-04	2.25E-02	M7.3_Not.Determined
A_22_P00023397	lnc-TMEM159-2	6.02	-0.58	2.47E-04	2.78E-02	NA
A_33_P3266444	MRPS25	8.23	-0.37	7.15E-05	1.51E-02	M5.11_Not.Determined
A_23_P166716	TRMT10C	11.39	-0.40	4.76E-04	3.74E-02	M5.6_Mitochondrial.Stress/Proteasome
A_24_P302574	OSGEPL1	7.38	-0.50	2.36E-04	2.75E-02	M7.12_Undetermined
A_21_P0012663	XLOC_l2_011102	5.79	-0.72	3.71E-05	1.09E-02	NA
A_23_P389692	KIAA1328	5.64	-0.73	1.84E-05	7.72E-03	NA
A_32_P357301	PPHLN1	5.21	-0.52	7.64E-05	1.57E-02	M6.7_Not.Determined|M9.28_Undetermined
A_22_P00024159	lnc-GAMT-1	4.25	-0.47	1.22E-04	2.00E-02	NA
A_19_P00321597	LINC01550	6.41	-0.95	8.97E-06	5.66E-03	NA

A_21_P0000840	PXN-AS1	5.33	-0.34	2.99E-04	3.03E-02	NA
A_23_P202170	MGEA5	14.24	-0.30	7.09E-04	4.52E-02	M7.2_Not.Determined
A_23_P135357	RNMTL1	9.29	-0.33	6.10E-04	4.21E-02	M4.12_Not.Determined
A_33_P3311770	ZNF789	8.16	-0.39	4.05E-04	3.50E-02	M5.11_Not.Determined
A_21_P0008484	LINC01550	8.49	-0.86	4.05E-06	4.38E-03	NA
A_23_P422766	KLHDC1	6.21	-0.54	2.16E-04	2.63E-02	M7.12_Undetermined
A_23_P12336	PRMT6	7.07	-0.47	7.02E-04	4.51E-02	M6.9_Not.Determined
A_21_P0000118	LEKR1	4.05	-0.48	3.38E-04	3.20E-02	NA
A_23_P258190	AKR1B1	10.27	-0.27	6.11E-04	4.22E-02	M3.5_Cell.Cycle
A_24_P93741	RFT1	8.34	-0.35	7.29E-04	4.57E-02	NA
A_23_P320530	ZNF780A	4.98	-0.40	5.36E-04	3.98E-02	NA
A_23_P250212	SGK223	9.78	-1.00	5.29E-05	1.29E-02	M4.1_T.cell
A_32_P100258	FLJ37453	9.89	-0.30	2.67E-04	2.85E-02	NA
A_33_P3234202	DNASE1L3	6.60	-0.62	2.84E-04	2.96E-02	M9.30_Undetermined
A_24_P184799	COCH	5.18	-0.61	8.50E-04	4.93E-02	M9.17_Undetermined
A_24_P347480	NEK9	10.21	-0.51	1.94E-04	2.50E-02	NA
A_22_P00015880	lnc-TC2N-1	8.19	-0.89	6.94E-05	1.48E-02	NA
A_23_P82047	STXBP5	5.94	-0.45	3.28E-04	3.18E-02	M5.7_Inflammation
A_33_P3383261	SIKE1	10.16	-0.26	4.56E-04	3.68E-02	M9.21_Undetermined
A_33_P3259135	NSG1	7.51	-1.11	3.92E-05	1.11E-02	M4.1_T.cell
A_21_P0014835		4.12	-0.47	7.19E-05	1.51E-02	NA
A_33_P3283213	MGC57346	5.29	-0.38	5.08E-04	3.88E-02	M6.15_Not.Determined
A_21_P0010084	LOC100270804	8.76	-0.57	1.30E-06	2.97E-03	NA
A_33_P3210139	PCF11	11.34	-0.41	5.46E-04	4.03E-02	M6.3_Not.Determined
A_21_P0014589	LOC101929112	5.68	-0.39	8.22E-04	4.84E-02	NA
A_33_P3315410	COIL	10.82	-0.36	1.64E-04	2.30E-02	M5.5_Not.Determined
A_21_P0008877	LINC01569	5.03	-0.40	8.67E-04	4.99E-02	NA
A_33_P3357097	LOC100132741	6.99	-0.47	4.65E-05	1.19E-02	NA
A_21_P0000668	ADAM1A	7.31	-0.62	4.70E-05	1.19E-02	NA
A_24_P277295	RAB43	11.44	-0.34	1.25E-04	2.01E-02	M8.88_Undetermined|M9.22_Undetermined
A_33_P3385750	ZNF793	5.85	-0.75	3.10E-04	3.06E-02	NA
A_23_P387523	ZBTB40	11.10	-0.34	3.26E-04	3.17E-02	M8.54_Undetermined
A_33_P3334220	ACACB	8.52	-0.62	4.27E-05	1.15E-02	M7.13_Not.Determined
A_24_P186124	MTERF4	10.52	-0.48	2.98E-06	4.30E-03	NA
A_32_P146659	ATP6V0E2-AS1	5.79	-1.27	5.27E-06	4.52E-03	NA
A_33_P3248992	ACADSB	9.74	-0.51	1.60E-04	2.28E-02	NA
A_21_P0010461	LOC101928824	5.16	-0.28	1.71E-04	2.34E-02	NA
A_23_P205738	BCL11B	12.29	-0.66	3.85E-05	1.11E-02	M4.1_T.cell
A_19_P00803019		7.85	-0.88	1.25E-05	6.53E-03	NA
A_23_P255805	ZNF7	8.16	-0.33	6.51E-04	4.35E-02	M6.7_Not.Determined
A_33_P3305655	NBEAP1	4.52	-0.43	3.33E-04	3.19E-02	NA
A_23_P93499	TFB1M	8.36	-0.53	1.41E-04	2.15E-02	M8.5_Undetermined
A_23_P59855	ZNF138	6.60	-0.63	5.17E-06	4.52E-03	M9.6_Undetermined
A_23_P255076	RWDD2A	7.42	-0.47	1.29E-04	2.05E-02	M6.12_Mitochondrial.Stress
A_23_P129358	SETD6	8.52	-0.36	1.16E-04	1.95E-02	M8.32_Undetermined
A_23_P34568	ADPRHL2	8.73	-0.30	6.08E-04	4.20E-02	M7.21_Undetermined
A_23_P357248	ZNF343	4.56	-0.42	5.17E-04	3.90E-02	M8.40_Undetermined
A_24_P208737	GHRLOS	8.94	-0.47	2.28E-04	2.69E-02	NA
A_23_P90911	RDH14	9.67	-0.36	1.04E-04	1.85E-02	NA
A_23_P7562	ACSL6	7.66	-0.52	4.41E-05	1.17E-02	M6.18_Erythrocytes
A_33_P3628409	PKI55	7.41	-0.55	1.03E-04	1.85E-02	NA
A_21_P0012912	ANKRD31	4.56	-0.61	4.39E-06	4.41E-03	NA
A_23_P125717	NAP1L3	6.28	-0.57	1.47E-04	2.19E-02	M8.58_Undetermined
A_23_P126605	TMOD4	5.79	-0.73	7.36E-05	1.54E-02	M9.5_Undetermined
A_23_P7402	PDZD2	4.44	-0.54	4.72E-05	1.20E-02	NA
A_21_P0007814		4.87	-0.37	6.62E-04	4.38E-02	NA
A_21_P0014090	LOC101927055	4.52	-0.68	8.20E-05	1.63E-02	NA
A_23_P58443	ANKHD1-EIF4EBP3	9.72	-0.23	3.75E-04	3.34E-02	NA
A_23_P93750	LSM5	10.80	-0.28	4.08E-05	1.13E-02	M6.12_Mitochondrial.Stress
A_21_P0006454	lnc-ACRC-1	6.65	-0.74	1.05E-05	6.09E-03	NA
A_23_P35645	RBM17	11.60	-0.25	4.74E-04	3.74E-02	M5.5_Not.Determined
A_33_P3263317		5.32	-0.75	4.28E-06	4.38E-03	NA
A_23_P157679	UTP23	11.01	-0.26	2.49E-04	2.78E-02	M8.54_Undetermined
A_32_P18159	LYRM7	5.64	-0.41	2.27E-04	2.69E-02	M7.12_Undetermined
A_24_P61772	TBC1D27	4.65	-0.38	2.80E-04	2.93E-02	NA

A_22_P00012878	LOC102723373	5.00	-0.56	1.05E-04	1.86E-02	NA
A_21_P0010430	lnc-MAPK8IP2-1	6.15	-0.77	1.25E-04	2.01E-02	NA
A_22_P00022896	LOC101927596	8.49	-0.79	3.98E-04	3.46E-02	NA
A_21_P0000857	MORF4L2-AS1	4.88	-0.53	5.92E-05	1.36E-02	NA
A_23_P154840	SOD1	14.58	-0.29	6.40E-04	4.32E-02	M8.73_Undetermined
A_32_P132317	GPR155	8.80	-0.58	3.22E-04	3.14E-02	M7.14_Undetermined
A_23_P115861	ZNF485	5.20	-0.48	6.32E-04	4.29E-02	M6.19_Not.Determined
A_32_P36046	C2orf68	8.62	-0.36	5.16E-04	3.89E-02	NA
A_33_P3300117		5.97	-0.42	8.52E-06	5.57E-03	NA
A_23_P321034	INADL	5.71	-0.46	5.95E-04	4.17E-02	NA
A_32_P134209	ACVR2B	5.75	-0.61	2.06E-04	2.58E-02	NA
A_22_P00023318	lnc-TPX2-1	5.15	-0.56	3.57E-05	1.08E-02	NA
A_23_P92362	NDUFC1	12.85	-0.22	7.36E-04	4.60E-02	M5.6_Mitochondrial.Stress/Proteasome
A_22_P00009378		5.02	-0.44	1.30E-05	6.57E-03	NA
A_23_P92012	TSEN2	7.28	-0.48	2.46E-04	2.78E-02	NA
A_33_P3261927	ZNF789	8.05	-0.38	1.96E-04	2.51E-02	M5.11_Not.Determined
A_21_P0004683		4.69	-0.44	1.70E-04	2.33E-02	NA
A_33_P3281403	TRAF3IP3	12.45	-0.57	1.06E-05	6.09E-03	M5.5_Not.Determined
A_22_P00013415	LINC01550	7.80	-0.89	9.39E-05	1.74E-02	NA
A_23_P369328	C10orf35	7.99	-0.80	7.24E-05	1.52E-02	NA
A_24_P97001	PRPF38A	10.69	-0.27	1.44E-04	2.17E-02	M5.10_Mitochondrial.Respiration|
A_23_P143047	ATP6V1E2	7.89	-0.57	4.13E-04	3.54E-02	M5.5_Not.Determined
A_19_P00320727	LOC101927237	4.88	-0.68	2.93E-04	3.01E-02	NA
A_33_P3256391	CRB3	5.90	-0.60	4.28E-06	4.38E-03	NA
A_22_P00021589	LOC101927837	4.59	-0.55	3.39E-04	3.20E-02	NA
A_22_P00006379		5.91	-0.46	5.53E-04	4.06E-02	NA
A_33_P3326256	MRPS16	8.90	-0.20	4.68E-04	3.72E-02	NA
A_22_P00009172	LOC100507577	11.03	-0.32	3.38E-04	3.20E-02	NA
A_19_P00328886	TUG1	6.12	-0.44	1.16E-04	1.94E-02	NA
A_23_P153524	C19orf73	6.52	-0.55	2.19E-04	2.65E-02	NA
A_23_P143374	NINL	7.13	-0.70	2.78E-05	9.44E-03	NA
A_23_P305877	TMEM261	5.81	-0.47	4.10E-05	1.13E-02	NA
A_21_P0006666		4.21	-0.59	9.68E-05	1.78E-02	NA
A_32_P93852	BOD1	8.50	-0.33	2.23E-04	2.67E-02	M4.3_Protein.Synthesis
A_24_P284584	ZNF559	5.78	-0.52	6.30E-04	4.29E-02	M4.7_Cell.Cycle
A_32_P60223	ING5	8.74	-0.36	4.37E-04	3.62E-02	M9.2_Undetermined
A_22_P00021130	lnc-TFB1M-1	5.30	-0.64	1.36E-04	2.12E-02	NA
A_33_P3365750	EML5	5.58	-0.54	2.16E-05	8.10E-03	NA
A_23_P149375	THEM4	8.47	-0.66	9.55E-05	1.76E-02	NA
A_33_P3227944	CRHR1-IT1	8.81	-0.53	2.32E-04	2.71E-02	NA
A_23_P323761	TRAF3IP3	13.33	-0.54	2.73E-05	9.37E-03	M5.5_Not.Determined
A_23_P205867	NR2E3	5.06	-0.42	6.92E-04	4.46E-02	NA
A_21_P0008485	LINC01550	6.62	-0.75	2.57E-05	8.94E-03	NA
A_23_P163278	PARP16	8.41	-0.46	2.03E-05	7.91E-03	M8.20_Undetermined
A_23_P169838	SUN1	9.92	-0.31	2.66E-04	2.84E-02	M4.7_Cell.Cycle
A_21_P0012708		5.98	-0.73	2.37E-04	2.75E-02	NA
A_21_P0014380		5.26	-0.66	2.51E-04	2.78E-02	NA
A_22_P00002959	lnc-C5orf63-1	4.03	-0.46	3.45E-04	3.23E-02	NA
A_33_P3390656	ACSL6	7.29	-0.49	2.59E-04	2.82E-02	M6.18_Erythrocytes
A_21_P0006005		6.63	-0.52	3.15E-05	1.01E-02	NA
A_24_P85243	FAM153A	7.59	-0.92	6.08E-05	1.38E-02	M4.1_T.cell
A_32_P89679	ALG10B	7.37	-0.33	1.14E-04	1.93E-02	NA
A_32_P449652		4.18	-0.45	3.33E-04	3.19E-02	NA
A_21_P0007549	lnc-FAM113B-1	5.07	-0.71	5.28E-06	4.52E-03	NA
A_33_P3335511	FCRL5	4.27	-0.57	5.90E-04	4.16E-02	NA
A_33_P3312799		4.11	-0.44	6.14E-04	4.22E-02	NA
A_33_P3328559	TBC1D10C	14.11	-0.49	6.08E-04	4.20E-02	M4.16_Not.Determined
A_32_P71113	SCAI	8.46	-0.84	5.22E-06	4.52E-03	NA
A_22_P00011951	lnc-PKIA-1	4.68	-0.41	1.91E-04	2.48E-02	NA
A_33_P3387621	RHPN2	6.36	-0.56	2.98E-04	3.02E-02	M9.6_Undetermined
A_33_P3274935	HID1	7.36	-0.51	5.79E-04	4.13E-02	NA
A_33_P8983845	LOC284191	5.42	-0.84	3.71E-04	3.33E-02	NA
A_23_P216455	RLN2	5.29	-0.53	5.65E-04	4.11E-02	M9.11_Undetermined
A_21_P0008548	LINC01550	7.13	-0.94	8.76E-06	5.61E-03	NA
A_32_P224522	SLC25A23	8.26	-0.54	1.53E-04	2.24E-02	M7.24_Undetermined

A_24_P156267	SOX12	4.25	-0.68	4.82E-05	1.21E-02	NA
A_23_P255376	CCDC109B	11.73	-0.32	4.18E-04	3.55E-02	M5.6_Mitochondrial.Stress/Proteasome
A_22_P00005428		5.62	-0.72	7.42E-06	5.33E-03	NA
A_33_P6815667	RBM26-AS1	6.84	-0.49	3.93E-05	1.11E-02	NA
A_21_P0010838	XLOC_l2_001669	5.86	-0.42	2.24E-05	8.24E-03	NA
A_33_P3303385	NCAPD2	10.24	-0.46	6.90E-04	4.45E-02	M5.10_Mitochondrial.Respiration
A_24_P73599	IL16	8.80	-0.61	8.27E-06	5.57E-03	M8.16_Undetermined
A_22_P00020951		4.59	-0.55	2.20E-04	2.65E-02	NA
A_33_P3415663	MBLAC2	6.40	-0.58	8.36E-04	4.89E-02	M7.12_Undetermined
A_23_P38696	DSC1	5.35	-1.03	6.36E-05	1.43E-02	M9.11_Undetermined
A_32_P131143	CECR5-AS1	5.15	-0.53	1.47E-04	2.19E-02	NA
A_23_P114445	MAGEE1	6.39	-0.27	2.61E-04	2.82E-02	M9.9_Undetermined
A_22_P00010449	CLUAP1	6.54	-0.37	3.03E-04	3.04E-02	M6.19_Not.Determined|M7.25_Undetermined|
A_21_P0006563	ZC3H12B	5.65	-0.59	2.89E-06	4.30E-03	M9.11_Undetermined
A_24_P242299	ZRANB2	12.36	-0.38	5.48E-06	4.57E-03	M7.25_Undetermined
A_19_P00801823	XLOC_l2_014645	7.50	-1.18	5.68E-06	4.62E-03	NA
A_23_P7582	TCF7	12.71	-0.72	3.55E-05	1.08E-02	M4.1_T.cell|M9.12_Undetermined
A_23_P202458	ZNF22	10.14	-0.31	2.72E-04	2.87E-02	M4.3_Protein.Synthesis
A_21_P0014847	CYB561D2	9.53	-0.72	4.51E-06	4.41E-03	M6.2_Mitochondrial.Respiration
A_32_P84373	FAM153B	8.57	-0.92	4.31E-05	1.15E-02	NA
A_33_P3231858	MAP3K14-AS1	5.81	-0.49	5.57E-05	1.32E-02	NA
A_33_P3362372		7.24	-0.52	7.00E-05	1.49E-02	NA
A_23_P411723	PLAG1	9.47	-0.78	2.21E-05	8.17E-03	M9.6_Undetermined|M9.21_Undetermined
A_33_P3280993	HCG18	8.39	-0.59	4.42E-04	3.62E-02	M7.12_Undetermined
A_33_P3377190	LOC100131662	7.05	-0.67	9.37E-05	1.74E-02	M9.11_Undetermined
A_22_P00016562	LOC284191	5.60	-0.90	1.45E-04	2.18E-02	NA
A_23_P383435	ZNHIT3	12.01	-0.35	6.91E-05	1.48E-02	M5.5_Not.Determined|M5.10_Mitochondrial.Respiration
A_23_P428887	KLHL34	5.59	-0.54	4.25E-05	1.15E-02	M9.11_Undetermined
A_24_P200427	PAICS	8.57	-0.37	5.60E-04	4.10E-02	M3.5_Cell.Cycle
A_22_P00016779	lnc-TRIM41-3	6.28	-0.52	1.45E-04	2.18E-02	NA
A_22_P00003031	lnc-C7orf49-1	4.51	-0.65	3.37E-05	1.05E-02	NA
A_23_P117734	LYSMD4	8.65	-0.51	5.35E-06	4.54E-03	NA
A_24_P115007	ALDH5A1	6.04	-0.64	1.84E-05	7.72E-03	M6.18_Erythrocytes
A_24_P940310	URB1	4.45	-0.54	1.91E-04	2.48E-02	NA
A_32_P147622	MCF2L-AS1	7.40	-0.60	4.23E-04	3.56E-02	M9.11_Undetermined
A_21_P0000989	LOC101927412	8.03	-1.03	1.96E-04	2.51E-02	NA
A_23_P37005	MTRF1	8.76	-0.57	1.06E-05	6.09E-03	NA
A_33_P3381245	PDCD5	12.07	-0.33	1.86E-04	2.45E-02	M5.6_Mitochondrial.Stress/Proteasome
A_33_P3350853	PAXIP1-AS1	6.90	-0.43	4.10E-04	3.53E-02	NA
A_23_P346982	DTWD2	5.17	-0.51	5.65E-04	4.11E-02	M9.37_Undetermined
A_23_P88095	TBC1D4	8.97	-0.74	9.36E-06	5.83E-03	M4.1_T.cell
A_33_P3503537	LOC285178	8.44	-0.50	2.67E-04	2.85E-02	NA
A_33_P3462422	THEMIS	8.87	-0.69	4.14E-04	3.54E-02	M4.15_T.cells
A_33_P3248953	C5orf63	4.65	-0.46	5.94E-04	4.16E-02	NA
A_22_P00020493	SMAD2	4.28	-0.47	5.27E-04	3.94E-02	NA
A_33_P3662000	lnc-COL6A3-5	4.33	-0.58	3.36E-04	3.19E-02	NA
A_23_P111112	VARS2	10.80	-0.35	4.91E-04	3.82E-02	M4.12_Not.Determined
A_24_P727501		6.85	-0.44	9.45E-06	5.84E-03	NA
A_23_P339053		8.28	-0.61	6.27E-04	4.28E-02	NA
A_24_P74064	ZBTB14	8.40	-0.29	3.48E-04	3.24E-02	M5.5_Not.Determined
A_23_P105619	TMEM116	9.02	-0.42	5.42E-04	4.00E-02	M4.7_Cell.Cycle
A_32_P84369	FAM153C	10.05	-1.01	2.17E-05	8.10E-03	NA
A_23_P48088	CD27	10.86	-0.69	4.40E-04	3.62E-02	M4.15_T.cells
A_33_P3362869	DNAJC19	10.35	-0.31	4.69E-04	3.72E-02	NA
A_32_P163147	VSIG1	6.29	-0.69	6.31E-04	4.29E-02	M6.19_Not.Determined
A_24_P256552	CSTF3	6.98	-0.51	7.07E-04	4.52E-02	M5.10_Mitochondrial.Respiration|
A_33_P3212432		6.40	-0.56	5.78E-04	4.13E-02	NA
A_33_P3218410	ATM	7.40	-0.40	2.96E-04	3.02E-02	NA
A_32_P49350		14.98	-0.24	5.37E-04	3.99E-02	NA
A_23_P117558	FKBP3	11.15	-0.32	7.76E-06	5.37E-03	M7.19_Undetermined
A_24_P935881	SERF1B	9.88	-0.39	7.23E-04	4.56E-02	M5.9_Protein.Synthesis
A_22_P00017197	LOC101927121	6.24	-1.07	1.22E-05	6.47E-03	NA
A_23_P102471	MSH2	8.22	-0.62	7.23E-04	4.56E-02	M9.6_Undetermined
A_24_P674924	LRPPRC	6.29	-0.42	8.09E-04	4.80E-02	M4.7_Cell.Cycle
A_23_P258612	ATP8A2	5.14	-0.67	8.15E-05	1.63E-02	NA

A_32_P794272		5.69	-0.45	2.58E-04	2.82E-02	NA
A_33_P3343432	THEM4	8.74	-0.50	3.75E-04	3.34E-02	NA
A_23_P145935	EPHB6	8.85	-0.65	5.01E-05	1.24E-02	M7.18_Undetermined
A_23_P406385	FBXL16	9.32	-0.80	7.23E-04	4.56E-02	M6.15_Not.Determined
A_23_P53476	LDHB	14.98	-0.32	6.12E-04	4.22E-02	M4.15_T.cells
A_33_P3300941	NPCDR1	6.62	-0.75	6.69E-04	4.39E-02	M8.71_Undetermined
A_23_P68868	TUG1	12.98	-0.29	7.11E-05	1.51E-02	NA
A_19_P00812310	lnc-ITSN1-2	6.53	-0.89	2.43E-04	2.77E-02	NA
A_23_P77430	PRMT7	11.19	-0.43	1.50E-04	2.21E-02	M4.12_Not.Determined
A_32_P195401	FAM117B	10.69	-0.46	6.36E-04	4.30E-02	M8.83_Immune.Responses
A_23_P6762	JAGN1	11.02	-0.28	5.93E-04	4.16E-02	NA
A_22_P00013804	NUPR1L	5.67	-0.31	7.12E-04	4.52E-02	NA
A_33_P3252369	TMEM182	4.35	-0.57	4.62E-04	3.72E-02	NA
A_21_P0011488	XLOC_l2_005553	4.31	-0.43	8.17E-04	4.82E-02	NA
A_23_P77459	NAE1	11.14	-0.38	2.59E-04	2.82E-02	M5.5_Not.Determined
A_33_P3340990	AKTIP	6.44	-0.48	4.38E-04	3.62E-02	M8.10_Undetermined
A_23_P54556	MKL2	8.08	-0.61	8.62E-05	1.69E-02	M9.27_Undetermined
A_33_P3316310	MTERF4	9.36	-0.38	2.23E-04	2.67E-02	NA
A_33_P3421351	TRAF3IP3	13.25	-0.62	2.69E-05	9.27E-03	M5.5_Not.Determined
A_33_P6505283	LOC100507316	9.17	-0.30	6.64E-04	4.38E-02	NA
A_33_P3238052	FAM216A	9.04	-0.54	1.58E-04	2.27E-02	M5.5_Not.Determined
A_33_P3276301		6.01	-0.52	2.25E-04	2.68E-02	NA
A_33_P3424577		14.54	-0.49	6.60E-04	4.37E-02	NA
A_24_P333421	ZNF862	10.18	-0.75	5.48E-06	4.57E-03	NA
A_33_P3245665		8.88	-0.61	1.78E-05	7.72E-03	NA
A_21_P0000807	LINC00861	6.77	-0.69	1.89E-05	7.80E-03	NA
A_21_P0010470	lnc-MAPK8IP2-1	5.96	-0.79	5.03E-05	1.24E-02	NA
A_33_P3416822	HSF5	5.20	-0.49	7.17E-04	4.54E-02	M8.100_Undetermined
A_21_P0000899	LOC100506990	5.81	-0.55	1.58E-05	7.28E-03	NA
A_23_P66137	SOX8	7.35	-0.70	4.22E-04	3.56E-02	M6.19_Not.Determined
A_23_P393034	HAS3	5.94	-0.56	2.07E-04	2.58E-02	M9.13_Undetermined
A_21_P0005917	LOC100507316	7.24	-0.53	8.23E-04	4.84E-02	NA
A_22_P00025114	lnc-POU5F1B-3	5.22	-0.39	4.16E-04	3.55E-02	NA
A_23_P434430	ZNF439	6.81	-0.57	8.10E-04	4.80E-02	M7.12_Undetermined
A_19_P00812582	TUG1	5.44	-0.25	7.52E-04	4.64E-02	NA
A_33_P3295655	APBA1	4.30	-0.48	2.08E-04	2.58E-02	NA
A_32_P101570	TPTE2P5	4.86	-0.55	2.29E-04	2.70E-02	NA
A_22_P00015596	STXBP4	4.38	-0.65	3.78E-04	3.35E-02	NA
A_33_P3266993		8.62	-0.60	3.12E-04	3.08E-02	NA
A_33_P3362826	ANKRD31	4.74	-0.68	1.44E-05	6.89E-03	NA
A_23_P171074	ITM2A	12.13	-0.39	3.77E-04	3.35E-02	M4.15_T.cells
A_21_P0010236	LOC101928126	6.34	-0.66	7.15E-04	4.53E-02	NA
A_21_P0000823	PAXBP1-AS1	7.39	-0.62	3.96E-05	1.12E-02	NA
A_24_P28977	TRPC1	6.62	-0.58	1.77E-04	2.40E-02	M8.15_Undetermined
A_19_P00804417		5.54	-0.34	6.89E-04	4.45E-02	NA
A_33_P3356022		5.52	-0.51	1.25E-04	2.01E-02	NA
A_33_P3345016	HTR6	4.12	-0.34	5.40E-04	4.00E-02	NA
A_23_P250102	CAND2	6.50	-0.54	3.07E-04	3.06E-02	NA
A_21_P0006827	lnc-AL137145.1-3	6.39	-0.97	2.85E-05	9.48E-03	NA
A_23_P22672	ALG13	10.56	-0.52	2.81E-04	2.94E-02	M5.11_Not.Determined|M7.11_Undetermined
A_23_P20752	CDK20	7.45	-0.49	8.19E-04	4.83E-02	NA
A_21_P0012873	LOC100507387	8.28	-0.82	6.81E-05	1.48E-02	NA
A_33_P3256920	WNT7B	7.08	-0.67	4.23E-04	3.56E-02	NA
A_33_P3226605	PSIP1	11.69	-0.44	4.53E-05	1.18E-02	M5.5_Not.Determined|M9.1_Undetermined
A_23_P14165	GPR18	9.26	-0.56	4.97E-04	3.84E-02	M4.15_T.cells
A_23_P6293	UBASH3A	9.42	-0.63	7.15E-04	4.53E-02	NA
A_24_P323815	MYCBP2	11.80	-0.41	4.75E-05	1.20E-02	M7.3_Not.Determined
A_33_P3224735	ZC3H12B	6.26	-0.57	8.74E-05	1.69E-02	M9.11_Undetermined
A_23_P502371	PHF2	9.98	-0.22	7.69E-04	4.68E-02	M5.7_Inflammation|M9.4_Undetermined
A_23_P75380	AIP	12.28	-0.23	5.87E-04	4.16E-02	M5.10_Mitochondrial.Respiration
A_23_P133596	DROSHA	11.06	-0.43	8.03E-04	4.78E-02	M5.5_Not.Determined
A_33_P3260654		15.11	-0.51	2.58E-04	2.82E-02	NA
A_22_P00014730	lnc-SLC2A4RG-1	6.77	-0.47	5.09E-05	1.25E-02	NA
A_33_P3399911		5.42	-0.32	2.37E-04	2.75E-02	NA
A_33_P3348714	FGF9	6.87	-0.60	6.38E-04	4.31E-02	NA

A_23_P82738	RAD54B	5.16	-0.83	1.58E-05	7.28E-03	M9.2_Undetermined
A_22_P00007635	FAM13A-AS1	11.84	-0.29	4.10E-04	3.54E-02	NA
A_23_P382602	BCL9	6.08	-0.37	6.80E-04	4.42E-02	M8.73_Undetermined
A_33_P3347343	CCDC102B	5.29	-0.55	1.06E-04	1.86E-02	NA
A_23_P258410	WNT7A	7.27	-0.75	1.59E-04	2.28E-02	M9.2_Undetermined
A_23_P99967	BBS4	8.68	-0.41	7.73E-04	4.69E-02	M8.38_Undetermined
A_23_P384056	CCDC14	10.74	-0.43	7.60E-04	4.67E-02	M5.5_Not.Determined
A_23_P64650	TSFM	10.76	-0.38	5.77E-04	4.13E-02	M3.5_Cell.Cycle
A_33_P3607359	LOC399815	4.80	-0.60	2.79E-05	9.44E-03	NA
A_21_P0006645	LOC101928150	7.32	-0.89	2.43E-05	8.65E-03	NA
A_33_P3214393		6.11	-0.47	8.26E-04	4.85E-02	NA
A_33_P3792328	LSM3	5.96	-0.35	6.51E-04	4.35E-02	M5.13_Not.Determined
A_21_P0013517	XLOC_l2_014549	6.46	-0.50	3.62E-05	1.08E-02	NA
A_23_P17134	MAL	12.93	-0.55	5.86E-04	4.16E-02	M4.1_T.cell
A_22_P00012830	TMEM161B-AS1	7.48	-0.41	1.85E-04	2.45E-02	NA
A_22_P00010998	STX18-AS1	5.87	-0.31	4.80E-04	3.76E-02	NA
A_32_P167705	AGBL2	5.76	-0.65	8.68E-04	4.99E-02	NA
A_24_P20630	LEF1	13.34	-0.77	9.28E-06	5.81E-03	M4.1_T.cell
A_23_P48585	SALL2	7.69	-0.55	4.20E-04	3.56E-02	M9.11_Undetermined
A_32_P194072	TECPR1	11.11	-0.44	1.90E-04	2.48E-02	M8.31_Undetermined
A_23_P33196	COL5A2	4.52	-0.60	1.32E-05	6.60E-03	NA
A_22_P00010578	lnc-NDFIP2-2	4.91	-0.36	2.76E-04	2.90E-02	NA
A_22_P00010971	lnc-NRIP2-1	7.77	-0.29	1.03E-04	1.85E-02	NA
A_33_P3402474	ATAT1	9.12	-0.37	6.10E-04	4.21E-02	M9.1_Undetermined
A_23_P120194	ORMDL1	13.02	-0.31	2.12E-04	2.60E-02	M6.7_Not.Determined
A_23_P35916	ATM	8.62	-0.52	1.92E-05	7.84E-03	NA
A_23_P328621	UBQLNL	6.65	-0.56	4.49E-04	3.65E-02	M9.2_Undetermined
A_33_P3282556	TMEM204	9.56	-0.74	1.03E-04	1.85E-02	M4.1_T.cell
A_33_P3355474		6.69	-0.50	2.14E-05	8.10E-03	NA
A_23_P211957	TGFBR2	12.67	-0.36	5.72E-04	4.13E-02	M5.7_Inflammation
A_21_P0000232	SNORD109B	5.08	-0.57	5.36E-05	1.29E-02	NA
A_33_P3252359	BDH1	8.68	-0.59	3.62E-04	3.29E-02	NA
A_23_P62188	ZC4H2	8.84	-0.46	7.67E-04	4.68E-02	NA
A_22_P00001060	lnc-ALB-1	6.38	-0.57	4.42E-04	3.62E-02	NA
A_33_P3291569	LUC7L3	13.15	-0.34	9.09E-05	1.72E-02	M5.11_Not.Determined
A_19_P00327035	HAR1A	7.14	-0.51	1.71E-05	7.55E-03	NA
A_23_P323196	MDS2	7.03	-0.97	1.32E-04	2.08E-02	NA
A_23_P306941	RGL4	10.25	-0.42	5.61E-04	4.10E-02	M3.2_Inflammation
A_23_P502170	DYNC2LI1	4.25	-0.29	8.49E-04	4.93E-02	M9.9_Undetermined
A_23_P40049	CAD	8.33	-0.49	5.77E-04	4.13E-02	M6.12_Mitochondrial.Stress
A_21_P0013528		8.37	-0.41	2.05E-04	2.57E-02	NA
A_33_P3378491		7.02	-0.61	2.45E-05	8.68E-03	NA
A_22_P00018189	lnc-ZNF609-1	6.60	-0.54	7.41E-04	4.61E-02	NA
A_33_P3221458	ZNF204P	8.59	-0.79	4.60E-05	1.19E-02	NA
A_33_P3240966		4.47	-0.46	5.17E-04	3.89E-02	NA
A_24_P171983	NDUFAF4	9.40	-0.36	1.12E-04	1.92E-02	M6.12_Mitochondrial.Stress
A_23_P57760	PXYLP1	8.80	-0.41	1.40E-04	2.15E-02	NA
A_33_P3267330	HAR1B	5.30	-0.52	8.04E-04	4.78E-02	NA
A_33_P3261902	ENOSF1	8.95	-0.52	2.15E-05	8.10E-03	M9.2_Undetermined
A_33_P3360917	IPO9	5.99	-0.48	4.40E-04	3.62E-02	M7.5_Undetermined
A_24_P319374	GPA33	8.46	-0.82	3.02E-04	3.04E-02	M6.19_Not.Determined
A_33_P3274832	LOC283440	5.62	-0.45	2.35E-05	8.48E-03	NA
A_32_P46981	HSBP1L1	8.40	-0.34	5.20E-04	3.90E-02	NA
A_21_P0014850		6.25	-0.81	1.65E-04	2.30E-02	NA
A_23_P209032	ZNF302	7.19	-0.50	1.43E-04	2.17E-02	M9.28_Undetermined
A_24_P90097	ADD3	12.18	-0.41	4.47E-04	3.64E-02	M8.54_Undetermined|M8.109_Undetermined
A_33_P3422679	FAM149B1	8.77	-0.33	6.55E-04	4.36E-02	NA
A_22_P00000987	PRKCQ-AS1	6.88	-0.65	7.10E-04	4.52E-02	M4.1_T.cell
A_21_P0006902		5.32	-0.49	2.02E-04	2.56E-02	NA
A_33_P3285987	METTL15	7.25	-0.55	3.82E-04	3.37E-02	NA
A_23_P88106	MCF2L	5.42	-0.63	6.94E-05	1.48E-02	NA
A_24_P215765	ATP10A	9.69	-0.63	1.66E-04	2.31E-02	NA
A_22_P00011090	lnc-NUDT11-2	7.49	-0.54	1.94E-04	2.50E-02	NA
A_22_P00009162	LMO7	6.88	-0.38	2.68E-04	2.85E-02	NA
A_22_P00015054	lnc-SNPH-1	5.82	-0.59	3.08E-05	9.95E-03	NA

A_21_P0012835	XLOC_l2_011649	6.18	-0.99	2.61E-04	2.82E-02	NA
A_21_P0006828	lnc-AL137145.1-4	6.55	-0.88	4.28E-05	1.15E-02	NA
A_23_P39116	LIG1	10.62	-0.49	2.51E-05	8.84E-03	M9.5_Undetermined
A_22_P00016450	lnc-TMEM63A-1	12.11	-0.52	5.67E-05	1.33E-02	NA
A_24_P303145	ANKH	6.90	-0.77	6.31E-04	4.29E-02	M9.33_Undetermined
A_24_P391526	MAGED1	9.00	-0.32	5.58E-04	4.08E-02	M3.5_Cell.Cycle
A_23_P29836	TMEM42	10.97	-0.60	2.45E-04	2.78E-02	M4.3_Protein.Synthesis
A_33_P3879920	TRIM39-RPP21	12.97	-0.25	3.48E-04	3.24E-02	NA
A_23_P326931	CFAP70	7.74	-0.50	2.35E-05	8.48E-03	NA
A_21_P0009993	LOC100505771	8.82	-0.39	3.82E-04	3.37E-02	NA
A_23_P205389	MOAP1	11.26	-0.40	5.30E-05	1.29E-02	M5.5_Not.Determined
A_24_P921897	HOOK1	6.34	-0.50	2.89E-04	2.99E-02	M4.1_T.cell
A_33_P3234804	CBR4	9.50	-0.34	5.99E-04	4.17E-02	M6.7_Not.Determined
A_23_P207742	THRA	11.67	-0.53	1.95E-05	7.84E-03	M9.29_Undetermined
A_32_P86118	PM20D2	7.75	-0.37	6.52E-04	4.35E-02	M7.6_Undetermined
A_33_P3386621		4.86	-0.50	7.06E-04	4.52E-02	NA
A_33_P3418611	ZNF729	10.52	-0.36	8.11E-04	4.80E-02	NA
A_23_P210176	ITGA6	8.88	-0.75	2.10E-04	2.59E-02	NA
A_33_P3308332	PLEKHB1	10.01	-0.98	6.70E-05	1.47E-02	M6.19_Not.Determined
A_21_P0010097	lnc-ZNF831-1	5.00	-0.49	5.32E-05	1.29E-02	NA
A_33_P3297205	C22orf29	10.46	-0.53	8.97E-05	1.71E-02	NA
A_32_P42964	NUPR1L	6.75	-0.53	8.73E-05	1.69E-02	NA
A_21_P0000054	PET117	10.82	-0.30	7.93E-04	4.75E-02	NA
A_23_P92281	GTPBP8	12.01	-0.34	9.70E-05	1.78E-02	M7.5_Undetermined
A_19_P00813085	lnc-SNURF-1	6.49	-0.62	1.50E-04	2.21E-02	NA
A_33_P3409347	C19orf53	5.84	-0.37	1.69E-04	2.32E-02	M5.10_Mitochondrial.Respiration
A_23_P202427	HKDC1	6.09	-0.76	4.87E-04	3.79E-02	M8.58_Undetermined
A_21_P0006825	PRKCQ-AS1	7.00	-0.61	4.13E-04	3.54E-02	M4.1_T.cell
A_23_P22352	FRMD4A	4.86	-0.64	1.24E-04	2.01E-02	M9.33_Undetermined
A_21_P0010469	CHKB-AS1	5.07	-0.39	7.80E-04	4.71E-02	NA
A_24_P237389	EIF1AX	10.40	-0.34	1.80E-05	7.72E-03	M4.5_Protein.Synthesis|M5.6_Mitochondrial.Stress/Proteasome
A_22_P00025871	HAR1B	4.58	-0.62	1.52E-05	7.17E-03	NA
A_22_P00006106	IRAIN	4.62	-0.55	7.74E-05	1.58E-02	NA
A_23_P70897	ZCWPW1	10.38	-0.42	4.94E-04	3.84E-02	M7.25_Undetermined
A_22_P00005417		7.50	-0.39	7.17E-04	4.54E-02	NA
A_33_P3351524		9.48	-0.36	7.80E-05	1.58E-02	NA
A_23_P63067	DAP3	13.83	-0.24	3.08E-04	3.06E-02	M5.10_Mitochondrial.Respiration|M8.6_Undetermined
A_33_P3255329	ACACB	4.64	-0.35	5.88E-04	4.16E-02	M7.13_Not.Determined
A_23_P24960	NARS2	7.55	-0.42	1.60E-04	2.28E-02	M6.12_Mitochondrial.Stress
A_33_P3243554		10.82	-0.30	2.27E-04	2.69E-02	M8.100_Undetermined|M9.7_Undetermined
A_33_P3510837		7.91	-0.59	3.88E-04	3.40E-02	NA
A_33_P3334308	ZXDB	10.46	-0.39	1.57E-04	2.27E-02	M4.7_Cell.Cycle
A_23_P213153	HNRNPDL	12.27	-0.22	1.73E-04	2.36E-02	M5.8_Not.Determined|M6.9_Not.Determined
A_23_P203115	TMEM25	8.39	-0.64	3.44E-04	3.23E-02	NA
A_23_P391926	LPHN1	7.65	-0.38	8.21E-04	4.83E-02	M8.58_Undetermined
A_23_P139500	BHLHE41	4.80	-0.54	8.47E-04	4.93E-02	NA
A_33_P3387691	SCML4	11.72	-0.74	4.56E-05	1.18E-02	M9.25_Undetermined
A_23_P343398	CCR7	14.34	-0.64	6.77E-04	4.41E-02	M4.1_T.cell
A_33_P3290853		6.87	-0.69	4.47E-05	1.18E-02	NA
A_23_P6413	SELM	9.56	-0.45	3.65E-04	3.30E-02	M4.1_T.cell
A_24_P203964	SMA4	9.47	-0.52	1.38E-04	2.14E-02	M4.8_Not.Determined|M5.11_Not.Determined
A_21_P0001106		6.00	-0.64	1.65E-04	2.30E-02	NA
A_19_P00811048	ZEB1-AS1	5.48	-0.39	1.94E-04	2.50E-02	M7.23_Undetermined
A_32_P179998	DMRTC1	7.15	-0.64	1.92E-04	2.48E-02	NA
A_23_P103486	CYP2J2	5.04	-0.83	5.79E-04	4.13E-02	M9.11_Undetermined
A_33_P3501900	ZNF582-AS1	7.92	-0.60	2.21E-04	2.65E-02	NA
A_22_P00000741	LOC642852	9.26	-0.46	4.25E-04	3.57E-02	M9.27_Undetermined
A_32_P67623	FAM120C	9.00	-0.41	6.71E-04	4.40E-02	M7.12_Undetermined
A_23_P138125	FAIM3	10.49	-0.59	2.42E-04	2.76E-02	M4.1_T.cell
A_23_P210726	CDC25B	11.09	-0.51	2.97E-04	3.02E-02	M4.7_Cell.Cycle
A_33_P3495234	ORF1	4.03	-0.53	2.66E-05	9.17E-03	NA
A_33_P3418668	PWARSN	9.85	-0.49	2.98E-04	3.02E-02	NA
A_23_P34930	BCAS2	12.19	-0.39	6.68E-04	4.39E-02	M7.20_Undetermined
A_21_P0012393	XLOC_l2_009883	6.99	-0.55	1.77E-04	2.39E-02	NA
A_33_P3695899	FLJ31104	6.64	-0.64	4.22E-04	3.56E-02	NA

A_23_P10025	NELL2	11.43	-0.71	3.60E-04	3.29E-02	M4.1_T.cell
A_23_P44466	CCDC102B	4.16	-0.46	3.21E-04	3.14E-02	NA
A_23_P21673	FOCAD	9.52	-0.44	4.74E-04	3.74E-02	M5.10_Mitochondrial.Respiration
A_23_P362183	ANKS6	9.38	-0.60	3.03E-04	3.04E-02	NA
A_21_P0000682	LHX4-AS1	9.05	-0.73	7.57E-04	4.66E-02	NA
A_19_P00321473	HCG18	9.31	-0.46	4.44E-04	3.63E-02	M7.12_Undetermined
A_21_P0009730	ZNF582-AS1	5.81	-0.51	2.98E-04	3.02E-02	NA
A_23_P98483	ZBED5	11.90	-0.37	4.69E-04	3.72E-02	NA
A_22_P00025545	CECR7	4.51	-0.58	3.97E-04	3.45E-02	NA
A_32_P114215	COMMD6	13.69	-0.26	1.43E-04	2.17E-02	M5.5_Not.Determined
A_22_P00006033		5.29	-0.51	6.68E-04	4.39E-02	NA
A_21_P0014663	ZNF605	4.42	-0.41	1.08E-04	1.87E-02	M9.2_Undetermined
A_33_P3311917		5.63	-0.58	1.11E-04	1.91E-02	NA
A_21_P0001760	lnc-C1orf198-2	6.57	-0.62	6.20E-04	4.25E-02	NA
A_33_P3397127		8.27	-0.66	7.01E-05	1.49E-02	NA
A_23_P203920	SSPN	5.02	-0.97	2.22E-04	2.66E-02	M9.30_Undetermined
A_33_P3645465	PDCD4-AS1	10.22	-0.38	9.13E-05	1.72E-02	NA
A_24_P37264	RNF144A	6.98	-0.61	1.27E-04	2.03E-02	M7.12_Undetermined
A_21_P0013780	ARMCX4	5.40	-0.38	6.58E-04	4.37E-02	NA
A_24_P626931	UBE3D	5.55	-0.60	1.54E-04	2.24E-02	NA
A_23_P340263	RNF175	5.87	-0.78	1.43E-04	2.17E-02	M5.3_Not.Determined
A_23_P145711	SUGCT	4.59	-0.51	2.31E-04	2.70E-02	M9.1_Undetermined
A_21_P0004475	lnc-PROP1-3	4.27	-0.48	3.71E-04	3.33E-02	NA
A_21_P0000572	PITPNA-AS1	10.39	-0.41	2.67E-04	2.85E-02	NA
A_24_P90878	THUMPD1	8.59	-0.30	5.32E-05	1.29E-02	M4.5_Protein.Synthesis
A_24_P191781	PARM1	4.63	-0.61	6.24E-04	4.27E-02	M8.92_Undetermined
A_32_P32254	COL6A1	8.04	-0.75	1.59E-04	2.28E-02	NA
A_23_P31376	LRRN3	8.59	-1.32	1.04E-04	1.85E-02	M4.1_T.cell
A_23_P94141	RAD54B	5.56	-0.44	6.60E-04	4.37E-02	M9.2_Undetermined
A_23_P103601	MAN1C1	11.13	-0.88	1.99E-04	2.54E-02	M4.1_T.cell
A_32_P122940	LOC642852	6.76	-0.50	2.97E-04	3.02E-02	M9.27_Undetermined
A_24_P159635	LIMD2	9.21	-0.43	5.34E-05	1.29E-02	M9.3_Undetermined
A_23_P95736	ZNF429	12.28	-0.25	6.00E-04	4.18E-02	M8.37_Undetermined
A_33_P3340655	KLHL32	4.58	-0.68	3.92E-05	1.11E-02	NA
A_33_P3235340	DDX18	11.02	-0.30	6.51E-04	4.35E-02	M4.3_Protein.Synthesis
A_33_P3241786	ADD2	7.33	-0.83	8.57E-05	1.68E-02	NA
A_24_P630490	DFNB59	6.04	-0.38	8.70E-04	5.00E-02	NA
A_23_P88099	MCF2L	7.79	-0.50	3.24E-04	3.16E-02	NA
A_33_P3256957		4.44	-0.36	5.56E-04	4.08E-02	NA
A_33_P3364904	ZNF662	4.83	-0.60	7.27E-04	4.57E-02	NA
A_33_P3291154	ZBTB20	5.70	-0.42	4.22E-04	3.56E-02	M7.3_Not.Determined
A_33_P3424010		7.21	-0.52	8.06E-04	4.79E-02	NA
A_24_P237778	MAN1C1	6.11	-0.66	2.23E-04	2.67E-02	M4.1_T.cell
A_21_P0000674	LOC100289473	6.50	-0.42	3.42E-04	3.22E-02	NA
A_23_P316150	IFT80	6.61	-0.61	3.15E-04	3.09E-02	NA
A_23_P80156	PRMT2	9.50	-0.49	9.09E-05	1.72E-02	M7.18_Undetermined|M9.17_Undetermined
A_32_P30271	ARRDC5	7.69	-0.35	7.06E-04	4.52E-02	NA
A_33_P3378915	ARHGEF18	7.56	-0.38	7.58E-04	4.66E-02	M5.5_Not.Determined
A_33_P3287502	MSH2	7.45	-0.54	7.88E-04	4.73E-02	M9.6_Undetermined
A_23_P350551	C12orf57	13.89	-0.39	1.12E-04	1.92E-02	M6.15_Not.Determined
A_33_P3386117	RER1	10.45	-0.47	7.48E-04	4.62E-02	M5.13_Not.Determined
A_33_P3375467	GPLD1	4.06	-0.42	3.33E-04	3.19E-02	NA
A_22_P00002416		4.78	-0.78	7.65E-05	1.57E-02	NA
A_23_P96590	GPRASP1	10.93	-0.62	2.24E-04	2.67E-02	M9.1_Undetermined
A_23_P345460	PLEKHG4	7.59	-0.83	7.65E-04	4.67E-02	M9.11_Undetermined
A_21_P0011654	NPIPA2	12.10	-0.33	2.09E-04	2.59E-02	NA
A_22_P00011301	TUG1	11.25	-0.23	4.72E-04	3.73E-02	NA
A_21_P0013820	XLOC_l2_015762	13.04	-0.34	6.27E-04	4.28E-02	NA
A_21_P0004293	lnc-ADAMTS19-2	4.37	-0.44	3.48E-04	3.24E-02	NA
A_19_P00321911	IPW	5.40	-0.40	2.03E-04	2.56E-02	NA
A_24_P359322	C21orf62-AS1	4.55	-0.46	8.29E-04	4.86E-02	NA
A_22_P00017514	INTS6-AS1	8.31	-0.29	7.10E-04	4.52E-02	NA
A_23_P50517	ZNF541	6.52	-0.58	8.94E-05	1.71E-02	NA
A_24_P192627	MLLT3	6.66	-0.48	3.15E-04	3.09E-02	M2.2_Cell.Cycle
A_21_P0012391		7.52	-0.50	6.44E-05	1.43E-02	NA

A_21_P0014503	INTS6-AS1	10.19	-0.34	4.13E-04	3.54E-02	NA
A_23_P162766	DOCK9	8.45	-0.56	1.04E-04	1.85E-02	M4.1_T.cell
A_33_P3415698	TMIGD2	10.80	-0.66	2.41E-04	2.76E-02	M9.3_Undetermined
A_22_P00004825		7.24	-0.57	6.01E-05	1.38E-02	NA
A_24_P602507	HYKK	6.53	-0.70	1.13E-04	1.93E-02	NA
A_21_P0004417	RASGRF2-AS1	4.92	-0.58	5.69E-05	1.33E-02	NA
A_22_P00006161	SUCLG2-AS1	5.10	-0.53	3.21E-04	3.14E-02	NA
A_33_P3250671	TCF7	10.38	-0.58	2.49E-04	2.78E-02	M4.1_T.cell|M9.12_Undetermined
A_23_P58529	DIMT1	10.43	-0.28	3.83E-04	3.37E-02	M4.12_Not.Determined
A_24_P125871	RIPK4	4.77	-0.73	6.71E-05	1.47E-02	NA
A_23_P151459	MYCBP2	13.02	-0.40	1.58E-04	2.27E-02	M7.3_Not.Determined
A_23_P63660	FAM213A	7.41	-0.47	1.60E-04	2.28E-02	M7.12_Undetermined
A_24_P340776		10.43	-0.37	8.48E-04	4.93E-02	NA
A_24_P133017	TMEM25	5.77	-0.43	4.50E-04	3.65E-02	NA
A_32_P144908	ZNF254	13.62	-0.29	6.31E-04	4.29E-02	M9.12_Undetermined
A_21_P0001481	lnc-C1orf201-3	8.18	-0.48	2.98E-04	3.02E-02	NA
A_23_P144778	CKMT2	4.02	-0.47	4.53E-04	3.67E-02	NA
A_33_P3358392	BCL11B	8.41	-0.43	1.18E-04	1.96E-02	M4.1_T.cell
A_23_P346093	TMC8	13.27	-0.37	6.70E-04	4.39E-02	M7.25_Undetermined
A_32_P206735	PRO1082	6.33	-0.53	8.28E-04	4.86E-02	NA
A_22_P00000241		4.71	-0.65	2.20E-04	2.65E-02	NA
A_23_P329375	POU6F1	7.37	-0.42	4.95E-04	3.84E-02	NA
A_22_P00011001	lnc-NSMCE1-1	5.59	-0.83	8.70E-05	1.69E-02	NA
A_33_P3301897		6.26	-0.54	1.26E-04	2.01E-02	NA
A_23_P251795	GPC2	8.58	-0.58	5.99E-05	1.38E-02	M9.5_Undetermined
A_33_P6468355	TP73-AS1	7.47	-0.45	3.64E-04	3.30E-02	M5.11_Not.Determined
A_24_P409857	HMGN1	13.05	-0.23	7.82E-04	4.71E-02	M5.6_Mitochondrial.Stress/Proteasome|
A_21_P0005657		7.01	-0.52	1.18E-04	1.96E-02	NA
A_23_P163408	SCAPER	7.18	-0.47	1.83E-04	2.43E-02	M9.6_Undetermined
A_24_P365365	TCF3	11.54	-0.43	6.25E-04	4.27E-02	NA
A_33_P3211153	ANKS3	10.85	-0.44	8.47E-04	4.93E-02	M8.28_Undetermined
A_33_P3362812		13.96	-0.25	5.49E-04	4.04E-02	NA
A_23_P120710	TTC3	10.31	-0.30	5.39E-04	4.00E-02	M4.7_Cell.Cycle
A_23_P258483	ANKRD55	6.56	-0.79	4.71E-04	3.72E-02	M7.10_Undetermined
A_24_P19268	ZNF714	12.95	-0.30	5.20E-04	3.90E-02	NA
A_33_P3414880	LOC339192	12.17	-0.40	8.42E-04	4.92E-02	NA
A_23_P154875	BACE2	7.14	-0.69	7.25E-04	4.56E-02	M8.110_Undetermined
A_21_P0003719	lnc-SLC2A9-1	7.30	-0.46	2.14E-04	2.62E-02	NA
A_21_P0002569	lnc-RNF144A-1	4.98	-0.48	1.68E-04	2.32E-02	NA
A_19_P00808461	ZNF37A	9.90	-0.44	8.50E-04	4.93E-02	NA
A_22_P00015075	lnc-SNURF-1	4.45	-0.45	4.85E-04	3.79E-02	NA
A_22_P00023206	MORF4L2-AS1	5.93	-0.45	1.31E-04	2.06E-02	NA
A_23_P130149	ENO3	9.67	-0.38	2.41E-04	2.76E-02	M7.13_Not.Determined
A_23_P82412	NSUN5	11.93	-0.40	4.32E-04	3.59E-02	M5.11_Not.Determined|M7.25_Undetermined
A_21_P0013505		5.36	-0.43	2.24E-04	2.67E-02	NA
A_23_P43141	EIF3E	14.71	-0.24	4.68E-04	3.72E-02	M5.5_Not.Determined
A_21_P0000231	SNORD64	9.33	-0.50	7.75E-05	1.58E-02	NA
A_22_P00007533	lnc-HADH-1	6.00	-0.73	2.80E-04	2.93E-02	NA
A_19_P00811348	lnc-SNURF-1	6.23	-0.35	2.24E-04	2.67E-02	NA
A_33_P3420204	CRTC1	10.76	-0.50	3.76E-04	3.34E-02	M9.3_Undetermined
A_23_P65278	NBEA	7.35	-0.68	7.71E-04	4.69E-02	M9.6_Undetermined
A_24_P936122	STX16	12.14	-0.27	5.19E-04	3.90E-02	M8.2_Not.Determined|M9.10_Undetermined
A_21_P0005658		7.08	-0.45	3.42E-04	3.22E-02	NA
A_23_P50357	ARHGEF18	13.00	-0.47	1.53E-04	2.24E-02	M5.5_Not.Determined
A_24_P194017	NOSIP	10.47	-0.47	3.08E-04	3.06E-02	M5.5_Not.Determined
A_23_P56703	TRABD2A	11.71	-0.68	1.29E-04	2.05E-02	NA
A_19_P00317054	SATB1-AS1	7.57	-0.57	1.44E-04	2.17E-02	NA
A_23_P84705	TNFRSF13B	4.83	-0.60	1.07E-04	1.87E-02	M7.32_Undetermined
A_33_P3262028	XLOC_l2_010082	6.92	-0.63	4.66E-04	3.72E-02	NA
A_33_P3316661	C12orf42	5.72	-0.40	6.69E-04	4.39E-02	NA
A_23_P160240	ACP6	5.50	-0.47	1.40E-04	2.15E-02	M8.45_Undetermined
A_33_P3238579		5.61	-0.57	1.32E-04	2.08E-02	NA
A_19_P00804489	lnc-SNURF-1	6.11	-0.37	3.13E-04	3.08E-02	NA
A_23_P79818	OSER1	12.51	-0.32	8.52E-04	4.94E-02	M8.72_Undetermined
A_24_P363087	C5orf45	10.88	-0.55	1.23E-04	2.01E-02	NA

A_24_P143492	BCAS4	7.72	-0.52	1.58E-04	2.27E-02	M6.15_Not.Determined
A_33_P3227284	OGT	13.42	-0.35	6.72E-04	4.40E-02	M5.11_Not.Determined
A_21_P0008383	lnc-VRK1-5	8.71	-0.56	3.48E-04	3.24E-02	NA
A_22_P00009053	LOC101928236	5.08	-0.50	7.71E-04	4.69E-02	NA
A_24_P416159	RBL2	10.54	-0.34	3.39E-04	3.20E-02	M5.8_Not.Determined
A_33_P3357332	lnc-C9orf147-1	4.37	-0.45	2.37E-04	2.75E-02	NA
A_22_P00006676	lnc-FPGS-1	5.75	-0.50	2.30E-04	2.70E-02	NA
A_23_P129466	ATF7IP2	9.80	-0.71	4.31E-04	3.59E-02	M6.15_Not.Determined
A_22_P00017346	LOC101928000	8.49	-0.47	4.38E-04	3.62E-02	NA
A_23_P500410	ATP6V1G2	6.71	-0.50	1.80E-04	2.42E-02	M9.7_Undetermined
A_23_P313632	FUT8	8.88	-0.59	1.91E-04	2.48E-02	M7.6_Undetermined
A_32_P210252	RPL22	14.50	-0.25	3.28E-04	3.18E-02	M4.3_Protein.Synthesis|M6.9_Not.Determined
A_21_P0000230	SNORD107	8.09	-0.41	5.97E-04	4.17E-02	NA
A_21_P0005819		5.47	-0.35	2.59E-04	2.82E-02	NA
A_22_P00002525	LOC339192	9.57	-0.38	6.16E-04	4.23E-02	NA
A_21_P0012664	LOC102723415	6.48	-0.65	3.04E-04	3.04E-02	NA
A_21_P0013364	ZNF890P	6.76	-0.72	2.89E-04	2.99E-02	NA
A_33_P3258712	LOC101928000	8.48	-0.47	5.92E-04	4.16E-02	NA
A_21_P0001153	LOC100131564	8.71	-0.35	1.68E-04	2.32E-02	NA
A_33_P3410284	DOCK9	5.85	-0.40	7.61E-04	4.67E-02	M4.1_T.cell
A_23_P107166	ACBD4	7.20	-0.31	8.46E-04	4.93E-02	M9.5_Undetermined
A_32_P209230	CITED4	13.05	-0.60	4.47E-04	3.64E-02	M9.8_Undetermined
A_33_P3278813		5.26	-0.40	4.28E-04	3.59E-02	NA
A_33_P3222105	EIF1AX	12.67	-0.23	3.03E-04	3.04E-02	M4.5_Protein.Synthesis|M5.6_Mitochondrial.Stress/Proteasome|
A_33_P3252588	LOC100130093	6.12	-0.45	5.34E-04	3.98E-02	NA
A_21_P0013792	LINC00086	5.93	-0.36	4.78E-04	3.75E-02	NA
A_24_P298360	LTBP3	9.71	-0.47	4.95E-04	3.84E-02	M4.1_T.cell
A_23_P105664	CCDC59	12.35	-0.30	8.65E-04	4.98E-02	M7.19_Undetermined
A_33_P3216955	ANAPC16	8.75	-0.52	7.92E-04	4.74E-02	M5.9_Protein.Synthesis
A_23_P216501	TPM2	11.05	-0.52	2.55E-04	2.81E-02	M7.13_Not.Determined
A_24_P100830	AMN1	5.25	-0.36	8.26E-04	4.85E-02	M8.72_Undetermined
A_23_P3911	PLXDC1	9.52	-0.69	5.49E-04	4.04E-02	M9.5_Undetermined
A_33_P3361393	EIF1AX	12.22	-0.23	2.98E-04	3.02E-02	M4.5_Protein.Synthesis|M5.6_Mitochondrial.Stress/Proteasome|
A_23_P22614		11.75	-0.30	5.86E-04	4.16E-02	M8.100_Undetermined|M9.7_Undetermined
A_33_P3361388	MYCBPAP	5.67	-0.55	6.95E-04	4.48E-02	NA
A_33_P3311775	ZNF789	8.15	-0.33	7.45E-04	4.61E-02	M5.11_Not.Determined
A_19_P00320622	MIATNB	6.57	-0.36	5.18E-04	3.90E-02	NA
A_23_P146849	APBA2	8.22	-0.51	7.05E-04	4.52E-02	M9.11_Undetermined
A_33_P3270599	TPM2	10.71	-0.49	4.47E-04	3.64E-02	M7.13_Not.Determined
A_21_P0011811	ANKRD36BP2	7.54	-0.50	6.26E-04	4.27E-02	M9.32_Undetermined
A_32_P156373	LOC102725134	7.15	-0.59	4.68E-04	3.72E-02	NA
A_22_P00002439		4.35	-0.56	6.81E-04	4.42E-02	NA

Supplementary Table 5. Probes up in 'Metastasis' v 'Primary'

ProbeName	GENE_SYMBOL	Avg. log2 exp.	log2 FC	p.value	adjusted.p.value	GeneSets.Modules
A_22_P00003343	lnc-CBFA2T3-2	5.30	0.40	2.5253E-05	0.008874894	NA
A_22_P00012949		4.91	0.36	3.03571E-05	0.009891479	NA
A_33_P3323136	ENKUR	9.72	0.63	8.54534E-05	0.016790962	M6.14_Not.Determined
A_33_P3264364	DNM3	9.87	0.66	0.000151958	0.022318099	M1.1_Platelets
A_23_P316850	ODF3L2	9.02	0.51	0.000171473	0.02343541	NA
A_19_P00811843	ARHGAP32	6.36	0.33	0.000181813	0.02420965	M8.25_Undetermined
A_21_P0014395	lnc-ZNF100-2	6.15	0.92	0.000220292	0.026532879	NA
A_21_P0010671	LYPLAL1-AS1	7.32	0.65	0.000257714	0.028169994	NA
A_24_P10884	GRAP2	8.24	0.45	0.000286721	0.029782806	M1.1_Platelets
A_23_P429998	FOSB	13.01	0.79	0.000307099	0.030555602	M8.69_Undetermined
A_22_P00010905	LOC100294362	4.67	0.30	0.000333979	0.031926111	NA
A_23_P167983	HIST1H2AC	11.54	0.62	0.000353675	0.032636681	M4.9_Not.Determined
A_24_P215240	ENKUR	8.82	0.59	0.000353885	0.032636681	M6.14_Not.Determined
A_23_P72668	SDPR	11.34	0.67	0.000375451	0.033418899	M1.1_Platelets
A_23_P105957	ACTN1	11.42	0.48	0.00038699	0.034000884	M4.13_Inflammation
A_33_P3377194	ADRA1A	10.60	0.41	0.000417394	0.035509032	M2.2_Cell.Cycle
A_21_P0010663	XLOC_l2_001206	12.01	0.40	0.000422257	0.03557475	NA
A_33_P3262020	C8G	10.57	0.44	0.000465744	0.037232052	NA
A_23_P7342	UGT2B10	4.94	0.35	0.00047441	0.037377879	NA
A_22_P00012227	lnc-PPIA-1	9.78	0.40	0.00047612	0.037405978	NA
A_23_P164047	MMD	11.91	0.53	0.000485953	0.037900665	M1.1_Platelets
A_22_P00013904	LINC00856	9.30	0.44	0.000494851	0.038361321	NA
A_23_P128084	ITGA7	10.52	0.45	0.000497824	0.038361321	NA
A_33_P3292478	CCL16	10.54	0.44	0.000505315	0.038669168	NA
A_33_P3324086	MCUR1	11.79	0.39	0.000515485	0.038912744	M8.51_Undetermined
A_33_P3323699	NPPA	6.39	0.26	0.000525393	0.039285038	M9.51_Undetermined
A_33_P3849275	FHL1	10.21	0.38	0.000593237	0.041641944	M1.1_Platelets
A_22_P00024602	LOC101927437	5.09	0.25	0.00062244	0.042623498	NA
A_22_P00010511	lnc-NBPF3-4	8.90	0.24	0.000645745	0.043391964	NA
A_33_P3231677		8.20	0.52	0.000647744	0.043419556	NA
A_21_P0001087	C1orf86	4.80	0.38	0.000673863	0.044059869	M5.8_Not.Determined
A_23_P333951	DNAH14	4.99	0.37	0.000675025	0.044072389	NA
A_33_P8911753	ITGA9-AS1	5.64	0.44	0.000728971	0.045718902	NA
A_33_P3312754	LOC102467146	11.12	0.42	0.000762056	0.046691838	NA
A_33_P3368339	NUTM2G	10.46	0.54	0.000771588	0.046870168	NA
A_33_P3366754	LOC100128670	8.85	0.52	0.000774978	0.046949628	NA
A_23_P96623	OPN1MW	5.70	0.36	0.00078098	0.04707844	NA
A_22_P00011727		9.57	0.54	0.000784033	0.047129627	NA
A_21_P0000337	SNORA55	5.73	0.34	0.000788772	0.047298947	NA
A_21_P0014061	LINC00083	10.90	0.59	0.000797172	0.04755026	NA
A_33_P3343845	CBX7	8.59	0.44	0.000852618	0.049353041	M7.18_Undetermined
A_33_P3353343	SRRM2	9.71	0.39	0.000856626	0.049555918	M9.5_Undetermined
A_24_P177553		5.44	0.51	0.000860374	0.049714259	NA
A_23_P315286	R3HDM4	12.56	0.30	0.000862826	0.04979809	M3.1_Erythrocytes
A_23_P131825	TNNC2	9.90	0.47	0.000865183	0.049849786	M1.1_Platelets
A_33_P3370600	SMIM6	4.74	0.51	7.51155E-06	0.005356228	NA
A_22_P00013971	lnc-RTN2-1	7.38	0.81	1.76226E-05	0.007707178	NA
A_23_P309837	STON2	5.63	0.75	2.34322E-05	0.008477342	NA
A_22_P00002271	lnc-C10orf31-2	4.78	0.41	4.1651E-05	0.011406166	NA
A_24_P128308	KLF6	8.00	0.60	7.78918E-05	0.015824041	M7.2_Not.Determined|M7.15_Undetermined|
A_32_P198923	YWHAZ	11.61	0.37	0.000106101	0.018644088	M4.9_Not.Determined|M9.44_Undetermined
A_33_P3258274	TFPI	5.93	0.69	0.000112723	0.019191864	M1.1_Platelets|M8.39_Undetermined
A_23_P151662	MAX	11.05	0.33	0.000122982	0.020080023	M6.14_Not.Determined|M7.30_Undetermined|
A_33_P3322539	BEND2	8.01	0.63	0.00012366	0.020080023	NA
A_23_P2414	SPX	7.04	0.72	0.000138721	0.021398952	NA
A_24_P414658	HIST1H2AG	5.86	0.61	0.000149876	0.022135108	M1.1_Platelets
A_23_P90357	TBXA2R	9.28	0.69	0.000156193	0.022642288	M9.41_Undetermined
A_23_P169437	LCN2	8.13	0.77	0.000165418	0.023023451	NA
A_21_P0009522		5.10	0.52	0.000175569	0.023829656	NA
A_33_P3341429	NEXN	8.10	0.63	0.000184127	0.024385843	M8.18_Undetermined

A_22_P00016935	TSPAN33	9.75	0.56	0.000191006	0.024835605	M1.1_Platelets
A_23_P141974	TPM4	11.51	0.42	0.00021605	0.026344461	NA
A_22_P00005011	FAM212B-AS1	5.61	0.59	0.000221028	0.026556527	NA
A_23_P62953	PBX1	4.93	0.55	0.000225496	0.026798849	M3.1_Erythrocytes
A_23_P143902	P2RY12	7.60	0.66	0.000250963	0.02784477	M9.21_Undetermined
A_23_P405295	LCE3C	4.66	0.43	0.000261177	0.028222508	NA
A_21_P0000061	CGREF1	6.80	0.40	0.000262123	0.028223918	NA
A_23_P67864	ADCY3	10.91	0.33	0.000264775	0.028382019	M7.29_Not.Determined
A_24_P95822	NPTN	9.07	0.45	0.000269398	0.028504905	M8.2_Not.Determined
A_33_P3273136	MCUR1	9.92	0.42	0.000300838	0.030385148	M8.51_Undetermined
A_23_P380208	VEPH1	6.36	0.72	0.000303531	0.030410542	M9.21_Undetermined
A_33_P3231670	RNF208	7.87	0.63	0.000304165	0.030417459	NA
A_33_P3396370	ACRBP	12.64	0.61	0.000321034	0.031371074	M1.1_Platelets
A_23_P216845	GFI1B	8.74	0.72	0.000326667	0.031701163	M6.14_Not.Determined
A_33_P3304983	PRKAR2B	11.59	0.76	0.000329316	0.031762592	NA
A_23_P501831	FAXDC2	10.65	0.77	0.000329355	0.031762592	M3.1_Erythrocytes|M4.4_Not.Determined
A_19_P00317360	ATP2C1	6.66	0.57	0.00037942	0.03357561	M7.17_Undetermined|M8.36_Undetermined
A_22_P00002303	lnc-C11orf30-1	8.49	0.90	0.000382753	0.033705206	NA
A_33_P3275722	LY6G6D	6.48	0.42	0.000395088	0.034475508	M9.21_Undetermined
A_21_P0012452		5.27	0.71	0.000407855	0.035205392	NA
A_33_P3236858	TGFB1I1	8.35	0.62	0.000414729	0.035425882	M9.19_Undetermined
A_33_P3363620	TMEM91	10.26	0.49	0.000417848	0.035509032	NA
A_33_P3379669	RNF208	6.06	0.51	0.000424134	0.03564136	NA
A_33_P3244274	RNF208	7.89	0.61	0.000433704	0.035984613	NA
A_23_P251173	EIF2AK1	11.05	0.26	0.000439322	0.036162723	M4.4_Not.Determined
A_33_P3223116	HIPK2	7.04	0.46	0.000439331	0.036162723	M7.26_Undetermined
A_33_P3247858	MPP1	8.68	0.66	0.000459491	0.037001062	M7.33_Undetermined
A_24_P365901	TSPAN33	10.44	0.52	0.000464849	0.037232052	M1.1_Platelets
A_24_P123408	ABLIM3	5.40	0.74	0.000475085	0.037399834	M1.1_Platelets
A_22_P00005519	lnc-EBF3-6	8.58	0.63	0.000481983	0.037701531	NA
A_23_P145238	HIST1H2BK	11.63	0.51	0.000490006	0.038147208	M7.16_Not.Determined
A_23_P420831	TRIM10	6.23	0.49	0.000497809	0.038361321	M2.3_Erythrocytes|M4.4_Not.Determined
A_33_P3398526	BCL2L11	10.36	0.50	0.000501275	0.03855304	NA
A_23_P142631	FKBP1B	8.41	0.51	0.000514266	0.038911264	NA
A_23_P210358	LIMS1	10.74	0.49	0.000517643	0.038960195	M6.14_Not.Determined|M8.39_Undetermined
A_33_P3337019	LOC728975	9.20	0.67	0.000541054	0.040040156	NA
A_23_P104199	ITGB1	10.24	0.33	0.000544572	0.040200714	M5.4_Not.Determined|M7.3_Not.Determined
A_23_P202004	PRTFDC1	5.94	0.58	0.000548305	0.04035634	M8.18_Undetermined
A_33_P3235400	HDGF	8.96	0.38	0.000574811	0.04133617	M4.4_Not.Determined
A_33_P3263666	ANKRD9	10.48	0.66	0.000575091	0.04133617	M9.26_Undetermined
A_23_P155979	EGF	6.32	0.80	0.000578048	0.04133617	M1.1_Platelets
A_33_P3249414	TRIM58	11.31	0.74	0.000587547	0.041641944	NA
A_23_P107612	RAB27B	7.81	0.52	0.000605341	0.04196584	M1.1_Platelets|M6.14_Not.Determined
A_23_P152906	ALOX12	8.24	0.85	0.000606181	0.04196584	M1.1_Platelets
A_23_P128598	TUBA3C	8.59	0.49	0.000635739	0.043010142	NA
A_33_P3232955	F2RL3	8.42	0.60	0.000646617	0.043391964	NA
A_33_P3381777	TREML1	9.94	0.87	0.000652535	0.043474196	M1.1_Platelets
A_22_P00019581		6.09	0.55	0.000659282	0.043735075	NA
A_23_P116264	NRGN	13.88	0.69	0.00066316	0.043838211	M1.1_Platelets
A_23_P102731	SMOX	9.95	0.70	0.000677912	0.044149328	M7.33_Undetermined
A_33_P3423270	TMEM40	8.15	0.61	0.000682891	0.044267776	M1.1_Platelets
A_23_P120435	WFDC3	6.63	0.28	0.000696523	0.044826626	NA
A_33_P3342528	P2RY1	7.32	0.76	0.000728823	0.045718902	M9.21_Undetermined
A_23_P45304	XK	7.93	0.85	0.000730616	0.045734622	M2.3_Erythrocytes
A_23_P25974	TTC7B	9.36	0.69	0.000768076	0.046827207	NA
A_23_P217319	FGF13	4.34	0.46	0.000773192	0.046897455	M7.29_Not.Determined|M9.15_Undetermined
A_24_P941353	PCYT1B	4.75	0.69	0.000778307	0.047044051	NA
A_24_P362540	ASAP2	6.85	0.65	0.000779538	0.047073316	M1.1_Platelets
A_19_P00321743	LOC100130938	9.09	0.66	0.000787922	0.04729161	NA
A_23_P19987	IGF2BP3	10.13	0.51	0.000806814	0.047913657	M7.16_Not.Determined
A_23_P113701	PDGFA	6.98	0.66	0.000809701	0.048002032	NA
A_33_P3416097	F13A1	7.57	0.74	0.000810254	0.048002032	M1.1_Platelets
A_33_P3343316	SH3BGRL2	7.09	0.69	0.000862837	0.04979809	NA

Supplementary Table 6. Probes down in 'Metastasis' v 'Primary'

ProbeName	GENE_SYMBOL	Avg. log2 exp.	log2 FC	p.value	adjusted.p.value	GeneSets.Modules
A_21_P0014136		5.27	-0.52	5.55729E-05	0.013209035	NA
A_23_P338233	BCDIN3D	7.97	-0.42	0.000360201	0.032910693	M7.24_Undetermined
A_23_P33607	TEFM	7.62	-0.30	0.000530189	0.039524401	NA
A_23_P501372	MIEF2	7.84	-0.29	0.000591139	0.041641944	NA
A_24_P548060		6.77	-0.68	0.000646891	0.043391964	NA
A_33_P3235731	LOC101930072	4.95	-0.43	0.00077579	0.046949628	NA
A_33_P3274194	KCNIP4	4.85	-0.46	8.91633E-05	0.017069908	NA
A_33_P3405168	MMAA	6.38	-0.43	0.000181499	0.02420965	NA
A_33_P3317576	DHFRL1	5.28	-0.50	0.000204162	0.025657969	NA
A_23_P81212	MRPS18C	10.71	-0.51	0.000207998	0.025822209	M5.13_Not.Determined
A_21_P0007249	RAB30-AS1	6.14	-0.35	0.000268684	0.028461171	NA
A_21_P0000830	RAB30-AS1	5.60	-0.33	0.000425118	0.035663183	NA
A_23_P336796	GXYLT1	6.81	-0.35	0.000462709	0.037168933	M7.3_Not.Determined
A_33_P3277527	LAMC3	4.08	-0.63	0.000635645	0.043010142	NA
A_33_P3214745	FBXO48	4.98	-0.38	0.00066379	0.043838211	NA
A_33_P3407314	PAXIP1-AS2	5.89	-0.47	0.000680255	0.044200216	NA
A_22_P00002000	FBXL19-AS1	5.69	-0.33	0.000683817	0.044298636	NA
A_24_P316305	AQR	8.70	-0.42	0.000837136	0.048975429	M6.2_Mitochondrial.Respiration
A_23_P218358	CDRT1	4.15	-0.36	0.000843117	0.049177224	NA
A_23_P26976	CHAD	4.41	-0.23	0.000865252	0.049849786	NA
A_21_P0002200	lnc-QPCT-3	4.23	-0.58	0.000868518	0.049921008	NA
A_23_P329261	KCNJ2	5.22	-0.89	0.000343207	0.032225735	M7.16_Not.Determined
A_22_P00024322	lnc-GBP6-1	6.60	-0.69	0.000416725	0.035509032	NA

Supplementary Table 7. Genes up in [‘Primary’ v ‘Unaffected’] ONLY

KCNJ2
lnc-GBP6-1
GBP1
CXCL10
SCUBE2
LACC1
CDYL2
MR1
INPP1
FAM45A
ACBD5
PARP9
IL15RA
lnc-SIPA1L1-1
AP3S2
LOC100507006

Supplementary Table 8. Genes up in [‘Primary’ v ‘Unaffected’] AND [‘Metastasis’ v ‘Unaffected’]

MUC1
CDKN2A
GREM2
PSMD2
lnc-MYO1G-1

Supplementary Table 9. Genes up in [‘Metastasis’ v ‘Unaffected’] ONLY

ESAM
ANGPT1
CLIP2
MTURN
LOC100130264
ABCC4
LTBP1
MPST
BMP6
lnc-SHANK2-1
PTCRA
LINC00958
MYLK
C6orf25
SELP
lnc-CCDC68-1
GP1BB
PLXNA4
LOC101928489
TUBA8
GMPR
KCNAB2
lnc-VAMP1-1
lnc-CYP4A22-2
lnc-LUC7L3-1
HOMER2
GUCY1B3
CMTM5
LINC01016
lnc-C14orf101-1
C2orf88
MOB1B
LOC101929089
PCSK6
ZNF185
TUBA4A
C19orf26
FGD5-AS1
GDI1
FRMD3
PDLIM7
SLC6A4
GP9
ARHGAP6
PTGS1
CXCL5
ELOVL7
DGKD
CLEC1B
MEIS1
NT5M
CCPG1
GP1BA
LINC00152
LFNG
HSF4
GOLGA2
TPM1
USF2
GATA1
AZU1
C2orf73
CD226
CALD1
SFXN5
LRP12
AVPR1A
PEAR1
EGFL7
lnc-SLC16A3-1
EHD2
SNCA
LINC00853
PARD3
MFAP3L
GP6
VWF
CLU
PPP1R14A
TCTEX1D4
SPARC
CTDSPL
RTN2
ITGB5
TSPAN9
PLA2G12A
MSANTD3
CDC14B
LY6G6F
ZBTB16
DENND4C
HEXIM2
NEAT1
TMEM140
ITGB3
lnc-MBL2-3
IGF2BP2
SENCR
MYCT1
SEC14L1
XKR5
CALM3
CTTN
MYEOV
WASF3
FAM63A
KCND3
ACSBG1
TBXAS1
NAT8B
HEMGN
SDC1
FERMT3
ST3GAL6-AS1
ULK1
DNAAF3
UBE2C
EIF4G3
STRN4
LINC00642
lnc-NCOA5-1
WIPI1
lnc-UGT8-4
HDGFRP3
FNBP1L
CCDC3
HRASLS
AQP10
CALML3
GNG11
C15orf26
LINC00534
PARVB
MYL9
CYB5R3
FAM65C
PTPRF
PROS1
SLA2
PF4
FUBP3
SLC8A3
FLNA
ADIPOR1
ITGA2B
RHOBTB1
FAH
INAFM2
RAB6B
lnc-ROM1-3
TGFB1
LINC00211
LGALSL
LGALS12
lnc-OBFC2A-5
AGFG1
NEXN-AS1
GAS2L1
VCL
LIPH
DMTN
GAS2L1P2
LAPTM4B
SSX2IP
LOC100133669
lnc-C6orf146-2
EPS15L1
SPTB
CCDC6
NYNRIN
ZC3HAV1L
LOC102725057
VEGFC
SEC16A
GOLGA8O
YWHAH
TTC7A
LOC100288846
LINC00092
DNAH2
PTPN12
GOLGA6L9
RSPH1
SLC24A3
ABCC3
PXK
VIL1
TMEM63B
OR2W3
PHC2
WDR44
WRB
CTSA
lnc-SLA2-2
PDLIM1
F11R
SMIM3
MLXIP
BCL2L1
C9orf16
LINC00635
PDGFC
PLXNB3
FAM91A1
ENDOD1
ASPH
LINC01126
FSTL1
CMIP
MGLL
DAPP1
SCYL2
CETP
TAGLN2
RSPH9
BCL2L2
C19orf33
UBL4A
PTTG1IP
SPANXN4
C8orf60
SAMD14
UBE2Q2P1
SH3TC1
GPD2
lnc-GCNT3-1
ILK
CD9
RAB11A
RDH11
MAP1LC3B
MIR4435-1HG
NID2
PLEKHB2
GPR137
NF1
lnc-POFUT2-3
SEC14L5
LOC100132287
lnc-LRCH1-1
AQP1
XPNPEP1
ZFAND3
RAB7A
RNASE1
ELK3
TNFRSF6B
lnc-SLC9A4-1
RAB1B
LGALS8
CDS2
ZDHHC20
SPIRE1
EPOR
CHRNA7
BRK1
lnc-FARP1-1
PIM1
RELL1
DSC2
MARK2
SSPO
ZCCHC17
F2R
CLEC2L
LOC100133299
PLIN3
PAPSS1
ARNT
GOLGA8R
CREB3L3
XLOC_l2_001569
MALL
NCKAP1
DRC7
GP5
PLOD2
TMEM189
CASZ1
SLC15A4
MGRN1
FAR1
ST7
CHRFAM7A
KIFC3
PHTF1
CREB3L2
UBTD1
lnc-SCRG1-1
ANKDD1A
MCTP2
E2F1
lnc-SERPINC1-3
ANO2
MYO9B
ABAT
MMP1
TMSB15A
CHADL
CCAR2
RGS6
VIM-AS1
MTMR3
BROX
NPDC1
GAS2L2
MIR612
lnc-IDH3G-1
NFIB
PCGF3
MAP2K3
DIAPH1
MMRN1
FGFR1OP2
FAM53B
lnc-ZNF37A-3
LPAR5
CLDN5
lnc-CHADL-1
C1orf116
KMT2E-AS1
CAB39
SH3BGRL3
LOC100130587
GLA
TIRAP
DSCR3
IKBKG
ELK1
ATG2A
P2RX1
MAP3K5
LRRFIP2
SMR3A
LOC101927272
SLCO3A1
lnc-NLRP12-2
FBXW9
CCIN
PLCD3
PXN
STOM
ITPRIPL1
PRDM1
RAP1GAP2
BMP1
LOC101928173
NOL10
AGXT
PCYT1A

Supplementary Table 10. Genes up in [‘Metastasis’ v ‘Unaffected’] AND [‘Metastasis’ v ‘Primary’]

TPM4	MAX	TMEM91	WFDC3
LOC100130938	SPX	EIF2AK1	XK
P2RY1	HIST1H2AG	MPP1	TTC7B
NEXN	TBXA2R	lnc-EBF3-6	FGF13
TMEM40	LCN2	HIST1H2BK	ASAP2
lnc-NBPF3-4	TSPAN33	TRIM10	IGF2BP3
PDGFA	FAM212B-AS1	BCL2L11	F13A1
PCYT1B	PBX1	FKBP1B	
ABLIM3	P2RY12	LIMS1	
BEND2	LCE3C	LOC728975	
SH3BGRL2	CGREF1	ITGB1	
PRKAR2B	ADCY3	PRTFDC1	
HDGF	MCUR1	ANKRD9	
HIPK2	VEPH1	EGF	
TFPI	RNF208	TRIM58	
NPTN	ACRBP	RAB27B	
SMIM6	GFI1B	ALOX12	
lnc-RTN2-1	FAXDC2	TUBA3C	
STON2	ATP2C1	F2RL3	
lnc-C10orf31-2	lnc-C11orf30-1	TREML1	
KLF6	LY6G6D	NRGN	
YWHAZ	TGFB1I1	SMOX	

Supplementary Table 11. Genes up in [‘Metastasis’ v ‘Primary’] ONLY

lnc-CBFA2T3-2	lnc-PPIA-1	CBX7
ENKUR	MMD	SRRM2
DNM3	LINC00856	R3HDM4
ODF3L2	ITGA7	TNNC2
ARHGAP32	CCL16	
lnc-ZNF100-2	NPPA	
LYPLAL1-AS1	FHL1	
GRAP2	LOC101927437	
FOSB	C1orf86	
LOC100294362	DNAH14	
HIST1H2AC	ITGA9-AS1	
SDPR	LOC102467146	
ACTN1	NUTM2G	
ADRA1A	LOC100128670	
XLOC_l2_001206	OPN1MW	
C8G	SNORA55	
UGT2B10	LINC00083	

Supplementary Table 12. Genes down in [‘Primary’ v ‘Unaffected’] ONLY

FLJ36777	PIK3IP1-AS1	C1QTNF6
OTUD7A	SDR39U1	FBLN2
lnc-EIF2S3L.1-2	lnc-TMED5-1	CTSF
ASIC1	SDCCAG8	LINC00304
JPH3	CCDC7	
SNORD22	ANTXRL	
lnc-ARFGEF2-2	SATB1	

Supplementary Table 13. Genes down in [‘Primary’ v ‘Unaffected’] AND [‘Metastasis’ v ‘Unaffected’]

NR3C2	ZC3H12B	NUCB2	STMN3	TRAF3IP2-AS1	LRP6
COL4A3	AK5	LOC101927056	NRCAM	FBXO25	LOC102723346
LIPT2	EDAR	FBXO15	lnc-EXD2-1	IQCH-AS1	FAM90A1
LOC101060038	LOC101928803	lnc-DCTD-1	SHF	TXNRD3	TTC14
COL4A4	PLXDC1	HSPG2	XLOC_l2_014098	BTNL9	KRT73-AS1
LOC256880	TMIE	MMP28	TMEM27	lnc-FPGS-1	PRMT2
KLF3-AS1	RNF157-AS1	lnc-AC009113.1-1	COL18A1	SATB1-AS1	TLE2
MGC40069	TNK1	MAML2	CD248	LEF1-AS1	LOC100506990
NMT2	lnc-PRAGMIN.1-3	CELA1	DNMT3A	LOC101927372	CXorf67
LINC00282	XLOC_l2_013267	ATHL1	RASGRP2	SNORD116-26	LMF1
NOG	SNORD116-29	SDCBP2-AS1	HULC	lnc-WDR7-2	KLHL3
lnc-ZC3H12B-2	TEPP	COPG2IT1	CACHD1	EPHX2	KLHL29
FCGBP	XLOC_l2_009639	LMO7	RBM19	lnc-C1orf201-2	MTERF4
LOC100270804	ACTN1-AS1	SPEG		PPP1R3E	SCARNA10
LINC01089	SLC16A10	IGF1R		POLI	TATDN1
lnc-HADH-1	ATM	SLC5A2		OBSCN	SCML4
HNRNPDL	TCEA3	SERINC5		ASNSD1	SNORD116-27

Supplementary Table 14. Genes down in [‘Metastasis’ v ‘Unaffected’] ONLY

EXPH5	DNPEP	TYSND1	XLOC_l2_015213	PRKCQ-AS1	C21orf62-AS1
SRP14-AS1	MRPS36	FAM220A	lnc-WDR1-1	METTL15	INTS6-AS1
UNC50	PDE7B	FAM178A	ALDH8A1	MCF2L	ZNF541
ZNF770	NAIF1	PLEKHG7	RAPGEF6	ATP10A	MLLT3
ZC3H14	MDH1	LOC101927531	CNOT7	lnc-NUDT11-2	DOCK9
NUPR1L	C17orf51	ZNF671	ATP5O	lnc-SNPH-1	TMIGD2
HINT3	CENPJ	lnc-UTS2D-1	ING5	XLOC_l2_011649	HYKK
SLC3A1	lnc-C2orf78-1	lnc-SREK1-2	lnc-TFB1M-1	lnc-AL137145.1-4	RASGRF2-AS1
PXMP4	EDRF1	MAGI3	EML5	LIG1	SUCLG2-AS1
USP44	RPUSD2	ZNF507	THEM4	lnc-TMEM63A-1	DIMT1
USP9X	PRKAA1	C14orf169	CRHR1-IT1	ANKH	RIPK4
DOCK9-AS2	LINC00667	SLC35B4	NR2E3	MAGED1	FAM213A
ZSWIM5	LOC729683	lnc-FAM98A-1	PARP16	TMEM42	ZNF254
ZNF561	GLS2	SETMAR	SUN1	TRIM39-RPP21	lnc-C1orf201-3
ZNF765	LOC100131581	PP7080	lnc-C5orf63-1	CFAP70	CKMT2
THAP1	lnc-RASA1-3	lnc-STX3-2	FAM153A	LOC100505771	TMC8
TAS2R5	TCEANC	ZFP2	ALG10B	MOAP1	PRO1082
SDHC	THAP6	CLUAP1	lnc-FAM113B-1	HOOK1	POU6F1
UTP14C	PAXIP1-AS1	SPRYD4	FCRL5	CBR4	lnc-NSMCE1-1
SNHG21	ARL14EP	EXOSC3	TBC1D10C	THRA	GPC2
RNF114	CHKB-AS1	LOC101928101	SCAI	PM20D2	TP73-AS1
C16orf91	CSRP2BP	RAB15	lnc-PKIA-1	ZNF729	HMGN1
SNRPG	IPP	AHSA2	RHPN2	MYCBPAP	lnc-VRK1-5

GIMAP7
ACAT2
C12orf29
BAG2
lnc-TMEM35-1
ZNF582
TPBGL
ZNF813
ANKRD46
KIAA1279
GOPC
LINC00087
SACS
ASPRV1
DNAJC21
ZNF92
SAYSD1
EID3
STXBP5
ERLIN2
ZNF879
lnc-PPM1D-1
HNRNPH3
DCBLD2
ZNHIT3
KLHL34
PAICS
lnc-TRIM41-3
lnc-C7orf49-1
LYSMD4
ALDH5A1
URB1
MCF2L-AS1
TFB1M
ZNF138
RWDD2A
SETD6
ADPRHL2
ZNF343
GHRLOS
RDH14
ACSL6
PKI55
ANKRD31
NAP1L3
TMOD4
PDZD2
LOC101927055
ANKHD1-EIF4EBP3
LSM5
lnc-ACRC-1
RBM17
UTP23
LYRM7
TBC1D27
LOC102723373
lnc-MAPK8IP2-1
LOC101927596
MORF4L2-AS1
SOD1
ZNF485
C2orf68
INADL
ACVR2B
lnc-TPX2-1
LOC101927156
PPAPDC2
C1orf145
AMIGO1
ZFP62
BTRC
KRR1
CCDC90B
OBFC1
LINC01395
KRIT1
YAE1D1
lnc-C8orf56-1
HCG25
MAGOH
ZNF519
TSGA10
lnc-RGS5-1
ANKRD20A12P
DOLK
ARMCX5
lnc-MAP3K3-1
VAPA
YRDC
LOC101927837
MRPS16
LOC100507577
TUG1
C19orf73
NINL
TMEM261
BOD1
ZNF559
ING5
lnc-TFB1M-1
EML5
THEM4
CRHR1-IT1
NR2E3
PARP16
SUN1
lnc-C5orf63-1
FAM153A
ALG10B
lnc-FAM113B-1
FCRL5
TBC1D10C
SCAI
lnc-PKIA-1
RHPN2
HID1
LOC284191
RLN2
SLC25A23
SOX12
CCDC109B
RBM26-AS1
XLOC_l2_001669
NCAPD2
IL16
MBLAC2
DSC1
CECR5-AS1
MAGEE1
ZRANB2
HARBI1
BAIAP2L2
LOC101928714
NIFK
SLAIN1
BTN3A2
LINC01550
USP13
PCMTD2
CDC42SE2
RBM11
NT5E
LINC00954
LOC101929132
SLC46A1
UBTF
ZNF69
CCDC85C
RASGRF2
KDM4C
SLC9B1
IPW
LOC286437
CDHR3
ZNHIT3
KLHL34
PAICS
lnc-TRIM41-3
lnc-C7orf49-1
LYSMD4
ALDH5A1
URB1
MCF2L-AS1
LOC101927412
MTRF1
PDCD5
DTWD2
TBC1D4
LOC285178
THEMIS
C5orf63
SMAD2
lnc-COL6A3-5
VARS2
ZBTB14
TMEM116
FAM153C
CD27
DNAJC19
VSIG1
CSTF3
FKBP3
SERF1B
LOC101927121
MSH2
LRPPRC
ATP8A2
EPHB6
FBXL16
LDHB
NPCDR1
lnc-ITSN1-2
PRMT7
FAM117B
JAGN1
HID1
LOC284191
RLN2
SLC25A23
SOX12
CCDC109B
RBM26-AS1
XLOC_l2_001669
NCAPD2
IL16
MBLAC2
DSC1
CECR5-AS1
MAGEE1
ZRANB2
XLOC_l2_014645
TCF7
ZNF22
CYB561D2
FAM153B
MAP3K14-AS1
PLAG1
HCG18
LOC100131662
HSF5
SOX8
HAS3
lnc-POU5F1B-3
ZNF439
APBA1
TPTE2P5
STXBP4
ITM2A
LOC101928126
PAXBP1-AS1
TRPC1
HTR6
CAND2
lnc-AL137145.1-3
ALG13
CDK20
LOC100507387
WNT7B
PSIP1
GPR18
UBASH3A
MYCBP2
PHF2
AIP
DROSHA
lnc-SLC2A4RG-1
FGF9
RAD54B
FAM13A-AS1
BCL9
CCDC102B
WNT7A
BBS4
CCDC14
TSFM
LOC399815
LOC101928150
LSM3
XLOC_l2_014549
MAL
MIATNB
APBA2
ANKRD36BP2
LOC102725134FAIM3
CDC25B
ORF1
PWARSN
BCAS2
XLOC_l2_009883
FLJ31104
NELL2
FOCAD
ANKS6
LHX4-AS1
ZBED5
CECR7
COMMD6
ZNF605
lnc-C1orf198-2
SSPN
PDCD4-AS1
RNF144A
ARMCX4
UBE3D
RNF175
TECPR1
COL5A2
lnc-NDFIP2-2
lnc-NRIP2-1
SCAPER
TCF3
ANKS3
TTC3
ANKRD55
ZNF714
LOC339192
BACE2
lnc-SLC2A9-1
lnc-RNF144A-1
ZNF37A
ENO3
NSUN5
EIF3E
SNORD64
CRTC1
NBEA
STX16
NOSIP
TRABD2A
TNFRSF13B
XLOC_l2_010082
C12orf42
ACP6
OSER1
C5orf45
BCAS4
OGT
HAR1A
MDS2
RGL4
DYNC2LI1
CAD
lnc-ZNF609-1
ZNF204P
NDUFAF4
LOC101928236
RBL2
lnc-C9orf147-1
ATF7IP2
LOC101928000
ATP6V1G2
FUT8
RPL22
SNORD107
LOC102723415
ZNF890P
LOC100131564
ACBD4
CITED4
LOC100130093
LINC00086
LTBP3
CCDC59
ANAPC16
TPM2
AMN1
THUMPD1
PARM1
COL6A1
LRRN3
MAN1C1
LIMD2
ZNF429
KLHL32
DDX18
ADD2
DFNB59
ZNF662
ZBTB20
LOC100289473
IFT80
ARRDC5
ARHGEF18
C12orf57
RER1
GPLD1
GPRASP1
PLEKHG4
NPIPA2
XLOC_l2_015762
lnc-ADAMTS19-2
lnc-ZNF831-1
C22orf29
PET117
GTPBP8
lnc-SNURF-1
C19orf53
HKDC1
FRMD4A
EIF1AX
IRAIN
ZCWPW1
DAP3
NARS2
ZXDB
TMEM25
LPHN1
BHLHE41
CCR7
SELM

NDUFC1
TSEN2
TRAF3IP3
C10orf35
PRPF38A
ATP6V1E2
LOC101927237
CRB3
ATAT1
ORMDL1
UBQLNL
TMEM204
XLOC_l2_014645
TCF7
ZNF22
CYB561D2
FAM153B
MAP3K14-AS1
PLAG1
HCG18
LOC100131662
ITGA6
PLEKHB1
TMEM182
XLOC_l2_005553
NAE1
AKTIP
MKL2
LOC100507316
FAM216A
ZNF862
LINC00861
SUGCT
lnc-PROP1-3
PITPNA-AS1
TMEM161B-AS1
STX18-AS1
AGBL2
LEF1
SALL2
TGFBR2
SNORD109B
BDH1
ZC4H2
lnc-ALB-1
LUC7L3
PXYLP1
HAR1B
ENOSF1
IPO9
GPA33
LOC283440
HSBP1L1
ZNF302
ADD3
FAM149B1
SMA4
ZEB1-AS1
DMRTC1
CYP2J2
ZNF582-AS1
LOC642852
FAM120C

Supplementary Table 15. Genes down in [‘Metastasis’ v ‘Unaffected’] AND [‘Metastasis’ v ‘Primary’]

BCDIN3D
TEFM
MIEF2
LOC101930072

Supplementary Table 16. Genes down in [‘Metastasis’ v ‘Primary’] ONLY

KCNIP4
MMAA
DHFRL1
MRPS18C
RAB30-AS1
GXYLT1
LAMC3
FBXO48
PAXIP1-AS2
FBXL19-AS1
AQR
CDRT1
CHAD
lnc-QPCT-3
KCNJ2
lnc-GBP6-1

Supplementary Table 17 GO biological process enrichment in 73 genes up in [‘Metastasis’ v ‘Unaffected’] AND [‘Metastasis’ v ‘Primary’]

GO biological process	Fold Enrichment	FDR
learning (GO:0007612)	13.76	1.90E-02
platelet degranulation (GO:0002576)	12.45	4.70E-02
blood coagulation (GO:0007596)	8.65	3.56E-02
coagulation (GO:0050817)	8.59	2.49E-02
hemostasis (GO:0007599)	8.5	2.01E-02
regulation of body fluid levels (GO:0050878)	7.67	8.31E-04
cellular calcium ion homeostasis (GO:0006874)	6.64	3.53E-02
calcium ion homeostasis (GO:0055074)	6.44	3.79E-02
cellular divalent inorganic cation homeostasis (GO:0072503)	6.33	3.77E-02
wound healing (GO:0042060)	6.14	2.34E-02
divalent inorganic cation homeostasis (GO:0072507)	6.03	4.72E-02
cellular metal ion homeostasis (GO:0006875)	5.82	3.26E-02
metal ion homeostasis (GO:0055065)	5.74	1.86E-02
response to wounding (GO:0009611)	5.72	1.53E-02
cation homeostasis (GO:0055080)	4.99	3.49E-02
inorganic ion homeostasis (GO:0098771)	4.87	3.71E-02
ion homeostasis (GO:0050801)	4.68	4.60E-02
chemical homeostasis (GO:0048878)	4.28	2.02E-02
homeostatic process (GO:0042592)	3.47	1.69E-02

Supplementary Table 18. GO biological process enrichment in 350 genes up in [‘Metastasis’ v ‘Unaffected’] ONLY

GO biological process	Fold Enrichment	FDR
blood coagulation, intrinsic pathway (GO:0007597)	20.09	4.64E-03
copulation (GO:0007620)	19.28	2.52E-02
negative regulation of neural precursor cell proliferation (GO:2000178)	14.46	4.90E-02
platelet aggregation (GO:0070527)	14.46	2.21E-04
blood coagulation, fibrin clot formation (GO:0072378)	13.91	1.55E-02
actin filament polymerization (GO:0030041)	13.91	1.53E-02
homotypic cell-cell adhesion (GO:0034109)	12.52	1.23E-04
platelet degranulation (GO:0002576)	12.43	1.79E-12
platelet activation (GO:0030168)	10.18	4.42E-10
negative regulation of protein depolymerization (GO:1901880)	7.75	3.71E-02
myelination (GO:0042552)	7.69	1.04E-03
ensheathment of neurons (GO:0007272)	7.38	1.31E-03
axon ensheathment (GO:0008366)	7.38	1.26E-03
protein polymerization (GO:0051258)	6.97	1.08E-02
regulation of protein depolymerization (GO:1901879)	6.84	2.55E-02
positive regulation of endothelial cell proliferation (GO:0001938)	6.49	3.24E-02
negative regulation of supramolecular fiber organization (GO:1902904)	6.34	3.16E-03
blood coagulation (GO:0007596)	5.88	4.65E-08
coagulation (GO:0050817)	5.84	4.42E-08
hemostasis (GO:0007599)	5.78	4.60E-08
regulation of endothelial cell proliferation (GO:0001936)	5.36	3.67E-02
cell-matrix adhesion (GO:0007160)	5.33	1.94E-02
cell-substrate adhesion (GO:0031589)	5.23	2.92E-03
cell junction assembly (GO:0034329)	5.2	1.15E-02
wound healing (GO:0042060)	5.11	5.92E-10
response to organophosphorus (GO:0046683)	4.89	2.99E-02
regulation of wound healing (GO:0061041)	4.75	3.55E-02
cell junction organization (GO:0034330)	4.7	3.20E-03
regulation of muscle contraction (GO:0006937)	4.64	2.27E-02
regulation of response to wounding (GO:1903034)	4.52	2.57E-02
regulation of body fluid levels (GO:0050878)	4.35	9.57E-08
response to wounding (GO:0009611)	4.28	2.79E-08
cell-cell junction organization (GO:0045216)	4.25	3.65E-02
actin filament organization (GO:0007015)	4.19	1.45E-02
regulation of supramolecular fiber organization (GO:1902903)	3.89	1.89E-03
supramolecular fiber organization (GO:0097435)	3.54	1.93E-03
positive regulation of cell migration (GO:0030335)	3.37	2.03E-03
regulated exocytosis (GO:0045055)	3.36	8.32E-06
blood circulation (GO:0008015)	3.27	9.91E-03
positive regulation of cell motility (GO:2000147)	3.25	3.02E-03
circulatory system process (GO:0003013)	3.23	1.08E-02
positive regulation of locomotion (GO:0040017)	3.18	2.55E-03
actin cytoskeleton organization (GO:0030036)	3.17	5.81E-03
positive regulation of cellular component movement (GO:0051272)	3.16	3.84E-03
regulation of actin filament-based process (GO:0032970)	3.13	2.99E-02
actin filament-based process (GO:0030029)	3.13	2.07E-03
exocytosis (GO:0006887)	3.09	2.52E-05
cell adhesion (GO:0007155)	2.9	3.37E-05
regulation of cytoskeleton organization (GO:0051493)	2.9	1.47E-02
biological adhesion (GO:0022610)	2.88	3.61E-05
regulation of anatomical structure size (GO:0090066)	2.79	2.69E-02
cell-cell adhesion (GO:0098609)	2.78	3.77E-02
secretion (GO:0046903)	2.7	2.42E-05
secretion by cell (GO:0032940)	2.64	2.41E-04
cytoskeleton organization (GO:0007010)	2.6	3.03E-04
cell activation (GO:0001775)	2.48	9.98E-04
regulation of cell migration (GO:0030334)	2.47	1.76E-02
regulation of locomotion (GO:0040012)	2.45	5.73E-03
regulation of cell motility (GO:2000145)	2.4	1.58E-02
regulation of cellular component movement (GO:0051270)	2.36	1.15E-02
vesicle-mediated transport (GO:0016192)	2.31	7.65E-06
locomotion (GO:0040011)	2.04	2.51E-02
movement of cell or subcellular component (GO:0006928)	2.03	7.82E-03
regulation of cell proliferation (GO:0042127)	1.87	2.73E-02

regulation of cell differentiation (GO:0045595)	1.86	2.54E-02
regulation of biological quality (GO:0065008)	1.79	1.93E-05
regulation of multicellular organismal process (GO:0051239)	1.78	1.33E-03
cell surface receptor signaling pathway (GO:0007166)	1.75	1.52E-02
response to stress (GO:0006950)	1.74	2.57E-04
regulation of developmental process (GO:0050793)	1.73	1.49E-02
anatomical structure morphogenesis (GO:0009653)	1.72	4.91E-02
regulation of cellular component organization (GO:0051128)	1.7	2.51E-02
cellular component assembly (GO:0022607)	1.66	4.26E-02
establishment of localization (GO:0051234)	1.6	5.51E-04
transport (GO:0006810)	1.59	1.12E-03
localization (GO:0051179)	1.58	2.90E-05
regulation of cell communication (GO:0010646)	1.52	4.89E-02
signal transduction (GO:0007165)	1.4	4.94E-02
anatomical structure development (GO:0048856)	1.39	4.79E-02
cell communication (GO:0007154)	1.38	4.70E-02
multicellular organismal process (GO:0032501)	1.35	1.99E-02
response to stimulus (GO:0050896)	1.31	1.52E-02
cellular nitrogen compound metabolic process (GO:0034641)	0.63	3.67E-02
organic cyclic compound metabolic process (GO:1901360)	0.56	5.37E-03
nucleobase-containing compound metabolic process (GO:0006139)	0.55	9.46E-03
cellular macromolecule biosynthetic process (GO:0034645)	0.55	3.55E-02
cellular aromatic compound metabolic process (GO:0006725)	0.54	4.02E-03
heterocycle metabolic process (GO:0046483)	0.53	3.06E-03
gene expression (GO:0010467)	0.52	1.51E-02
nucleic acid metabolic process (GO:0090304)	0.49	3.08E-03
RNA metabolic process (GO:0016070)	0.48	9.50E-03
RNA processing (GO:0006396)	0.08	2.13E-02

Supplementary Table 19. GO biological process enrichment in 592 genes down in [‘Metastasis’ v ‘Unaffected’] ONLY

GO biological process	**Fold Enrichment**	**FDR**
gene expression (GO:0010467)	1.64	6.52E-05
RNA metabolic process (GO:0016070)	1.64	2.20E-04
transcription, DNA-templated (GO:0006351)	1.62	7.46E-03
nucleic acid-templated transcription (GO:0097659)	1.62	6.83E-03
RNA biosynthetic process (GO:0032774)	1.62	8.86E-03
nucleic acid metabolic process (GO:0090304)	1.55	4.65E-04
nucleobase-containing compound biosynthetic process (GO:0034654)	1.52	2.72E-02
nucleobase-containing compound metabolic process (GO:0006139)	1.51	4.72E-04
aromatic compound biosynthetic process (GO:0019438)	1.5	4.11E-02
cellular nitrogen compound biosynthetic process (GO:0044271)	1.48	2.23E-02
heterocycle metabolic process (GO:0046483)	1.48	5.46E-04
cellular aromatic compound metabolic process (GO:0006725)	1.48	5.07E-04
cellular macromolecule biosynthetic process (GO:0034645)	1.48	1.70E-02
organic cyclic compound metabolic process (GO:1901360)	1.47	4.23E-04
cellular nitrogen compound metabolic process (GO:0034641)	1.47	3.69E-04
macromolecule biosynthetic process (GO:0009059)	1.46	1.83E-02
response to stimulus (GO:0050896)	0.72	4.89E-03

Supplementary Table 20 Clusters of differentially expressed in ‘metastasis’ compared to ‘primary’

Cluster	Number of Probes	Gene or Probe	Module
C1	1	**KCNJ2**	
C2	22	A_21_P0014136	NA
		KCNIP4	NA
		MMAA	NA
		DHFRL1	NA
		MRPS18C	M5.13_Not.Determined
		RAB30-AS1	NA
		BCDIN3D	M7.24_Undetermined
		lnc-GBP6-1	NA
		GXYLT1	M7.3_Not.Determined
		TEFM	NA
		MIEF2	NA
		LAMC3	NA
			NA
		FBXO48	NA
		PAXIP1-AS2	NA
		FBXL19-AS1	NA
		LOC101930072	NA
		AQR	M6.2_Mitochondrial.Respiration
		CDRT1	NA
		CHAD	NA
		lnc-QPCT-3	NA
C3	49	**STON2**	NA
		ENKUR	M6.14_Not.Determined
		BEND2	NA
		SPX	NA

DNM3	M1.1_Platelets
TBXA2R	M9.41_Undetermined
LCN2	NA
NEXN	M8.18_Undetermined
lnc-ZNF100-2	NA
PBX1	M3.1_Erythrocytes
P2RY12	M9.21_Undetermined
VEPH1	M9.21_Undetermined
RNF208	NA
ACRBP	M1.1_Platelets
GFI1B	M6.14_Not.Determined
PRKAR2B	NA
FAXDC2	M3.1_Erythrocytes|M4.4_Not.Determined
HIST1H2AC	M4.9_Not.Determined
SDPR	M1.1_Platelets
lnc-C11orf30-1	NA
	NA
TGFB1I1	M9.19_Undetermined
RNF208	NA
ABLIM3	M1.1_Platelets
lnc-EBF3-6	NA
LIMS1	M6.14_Not.Determined|M8.39_Undetermined
LOC728975	NA
PRTFDC1	M8.18_Undetermined
EGF	M1.1_Platelets
TRIM58	NA
RAB27B	M1.1_Platelets|M6.14_Not.Determined
ALOX12	M1.1_Platelets

		F2RL3	NA
		TREML1	M1.1_Platelets
			NA
		NRGN	M1.1_Platelets
		TMEM40	M1.1_Platelets
		P2RY1	M9.21_Undetermined
		XK	M2.3_Erythrocytes
		TTC7B	NA
		PCYT1B	NA
		ASAP2	M1.1_Platelets
		LOC100130938	NA
		IGF2BP3	M7.16_Not.Determined
		PDGFA	NA
		F13A1	M1.1_Platelets
		SH3BGRL2	NA
		SMIM6	NA
		lnc-CBFA2T3-2	NA
			NA
		lnc-C10orf31-2	NA
		YWHAZ	M4.9_Not.Determined|M9.44_Undetermined
		TFPI	M1.1_Platelets|M8.39_Undetermined
C4	56	**MAX**	M6.14_Not.Determined|M7.30_Undetermined|M9.4_Undetermined|M9.10_Undetermined
		HIST1H2AG	M1.1_Platelets
		ODF3L2	NA
			NA
		ARHGAP32	M8.25_Undetermined
		TSPAN33	M1.1_Platelets
		TPM4	NA

FAM212B-AS1	NA
LYPLAL1-AS1	NA
LCE3C	NA
CGREF1	NA
ADCY3	M7.29_Not.Determined
NPTN	M8.2_Not.Determined
GRAP2	M1.1_Platelets
MCUR1	M8.51_Undetermined
LOC100294362	NA
ATP2C1	M7.17_Undetermined|M8.36_Undetermined
ACTN1	M4.13_Inflammation
LY6G6D	M9.21_Undetermined
TMEM91	NA
EIF2AK1	M4.4_Not.Determined
HIPK2	M7.26_Undetermined
MPP1	M7.33_Undetermined
UGT2B10	NA
MMD	M1.1_Platelets
HIST1H2BK	M7.16_Not.Determined
TRIM10	M2.3_Erythrocytes|M4.4_Not.Determined
BCL2L11	NA
FKBP1B	NA
MCUR1	M8.51_Undetermined
NPPA	M9.51_Undetermined
ITGB1	M5.4_Not.Determined|M7.3_Not.Determined
HDGF	M4.4_Not.Determined
ANKRD9	M9.26_Undetermined
FHL1	M1.1_Platelets

C5	18	**LOC101927437**	NA
		TUBA3C	NA
		lnc-NBPF3-4	NA
		C1orf86	M5.8_Not.Determined
		DNAH14	NA
		SMOX	M7.33_Undetermined
		WFDC3	NA
		ITGA9-AS1	NA
		FGF13	M7.29_Not.Determined|M9.15_Undetermined
		OPN1MW	NA
		SNORA55	NA
		SRRM2	M9.5_Undetermined
		R3HDM4	M3.1_Erythrocytes
		TNNC2	M1.1_Platelets
		lnc-RTN2-1	NA
		KLF6	M7.2_Not.Determined|M7.15_Undetermined|M7.23_Undetermined
		FOSB	M8.69_Undetermined
		ADRA1A	M2.2_Cell.Cycle
		XLOC_l2_001206	NA
		C8G	NA
		lnc-PPIA-1	NA
		LINC00856	NA
		ITGA7	NA
		CCL16	NA
			NA
		LOC102467146	NA
		NUTM2G	NA
		LOC100128670	NA

	NA
LINC00083	NA
CBX7	M7.18_Undetermined
	NA

Supplementary Table 21 IRGs up ‘Primary’ v ‘Unaffected’

Ensembl Id	Gene Name	Description
ENSG00000107897	ACBD5	acyl-CoA binding domain containing 5 [Source:HGNC Symbol;Acc:23338]
ENSG00000157823	AP3S2	adaptor-related protein complex 3, sigma 2 subunit [Source:HGNC Symbol;Acc:571]
ENSG00000147889	CDKN2A	cyclin-dependent kinase inhibitor 2A [Source:HGNC Symbol;Acc:1787]
ENSG00000166446	CDYL2	chromodomain protein, Y-like 2 [Source:HGNC Symbol;Acc:23030]
ENSG00000169245	CXCL10	chemokine (C-X-C motif) ligand 10 [Source:HGNC Symbol;Acc:10637]
ENSG00000117228	GBP1	guanylate binding protein 1, interferon-inducible [Source:HGNC Symbol;Acc:4182]
ENSG00000225492	GBP1P1	guanylate binding protein 1, interferon-inducible pseudogene 1 [Source:HGNC Symbol;Acc:39561]
ENSG00000180875	GREM2	gremlin 2, DAN family BMP antagonist [Source:HGNC Symbol;Acc:17655]
ENSG00000134470	IL15RA	interleukin 15 receptor, alpha [Source:HGNC Symbol;Acc:5978]
ENSG00000151689	INPP1	inositol polyphosphate-1-phosphatase [Source:HGNC Symbol;Acc:6071]
ENSG00000123700	KCNJ2	potassium inwardly-rectifying channel, subfamily J, member 2 [Source:HGNC Symbol;Acc:6263]
ENSG00000153029	MR1	major histocompatibility complex, class I-related [Source:HGNC Symbol;Acc:4975]
ENSG00000185499	MUC1	mucin 1, cell surface associated [Source:HGNC Symbol;Acc:7508]
ENSG00000138496	PARP9	poly (ADP-ribose) polymerase family, member 9 [Source:HGNC Symbol;Acc:24118]
ENSG00000261128	RP11-18F14.2	
ENSG00000175356	SCUBE2	signal peptide, CUB domain, EGF-like 2 [Source:HGNC Symbol;Acc:30425]

Supplementary Table 22 IRGs down ‘Primary’ v ‘Unaffected’

Ensembl Id	Gene Name	Description
ENSG00000154027	AK5	adenylate kinase 5 [Source:HGNC Symbol;Acc:365]
ENSG00000110881	ASIC1	acid-sensing (proton-gated) ion channel 1 [Source:HGNC Symbol;Acc:100]
ENSG00000149311	ATM	ataxia telangiectasia mutated [Source:HGNC Symbol;Acc:795]
ENSG00000133466	C1QTNF6	C1q and tumor necrosis factor related protein 6 [Source:HGNC Symbol;Acc:14343]
ENSG00000174807	CD248	CD248 molecule, endosialin [Source:HGNC Symbol;Acc:18219]
ENSG00000169031	COL4A3	collagen, type IV, alpha 3 (Goodpasture antigen) [Source:HGNC Symbol;Acc:2204]
ENSG00000119772	DNMT3A	DNA (cytosine-5-)-methyltransferase 3 alpha [Source:HGNC Symbol;Acc:2978]
ENSG00000120915	EPHX2	epoxide hydrolase 2, cytoplasmic [Source:HGNC Symbol;Acc:3402]
ENSG00000141665	FBXO15	F-box protein 15 [Source:HGNC Symbol;Acc:13617]
ENSG00000152795	HNRNPDL	heterogeneous nuclear ribonucleoprotein D-like [Source:HGNC Symbol;Acc:5037]
ENSG00000140443	IGF1R	insulin-like growth factor 1 receptor [Source:HGNC Symbol;Acc:5465]
ENSG00000119771	KLHL29	kelch-like family member 29 [Source:HGNC Symbol;Acc:29404]
ENSG00000146021	KLHL3	kelch-like family member 3 [Source:HGNC Symbol;Acc:6354]
ENSG00000070018	LRP6	low density lipoprotein receptor-related protein 6 [Source:HGNC Symbol;Acc:6698]
ENSG00000184384	MAML2	mastermind-like 2 (Drosophila) [Source:HGNC Symbol;Acc:16259]
ENSG00000152465	NMT2	N-myristoyltransferase 2 [Source:HGNC Symbol;Acc:7858]
ENSG00000151623	NR3C2	nuclear receptor subfamily 3, group C, member 2 [Source:HGNC Symbol;Acc:7979]
ENSG00000091129	NRCAM	neuronal cell adhesion molecule [Source:HGNC Symbol;Acc:7994]
ENSG00000101751	POLI	polymerase (DNA directed) iota [Source:HGNC Symbol;Acc:9182]
ENSG00000122965	RBM19	RNA binding motif protein 19 [Source:HGNC Symbol;Acc:29098]
ENSG00000182568	SATB1	SATB homeobox 1 [Source:HGNC Symbol;Acc:10541]
ENSG00000164300	SERINC5	serine incorporator 5 [Source:HGNC Symbol;Acc:18825]
ENSG00000112394	SLC16A10	solute carrier family 16 (aromatic amino acid transporter), member 10 [Source:HGNC Symbol;Acc:17027]
ENSG00000072195	SPEG	SPEG complex locus [Source:HGNC Symbol;Acc:16901]
ENSG00000147003	TMEM27	transmembrane protein 27 [Source:HGNC Symbol;Acc:29437]

ENSG00000174292	TNK1	tyrosine kinase, non-receptor, 1 [Source:HGNC Symbol;Acc:11940]
ENSG00000197763	TXNRD3	thioredoxin reductase 3 [Source:HGNC Symbol;Acc:20667]
ENSG00000206483	TXNRD3NB	thioredoxin reductase 3 neighbor [Source:HGNC Symbol;Acc:33870]

Supplementary Table. 23 IRGs up in ‘Metastasis’ v ‘Unaffected’

Ensembl Id	Gene Name	Description
ENSG00000183044	ABAT	4-aminobutyrate aminotransferase [Source:HGNC Symbol;Acc:23]
ENSG00000108846	ABCC3	ATP-binding cassette, sub-family C (CFTR/MRP), member 3 [Source:HGNC Symbol;Acc:54]
ENSG00000125257	ABCC4	ATP-binding cassette, sub-family C (CFTR/MRP), member 4 [Source:HGNC Symbol;Acc:55]
ENSG00000172482	AGXT	alanine-glyoxylate aminotransferase [Source:HGNC Symbol;Acc:341]
ENSG00000108839	ALOX12	arachidonate 12-lipoxygenase [Source:HGNC Symbol;Acc:429]
ENSG00000154188	ANGPT1	angiopoietin 1 [Source:HGNC Symbol;Acc:484]
ENSG00000156381	ANKRD9	ankyrin repeat domain 9 [Source:HGNC Symbol;Acc:20096]
ENSG00000047648	ARHGAP6	Rho GTPase activating protein 6 [Source:HGNC Symbol;Acc:676]
ENSG00000151693	ASAP2	ArfGAP with SH3 domain, ankyrin repeat and PH domain 2 [Source:HGNC Symbol;Acc:2721]
ENSG00000110046	ATG2A	autophagy related 2A [Source:HGNC Symbol;Acc:29028]
ENSG00000123810	B9D2	B9 protein domain 2 [Source:HGNC Symbol;Acc:28636]
ENSG00000171552	BCL2L1	BCL2-like 1 [Source:HGNC Symbol;Acc:992]
ENSG00000153094	BCL2L11	BCL2-like 11 (apoptosis facilitator) [Source:HGNC Symbol;Acc:994]
ENSG00000153162	BMP6	bone morphogenetic protein 6 [Source:HGNC Symbol;Acc:1073]
ENSG00000156206	C15orf26	chromosome 15 open reading frame 26 [Source:HGNC Symbol;Acc:26782]
ENSG00000135932	CAB39	calcium binding protein 39 [Source:HGNC Symbol;Acc:20292]
ENSG00000160014	CALM3	calmodulin 3 (phosphorylase kinase, delta) [Source:HGNC Symbol;Acc:1449]
ENSG00000178363	CALML3	calmodulin-like 3 [Source:HGNC Symbol;Acc:1452]
ENSG00000130940	CASZ1	castor zinc finger 1 [Source:HGNC Symbol;Acc:26002]
ENSG00000260916	CCPG1	cell cycle progression 1 [Source:HGNC Symbol;Acc:24227]
ENSG00000150637	CD226	CD226 molecule [Source:HGNC Symbol;Acc:16961]
ENSG00000010278	CD9	CD9 molecule [Source:HGNC Symbol;Acc:1709]

ENSG00000081377	CDC14B	cell division cycle 14B [Source:HGNC Symbol;Acc:1719]
ENSG00000147889	CDKN2A	cyclin-dependent kinase inhibitor 2A [Source:HGNC Symbol;Acc:1787]
ENSG00000101290	CDS2	CDP-diacylglycerol synthase (phosphatidate cytidylyltransferase) 2 [Source:HGNC Symbol;Acc:1801]
ENSG00000087237	CETP	cholesteryl ester transfer protein, plasma [Source:HGNC Symbol;Acc:1869]
ENSG00000165682	CLEC1B	C-type lectin domain family 1, member B [Source:HGNC Symbol;Acc:24356]
ENSG00000120885	CLU	clusterin [Source:HGNC Symbol;Acc:2095]
ENSG00000153815	CMIP	c-Maf inducing protein [Source:HGNC Symbol;Acc:24319]
ENSG00000182158	CREB3L2	cAMP responsive element binding protein 3-like 2 [Source:HGNC Symbol;Acc:23720]
ENSG00000060566	CREB3L3	cAMP responsive element binding protein 3-like 3 [Source:HGNC Symbol;Acc:18855]
ENSG00000144677	CTDSPL	CTD (carboxy-terminal domain, RNA polymerase II, polypeptide A) small phosphatase-like [Source:HGNC Symbol;Acc:16890]
ENSG00000064601	CTSA	cathepsin A [Source:HGNC Symbol;Acc:9251]
ENSG00000085733	CTTN	cortactin [Source:HGNC Symbol;Acc:3338]
ENSG00000163735	CXCL5	chemokine (C-X-C motif) ligand 5 [Source:HGNC Symbol;Acc:10642]
ENSG00000100243	CYB5R3	cytochrome b5 reductase 3 [Source:HGNC Symbol;Acc:2873]
ENSG00000070190	DAPP1	dual adaptor of phosphotyrosine and 3-phosphoinositides [Source:HGNC Symbol;Acc:16500]
ENSG00000137145	DENND4C	DENN/MADD domain containing 4C [Source:HGNC Symbol;Acc:26079]
ENSG00000077044	DGKD	diacylglycerol kinase, delta 130kDa [Source:HGNC Symbol;Acc:2851]
ENSG00000134755	DSC2	desmocollin 2 [Source:HGNC Symbol;Acc:3036]
ENSG00000261771	DYX1C1-CCPG1	DYX1C1-CCPG1 readthrough (non-protein coding) [Source:HGNC Symbol;Acc:43019]
ENSG00000075151	EIF4G3	eukaryotic translation initiation factor 4 gamma, 3 [Source:HGNC Symbol;Acc:3298]
ENSG00000164181	ELOVL7	ELOVL fatty acid elongase 7 [Source:HGNC Symbol;Acc:26292]
ENSG00000149218	ENDOD1	endonuclease domain containing 1 [Source:HGNC Symbol;Acc:29129]
ENSG00000262523	ENDOD1	endonuclease domain containing 1 [Source:HGNC Symbol;Acc:29129]
ENSG00000187266	EPOR	erythropoietin receptor [Source:HGNC Symbol;Acc:3416]
ENSG00000158769	F11R	F11 receptor [Source:HGNC Symbol;Acc:14685]
ENSG00000124491	F13A1	coagulation factor XIII, A1 polypeptide [Source:HGNC Symbol;Acc:3531]
ENSG00000181104	F2R	coagulation factor II (thrombin) receptor [Source:HGNC Symbol;Acc:3537]
ENSG00000103876	FAH	fumarylacetoacetate hydrolase (fumarylacetoacetase) [Source:HGNC Symbol;Acc:3579]

ENSG00000189319	FAM53B	family with sequence similarity 53, member B [Source:HGNC Symbol;Acc:28968]
ENSG00000143409	FAM63A	family with sequence similarity 63, member A [Source:HGNC Symbol;Acc:25648]
ENSG00000197601	FAR1	fatty acyl CoA reductase 1 [Source:HGNC Symbol;Acc:26222]
ENSG00000170271	FAXDC2	fatty acid hydroxylase domain containing 2 [Source:HGNC Symbol;Acc:1334]
ENSG00000132004	FBXW9	F-box and WD repeat domain containing 9 [Source:HGNC Symbol;Acc:28136]
ENSG00000129682	FGF13	fibroblast growth factor 13 [Source:HGNC Symbol;Acc:3670]
ENSG00000119782	FKBP1B	FK506 binding protein 1B, 12.6 kDa [Source:HGNC Symbol;Acc:3712]
ENSG00000196924	FLNA	filamin A, alpha [Source:HGNC Symbol;Acc:3754]
ENSG00000172159	FRMD3	FERM domain containing 3 [Source:HGNC Symbol;Acc:24125]
ENSG00000107164	FUBP3	far upstream element (FUSE) binding protein 3 [Source:HGNC Symbol;Acc:4005]
ENSG00000185340	GAS2L1	growth arrest-specific 2 like 1 [Source:HGNC Symbol;Acc:16955]
ENSG00000102145	GATA1	GATA binding protein 1 (globin transcription factor 1) [Source:HGNC Symbol;Acc:4170]
ENSG00000102393	GLA	galactosidase, alpha [Source:HGNC Symbol;Acc:4296]
ENSG00000137198	GMPR	guanosine monophosphate reductase [Source:HGNC Symbol;Acc:4376]
ENSG00000203618	GP1BB	glycoprotein Ib (platelet), beta polypeptide [Source:HGNC Symbol;Acc:4440]
ENSG00000115159	GPD2	glycerol-3-phosphate dehydrogenase 2 (mitochondrial) [Source:HGNC Symbol;Acc:4456]
ENSG00000180875	GREM2	gremlin 2, DAN family BMP antagonist [Source:HGNC Symbol;Acc:17655]
ENSG00000061918	GUCY1B3	guanylate cyclase 1, soluble, beta 3 [Source:HGNC Symbol;Acc:4687]
ENSG00000234289	H2BFS	H2B histone family, member S (pseudogene) [Source:HGNC Symbol;Acc:4762]
ENSG00000166503	HDGFRP3	Hepatoma-derived growth factor-related protein 3 [Source:UniProtKB/Swiss-Prot;Acc:Q9Y3E1]
ENSG00000064393	HIPK2	homeodomain interacting protein kinase 2 [Source:HGNC Symbol;Acc:14402]
ENSG00000197903	HIST1H2BK	histone cluster 1, H2bk [Source:HGNC Symbol;Acc:13954]
ENSG00000073792	IGF2BP2	insulin-like growth factor 2 mRNA binding protein 2 [Source:HGNC Symbol;Acc:28867]
ENSG00000136231	IGF2BP3	insulin-like growth factor 2 mRNA binding protein 3 [Source:HGNC Symbol;Acc:28868]
ENSG00000166333	ILK	integrin-linked kinase [Source:HGNC Symbol;Acc:6040]
ENSG00000005961	ITGA2B	integrin, alpha 2b (platelet glycoprotein IIb of IIb/IIIa complex, antigen CD41) [Source:HGNC Symbol;Acc:6138]
ENSG00000259207	ITGB3	integrin, beta 3 (platelet glycoprotein IIIa, antigen CD61) [Source:HGNC Symbol;Acc:6156]
ENSG00000082781	ITGB5	integrin, beta 5 [Source:HGNC Symbol;Acc:6160]

ENSG00000069424	KCNAB2	potassium voltage-gated channel, shaker-related subfamily, beta member 2 [Source:HGNC Symbol;Acc:6229]
ENSG00000171385	KCND3	potassium voltage-gated channel, Shal-related subfamily, member 3 [Source:HGNC Symbol;Acc:6239]
ENSG00000067082	KLF6	Kruppel-like factor 6 [Source:HGNC Symbol;Acc:2235]
ENSG00000148346	LCN2	lipocalin 2 [Source:HGNC Symbol;Acc:6526]
ENSG00000106003	LFNG	LFNG O-fucosylpeptide 3-beta-N-acetylglucosaminyltransferase [Source:HGNC Symbol;Acc:6560]
ENSG00000116977	LGALS8	lectin, galactoside-binding, soluble, 8 [Source:HGNC Symbol;Acc:6569]
ENSG00000119862	LGALSL	lectin, galactoside-binding-like [Source:HGNC Symbol;Acc:25012]
ENSG00000169756	LIMS1	LIM and senescent cell antigen-like domains 1 [Source:HGNC Symbol;Acc:6616]
ENSG00000240428	LIMS1	LIM and senescent cell antigen-like-containing domain protein 3; LIM and senescent cell antigen-like-containing domain protein 3-like; Uncharacterized protein; cDNA FLJ59124, highly similar to Particularly interesting newCys-His protein; cDNA, FLJ79109, highly similar to Particularly interesting newCys-His protein [Source:UniProtKB/TrEMBL;Acc:B4DPH6]
ENSG00000256977	LIMS3	LIM and senescent cell antigen-like domains 3 [Source:HGNC Symbol;Acc:30047]
ENSG00000257207	LIMS3	LIM and senescent cell antigen-like-containing domain protein 3; Uncharacterized protein; cDNA FLJ59124, highly similar to Particularly interesting newCys-His protein; cDNA, FLJ79109, highly similar to Particularly interesting newCys-His protein [Source:UniProtKB/TrEMBL;Acc:B4DPH6]
ENSG00000147650	LRP12	low density lipoprotein receptor-related protein 12 [Source:HGNC Symbol;Acc:31708]
ENSG00000093167	LRRFIP2	leucine rich repeat (in FLII) interacting protein 2 [Source:HGNC Symbol;Acc:6703]
ENSG00000049323	LTBP1	latent transforming growth factor beta binding protein 1 [Source:HGNC Symbol;Acc:6714]
ENSG00000140941	MAP1LC3B	microtubule-associated protein 1 light chain 3 beta [Source:HGNC Symbol;Acc:13352]
ENSG00000034152	MAP2K3	mitogen-activated protein kinase kinase 3 [Source:HGNC Symbol;Acc:6843]
ENSG00000197442	MAP3K5	mitogen-activated protein kinase kinase kinase 5 [Source:HGNC Symbol;Acc:6857]
ENSG00000125952	MAX	MYC associated factor X [Source:HGNC Symbol;Acc:6913]
ENSG00000050393	MCUR1	mitochondrial calcium uniporter regulator 1 [Source:HGNC Symbol;Acc:21097]
ENSG00000198948	MFAP3L	microfibrillar-associated protein 3-like [Source:HGNC Symbol;Acc:29083]
ENSG00000205639	MFSD2B	major facilitator superfamily domain containing 2B [Source:HGNC Symbol;Acc:37207]
ENSG00000074416	MGLL	monoglyceride lipase [Source:HGNC Symbol;Acc:17038]
ENSG00000175727	MLXIP	MLX interacting protein [Source:HGNC Symbol;Acc:17055]
ENSG00000196611	MMP1	matrix metallopeptidase 1 (interstitial collagenase) [Source:HGNC Symbol;Acc:7155]
ENSG00000130830	MPP1	membrane protein, palmitoylated 1, 55kDa [Source:HGNC Symbol;Acc:7219]
ENSG00000066697	MSANTD3	Myb/SANT-like DNA-binding domain containing 3 [Source:HGNC Symbol;Acc:23370]
ENSG00000100330	MTMR3	myotubularin related protein 3 [Source:HGNC Symbol;Acc:7451]

ENSG00000180354	MTURN	maturin, neural progenitor differentiation regulator homolog (Xenopus) [Source:HGNC Symbol;Acc:25457]
ENSG00000185499	MUC1	mucin 1, cell surface associated [Source:HGNC Symbol;Acc:7508]
ENSG00000065534	MYLK	myosin light chain kinase [Source:HGNC Symbol;Acc:7590]
ENSG00000162614	NEXN	nexilin (F actin binding protein) [Source:HGNC Symbol;Acc:29557]
ENSG00000196712	NF1	neurofibromin 1 [Source:HGNC Symbol;Acc:7765]
ENSG00000147862	NFIB	nuclear factor I/B [Source:HGNC Symbol;Acc:7785]
ENSG00000115761	NOL10	nucleolar protein 10 [Source:HGNC Symbol;Acc:25862]
ENSG00000156642	NPTN	neuroplastin [Source:HGNC Symbol;Acc:17867]
ENSG00000154146	NRGN	neurogranin (protein kinase C substrate, RC3) [Source:HGNC Symbol;Acc:8000]
ENSG00000108405	P2RX1	purinergic receptor P2X, ligand-gated ion channel, 1 [Source:HGNC Symbol;Acc:8533]
ENSG00000138801	PAPSS1	3'-phosphoadenosine 5'-phosphosulfate synthase 1 [Source:HGNC Symbol;Acc:8603]
ENSG00000148498	PARD3	par-3 family cell polarity regulator [Source:HGNC Symbol;Acc:16051]
ENSG00000185630	PBX1	pre-B-cell leukemia homeobox 1 [Source:HGNC Symbol;Acc:8632]
ENSG00000140479	PCSK6	proprotein convertase subtilisin/kexin type 6 [Source:HGNC Symbol;Acc:8569]
ENSG00000161217	PCYT1A	phosphate cytidylyltransferase 1, choline, alpha [Source:HGNC Symbol;Acc:8754]
ENSG00000197461	PDGFA	platelet-derived growth factor alpha polypeptide [Source:HGNC Symbol;Acc:8799]
ENSG00000145431	PDGFC	platelet derived growth factor C [Source:HGNC Symbol;Acc:8801]
ENSG00000107438	PDLIM1	PDZ and LIM domain 1 [Source:HGNC Symbol;Acc:2067]
ENSG00000196923	PDLIM7	PDZ and LIM domain 7 (enigma) [Source:HGNC Symbol;Acc:22958]
ENSG00000116793	PHTF1	putative homeodomain transcription factor 1 [Source:HGNC Symbol;Acc:8939]
ENSG00000137193	PIM1	pim-1 oncogene [Source:HGNC Symbol;Acc:8986]
ENSG00000123739	PLA2G12A	phospholipase A2, group XIIA [Source:HGNC Symbol;Acc:18554]
ENSG00000115762	PLEKHB2	pleckstrin homology domain containing, family B (evectins) member 2 [Source:HGNC Symbol;Acc:19236]
ENSG00000152952	PLOD2	procollagen-lysine, 2-oxoglutarate 5-dioxygenase 2 [Source:HGNC Symbol;Acc:9082]
ENSG00000057657	PRDM1	PR domain containing 1, with ZNF domain [Source:HGNC Symbol;Acc:9346]
ENSG00000005249	PRKAR2B	protein kinase, cAMP-dependent, regulatory, type II, beta [Source:HGNC Symbol;Acc:9392]
ENSG00000184500	PROS1	protein S (alpha) [Source:HGNC Symbol;Acc:9456]
ENSG00000095303	PTGS1	prostaglandin-endoperoxide synthase 1 (prostaglandin G/H synthase and cyclooxygenase) [Source:HGNC Symbol;Acc:9604]

ENSG00000127947	PTPN12	protein tyrosine phosphatase, non-receptor type 12 [Source:HGNC Symbol;Acc:9645]
ENSG00000168297	PXK	PX domain containing serine/threonine kinase [Source:HGNC Symbol;Acc:23326]
ENSG00000041353	RAB27B	RAB27B, member RAS oncogene family [Source:HGNC Symbol;Acc:9767]
ENSG00000132359	RAP1GAP2	RAP1 GTPase activating protein 2 [Source:HGNC Symbol;Acc:29176]
ENSG00000072042	RDH11	retinol dehydrogenase 11 (all-trans/9-cis/11-cis) [Source:HGNC Symbol;Acc:17964]
ENSG00000072422	RHOBTB1	Rho-related BTB domain containing 1 [Source:HGNC Symbol;Acc:18738]
ENSG00000129538	RNASE1	ribonuclease, RNase A family, 1 (pancreatic) [Source:HGNC Symbol;Acc:10044]
ENSG00000240912	RP11-274J15.2	
ENSG00000270149	RP11-544M22.13	Uncharacterized protein [Source:UniProtKB/TrEMBL;Acc:R4GMV9]
ENSG00000136021	SCYL2	SCY1-like 2 (S. cerevisiae) [Source:HGNC Symbol;Acc:19286]
ENSG00000115884	SDC1	syndecan 1 [Source:HGNC Symbol;Acc:10658]
ENSG00000129657	SEC14L1	SEC14-like 1 (S. cerevisiae) [Source:HGNC Symbol;Acc:10698]
ENSG00000184702	Sep-05	septin 5 [Source:HGNC Symbol;Acc:9164]
ENSG00000198478	SH3BGRL2	SH3 domain binding glutamic acid-rich protein like 2 [Source:HGNC Symbol;Acc:15567]
ENSG00000142669	SH3BGRL3	SH3 domain binding glutamic acid-rich protein like 3 [Source:HGNC Symbol;Acc:15568]
ENSG00000125089	SH3TC1	SH3 domain and tetratricopeptide repeats 1 [Source:HGNC Symbol;Acc:26009]
ENSG00000101082	SLA2	Src-like-adaptor 2 [Source:HGNC Symbol;Acc:17329]
ENSG00000139370	SLC15A4	solute carrier family 15 (oligopeptide transporter), member 4 [Source:HGNC Symbol;Acc:23090]
ENSG00000100678	SLC8A3	solute carrier family 8 (sodium/calcium exchanger), member 3 [Source:HGNC Symbol;Acc:11070]
ENSG00000176463	SLCO3A1	solute carrier organic anion transporter family, member 3A1 [Source:HGNC Symbol;Acc:10952]
ENSG00000088826	SMOX	spermine oxidase [Source:HGNC Symbol;Acc:15862]
ENSG00000145335	SNCA	synuclein, alpha (non A4 component of amyloid precursor) [Source:HGNC Symbol;Acc:11138]
ENSG00000113140	SPARC	secreted protein, acidic, cysteine-rich (osteonectin) [Source:HGNC Symbol;Acc:11219]
ENSG00000004866	ST7	suppression of tumorigenicity 7 [Source:HGNC Symbol;Acc:11351]
ENSG00000148175	STOM	stomatin [Source:HGNC Symbol;Acc:3383]
ENSG00000140022	STON2	stonin 2 [Source:HGNC Symbol;Acc:30652]
ENSG00000158710	TAGLN2	transgelin 2 [Source:HGNC Symbol;Acc:11554]
ENSG00000059377	TBXAS1	thromboxane A synthase 1 (platelet) [Source:HGNC Symbol;Acc:11609]

ENSG00000003436	TFPI	tissue factor pathway inhibitor (lipoprotein-associated coagulation inhibitor) [Source:HGNC Symbol;Acc:11760]
ENSG00000105329	TGFB1	transforming growth factor, beta 1 [Source:HGNC Symbol;Acc:11766]
ENSG00000146859	TMEM140	transmembrane protein 140 [Source:HGNC Symbol;Acc:21870]
ENSG00000240849	TMEM189	transmembrane protein 189 [Source:HGNC Symbol;Acc:16735]
ENSG00000137216	TMEM63B	transmembrane protein 63B [Source:HGNC Symbol;Acc:17735]
ENSG00000142046	TMEM91	transmembrane protein 91 [Source:HGNC Symbol;Acc:32393]
ENSG00000158164	TMSB15A	thymosin beta 15a [Source:HGNC Symbol;Acc:30744]
ENSG00000140416	TPM1	tropomyosin 1 (alpha) [Source:HGNC Symbol;Acc:12010]
ENSG00000161911	TREML1	triggering receptor expressed on myeloid cells-like 1 [Source:HGNC Symbol;Acc:20434]
ENSG00000204613	TRIM10	tripartite motif containing 10 [Source:HGNC Symbol;Acc:10072]
ENSG00000158457	TSPAN33	tetraspanin 33 [Source:HGNC Symbol;Acc:28743]
ENSG00000165914	TTC7B	tetratricopeptide repeat domain 7B [Source:HGNC Symbol;Acc:19858]
ENSG00000127824	TUBA4A	tubulin, alpha 4a [Source:HGNC Symbol;Acc:12407]
ENSG00000175063	UBE2C	ubiquitin-conjugating enzyme E2C [Source:HGNC Symbol;Acc:15937]
ENSG00000102178	UBL4A	ubiquitin-like 4A [Source:HGNC Symbol;Acc:12505]
ENSG00000165886	UBTD1	ubiquitin domain containing 1 [Source:HGNC Symbol;Acc:25683]
ENSG00000177169	ULK1	unc-51 like autophagy activating kinase 1 [Source:HGNC Symbol;Acc:12558]
ENSG00000105698	USF2	upstream transcription factor 2, c-fos interacting [Source:HGNC Symbol;Acc:12594]
ENSG00000035403	VCL	vinculin [Source:HGNC Symbol;Acc:12665]
ENSG00000150630	VEGFC	vascular endothelial growth factor C [Source:HGNC Symbol;Acc:12682]
ENSG00000110799	VWF	von Willebrand factor [Source:HGNC Symbol;Acc:12726]
ENSG00000131725	WDR44	WD repeat domain 44 [Source:HGNC Symbol;Acc:30512]
ENSG00000070540	WIPI1	WD repeat domain, phosphoinositide interacting 1 [Source:HGNC Symbol;Acc:25471]
ENSG00000182093	WRB	tryptophan rich basic protein [Source:HGNC Symbol;Acc:12790]
ENSG00000108039	XPNPEP1	X-prolyl aminopeptidase (aminopeptidase P) 1, soluble [Source:HGNC Symbol;Acc:12822]
ENSG00000109906	ZBTB16	zinc finger and BTB domain containing 16 [Source:HGNC Symbol;Acc:12930]
ENSG00000156639	ZFAND3	zinc finger, AN1-type domain 3 [Source:HGNC Symbol;Acc:18019]

Supplementary Table 24 IRGs down in ‘Metastasis’ v ‘Unaffected’

Ensembl Id	Gene Name	Description
ENSG00000170468	AC005280.1	
ENSG00000076555	ACACB	acetyl-CoA carboxylase beta [Source:HGNC Symbol;Acc:85]
ENSG00000120437	ACAT2	acetyl-CoA acetyltransferase 2 [Source:HGNC Symbol;Acc:94]
ENSG00000164398	ACSL6	acyl-CoA synthetase long-chain family member 6 [Source:HGNC Symbol;Acc:16496]
ENSG00000148700	ADD3	adducin 3 (gamma) [Source:HGNC Symbol;Acc:245]
ENSG00000116863	ADPRHL2	ADP-ribosylhydrolase like 2 [Source:HGNC Symbol;Acc:21304]
ENSG00000110711	AIP	aryl hydrocarbon receptor interacting protein [Source:HGNC Symbol;Acc:358]
ENSG00000154027	AK5	adenylate kinase 5 [Source:HGNC Symbol;Acc:365]
ENSG00000085662	AKR1B1	aldo-keto reductase family 1, member B1 (aldose reductase) [Source:HGNC Symbol;Acc:381]
ENSG00000166971	AKTIP	AKT interacting protein [Source:HGNC Symbol;Acc:16710]
ENSG00000112294	ALDH5A1	aldehyde dehydrogenase 5 family, member A1 [Source:HGNC Symbol;Acc:408]
ENSG00000118514	ALDH8A1	aldehyde dehydrogenase 8 family, member A1 [Source:HGNC Symbol;Acc:15471]
ENSG00000101901	ALG13	ALG13, UDP-N-acetylglucosaminyltransferase subunit [Source:HGNC Symbol;Acc:30881]
ENSG00000154122	ANKH	ANKH inorganic pyrophosphate transport regulator [Source:HGNC Symbol;Acc:15492]
ENSG00000131503	ANKHD1	ankyrin repeat and KH domain containing 1 [Source:HGNC Symbol;Acc:24714]
ENSG00000254996	ANKHD1-EIF4EBP3	ANKHD1-EIF4EBP3 readthrough [Source:HGNC Symbol;Acc:33530]
ENSG00000230006	ANKRD36BP2	ankyrin repeat domain 36B pseudogene 2 [Source:HGNC Symbol;Acc:33607]
ENSG00000164512	ANKRD55	ankyrin repeat domain 55 [Source:HGNC Symbol;Acc:25681]
ENSG00000165138	ANKS6	ankyrin repeat and sterile alpha motif domain containing 6 [Source:HGNC Symbol;Acc:26724]
ENSG00000166669	ATF7IP2	activating transcription factor 7 interacting protein 2 [Source:HGNC Symbol;Acc:20397]
ENSG00000149311	ATM	ataxia telangiectasia mutated [Source:HGNC Symbol;Acc:795]
ENSG00000206190	ATP10A	ATPase, class V, type 10A [Source:HGNC Symbol;Acc:13542]
ENSG00000182240	BACE2	beta-site APP-cleaving enzyme 2 [Source:HGNC Symbol;Acc:934]
ENSG00000140463	BBS4	Bardet-Biedl syndrome 4 [Source:HGNC Symbol;Acc:969]
ENSG00000127152	BCL11B	B-cell CLL/lymphoma 11B (zinc finger protein) [Source:HGNC Symbol;Acc:13222]

ENSG00000161267	BDH1	3-hydroxybutyrate dehydrogenase, type 1 [Source:HGNC Symbol;Acc:1027]
ENSG00000186470	BTN3A2	butyrophilin, subfamily 3, member A2 [Source:HGNC Symbol;Acc:1139]
ENSG00000111801	BTN3A3	butyrophilin, subfamily 3, member A3 [Source:HGNC Symbol;Acc:1140]
ENSG00000166167	BTRC	beta-transducin repeat containing E3 ubiquitin protein ligase [Source:HGNC Symbol;Acc:1144]
ENSG00000133641	C12orf29	chromosome 12 open reading frame 29 [Source:HGNC Symbol;Acc:25322]
ENSG00000111678	C12orf57	chromosome 12 open reading frame 57 [Source:HGNC Symbol;Acc:29521]
ENSG00000255242	C14orf169	chromosome 14 open reading frame 169 [Source:HGNC Symbol;Acc:20968]
ENSG00000212719	C17orf51	chromosome 17 open reading frame 51 [Source:HGNC Symbol;Acc:27904]
ENSG00000104979	C19orf53	chromosome 19 open reading frame 53 [Source:HGNC Symbol;Acc:24991]
ENSG00000221916	C19orf73	chromosome 19 open reading frame 73 [Source:HGNC Symbol;Acc:25534]
ENSG00000161010	C5orf45	chromosome 5 open reading frame 45 [Source:HGNC Symbol;Acc:30817]
ENSG00000144712	CAND2	cullin-associated and neddylation-dissociated 2 (putative) [Source:HGNC Symbol;Acc:30689]
ENSG00000150636	CCDC102B	coiled-coil domain containing 102B [Source:HGNC Symbol;Acc:26295]
ENSG00000005059	CCDC109B	coiled-coil domain containing 109B [Source:HGNC Symbol;Acc:26076]
ENSG00000175455	CCDC14	coiled-coil domain containing 14 [Source:HGNC Symbol;Acc:25766]
ENSG00000133773	CCDC59	coiled-coil domain containing 59 [Source:HGNC Symbol;Acc:25005]
ENSG00000126353	CCR7	chemokine (C-C motif) receptor 7 [Source:HGNC Symbol;Acc:1608]
ENSG00000174807	CD248	CD248 molecule, endosialin [Source:HGNC Symbol;Acc:18219]
ENSG00000139193	CD27	CD27 molecule [Source:HGNC Symbol;Acc:11922]
ENSG00000101224	CDC25B	cell division cycle 25B [Source:HGNC Symbol;Acc:1726]
ENSG00000158985	CDC42SE2	CDC42 small effector 2 [Source:HGNC Symbol;Acc:18547]
ENSG00000156345	CDK20	cyclin-dependent kinase 20 [Source:HGNC Symbol;Acc:21420]
ENSG00000151849	CENPJ	centromere protein J [Source:HGNC Symbol;Acc:17272]
ENSG00000198791	CNOT7	CCR4-NOT transcription complex, subunit 7 [Source:HGNC Symbol;Acc:14101]
ENSG00000100473	COCH	cochlin [Source:HGNC Symbol;Acc:2180]
ENSG00000169031	COL4A3	collagen, type IV, alpha 3 (Goodpasture antigen) [Source:HGNC Symbol;Acc:2204]
ENSG00000204262	COL5A2	collagen, type V, alpha 2 [Source:HGNC Symbol;Acc:2210]
ENSG00000142156	COL6A1	collagen, type VI, alpha 1 [Source:HGNC Symbol;Acc:2211]

ENSG00000188243	COMMD6	COMM domain containing 6 [Source:HGNC Symbol;Acc:24015]
ENSG00000130545	CRB3	crumbs homolog 3 (Drosophila) [Source:HGNC Symbol;Acc:20237]
ENSG00000149474	CSRP2BP	CSRP2 binding protein [Source:HGNC Symbol;Acc:15904]
ENSG00000176102	CSTF3	cleavage stimulation factor, 3' pre-RNA, subunit 3, 77kDa [Source:HGNC Symbol;Acc:2485]
ENSG00000226432	CTD-2015B23.2	
ENSG00000134716	CYP2J2	cytochrome P450, family 2, subfamily J, polypeptide 2 [Source:HGNC Symbol;Acc:2634]
ENSG00000057019	DCBLD2	discoidin, CUB and LCCL domain containing 2 [Source:HGNC Symbol;Acc:24627]
ENSG00000168724	DNAJC21	DnaJ (Hsp40) homolog, subfamily C, member 21 [Source:HGNC Symbol;Acc:27030]
ENSG00000163687	DNASE1L3	deoxyribonuclease I-like 3 [Source:HGNC Symbol;Acc:2959]
ENSG00000119772	DNMT3A	DNA (cytosine-5-)-methyltransferase 3 alpha [Source:HGNC Symbol;Acc:2978]
ENSG00000123992	DNPEP	aspartyl aminopeptidase [Source:HGNC Symbol;Acc:2981]
ENSG00000088387	DOCK9	dedicator of cytokinesis 9 [Source:HGNC Symbol;Acc:14132]
ENSG00000138036	DYNC2LI1	dynein, cytoplasmic 2, light intermediate chain 1 [Source:HGNC Symbol;Acc:24595]
ENSG00000107938	EDRF1	erythroid differentiation regulatory factor 1 [Source:HGNC Symbol;Acc:24640]
ENSG00000255150	EID3	EP300 interacting inhibitor of differentiation 3 [Source:HGNC Symbol;Acc:32961]
ENSG00000173674	EIF1AX	eukaryotic translation initiation factor 1A, X-linked [Source:HGNC Symbol;Acc:3250]
ENSG00000243056	EIF4EBP3	eukaryotic translation initiation factor 4E binding protein 3 [Source:HGNC Symbol;Acc:3290]
ENSG00000108515	ENO3	enolase 3 (beta, muscle) [Source:HGNC Symbol;Acc:3354]
ENSG00000132199	ENOSF1	enolase superfamily member 1 [Source:HGNC Symbol;Acc:30365]
ENSG00000120915	EPHX2	epoxide hydrolase 2, cytoplasmic [Source:HGNC Symbol;Acc:3402]
ENSG00000162894	FAIM3	Fas apoptotic inhibitory molecule 3 [Source:HGNC Symbol;Acc:14315]
ENSG00000138439	FAM117B	family with sequence similarity 117, member B [Source:HGNC Symbol;Acc:14440]
ENSG00000138286	FAM149B1	family with sequence similarity 149, member B1 [Source:HGNC Symbol;Acc:29162]
ENSG00000204677	FAM153C	family with sequence similarity 153, member C [Source:HGNC Symbol;Acc:33936]
ENSG00000119906	FAM178A	family with sequence similarity 178, member A [Source:HGNC Symbol;Acc:17814]
ENSG00000122378	FAM213A	family with sequence similarity 213, member A [Source:HGNC Symbol;Acc:28651]
ENSG00000204856	FAM216A	family with sequence similarity 216, member A [Source:HGNC Symbol;Acc:30180]
ENSG00000141665	FBXO15	F-box protein 15 [Source:HGNC Symbol;Acc:13617]

ENSG00000102678	FGF9	fibroblast growth factor 9 [Source:HGNC Symbol;Acc:3687]
ENSG00000151474	FRMD4A	FERM domain containing 4A [Source:HGNC Symbol;Acc:25491]
ENSG00000033170	FUT8	fucosyltransferase 8 (alpha (1,6) fucosyltransferase) [Source:HGNC Symbol;Acc:4019]
ENSG00000179144	GIMAP7	GTPase, IMAP family member 7 [Source:HGNC Symbol;Acc:22404]
ENSG00000163328	GPR155	G protein-coupled receptor 155 [Source:HGNC Symbol;Acc:22951]
ENSG00000125245	GPR18	G protein-coupled receptor 18 [Source:HGNC Symbol;Acc:4472]
ENSG00000163607	GTPBP8	GTP-binding protein 8 (putative) [Source:HGNC Symbol;Acc:25007]
ENSG00000111911	HINT3	histidine triad nucleotide binding protein 3 [Source:HGNC Symbol;Acc:18468]
ENSG00000156510	HKDC1	hexokinase domain containing 1 [Source:HGNC Symbol;Acc:23302]
ENSG00000152795	HNRNPDL	heterogeneous nuclear ribonucleoprotein D-like [Source:HGNC Symbol;Acc:5037]
ENSG00000140443	IGF1R	insulin-like growth factor 1 receptor [Source:HGNC Symbol;Acc:5465]
ENSG00000172349	IL16	interleukin 16 [Source:HGNC Symbol;Acc:5980]
ENSG00000198700	IPO9	importin 9 [Source:HGNC Symbol;Acc:19425]
ENSG00000261796	ISY1-RAB43	ISY1-RAB43 readthrough [Source:HGNC Symbol;Acc:42969]
ENSG00000078596	ITM2A	integral membrane protein 2A [Source:HGNC Symbol;Acc:6173]
ENSG00000119771	KLHL29	kelch-like family member 29 [Source:HGNC Symbol;Acc:29404]
ENSG00000146021	KLHL3	kelch-like family member 3 [Source:HGNC Symbol;Acc:6354]
ENSG00000185915	KLHL34	kelch-like family member 34 [Source:HGNC Symbol;Acc:26634]
ENSG00000111716	LDHB	lactate dehydrogenase B [Source:HGNC Symbol;Acc:6541]
ENSG00000105486	LIG1	ligase I, DNA, ATP-dependent [Source:HGNC Symbol;Acc:6598]
ENSG00000070018	LRP6	low density lipoprotein receptor-related protein 6 [Source:HGNC Symbol;Acc:6698]
ENSG00000138095	LRPPRC	leucine-rich pentatricopeptide repeat containing [Source:HGNC Symbol;Acc:15714]
ENSG00000173114	LRRN3	leucine rich repeat neuronal 3 [Source:HGNC Symbol;Acc:17200]
ENSG00000170860	LSM3	LSM3 homolog, U6 small nuclear RNA associated (S. cerevisiae) [Source:HGNC Symbol;Acc:17874]
ENSG00000179222	MAGED1	melanoma antigen family D, 1 [Source:HGNC Symbol;Acc:6813]
ENSG00000184384	MAML2	mastermind-like 2 (Drosophila) [Source:HGNC Symbol;Acc:16259]
ENSG00000117643	MAN1C1	mannosidase, alpha, class 1C, member 1 [Source:HGNC Symbol;Acc:19080]
ENSG00000014641	MDH1	malate dehydrogenase 1, NAD (soluble) [Source:HGNC Symbol;Acc:6970]

ENSG00000123427	METTL21B	methyltransferase like 21B [Source:HGNC Symbol;Acc:24936]
ENSG00000198408	MGEA5	meningioma expressed antigen 5 (hyaluronidase) [Source:HGNC Symbol;Acc:7056]
ENSG00000186260	MKL2	MKL/myocardin-like 2 [Source:HGNC Symbol;Acc:29819]
ENSG00000165943	MOAP1	modulator of apoptosis 1 [Source:HGNC Symbol;Acc:16658]
ENSG00000037757	MRI1	methylthioribose-1-phosphate isomerase 1 [Source:HGNC Symbol;Acc:28469]
ENSG00000095002	MSH2	mutS homolog 2 [Source:HGNC Symbol;Acc:7325]
ENSG00000005810	MYCBP2	MYC binding protein 2, E3 ubiquitin protein ligase [Source:HGNC Symbol;Acc:23386]
ENSG00000186310	NAP1L3	nucleosome assembly protein 1-like 3 [Source:HGNC Symbol;Acc:7639]
ENSG00000010292	NCAPD2	non-SMC condensin I complex, subunit D2 [Source:HGNC Symbol;Acc:24305]
ENSG00000109390	NDUFC1	NADH dehydrogenase (ubiquinone) 1, subcomplex unknown, 1, 6kDa [Source:HGNC Symbol;Acc:7705]
ENSG00000184613	NELL2	NEL-like 2 (chicken) [Source:HGNC Symbol;Acc:7751]
ENSG00000101004	NINL	ninein-like [Source:HGNC Symbol;Acc:29163]
ENSG00000152465	NMT2	N-myristoyltransferase 2 [Source:HGNC Symbol;Acc:7858]
ENSG00000254852	NPIPA2	nuclear pore complex interacting protein family, member A2 [Source:HGNC Symbol;Acc:41979]
ENSG00000183793	NPIPA5	nuclear pore complex interacting protein family, member A5 [Source:HGNC Symbol;Acc:41980]
ENSG00000233024	NPIPA7	LOC339047 protein; Nuclear pore complex-interacting protein family member A3; Nuclear pore complex-interacting protein family member A5; Protein PKD1P1 [Source:UniProtKB/TrEMBL;Acc:Q0P618]
ENSG00000151623	NR3C2	nuclear receptor subfamily 3, group C, member 2 [Source:HGNC Symbol;Acc:7979]
ENSG00000091129	NRCAM	neuronal cell adhesion molecule [Source:HGNC Symbol;Acc:7994]
ENSG00000135318	NT5E	5'-nucleotidase, ecto (CD73) [Source:HGNC Symbol;Acc:8021]
ENSG00000128694	OSGEPL1	O-sialoglycoprotein endopeptidase-like 1 [Source:HGNC Symbol;Acc:23075]
ENSG00000128050	PAICS	phosphoribosylaminoimidazole carboxylase, phosphoribosylaminoimidazole succinocarboxamide synthetase [Source:HGNC Symbol;Acc:8587]
ENSG00000169116	PARM1	prostate androgen-regulated mucin-like protein 1 [Source:HGNC Symbol;Acc:24536]
ENSG00000203880	PCMTD2	protein-L-isoaspartate (D-aspartate) O-methyltransferase domain containing 2 [Source:HGNC Symbol;Acc:15882]
ENSG00000171408	PDE7B	phosphodiesterase 7B [Source:HGNC Symbol;Acc:8792]
ENSG00000133401	PDZD2	PDZ domain containing 2 [Source:HGNC Symbol;Acc:18486]
ENSG00000236618	PITPNA-AS1	PITPNA antisense RNA 1 [Source:HGNC Symbol;Acc:44116]
ENSG00000196155	PLEKHG4	pleckstrin homology domain containing, family G (with RhoGef domain) member 4 [Source:HGNC Symbol;Acc:24501]
ENSG00000146281	PM20D2	peptidase M20 domain containing 2 [Source:HGNC Symbol;Acc:21408]

ENSG00000101751	POLI	polymerase (DNA directed) iota [Source:HGNC Symbol;Acc:9182]
ENSG00000184271	POU6F1	POU class 6 homeobox 1 [Source:HGNC Symbol;Acc:9224]
ENSG00000132356	PRKAA1	protein kinase, AMP-activated, alpha 1 catalytic subunit [Source:HGNC Symbol;Acc:9376]
ENSG00000132600	PRMT7	protein arginine methyltransferase 7 [Source:HGNC Symbol;Acc:25557]
ENSG00000164985	PSIP1	PC4 and SFRS1 interacting protein 1 [Source:HGNC Symbol;Acc:9527]
ENSG00000172780	RAB43	RAB43, member RAS oncogene family [Source:HGNC Symbol;Acc:19983]
ENSG00000197275	RAD54B	RAD54 homolog B (S. cerevisiae) [Source:HGNC Symbol;Acc:17228]
ENSG00000103479	RBL2	retinoblastoma-like 2 (p130) [Source:HGNC Symbol;Acc:9894]
ENSG00000185272	RBM11	RNA binding motif protein 11 [Source:HGNC Symbol;Acc:9897]
ENSG00000122965	RBM19	RNA binding motif protein 19 [Source:HGNC Symbol;Acc:29098]
ENSG00000163933	RFT1	RFT1 homolog (S. cerevisiae) [Source:HGNC Symbol;Acc:30220]
ENSG00000131941	RHPN2	rhophilin, Rho GTPase binding protein 2 [Source:HGNC Symbol;Acc:19974]
ENSG00000124226	RNF114	ring finger protein 114 [Source:HGNC Symbol;Acc:13094]
ENSG00000151692	RNF144A	ring finger protein 144A [Source:HGNC Symbol;Acc:20457]
ENSG00000238923	RNU7-1	RNA, U7 small nuclear 1 [Source:HGNC Symbol;Acc:34033]
ENSG00000261512	RP11-46D6.1	
ENSG00000213178	RP11-641D5.1	
ENSG00000218227	RP11-889L3.1	
ENSG00000116251	RPL22	ribosomal protein L22 [Source:HGNC Symbol;Acc:10315]
ENSG00000151835	SACS	spastic ataxia of Charlevoix-Saguenay (sacsin) [Source:HGNC Symbol;Acc:10519]
ENSG00000173611	SCAI	suppressor of cancer cell invasion [Source:HGNC Symbol;Acc:26709]
ENSG00000140386	SCAPER	S-phase cyclin A-associated protein in the ER [Source:HGNC Symbol;Acc:13081]
ENSG00000198832	SELM	Selenoprotein M [Source:UniProtKB/Swiss-Prot;Acc:Q8WWX9]
ENSG00000164300	SERINC5	serine incorporator 5 [Source:HGNC Symbol;Acc:18825]
ENSG00000182319	SGK223	Tyrosine-protein kinase SgK223 [Source:UniProtKB/Swiss-Prot;Acc:Q86YV5]
ENSG00000112394	SLC16A10	solute carrier family 16 (aromatic amino acid transporter), member 10 [Source:HGNC Symbol;Acc:17027]
ENSG00000125648	SLC25A23	solute carrier family 25 (mitochondrial carrier; phosphate carrier), member 23 [Source:HGNC Symbol;Acc:19375]
ENSG00000205060	SLC35B4	solute carrier family 35 (UDP-xylose/UDP-N-acetylglucosamine transporter), member B4 [Source:HGNC Symbol;Acc:20584]

ENSG00000138079	SLC3A1	solute carrier family 3 (amino acid transporter heavy chain), member 1 [Source:HGNC Symbol;Acc:11025]
ENSG00000076351	SLC46A1	solute carrier family 46 (folate transporter), member 1 [Source:HGNC Symbol;Acc:30521]
ENSG00000239169	SNORD109B	small nucleolar RNA, C/D box 109B [Source:HGNC Symbol;Acc:32774]
ENSG00000005513	SOX8	SRY (sex determining region Y)-box 8 [Source:HGNC Symbol;Acc:11203]
ENSG00000072195	SPEG	SPEG complex locus [Source:HGNC Symbol;Acc:16901]
ENSG00000123096	SSPN	sarcospan [Source:HGNC Symbol;Acc:11322]
ENSG00000127366	TAS2R5	taste receptor, type 2, member 5 [Source:HGNC Symbol;Acc:14912]
ENSG00000175463	TBC1D10C	TBC1 domain family, member 10C [Source:HGNC Symbol;Acc:24702]
ENSG00000136111	TBC1D4	TBC1 domain family, member 4 [Source:HGNC Symbol;Acc:19165]
ENSG00000071564	TCF3	transcription factor 3 [Source:HGNC Symbol;Acc:11633]
ENSG00000101190	TCFL5	transcription factor-like 5 (basic helix-loop-helix) [Source:HGNC Symbol;Acc:11646]
ENSG00000163513	TGFBR2	transforming growth factor, beta receptor II (70/80kDa) [Source:HGNC Symbol;Acc:11773]
ENSG00000159445	THEM4	thioesterase superfamily member 4 [Source:HGNC Symbol;Acc:17947]
ENSG00000126351	THRA	thyroid hormone receptor, alpha [Source:HGNC Symbol;Acc:11796]
ENSG00000167895	TMC8	transmembrane channel-like 8 [Source:HGNC Symbol;Acc:20474]
ENSG00000198270	TMEM116	transmembrane protein 116 [Source:HGNC Symbol;Acc:25084]
ENSG00000147003	TMEM27	transmembrane protein 27 [Source:HGNC Symbol;Acc:29437]
ENSG00000174292	TNK1	tyrosine kinase, non-receptor, 1 [Source:HGNC Symbol;Acc:11940]
ENSG00000198467	TPM2	tropomyosin 2 (beta) [Source:HGNC Symbol;Acc:12011]
ENSG00000009790	TRAF3IP3	TRAF3 interacting protein 3 [Source:HGNC Symbol;Acc:30766]
ENSG00000154743	TSEN2	TSEN2 tRNA splicing endonuclease subunit [Source:HGNC Symbol;Acc:28422]
ENSG00000123297	TSFM	Ts translation elongation factor, mitochondrial [Source:HGNC Symbol;Acc:12367]
ENSG00000182670	TTC3	tetratricopeptide repeat domain 3 [Source:HGNC Symbol;Acc:12393]
ENSG00000215105	TTC3P1	tetratricopeptide repeat domain 3 pseudogene 1 [Source:HGNC Symbol;Acc:23318]
ENSG00000197763	TXNRD3	thioredoxin reductase 3 [Source:HGNC Symbol;Acc:20667]
ENSG00000206483	TXNRD3NB	thioredoxin reductase 3 neighbor [Source:HGNC Symbol;Acc:33870]
ENSG00000118420	UBE3D	ubiquitin protein ligase E3D [Source:HGNC Symbol;Acc:21381]
ENSG00000175518	UBQLNL	ubiquilin-like [Source:HGNC Symbol;Acc:28294]

ENSG00000108312	UBTF	upstream binding transcription factor, RNA polymerase I [Source:HGNC Symbol;Acc:12511]
ENSG00000058056	USP13	ubiquitin specific peptidase 13 (isopeptidase T-3) [Source:HGNC Symbol;Acc:12611]
ENSG00000188064	WNT7B	wingless-type MMTV integration site family, member 7B [Source:HGNC Symbol;Acc:12787]
ENSG00000204789	ZNF204P	zinc finger protein 204, pseudogene [Source:HGNC Symbol;Acc:12995]
ENSG00000197782	ZNF780A	zinc finger protein 780A [Source:HGNC Symbol;Acc:27603]
ENSG00000198455	ZXDB	zinc finger, X-linked, duplicated B [Source:HGNC Symbol;Acc:13199]

Supplementary Table 25 IRGs up in ‘Metastasis’ v ‘Primary’

Ensembl Id	Gene Name	Description
ENSG00000072110	ACTN1	actinin, alpha 1 [Source:HGNC Symbol;Acc:163]
ENSG00000108839	ALOX12	arachidonate 12-lipoxygenase [Source:HGNC Symbol;Acc:429]
ENSG00000156381	ANKRD9	ankyrin repeat domain 9 [Source:HGNC Symbol;Acc:20096]
ENSG00000151693	ASAP2	ArfGAP with SH3 domain, ankyrin repeat and PH domain 2 [Source:HGNC Symbol;Acc:2721]
ENSG00000153094	BCL2L11	BCL2-like 11 (apoptosis facilitator) [Source:HGNC Symbol;Acc:994]
ENSG00000100307	CBX7	chromobox homolog 7 [Source:HGNC Symbol;Acc:1557]
ENSG00000197959	DNM3	dynamin 3 [Source:HGNC Symbol;Acc:29125]
ENSG00000124491	F13A1	coagulation factor XIII, A1 polypeptide [Source:HGNC Symbol;Acc:3531]
ENSG00000170271	FAXDC2	fatty acid hydroxylase domain containing 2 [Source:HGNC Symbol;Acc:1334]
ENSG00000129682	FGF13	fibroblast growth factor 13 [Source:HGNC Symbol;Acc:3670]
ENSG00000022267	FHL1	four and a half LIM domains 1 [Source:HGNC Symbol;Acc:3702]
ENSG00000119782	FKBP1B	FK506 binding protein 1B, 12.6 kDa [Source:HGNC Symbol;Acc:3712]
ENSG00000125740	FOSB	FBJ murine osteosarcoma viral oncogene homolog B [Source:HGNC Symbol;Acc:3797]
ENSG00000234289	H2BFS	H2B histone family, member S (pseudogene) [Source:HGNC Symbol;Acc:4762]
ENSG00000064393	HIPK2	homeodomain interacting protein kinase 2 [Source:HGNC Symbol;Acc:14402]
ENSG00000180573	HIST1H2AC	histone cluster 1, H2ac [Source:HGNC Symbol;Acc:4733]
ENSG00000197903	HIST1H2BK	histone cluster 1, H2bk [Source:HGNC Symbol;Acc:13954]
ENSG00000136231	IGF2BP3	insulin-like growth factor 2 mRNA binding protein 3 [Source:HGNC Symbol;Acc:28868]
ENSG00000067082	KLF6	Kruppel-like factor 6 [Source:HGNC Symbol;Acc:2235]

ENSG00000148346	LCN2	lipocalin 2 [Source:HGNC Symbol;Acc:6526]
ENSG00000169756	LIMS1	LIM and senescent cell antigen-like domains 1 [Source:HGNC Symbol;Acc:6616]
ENSG00000240428	LIMS1	LIM and senescent cell antigen-like-containing domain protein 3; LIM and senescent cell antigen-like-containing domain protein 3-like; Uncharacterized protein; cDNA FLJ59124, highly similar to Particularly interesting newCys-His protein; cDNA, FLJ79109, highly similar to Particularly interesting newCys-His protein [Source:UniProtKB/TrEMBL;Acc:B4DPH6]
ENSG00000256977	LIMS3	LIM and senescent cell antigen-like domains 3 [Source:HGNC Symbol;Acc:30047]
ENSG00000257207	LIMS3	LIM and senescent cell antigen-like-containing domain protein 3; Uncharacterized protein; cDNA FLJ59124, highly similar to Particularly interesting newCys-His protein; cDNA, FLJ79109, highly similar to Particularly interesting newCys-His protein [Source:UniProtKB/TrEMBL;Acc:B4DPH6]
ENSG00000125952	MAX	MYC associated factor X [Source:HGNC Symbol;Acc:6913]
ENSG00000050393	MCUR1	mitochondrial calcium uniporter regulator 1 [Source:HGNC Symbol;Acc:21097]
ENSG00000205639	MFSD2B	major facilitator superfamily domain containing 2B [Source:HGNC Symbol;Acc:37207]
ENSG00000108960	MMD	monocyte to macrophage differentiation-associated [Source:HGNC Symbol;Acc:7153]
ENSG00000130830	MPP1	membrane protein, palmitoylated 1, 55kDa [Source:HGNC Symbol;Acc:7219]
ENSG00000162614	NEXN	nexilin (F actin binding protein) [Source:HGNC Symbol;Acc:29557]
ENSG00000156642	NPTN	neuroplastin [Source:HGNC Symbol;Acc:17867]
ENSG00000154146	NRGN	neurogranin (protein kinase C substrate, RC3) [Source:HGNC Symbol;Acc:8000]
ENSG00000185630	PBX1	pre-B-cell leukemia homeobox 1 [Source:HGNC Symbol;Acc:8632]
ENSG00000197461	PDGFA	platelet-derived growth factor alpha polypeptide [Source:HGNC Symbol;Acc:8799]
ENSG00000005249	PRKAR2B	protein kinase, cAMP-dependent, regulatory, type II, beta [Source:HGNC Symbol;Acc:9392]
ENSG00000041353	RAB27B	RAB27B, member RAS oncogene family [Source:HGNC Symbol;Acc:9767]
ENSG00000240912	RP11-274J15.2	
ENSG00000198478	SH3BGRL2	SH3 domain binding glutamic acid-rich protein like 2 [Source:HGNC Symbol;Acc:15567]
ENSG00000088826	SMOX	spermine oxidase [Source:HGNC Symbol;Acc:15862]
ENSG00000140022	STON2	stonin 2 [Source:HGNC Symbol;Acc:30652]
ENSG00000003436	TFPI	tissue factor pathway inhibitor (lipoprotein-associated coagulation inhibitor) [Source:HGNC Symbol;Acc:11760]
ENSG00000142046	TMEM91	transmembrane protein 91 [Source:HGNC Symbol;Acc:32393]
ENSG00000101470	TNNC2	troponin C type 2 (fast) [Source:HGNC Symbol;Acc:11944]
ENSG00000161911	TREML1	triggering receptor expressed on myeloid cells-like 1 [Source:HGNC Symbol;Acc:20434]
ENSG00000204613	TRIM10	tripartite motif containing 10 [Source:HGNC Symbol;Acc:10072]
ENSG00000158457	TSPAN33	tetraspanin 33 [Source:HGNC Symbol;Acc:28743]

ENSG00000165914	TTC7B	tetratricopeptide repeat domain 7B [Source:HGNC Symbol;Acc:19858]

Supplementary Table 26 IRGs down in ‘Metastasis’ v ‘Primary’

Ensembl Id	Gene Name	Description
ENSG00000241322	CDRT1	CMT1A duplicated region transcript 1 [Source:HGNC Symbol;Acc:14379]
ENSG00000171931	FBXW10	F-box and WD repeat domain containing 10 [Source:HGNC Symbol;Acc:1211]
ENSG00000123700	KCNJ2	potassium inwardly-rectifying channel, subfamily J, member 2 [Source:HGNC Symbol;Acc:6263]
ENSG00000151611	MMAA	methylmalonic aciduria (cobalamin deficiency) cblA type [Source:HGNC Symbol;Acc:18871]
ENSG00000251537	RP11-385D13.1	Uncharacterized protein [Source:UniProtKB/TrEMBL;Acc:H0Y626]

Supplementary Table 27 Subgroups of IRGs

I. Chronic disease	II. Cancer-associated	III. Acute cancer/disease- associated			IV. Metastasis-specific	V. Non-primary
ACBD5	CDKN2A	ABAT	SEC14L1	EIF4EBP3	PXK	ALOX12	ACTN1
AP3S2	GREM2	ABCC3	Sep-05	ENO3	RAP1GAP2	ANKRD9	CBX7
CDYL2	MUC1	ABCC4	SH3BGRL3	ENOSF1	RDH11	ASAP2	DNM3
CXCL10	AK5	AGXT	SH3TC1	FAIM3	RHOBTB1	BCL2L11	FHL1
GBP1	ATM	ANGPT1	SLA2	FAM117B	RNASE1	F13A1	FOSB
GBP1P1	CD248	ARHGAP6	SLC15A4	FAM149B1	RP11-544M22.13	FAXDC2	HIST1H2AC
IL15RA	COL4A3	ATG2A	SLC8A3	FAM153C	SCYL2	FGF13	MMD
INPP1	DNMT3A	B9D2	SLCO3A1	FAM178A	SDC1	FKBP1B	TNNC2
MR1	EPHX2	BCL2L1	SNCA	FAM213A	UBE3D	H2BFS	CDRT1
PARP9	FBXO15	BMP6	SPARC	FAM216A	UBQLNL	HIPK2	FBXW10
RP11-18F14.2	HNRNPDL	C15orf26	ST7	FGF9	UBTF	HIST1H2BK	MMAA
SCUBE2	IGF1R	CAB39	STOM	FRMD4A	USP13	IGF2BP3	RP11-385D13.1
ASIC1	KLHL29	CALM3	TAGLN2	FUT8	WNT7B	KLF6	
C1QTNF6	KLHL3	CALML3	TBXAS1	GIMAP7	ZNF204P	LCN2	
SATB1	LRP6	CASZ1	TGFB1	GPR155	ZNF780A	LIMS1	
	MAML2	CCPG1	TMEM140	GPR18	ZXDB	LIMS3	
	NMT2	CD226	TMEM189	GTPBP8		MAX	
	NR3C2	CD9	TMEM63B	HINT3		MCUR1	
	NRCAM	CDC14B	TMSB15A	HKDC1		MFSD2B	
	POLI	CDS2	TPM1	IL16		MPP1	
	RBM19	CETP	TUBA4A	IPO9		NEXN	
	SERINC5	CLEC1B	UBE2C	ISY1-RAB43		NPTN	
	SLC16A10	CLU	UBL4A	ITM2A		NRGN	
	SPEG	CMIP	UBTD1	KLHL34		PBX1	
	TMEM27	CREB3L2	ULK1	LDHB		PDGFA	
	TNK1	CREB3L3	USF2	LIG1		PRKAR2B	
	TXNRD3	CTDSPL	VCL	LRPPRC		RAB27B	
	TXNRD3NB	CTSA	VEGFC	LRRN3		RP11-274J15.2	
		CTTN	VWF	LSM3		SH3BGRL2	
		CXCL5	WDR44	MAGED1		SMOX	
		CYB5R3	WIPI1	MAN1C1		STON2	
		DAPP1	WRB	MDH1		TFPI	
		DENND4C	XPNPEP1	METTL21B		TMEM91	
		DGKD	ZBTB16	MGEA5		TREML1	
		DSC2	ZFAND3	MKL2		TRIM10	
		DYX1C1-CCPG1	AC005280.1	MOAP1		TSPAN33	
		EIF4G3	ACACB	MRI1		TTC7B	

ELOVL7
ENDOD1
EPOR
F11R
F2R
FAH
FAM53B
FAM63A
FAR1
FBXW9
FLNA
FRMD3
FUBP3
GAS2L1
GATA1
GLA
GMPR
GP1BB
GPD2
GUCY1B3
HDGFRP3
IGF2BP2
ILK
ITGA2B
ITGB3
ITGB5
KCNAB2
KCND3
LFNG
LGALS8
LGALSL
LRP12
LRRFIP2
LTBP1
MAP1LC3B
MAP2K3
MAP3K5
MFAP3L
MGLL
MLXIP
MMP1
MSANTD3
MTMR3
MTURN
MYLK
NF1
NFIB
NOL10
P2RX1
PAPSS1
PARD3
PCSK6
PCYT1A
PDGFC
PDLIM1
PDLIM7
PHTF1
PIM1
PLA2G12A
PLEKHB2
PLOD2
PRDM1
PROS1
PTGS1
PTPN12
ACAT2
ACSL6
ADD3
ADPRHL2
AIP
AKR1B1
AKTIP
ALDH5A1
ALDH8A1
ALG13
ANKH
ANKHD1
ANKHD1-EIF4EBP3
ANKRD36BP2
ANKRD55
ANKS6
ATF7IP2
ATP10A
BACE2
BBS4
BCL11B
BDH1
BTN3A2
BTN3A3
BTRC
C12orf29
C12orf57
C14orf169
C17orf51
C19orf53
C19orf73
C5orf45
CAND2
CCDC102B
CCDC109B
CCDC14
CCDC59
CCR7
CD27
CDC25B
CDC42SE2
CDK20
CENPJ
CNOT7
COCH
COL5A2
COL6A1
COMMD6
CRB3
CSRP2BP
CSTF3
CTD-2015B23.2
CYP2J2
DCBLD2
DNAJC21
DNASE1L3
DNPEP
DOCK9
DYNC2LI1
EDRF1
EID3
EIF1AX
MSH2
MYCBP2
NAP1L3
NCAPD2
NDUFC1
NELL2
NINL
NPIPA2
NPIPA5
NPIPA7
NT5E
OSGEPL1
PAICS
PARM1
PCMTD2
PDE7B
PDZD2
PITPNA-AS1
PLEKHG4
PM20D2
POU6F1
PRKAA1
PRMT7
PSIP1
RAB43
RAD54B
RBL2
RBM11
RFT1
RHPN2
RNF114
RNF144A
RNU7-1
RP11-46D6.1
RP11-641D5.1
RP11-889L3.1
RPL22
SACS
SCAI
SCAPER
SELM
SGK223
SLC25A23
SLC35B4
SLC3A1
SLC46A1
SNORD109B
SOX8
SSPN
TAS2R5
TBC1D10C
TBC1D4
TCF3
TCFL5
TGFBR2
THEM4
THRA
TMC8
TMEM116
TPM2
TRAF3IP3
TSEN2
TSFM
TTC3
TTC3P1

Supplementary Table 28 GO enrichment of 348 ‘metastasis’ associated differentially expressed IRGs (combined subgroups III, IV & V)

GO biological process	Fold Enrichment	FDR
platelet degranulation (GO:0002576)	9.13	1.16E-08
homotypic cell-cell adhesion (GO:0034109)	7.87	3.74E-02
platelet activation (GO:0030168)	5.76	1.29E-03
cell junction assembly (GO:0034329)	5.05	1.39E-02
regulation of muscle contraction (GO:0006937)	4.5	2.48E-02
cell junction organization (GO:0034330)	4.38	6.10E-03
blood coagulation (GO:0007596)	3.96	1.14E-03
coagulation (GO:0050817)	3.94	1.08E-03
hemostasis (GO:0007599)	3.9	1.10E-03
wound healing (GO:0042060)	3.88	3.47E-06
response to wounding (GO:0009611)	3.36	3.38E-05
regulation of body fluid levels (GO:0050878)	2.93	5.68E-03
positive regulation of protein kinase activity (GO:0045860)	2.74	1.78E-02
hemopoiesis (GO:0030097)	2.7	1.84E-02
hematopoietic or lymphoid organ development (GO:0048534)	2.58	2.34E-02
positive regulation of kinase activity (GO:0033674)	2.55	3.24E-02
regulated exocytosis (GO:0045055)	2.46	1.95E-02
immune system development (GO:0002520)	2.44	5.11E-02
positive regulation of transferase activity (GO:0051347)	2.37	2.98E-02
cell activation (GO:0001775)	2.18	1.46E-02
secretion by cell (GO:0032940)	2.13	3.00E-02
secretion (GO:0046903)	2.13	1.86E-02
response to stress (GO:0006950)	1.69	5.87E-04
regulation of multicellular organismal process (GO:0051239)	1.61	2.58E-02
regulation of biological quality (GO:0065008)	1.5	3.89E-02
biological_process (GO:0008150)	1.09	5.03E-02
Unclassified (UNCLASSIFIED)	0.56	4.85E-02
GO biological process complete	9.13	1.16E-08
platelet degranulation (GO:0002576)	7.87	3.74E-02
homotypic cell-cell adhesion (GO:0034109)	5.76	1.29E-03
platelet activation (GO:0030168)	5.05	1.39E-02
cell junction assembly (GO:0034329)	4.5	2.48E-02
regulation of muscle contraction (GO:0006937)	4.38	6.10E-03
cell junction organization (GO:0034330)	3.96	1.14E-03
blood coagulation (GO:0007596)	3.94	1.08E-03
coagulation (GO:0050817)	3.9	1.10E-03
hemostasis (GO:0007599)	3.88	3.47E-06

Appendix IV - Patent: Interferon Epsilon, as an Anti-Cancer Agent

A METHOD OF TREATMENT

FIELD

[0001] The present invention relates to the field of cancer treatment and formulations useful for same.

BACKGROUND

[0002] Bibliographic details of the publications referred to by author in this specification are collected alphabetically at the end of the description.

[0003] The reference in this specification to any prior publication (or information derived from it), or to any matter which is known, is not, and should not be taken as an acknowledgement or admission or any form of suggestion that the prior publication (or information derived from it) or known matter forms part of the common general knowledge in the field of endeavor to which this specification relates.

[0004] Cancer is a complex, multifaceted, cellular disorder. It can lead to debilitating levels of disease with potentially significant morbidity and mortality rates. The economic cost to the healthcare sector in the treatment of cancer, not to mention the emotional burden to individuals and families, is substantial. Much effort has been invested in understanding cancer biology and endogenous and exogenous factors which retard its development. Despite great advances over the decades, further research is crucial in order to fully understand this disease.

[0005] Ovarian cancer, for example, is a complex, heterogeneous disease comprising a number of molecularly distinct tumors that arise not only from ovarian cells but also cells

of the fallopian tubes and/or surrounding tissue (Jayson *et al*. (2014) *The Lancet 384(9951)*:1376-88). Many women are first diagnosed when they already have reached advanced stage disease and of those who respond to treatment, more than half will relapse and die within 5 years (AIHW. (2010) *Cancer series 52 Cat No. CAN48*).

[0006] The vast majority of ovarian cancers are of epithelial origin (EOC) and have the fourth highest female cancer fatality rate (Jayson *et al*. (2014) *supra*). EOC is classified based on histological subtype including mucinous, clear cell, endometroid and serous carcinomas, each of which is associated with a distinct morphology, mutational profile, cell of origin and prognosis. Serous carcinomas are the most commonly diagnosed EOC and there is increasing evidence to suggest that EOC is derived from the secretory epithelial lining of the distal fallopian tube. The standard therapeutic options, surgical resection and platinum-based chemotherapy, are often ineffective as many women with advanced disease are not surgical candidates and chemoresistence leads to increasing rates of recurrence (Jayson *et al*. (2014) *supra*).

[0007] Extensive molecular profiling of ovarian cancers has shown that mutations in BRCA1/2 genes confer significantly increased risk of high-grade serous carcinoma (HGSC), the most common and lethal EOC (Bowtell *et al*. (2010) *Nature Rev Cancer 10(11)*:803-8). BRCA1 and BRCA2 are both documented interferon (IFN) regulated genes (IRGs) and play an important role in the homologous recombination repair pathway of DNA (Venkitaraman (2014) *Science 343(6178)*:1470-5), somatic and germline mutations of which contribute to overall chromosomal instability. Molecular profiling has also identified that high grade serous carcinoma (HGSC) with higher expression of immune-associated genes such as CD8A, Granzyme B and CXCL9, designated the immunologic subtype, demonstrate the best overall survival (Tothill *et al*. (2008) *Clin Cancer Res. 14(16)*:5198-208), highlighting the potential benefit of immune-driven suppression in this cancer, Molecular profiling has identified similarities in the mutational

profile of basal-like breast cancers and serous ovarian cancers with high frequency TP53, BRCA1 and BRCA2 mutations, down-regulation of RB1 and amplification of cyclin E1 common to both (Kobolt *et al*. (2012) *Nature* 490(7418):61-70). Additionally, while the role of hormones in ovarian cancer tumorigenesis remains unclear, there is evidence of poor prognosis in progesterone receptor (PR) negative patients irrespective of estrogen receptor (ER) expression (Sieh *et al*. (2013) *The Lancet Oncology 14(9)*:853-62), which bears similarities to the reports of poor prognosis in breast cancer patients with either triple negative breast cancer (TNBC) or estrogen receptor positive/progesterone receptor negative (ER^+/PR^-) cancers (Thakkar and Mehta (2011) *Oncologist 16(3)*:276-85). Much is still unknown about the common drivers in these two cancers, both have common elements of oncogene and tumor suppressor gene expression, hormone sensitivity and immune cell involvement.

[0008] There is a need to further examine the effect of immune modulation in regulating the development and ? treatment of ovarian cancer as well as other cancer types.

[0009] This is particularly the case with respect to the interplay between innate and adaptive immunity. The innate immune response represents pre-existing, inherent, first line and rapidly inducible defence to pathogens and responses to homeostatic cues (Mangan *et al.* (2007) *Eur J Immunol* 37(5):1302-12; Smith *et al.* (2007) *J Immunol* 178(7):4557-66). This is mediated through resident cells such as macrophages, natural killer (NK) and epithelial cells. Adaptive immune responses encompass the recognition, and response to antigens with elicited responses being gradual and specific, mediated through antibody secreting B lymphocytes and T helper and effector lymphocytes. The adaptive response is sculpted by the innate system. In the reproductive tract, both arms of the immune system must balance the presence of an allogenic fetus, essentially containing "foreign" proteins, with the control of harmful pathogens e.g. viruses and bacteria. It must also maintain homeostasis against a background of cyclical hormonal milieu and structural changes that occur in the mucosa.

[0010] The innate and adaptive immune cells of the female reproductive tract (FRT) produce cytokines and chemokines, thereby influencing various reproductive processes including sperm migration, fertilization, implantation, endometrial remodelling and immune response to infectious or other challenge (Salamonsen *et al.* (2007) *Semin Reprod Med* 25(6):437-44).

[0011] In its simplest form, the innate response includes physicochemical barriers such as mucous secretions, pH and redox state. In its most sophisticated form it is represented by the innate immune response which senses pathogens within minutes and starts a series of reactions, culminating in the production of products like antimicrobial defensins, NOS enzymes, chemokines that recruit and activate inflammatory cells and cytokines that modulate cell behavior. One family of modulators having pleiotropic activity is the type I interferons (IFNs).

[0012] Clinical trials for the treatment of ovarian cancer using type I IFNs, specifically IFNα and IFNβ have been underwhelming, largely due to the dose-limiting toxicity preventing high-dose therapy in late stage disease as is the case with other solid tumours?? (Berek *et al*. (1985) *Cancer Res. 45*:4447-53; Willemse *et al*. (1990) *Eur J Cancer Clin Oncol 26(3)*:353-8; Markman *et al*. (1992) *Gynecol Oncol. 45(1)*:3-8; Frasci *et al*. (1994) *Eur J Cancer 30(7)*:946-50; Bruzzone *et al*. (1997) *Gynecol Oncol. 65(3)*:499-505; Moore *et al*. (1995) *Gynecol Oncol. 59(2)*:267-72; Berek *et al*. (1999) *Gynecol Oncol. 75(1)*:10-4; Markman *et al*. (2004) *Oncology 66(5)*:343-6). Some success, however, has been reported using intraperitoneal IFNα in the treatment of malignancy ascites from ovarian cancer notwithstanding that the mechanisms underlying IFN's efficacy against ascites remain unclear (Berek *et al*. (1985) *Cancer Res. 45*:4447-53). It is important to understand the role of IFNs in disease pathogenesis in order to best direct therapy.

[0013] IFN epsilon (IFNε) is a type I IFN (Fung *et al*. (2013) *Science 339(123)*:1088-1092; Peng *et al*. (2007) *Prot Expr Purif 53(2)*:356-362). The *lfnε* gene is located on chromosome 9p in the type I IFN locus (Hardy *et al.* (2004) *Genomics 84(2):*331-45). IFNε shares roughly 30% amino acid sequence homology with IFNα and IFNβ, and *in vitro* studies demonstrated that IFNε signals through the characteristic type I IFN receptors lFNAR1 and lFNAR2, however, its potential anti-tumor properties have hitherto not been addressed.

[0014] Interestingly, unlike other type I IFNs which remain at undetectable levels until pathogen-induced, IFNε has been found to be constitutively expressed primarily in organs of the FRT such as uterus, cervix vagina and ovary. IFNε produced by luminal and glandular epithelial cells of the FRT and is unaltered in the absence of hemopoietic cells..

[0015] Additionally, regulation of IFNε is distinct from other type I IFNs. Unlike *lfnα* and *lfnβ*, murine *lfnε* expression is largely unaltered in response to pathogenic stimuli

[0016] Instead, IFNε levels vary significantly across stages of the murine estrous cycle, with expression levels 30-fold higher during estrus than diestrus, an expression pattern that is reflected in human tissue during the menstrual cycle. This indicates that unlike other type I IFNs, IFNε is hormonally regulated.

[0017] There is a need to investigate the role of IFNε in cancer biology.

SUMMARY

[0018] Nucleotide sequences are referred to by a sequence identifier number (SEQ ID NO). The SEQ ID NOs correspond numerically to the sequence identifiers <400>1 (SEQ ID NO:1), <400>2 (SEQ ID NO:2), etc. A Sequence Listing is provided after the claims. A summary of the sequence identifiers is provided in Table 2.

[0019] The present invention is predicated in part on the determination that IFNε has a role in inhibiting cancer cells. Such an inhibition includes directly or indirectly inducing cancer cell death, including by apoptotic processes, as well as arresting OR SLOWING (? INHIBIT) development, proliferation, motility and/or migration of cancer cells. IFNε may act directly on the cancer cell or it may induce immune response that via particular cell types of production of regulators or other factors which in turn induce a cytotoxic or cytostatic effect on cancer cells. Whilst the present invention was elucidated following an investigation of ovarian cancer, the findings apply to other cancers of the female reproductive tract (FRT) as well as cancers elsewhere in the body of female or male subjects in any mammals, in particular, humans.

[0020] Hence, the present invention provides a method for inhibiting viability, growth, development and spread of cancer cells in a subject including a human.

[0021] Accordingly, taught herein is a method for inhibiting a cancer cell in a subject, the method comprising contacting the cancer cell with an amount of interferon epsilon (IFNε) or a functional natural or synthetic variant or hybrid form thereof or an modulator of *lfnε* expression or IFNε activity effective to directly or indirectly induce apoptosis of the cancer cell or inhibit cancer cell proliferation, motility and/or migration. This can lead to a reduction in the localized growth and invasion of cancer cells as well as their metastasis to other parts of the body.

[0022] Further enabled herein is a method for treating a subject with cancer, the method comprising administering to the subject an effective amount of IFNε or a functional natural or synthetic variant or hybrid form thereof or a modulator of *lfnε* expression or IFNε activity for a time and under conditions sufficient to directly or indirectly induce apoptosis of cancer cells or inhibit cancer cell proliferation, motility and/or mitigation.

[0023] The present specification is instructional on the use of IFNε or a functional natural or synthetic variant or hybrid form thereof or a modulator of *lfnε* expression or IFNε activity in the manufacture of a medicament in the treatment of cancer in a subject. In an embodiment, taught herein is IFNε or a functional natural or synthetic variant or hybrid form thereof or a modulator of *lfnε* expression or IFNε activity for use in the treatment of cancer in a subject. The medicament includes an anti-cancer vaccine comprising IFNε or its variant or hybrid or modulator as the primary active ingredient or where it acts as an adjuvant for another anti-cancer agent. Examples of other anti-cancer agents which may be used in conjunction with IFNε or its variant or hybrid or modulator include antimetabolites, anti-tumor antibiotics, mitotic inhibitors, steroids, sex hormones or hormone-like drugs, alkylating agents, nitrogen mustard, nitrosoureas, hormone agonists and microtubular inhibitors. Recombinant cells may also be engineered to produce IFNε or its variant, hybrid or modulator or recombinant viruses engineered to direct infected cells to produce IFNε, its variant, hybrid or modulator.

[0024] Formulations comprising IFNε or a functional natural or synthetic variant or hybrid form thereof or a modulator of *lfnε* expression or IFNε activity and one or more carriers, adjuvants and/or excipients for use in the treatment of cancer. The IFNε or its functional natural or synthetic variant or hybrid form thereof may also be used as a vaccine adjuvant in conjunction with an anti-cancer agent or cancer cell regulating molecules.

[0025] Abbreviations used herein are defined in Table 1.

Table 1

Abbreviations

Abbreviation	Definition
EOC	Epithelial origin
ER	Estrogen receptor
FCS	Fetal calf serum
FRT	Female reproductive tract
HGSC	High grade serous carcinoma
HuIFNε	Human interferon epsilon
IFN	Interferon
IFNε	Interferon epsilon
IRG	Interferon regulated gene
Ifnε	Gene encoding IFNε
LGSC	Low grade serous carcinoma
MuIFNε	Mouse interferon epsilon
PEC	Peritoneal exudate cells
PR	Progesterone receptor
TNBC	Triple negative breast cancer

BRIEF DESCRIPTION OF THE FIGURES

[0026] Some figures contain color representations or entities. Color photographs are available from the Patentee upon request or from an appropriate Patent Office. A fee may be imposed if obtained from a Patent Office.

[0027] Figures 1A through C are graphical representations showing induction of interferon regulating genes (IRGs) in ID8 cells by IFNε and IFNβ. The graphs show a 3 hour dose response of 10-1000 IU/ml IFNε (left panels shown in black) and IFNβ (right panels in grey) induction of CXCL10 (A), lfit1 (B) and Isg15 (C). Gene expression is measured by qRT-PCR, expression calculated by dCT standardized to 18s and relative expression shown here determined in relation to expression at t0. Data are shown as mean +/- SEM of n=3 independent experiments, each done in technical triplicates. Significance was determined by Student's T test ****$p<0.0001$.

[0028] Figures 2A through E are graphical representations showing regulation of genes involved in cancer-related biological functions. Graph shows expression of Bcl-2 (A), Ccne1 (B), Cdc20 (C), Tap1 (D) and Casp1 (E) in response to stimulation with 1000 IU/ml of IFNε (middle bar?) or IFNβ (right bar?) for 3 hours. Data are shown as mean +/- SEM of n=3 independent experiments, each done in technical triplicates. Significance was determined by Student's T test *$p<0.05$, **$p<0.01$, ***$p<0.001$, ****$p<0.0001$.

[0029] Figures 3A and B aGraphs show the mean cell index measurements, a correlate of cell number,at 30min intervlals over the 72h of treatment of ID8 cells with interferon; showing inhibition of ID8 cell proliferation by IFNε (A) but not?? IFNβ (B). Graphs show inhibition of proliferation of ID8 cells treated with 100-1000 IU/ml of: a) IFNε; b) IFNβ for 48 hours. Cell proliferation is measured by xCELLigence. Graphs show the mean cell index across each well +/- SD. Each cell index is normalized after 24 hours (arrow) of

cells plated in serum free media and compared to untreated and buffer-treated controls. Representative of n=3 independent experiments each done in technical triplicate. Legend (a) – untreated (red), control (green), 100 IU/ml IFNε (pink) and 1000 IU/ml IFNε (blue); (b) untreated (red), control (green), 100 IU/ml IFNβ (blue) and 1000 IU/ml IFNβ (pink).

[0030] Figures 4A through C are graphical representations showing IFN induced inhibition of ID8 cell growth. ID8 cells were plated onto a 96 well E plate coated with electrodes to measure cell impedence. Cells were serum starved for 24 h then treated with 0 - 1000 IU/ml of either: (A) IFNε; or (B) IFNβ for 48 h. The cell index (CI – a measurement of impedance) was normalized to time of treatment and doubling time was calculated over 48h post treatment using the RTCA software. (C) the slope (1 hr – representative of rate of proliferation) of the growth curves was also calculated from normalized Cl to 48h post treatment using the RTCA software. Data representative of n=3 independent experiments done in technical quadruplicate. Data are expressed as mean +SD of N=3 independent experiments, analyzed using 2-way ANOVA with Sidak's multiple comparisons test, ****p,0.0001.

[0031] Figure 5 is a graphical representation showing that IFNε treatment inhibits? cell migration of ID8 cells. ID8 cells were treated with 1-100 IU/ml of IFNε or buffer control and migration was measured after 12h of treatment. Fetal calf serum (FCS) was used as the chemoattractant. Serum free media (SFM) was used as a negative control. Data are representative of one independent experiment, performed in technical triplicate, and expressed as mean +SD of technical replicates. Significance was determined using a one-way ANOVA with Tukey's multiple comparisons; *p<0.05; **p,0.01; ***p<0.001; ****p,0.0001.

[0032] Figures 6A through D are graphical representations showing that IFNε treatment induces apoptosis of ID8 cells. Data show analysis of Annexin V/PI staining for ID8 cells

treated with 40-400 IU/ml of IFNε for 4 hours compared to PBS and buffer treated controls. H_2O_2 is used as a positive control. (A) Live cells; (B) necrotic cells; (C) early apoptosis; (D) late apoptosis. Data are representative of N=3 independent experiments, performed in technical duplicate, and expressed as mean +SD of technical replicates. Significance was determined using Student's T test; *p,0.05; **p<0.01.

[0033] Figure 7 is a graphical representation of IFNε staining intensity in benign human epithelium and serous carcinoma samples. Immunohistochemical staining for IFNε expression in human control epithelium low grade (LG) and high grade (HG) serous carcinoma (SC) samples were analyzed using positive pixel analysis in Imagescope software to quantify staining intensity in epithelial derived tissue components. Data are expressed as intensity scores for each sample stained in technical duplicates. 'fields analysed per sample? on tissue microarrays., Data presented as a dot plot of n=30 samples of control epithelium (??) and epithelium from low (n=6) and high grade serous carcinoma samples (n=70), mean indicated by a bar. Data were analyzed using individual Mann-Whitney tests, **p<0.01, ***p<0.001.

[0034] Figures 8A through E are graphical representations of advanced disseminated ovarian cancer metastases from orthotopic primary tumor. At 13 weeks post-intrabursal ID8 injection WT and *lfnε* deficient mice demonstrate advanced primary tumors and metastatic ovarian cancer. A-B) left ovaries and spleens were weighed from non-tumor and ID8 injected mice; C) ascites fluid was drained from the peritoneum; and E) measured for red blood cell content; D) number of metastatic deposits on the peritoneal wall were recorded. Data shows n=3 non-tumor bearing and n=6 ID8 injected mice per genotype, analyzed using unpaired Student's T test *p<0.05.

[0035] Figure 9A through D are graphical representations showing the recombinant IFNε regulates peritoneal immune cell populations *in vivo*. Healthy C57BL/6 wild-type mice (6

to 8 weeks of age) were treated with recombinant murine IFNε or IFNβ (at 500 IU/dose) *via* intraperitoneal injection, three times weekly for 8 weeks. Peritoneal exudate cells were collected in PBS *via* peritoneal lavage and analyzed using flow cytometry for immune cell populations include: A) CD45+ CD8+ T cells; B) CD45+ CD4+ T cells; C) CD45+ CD11b+ Ly6C+ inflammatory monocytes; and D) CD45+ CD4+ PD1+ T cells. Data are presented as mean +/- SEM of n=5 mice per group, analyzed using unpaired Student T tests *p<0.05, **p<0.01.

[0036] Figures 10A through C are graphical representations showing that IFNε suppresses malignant ascites development in a disseminated ovarian cancer model. A) image shows the volume of ascites drained from the peritoneum of mice 8 weeks post-ID8 injection treated with PBS, IFNε or IFNβ (500 IU/dose 3 times weekly); B) the number of epithelial (pan-cytokeratin positive) tumor cells in ascites fluid was measured using flow cytometry; C) the concentration of red blood cells in ascites fluid was measured using Sysmex Cell Counter. Data show n=3 PBS control mice and n=5 mice per treatment group, analyzed using unpaired Student's T test *p,0.05, **p,0.01, ***p<0.001.

[0037] Figures 11A through C are graphical representations showing changes in inflammatory cytokine levels in tumour bearing mice treated with IFNe or IFNb. Images show concentrations for MCP-1 (A), IL6 (B) and IL-10 (C) in ascites drained from the peritoneum of mice 8 weeks post-ID8 injection treated with PBS, IFNε or IFNβ (500 IU/dose 3 times weekly) measured by BD cytometric bead array (CBA). Data show are presented as mean +/- SEM of n=3 PBS control mice and n=5 mice per treatment group, analyzed using unpaired Student T test *p,0.05.

[0038] Figure 12 is a graphical representation showing that recombinant IFNε regulates peritoneal immune cell populations in a disseminated ovarian cancer model. C57BL/6 wild-type mice (6 to 8 weeks of age) were injected intraperitoneally with ID8 cells and

treated with recombinant murine IFNε or IFNβ (at 500 IU/dose) *via* intraperitoneal injection, three times weekly for 8 weeks. Peritoneal exudate cells were collected in PBS *via* peritoneal lavage and analyzed using flow cytometry for immune cell populations. Data presented as mean +/- SEM of n=5 mice per group, analyzed using unpaired Student T tests *p<0.05; **p<0.01.

[0039] Figures 13A through D are graphical representations showing growth and ascites development in murine cancers of epithelial origin (EOC) treated with recombinant interferon. A) body weights of mice were monitored over 8 weeks post-ID8 cell injection and the percentage weight increase of each treatment group was calculated relative to the average of all mice on day 1, distance from the mean weight at the start of the experiment was incorporated into the overall percentage increase of each mouse. B) overall growth curves measuring total body weight of mice 8-weeks post-ID8 cell injection treated with or without recombinant IFN 3 times weekly. C) abdominal circumferences were measured at 8weeks post-ID8 cell injection. D) total volume of ascites fluid was drained from the peritoneal cavity of each mouse 8-weeks post-ID8 cell injection. To determine significance across multiple groups an ordinary one-way ANOVA with Tukey's multiple comparisons test was performed (A) while unpaired Student T tests were used to compare two means (C and D) ***p<0.001, **p<0.01, *p<0.05. Data presented as mean +/- SEM of n=3-5 mice per group.

[0040] Figures 14A through D are graphical representations showing evidence of the effect of IFN on systemic anemia, peritoneal hemorrhaging and splenomegaly in murine EOC. A) clinical signs of anemia in mice at 8-weeks post-ID8 cell injection include pallor of the hind paws which was graded, 0 – normal perfusion, 1- slight pallor, 2 – extremely pale. B) peritoneal lavages were performed suing 5ml PBS and graded for hemorrhaging, 0 – no hemorrhaging to 3 – extensive hemorrhaging, dark red and completely opaque fluid. C) a cell count was performed on peritoneal exudate cells (PEC) including red blood cell

(RBC) count. D) splenic weights from mice 8-weeks post-ID8 cell injection. Data presented as mean +/- SEM of n=3-5 mice per group. Significance was determined using unpaired Student's T tests ****p,0.0001, **p<0.01, *p<0.05.

[0041] Figures 15A through F are graphical representations showing effects on tumor burden in murine EOC treated with recombinant IFNε. A) the extent of mesenteric tumor burden was grade, 0 – no macroscopic disease to 4- extensive tumor formation evident as a large nodular sub-phrenic tumor mass as well as countless tumor deposits throughout the mesentery. B) macroscopic tumor deposits attached to the peritoneal wall were counted. These included tumors of varied sizes. C) macroscopic tumor deposits attached to the diaphragm were counted. These included tumors of varied sizes. D) macroscopic tumor deposits attached to the liver lobes were counted. E) free-floating spheroids were counted. F) surface area measurements of the largest representative tumor nodule per mouse. Data presented as mean +/- SEM of n=3-5 mice per group. Significance was determined using unpaired Student T tests ***p<0.001, **p<0.01, *p<0.05.

DETAILED DESCRIPTION

[0042] Throughout this specification, unless the context requires otherwise, the word "comprise", or variations such as "comprises" or "comprising", will be understood to imply the inclusion of a stated element or integer or method step or group of elements or integers or method steps but not the exclusion of any other element or integer or method steps or group of elements or integers or method steps.

[0043] As used in the subject specification, the singular forms "a", "an" and "the" include plural aspects unless the context clearly dictates otherwise. Thus, for example, reference to "a cancer cell" includes a single cancer cell, as well as two or more cancer cells; reference to "an IFNε" includes a single IFNε molecule, as well as two or more IFNε molecules; reference to "the disclosure" includes single and multiple aspects taught by the disclosure; and so forth. Aspects taught and enabled herein are encompassed by the term "invention". Any variants and derivatives contemplated herein are encompassed by "forms" of the invention. All aspects of the invention are enabled across the width of the claims.

[0044] The present invention teaches the use of interferon epsilon (IFNε) in the treatment of cancer in a subject. This includes a functional natural or synthetic variant or hybrid form of IFNε. Further taught herein is the use of a modulator of *lfnε* expression or IFNε activity in the treatment of cancer. Hence, IFNε or its functional natural or synthetic variant or hybrid form may act directly on a cancer cell or may act indirectly *via* innate or adaptive immune cells or regulators or processes induced by IFNε.

[0045] Hence, enabled herein is the use of:

(i) natural purified IFNε;

(ii) recombinant IFNε;

(iii) a functional natural variant of IFNε;

(iv) a functional synthetic variant of IFNε;

(v) a hybrid of two or more IFNε from different species; and/or

(vi) a modulator of *Ifnε* expression or IFNε activity,

to directly or indirectly inhibit a cancer cell. The present invention may use any one of (i) through (vi), that is an agent selected from the group consisting of (i) through (vi), or use combination of two or more of (i) through (vi) to treat cancer.

[0046] The treatment of cancer comprises the inhibition of a single or multiple cancer cells. This comprises any one or more of directly or indirectly inducing apoptosis of a cancer cell, directly or indirectly acting as a cytotoxic agent, directly or indirectly inhibiting replication, growth, development, motility, proliferation, survival and/or migration of a cancer cell and/or directly or indirectly inducing cytostasis of a cancer cell.

[0047] In addition, the IFNε or its functional natural or synthetic variant or modulator may directly or indirectly prevent localized growth or invasion of a cancer cell and/or prevent metastasis of cancer cells elsewhere in the body of a subject including regions distant to the original foci of cancer cell development.

[0048] The present invention arose in part from an investigation of ovarian cancer. However, the anti-cancer effects of IFNε are applicable to any of a range of cancers including cancers derived from epithelial tissue, connective tissue, glandular tissue, embryonic tissue, blood borne cancers and cancers comprising hemopoietic cells, lymphatic tissue and bone marrow or cells from which such cells are derived. The present invention is not to be limited to the treatment of any one type of cancer or organ or anatomical compartment or region affected by cancer. Hence, the present invention extends to the treatment of cancers from any of the ovary, uterus, fallopian tube, endometrium, placenta, breast, testis, prostate, brain, stomach, liver, spleen, pancreas, thymus, colon, lung, kidney, heart, thyroid and smooth muscle. This is not intended to be

an exhaustive list but representative of the types of cancers that can be treated by IFNε or a functional natural or synthetic variant or hybrid thereof or a modulator of IFNε expression or activity.

[0049] In an embodiment, however, the present invention extends to cancer affecting the female reproductive tract (FRT) such as but not limited to ovarian cancer. As indicated above, the IFNε or its functional natural or synthetic variant or hybrid form may act directly on a cancer cell inducing any one or more of apoptosis, cytoxicity, senescence, lysis or other form of cell death or may retard, inhibit or otherwise inhibit cell growth, proliferation, replication, development, migration or motility. The IFNε or its functional natural or synthetic variant or hybrid form may also act indirectly on a cancer cell inducing any one or more of apoptosis, cytoxicity, senescence, lysis or other form of cell death or may retard, inhibit or otherwise arrest cell growth, proliferation, replication, development, migration or motility. Without limiting the present invention to any theory or mode of action, indirect activity includes the induction of innate and adaptive immune regulators and processes.

[0050] The subject being treated includes a human and a non-human mammal. Non-human animals include those useful in animal models. Hence, the present invention has applications in human and veterinary medicine and as a research tool.

[0051] Reference to a human subject includes a human of any gender or age. In an embodiment, the human is a female with a cancer affecting the FRT such as but not limited to ovarian cancer.

[0052] Whilst not intending to limit the scope of the present invention to any type of cancer, it extends to carcinoma, sarcoma, adenocarcinoma, blastoma, leukemia, lymphoma and myeloma. The term "cancer" is not to be construed as distinguish from a "tumor" and

both terms are used herein to mean the same cell type. A cancer may be of any grade and any stage, regardless of how the staging is classified. Hence, the cancer may be a solid tumor or blood or lymph fluid borne or bone marrow derived and may be defined in terms of cell type, location, tumor size, degree of local, regional or distant metastasis. For example, in relation to ovarian cancer, this may be serous, mucinous, clear cell or endometroid of high grade or low grade or a grade inbetween.

[0053] Accordingly, enabled herein is a method for inhibiting a cancer cell in a subject, the method comprising contacting the cancer cell with an amount of interferon epsilon (IFNε) or a functional natural or synthetic variant or hybrid form thereof or a modulator of *lfnε* expression or IFNε activity effective to indirectly or indirectly induce apoptosis of the cancer cell survival, proliferation, motility and/or migration.

[0054] Further enabled herein is a method for treating a subject with cancer, the method comprising administering to the subject an effective amount of IFNε or a functional natural or synthetic variant or hybrid form thereof or a modulator of *lfnε* expression or IFNε activity for a time and under conditions sufficient to induce apoptosis of cancer cells or inhibit cancer cell proliferation motility and/or migration.

[0055] Taught herein is the use of IFNε or a functional natural or synthetic variant or hybrid form thereof or a modulator of *lfnε* expression or IFNε activity in the manufacture of a medicament in the treatment of cancer in a subject.

[0056] Further taught herein is IFNε or a functional natural or synthetic variant or hybrid form thereof or a modulator of *lfnε* expression or IFNε activity for use in the treatment of cancer in a subject.

[0057] The IFNε or its functional natural or synthetic variant or hybrid form may also be

employed as an adjuvant for use with an anti-cancer agent such as a chemotherapeutic agent, another type I interferon such as IFNα or IFNβ or another biological molecule. By "adjuvant" in this context means that the IFNε or variant or hybrid acts in synergy with another anti-cancer agent.

[0058] Hence, enabled herein is a method for inhibiting a cancer cell in a subject, the method comprising contacting the cancer cell with an amount of interferon epsilon (IFNε) or a functional natural or synthetic variant or hybrid form thereof or a modulator of *lfnε* expression or IFNε activity in combination with another anti-cancer agent effective to indirectly or indirectly induce apoptosis of the cancer cell survival, proliferation, motility and/or migration.

[0059] Further enabled herein is a method for treating a subject with cancer, the method comprising administering to the subject an effective amount of IFNε or a functional natural or synthetic variant or hybrid form thereof or a modulator of *lfnε* expression or IFNε activity in combination with another anti-cancer agent for a time and under conditions sufficient to induce apoptosis of cancer cells or inhibit cancer cell proliferation motility and/or migration.

[0060] Taught herein is the use of IFNε or a functional natural or synthetic variant or hybrid form thereof or a modulator of *lfnε* expression or IFNε activity in combination with another anti-cancer agent in the manufacture of a medicament in the treatment of cancer in a subject. The medicament may be a single entity or a collocation of pharmaceutically effective agents which are used in combination with each other.

[0061] Reference to another anti-cancer agent includes but is not limited to an antimetabolite, an antitumor antibolite, a mitototoxic inhibitor, a steroid, a sex hormone or hormone-like drug, an alkylating agent, nitrogen mustard, nitrosourea, a hormone agonist

and/or a microtubular inhibitor.

[0062] Antimetabolites are substances that interfere with the body's chemical processes, such as creating proteins, DNA, and other chemicals needed for cell growth and reproduction; in cancer treatment, antimetabolite drugs disrupt DNA production, which in turn prevents cell division. Examples include Azaserine, D-Cycloserine, Mycophenolic acid, Trimethoprim, 5-fluorouracil, capecitabine, methotrexate, gemcitabine, cytarabine (ara-C) and fludarabine.

[0063] Antitumor antibiotics interfere with DNA by stopping enzymes and mitosis or altering the membranes that surround cells. These agents work in all phases of the cell cycle. Thus, they are widely used for a variety of cancers. Examples of antitumor antibiotics include dactinomycin, daunorubicin, doxorubicin (Adriamycin), idarubicin, and mitoxantrone.

[0064] Mitotic inhibitors are plant alkaloids and other compounds derived from natural products. They can inhibit, or stop, mitosis or inhibit enzymes for making proteins needed for reproduction of the cell. These work during the M phase of the cell cycle. Examples of mitotic inhibitors include paclitaxel, docetaxel, etoposide (VP-16), vinblastine, vincristine, and vinorelbine.

[0065] Steroids are natural and synthetic hormones that are useful in treating some types of cancer (lymphoma, leukemias, and multiple myeloma) as well as other illnesses. They can kill cancer cells or slow their growth. Examples include prednisone and dexamethasone.

[0066] Sex hormones, or hormone-like drugs, alter the action or production of female or male hormones. They are used to slow the growth of breast, prostate, and endometrial cancers, which normally grow in response to hormone levels in the body. Examples include anti-estrogens (tamoxifen, fulvestrant), aromatase inhibitors (anastrozole,

letrozole), progestins (megestrol acetate), anti-androgens (bicalutamide, flutamide), and LHRH agonists (leuprolide, goserelin).

[0067] Alkylating agents work directly on DNA to prevent the cancer cell from reproducing. As a class of drugs, these agents are not phase-specific (in other words, they work in all phases of the cell cycle). These drugs are active against chronic leukemias, non-Hodgkin's lymphoma, Hodgkin's disease, multiple myeloma, and certain cancers of the lung, breast, and ovary. Examples of alkylating agents include busulfan, cisplatin, carboplatin, chlorambucil, cyclophosphamide, ifosfamide, dacarbazine (DTIC), mechlorethamine (nitrogen mustard), and melphalan.

[0068] Nitrogen mustard in the form of its crystalline hydrochloride it is used as a drug in the treatment of Hodgkin's disease, non-Hodgkin's lymphomas, and brain tumors. Nitrogen mustards cause mutations in the genetic material of cells, thereby disrupting mitosis, or cell division. Cells vary in their susceptibility to nitrogen mustards, with rapidly proliferating tumor and cancer cells most sensitive; bone marrow, which produces red blood cells, is also sensitive, and depression of red blood cell production is a frequent side effect of nitrogen mustard therapy. The nitrogen mustards also suppress the immune response (see immunity). Other types include the aromatic mustards melphalan and chlorambucil, cyclophosphamide, HN1, *bis*-(2-chloroethyl), ethylamine; HN2, *bis*-(2-chloroethyl), methylamine and HN3, *tris*-(2-chloroethyl), amine.

[0069] Nitrosoureas act in a similar way to alkylating agents. They interfere with enzymes that help repair DNA . These agents are able to travel to the brain so they are used to treat brain tumors as well as non-Hodgkin's lymphomas, multiple myeloma, and malignant melanoma. Examples of nitrosoureas include carmustine (BCNU) and lomustine (CCNU).

[0070] Hormone agonists include leuprolide (Lupron, Viadur, Eligard) for prostate cancer, Goserelin (Zoladex) for breast and prostate cancers and Triptorelin (Trelstar) for ovarian

and prostate cancers and nafarelin acetate (Synarel).

[0071] Microtubule inhibitors include “Vinca” alkaloids, taxoids and benzimidazoles

[0072] Inducing *lfnε* expression or IFNε activity includes the use of IFNε modulatory agents. Such agents include proteinaceous and non-proteinaceous agents. These agents may bind either the *lfnε* nucleic acid or expression product itself (including mature or precursor forms of IFNε) or modulate the expression of an upstream molecule, which upstream molecule subsequently modulates *lfnε* expression or expression product activity. Accordingly, contemplated herein are agents which either directly or indirectly induce or modify *lfnε* expression and/or IFNε activity.

[0073] Without limiting the present invention in any way, *lfnε* expression is known to be hormonally regulated. Accordingly, in one embodiment the use of estrogen and estrogen mimetics provides a useful means of upregulating IFNε levels. In another example, TGFβ can be utilized. Similarly bioinformatic analysis has identified glucocorticoid receptor response elements and Ets factor binding elements within the IFNε promoter. The putative transcription factor binding site BRCA1 has also been identified in the human *lfnε* promoter. Accordingly, molecules which activate transcription *via* these sites, such as Elf3 and Elf5, could be utilized to upregulate *lfnε* expression.

[0074] The modulatory agents which are utilized in accordance with this aspect of the present invention may take any suitable form. For example, proteinaceous agents may be glycosylated or unglycosylated, phosphorylated or dephosphorylated to various degrees and/or may contain a range of other molecules used, linked, bound or otherwise associated with the proteins such as amino acids, lipid, carbohydrates or other peptides, polypeptides or proteins. Similarly, non-proteinaceous molecules may also take any suitable form. Both the proteinaceous and non-proteinaceous agents herein described may be linked,

bound otherwise associated with any other proteinaceous or non-proteinaceous molecules. For example, in one embodiment of the present invention the agent is associated with a molecule which permits its targeting to a localized region.

[0075] The term "expression" refers to the transcription and/or translation of a nucleic acid molecule. Reference to "expression product" is a reference to the product produced from the transcription and translation of a nucleic acid molecule. Reference to "modulation" should be understood as a reference to up-regulation or down-regulation. Generally, a modulator results in up-regulation of IFNε synthesis.

[0076] "Variants" of the molecules herein described include fragments, parts, portions or derivatives either naturally occurring or synthetically prepared. Non-natural sources include, for example, recombinant or synthetic sources. By "recombinant sources" is meant that the cellular source from which the IFNε is harvested has been genetically altered. This may occur, for example, in order to increase or otherwise enhance the rate and volume of production by that particular cellular source. Parts or fragments include, for example, active regions of IFNε. Derivatives may be derived from insertion, deletion or substitution of amino acids. Amino acid insertional derivatives include amino and/or carboxylic terminal fusions as well as intrasequence insertions of single or multiple amino acids. Insertional amino acid sequence variants are those in which one or more amino acid residues are introduced into a predetermined site in the protein although random insertion is also possible with suitable screening of the resulting product. Deletional variants are characterized by the removal of one or more amino acids from the sequence. Substitutional amino acid variants are those in which at least one residue in a sequence has been removed and a different residue inserted in its place. Additions to amino acid sequences include fusions with other peptides, polypeptides or proteins, as detailed above.

[0077] Variants also include fragments having particular epitopes or parts of the entire

IFNε protein fused to peptides, polypeptides or other proteinaceous or non-proteinaceous molecules. Analogs of the molecules contemplated herein include, but are not limited to, modification to side chains, incorporating of unnatural amino acids and/or their derivatives during peptide, polypeptide or protein synthesis and the use of crosslinkers and other methods which impose conformational constraints on the proteinaceous molecules or their analogs.

[0078] A "variant" or "mutant" of IFNε should be understood to mean molecules which exhibit at least some of the functional activity of IFNε (i.e. direct or indirect anti-cancer activity) of which it is a variant or mutant. A variation or mutation may take any form and may be naturally or non-naturally occurring. In an embodiment, the variant is a hybrid of two or more IFNε molecules. For example, an IFNε derived from the species of the subject being treated may be modified to incorporate aspects of an IFNε from another species or *vice versa*. In one example, murine IFNε can have greater human IFNRI binding capacity than human IFNε. Hence, a hybrid murine IFNε which incorporates elements of human IFNε to render it non-immunogenic (or *vice versa*) may be generated.

[0079] Variants include chemical and functional equivalents of IFNε which include molecules exhibiting any one or more of the functional activities (i.e. direct or indirect anti-cancer activity) of the IFNε, which functional equivalents may be derived from any source such as being chemically synthesized or identified *via* screening processes such as natural product screening. For example chemical or functional equivalents can be designed and/or identified utilizing well known methods such as combinatorial chemistry or high throughput screening of recombinant libraries or following natural product screening.

[0080] For example, libraries containing small organic molecules may be screened, wherein organic molecules having a large number of specific parent group substitutions are

used. A general synthetic scheme may follow published methods (e.g. Bunin *et al.* (1994) *Proc. Natl. Acad. Sci. USA*, 91:4708-4712; DeWitt *et al.* (1993) *Proc. Natl. Acad. Sci. USA*, 90:6909-6913). Briefly, at each successive synthetic step, one of a plurality of different selected substituents is added to each of a selected subset of tubes in an array, with the selection of tube subsets being such as to generate all possible permutation of the different substituents employed in producing the library. One suitable permutation strategy is outlined in US. Patent No. 5,763,263.

[0081] There is currently widespread interest in using combinational libraries of random organic molecules to search for biologically active compounds (see for example U.S. Patent No. 5,763,263). Ligands discovered by screening libraries of this type may be useful in mimicking or blocking natural ligands or interfering with the naturally occurring ligands of a biological target. In the present context, for example, they may be used as a starting point for developing IFNε analogs which exhibit properties such as more potent pharmacological effects. IFNε or a functional part thereof may according to the present invention be used in combination libraries formed by various solid-phase or solution-phase synthetic methods (see for example U.S. Patent No. 5,763,263 and references cited therein). By use of techniques, such as that disclosed in U.S. Patent No. 5,753,187, millions of new chemical and/or biological compounds may be routinely screened in less than a few weeks. Of the large number of compounds identified, only those exhibiting appropriate biological activity are further analyzed.

[0082] With respect to high throughput library screening methods, oligomeric or small-molecule library compounds capable of interacting specifically with a selected biological agent, such as a biomolecule, a macromolecule complex, or cell, are screened utilizing a combinational library device which is easily chosen by the person of skill in the art from the range of well-known methods, such as those described above. In such a method, each member of the library is screened for its ability to interact specifically with the selected

agent. In practising the method, a biological agent is drawn into compound-containing tubes and allowed to interact with the individual library compound in each tube. The interaction is designed to produce a detectable signal that can be used to monitor the presence of the desired interaction.

[0083] Analogs of IFNε contemplated herein include, but are not limited to, modifications to side chains, incorporating unnatural amino acids and/or derivatives during peptide, polypeptide or protein synthesis and the use of crosslinkers and other methods which impose conformational constraints on the analogues. The specific form which such modifications can take will depend on whether the subject molecule is proteinaceous or non-proteinaceous. The nature and/or suitability of a particular modification can be routinely determined by the person of skill in the art.

[0084] As indicated above, the present invention extends to a formulation wherein the IFNε is a hybrid between human and murine IFNε. Administration of the formulation comprising IFNε or a functional natural or synthetic variant or hybrid thereof or a modulator of *lfnε* expression or IFNε activity alone or in combination with another anti-cancer agent of the present invention may also be referred to as a pharmaceutical composition. Such a formulation may be prepared by any convenient means. The components of the formulation are contemplated to exhibit anti-cancer activity when administered in an amount which depends on the particular case. The amount of IFNε or variant, hybrid or modulator adequate to accomplish anti-cancer activity is defined as a "therapeutically effective dose" or "effective amount". The dosage schedule and amounts effective for this use, i.e., the "dosing regimen", will depend upon a variety of factors, including the stage of the disease or condition, the severity of the disease or condition, the general state of the patient's health, the patient's physical status, age, pharmaceutical formulation and concentration of active agent (e.g. IFNε), and the like. In calculating the dosage regimen for a patient, the mode of administration is also taken into consideration.

The dosge regimen must also take into consideration the pharmacokinetics, i.e., the pharmaceutical composition's rate of absorption, bioavailability, metabolism, clearance, and the like. See, e.g., Egleton (1997) *Peptides* 18:1431-1439; Langer (1990) *Science* 249:1527-1533. A broad range of doses may be applicable. Dosage regimes may be adjusted to provide the optimum therapeutic response. For example, several divided doses may be administered daily, weekly, monthly or other suitable time intervals or the dose may be proportionally reduced as indicated by the exigencies of the situation. In an example, an amount of from 10 Ul/dose to 1,000,000 Ul/dose may be administered 1 to 3 times a week per subject. Exemplary dosage regimes include 10, 11, 12, 13, 14, 15, 16, 17, 18, 19, 20, 21, 22, 23, 24, 25, 26, 27, 28, 29, 30, 31, 32, 33, 34, 35, 36, 37, 38, 39, 40, 41, 42, 43, 44, 45, 46, 47, 48, 49, 50, 51, 52, 53, 54, 55, 56, 57, 58, 59, 60, 61, 62, 63, 64, 65, 66, 67, 68, 69, 70, 71, 72, 73, 74, 75, 76, 77, 78, 79, 80, 81, 82, 83, 84, 85, 86, 87, 88, 89, 90, 91, 92, 93, 94, 95, 96, 97, 98, 99, 100 IU/dose, 100, 200, 300, 400, 500, 600, 700, 800, 900, 1000 IU/dose or 10^3, 10^4, 10^5, 10^6 IU/dose. This may be from 1, 2, 3, 4, 5, 6 or 7 times per week. Doses may also be calculated based on IU/kg body weight of the subject. In an embodiment, dosages are given by any convenient means.

[0085] The pharmaceutical forms suitable for injectable use include sterile aqueous solutions (where water soluble) or dispersions and sterile powders for the extemporaneous preparation of sterile injectable solutions or dispersion or may be in the form of a cream or other form suitable for topical application. It must be stable under the conditions of manufacture and storage and must be preserved against the contaminating action of microorganisms such as bacteria and fungi. The carrier can be a solvent or dispersion medium containing, for example, water, ethanol, polyol (for example, glycerol, propylene glycol and liquid polyethylene glycol, and the like), suitable mixtures thereof, and vegetable oils. The proper fluidity can be maintained, for example, by the use of a coating such as lecithin, by the maintenance of the required particle size in the case of dispersion and by the use of superfactants. The preventions of the action of microorganisms can be brought about by various antibacterial and antifungal agents, for example, parabens,

chlorobutanol, phenol, sorbic acid, thimerosal and the like. In many cases, it will be preferable to include isotonic agents, for example, sugars or sodium chloride. Prolonged absorption of the injectable compositions can be brought about by the use in the compositions of agents delaying absorption, for example, aluminium monostearate and gelatin.

[0086] Sterile injectable solutions are prepared by incorporating the active compounds in the required amount in the appropriate solvent with various of the other ingredients enumerated above, as required, followed by filtered sterilization. Generally, dispersions are prepared by incorporating the various sterilized active ingredient into a sterile vehicle which contains the basic dispersion medium and the required other ingredients from those enumerated above. In the case of sterile powders for the preparation of sterile injectable solutions, the preferred methods of preparation are vacuum drying and the freeze-drying technique which yield a powder of the active ingredient plus any additional desired ingredient from previously sterile-filtered solution thereof.

[0087] The formulation may be administered in a convenient manner such as by the oral, intraperitoneal, intravenous, subcutaneous, inhaled, suppository routes or implanting (e.g. using slow release molecules). The formulation may be administered in the form of pharmaceutically acceptable nontoxic salts, such as acid addition salts or metal complexes, e.g. with zinc, iron or the like (which are considered as salts for purposes of this application). Illustrative of such acid addition salts are hydrochloride, hydrobromide, sulphate, phosphate, maleate, acetate, citrate, benzoate, succinate, malate, ascorbate, tartrate and the like. If the active ingredient is to be administered in tablet form, the tablet may contain a binder such as tragacanth, corn starch or gelatin; a disintegrating agent, such as alginic acid; and a lubricant, such as magnesium stearate.

[0088] The IFNε or its variant, hybrid or modulator of the present invention can be combined with a pharmaceutically acceptable carrier (excipient) to form a pharmacological composition. Pharmaceutically acceptable carriers can contain a physiologically acceptable compound that acts to, e.g., stabilize, or increase or decrease the absorption or clearance rates of the pharmaceutical compositions of the subject invention. Physiologically acceptable compounds can include, e.g., carbohydrates, such as glucose, sucrose, or dextrans, antioxidants, such as ascorbic acid or glutathione, chelating agents, low molecular weight proteins, compositions that reduce the clearance or hydrolysis of the peptides or polypeptides, or excipients or other stabilizers and/or buffers. Detergents can also used to stabilize or to increase or decrease the absorption of the pharmaceutical composition, including liposomal carriers. Pharmaceutically acceptable carriers and formulations for peptides and polypeptide are known to the skilled artisan and are described in detail in the scientific and patent literature.

[0089] As indicated above, the IFNε may also be added as an adjuvant for another anti-cancer agent. In this regard, the "medicament" includes IFNε or a variant or hybrid thereof alone or in combination with another anti-cancer agent.

[0090] Solid formulations can be used for enteral (oral) administration. They can be formulated as, e.g., pills, tablets, powders or capsules. For solid compositions, conventional nontoxic solid carriers can be used which include, e.g., pharmaceutical grades of mannitol, lactose, starch, magnesium stearate, sodium saccharin, talcum, cellulose, glucose, sucrose, magnesium carbonate, and the like. For oral administration, a pharmaceutically acceptable nontoxic composition is formed by incorporating any of the normally employed excipients, such as those carriers previously listed. A non-solid formulation can also be used for enteral administration. The carrier can be selected from various oils including those of petroleum, animal, vegetable or synthetic origin, e.g., peanut oil, soybean oil, mineral oil, sesame oil, and the like. Suitable pharmaceutical

excipients include e.g., starch, cellulose, talc, glucose, lactose, sucrose, gelatin, malt, rice, flour, chalk, silica gel, magnesium stearate, sodium stearate, glycerol monostearate, sodium chloride, dried skim milk, glycerol, propylene glycol, water and ethanol.

[0091] The composition of the subject invention, when administered orally, can be protected from digestion. This can be accomplished either by complexing the composition with a composition to render it resistant to acidic and enzymatic hydrolysis or by packaging these molecules in an appropriately resistant carrier such as a liposome. Means of protecting compounds from digestion are well known in the art, see, e.g., Fix (1996) *Pharm Res*. 13:1760-1764; Samanen (1996) *J. Pharm. Pharmacol*. 48:119-135; U.S. Patent 5,391,377, describing lipid compositions for oral delivery of therapeutic agents (liposomal delivery is discussed in further detail, infra).

[0092] The composition of the present invention can also be administered in sustained delivery or sustained release mechanisms, which can deliver the formulation internally. For example, biodegradable microspheres or capsules or other biodegradable polymer configurations capable of sustained delivery of a peptide can be included in the formulations of the invention (see, e.g., Putney (1998) *Nat. Biotechnol*. 16:153-157).

[0093] For inhalation, the composition of the invention can be delivered using any system known in the art, including dry powder aerosols, liquid delivery systems, air jet nebulizers, propellant systems, and the like. See, e.g. Patton (1998) *Biotechniques* 16:141-143; product and inhalation delivery systems for polypeptide macromolecules by, e.g., Dura Pharmaceuticals (San Diego, CA) , Aradigm (Hayward, CA), Aerogen (Santa Clara, CA), Inhale Therapeutic Systems (San Carlos, CA), and the like. For example, the IFNε formulation can be administered in the form of an aerosol or mist. For aerosol administration, the formulation can be supplied in finely divided form along with a surfactant and propellant. In another aspect, the device for delivering the formulation to

respiratory tissue is an inhaler in which the formulation vaporizes. Other liquid delivery systems include, e.g., air jet nebulizers.

[0094] The IFNε can also be formulated in pharmaceutically acceptable compositions suitable for pulmonary or respiratory delivery to a patient. Particular formulations include dry powders, liquid solutions or suspensions suitable for nebulisation, and propellant formulations suitable for use in metered dose inhalers (MDI's). The preparation of such formulations is well described in the patent, scientific, and medical literatures, and the following descriptions are intended to be exemplary only.

[0095] Liquid formulations of IFNε for use in nebulizer systems can include components to enhance or maintain chemical stability, including chelating agents, protease inhibitors, isotonic modifiers, inert gases, and the like.

[0096] For use in metered dose inhalers, the IFNε of the present invention is dissolved or suspended in a suitable aerosol propellant, such as a chlorofluorocarbon (CFC) or a hydrofluorocarbon (HFC). Suitable CFC's include trichloromonofluoromethane (propellant 11), dichlorotetrafluoroethane (propellant 114), and dichlorodifluoromethane (propellant 12). Suitable HFC's include tetrafluoroethane (HFC-134a) and heptafluoropropane (HFC-227).

[0097] In an embodiment, for incorporation into the aerosol propellant, the IFNε of the present invention is processed into respirable particles as described below for the dry powder formulations. The particles are then suspended in the propellant, typically being coated with a surfactant to enhance their dispersion. Suitable surfactants include oleic acid, sorbitan trioleate, and various long chain diglycerides and phospholipids.

[0098] Such aerosol propellant formulations may further include a lower alcohol, such as ethanol (up to 30% by weight) and other additives to maintain or enhance chemical stability and physiological acceptability.

[0099] Dry powder formulations typically comprises the IFNε in a dry, usually lyophilized, form with a particular size within a preferred range for deposition within the alveolar region of the lung. Respirable powders of IFNε within the preferred size range can be produced by a variety of conventional techniques, such as jet-milling, spray-drying, solvent precipitation, and the like. Dry powders can then be administered to the patient in conventional dry powder inhalers (DPI's) that use the inspiratory breath through the device to disperse the powder or in air-assisted devices that use an external power source to disperse the powder into an aerosol cloud. In the above description, reference to "IFNε" includes its variants, hybrids and modulators.

[0100] In preparing pharmaceutical formulations of the present invention, a variety of modifications can be used and manipulated to alter pharmacokinetics and biodistribution. A number of methods for altering pharmacokinetics and biodistribution are known to one of ordinary skill in the art.

[0101] In an embodiment, modulation of the expression of *lfnε* is achieved by directly effecting expression of *lfnε*. This can be achieved by the introduction directly to cancer cells in a solid tumor of a construct with the gene comprising *lfnε* which will allow for modulation of the levels of IFNε upon expression or even *de novo* expression and thereby effect the biological functions for which it is directed. Hence, recombinant cellular or viral means may be employed to generate IFNε or its variant, hybrid or modulator at or near or within cancer cells.

[0102] The present invention further contemplates a combination of methods in the treatment of cancer. For example, IFNε treatment or treatment by a variant or hybrid or modulator of IFNε may be used in combination with surgical or chemical ablation of a cancer or cancer-affected organ or tissue.

EXAMPLES

[0103] Aspects disclosed herein are further described by the following non-limiting Examples.

Methods

Cell lines and cell culture

[0104] Ovarian cancer lines ID8 (murine; Roby *et al*. (2000) *Carcinogenesis 21(4)*:585-591), CAOV3 (human; ATCC, USA), and OVCAR4 (human; National Cancer Institute, USA) were used for *in vitro* assays. ID8 & OVCAR4 cell lines were cultured in RPMI 1640 (GibcoBRL, Ontario, Canada) and CAOV3 in DMEM (GibcoBRL) supplemented with 4% v/v (ID8) or 10% v/v (CaOV3, OVCAR4) heat-activated fetal calf serum (FCS; GibcoBRL). All cells were cultured at 37°C in an atmosphere of 5% v/v carbon dioxide (CO_2). Cells were Mycoplasma negative according to MycoAlert (Trade Mark) PLUS Mycoplasma Detection Kit (ratio <1; Lonza, Basel).

Cell stimulation for gene expression studies

[0105] Cell lines were plated ($1.5x10^5$ cells/well) in a 12 well plate 24 hour prior to stimulation with recombinant IFNε or IFNβ (described below) at 0 – 1000IU/ml with resuspension buffer (described below) or PBS as vehicle controls. Cells were then incubated at 37°C for 3 hrs prior to mRNA extraction.

mRNA extraction and purification

[0106] RNA was extracted using a QIAGEN RNeasy mini-kit (Invitrogen, USA) as per the manufacturer's protocol (see appendix B for detailed protocol). Cells were harvested in betamercaptoethanol/RLT (10µl –ME per 1ml of RLT buffer) and using a 1 mL syringe and a 23-gauge needle, each sample was syringed up and down ten times to homogenize

the cells. RNA was on-column DNase treated using the QIAGEN RNase-free DNase Set (Invitrogen, USA) according to manufacturer's instructions. RNA yield and quality was then assessed using a NanoDrop (Registered Trade Mark) ND-1000 spectrophotometer (acceptable ranges for RNA purity 260/280 ratio ~2.0 & 260/230 ratio between 2.0 – 2.2) and stored at -80°C.

cDNA synthesis

[0107] A total of 500ng of RNA was made up to 7µl with diethylpyrocarbonate (DEPC) treated Milli-Q H_2O. RNA was then reverse-transcribed into cDNA using M-MLV reverse transcriptase (Promega, USA), according to manufacturer's instructions. cDNA samples were stored at -20°C until use

GAPDH polymerase chain reaction PCR)

[0108] A GAPDH PCR was performed on samples from cDNA synthesis in the presence or absence of reverse transcriptase enzyme (+/- RT). The absence of product generated by GAPDH PCR for negative RT samples ruled out the presence of genomic DNA contamination. An aliquot of 1µl of cDNA was added to 5xgreen GoTaq buffer, magnesium chloride, forward and reverse GAPDH primers, 10mM dNTPs, GoTaq enzyme (Promega, USA) and a total volume of 25µl was made up with DEPC treated H_2O.

[0109] All PCR reactions were carried out in a MyCycler (Trade Mark) Thermal Cycler (BIO-RAD) using the following cycle reaction conditions:

-	Denaturation: 94°C, 2 mins	1 cycle
-	Denaturation: 94°C, 30 secs	35 cycles
-	Annealing: 55°C, 30 secs	
-	Extension: 72°C, 30 secs	
-	Extension: 72°C, 7 mins	1 cycle

[0110] Each PCR product was then loaded onto a 1.5% w/v agarose gel and run at 100V for 30 minutes.

Quantitative real time PCR (qRT-PCR)

[0111] Primers were designed to be intron-spanning where possible. This ensures that cDNA band would be distinguished from genomic DNA on the basis of size. Primers were designed using Primer Express (Registered Trade Mark) v3.0 software (Applied Biosystems, USA). Each reaction was performed in a total of 10µl comprising 2µl of cDNA, 5µl Sybr Green PCR Master Mix (Applied Biosystems, USA), 0.2µl of each 10mM stocks of relevant forward and reverse primers and DEPC H_2O. All gene amplifications were normalized to the expression of 18S, an internal control gene stably expressed in cells. Samples were loaded in triplicate onto a MicroAmp (Trade Mark) Optical 384-well reaction plate and sealed with MicroAmp (Trade Mark) Optical adhesive film. Additionally, two RT negative reactions were used as well as a no transcript control where DEPC treated H_2O was used to replace cDNA. Amplification of a single PCR product was confirmed by analyzing dissociations curves and visualization on agarose gels. A list of primers sequences is provided in Table 2.

Table 2

Summary of sequence identifiers

GAPDH primers

5’ GAPDH primer	5’- GAACGGGAAGCTTGTCATCAA -3’ (SEQ ID NO:1)
3’ GAPDH primer	3’- CTAAGCAGTTGGTGGTGCAG -5’ (SEQ ID NO:2)

qRT-PCR SYBR primers

5’ 18S primer	5’- GTAACCCGTTGAACCCCATT -3’ (SEQ ID NO:3)
3’ 18S primer	3’- CCATCCAATCGGTAGTAGCG -5’ (SEQ ID NO:4)

Mouse

5’ Isg15 primer	5’- TGAGAGCAAGCAGCCAGAAG -3’ (SEQ ID NO:5)
3’ Isg15 primer	3’- ACGGACACCAGGAAATCGTT -5’ (SEQ ID NO:6)
5’ Tap1 primer	5’ – CGCAACATATGGCTCATGTC – 3’ (SEQ ID NO:7)
3’ Tap1 primer	3’ – GCCCGAAACACCTCTCTGT – 5’ (SEQ ID NO:8)
5’ Cdc20 primer	5’ – GTCACTCCGCTCGAGTAAGC – 3’ (SEQ ID NO:9)
3’ Cdc20 primer	3’ – GCCCACATACTTCCTGGCTA – 5’ (SEQ ID NO:10)
5’ Ccne1 primer	5’ – CCTCCAAAGTTGCACCAGTT – 3’ (SEQ ID NO:11)
3’ Ccne1 primer	3’ – AGAGGGCTTAGACGCCACTT – 5’ (SEQ ID NO:12)
5’ Cxcl10 primer	5’- CTGAATCCGGAATCTAAGACCA -3’ (SEQ ID NO:13)
3’ Cxcl10 primer	3’- GAGGCTCTCTGCTGTCCATC -5’ (SEQ ID NO:14)
5’ Ifit1 primer	5’- TCAAGGCAGGTTTCTGAGGA -3’ (SEQ ID NO:15)
3’ Ifit1 primer	3’- ACCTGGTCACCATCAGCATT -5’ (SEQ ID NO:16)
5’ Casp1 primer	5’ – ACGCCATGGCTGACAAGATCCTG – 3’ (SEQ ID NO:17)
3’ Casp1 primer	3’ – GGTCCCGTGCCTTGTCCATAGC – 5’ (SEQ ID NO: 18)
5’ Ifnε primer	5’ – GAAACGGATTCCCTTCCAAT – 3’ (SEQ ID NO:19)
3’ Ifnε primer	3’ – ACTGCTGGACTGACGAGCTT – 5’ (SEQ ID NO:20)

Human

5’ ISG15 primer	5’- GCGAACTCATCTTTGCCAGT -3’ (SEQ ID NO:21)
3’ ISG15 primer	3’- AGCATCTTCACCGTCAGGTC -5’ (SEQ ID NO:22)
5’ IFIT1 primer	5’ – AGCTTACACCATTGGCTGCT – 3’ (SEQ ID NO:23)

3’ IFIT1 primer 3’ – CCATTTGTACTCATGGTTGCTGT – 5’ (SEQ ID NO:24)

5’ IFNε primer 5’ – AGGACACACTCTGGCCATTC -3’ (SEQ ID NO:25)
3’ IFNε primer 3’ – CTCCCAACCATCCAGAGAAA – 5’ (SEQ ID NO:26)

[0112] All reactions were processed using a 7900HT Fast Real Time PCR machine (Applied Biosystems, USA) using the following thermal cycling protocol: 50°C for 2 minutes, 95°C for 10 minutes followed by 40 cycles of 95°C for 15 seconds and 60°C for 1 minute. Cycle threshold (Ct) values for all probes were exported and data analysis was carried out using the $2-\Delta\Delta CT$ method. For figures, gene amplifications were normalized to the expression of 18S, an internal control gene stably expressed in cells. Then values of fold-change after IFN treatment, were expressed relative to value for untreated samples (which was 1).

Cellular growth assays

[0113] Cellular proliferation was measured using the xCELLigence system (ACEA Biosciences, Inc., San Diego, CA, USA) for real-time cell analysis (RTCA). Fifty microliters of cell culture medium was added to each well in a 96 well E- plate (ACEA Biosciences, Inc.) for the impedance background measurement. Cells were then added (ID8 – $6x10^3$ cells/well, CAOV3 & OVCAR4 – $1x10^5$ cells/well) to a volume of 100µL in serum-free culture media and allowed to adhere overnight. Recombinant IFN or vehicle was added to the cells up to a final volume of 200µL of normal culture media. The E-Plates were incubated at 37°C with 5% v/v CO_2 and impedance measured on the RTCA system at 15-minute time intervals for up to 72 hours with or without treatment. For data analysis, the baseline cell index (CI) is determined by subtracting the CI for a cell-containing well from the CI of a well with only culture media. To facilitate the statistical evaluation of the results, impedance measurements from each well were normalized to the time of stimulation with IFN, termed 'normalized cell index'. Three independent experiments were performed in technical quadruplicate and analyzed for doubling-time and slope (1/hr) of growth curves, indicative of rate of proliferation, using RCTA software. Data was analyzed using 2-way ANOVA with Sidak's multiple comparisons test, ****$p<0.0001$, ***$p<0.001$.

Migration assays

[0114] For single cell tracking, ID8 cells were plated in serum free media at $2.5x10^4$ cells/well in a 48 well plate and left to adhere overnight. For scratch assays, ID8 cells were plated in a 48 well plate and allowed to reach confluence. Coated wells were scratched using a P10 filter tip (Axygen Scientific, California). Cells were stained using CellTrace (Trade Mark) CFSE Cell Proliferation Kit (ThermoFischer Scientific, Massachusetts) as per the manufacturer's instructions, then washed in PBS and treated with recombinant IFN. Fluorescent images were captured every 30 minutes for 12 hours using a confocal microscope and analyzed using Imaris software. For single cell tracking, individual cells were tracked *via* fluorescence to measure the overall distance traveled by each cell (track length) and direct displacement length from the initial to final position of each cell (track displacement) over 12 hours. Significance was determined by Student's T test comparing the mean distances traveled $2.5x10^4$ cells plated in technical triplicate. For scratch assays, cellular migration was measured as the percentage surface area closure of the scratch (empty space) over 12 hours. Significance was determined by one-way ANOVA with Tukey's multiple comparisons; *p<0.05, **p<0.01, ***p<0.001, ****p<0.0001.

Apoptosis assays

[0115] ID8 cells were plated in a 12 well plate ($3.5x10^4$ cells/well) in 2ml and left to adhere overnight. Cells were stimulated with recombinant murine *Ifnε* or vehicle control for 48 hours. Hydrogen peroxide (H_2O_2) was used a positive control for induction of apoptosis at 1 – 5mM. Following stimulation, cells were trypsinized and washed in PBS. Single cell suspensions were stained with FITC conjugated Annexin V and propidium iodide (PI) using the FITC Annexin V Apoptosis Detection kit II (BD Biosciences, New Jersey), as per the manufacturer's instructions and analyzed by flow cytometry using a FACSCanto (Trade Mark) II flow cytometer (BD Biosciences) and Flo-Jo software. The different phases of apoptosis were defined as i) live cells (FITC Annexin V-/PI-), ii) early apoptotic (FITC Annexin V+/PI-), iii) late apoptotic (FITC AnnexinV+/PI+), and iv) necrotic cells (FITC Annexin V-/PI+).

Immunohistochemistry

[0116] Human fallopian tubes, mouse organs and tumor samples were fixed for 24 hours in 10% v/v neutral buffered formalin, then washed in 70% v/v ethanol, and embedded in paraffin. Tissue was sectioned at 4-μm thickness and stained for H&E, smooth muscle actin (SMa), cytokeratin 18(Ck18) and IFNε. Briefly, histological tissue sections were deparaffinized and rehydrated. Antigen retrieval was performed by heat in 10 mM Tris/1 mM EDTA (pH 9.0) for 6 mins. After inhibition of endogenous peroxidase activity with 3% v/v hydrogen peroxide, tissues were blocked in CAS-Block [Trade Mark] (ThermoFisher Scientific) for 1 hour. Tissues were then incubated overnight at 4°C with anti-IFNε (1:200; Novus Biologicals, Colorado), anti-SMa (1:100; Dako Omnis, Santa Clara), anti-Ck18 (1:50; Dako Omnis) and rabbit IgG (1:200; Vector Laboratories, California) or mouse IgG1 (1:37; Vector Laboratories) as isotype controls. Biotinylated anti-rabbit or anti-mouse IgGs (both 1:250 dilution; Vector Laboratories) were diluted in the same buffer and incubated for 1 hour. Slides were then washed in 0.05% v/v Tween/PBS and incubated with avidin and biotinylated horseradish peroxidase (VECTASTAIN (Registered Trade Mark) Elite (Registered Trade Mark) ABC Kit, Vector Laboratories) as per the manufacturer's instructions and washed again. Slides were then incubated with diaminobenzidine tetrahydrochloride (DAB; DAB+ Substrate Chromogen System, Dako Omnis) as per the manufacturer's instructions. Sections were counterstained with Haematoxylin for 45 seconds then dehydrated and placed under coverslip with dibutylphthalate dolystyrene xylene (DPX; Merck, Germany). Staining intensity was calculated using the positive pixel analysis tool in Imagescope software and significance was determined using Mann-Whitney tests, **$p<0.01$, ****$p<0.0001$.

Immunophenotyping

[0117] Single cell suspensions were obtained from peritoneal lavage cells of C57BL/J mice studied for surface antigen expression using a panel of monoclonal antibodies

directly conjugated with fluorochromes. In order to prevent non-specific binding, cell surface receptors were blocked with Anti-mouse CD16/CD32 Fcγ III/II Receptor blocking antibody (BD PharMingen, California). For surface staining, cells were stained with the various combinations of fluorochrome-labeled antibodies: panel 1 – APC conjugated CD45, APC-Cy7 conjugated CD8, FITC conjugated NK-1.1, PE conjugated CD69, Pacific Blue conjugated CD4; panel 2 – APC conjugated CD25, APC-Cy7 conjugated CD8, FITC conjugated CD45, PE conjugated Pan CK, PE-Cy7 conjugated CD4 and Pacific Blue conjugated FoxP3; panel 3 – APC conjugated CD45, APC-Cy7 conjugated CD11b, FITC conjugated Ly6C, PE conjugated I-Ab, PE-Cy7 conjugated CD11c and Pacific Blue Ly6G. Cells were analyzed using a FACSCanto (Trade Mark) II flow cytometer (BD Biosciences) and Flo-Jo software.

Cytometric bead array (CBA)

[0118] Cytometric bead array (BD CBA Mouse Inflammation Kit; BD Pharmingen) was used to determine cytokine levels in the supernatant of peritoneal exudate cells from mice injected with ID8 cells (see intraperitoneal model of ovarian cancer below) as per the manufacturer's instructions. Flow cytometry was used to detect PE-conjugated detection antibodies forming sandwich complexes with capture beads for IL-8, IL-1β, IL-6, IL-10, IL-12p70, or TNF-α. PE fluorescent intensities for each sandwich complex was acquired using a FACSCanto (Trade Mark) II flow cytometer (BD Biosciences) and Flo-Jo software.

Mice

[0119] The *Ifnε*$^{-/-}$ mice (Fung *et al*. (2013) *supra*) on a C57bl/6 background and wild-type mice (Monash Animal Research Facility, Monash University, Clayton, Australia) were housed in standard specific pathogen free (SPF) conditions.

Intrabursal (orthotropic) ovarian cancer model

[0120] Female (10 weeks of age) C57BL/6 wild-type (*Ifnε*$^{+/+}$) and Ifnε deficient mice (Ifnε$^{-/-}$) were used in these experiments. Mice were anaesthetized by inhalation of isoflurane (5% in oxygen) in an induction chamber, and anaesthesia maintained at 2.5-3.0% isoflurane delivered *via* nosecone during all procedures. Mice were subcutaneously injected with Carprofen (5mg/kg) prior to surgery. A small incision was made at the dorso-medial position directly above the ovarian fat pad, with a secondary small incision through the peritoneal wall. The ovarian fat pad was externalized and stabilized with a bull clip, and a dissecting microscope used to locate the oviduct in the exposed ovary. ID8 cells ($1x10^6$) were injected underneath the left ovarian bursa. The peritoneal wall was sutured closed using 6/0 suture prior to topical Bupivacaine administration and closure of the incision closed with surgical staples. Analgesia (Carprofen 5mg/kg body weight) was provided in drinking water for 3 days thereafter. Mice were monitored for body weight, Body Condition Score (BCS) defined as: BCS 1 Thin – Skeletal structure prominent and vertebral bodies protruding, BCS 2 Under-conditioned – segmentation of vertebral column evident but not protruding, and BCS3 Well-conditioned – vertebrae not evident without palpation, as well as clinical signs and culled 13 weeks post-ID8 injection. Do we need something on samples collected at experiments end? At autopsy, the overall spread and tumor burden of each mouse was documented (number of tumor nodules, sites of nodule deposits recorded and photographed), ascites fluid was drained from the peritoneum for volume measurement and cell counts and tissue harvested (spleen, diaphragm, peritoneal wall, mesenteric fat, female reproductive tract) for weight measurements and immunohistochemical analysis.

Intraperitoneal (disseminated) ovarian cancer model

[0121] Female (6 to 8 weeks of age) C57BL/6 wild-type (Ifnε$^{+/+}$) mice were used in these experiments. Mice were injected intraperitoneally with $5x10^6$ ID8 cells using a 30-gauge needle. Mice were monitored for body weight, BCS and clinical signs and culled 8 weeks post-ID8 injection. At autopsy, the overall spread and tumor burden of each mouse was documented (number of tumor nodules, sites of nodule deposits recorded and

photographed), ascites fluid was drained from the peritoneum for volume measurement and cell counts and tissue harvested (spleen, diaphragm, peritoneal wall, mesenteric fat, female reproductive tract) for weight measurements and immunohistochemical analysis.

Intraperitoneal recombinant IFN therapy

[0122] IFN treatments were commenced 3 days post-intraperitoneal ID8 cell injections. Mice either received recombinant murine *Ifnε* injected intraperitoneally 3 times a week at a dose of 2 – 500IU/injection or *Ifnβ* at 500IU/injection or vehicle for 8 weeks. At autopsy, the orthotropic ‘primary" tumor was collected along with metastases (diaphragmatic & peritoneal), spleen, ascites fluid (volume and cell counts) and peritoneal lavage and samples weighed, photographed and processed for immunohistochemical analysis.

Recombinant IFN production

Mouse

Production and purification of mulFNε

[0123] The generation and PCR screening of recombinant bacmids containing the IFNε gene and baculovirus was carried out as described elsewhere . Briefly, PCR-positive colonies were expanded and recombinant bacmid isolated using an EndoFree Maxi-Prep kit according to the manufacturer’s instructions (Qiagen). Recombinant baculovirus was generated by transfection of the purified bacmid into Sf9 insect cells and high titre baculovirus generated. IFNε was expressed as a soluble protein and secreted into the culture media.

[0124] Insect cell expression supernatants were clarified of cells by centrifugation as described, supplemented with phenylmethanesulfonyl fluoride (PMSF) at a final concentration of 1mM before dialysis against TBS (10mM Tris-HCl, 150mM NaCl, pH8.0) overnight at 4°C using 12.5kDa cut-off dialysis tubing (Sigma-Aldrich).

Particulates were removed by filtration of the dialysate through a 0.8µm syringe driven filter (Sartorius). An anti-IFNε monoclonal antibody affinity column was prepared by coupling 10mg of anti-IFNε antibody to 1ml of AminoLink Plus resin according to the manufacturer's instructions (Thermo Scientific). The filtrate was applied to this column and then the column washed with five column volumes (CV) of TBS to remove non-specifically bound proteins and rIFNε eluted with 0.1M Glycine pH3.0 in 0.5CV fractions. Collected fractions were immediately neutralized with 1/10th CV of 1M Tris-HCl pH8.0 and buffer exchanged by addition of 10x TBS (100mM Tris-HCl, 1.5M NaCl, pH8.0). Protein containing fractions, as determined by absorbance at 280nm, were further supplemented with 10% v/v glycerol. Purified IFNε was subsequently further purified by gel filtration on a S75 10/30 size exclusion column (GE Healthcare) connected to an AKTA PrimePlus (GE Healthcare) using TBS pH8.0 containing 10% v/v glycerol. Purified fractions were filter sterilized and stored at 4°C or snap-frozen in liquid nitrogen for long-term storage at -80ºC.

Human

Production of huIFNε using bacterial system

[0125] Human IFNε (tagless native 187 residue sequence) was expressed from a pET-28a expression vector (Novagen) in *Escherichia coli* BL21 (DE3). A single colony of the freshly transformed cells was inoculated into L-Broth containing 50 µg/mL kanamycin. The culture was grown overnight at 37°C with constant shaking at 250 rpm. After 16 h, the cell culture was diluted 50-fold with fresh L-Broth containing 50 µg/mL kanamycin. The mixture was incubated with shaking at 37°C until the optical density (OD_{600}) reached 0.6 – 0.8 when the cells were induced with 1 mM isopropyl β-D-1-thiogalactopyranoside (IPTG). The cells were allowed to grow for 3 h before harvesting by centrifugation at 5000 g for 15 mins. The cell pellets were frozen at -20°C until further use.

Preparation of inclusion bodies

[0126] Frozen cells were thawed at room temperature for 30 mins. Each gram of cell pellet was resuspended with 10 mL of BugBuster Master Mix (Merck Millipore) with added 10 mM dithiothreitol (DTT), 5 mM ethylenediaminetetraacetic acid (EDTA) and 0.5 % w/v complete Mini protease inhibitor cocktail tablet (Roche), and incubated at room temperature for 2 h with gentle agitation. The lysate was centrifuged at 30000 *g* for 20 mins, and the supernatant was decanted. The inclusion bodies (IBs) were then washed multiple times using different buffers (70 mL for each gram of IBs) all containing 10 mM DTT and 5 mM EDTA: (1) 1:10 diluted BµgBuster Master Mix (with MilliQ water), (2) 10 mM tris(hydroxymethyl)aminomethane (Tris) buffer pH 8.0 with 150 mM NaCl and 2 M urea, (3) 10 mM Tris buffer pH 8.0 with 150 mM NaCl and 5 % v/v Triton X-100. Each wash was followed by centrifugation of 30000 *g* for 20 mins to remove the supernatant. Thereafter, the IBs were washed twice with 10 mM Tris pH 8.0 with 150 mM NaCl (70 mL for each gram of IB) to remove EDTA in the product. The IBs were then solubilized using buffer containing 6 M guanidine hydrochloride (Gdn-HCl) pH 7.4, 100 mM Na_2HPO_4 and 10 mM Tris overnight at cold room under constant agitation. The resulting mixture was centrifuged at 30000 *g* for 20 mins, and the solution was 0.2 µm-filtered.

Refolding of huIFNε

[0127] DTT was added into the denatured huIFNε solution at concentration of 5 mM, and the mixture was incubated at room temperature (25°C) under mild agitation for 2 h. Thereafter, the mixture was chilled to 4 °C before it was added dropwise into 50 volumes of refold buffer (20 mM phosphate buffer pH 7.4, 150 mM NaCl, 0.8 M L-Arginine (L-Arg) and 10 µM $CuSO_4$) at 4 °C with gentle stirring, and the refolding was allowed to proceed for 16 h.

Protein purification

[0128] EDTA was added into the refold mixture at 5 mM concentration, and the pH of the refold solution was adjusted to pH 6.0 before it was concentrated using both Vivaspin 200 tangential flow filter (MWCO 10 kDa) and Vivaspin 20 concentrator (MWCO 10 kDa) at 4°C. The sample was then purified using gel filtration (HiLoad 16/60 Superdex 200) at flow rate of 1.0 mL/min with 20 mM phosphate buffer pH 6.0 containing 150 mM NaCl and 0.8 M L-Arg as running buffer. Fractions containing huIFNε were combined and 1 mL of anion-exchange resin (Q Sepharose fast flow) was added into it. The mixture was incubated at 4°C under constant agitation for 18 h. The flow through was then collected and concentrated using Vivaspin 20 concentrator.

Gel electrophoresis and Western blot

[0129] Sodium dodecyl sulfate polyacrylamide gel electrophoresis (SDS-PAGE) and western blot were performed using Bolt Bis-Tris plus 4 – 12 % gradient gel (Life Technologies) and Bolt MOPS SDS running buffer (Life Technologies) at 165 V for 50 mins. For SDS-PAGE analysis, the gel was stained with Coomassie Blue solution (0.25 % w/v Coomassie Blue R-250, 50 % v/v methanol and 10 % v/v acetic acid) for 2 h before destained with solution containing 40 % v/v ethanol and 10 % v/v acetic acid. For western blot, protein bands were transferred to Immobilon-FL Polyvinylidene Difluoride (PVDF) membrane using Bolt transfer buffer (Life Technologies) at 30 V for 45 mins. The membrane was incubated in Odyssey blocking buffer (PBS) [LI-COR Biosciences] at room temperature for 1 h. The buffer was decanted and rabbit polyclonal anti-huIFNε antibody (Novus Biological) at 1:500 dilution was added onto the membrane and incubated for 16 h at 4 °C. Thereafter, the antibody solution was removed and the membrane was washed three times with phosphate-buffered saline (PBS) pH 7.4 containing 0.1 % v/v Tween 20. Anti-rabbit IgG (H&L) (GOAT) antibody IR dye 800 conjugated (Rockland) at 1:1000 dilution was added onto the membrane and incubated at room temperature for 1 h. The membrane was washed as before with PBS pH 7.4 containing 0.1 % v/v Tween 20. Western blot analysis was performed using Odyssey infrared imaging system (LI-COR Biosciences) using both 700 and 800 channels.

Endotoxin testing

[0130] Endotoxin levels in a sample were tested using limulus amebocyte lysate (LAL) test. The testing system and reagents were purchased from Charles River. Protein sample was first diluted 1:10 with LAL reagent water, and then further diluted 1:10 with Endotoxin-specific buffer. Sample was then loaded onto the LAL cartridge (sensitivity 0.05 to 5 EU/mL for neat sample) and the absorbance was recorded using Endosafe-PTS.

Circular dichrosim

[0131] Human IFNε sample was prepared in 20 mM phosphate buffer pH 6.0 containing 500 mM NaCl, 5 mM EDTA and 10 % v/v glycerol. Circular Dichroism (CD) experiments were performed at 25 °C on a Jasco J-810 spectrometer equipped with a Peltier temperature-controlled water circulator. Spectra ranging from 190 to 250 nm was measured using 1 mm path length quartz cell, accumulation cycle of 3 runs, 1 nm bandwidth, 0.1 nm data pitch and 1 s data integration time. The data were analyzed using Jasco Spectra Manager.

[0132] Biological activity (IU/ml) of the huIFNε sample was determined by comparison against a serial dilution of hIFNβ protein of known activity.

[0133] Specific activity (IU/mg) of the refolded huIFNε using this system is consistent with results obtained from an anti-viral protection assay (protection of WISH cells from infection with EMCV) and confirms: this refolded protein is biologically active; and the specific activity of huIFNε is of a similar order of magnitude to that of muIFNε expressed in an insect cell expression system (Table 3).

Table 3

Comparison of specific activity (IU/mg) of mouse and human interferon epsilon proteins as determined by either viral-protection assay or reporter cell line

Interferon	**Method**	**Specific Activity (IU/mg)**	**Reference**
muIFNε	Anti-viral protection assay (L929 cells and SFV)	2.1×10^5	Stifter, S. Unpublished data (Doctoral Thesis)
huIFNε	Anti-viral protection assay (WISH cells and EMCV)	1.12×10^4	Experimental data
huIFNε	Reporter cell line (HEK-Blue™)	5.26×10^4	Experimental data

[0134] Use of this reporter cell line has provided an easy and economical assay for the determination of the biological activity of huIFNε and should simplify identification of monoclonal antibodies capable of neutralising this activity.

[0135] The final IFNε formulation was in the following buffer that was used as the "vehicle control" in the *in vivo* and *in vitro* experiments: 20 mM phosphate buffer pH 6.0 containing 150 mM NaCl and 0.8 M L-Arg as running buffer.

EXAMPLE 1

The role of IFNε in ovarian cancer

[0136] The effects of treating both mouse and human tumor derived cell lines with recombinant IFNε was assessed and compared the effects with other, conventional type I IFNs.

[0137] The mouse cell lines examined were the murine ovarian epithelial cell line, ID8s, which are used for *in vivo* experiments (Example 2) to enable the comparison of *in vitro* with *in vivo* anti-tumor effects.

[0138] Also examined are the effects of IFNε on various human ovarian cancer cell lines. A number of human cell lines were used to investigate ovarian cancer *in vitro*, including OVCAR4 and CAOV3 cells. These represent cell lines that are classified as representative of high grade serous ovarian cancer (HGSC) as per systematic genomic comparison with tumor samples to be highly genetically similar to human HGSC (Domcke *et al*. (2013) *Nature Communications 4*:2126). Each of the cell lines used demonstrated the fundamental molecular characteristics of HGSC including a high fraction of genomic alterations, universal TP53 mutations and few, if any, other somatic mutations in protein-coding regions, and thus, represent some of the most suitable models for studying human ovarian cancer *in vitro*.

EXAMPLE 2

IFNε induces anti-tumor effects the murine ovarian cancer ID8 cell line

[0139] The aim was to use the ID8 cell line to characterize the anti-tumor effects of IFNε *in vivo* in a murine model of ovarian cancer. Initially, it was important to confirm that this cell could indeed respond to type I IFNs, including IFNε. ID8 cells were stimulated *in vitro* with different doses of either recombinant murine IFNε or IFNβ for 3h before quantification of three well characterized IFN regulated genes (IRGs), cxcl10, isg15 and ifit1 (Figure 1). IFNε significantly induced expression of all three IRGs in a dose dependent manner, similar to IFNβ (in IU/ml), thus confirming that these cells can respond to IFNε.

[0140] Having confirmed that ID8 cells can respond to IFNε, next investigated was whether IFNε could regulate the expression of IRGs-encoding proteins with roles in tumor-related properties, cell proliferation and apoptosis. It was found that treatment of ID8 cells with 1000 IU/ml of IFNε significantly down-regulated the expression of *bcl-2*, *ccne1* and *cdc20*, which encode for proteins with anti-apoptotic (*bcl-2*) and pro-proliferative functions (*ccne1, cdc20*) (Figure 2). Conversely, IFNε significantly induced expression of the IRGs *tap1* and *casp1*, genes which encode for pro-apoptotic proteins. Therefore, these data indicate that IFNε regulated genes are involved in cell cycle, proliferation and apoptosis.

[0141] Next assessed was the effect of IFNε on proliferation of ID8 cells using the Xcelligence (Registered Trade Mark) Real Time Cell Analysis (RTCA) system (Acea Biosciences), which allows real-time, label-free monitoring of cell proliferation. Therefore, it was possible to monitor proliferation of ID8 cells treated with IFNε based on an impedance reading of cells in the wells every 30 mins. As cells proliferate, the impedance reading (cell index) increases. As evident in Figure 2, there is a dose-

dependent difference in cell index upon treatment with IFNε (Figure 3A) or IFNβ (Figure 3B).

[0142] From this software, this decrease can quantify cellular proliferation using two different measurements: (i) doubling time of the cells; and (ii) the slope of the growth curves of the cells indicative of growth rate. It was found that IFNε treatment increased the doubling time of ID8 cells in a dose dependent manner, similar to what was observed for IFNβ (Figures 4A and 4B). Also observed was a decrease in the slope of the growth curves of ID8 cells following treatment with IFNε or IFNβ (Figure 4C). Therefore, IFNε treatment could significantly inhibit the proliferation of the murine ovarian cancer cell line.

[0143] Having observed that IFNε treatment could decrease the proliferation of ID8 cell line, next analyzed was the effect on cell migration, as an indication of how IFNε may affect metastasis of tumor cells. To do this, a fluorescent cell dye (CellTrace (Trade Mark) CSFE, ThermoFisher Scientific) was used to stain and track ID8 cell migration during a scratch assay. Using this method of analysis, the percentage migration of ID8 cells was calculated based on the closure of a 'scratch' as ID8 cells migrate from a confluent are to an open space over a 12 h period. It was found that treatment of the cells with IFNε for 12 h could significantly decrease the percentage scratch closure (or migration) of ID8 cells thereby demonstrating that IFNε affects the tumor-related *in vitro* activity of ID8 cell motility, which would have implications for the metastatic potential of these cells (Figure 5).

[0144] Since it was observed that IFNε inhibited ID8 cell proliferation, mobility and migration, next assessed was whether IFNε could induce apoptosis of ID8 cells. To do this, Annexin/PI staining of treated cells was used with FACS analysis to identify whether dying cells are undergoing early or late apoptosis or necrosis. It was found that IFNε treatment decreased the number of live cells by roughly 40% in the assay and upon further

analysis that these cells were found to be in early & late apoptosis, as indicated by cells staining positive for both Annexin V only and both Annexin V and PI, respectively. Importantly, no necrosis was observed with any dose of IFNε assessed. The data from this FACS analysis is summarized in Figure 6.

EXAMPLE 3

The dysregulation of IFNε in ovarian cancer development: patient samples

[0145] IFNε expression was assayed in healthy *vs* ovarian cancer patients using immunohistochemistry in ovarian cancer patient samples. Tissue sections were formatted into tissue microarray (TMA) to minimize experimental error between staining. IHC analysis was commenced by staining sections from the healthy fallopian tube control samples obtained and generating control tissue blocks to stain along side the ovarian cancer patients. It was found that IFNε is highly expressed in the epithelium of the healthy fallopian tube. As controls, epithelium was stained with cytokeratin 18 and the underlying stromal cells with smooth muscle actin (SMA).

[0146] These sections of healthy control fallopian tubes were used to generate control blocks containing up to 8 samples per block for side-by-side simultaneous staining along side ovarian cancer patient biopsy TMAs. These TMAs contain biopsies of high grade serous carcinomas, low grade serous carcinomas, benign hyperplasia and borderline epithelium from 106 patients. It was found that IFNε expression is significantly suppressed in serous carcinoma samples compared to control benign epithelium (Figure 7).

EXAMPLE 4

The role of IFNε in ovarian cancer development and therapeutic benefit: mouse models

[0147] The role of endogenous IFNε in tumorigenesis of ovarian cancer was investigated.

[0148] C57BL/6 wild-type and *Ifnε* deficient mice were injected with ID8 cells into the left ovarian bursa. At 13 weeks post-injection these mice developed large orthotropic tumors and characteristic hemorrhagic ascites in the peritoneum associated with metastatic deposits on the peritoneal wall, diaphragm, spleen and mesentery. Importantly, this model of disease spread is characteristic of the progression and metastasis of advanced human ovarian cancer. At 13 weeks these mice had developed advanced disease and subsequently, it was found no difference in primary tumor size at this time between WT and $Ifn\varepsilon^{-/-}$ mice (Figure 8). Instead, a trend was observed towards more advanced disseminated disease in *Ifnε* deficient mice including splenomegaly (Figure 8B), ascites volume (Figure 8C), number of metastatic peritoneal deposits (Figure 8D) and red blood cells in drained ascites fluid (Figure 8E). Primary tumors and metastatic deposits were collected for immunohistochemical analysis. Hematoxylin and eosin stains demonstrated mixed glandular morphology with interspersed fibroblast-like cells and adipose tissue as well as invasion into the diaphragm and spleen. This is further analyzed using multiplexing for immune cell panels.

EXAMPLE 5

Additional data from recombinant IFNε therapy in a model of disseminated ovarian cancer

IFNε induces anti-tumor effects in human ovarian cancer cells

[0149] As it was demonstrated that IFNε has strong anti-tumor effects on a murine ovarian cancer cell line, next assessed was its effects on human ovarian cell line. As documented above, CaOV3 and OVCAR4 cells were chosen as these represent HGSC.

[0150] First, it was confirmed that these cell lines responded to type I IFN stimulation. CaOV3 and OVCAR4 cells were treated with recombinant human IFNε. IRG induction was measured after 3h of stimulation. It was found that both cell lines responded to type I IFN stimulation, although with different IRG induction observed across the different cell lines.

[0151] It was next determined if IFNε stimulation altered the proliferation of human ovarian cancer cell lines using the xCELLigence RTCA system. It was found that human ovarian cancer cells treated with IFNε had overall significantly lower cell index plots, had an increased doubling time and the slopes of their growth curves were significantly lower. This analysis demonstrates that IFNε treatment decreased proliferation of human ovarian cancer cell lines. This anti-proliferative effect of IFNε was demonstrated in CaOV3 and OVCAR4.

Immunomodulatory effects of intraperitoneal recombinant IFNε therapy in healthy mice

[0152] Healthy C57BL/6 wild-type mice (6 to 8 weeks of age) were treated with recombinant murine IFNε or IFNβ (at 500 IU/dose) *via* intraperitoneal injection, three times weekly for 8 weeks. Peritoneal exudate cells were collected in PBS *via* peritoneal lavage and analyzed using flow cytometry for immune cell populations. It was found that

IFNε therapy significantly regulated immune cell populations known to be important in anti-cancer immunity as well las their activation status including CD8+ T cells (Figure 9A), activation of CD4+ T cells (Figure 9B), inflammatory monocytes (Figure 9C) and PD1+ expression on CD4+ T cells (Figure 9D).

Efficacy of intraperitoneal recombinant IFNε therapy in a model of disseminated ovarian cancer

[0153] For a model of advanced disseminated ovarian cancer that accurately recapitulates the metastatic spread (diaphragm, peritoneal wall and mesentery) malignant ascites development, splenomegaly and anemia of human ovarian cancer an intraperitoneal ID8 mouse model was used. C57BL/6 wild-type mice (6 to 8 weeks of age) were intraperitoneally injected with ID8 cells (5×10^6 cells per mouse). At 3 days post-injection mice commenced intraperitoneal recombinant IFNε or IFNβ therapy (500 IU/dose three times weekly) for 8 weeks. It was found that mice treated with IFNε had significantly decreased tumor dissemination in the mesentery as well as fewer peritoneal and diaphragmatic deposits than PBS control mice or mice treated with IFNβ.

[0154] Also found was that mice treated with IFNε had significantly reduced ascites development (Figure 10A), with fewer detectable ascites tumor cells (Figure 10B) and a decreased red blood cell content (Figure 10C), indicative of less advanced disease. This was associated with suppressed inflammatory cytokine levels detectable in ascites fluid from these mice particularly MCP-1 (monocyte chemoattractant protein 1) [Figure 11] known to facilitate angiogenesis in this disease. Figure 12 provides data on the region of peritonea immune cell regulation by IFNε in a disseminated ovarian cancer model.

[0155] The results are shown in Figures 13 to 15.

Figure 13

[0156] Figure 13A shows that by 8 weeks this model had progressed enough for diffuse tumor development (as shown by weight gain and upon culling the mice) as well as hemorrhaging of the peritoneal fluid, however, this time point caught the mice just prior to advanced ascites development. None of the treatment groups showed significant weight gain difference? compared to non-tumor bearing controls indicative of little ascites development. However, every treatment group except high dose IFNε are trending towards significance compared to their own control. Additionally, significant differences can be seen between tumor-bearing treatment groups, showing the least amount of disease development in mice treated with 500 IU IFNε.

[0157] Figure 13B, significantly steeper curves can be seen in the final 2 weeks (week 6 to week 8). This time point represents progression of the disease just prior to advanced ascites development. Only mice treated with high does IFNε do not demonstrate a steeper growth rate than their non-tumor bearing controls in this period.

[0158] Figure 13C, none of the tumor-bearing mice showed significant differences across treatment groups, however, all of the treatment groups had significantly larger circumferences compared to their non-tumor bearing controls except mice treated with high dose IFNε. This trend is somewhat reflected by the drained ascites volumes.

[0159] Figure 13D, shows the volume of ascites fluid drained from the peritoneal cavity of each mice at the experimental endpoint of 8 weeks. Mice treated with high does IFNε constituted the only treatment group with significantly reduced ascites development (individual Mann-Whitney tests) and the only treatment group with tumor-bearing mice that had not yet developed ascites. All other tumor-bearing mice had started to develop ascites with the largest volume recorded from the low dose IFNε group (~3.5ml). At 8 weeks these mice are still in the early stages of ascites development.

Figure 15

[0160] Figure 15A shows the extent of tumor development and spread throughout the mesentery graded 0 to 4 (0 – no disease, 1 – very little obvious disease, some small tumor deposits upon exploration, 2 – obvious tumor but mainly localized to one deposit, 3 – large tumor nodule developed near spleen and some deposits throughout mesentery, 4 – large tumor nodule near spleen extending throughout the mesentery too numerous to count). Mice treated with high dose IFNε were the only treatment group with significantly less disease present in the mesenteric region.

[0161] Figure 15B, mice treated with high dose IFNε had the least peritoneal nodules.

[0162] Figure 15C, mice treated with high dose IFNε had the least diaphragmatic nodules, however, some variability in the PBS control mice prevented significance for this group.

[0163] Figure 15D, liver nodules were not as detectable as other sites (peritoneum, diaphragm), however, there is still a trend for a reduction in mice treated with high does IFNε.

[0164] Figure 15E is an early time point for the model by which the tumor had not had a chance to successfully adhere and colonize secondary sites. In the second model (which ran for 10 weeks with extensive ascites development), no spheroids were detected. As such spheroids may serve as a marker of less advanced disease in this model. In this current model, very few of these nodules were detected due to the reasonably advanced stage at 8 weeks (however, still earlier than last time) and while not significant, mice treated with high dose IFNε are showing the highest prevalence of non-attached spheroids. Perhaps another indicator of how IFNε may prevent the progression of this disease.

[0165] Figure 15F, given the varying size of some of the tumor deposits the surface area dimensions were measured of the largest single tumor nodule per mouse to see whether this would still reflect a trend towards IFNε disrupting tumor growth. While there was some variability in the PBS controls ($p=0.06$ with high dose IFNε) high dose IFNε significantly reduced the larges nodule compared to low dose IFNε demonstrating a dose reduction in tumor growth.

[0166] Those skilled in the art will appreciate that the disclosure described herein is susceptible to variations and modifications other than those specifically described. It is to be understood that the disclosure contemplates all such variations and modifications. The disclosure also enables all of the steps, features, compositions and compounds referred to or indicated in this specification, individually or collectively, and any and all combinations of any two or more of the steps or features or compositions or compounds.

[0167] All patents, applications, publications, test methods, literature, and other materials cited herein are hereby incorporated by reference in their entirety as if physically present in this specification.

BIBLIOGRAPHY

AIHW (2010) *Cancer series 52 Cat No. CAN48*

Berek *et al*. (1985) *Cancer Res. 45*:4447-53

Berek *et al*. (1999) *Gynecol Oncol. 75(1)*:10-4

Bowtell *et al*. (2010) *Nature Rev Cancer 10(11)*:803-8

Bruzzone *et al*. (1997) *Gynecol Oncol. 65(3)*:499-505

Bunin *et al.* (1994) *Proc. Natl. Acad. Sci. USA,* 91:4708-4712

DeWitt *et al*. (1993) *Proc. Natl. Acad. Sci. USA,* 90:6909-6913

Domcke *et al*. (2013) *Nature Communications 4*:2126

Egleton (1997) *Peptides* 18:1431-1439

Fix (1996) *Pharm Res*. 13:1760-1764

Frasci *et al*. (1994) *Eur J Cancer 30A(7)*:946-50

Fung *et al*. (2013) *Science 339(123)*:1088-1092

Jayson *et al*. (2014) *The Lancet 284(9951)*:1376-88

Kobolt *et al*. (2012) *Nature* 490(7418):61-70

Langer (1990) *Science* 249:1527-1533

Mangan *et al. Eur J Immunol*, 2007, 37(5):1302-12

Markman *et al*. (1992) *Gynecol Oncol. 45(1)*:3-8

Markman *et al*. (2004) *Oncology 66(5)*:343-6

Moore *et al*. (1995) *Gynecol Oncol. 59(2)*:267-72

Patton (1998) *Biotechniques* 16:141-143

Peng *et al*. (2007) *Prot Expr Purif 53*:356-364

Putney (1998) *Nat. Biotechnol*. 16:153-157

Roby *et al*. (2000) *Carcinogenesis 21(4)*:585-591

Salamonsen *et al. Semin Reprod Med*, 2007, 25(6):437-44

Samanen (1996) *J. Pharm. Pharmacol*. 48:119-135

Sieh *et al*. (2013) *The Lancet Oncology 14(9)*:853-62

Smith *et al. J Immunol*, 2007, 178(7):4557-66

Thakkar and Mehta (2011) *Oncologist 16(3)*:276-85

Tothill *et al*. (2008) *Clin Cancer Res. 14(16)*:5198-208

Venkitaraman (2014) *Science 343(6178)*:1470-5

Willemse *et al*. (1990) *Eur J Cancer Clin Oncol 26(3)*:353-8

CLAIMS:

1. A method for inhibiting a cancer cell in a subject, said method comprising contacting the cancer cell with an amount of interferon epsilon (IFNε) or a functional natural or synthetic variant or hybrid form thereof or a modulator of *lfnε* expression or IFNε activity effective to indirectly or indirectly induce apoptosis of the cancer cell proliferation, motility and/or migration.

2. The method of Claim 1 wherein the IFNε is derived from a species homologous to the species of the subject being treated.

3. The method of Claim 1 wherein the IFNε is derived from a species heterologous to the species of the subject being treated.

4. The method of Claim 1 or 2 or 3 wherein the subject is a human.

5. The method of Claim 4 wherein the IFNε is recombinant human IFNε or a modulator of *lfnε* expression.

6. The method of Claim 4 wherein the IFNε is recombinant non-human IFNε or a modulator of *lfnε* expression.

7. The method of Claim 4 wherein the IFNε is a hybrid between human and non-human IFNε.

8. The method of Claim 7 wherein the IFNε is a hybrid between human and murine IFNε.

9. The method of any one of Claims 1 to 8 wherein the cancer cell is derived from epithelial tissue, connective tissue, glandular tissue, embryonic tissue, hemopoietic cells, lymphatic tissue or bone marrow or cells from which such cells are derived.

10. The method of Claim 9 wherein the cell is a cancer cell from the ovary, uterus, fallopian tube, endometrium, placenta, breast, testis, prostate, brain, stomach, liver, spleen, pancreas, thymus, colon, lung, kidney, heart, thyroid or smooth muscle.

11. The method of Claim 10 wherein the cell is an ovarian cancer cell.

12. The method of Claim 11 wherein the ovarian cancer cell is a low to high grade serous carcinoma cell.

13. The method of Claim 12 wherein the ovarian cancer cell is a high grade serous carcinoma cell.

14. The method of any one of Claims 1 to 13 wherein the IFNε or functional natural or synthetic variant or hybrid form directly or indirectly induces apoptosis of the cancer cell.

15. The method of any one of Claim 1 to 14 wherein the IFNε or variant, hybrid or modulator is used in combination with another anti-cancer agent.

16. The method of Claim 15 wherein the anti-cancer agent is selected from the group consisting of an antimetabolites, anti-tumor antibiotics, mitotic inhibitors, steroids, sex hormones or hormone-like drugs, alkylating agents, nitrogen mustard, nitrosoureas, hormone agonists and microtubular inhibitors.

17. The method of any one of Claims 1 to 16 wherein the amount of IFNε or variant or hybrid is from 10 IU/dose to 10^6 IU/dose.

18. A method for treating a subject with cancer, said method comprising administering to said subject an effective amount of IFNε or a functional natural or synthetic variant or hybrid form thereof or a modulator of *lfnε* expression or IFNε activity for a time and under conditions sufficient to induce apoptosis of cancer cells or inhibit cancer cell proliferation motility and/or migration.

19. The method of Claim 18 wherein the IFNε is derived from a species homologous to the species of the subject being treated.

20. The method of Claim 18 wherein the IFNε is derived from a species heterologous to the species of the subject being treated.

21. The method of Claim 18 or 19 or 20 wherein the subject is a human.

22. The method of Claim 21 wherein the IFNε is recombinant human IFNε or a modulator of *lfnε* expression.

23. The method of Claim 21 wherein the IFNε is recombinant non-human IFNε or a modulator of *lfnε* expression.

24. The method of Claim 21 wherein the IFNε is a hybrid between human and non-human IFNε.

25. The method of Claim 24 wherein the IFNε is a hybrid between human and murine IFNε.

26. The method of any one of Claims 18 to 25 wherein the cancer is a cancer of epithelial tissue, connective tissue, glandular tissue, embryonic tissue, hemopoietic cells, lymphatic tissue or bone marrow.

27. The method of Claim 26 wherein the cancer is in the ovary, uterus, fallopian tube, endometrium, placenta, breast, testis, prostate, brain, stomach, liver, spleen, pancreas, thymus, colon, lung, kidney, heart, thyroid or smooth muscle.

28. The method of Claim 27 wherein the cancer is ovarian cancer.

29. The method of Claim 28 wherein the ovarian cancer is a high grade serous carcinoma.

30. The method of any one of Claim 1 to 29 wherein the IFNε or variant, hybrid or modulator is used in combination with another anti-cancer agent.

31. The method of Claim 30 wherein the anti-cancer agent is selected from the group consisting of an antimetabolites, anti-tumor antibiotics, mitotic inhibitors, steroids, sex hormones or hormone-like drugs, alkylating agents, nitrogen mustard, nitrosoureas, hormone agonists and microtubular inhibitors.

32. The method of any one of Claims 1 to 31 wherein the amount of IFNε or variant or hybrid is from 10 IU/dose to 10^6 IU/dose.

33. Use of IFNε or a functional natural or synthetic variant or hybrid form thereof or a modulator of *lfnε* expression or IFNε activity in the manufacture of a medicament in the treatment of cancer in a subject.

34. IFNε or a functional natural or synthetic variant or hybrid form thereof or a modulator of *lfnε* expression or IFNε activity for use in the treatment of cancer in a subject.

35. Use of Claim 33 or IFNε or a functional natural or synthetic variant or hybrid form thereof or a modulator of *lfnε* expression or IFNε activity of Claim 34 wherein the IFNε is derived from a species homologous to the species of the subject to be treated.

36. Use of Claim 33 or IFNε or a functional natural or synthetic variant or hybrid form thereof or a modulator of *lfnε* expression or IFNε activity of Claim 34 wherein the IFNε is derived from a species heterologous to the species of the subject to be treated.

37. Use or IFNε or a functional natural or synthetic variant or hybrid form thereof or a modulator of *lfnε* expression or IFNε activity of Claim 34 or 35 or 36 wherein the subject is a human.

38. Use or IFNε or a functional natural or synthetic variant or hybrid form thereof or a modulator of *lfnε* expression or IFNε activity of Claim 37 wherein the IFNε is recombinant human IFNε.

39. Use or IFNε or a functional natural or synthetic variant or hybrid form thereof or a modulator of *lfnε* expression or IFNε activity of Claim 37wherein the IFNε is recombinant non-human IFNε.

40. Use or IFNε or a functional natural or synthetic variant or hybrid form thereof or a modulator of *lfnε* expression or IFNε activity of Claim 34wherein the IFNε is a hybrid between human and non-human IFNε.

41. Use or IFNε or a functional natural or synthetic variant or hybrid form thereof or a modulator of *lfnε* expression or IFNε activity of Claim 40 wherein the IFNε is a hybrid between human and murine IFNε.

42. Use or IFNε or a functional natural or synthetic variant or hybrid form thereof or a modulator of *lfnε* expression or IFNε activity of any one of Claims 33 to 41 wherein the cancer is a cancer of epithelial tissue, connective tissue, glandular tissue, embryonic tissue, hemopoietic cells, lymphatic tissue or bone marrow.

43. Use or IFNε or a functional natural or synthetic variant or hybrid form thereof or a modulator of *lfnε* expression or IFNε activity of Claim 42 wherein the cancer is in the ovary, uterus, fallopian tube, endometrium, placenta, breast, testis, prostate, brain, stomach, liver, spleen, pancreas, thymus, colon, lung, kidney, heart, thyroid or smooth muscle.

44. Use or IFNε or a functional natural or synthetic variant or hybrid form thereof or a modulator of *lfnε* expression or IFNε activity or a modulator of *lfnε* expression or IFNε activity of Claim 43 wherein the cancer is ovarian cancer.

45. Use or IFNε or a functional natural or synthetic variant or hybrid form thereof or a modulator of *lfnε* expression or IFNε activity of Claim 44 wherein the ovarian cancer is a high grade serous carcinoma.

46. Use or IFNε or a functional natural or synthetic variant or hybrid form thereof or a modulator of *lfnε* expression or IFNε activity wherein the use is an adjuvant for another anti-cancer agent.

47. Use or IFNε or a functional natural or synthetic variant or hybrid form thereof or a modulator of *lfnε* expression or IFNε activity of Claim 46 wherein the anti-cancer agent is selected from the group consisting of an antimetabolites, anti-tumor antibiotics, mitotic inhibitors, steroids, sex hormones or hormone-like drugs, alkylating agents, nitrogen mustard, nitrosoureas, hormone agonists and microtubular inhibitors.

48. A formulation comprising IFNε or a functional natural or synthetic variant or hybrid form thereof or a modulator of *lfnε* expression or IFNε activity and one or more carriers, adjuvants and/or excipients for use in the treatment of cancer.

49. The formulation of Claim 48 wherein the cancer is cancer of the ovary, uterus, fallopian tube, endometrium, placenta, breast, testis, prostate, brain, stomach, liver, spleen,

pancreas, thymus, colon, lung, kidney, heart, thyroid or smooth muscle.

50. The formulation of Claim 49 wherein the cancer is ovarian cancer.

51. The formulation of any one of Claims 41 to 50 in combination with an anti-cancer agent.

52. The formulation of Claim 51 wherein the anti-cancer agent is selected from the group consisting of an antimetabolites, anti-tumor antibiotics, mitotic inhibitors, steroids, sex hormones or hormone-like drugs, alkylating agents, nitrogen mustard, nitrosoureas, hormone agonists and microtubular inhibitors.

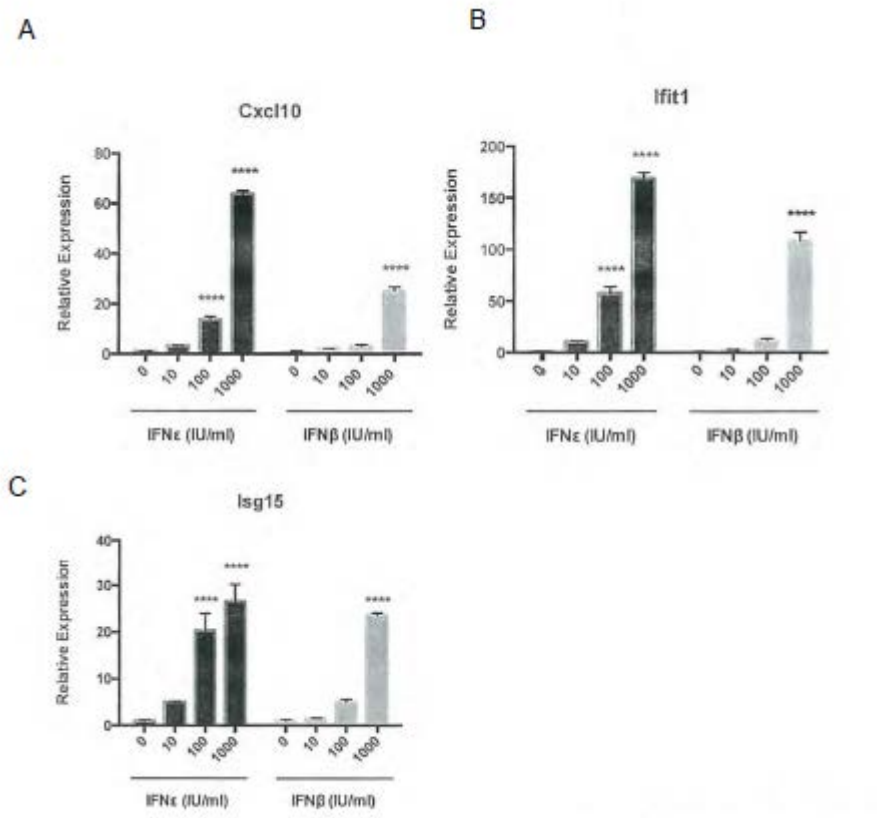
A
Cxcl10
Relative Expression
80
60
40
20
0
****
****
****
0
10
100
1000
0
10
100
1000
IFNε (IU/ml)
IFNβ (IU/ml)
B
Ifit1
Relative Expression
200
150
100
50
0
****
****
****
0
10
100
1000
0
10
100
1000
IFNε (IU/ml)
IFNβ (IU/ml)
C
Isg15
Relative Expression
40
30
20
10
0
****
****
****
0
10
100
1000
0
10
100
1000
IFNε (IU/ml)
IFNβ (IU/ml)

Figure 1

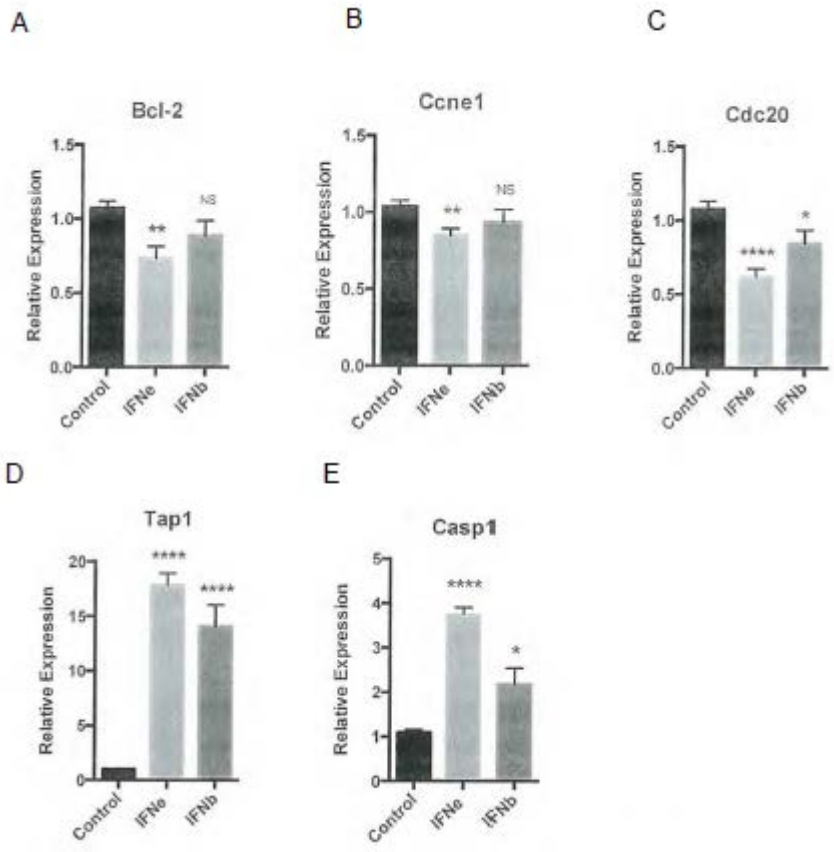
A
Bcl-2
Relative Expression
1.5
1.0
0.5
0.0
**
NS
Control
IFNe
IFNb
B
Ccne1
Relative Expression
1.5
1.0
0.5
0.0
**
NS
Control
IFNe
IFNb
C
Cdc20
Relative Expression
1.5
1.0
0.5
0.0
****
*
Control
IFNe
IFNb
D
Tap1
Relative Expression
20
15
10
5
0
****
****
Control
IFNe
IFNb
E
Casp1
Relative Expression
5
4
3
2
1
0
****
*
Control
IFNe
IFNb

Figure 2

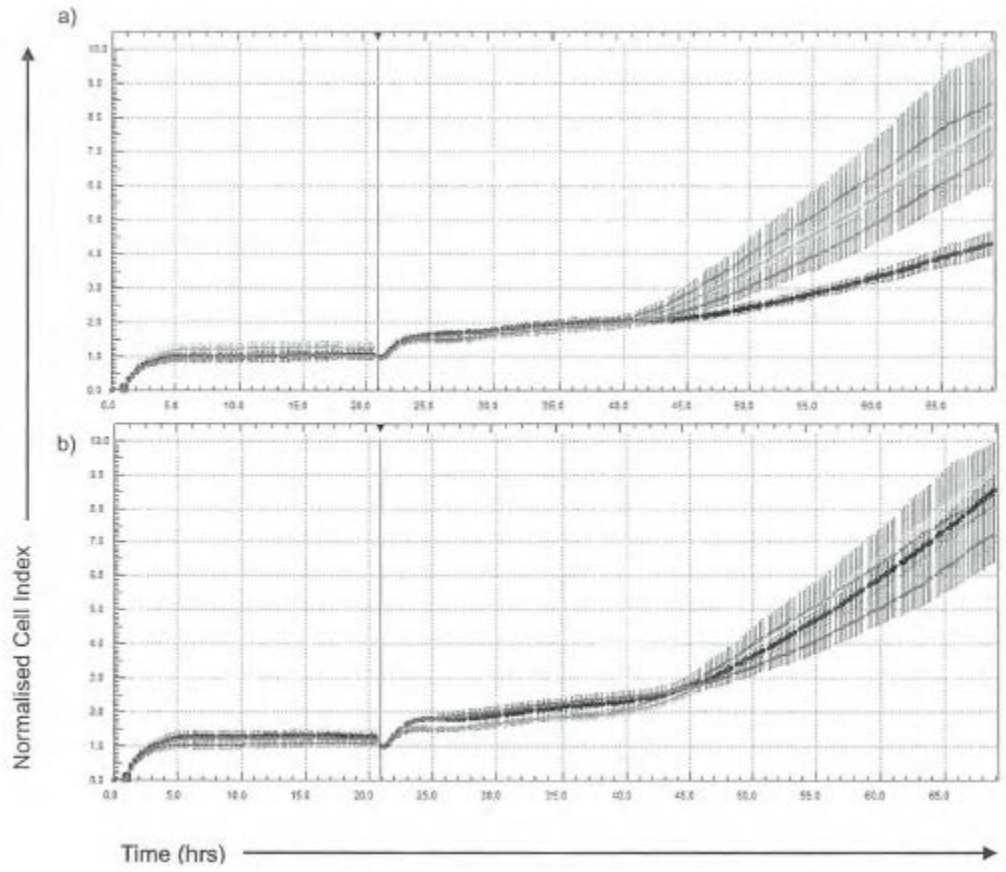

Figure 3

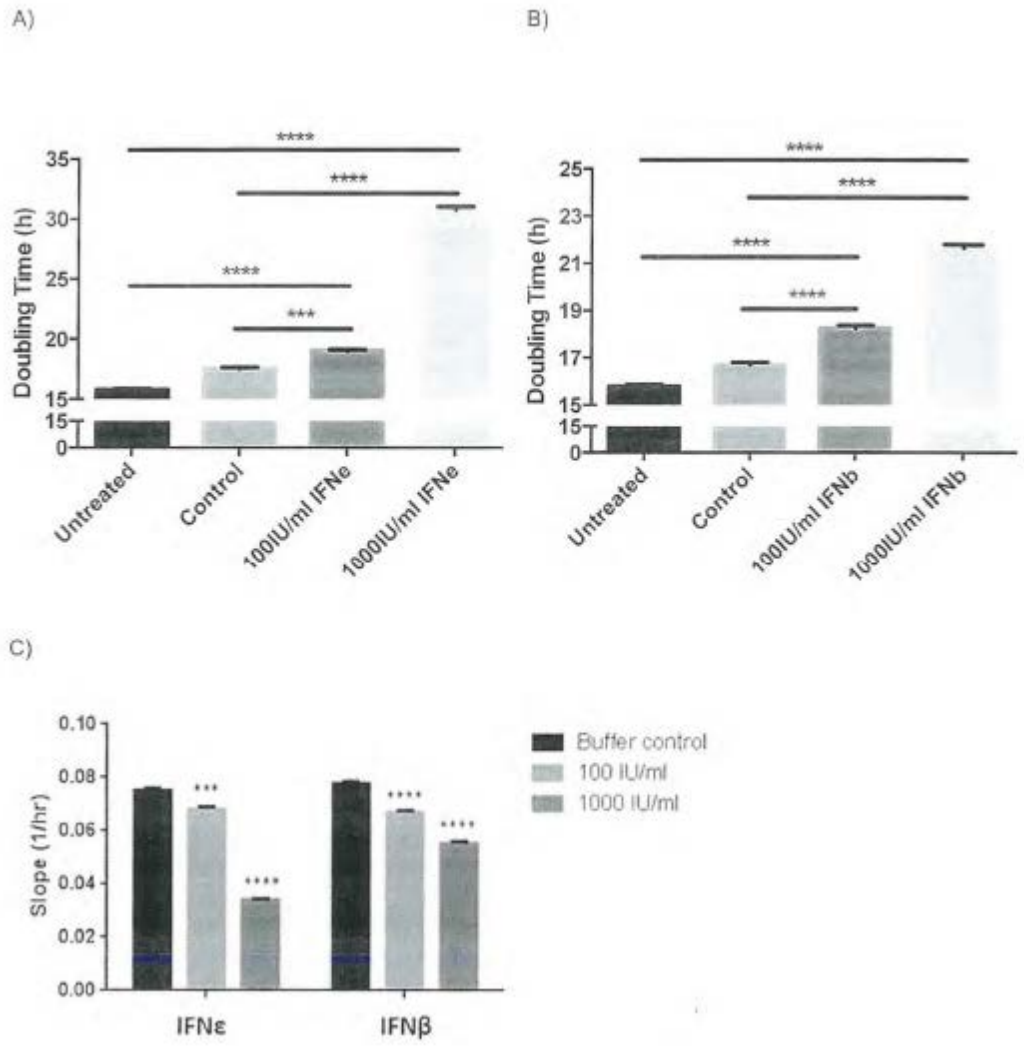
A)
B)
Doubling Time (h)
Untreated
Control
100IU/ml IFNe
1000IU/ml IFNe
100IU/ml IFNb
1000IU/ml IFNb
C)
Slope (1/hr)
IFNε
IFNβ
Buffer control
100 IU/ml
1000 IU/ml

Figure 4

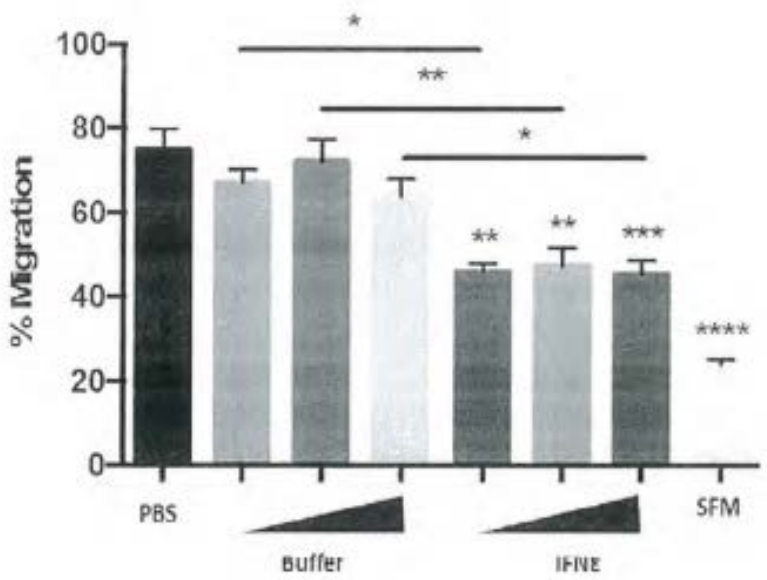

Figure 5

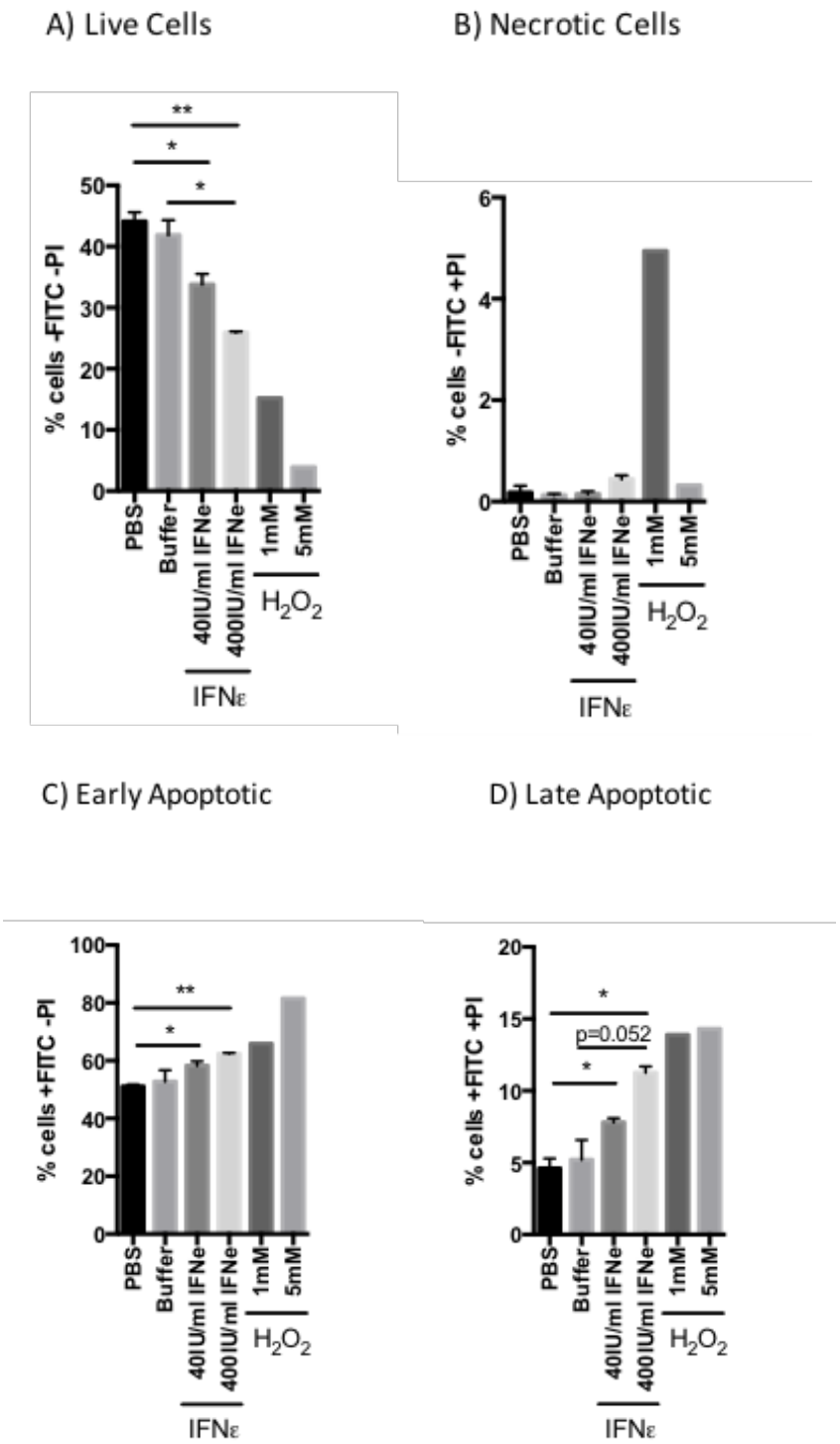
A) Live Cells
B) Necrotic Cells
C) Early Apoptotic
D) Late Apoptotic
% cells -FITC -PI
% cells -FITC +PI
% cells +FITC -PI
% cells +FITC +PI
PBS
Buffer
40IU/ml IFNε
400IU/ml IFNε
1mM
5mM
H2O2
IFNε
**
*
p=0.052

Figure 6

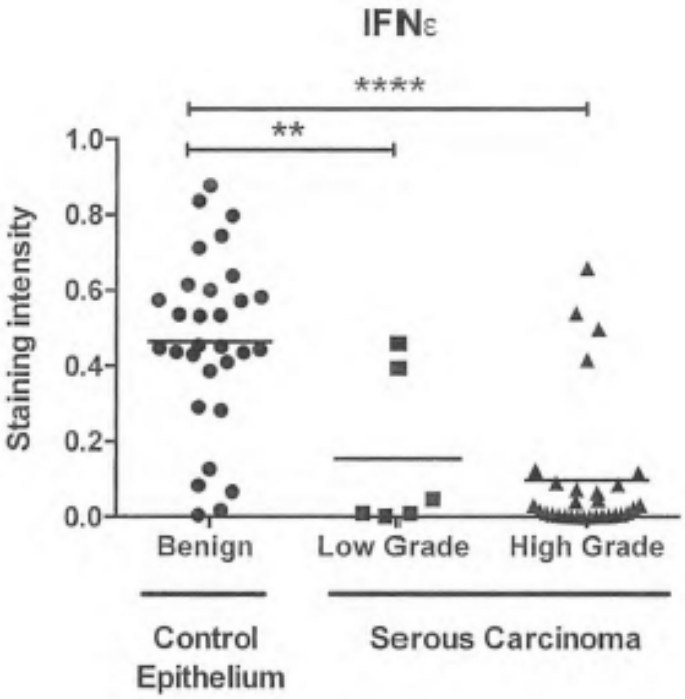
IFNε
****
**
1.0
0.8
0.6
0.4
0.2
0.0
Staining intensity
Benign
Low Grade
High Grade
Control Epithelium
Serous Carcinoma

Figure 7

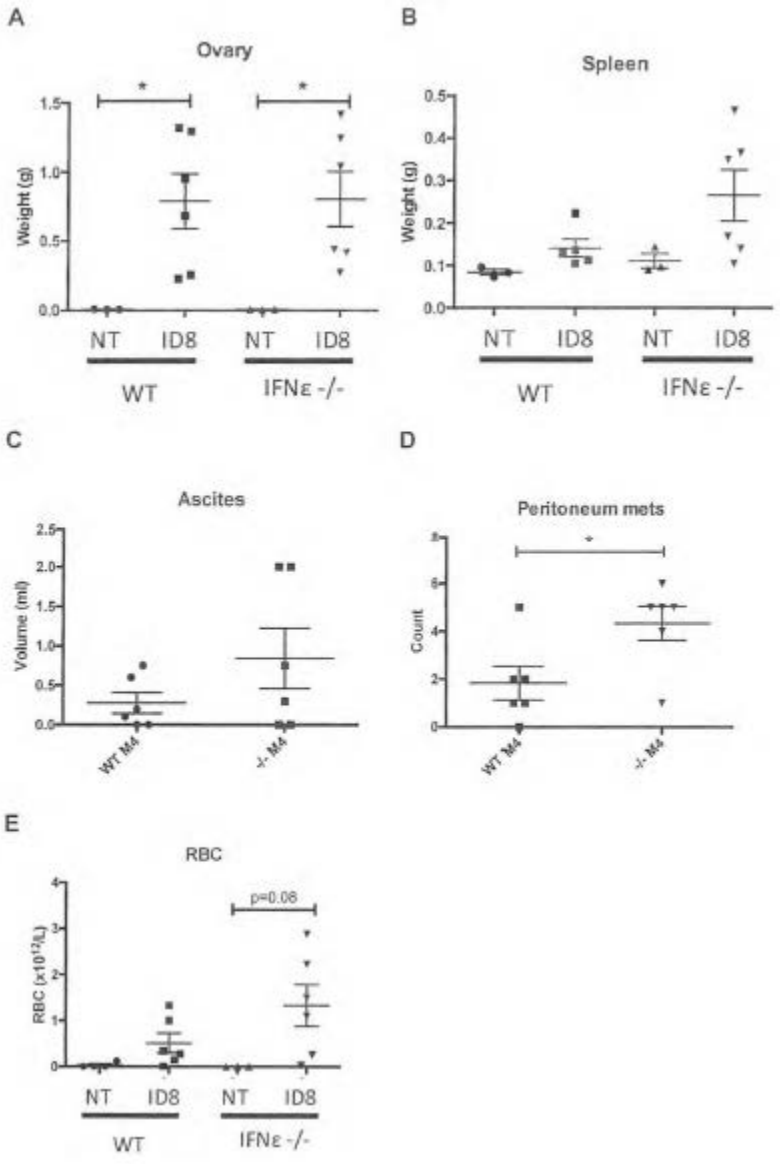
A
Ovary
Weight (g)
NT
ID8
NT
ID8
WT
IFNε -/-
B
Spleen
Weight (g)
NT
ID8
NT
ID8
WT
IFNε -/-
C
Ascites
Volume (ml)
WT M4
-/- M4
D
Peritoneum mets
Count
WT M4
-/- M4
E
RBC
p=0.06
RBC (x10^12/L)
NT
ID8
NT
ID8
WT
IFNε -/-

Figure 8

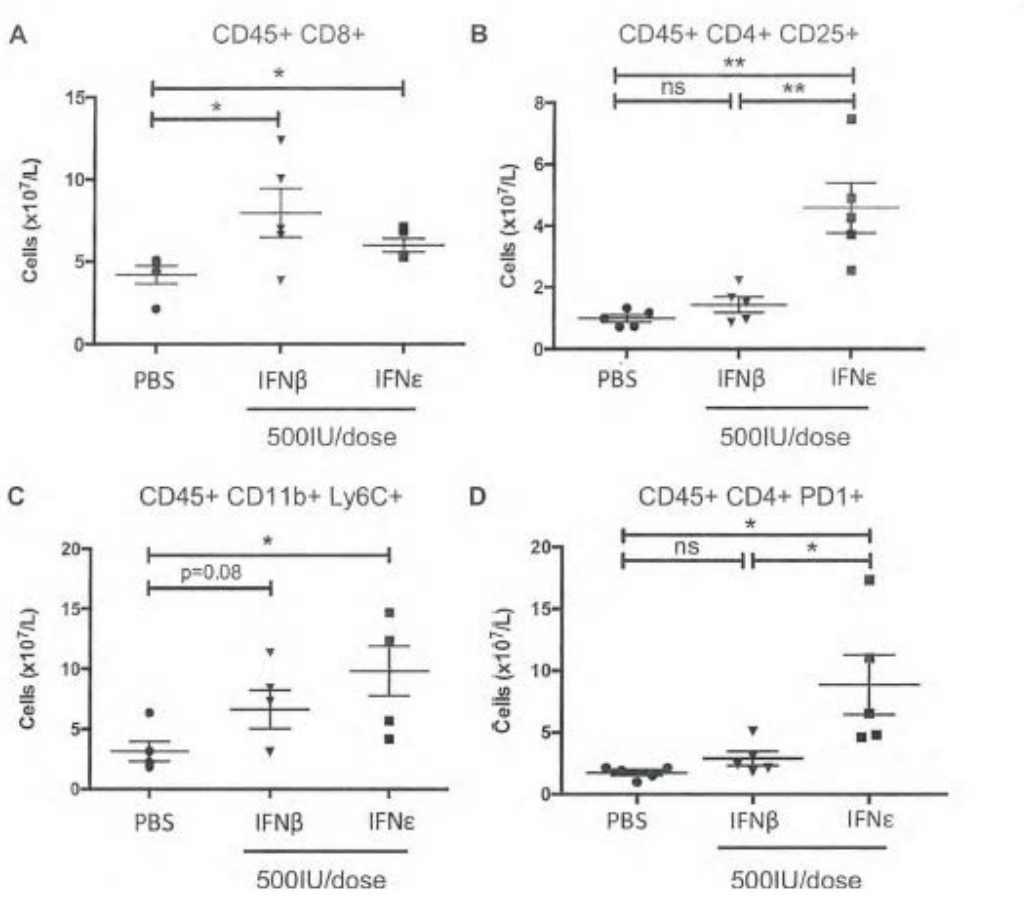
A
CD45+ CD8+
Cells (x10^7/L)
PBS
IFNβ
IFNε
500IU/dose
B
CD45+ CD4+ CD25+
ns
C
CD45+ CD11b+ Ly6C+
p=0.08
D
CD45+ CD4+ PD1+

Figure 9

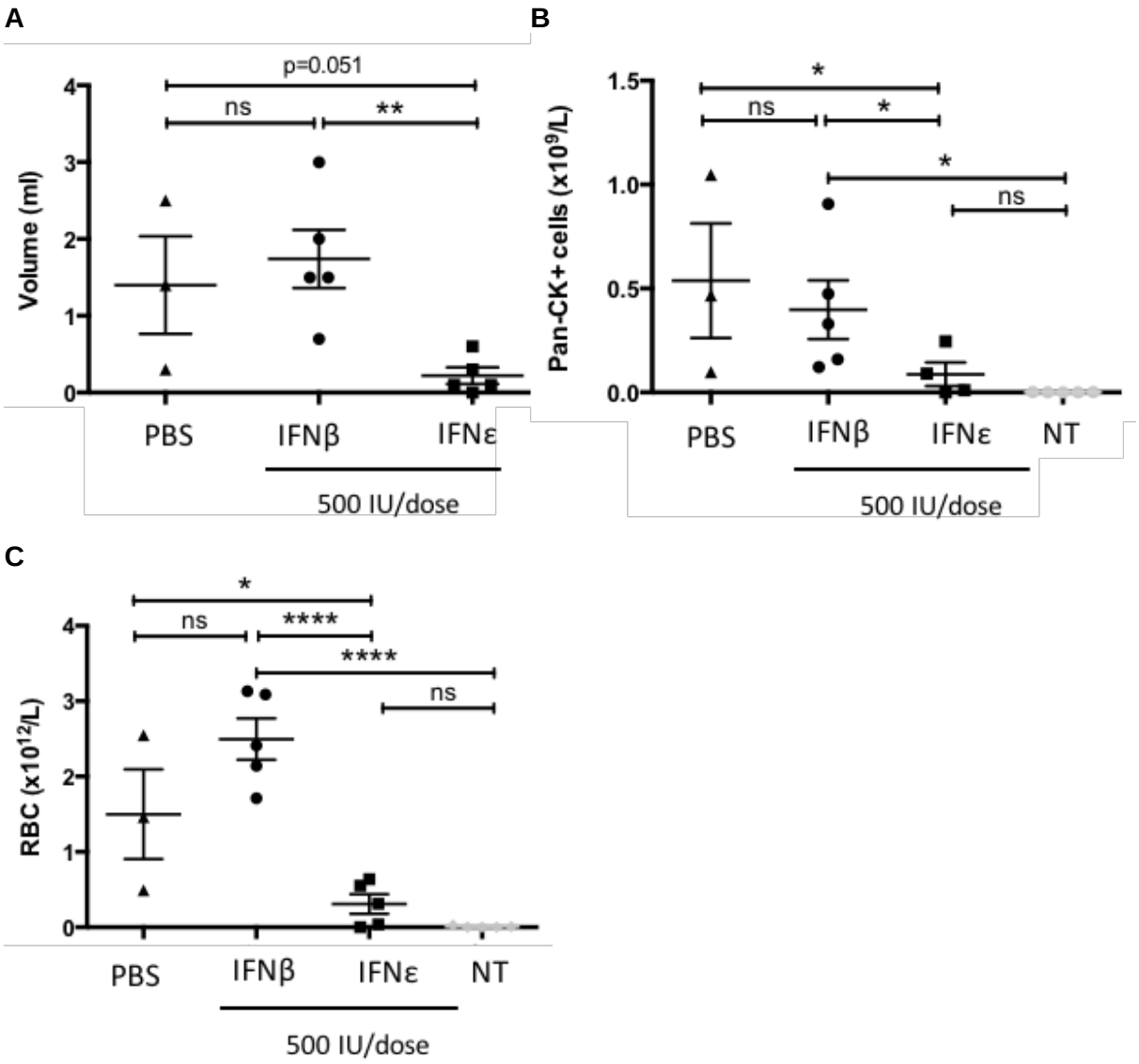
A
p=0.051
ns
**
Volume (ml)
4
3
2
1
0
PBS
IFNβ
IFNε
500 IU/dose
B
*
ns
*
*
ns
Pan-CK+ cells (x10⁹/L)
1.5
1.0
0.5
0.0
PBS
IFNβ
IFNε
NT
500 IU/dose
C
*
ns
****
****
ns
RBC (x10¹²/L)
4
3
2
1
0
PBS
IFNβ
IFNε
NT
500 IU/dose

Figure 10

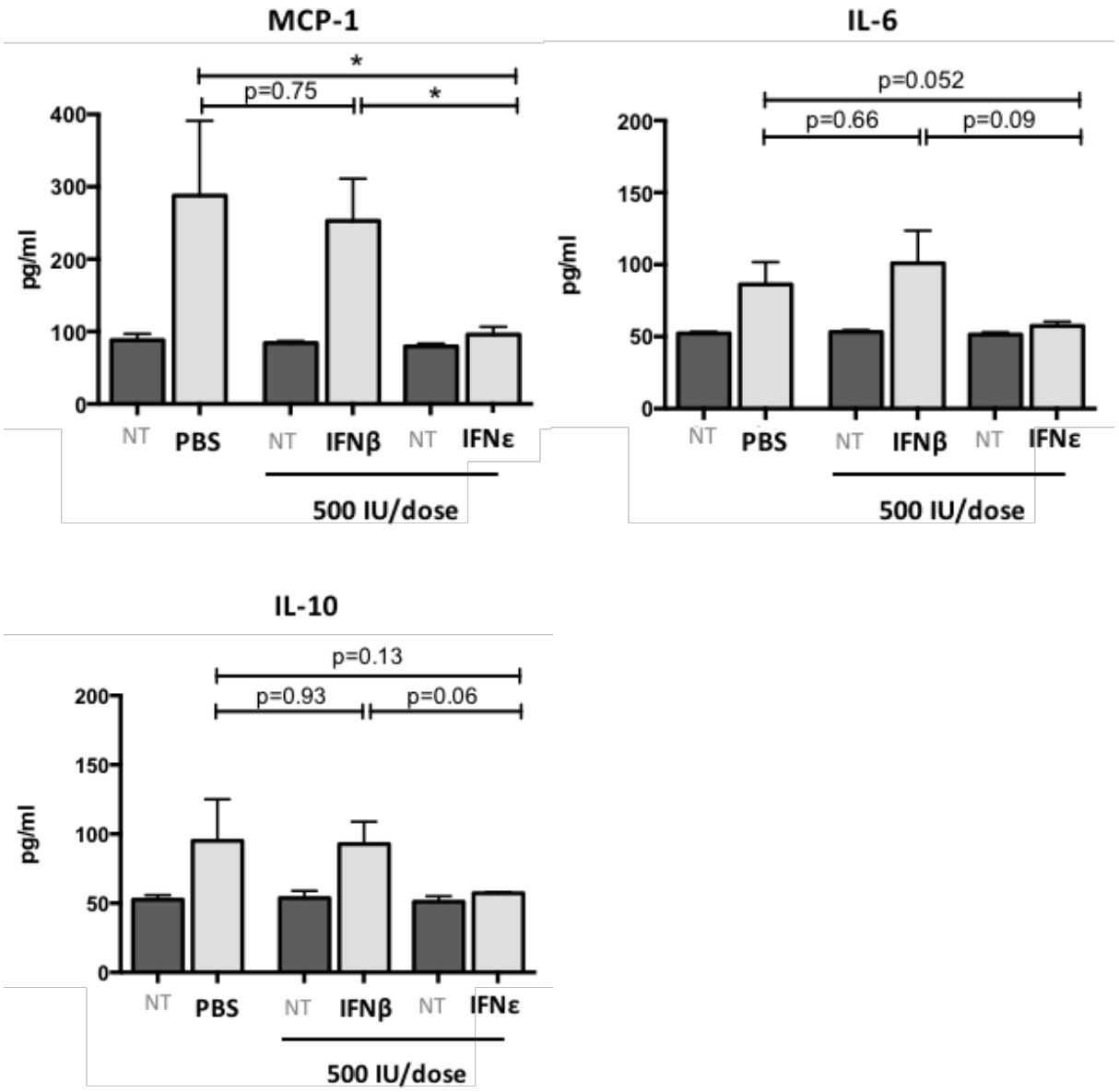
MCP-1
*
p=0.75
*
400
300
200
100
0
pg/ml
NT
PBS
NT
IFNβ
NT
IFNε
500 IU/dose
IL-6
p=0.052
p=0.66
p=0.09
200
150
100
50
0
pg/ml
NT
PBS
NT
IFNβ
NT
IFNε
500 IU/dose
IL-10
p=0.13
p=0.93
p=0.06
200
150
100
50
0
pg/ml
NT
PBS
NT
IFNβ
NT
IFNε
500 IU/dose

Figure 11

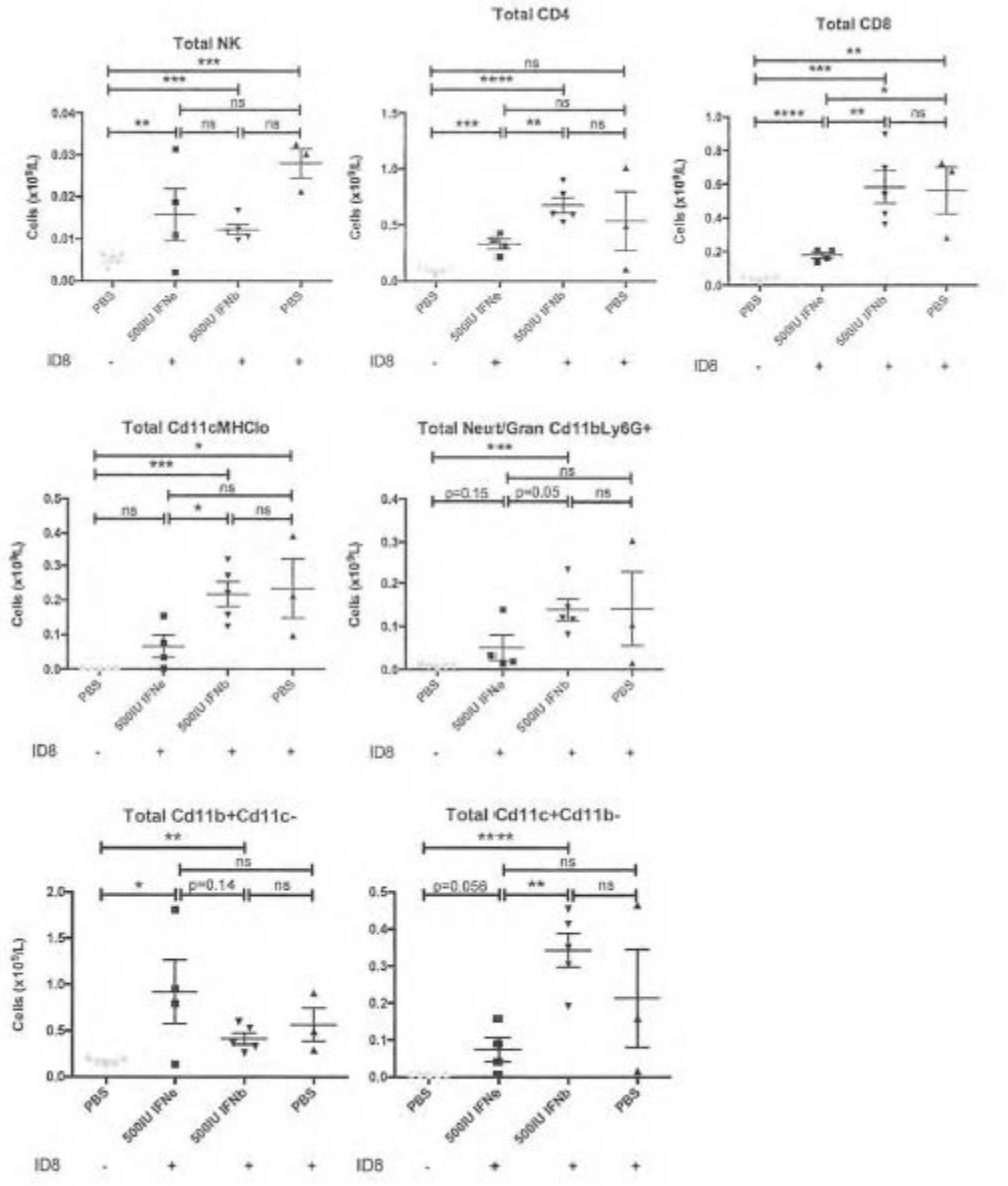
Total NK
Total CD4
Total CD8
Total Cd11cMHCIo
Total Neut/Gran Cd11bLy6G+
Total Cd11b+Cd11c-
Total Cd11c+Cd11b-
Cells (x10⁹/L)
PBS
500IU IFNα
500IU IFNb
PBS
ID8
p=0.15
p=0.05
p=0.14
p=0.056

Figure 12

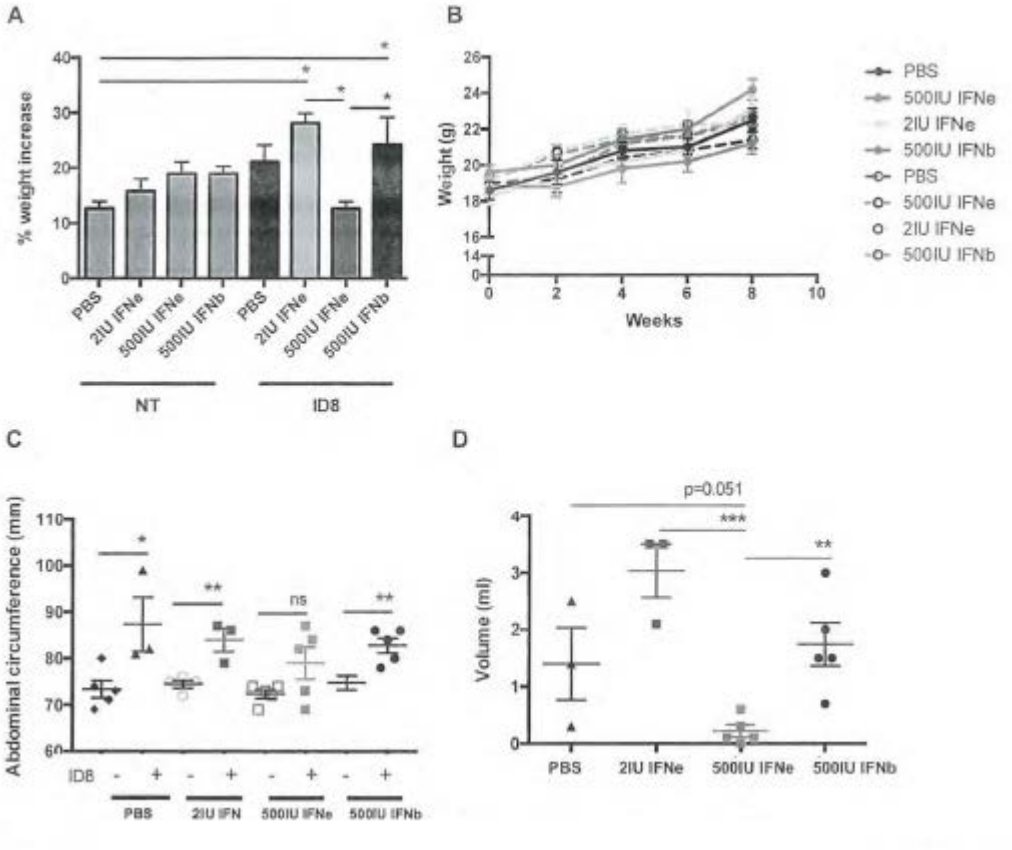
A
% weight increase
PBS
2IU IFNe
500IU IFNe
500IU IFNb
NT
ID8
B
Weight (g)
Weeks
PBS
500IU IFNe
2IU IFNe
500IU IFNb
C
Abdominal circumference (mm)
ID8
PBS
2IU IFN
500IU IFNe
500IU IFNb
ns
D
p=0.051
Volume (ml)
PBS
2IU IFNe
500IU IFNe
500IU IFNb

Figure 13

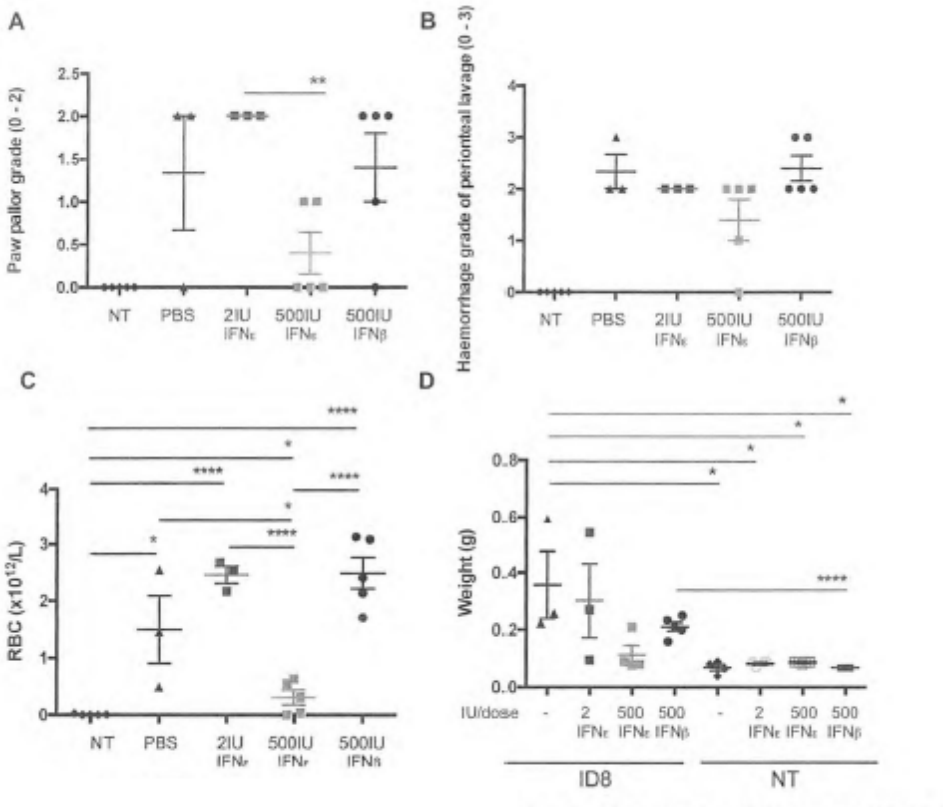
A
Paw pallor grade (0 - 2)
NT
PBS
2IU IFNε
500IU IFNε
500IU IFNβ
B
Haemorrhage grade of perionteal lavage (0 - 3)
C
RBC (x10^12/L)
D
Weight (g)
IU/dose
ID8
NT

Figure 14

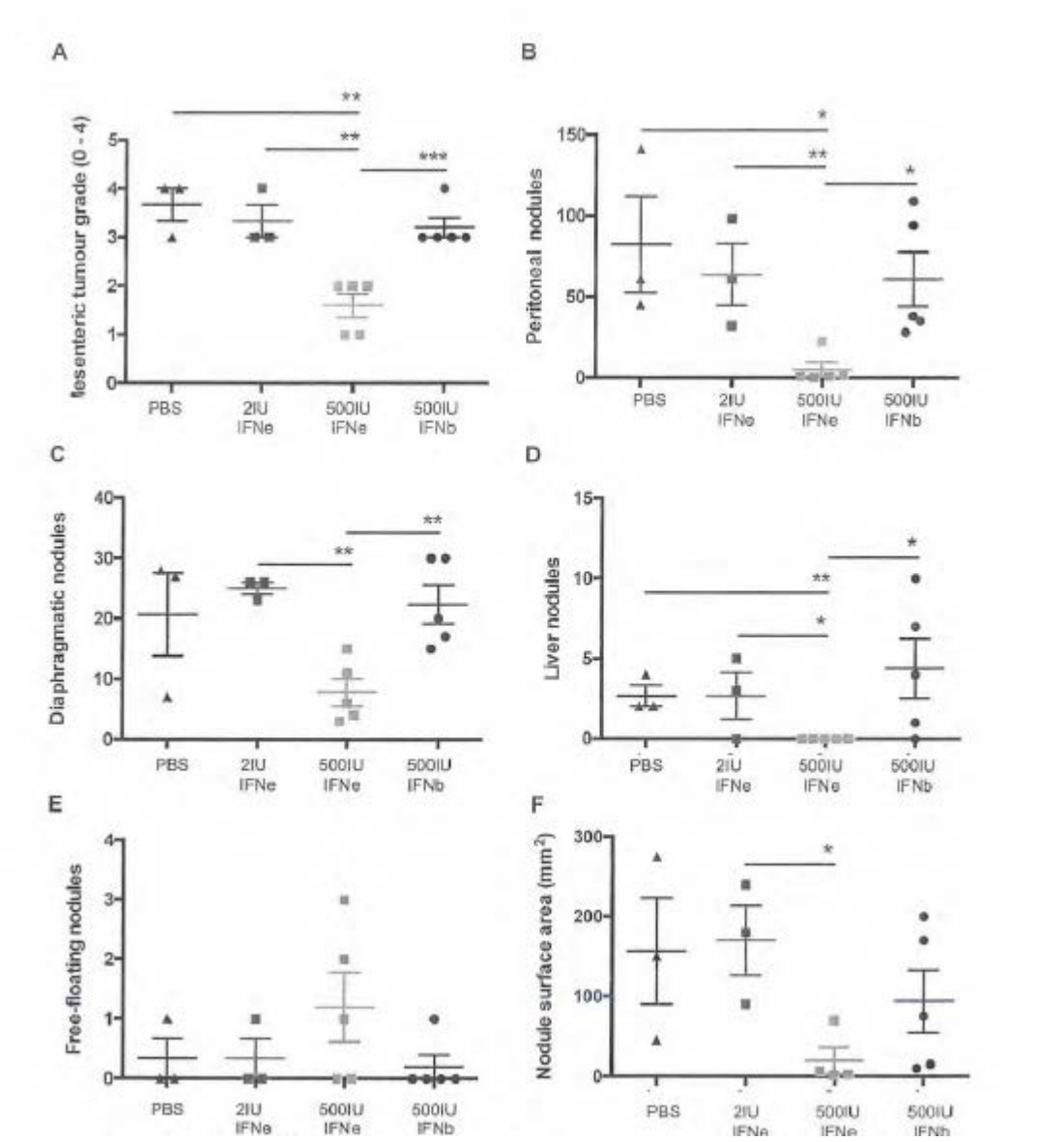
A
B
C
D
E
F
Mesenteric tumour grade (0 - 4)
Peritoneal nodules
Diaphragmatic nodules
Liver nodules
Free-floating nodules
Nodule surface area (mm²)
PBS
2IU IFNe
500IU IFNe
500IU IFNb

Figure 15